frontiers | Research Topics

Methods in alloimmunity and transplantation 2023

Edited by
Andreas Beilhack and Guido Moll

Published in
Frontiers in Immunology

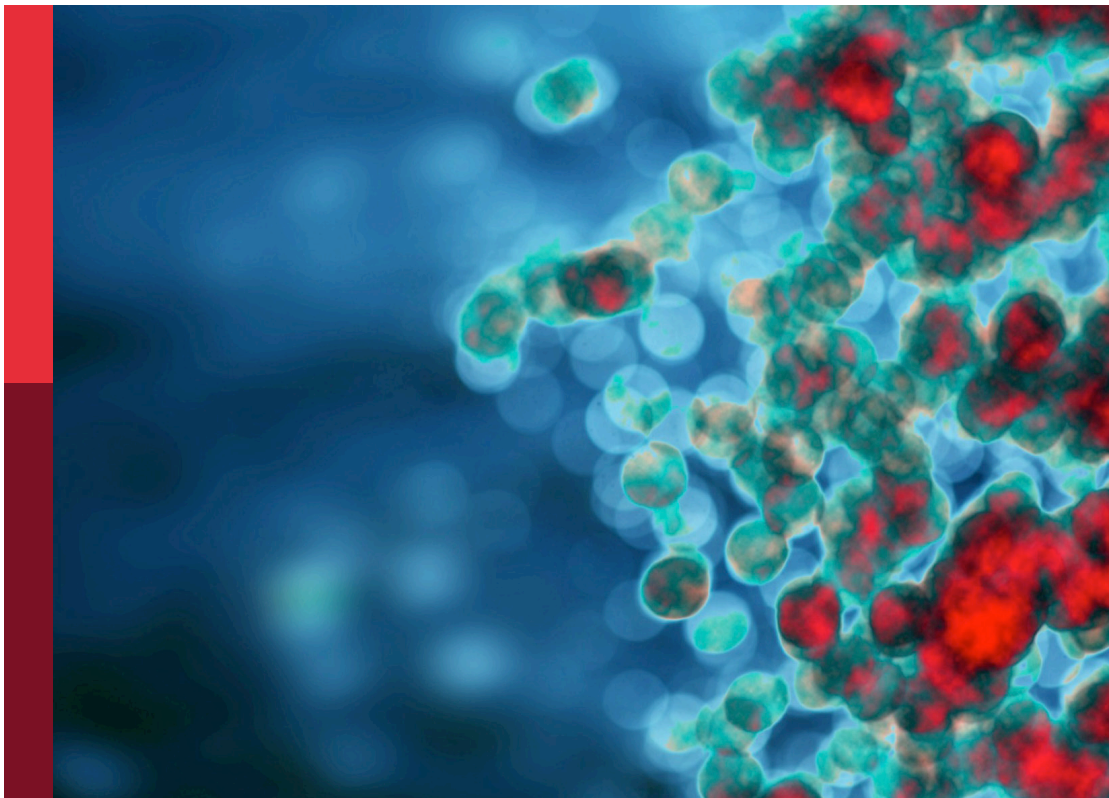

ISSN 1664-8714
ISBN 978-2-8325-5729-7
DOI 10.3389/978-2-8325-5729-7

About Frontiers

Frontiers is more than just an open access publisher of scholarly articles: it is a pioneering approach to the world of academia, radically improving the way scholarly research is managed. The grand vision of Frontiers is a world where all people have an equal opportunity to seek, share and generate knowledge. Frontiers provides immediate and permanent online open access to all its publications, but this alone is not enough to realize our grand goals.

Frontiers journal series

The Frontiers journal series is a multi-tier and interdisciplinary set of open-access, online journals, promising a paradigm shift from the current review, selection and dissemination processes in academic publishing. All Frontiers journals are driven by researchers for researchers; therefore, they constitute a service to the scholarly community. At the same time, the *Frontiers journal series* operates on a revolutionary invention, the tiered publishing system, initially addressing specific communities of scholars, and gradually climbing up to broader public understanding, thus serving the interests of the lay society, too.

Dedication to quality

Each Frontiers article is a landmark of the highest quality, thanks to genuinely collaborative interactions between authors and review editors, who include some of the world's best academicians. Research must be certified by peers before entering a stream of knowledge that may eventually reach the public - and shape society; therefore, Frontiers only applies the most rigorous and unbiased reviews. Frontiers revolutionizes research publishing by freely delivering the most outstanding research, evaluated with no bias from both the academic and social point of view. By applying the most advanced information technologies, Frontiers is catapulting scholarly publishing into a new generation.

What are Frontiers Research Topics?

Frontiers Research Topics are very popular trademarks of the *Frontiers journals series*: they are collections of at least ten articles, all centered on a particular subject. With their unique mix of varied contributions from Original Research to Review Articles, Frontiers Research Topics unify the most influential researchers, the latest key findings and historical advances in a hot research area.

Find out more on how to host your own Frontiers Research Topic or contribute to one as an author by contacting the Frontiers editorial office: frontiersin.org/about/contact

Methods in alloimmunity and transplantation: 2023

Topic editors

Andreas Beilhack — Julius Maximilian University of Würzburg, Germany

Guido Moll — Charité University Medicine Berlin, Germany

Citation

Beilhack, A., Moll, G., eds. (2024). *Methods in alloimmunity and transplantation: 2023*. Lausanne: Frontiers Media SA. doi: 10.3389/978-2-8325-5729-7

Table of contents

frontiers | Frontiers in Immunology

TYPE Editorial
PUBLISHED 11 November 2024
DOI 10.3389/fimmu.2024.1516554

OPEN ACCESS

EDITED AND REVIEWED BY
Antoine Toubert,
Université Paris Cité, France

*CORRESPONDENCE
Guido Moll
guido.moll@charite.de
Andreas Beilhack
beilhack_a@ukw.de

RECEIVED 24 October 2024
ACCEPTED 28 October 2024
PUBLISHED 11 November 2024

CITATION
Moll G and Beilhack A (2024)
Editorial: Methods in alloimmunity
and transplantation: 2023.
Front. Immunol. 15:1516554.
doi: 10.3389/fimmu.2024.1516554

Editorial: Methods in alloimmunity and transplantation: 2023

Guido Moll [1,2,3,4]* and Andreas Beilhack [5]*

[1]BIH Center for Regenerative Therapies (BCRT), [2]Berlin-Brandenburg School for Regenerative Therapies (BSRT), [3]Julius Wolff Institute (JWI) for Musculoskeletal Research, [4]Department of Nephrology and Internal Intensive Care Medicine, all three part of Charité Universitätsmedizin Berlin, corporate member of Freie Universität Berlin, Humboldt-Universität zu Berlin, and Berlin Institute of Health (BIH), Berlin, Germany, [5]Experimental Stem Cell Transplantation Group, Departments of Internal Medicine II and Department of Pediatrics, University Hospital Würzburg, Center of Experimental Molecular Medicine, Würzburg, Germany

KEYWORDS

transplantation, alloimmunity, rejection, inflammation, cell therapy, immunosuppression, immunomodulation, methods/technology

Editorial on the Research Topic
Methods in alloimmunity and transplantation: 2023

Introduction

This Research Topic is part of the "Methods in Immunology" series, which highlights cutting-edge techniques and methods used to investigate fundamental questions in immunology research, with a focus on Alloimmunity and Transplantation (Figure 1) (1, 2). Alloimmunity is the immune response to alloantigens – immunogenic molecules from members of the same species, including blood group antigens and the highly polymorphic antigens of the major histocompatibility complex/human leukocyte antigens (MHC/HLA) (Figure 1A) (3–5). Alloantigens can be classified as major and minor mismatch antigens, which is distinguished from xenoantigens/xenoreactivity against different species, and autoantigens/autoimmunity against self-antigens (1, 3–8). Alloantigens can trigger the formation of alloantibodies through alloantigen-primed B-cells and mature plasma cells (e.g. panel-reactive vs. donor-specific antibodies, PRA vs. DSA, respectively), as part of the humoral immune response, and the activation of effector T-lymphocytes, as part of the cellular immune response, with further amplification through secondary immune cell activation and infiltration (1, 3–8). Both, humoral and cellular alloimmune responses can lead to acute and chronic graft rejection in solid organ transplantation (SOT), and graft failure or graft-versus-host disease (GVHD) in hematopoietic (stem) cell transplantation (HCT/HSCT) (9–12). The most common SOT modalities include transplantation of kidneys (KTx), liver (LiTx), lungs (LuTx), heart (HTx), and vascularized composite allografts (VCA, e.g. hand, and face Tx) (1, 2, 13, 14). Successful allo-Tx requires precise "tissue matching" and optimal "IS protocols", to reduce the risk of immune rejection and to minimize IS toxicity (15). Current advancements in alloimmunity and transplantation (Figure 1B) include next generation sequencing (NGS) for transcriptome analysis at both bulk or single cell levels (RNAseq and scRNAseq) (16, 17), T- and B-cell receptor repertoire sequencing (TCRseq and BCRseq) (18–20), NGS analysis of donor-derived cell-free DNA (dd-cfDNA) (21–24),

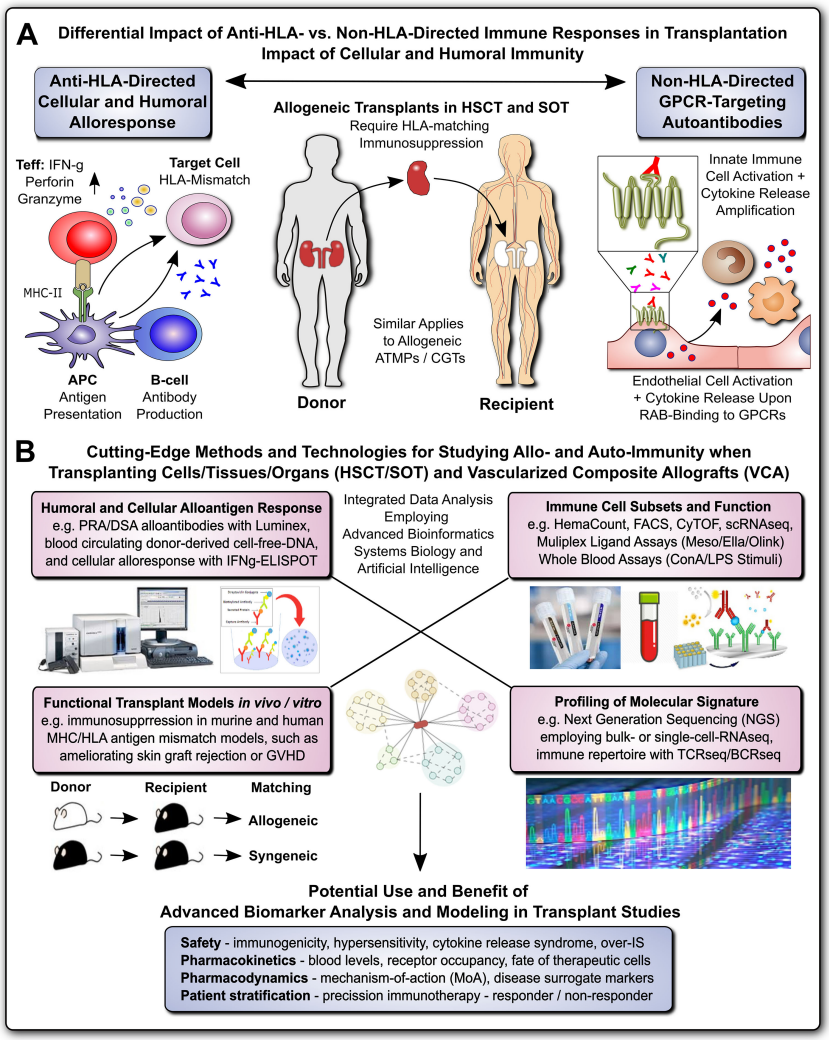

FIGURE 1
Methods for Studying Allo- and Auto-Immunity in Transplantation. **(A)** Differential Impact of Anti-HLA- and Non-HLA-directed Immune Responses in Transplantation: Allogeneic transplants in HSCT and SOT typically require HLA-matching and immunosuppression to prevent allograft rejection through anti-HLA-directed alloantigen-specific immune responses (e.g. T and B cell and alloantibody mediated), with a minor but significant contribution from non-HLA-directed auto-antigen-specific autoantibodies (e.g. GPCR-directed regulatory autoantibodies, RABs) (1, 7, 9). **(B)** Cutting-Edge Methods and Technologies for Studying Allo- and Auto-Immunity when Transplanting Cells/Tissues/Organs and Vascularized Composite Allografts (VACs): entailing at least four major important categories, such as detailed studies of: 1) Humoral and Cellular Alloantigen Responses, including monitoring of PRA/DSA with Luminex, blood circulating dd-cfDNA, and detection of cellular alloresponses with ELISpot typically IFNg-specific; 2) Functional Transplant Models *in vitro/in vivo*, including the study of novel immunosuppressive drugs and drug regimens in murine and human tissue MHC/HLA antigenic mismatch models, such as ameliorating allogeneic skin-graft rejection in mice or ameliorating GVHD in the HSCT setting; 3) Immune Cell Subsets and Function, including the use of hematology counters for absolute and relative cell quantification in whole blood, and targeted multiparametric analysis with flow cytometry/FACS and CyTOF with pre-defined panels, or broad-scale scRNAseq analysis for unbiased analysis of highly diverse cellular subsets, but also various multi-ligand-plex systems, (e.g. Mesoscale, Ella, and Olink) with different levels of sensitivity for specific ligands, and in addition whole blood assays (e.g. employing LPS or ConA stimulation for differential readout of cell type specific immune responses); and 4) Global Profiling of Molecular Signatures, including NGS-based analysis of bulk transcriptome with conventional RNAseq technology or at single-cell level with scRNAseq, and immune cell repertoire with TCRseq and BCRseq. In particular the integrated analysis of data from different analysis/modeling/readout platforms with advanced bioinformatics, including systems biology and artificial intelligence is of interest for optimal data interpretation and identification of suitable biomarkers. The potential use and benefit of advanced biomarker analysis and modeling in transplant studies entails multiple aspects, including: 1) Safety Assessment: such as immunogenicity, hypersensitivity, cytokine release syndrome, or over-immunosuppression (IS); 2) Pharmacokinetics: such as blood levels and receptor occupancy of specific ligands, or the fate of therapeutic cells; 3) Pharmacodynamics: such as studies on the mechanisms-of-action (MoA) and disease-specific surrogate markers; and 4) Patient Stratification: enabling precision immunotherapy by better understanding and distinguishing or restratifying responder and non-responder patients in advanced clinical trials. APC, antigen-presenting cell; ATMP, advanced therapy medicinal product; CGT, cell and gene therapy; MHC, major histocompatibility complex; HLA, human leukocyte antigen; HSCT, hematopoietic stem cell transplantation; SOT, solid organ transplantation; Teff and Treg, effector and regulatory T cells; GPCR, G-protein coupled receptor; RAB, regulatory autoantibodies of non-HLA type that are e.g. GPCR-directed, as distinguished from anti-HLA-directed panel-reactive alloantibodies (PRA) and donor-specific alloantibodies (DSA); dd-cfDNA, blood circulating donor-derived cell-free DNA; ELISpot-IFNg-specific, enzyme linked immune spot assay specific for release of interferon-gamma from activated T-cells; LPS, lipopolysaccharide pyrogen; ConA, concanavalin A mitogenic stimulus for T-cells; NGS, next-generation sequencing; TCRseq and BCRseq, T- and B-cell receptor sequencing, respectively.

sophisticated *in vitro* and *vivo* models to study transplant rejection (12, 25), but also novel concepts of transplantation (Tx), immunosuppression (IS), and patient care (15), including advanced therapy medicinal products and cell and gene therapies (ATMPs and CGTs) (1, 11, 15, 26–31). Adjunct technologies include machine perfusion of donor organs, novel renal replacement therapies (RRTs), but also the exponentially increasing use of advanced bioinformatics, systems biology, and artificial intelligence, for optimal analysis and interpretation of increasingly complex/large data sets (1, 31–37).

Clinical application of immune repertoire sequencing in SOT

Wong et al. from the University of British Columbia and Mc Gill University in Canada, reviewed the clinical use of TCRseq and BCRseq to monitor dynamic changes in donor-reactive clonal cell populations following Tx (20), which may enable therapy adjustments to prevent rejection, reduce excessive IS, and indicate the development of tolerance. The authors reviewed 37 articles - 16 on KTx (43%) and 21 on other types (57%) and they concluded that immune repertoire sequencing is a valuable emerging tool for pre- and post-Tx monitoring.

cfDNA quantification and qualification at the first month post lung transplant

Pedini et al. from Marseille in France conducted a prospective single-center study on 62 LuTx recipients to assess the relevance of dd-cfDNA for detecting acute and chronic rejection, or infection one month post LuTx (21–23). Total cfDNA was quantified with fluorimetry and digital PCR, cfDNA fragment size with BIABooster (Adelis), and dd-cfDNA with NGS (AlloSeq). While total cfDNA levels did not correlate with patient outcomes, higher dd-cfDNA were linked to graft injuries at d30 after LuTx (P=0.0004). A threshold of 1,72% dd-cfDNA effectively identified patients with healthy grafts, while higher levels of small dd-cfDNA indicated chronic injection or infection with 100% specificity.

Podocytes as glomerular sentinels at the crossroads of innate and adaptive immunity

Burke et al. from the Miami Transplant Institute in Florida reviewed the role of podocytes in in focal segmental glomerulosclerosis (FSGS), a common glomerular disorder that manifests as nephrotic syndrome after KTx. They focused on podocytes as targets of circulating factors which promote recurrence of proteinuria following KTx. They discussed the potential of pre-/post-reperfusion biopsies and podocyte *in vitro* assays to develop new treatments for FSGS.

Impact of deceased-donor characteristics on early graft function in KTx donor pairs

Mahler et al. from several Eurotransplant centers in Germany analyzed the outcomes from 328 cadaveric KTx recipients using 164 paired donor kidneys. They aimed to distinguish donor related risks from recipient and procedural variables, e.g. (a)symmetry of partner graft function, defined as early graft loss or impaired graft function (eGFR <30 ml/min) 3 months post KTx. They found that while donor factors impact early graft outcomes, they may play a limited role in long-term graft survival once the kidney graft has been accepted.

Predicting BKV infection post KTx

Bae et al. from the Catholic University of Korea investigated whether pre-KTx polyomavirus (BKV) serostatus and BK-specific cell mediated immunity (IFNg-ELISPOT against five BK viral antigens, LT, St, VP1, VP2, and VP3) could predict post-KTx BKV infection by evaluating 93 donor-recipient pairs who underwent KTx vs. 44 healthy controls. A combination of elevated donor BKV-IgG, low recipient BKV-IgG, and low BKV ELISPOT accurately predicted BKV infections in KTx recipients, helping clinicians to intervene earlier.

Autoantibodies from patients with KTx allograft vasculopathy promote inflammation

Moll et al. from Charité Berlin discovered that non-HLA-directed, protease activated receptor 1 (PAR1)-/G-protein coupled receptor (GPCR)-targeting regulatory autoantibodies (RABs) from KTx patients with transplant vasculopathy, but not IgG from KTx patients without vasculopathy or healthy controls, can exert immune stimulatory effects, triggering intracellular, and extracellular signaling in human microvascular endothelial cells and monocytic cells that may contribute to vasculopathy and graft failure, irrespective of alloantigen-directed responses.

Expanded hemodialysis ameliorates uremia-induced endothelial dysfunction

Zhao et al. from Charité Berlin found that expanded hemodialysis (HDx) with medium-cutoff (MCO) membranes can reduce endothelial dysfunction caused by uremia in HD patients. In turn, HDx therapy preserved the vasculoprotective Krüppel-like factor 2 (KLF2), which counteracts inflammation and promotes vascular health.

Better outcomes for HSCT recipients treated in home care versus hospital isolation

Ringdén et al. from Karolinska Institutet in Stockholm, Sweden, reviewed their >20-year "Karolinska Experience" providing home care to HSCT patients starting in 1998. Analyzing 252 allo-HSCT patient outcomes they found that home care is safe, reduces the risk of developing acute GVHD, lowers transplant-related mortality, improves survival, and decreases proinflammatory cytokine levels compared to hospital-treated controls.

Autoimmune encephalitis, neurological symptoms, and neuronal antibody in HSCT

Zhang et al. from Tongji Medical College in Wuhan, China, reported a case of neuronal surface antibody syndrome (NSAS)-related autoimmune neurological disorder, with presentation of autoimmune encephalitis (AE), in a 7-year-old girl following HSCT, diagnosed with anti-metabotropic glutamate receptor-5 (mGluR5) autoimmunity, a less common form of NSAS-related autoimmunity. Treatment with IVIG and methylprednisolone, followed by oral prednisone tablets, and levetiracetam as antiepileptic therapy led to significant improvement.

Ex vivo modeling of intestinal GVHD with a novel T-cell-organoid coculture system

Matthe et al. from the University Hospital Erlangen and University of Erlangen-Nuremberg in Germany developed a novel T-cell-organoid (co)culture system to study lympho-epithelial interactions in intestinal GvHD, which provides a valuable *ex vivo* platform for screening new therapeutic strategies on cellular and molecular level.

Novel preclinical mouse model for cGVDH

Verlaat et al. from Charité Berlin report the development of two murine cGvHD models, which display high long-term morbidity, but low mortality, and depict heterogeneous clinical manifestations seen of cGVDH pathophysiology seen in patients.

Author contributions

GM: Conceptualization, Data curation, Formal analysis, Funding acquisition, Investigation, Methodology, Project administration, Resources, Software, Supervision, Validation, Visualization, Writing – original draft, Writing – review & editing. AB: Conceptualization, Data curation, Formal analysis, Funding acquisition, Investigation, Methodology, Project administration, Resources, Software, Supervision, Validation, Visualization, Writing – original draft, Writing – review & editing.

Funding

The author(s) declare financial support was received for the research, authorship, and/or publication of this article. AB was supported by the Deutsche Forschungsgemeinschaft (DFG, German Research Foundation) – project number 324392634 – TRR 221. GM was supported by grants from the German Federal Ministry of Education and Research (BMBF) and the DFG (EXPAND-PD project #CA2816/1) and through the BIH Center for Regenerative Therapies (BCRT) and the Berlin-Brandenburg School for Regenerative Therapies (BSRT: GSC203), respectively, and in part by the European Union's Horizon 2020 Research and Innovation Program und the grant agreements No 733006 (PACE), 779293 (HIPGEN), 754995 (EU-TRAIN), and 101095635 (PROTO). We acknowledge financial support from the Open Access Publication Fund of Charité Universitätsmedizin Berlin and the DFG.

Acknowledgments

We would like to thank all authors who contributed submitting manuscripts to this Research Topic and all reviewers who provided insightful feedback and helpful comments. All listed authors have made a substantial direct intellectual contribution, approved it for publication, and declare that the research was conducted in the absence of any potential conflict of interest.

Conflict of interest

The authors declare that the research was conducted in the absence of any commercial or financial relationships that could be construed as a potential conflict of interest.

The author(s) declared that they were an editorial board member of Frontiers, at the time of submission. This had no impact on the peer review process and the final decision.

Publisher's note

References

1. Moll G, Lim WH, Penack O. Editorial: Emerging talents in alloimmunity and transplantation: 2022. *Front Immunol*. (2024) 15:1393026. doi: 10.3389/fimmu.2024.1393026

2. Moll G, Dai Z, Camara NOS. Editorial: advances in heart transplantation. *Front Immunol*. (2022) 13:960800. doi: 10.3389/fimmu.2022.960800

3. Rocha PN, Plumb TJ, Crowley SD, Coffman TM. Effector mechanisms in transplant rejection. *Immunol Rev*. (2003) 196:51–64. doi: 10.1046/j.1600-065X.2003.00090.x

4. Felix NJ, Allen PM. Specificity of T-cell alloreactivity. *Nat Rev Immunol*. (2007) 7:942–53. doi: 10.1038/nri2200

5. Ely LK, Burrows SR, Purcell AW, Rossjohn J, McCluskey J. T-cells behaving badly: structural insights into alloreactivity and autoimmunity. *Curr Opin Immunol*. (2008) 20:575–80. doi: 10.1016/j.coi.2008.07.006

6. Galili U. Xenotransplantation and ABO incompatible transplantation: the similarities they share. *Transfus Apher Sci*. (2006) 35:45–58. doi: 10.1016/j.transci.2006.05.007

7. Cabral-Marques O, Moll G, Catar R, Preuß B, Bankamp L, Pecher A-C, et al. Autoantibodies targeting G protein-coupled receptors: An evolving history in autoimmunity. Report of the 4th international symposium. *Autoimmun Rev*. (2023) 22:103310. doi: 10.1016/j.autrev.2023.103310

8. Moll G, Hult A, von Bahr L, Alm JJ, Heldring N, Hamad OA, et al. Do ABO blood group antigens hamper the therapeutic efficacy of mesenchymal stromal cells? *PLoS One*. (2014) 9:e85040. doi: 10.1371/journal.pone.0085040

9. Cordes S, Mokhtari Z, Bartosova M, Mertlitz S, Riesner K, Shi Y, et al. Endothelial damage and dysfunction in acute graft-versus-host disease. *Haematologica*. (2021) 106:2147–60. doi: 10.3324/haematol.2020.253716

10. Ullrich E, Beilhack A, Wolf D. Editorial: novel and improved methods for the prevention and treatment of graft-versus-host disease (GVHD). *Front Immunol*. (2022) 13:966389. doi: 10.3389/fimmu.2022.966389

11. Ringdén O, Moll G, Gustafsson B, Sadeghi B. Mesenchymal stromal cells for enhancing hematopoietic engraftment and treatment of graft-versus-host disease, Hemorrhages and Acute Respiratory Distress Syndrome. *Front Immunol*. (2022) 13:839844. doi: 10.3389/fimmu.2022.839844

12. Penack O, Marchetti M, Aljurf M, Arat M, Bonifazi F, Duarte RF, et al. Prophylaxis and management of graft-versus-host disease after stem-cell transplantation for haematological Malignancies: updated consensus recommendations of the European Society for Blood and Marrow Transplantation, The Lancet. *Haematology*. (2024) 11:e147–59. doi: 10.1016/S2352-3026(23)00342-3

13. Knoedler L, Dean J, Diatta F, Thompson N, Knoedler S, Rhys R, et al. Immune modulation in transplant medicine: a comprehensive review of cell therapy applications and future directions. *Front Immunol*. (2024) 15. doi: 10.3389/fimmu.2024.1372862

14. Kauke-Navarro M, Noel OF, Knoedler L, Knoedler S, Panayi AC, Stoegner VA, et al. Novel strategies in transplantation: genetic engineering and vascularized composite allotransplantation. *J Surg Res*. (2023) 291:176–86. doi: 10.1016/j.jss.2023.04.028

15. Roemhild A, Otto NM, Moll G, Abou-El-Enein M, Kaiser D, Bold G, et al. Regulatory T cells for minimising immune suppression in kidney transplantation: phase I/IIa clinical trial. *Bmj*. (2020) 371:m3734. doi: 10.1136/bmj.m3734

16. Andrzejewska A, Catar R, Schoon J, Qazi TH, Sass FA, Jacobi D, et al. Multi-parameter analysis of biobanked human bone marrow stromal cells shows little influence for donor age and mild comorbidities on phenotypic and functional properties. *Front Immunol*. (2019) 10:2474. doi: 10.3389/fimmu.2019.02474

17. Vandereyken K, Sifrim A, Thienpont B, Voet T. Methods and applications for single-cell and spatial multi-omics. *Nat Rev Genet*. (2023) 24:494–515. doi: 10.1038/s41576-023-00580-2

18. Freeman JD, Warren RL, Webb JR, Nelson BH, Holt RA. Profiling the T-cell receptor beta-chain repertoire by massively parallel sequencing. *Genome Res*. (2009) 19:1817–24. doi: 10.1101/gr.092924.109

19. Dziubianau M, Hecht J, Kuchenbecker L, Sattler A, Stervbo U, Rodelsperger C, et al. TCR repertoire analysis by next generation sequencing allows complex differential diagnosis of T cell-related pathology. *Am J Transplant*. (2013) 13:2842–54. doi: 10.1111/ajt.12431

20. Alachkar H, Mutonga M, Kato T, Kalluri S, Kakuta Y, Uemura M, et al. Quantitative characterization of T-cell repertoire and biomarkers in kidney transplant rejection. *BMC Nephrol*. (2016) 17:181. doi: 10.1186/s12882-016-0395-3

21. Tamkovich SN, Vlassov VV, Laktionov PP. Circulating DNA in the blood and its application in medical diagnosis. *Mol Biol*. (2008) 42:9–19. doi: 10.1134/S0026893308010020

22. Jiang P, Lo YMD. The long and short of circulating cell-free DNA and the ins and outs of molecular diagnostics. *Trends Genet*. (2016) 32:360–71. doi: 10.1016/j.tig.2016.03.009

23. Knight SR, Thorne A, Lo Faro ML. Donor-specific cell-free DNA as a biomarker in solid organ transplantation. A systematic review. *Transplantation*. (2019) 103:273–83. doi: 10.1097/TP.0000000000002482

24. Oellerich M, Sherwood K, Keown P, Schütz E, Beck J, Stegbauer J, et al. Liquid biopsies: donor-derived cell-free DNA for the detection of kidney allograft injury. *Nat Rev Nephrol*. (2021) 17:591–603. doi: 10.1038/s41581-021-00428-0

25. Jiang X, Shi QS, Wu C-Y, Xu L, Yang H, MedhatAskar. Investigative and laboratory assays for allogeneic rejection – A clinical perspective. *Transplant Rep*. (2023) 8:100133. doi: 10.1016/j.tpr.2023.100133

26. Moll G, Hoogduijn MJ, Ankrum JA. Editorial: safety, efficacy and mechanisms of action of mesenchymal stem cell therapies. *Front Immunol*. (2020) 11:243. doi: 10.3389/fimmu.2020.00243

27. Moll G, Ankrum JA, Kamhieh-Milz J, Bieback K, Ringden O, Volk HD, et al. Intravascular mesenchymal stromal/stem cell therapy product diversification: time for new clinical guidelines. *Trends Mol Med*. (2019) 25:149–63. doi: 10.1016/j.molmed.2018.12.006

28. Moll G, Ankrum JA, Olson SD, Nolta JA. Improved MSC minimal criteria to maximize patient safety: A call to embrace tissue factor and hemocompatibility assessment of MSC products. *Stem Cells Trans Med*. (2022) 11:2–13. doi: 10.1093/stcltm/szab005

29. Goldsobel G, von Herrath C, Schlickeiser S, Brindle N, Stähler F, Reinke P, et al. RESTORE survey on the public perception of advanced therapies and ATMPs in europe-why the european union should invest more! *Front Med (Lausanne)*. (2021) 8:739987. doi: 10.3389/fmed.2021.739987

30. Berishvili E, Piemonti L, de Koning EJP, Lindstedt S, Scholz H, Scott WE, et al. ESOT roadmap for advanced therapy medicinal products in transplantation: navigating regulatory challenges to enhance access and care. *Transplant Int*. (2024) 37. doi: 10.3389/ti.2024.13485

31. Silva-Sousa T, Usuda JN, Al-Arawe N, Frias F, Hinterseher I, Catar R, et al. The global evolution and impact of systems biology and artificial intelligence in stem cell research and therapeutics development: A scoping review. *Stem Cells*. (2024). doi: 10.1093/stmcls/sxae054

32. Tatum R, O'Malley TJ, Bodzin AS, Tchantchaleishvili V. Machine perfusion of donor organs for transplantation. *Artif organs*. (2021) 45:682–95. doi: 10.1111/aor.13894

33. Basile C, Davenport A, Mitra S, Pal A, Stamatialis D, Chrysochou C, et al. Frontiers in hemodialysis: Innovations and technological advances. *Artif organs*. (2021) 45:175–82. doi: 10.1111/aor.13798

34. Catar R, Moll G, Kamhieh-Milz J, Luecht C, Chen L, Zhao H, et al. Expanded hemodialysis therapy ameliorates uremia-induced systemic microinflammation and endothelial dysfunction by modulating VEGF, TNF-α and AP-1 signaling. *Front Immunol*. (2021) 12:774052. doi: 10.3389/fimmu.2021.774052

35. Loupy A, Mengel M, Haas M. Thirty years of the International Banff Classification for Allograft Pathology: the past, present, and future of kidney transplant diagnostics. *Kidney Int*. (2022) 101:678–91. doi: 10.1016/j.kint.2021.11.028

36. Yoo D, Goutaudier V, Divard G, Gueguen J, Astor BC, Aubert O, et al. An automated histological classification system for precision diagnostics of kidney allografts. *Nat Med*. (2023) 29:1211–20. doi: 10.1038/s41591-023-02323-6

37. Yoo D, Divard G, Raynaud M, Cohen A, Mone TD, Rosenthal JT, et al. A machine learning-driven virtual biopsy system for kidney transplant patients. *Nat Commun*. (2024) 15:554. doi: 10.1038/s41467-023-44595-z

frontiers | Frontiers in Immunology

TYPE Methods
PUBLISHED 24 January 2023
DOI 10.3389/fimmu.2022.1079921

OPEN ACCESS

EDITED BY
Andreas Beilhack,
Julius Maximilian University of Würzburg, Germany

REVIEWED BY
Olle Thor Hans Ringden,
Karolinska Institutet (KI), Sweden
Paul Joseph Martin,
Fred Hutchinson Cancer Research Center, United States

*CORRESPONDENCE
Olaf Penack
olaf.penack@charite.de

SPECIALTY SECTION
This article was submitted to Alloimmunity and Transplantation, a section of the journal Frontiers in Immunology

RECEIVED 25 October 2022
ACCEPTED 18 November 2022
PUBLISHED 24 January 2023

CITATION
Verlaat L, Riesner K, Kalupa M, Jung B, Mertlitz S, Schwarz C, Mengwasser J, Fricke C and Penack O (2023) Novel pre-clinical mouse models for chronic Graft-versus-Host Disease. *Front. Immunol.* 13:1079921. doi: 10.3389/fimmu.2022.1079921

Novel pre-clinical mouse models for chronic Graft-versus-Host Disease

Lydia Verlaat, Katarina Riesner, Martina Kalupa, Beate Jung, Sarah Mertlitz, Constanze Schwarz, Jörg Mengwasser, Claudine Fricke and Olaf Penack*

Department of Hematology, Oncology and Tumorimmunology, Charité – Universitätsmedizin Berlin, Corporate Member of Freie Universität Berlin and Humboldt-Universität zu Berlin, Berlin, Germany

Despite considerable progress in allogeneic hematopoietic cell transplantation (allo-HCT) has been achieved over the past years, chronic Graft-versus-Host Disease (cGvHD) still contributes to high morbidity rates, thus remaining a major hurdle in allo-HCT patients. To understand the complex pathophysiology of cGvHD and to develop refined prophylaxis and treatment strategies, improved pre-clinical models are needed. In this study, we developed two murine cGvHD models, which display high long-term morbidity but low mortality and depict the heterogeneous clinical manifestations of cGvHD seen in patients. We established a haploidentical C57BL/6→B6D2F1 allo-HCT model that uses myeloablative radiation and G-CSF-mobilized splenocytes as stem cell source and a sub-lethally irradiated Xenograft model, which utilizes the transfer of human peripheral blood mononuclear cells (PBMCs) into NOD scid gamma (NSG)-recipients. We characterized both mouse models to exhibit diverse clinical and histopathological signs of human cGvHD as extensive tissue damage, fibrosis/sclerosis, inflammation and B cell infiltration in cGvHD target organs skin, liver, lung and colon and found a decelerated immune cell reconstitution in the late phase after HCT. Our pre-clinical models can help to gain a deeper understanding of the target structures and mechanisms of cGvHD pathology and may enable a more reliable translation of experimental findings into the human setting of allo-HCT.

KEYWORDS

allogeneic hematopoietic stem cell transplantation, chronic Graft-versus-Host Disease, mouse models, G-CSF, xenogeneic transplantation, fibrosis, inflammation

Introduction

Allogeneic hematopoetic cell transplantation (allo-HCT) has emerged to the therapy of choice for a variety of hematologic, congenital and neoplastic disorders. Until 2020, nearly 50,000 allo-HCTs have been performed worldwide every year (1) with increasing numbers since 1990 (2). Although treatment outcomes have significantly improved, chronic Graft-versus-Host Disease (cGvHD) still occurs in up to 70% of transplanted patients and is accompanied with 25% of deaths after allo-HCT (3). Thus, cGvHD remains one of the major allo-HCT sequelae and contributes substantially to high long-term morbidity and non-relapse related mortality (NRM) rates (4, 5).

Due to the rising age of patients or unrelated-donor- and MHC-mismatched-transplantations, the overall incidence of cGvHD is increasing recently (6). Other major risk factors include prior acute GvHD and peripheral blood (PB) as hematopoietic cell (HC) source (7). Since HC collection from PB is easier to conduct, less invasive and bears a decreased risk for complications, it has recently become the standard choice in allo-HCT settings. Donors get administered with hematopoetic growth factors prior to apheresis, usually granulocyte colony-stimulating factor (G-CSF), which mobilizes bone marrow (BM) resident HCs into the PB circulation (8). However, several studies propose an increased risk of cGVHD development after G-CSF–mobilized allo-HCT (9, 10).

The pathophysiology of cGvHD development is highly complex (11) and still not fully understood. The establishment of mouse models has been of central importance for the identification and the general understanding of the cGvHD pathophysiology and the pre-clinical testing of reliable treatment strategies for translation into humans. Of big advantage, the genetically determined MHC variability between donors and recipients can be tightly controlled in murine models (12–14). For the majority of models, inbred mouse strain recipients are conditioned with total body irradiation and subsequently transplanted with HC grafts from BM, which is supplemented with T cells from donor mice (15). Hence, the severity and onset of GvHD can be adjusted by adaption of radiation doses and T cell numbers (16).

As reviewed elsewhere (15, 17, 18) several distinct mouse models were established, which helped to understand the intricate cGvHD pathophysiology and facilitated interventional treatment strategies. cGvHD mouse models can be broadly categorized into sclerodermatous/pro-fibrotic models, which exhibited fibrotic depositions in skin, lung or liver within 30 days after transplantation (19–21), autoantibody-mediated/lupus-like models that resemble human cGvHD, as they showed lupus-like manifestations as nephritis, liver cirrhosis, salivary gland fibrosis and skin involvement (22–24) and a transgenic thymic dysfunction model (25). Some mouse models manage to mimic a mixed cGvHD phenotype combining autoantibody production and scleroderma (26) or progressing from acute to chronic GvHD (27). Since this overlapping transformation is common in patients, mouse models can help to identify mechanisms of the causal link between allo- and autoreactivity.

Beyond classical murine models, xenogeneic (humanized) models have been developed, where human peripheral blood mononuclear cells (PBMCs) can be transplanted into immunodeficient mice. As one example, NOD/SCID gamma (NSG) mice are deficient in their Interleukin 2-receptor-function, resulting in a missing T-, B- and Natural Killer (NK) cell repertoire and deficient macrophage- and dendritic cell (DC) activity (28). In xeno-HCT experiments this model showed promising engraftment numbers and an acute GvHD phenotype with human T-cell infiltration of mouse skin, liver, intestine and lungs (29). Although this setup could be used to study and modify human GvHD *in vivo*, humanized models for simulation of cGvHD have not been further described.

Nonetheless, there is still no individual mouse model reliably comprising the highly diverse pathological and immunological characteristics of cGvHD seen in humans. So far, researchers may use more than one model to study cGvHD depending on ascientific hypothesis.Klicken Sie hier, um Text einzugeben.Furthermore, nearly all murine models are transplanted with HCs generated from BM, whereas the majority of clinical allo-HCTs are performed using G-CSF mobilized donor PB cells due to the simplified cell-collection procedure.

Objective

The present study attempts to establish pre-clinically relevant murine cGvHD models, which display high long-term morbidity but low mortality and resemble diverse manifestations of cGvHD seen in patients. The murine parent-into F1 model C57BL/6→B6D2F1 uses G-CSF-mobilized splenocytes as stem cell source, while the humanized model applies transplantation of human PBMCs → NSG mice. Those novel models can help to understand and describe the cGvHD pathology and to develop alternative therapeutic strategies in cGvHD prevention and management and guarantee a more reliable translation of the experimental findings into the human setting of allo-HCT.

Materials and methods

Mice

Female C57BL/6NCrl (B6) (H-2K^{b}) and B6D2F1 (BDF1) (H-2K$^{b/d}$) mice were purchased from Charles River Laboratories (Sulzfeld, Germany). Female immunodeficient NOD scid gamma (NSG) (NOD.Cg-Prkdc^{scid} Il2rg^{tm1Wjl}/SzJ) were bred and ordered from the group of Prof. Hans-Dieter Volk (Charité/

BIH, Berlin, Germany). All animals were housed in a 12-hour light-dark cycle under specified pathogen-free conditions in the Charité Animal Facility (Forschungseinrichtung für experimentelle Medizin). All experiments were approved by the local Ethics Committee for Animal Research (State Office of Health and Social Affairs, LaGeSo) and executed in compliance with the European Union guidelines.

Transplantation

Donor mice were aged >20 weeks, recipients were aged at least 8 to 10 weeks before HCT. B6 and BDF1 donors received daily subcutaneous injections of 10 mg/kg G-CSF (Filgrastim, 48 Mio. U.; Hexal, Germany) in 100 µl of sterile 5% glucose solution (Sigma-Aldrich, USA) for 5 consecutive days prior to transplantation to mobilize HCs. BDF1 underwent 1100 cGy total body irradiation on transplantation-day, split into two doses with a resting phase of at least 4 hours to reduce gut toxicity. NSGs were conditioned with reduced irradiation of 200 cGy on day -1 before HCT. On day 0, whole splenocytes were isolated from B6 donors (alternatively from BDF1-donors as syngeneic (syn) control group) and injected intravenously (i.v.) into conditioned BDF1 recipients. NSG mice were injected i.v. with human PBMCs, isolated from buffy coats from unknown donors provided by the German Red Cross, Berlin. Control NSG mice received only irradiation without injection of human PBMCs.

GvHD monitoring

cGvHD and control group animals were handled blinded to minimize experimental bias. HCT recipients were individually scored for four clinical parameters (posture, activity, fur, skin) on a scale from 0 to 2. Clinical GvHD score was assessed by summation of all parameters. Animals were sacrificed when exceeding a total GvHD score of 5 or a single GvHD score of >2. Weight loss was scored according to the 'body condition score' described by Ullman-Cullere (30) and animals were sacrificed when body condition score exceeded stadium (BC1 ≥ 20% total body weight loss)Survival was monitored daily. cGvHD experiments were run for 125 days before finalization.

Histological analyzes

Mice were euthanized and Tissue-Tek® cryo-embedding medium (Sakura Finetek, Alphen aan den Rijn, The Netherlands) was injected into the trachea to fill the lungs. Skin, liver, lung and colon were dissected and frozen in -80°C pre-cooled methylbutan (Carl Roth, Germany). 7 µm tissue cryosections were cut with a cryostat, fixed for 30 minutes in 10% ROTI®Histofix (Carl Roth, Germany) before Masson's Trichrome fibrosis staining was performed. Histopathologic and fibrotic grading of GvHD in murine tissue was performed blinded regarding cGvHD and control group in the stained sections after adapted Lerner citeria (31), as described with Cooke et al. (32) and Shulman et al. (33).

For immunohistofluorescence analyzes, 7 µm cryosections were fixed in -20°C methanol (Carl Roth, Germany), blocked (PBS + 3% BSA + 5% FCS) and incubated with primary antibodies (hamster CD3 (145-2C11; 1:200;BD Biosciences, USA), rat-B220 (6D5; 1:200; Biolegend, USA), hamster CD31 (2H8; 1:300; Invitrogen, USA) and rat-Endomucin (V.7C7; 1:200; Santa Cruz Biotech, USA) over night at 4°C. For visualization, sections were counter-stained with secondary antibodies donkey-anti-rat-AF488 (1:500; Invitrogen, USA) and goat-anti-hamster-Cy3 (1:1000; Jackson Laboratories, USA) for 2 hours at room temperature. Nuclei were stained with 2mg/ml 4',6-Diamidino-2-phenylindole (DAPI; Sigma-Aldrich, USA) before mounting with Fluoromount-G® (Southern Biotech, USA). Microscopy was performed using a Zeiss PALM MicroBeam with X-Cite® Xylis LED light source and Axiocam 305 color/Axiocam 712 mono cameras. Systems were using the ZEN blue software Version 3.1. Whole slide images were acquired from stitched tiles and processed and analyzed in FIJI Version 1.52p (34).

Flow cytometry

PB of mice was collected by facial vein or tail vein puncture. For analysing HC mobilization, blood was sampled before, on day 3 and 5 after G-CSF injection. Blood for engraftment checks was sampled at days +20 (+30 for NSG model), day+60 and day+125 after HCT. Spleens were harvested at day+125 and meshed through a 40µM cell strainer rinsed with isolation buffer (PBS + 2% FCS + 1 mM EDTA) for cell isolation. BM cells were harvested on day+125 by flushing of tibia and femur with isolation buffer through a 23G needle and subsequent filtering through a 70 µm cell strainer. After erythrocyte lysis (150 mM NH4Cl + 10 mM KHCO3 + 0.1 mM Na2EDTA), PB, splenic and BM cells were stained for 30 minutes with the following flow cytometry antibodies in MACS buffer (PBS + 0.5% BSA +1 mM EDTA): anti mouse H2kb-PE (1:100), Gr1-PE-Cy7 (1:200), CD80-APC (1:200), CD45-FITC (1:50; all Biolegend, USA), CD11c-PE (1:100; Invitrogen, USA), B220-PerCP-Cy5.5 (1:200), H2kd-FITC (1:50), CD3-APC (1:200), CD4-PE-Cy7 (1:200), CD8-APC-Cy7 (1:200) and CD11b-APC-Cy7 (1:200, all BD Biociences, USA). In NSG trials, the following anti-human antibodies were applied: CD3-APC (1:20), CD4-PerCP-Cy5.5 (1:20), CD8-APC-Cy7 (1:40), CD45-PE-Cy7 (1:20; all Biolegend, USA). Cells were detected with a FACSCanto II with BD FACSDiva™ Software v8.0.2 and the data was analyzed with FlowJo 10.6.1 Software (TreeStar Inc., Ashland, OR, USA).

Positive engraftment was defined as a minimum of 85% murine donor cells in the CD3+ fraction of the BDF1-recipients' blood at day+20, respectively the presence of human CD3+ cells in peripheral blood at d+30 after HCT and a minimum of 1% of human CD3+ cells or > 5% human CD45+ cells in the spleen of NSG mice upon the day of experiment abortion.

Mouse serum analysis

Blood from BDF1 and NSG mice was sampled by retro orbital bleeding under anesthesia. Blood was left to clot at room temperature 30 minutes and centrifuged to separate the serum fraction. Serum was analyzed with the LEGENDplex™ Mouse Inflammation Kit (Biolegend, USA) according to the manufacturer's protocol. Readings of the multiplex assays were performed at the BD FACS Aria II.

Statistics

Survival data were analyzed using the Kaplan–Meier method and the Mantel–Cox log-rank test. For analysis of all other data, unpaired Student's *t*-test was used, unless indicated otherwise. Error bars represent mean ± standard error of the mean (SEM). Values of $^{*}P \leq 0.05$ were considered statistically significant, with **P<0.01, ***P<0.001 and **** P<0.0001. All statistical analyzes were performed using GraphPad Prism software (GraphPad Software Inc., La Jolla, CA, USA).

Results

Mobilization of HCs by G-CSF treatment in mice

To determine the yield of donor HCs mobilized by G-CSF treatment, examine possible temporal differences in the recruitment of HCs between distinct mouse strains and to optimize the mobilization protocol in our B6→ BDF1 model, blood was sampled from B6- and BDF1-donors before G-CSF injection, at day 3 and day 5 after injection and analyzed by flow cytometry for the total cell count and the frequency of CD45+Gr1+ myeloid subset in PB (Figure 1). Flow cytometry highlighted a visible increase of myeloid cells, which were determined by staining of CD45+Gr1+ after 5 days of injection (Figure 1A). Cell frequencies (Figure 1B) as well as absolute cell counts (Figure 1C) of CD45+Gr1 positive cells and unstained myeloids were significantly increased after 5 day G-CSF treatment in all three mouse strains. Nonetheless, there was a time- and strain-dependence of HC-recruitment: CD45+ Gr1+ cells were recruited more efficiently in Balb/c mice compared to BDF1 and C57BL/6 mice, which showed slowest rise in cell frequency after 5 days of G-CSF treatment. While CD45+Gr1+ cell frequencies were more than doubled in Balb/c mice already at day 3 of G-CSF injection, BDF1 mice recruited cells in a linear manner, reaching maximum numbers around day 5. C56/BL6 showed only slightly elevated CD45+Gr1 cell numbers at day 3 and reached a peak not before day 5 (Figure 1D). Prolonged G-CSF administration was not necessary, because sufficient engraftment of 5 day -mobilized splenocytes was verified in the G-CSF-dependent models.

After 5 days of 10µg G-CSF recruitment, 33.22% CD45+ Sca1+cKit+ HCs accounted of all spleen PBMCs in G-CSF treated mice, while untreated wild type mice harbored only 8,76% of the same population (Figure 1E).

Cell dose dependency on cGvHD development after allo-HCT in B6D2F1-recipients

Aiming to develop a stable cGvHD phenotype in the C57BL/6→BDF1 model, variable numbers of splenocytes were transplanted into irradiated recipients, which were frequently scored with onset of first GvHD signs and transplant-engraftment was determined around day +20. Criteria for a successful transplantation with GvHD signs were defined the following: (1) development of moderate weight loss (<20%), (2) a moderate average GvHD score of 2 - 4 out of 6 maximum scoring points, (3) low mortality rates and (4) detection of >85% donor cells and <15% of recipient cells in the peripheral blood of recipients around day +20 after transplantation (engraftment). In the model C57BL/6→BDF1 the highest cell dose of $5x10^7$ splenocytes fulfilled all criteria, showing a moderate GvHD score, 100% survival and a reduced weight change compared to syn-controls or lower transplanted cell doses (Figure 2). Flow cytometry analysis of blood measured 99.8% $H2^b$-positive CD3+ cells from donors in all of the 5 recipients. In lower cell doses of $1x10^7$ ($5x10^6$), only 3 out of 5 (1 out of 5) recipients showed >85% $H2^b$+CD3+, while mixed chimerism was detected in two (one) mice, disqualifying them for further experiments.

Characterization of clinical cGvHD in the C57BL/6 ➔ BDF1 model

After cell dose evaluation, recipients were transplanted with $5x10^7$ allogeneic or syngeneic splenocytes and the developing cGvHD symptoms were monitored over 125 days, before tissues were harvested and histological and genetic analysis on the disease manifestations were conducted. Allo-transplanted

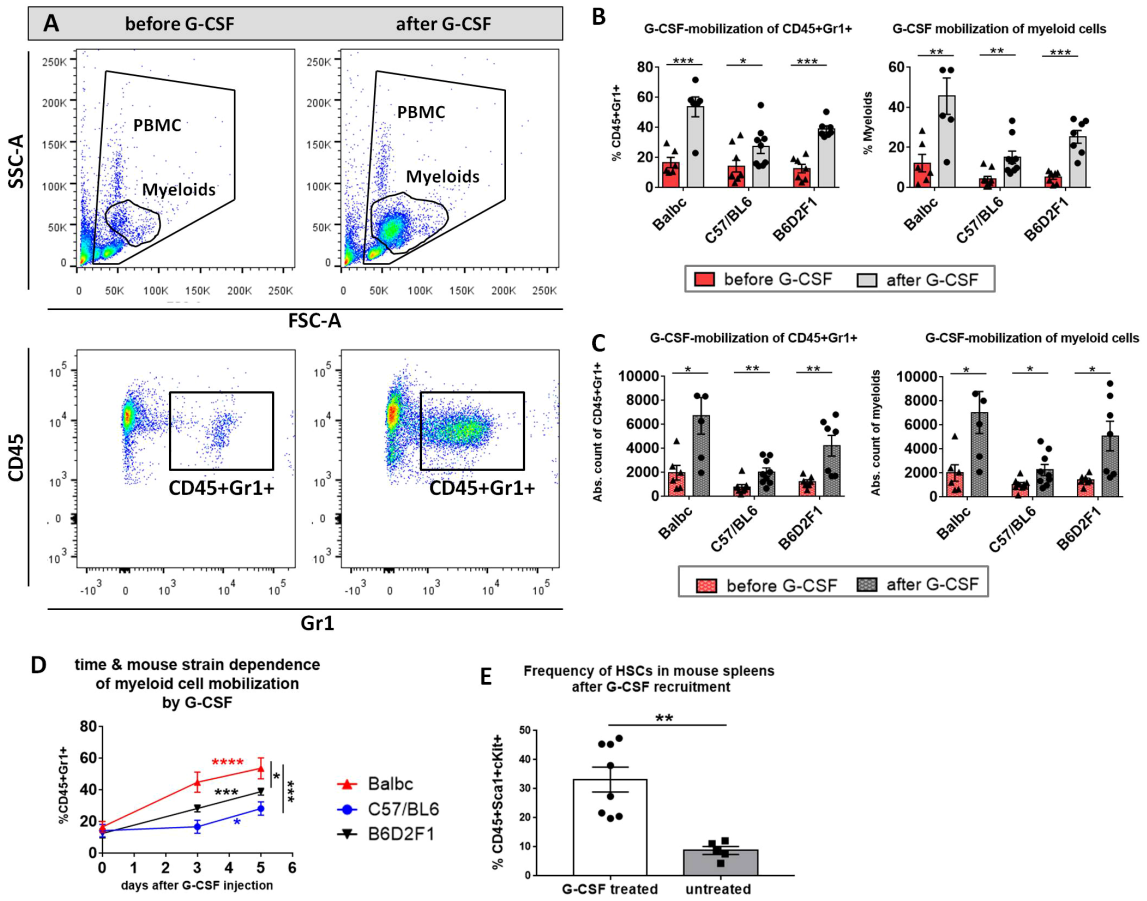

FIGURE 1
Myeloid cell-mobilization by G-CSF in peripheral blood of Balb/c, C57BL/6 and B6D2F1 mice. **(A)** FACS gating strategy of unstained myeloid cells in FSC/SSC and of stained CD45+Gr1+ cells. Example of a visible increase in myeloids and CD45+Gr1+ cells after 5 consecutive days 10 µg G-CSF injection in a BDF1-mouse. **(B)** Significant increase in % CD45+Gr1+ and % myeloids and **(C)** in the absolute cell count of CD45+Gr1+ and myeloids in the peripheral blood of different mouse strains before and after 5 day G-CSF treatment. **(D)** Temporal rise of % CD45+Gr1+ cells in the peripheral blood of different mouse strains from day 0 to 5 of G-CSF injection. Balb/c: n=6, BDF1: n=7, C57BL/6: n=9. **(E)** Frequency of CD45+Sca1+cKit+ HCs in the spleen of untreated vs. G-CSF treated mice. Cell frequencies were determined from isolated FACS-stained whole spleen PBMCs with or without 10 µg G-CSF treatment for 5 days. Pooled BDF1 (n=3), Balb/c (n=2) and C57BL/6 (n=3). Data pooled from three independent experiments. Error bars indicate mean+SEM. *P<0.05, **P<0.01, ***P<0.001, ****P<0.0001 by Holm-Sidak test **(B, C)** and unpaired students t-test with α=0,05 **(D, E)**.

cGvHD mice showed a significantly reduced weight gain and greater morbidity in contrast to the syn-transplanted control group, while the overall survival was not varying between groups. GvHD developed around day +20 in an acute form with high scores (~4.5) and progressed from day +60 with moderate scores of ~3 as robustly manifested cGvHD (Figure 3A). As depicted in Figure 3B, cGvHD mice (upper row) evinced diverse clinical cGvHD symptoms around day +120, which were not detected in syn-controls (bottom row): Posture and activity: a hunched, kyphotic posture with impaired movement and a stilt walk Fur: ruffled, erected fur and loss of whiskers, alopecia. Skin: erythema with scaling, small lesions, especially of hairless areas as mouth, ears or tail. Depigmentation of tail-skin. Eyes: blepharitis and dry, opaque eye lenses.

Clinical and histological manifestations of cGvHD in the C57BL/6➔BDF1 mouse model

The clinical cGvHD appearance in the C57BL/6→BDF1 model was correlated to analysis of Masson's trichrome staining, which was utilized to quantify fibrosis, immune cell infiltration and overall epithelial damage in cGvHD target organs. Organ fibrosis as well as tissue inflammation (Figure 4A) of liver and lungs were quantified to be considerably severe in the allo- than in the syn-transplanted group. In the skin the thickness of the dermis related to the underlying muscularis was elevated in cGvHD animals compared to controls (Figure 4C). Spleens of cGvHD mice

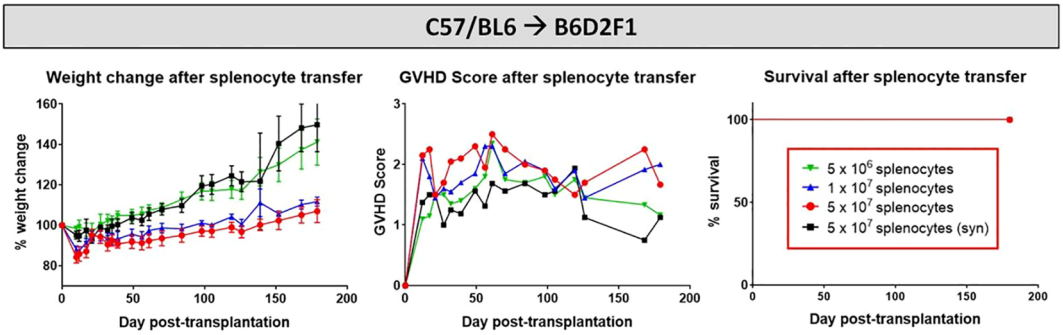

FIGURE 2
Cell dose titration for establishment of cGvHD in mouse models. C57BL/6 ➔ BDF1 model running for 180 days. Three different cell doses (1x106, 1x107 and 5x107) were transplanted in allo-setups and one as syn-control. Clinical GvHD was estimated by weight change (left), GvHD score (middle) and survival (right) Animals were regularly scored for five clinical parameters (weight loss, posture, activity, fur and skin) on a scale from 0 to 2. Clinical GvHD score was summarized of all five parameters. Error bars show mean ± SEM. n=5 per group.

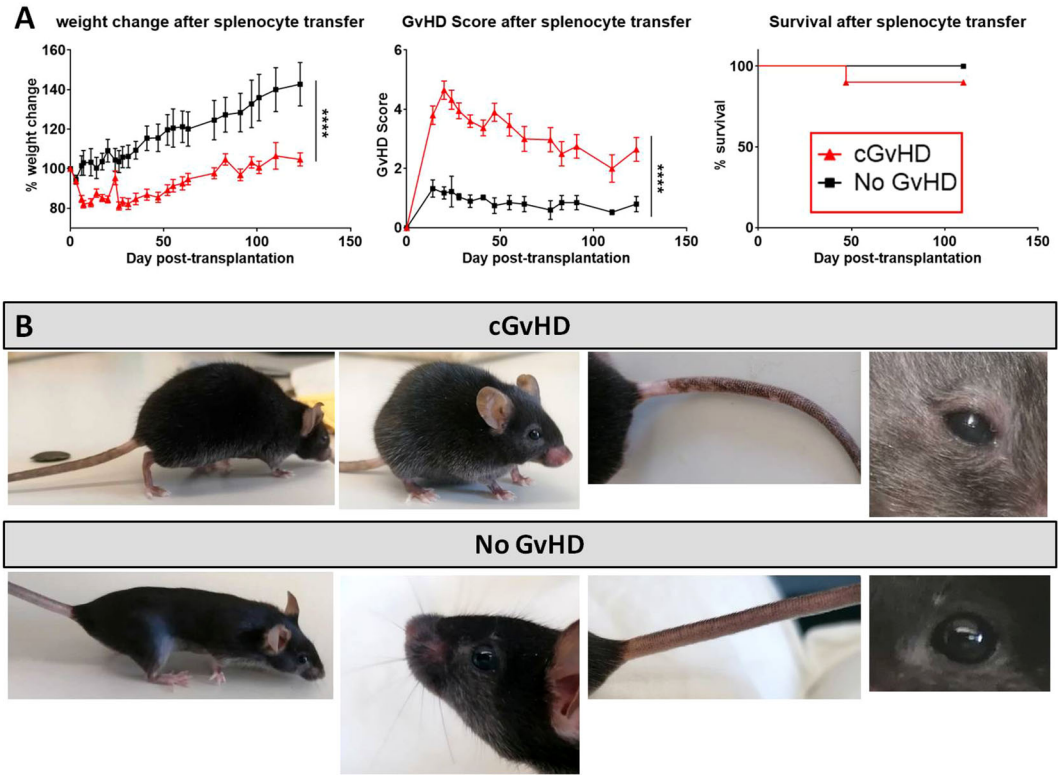

FIGURE 3
cGvHD morbidity and mortality over 125 days in C57BL/6 → BDF1. **(A)** Clinical cGvHD was estimated by frequently assessing weight change (left), GvHD score (middle) and survival (right). Animals were regularly scored for five clinical parameters (weight loss, posture, activity, fur and skin) on a scale from 0 to 2. Clinical GvHD score was summarized of all five parameters. Error bars show mean ± SEM. n=10 per group. Representative data from one out of four experiments. ****P<0.0001 by unpaired students t-test. Survival was tested by Mantel-Cox-log-rank test. **(B)** Frequently observed clinical manifestations of cGvHD in BDF1-recipients (upper): Kyphosis, ruffled fur, alopecia, skin-depigmentation and blepharitis were seen in allo-transplanted animals, while syn-mice did not show any cGvHD-symptoms (bottom).

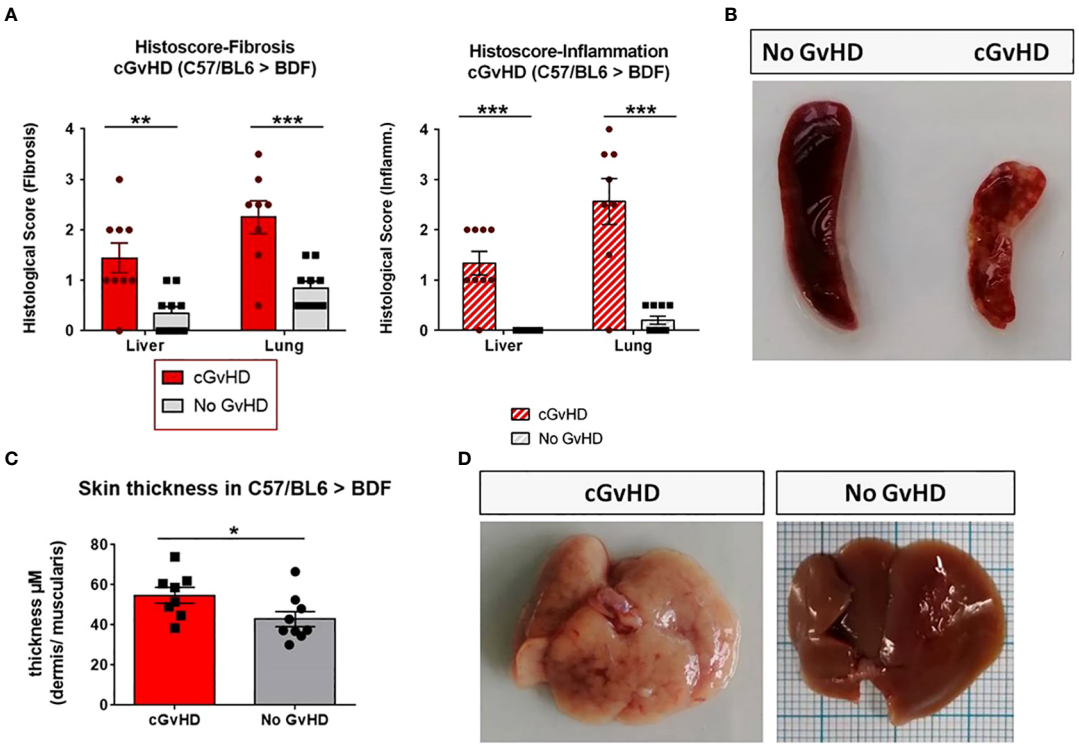

FIGURE 4
Clinical organ manifestations of cGvHD in C57BL/6➔BDF1 at day +125 after allo-HCT. **(A)** Histological quantification of fibrosis and inflammation in liver and lung of each individual mouse, based on histo-scoring ranging from 0=no to 4= severe fibrosis/inflammation. Error bars show mean ± SEM. n=9 (cGvHD); n=10 (No GvHD). Representative data from one out of four experiments. *P<0.05, **P<0.01, ***P<0.001by unpaired students t-test. **(B)** Spleen of cGvHD vs. non-GvHD mouse at d+125 after transplantation with visible sclerotic and apoptotic changes in cGvHD. **(C)** Skin thickness was increased in cGvHD vs. non-GvHD. Thickness was estimated by measurement of dermis-muscularis-ratio in Masson's Trichrome stainings. Error bars show mean ± SEM. n=8 (cGvHD); n=9 (No GvHD). Representative data from one out of four experiments. *P<0.05 by unpaired students t-test. **(D)** Livers of cGvHD vs. non-GvHD mouse at d+125 after transplantation with visible cirrhotic changes in cGvHD.

(Figure 4B) were marked of sclerotic tissue loss and necrotic foci and were notably smaller in size than spleens of syn-mice due to cellular apoptosis. cGvHD livers (Figure 4D) appeared pale, with intrahepatic bleedings and necrotic areas, emerging as cirrhotic changes, which were not detected in non-GvHD animals.

In the Masson's Trichrome staining, cGvHD lungs (Figure 5A) showed a massive immune cell infiltration around intrapulmonary bronchi (IPB) and pulmonary veins (PV). Infiltrates were surrounded by heavy collagen depositions, lining especially veins and small arteries, while syn-controls showed only minor collagen fibers around PV. The endothelial lining of large PV in cGvHD appeared superimposed by a visible blue collagen layer (yellow arrows), indicating an Endothelial tomesenchymal transition process in cGvHD mice. While syn-livers (Figure 5B) showed normal hepatic architecture without significant collagen emplacement, cGvHD manifested in marked portal vein inflammation, interspersed with fibrotic tissue. Fibrosis and inflammatory infiltrates were also detected around bile ducts and hepatic arteries. In perihepatic areas, superficial tissue exhibited remarkable hepatic steatosis. Cutaneous cGvHD occurred in the allo-HCT group (Figure 5C), with thickening, perivascular inflammation and sclerosis of the dermis. Single animals also exhibited vacuolization due to collagen degradation in dermal layers or showed epidermal desquamation.

With the objective to corroborate our findings from the Masson's stains, to characterize the extent of tissue inflammation in cGvHD target organs and to analyze differences between cGvHD and non-GvHD groups, additional immunohistofluorescence stainings on B- and T cells were performed. Figure 6 exemplarily describes massive immune cell accumulations in cGvHD lungs from allo-BDF1-recipients, which harbored dense B220+ B cell (left) and CD3+ T cell infiltrates (right). Similar results were also found exclusively in other examined cGvHD target organs, as liver, colon, skin and eyes but not in tissues from syn-recipients.

Due to the massive inflammatory cellular involvement in cGvHD target organs we hypothesized, that also systemic cytokine levels are affected, expecting especially higher levels of pro-inflammatory cytokines in serum during disease. We partly confirmed our assumption by detection of significantly increased

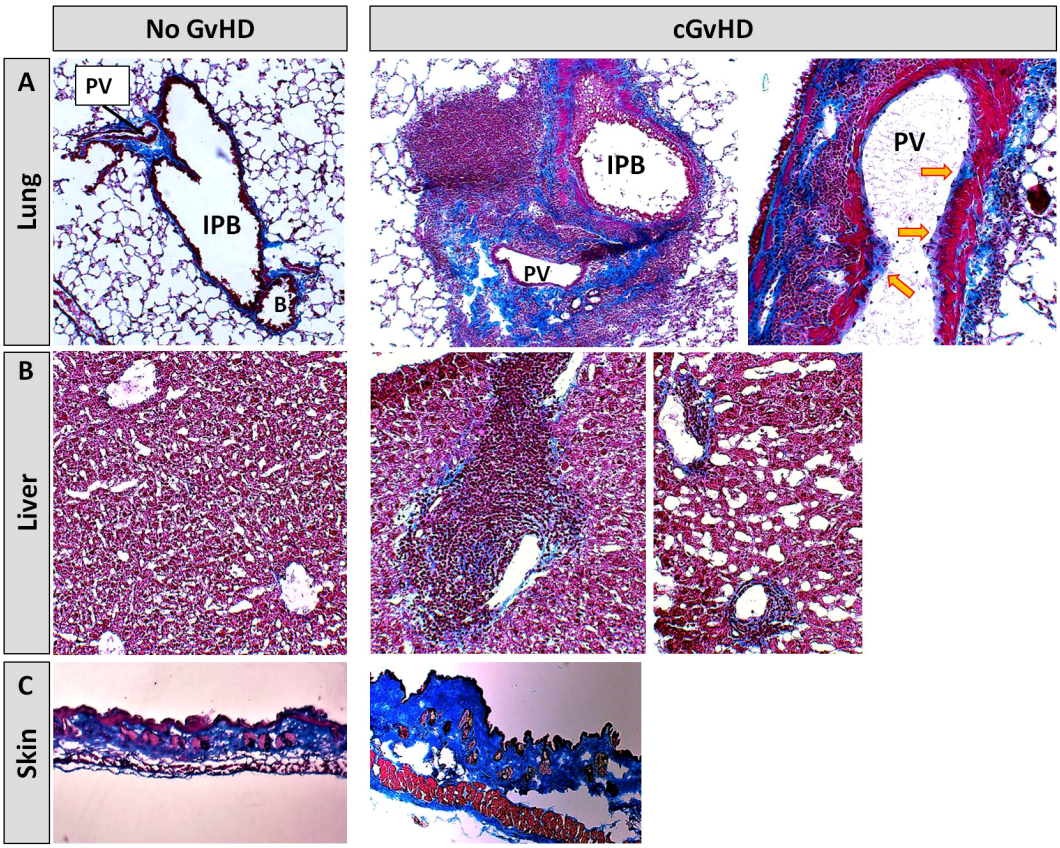

FIGURE 5
Histological characterization of murine cGvHD at day+125 after allo-HCT. Masson's trichrome fibrosis staining in cGvHD target organs **(A)** lung, **(B)** liver and **(C)** skin of syn- and allo-transplanted BDF1-recipients. Blue, collagen fibres (fibrosis); red, cytoplasm; keratin, muscle fibers and erythrocytes, dark red/black, nuclei; infiltrating immune cells. 20x magnification. PV, Pulmonary vein; IPB, Intrapulmonary bronchus; B, Bronchiolus.

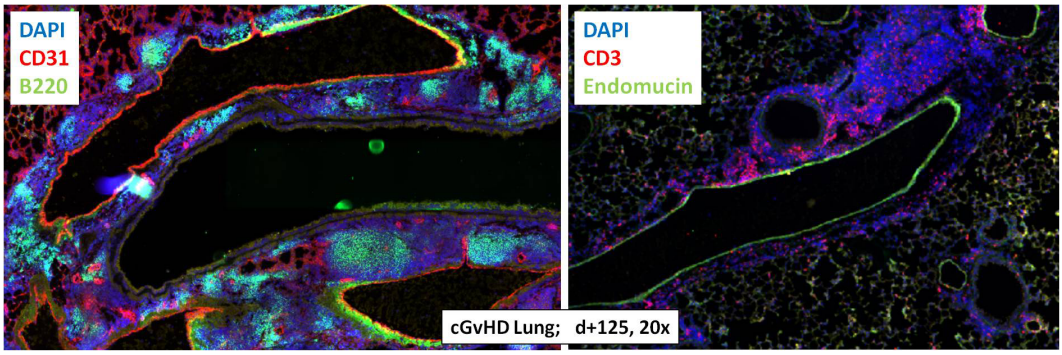

FIGURE 6
Tissue immune cell infiltration in lungs from C57BL/6 ➔ BDF1 during established cGvHD. Representative immunohistofluorescence images of cGvHD lungs at day +125 showed massive immune cell infiltrates (indicated by DAPI staining, blue) with dense foci of B220+ B cells (left, green) and CD3+ T cells (right, red). Magnification 20x.

levels of CXCL9 and CXCL10 exclusively in cGvHD-mice (Figure 7). Both markers are also frequently observed to be elevated in clinical cGvHD in patients. Other pro-inflammatory cytokines e.g. IFN-a, TNF-a or IL-6 were increased in cGvHD in tendency, but only few samples gave measurement results for these markers due to low cytokine threshold concentrations.

Engraftment of donor cells and immune reconstitution after allo-HCT in C57BL/6 B6D2F1

After transplantation, donor syn- or allo-HCs engrafted in myeloablative irradiated recipients. To address the question how immune reconstitution is altered in the BDF mouse model and if there are differences in immune cell recovery between syn- and allo-transplanted recipients, various immune cell subsets were tracked with flow cytometry of recipients blood over 125 days (Figure 8). With the onset of cGvHD around d+20, reconstitution of CD3+ and CD4+ T cell subsets was significantly decelerated in cGvHD animals, while especially CD8+ CTLs were massively expanded at d +20 in this group. Reappearance of B cells in cGvHD was first detected at day+60, while B cell numbers in cGvHD mice exceeded numbers in non-GvHD controls at day+125. At d+20 and d+60, CD11b+CD11c- myeloid and mature NK cells were elevated in the cGvHD-group, but cell numbers intensively dropped until d+125, reaching lower levels than the control-group. We detected a higher proportion of Gr1+ $^{diminished/high}$ and vice versa less Gr1+ ^{low} monocytes and macrophages in cGvHD mice than in controls at GvHD onset but no different cell numbers between cGvHD- and control group in late established cGvHD.

To estimate possible differences in cGvHD-immune cell reconstitution in various lymphatic niches, immune cell subsets were analyzed in PB, BM and spleens as the experiment was terminated at day+125 (Figure 9). CD3+, CD4+ and CD8+ T cell subsets were decreased in the PB, but increased in spleens of cGvHD mice. cGvHD spleens were also associated with massive B cell and neutrophil loads, which were lower in controls, while the presence of different APC subsets, such as myeloid and lymphoid DCs, monocytes and macrophages was decreased in cGvHD spleens. Interestingly, immune cell levels in the BM were generally low and no differences in cell numbers were measured between cGvHD and controls, encouraging the hypothesis that mature immune cells were hosted mainly in secondary lymphatic organs.

For single populations, e.g. DCs and NK cells the progression of their activation status in the PB from d+20 to d+125 (Figure 10A) and in BM and spleens at day+125 after HCT (Figure 10B) was analyzed by estimation of the expression of co-stimulatory receptor CD80+. Mice with cGvHD harbored significantly more activated myeloid (CD11b+CD11c+) and lymphoid (CD11b-CD11c+) DCs and myeloid NK cells (CD11b +CD11c-) than control mice especially at GvHD onset. Activation levels of DCs dropped until day +125 but still stayed markedly elevated in allo-recipients. Since no differences in cellular activation in BM and spleen were revealed, we assumed the recipients circulatory, respectively the vascular system to represent the major activation site in cGvHD pathophysiology.

Erythropoietic reconstitution during cGvHD in C57BL/6 ➔ BDF1

Aiming to investigate quantitative changes of nucleated and non-nucleated erythroid and lymphoid cells and associated features and to elucidate their relevance in cGvHD, a

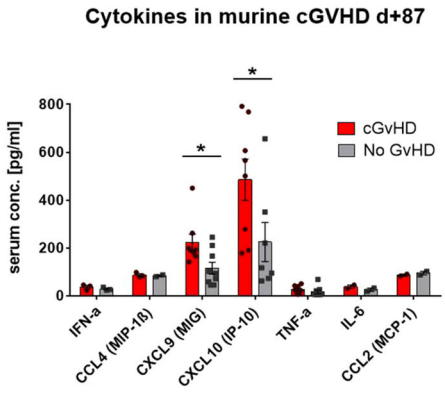

Marker	cGvHD			No GvHD		
	Mean	SD	n	Mean	SD	n
IFN-a	36,60	12,22	3	28,91	6,33	3
CCL4	86,99	10,24	3	84,34	5,73	2
CXCL9	222,48	98,20	8	115,81	73,99	9
CXCL10	485,32	244,86	8	225,16	215,80	7
TNF-a	26,26	16,21	8	17,00	21,10	9
IL-6	38,35	10,11	2	26,07	9,40	2
CCL2	86,71	6,05	2	95,09	10,70	2

FIGURE 7
Cytokine levels in serum of cGvHD vs. non-GvHD in C57BL/6➔ BDF1 model at day+87 after transplantation. Table shows mean+SD for each analyzed marker. Graph illustrates cytokine serum concentration in pg/mL. Error bars show mean ± SEM. Representative data from one experiment. *P<0.05, by unpaired students t-test.

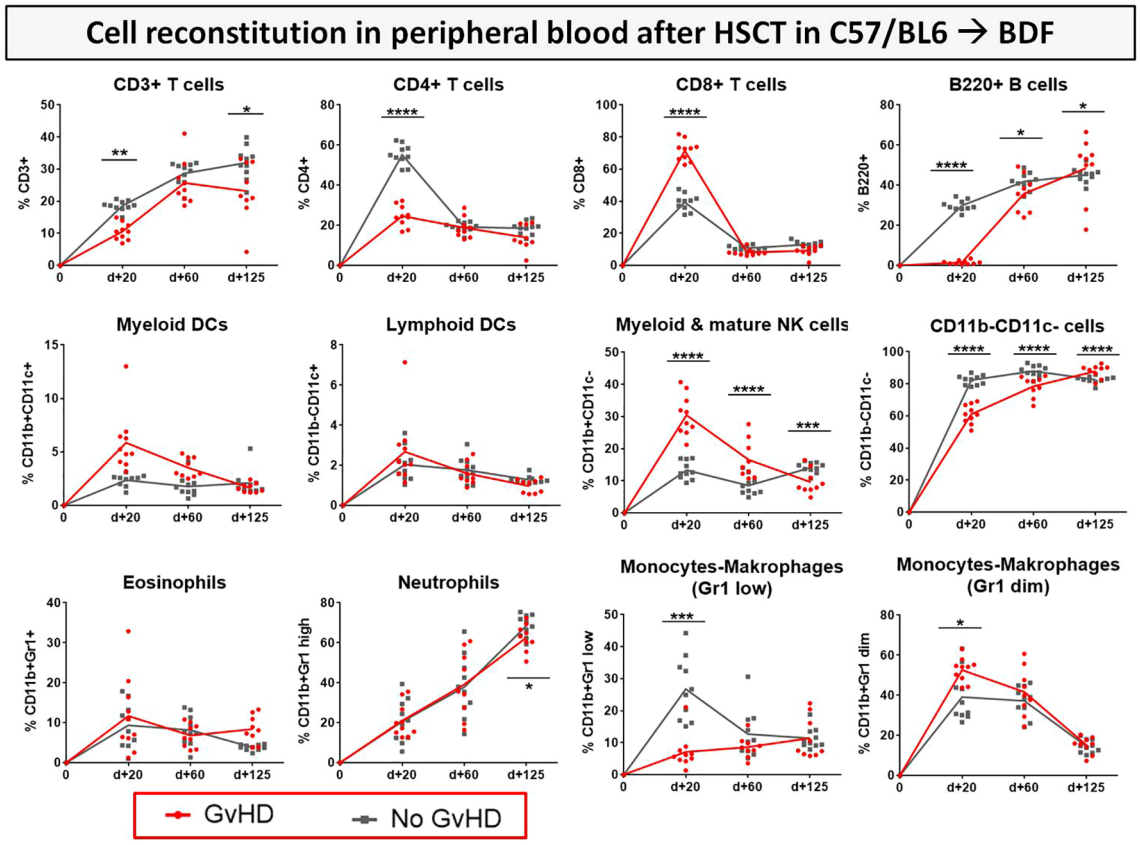

FIGURE 8
Immune cell reconstitution in peripheral blood of BDF1-recipients over 125 days after allo- vs. syn HCT. Tail vein blood was collected at three time points, PB cells were isolated, stained with the respective FACS-antibodies and samples were analyzed with flow cytometry. DCs, dendritic cells; NK, natural killer cells; dim, diminished. n=9 (cGvHD); n=10 (No GvHD). Representative data from one out of four experiments. *P<0.05, **P<0.01, ***P<0.001, ****P<0.0001 by unpaired students t-test.

differential blood count was performed at day +90 in syn- and allo-HCT recipients. In cGvHD, erythrocytes, hemoglobin and hematocrit were remarkably decreased, while mean corpuscular volume and –hemoglobin were elevated, clinically presenting as macrocytic anemia (Figure 11; Supplemental Figure 1). As of nucleated cells, only monocytes were detected to be diminished in cGvHD, which corresponds to the results from the flow cytometry analyzes in PB.

Cell dose- and huPBMC donor-dependency on cGvHD development after xeno-HCT in NSG-recipients

Similar to the murine cGvHD-models, variable numbers of huPBMCs of different donors were transplanted into sub-lethally irradiated, immunocompetent NSG mice and developing cGvHD was assessed by surveillance of weight change, GvHD score and survival. Criteria for a successful transplantation with GvHD signs were defined the following: (1) development of moderate weight loss (<20%), (2) a moderate average GvHD score of 2 - 4 out of 6 maximum scoring points, (3) low mortality rates and (4) detection of > 0.5% huPBMCs in the PB of recipients around day +30 after transplantation (engraftment) and of >5% huPBMCs in the spleen at the end of the experiment. Figure 12 gives an overview on the donor dependency of developing cGvHD in the NSG-model: the highest transplanted cell dose ($5x10^6$) resulted in high mortality and high morbidity independent from donor origin, while huPBMCs from donor C did not cause significant weight loss. Nearly no differences in weight change, GvHD scores and in survival were observed among the lower transplanted cell numbers ($1x10^6$, $5x10^5$ and $1x10^5$) of donor A, indicating that it requires a minimum threshold cell number for cGvHD development. The group of $1x10^6$ transplanted huPBMCs revealed the biggest variance between donors: while mice transplanted with cells from donor A developed the mildest cGvHD with a low average score of <2, 100% survival and no weight loss, cells from donor B caused rapid weight loss, high

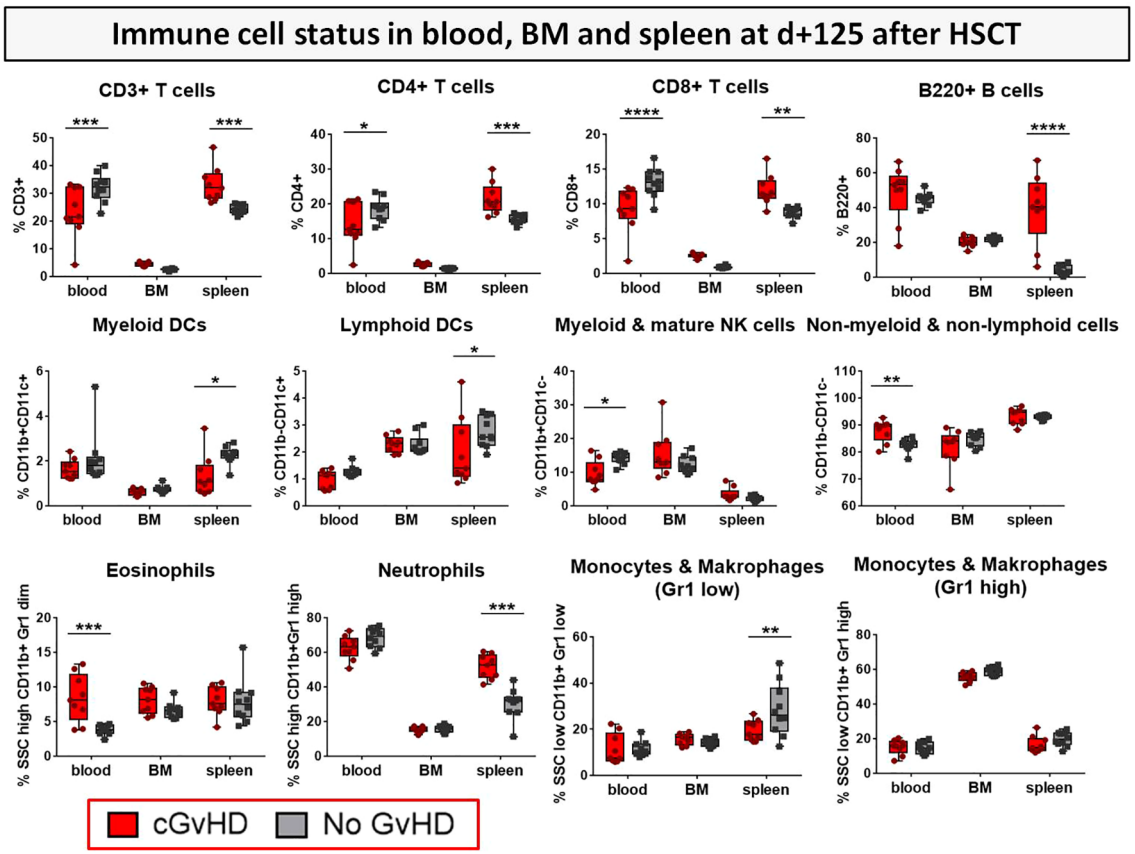

FIGURE 9
Immune cell status in peripheral blood, bone marrow and spleen of BDF1-recipients at day +125 after allo- vs. syn HCT. Blood was collected retrooribitally upon finalization. Spleens were harvested and BM flushed from tibia and femur. Immune cells were isolated, stained with the respective FACS-antibodies and samples were analyzed with flow cytometry DCs, dendritic cells; NK, natural killer cells; dim, diminished.n=9 (cGvHD); n=10 (No GvHD). Representative data from one out of four experiments. *P<0.05, **P<0.01, ***P<0.001, ****P<0.0001 by unpaired students t-test.

cGvHD morbidity and 100% mortality before day 60. NSG-recipients transplanted with $1x10^6$ huPBMCs from donor C developed moderate cGvHD scores of ~3 and moderate survival rates, designating this condition as most appropriate for further experiments. To estimate, if the donor-related differences in cGvHD severity cohere with the transplanted T cell numbers, isolated donor cells were stained for CD3+ and analyzed with FACS. Of whole PBMCs, donor A comprised a high frequency of 52.8% CD3+ T cells, while donor B showed 42.0% and donor C 31.3% CD3+ T cells. Thus, the transplanted donor T cell number alone did not seem to have a direct influence on the cGvHD severity.

To evaluate if the transplanted cell amount has an influence on the engraftment, the proportion of human T cells in the PB of NSGs transplanted with three different huPBMC doses after day +30 was checked by flow cytometry. Analyzes revealed that huCD3+ T cell persistence in the PB is independent from the transplanted huPBMC dose: 12 of 13 NSG-recipients (92,3%) from the group with the highest infused huPBMC number of $5x10^6$ cells per animal were found to have successfully engrafted with an average huCD3+ T cell frequency of 29.15 ± 8.81 in the PB, while in the group of $1x10^6$-transferred cells, only 20 out of 27 recipients (74.0%) harboured a minimum of >0.5 huCD3+ T cells, with an average frequency of 14,2 ± 2,48% huCD3+ in successfully engrafted recipients. The lower transplanted huPBMC dose of $5x10^5$ resulted in full engraftment of 8 out of 9 (88.9%) and a mean percentage of 22.05 ± 0.97% huCD3+ cells in the PB of NSG-recipients.

Characterization of clinical cGvHD in the huPBMCs➔ NSG model

Aiming to evaluate and describe the clinical manifestations in developing cGvHD after xeno-transplantation, one group of NSG-recipients received huPBMC-transfers of $1x10^6$ cells from donor C

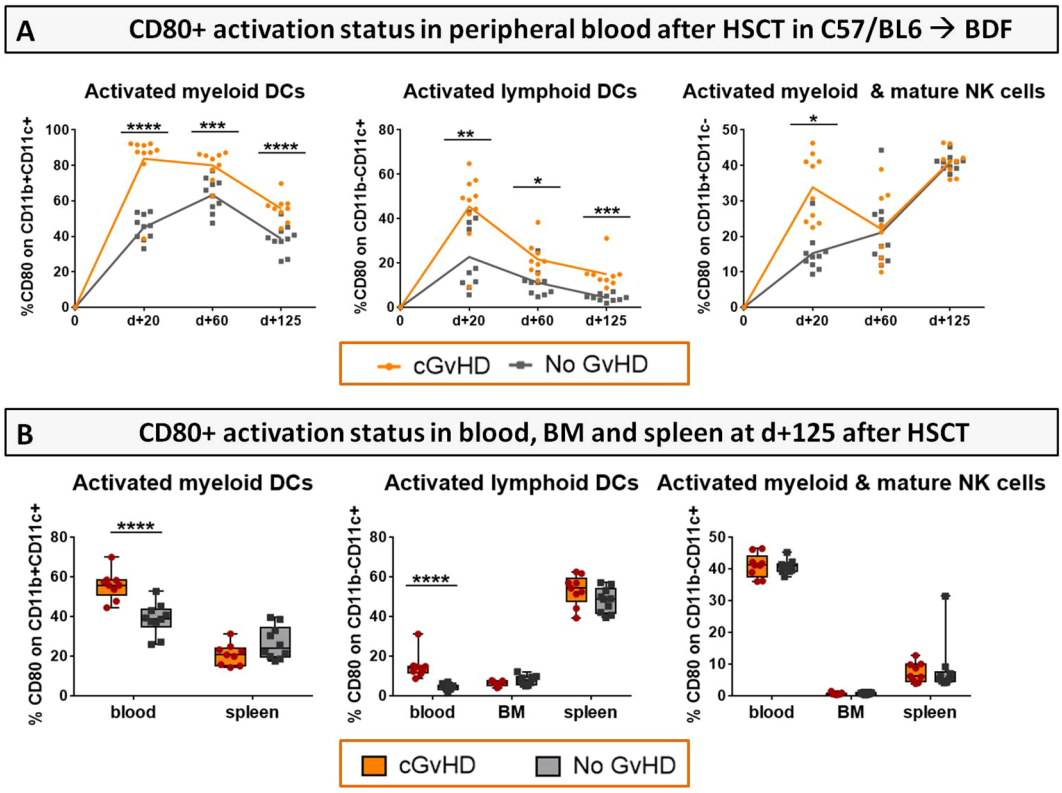

FIGURE 10
Activation status (CD80+) of DCs and NK cells in cGvHD in C57BL/6→BDF1. **(A)** CD80+ expression on immune cell subsets in the PB over 125 days and **(B)** in PB, BM and spleen at d+125 after syn- and allo HCT. Blood was collected by tail vein bleeding or retrooribitally upon finalization. Spleens were harvested and BM flushed from tibia and femur. Immune cells were isolated, stained with the respective FACS-antibodies and samples were analyzed with flow cytometry DCs, dendritic cells; NK, natural killer cells. n=9 (cGvHD); n=10 (No GvHD).Error bars represent mean ± SEM. Representative data from one out of four experiments. *P<0.05, **P<0.01, ***P<0.001, ****P<0.0001 by unpaired students t-test.

after non-lethal irradiation, while the 'No GvHD' control group was only irradiated without further cell infusion. Both groups were monitored and scored over 125 days equally to the previously described BDF1-model. While weight loss was no frequently recorded symptom occurring in xeno-cGvHD, transplanted mice exhibit steadily increasing cGvHD with scores to a maximum of ~4.5 and a higher transplant-related mortality compared to controls, emerging from day +50 and stabilizing around day+70 (Figure 13A). Transplanted NSG-recipients were recurrently encountered with classic cGvHD symptoms as kyphosis, reduced activity, sporadic alopecia, severe skin scaling and dryness as well as opacity of the eye lenses and blepharitis (Figure 13C). In histological analyzes of liver and lungs of xeno-cGvHD, significantly augmented fibrosis was detected in the majority of transplanted NSGs, while a severe inflammation was not regularly detected in all recipients, respectively was not found in xeno-cGvHD but also in few controls. The current results indicated that lungs immune cell infiltration might at least be partly induced by irradiation and further aggravated by cGvHD (Figure 13B). The observation of higher transplanted cell doses to not causally worsen cGvHD-morbidity until a certain cell number threshold is reached, was supported by the finding that there were no differences measured in epidermal thickness in NSGs receiving varying huPBMC numbers (Figure 13D), but epidermis is distinctly thickened in animals receiving $1x10^6$ huPBMCs, compared to controls (Figure 13E).

Further cGvHD organ manifestations were illustrated performing Masson's Trichrome fibrosis stainings. Clinical features of gastrointestinal involvement, similar to the human cGvHD pathology, were detected exclusively in cGvHD but not in controls, such as mucosa inflammation with mild crypt and gland apoptosis (Figure 14A). Hepatic cGvHD mainly appeared as moderate fibrotic fibre incorporations around vessels, veins and bile ducts (Figure 14B), with minor signs of immune cell infiltrates surrounding only bigger vascular tissues. Lungs of control-group-NSGs showed mild fibrosis around pulmonary veins and arteries without significant inflammation signs. Xeno-transplanted animals depicted altered lung parenchyma, damaged by dense infiltration-foci interspersed by fibrotic fiber-networks mainly around pulmonary veins and bigger bronchioles (Figure 14C).

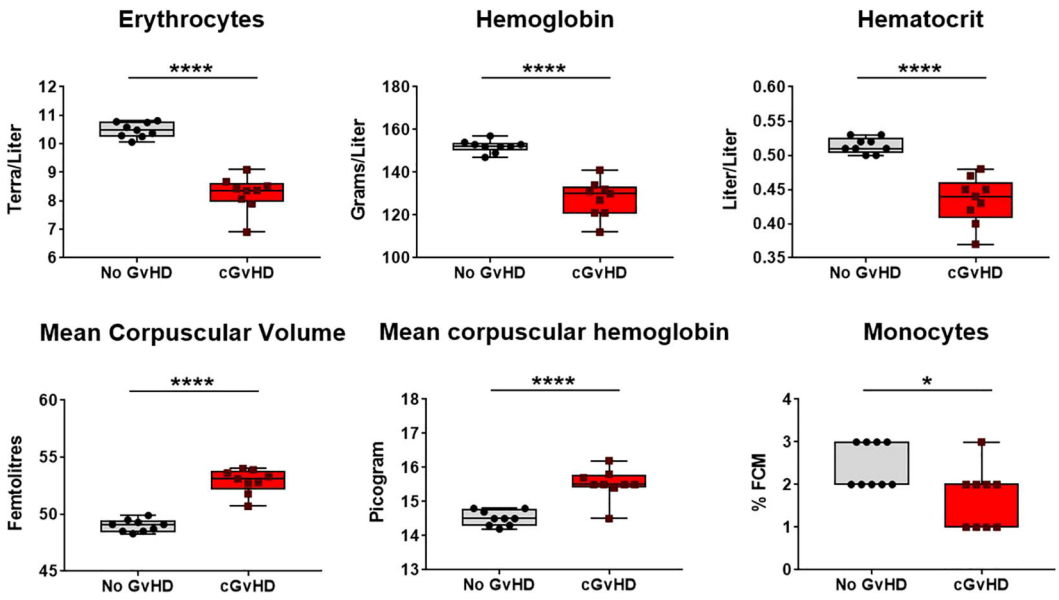

FIGURE 11
Recovery of red blood cells and related factors in cGvHD at d+90 after transplantation in C57BL/6➔BDF1. Blood was sampled from mice and differential blood count was performed by Synlab, Berlin. Data pooled from 2 independent experiments. n=9. Error bars represent mean ± SEM. *P<0.05, ****P<0.0001 by unpaired students t-test.

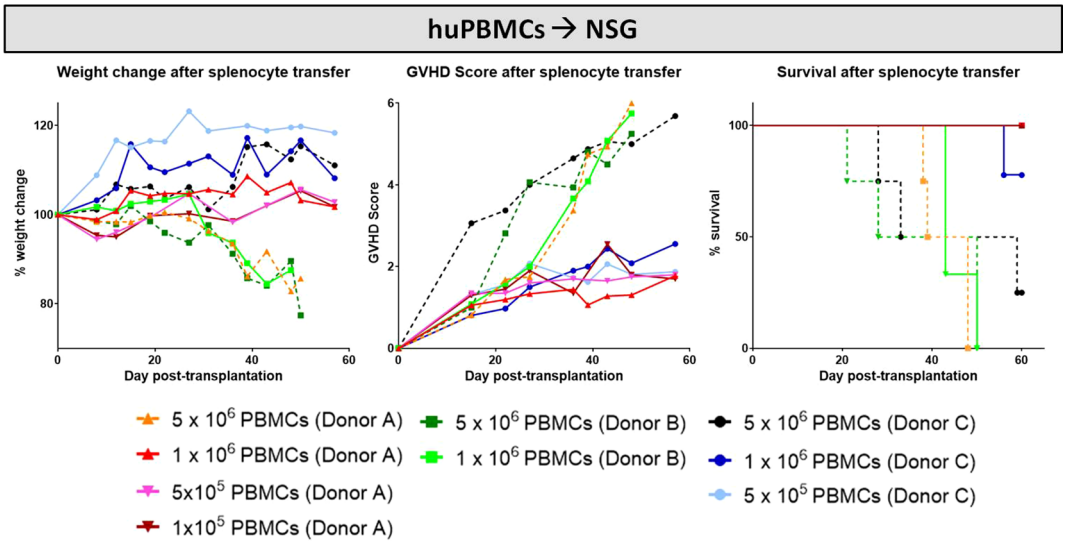

FIGURE 12
HuPBMC dose titration from three different donors for establishment of xeno-cGvHD in NSG-recipients over 60 days. Four different cell doses (5x106, 1x106, 5x105 and 1x105) from three different donors were transplanted into sub-lethally irradiated NSG. Clinical GvHD was estimated by weight change (left), GvHD score (middle) and survival (right). Animals were regularly scored for five clinical parameters (weight loss, posture, activity, fur and skin) on a scale from 0 to 2. Clinical GvHD score was summarized of all five parameters. A high variance in weight change and GvHD scores was observed not only between the cell doses, but among donors. Dotted lines indicate highest cell doses.

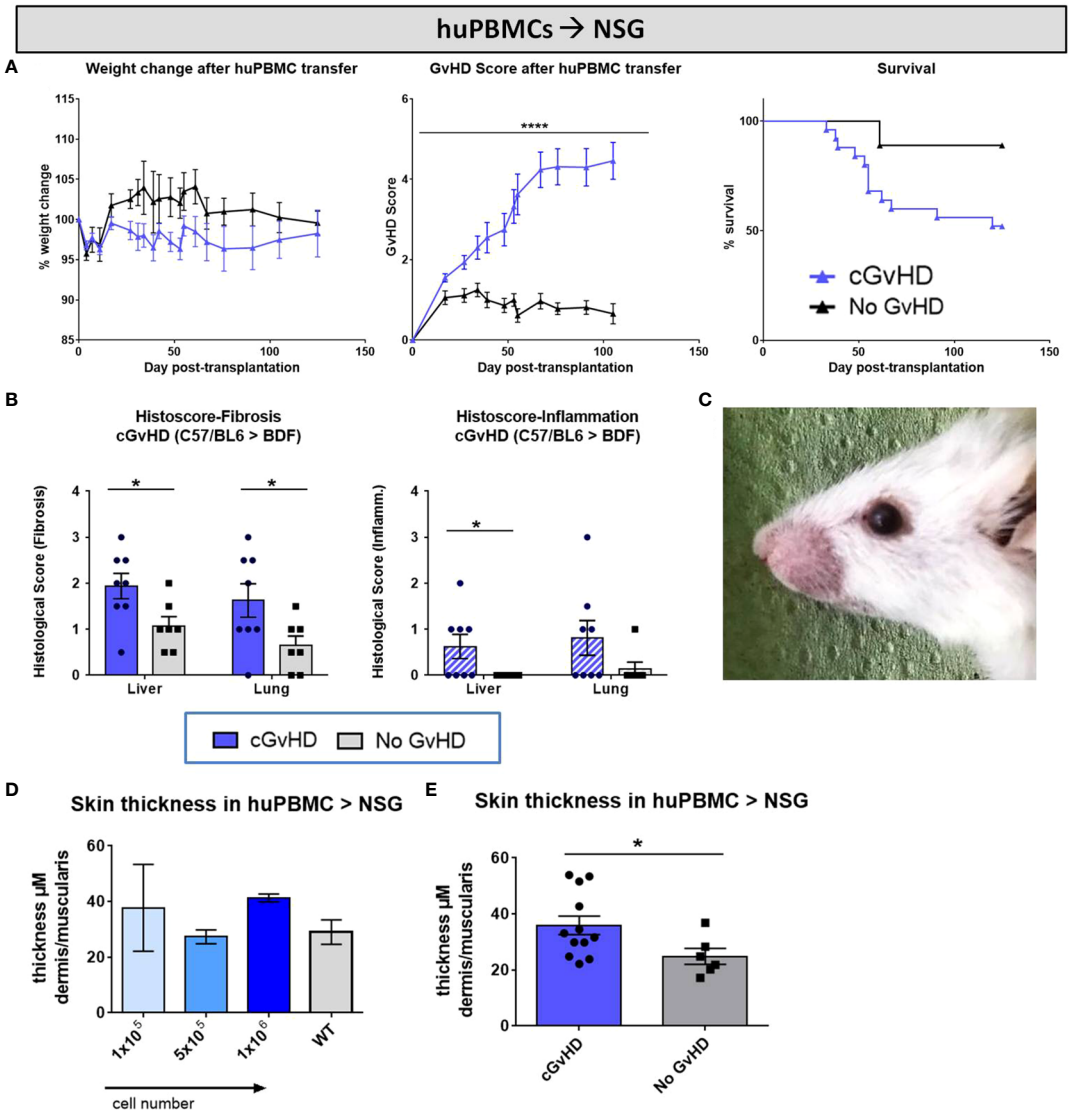

FIGURE 13
Clinical organ manifestations of cGvHD in huPBMCs➔ NSG at day +125 after allo-HCT. **(A)** Clinical cGvHD was estimated by frequently assessing weight change (left), GvHD score (middle) and survival (right). Animals were regularly scored for five clinical parameters (weight loss, posture, activity, fur and skin) on a scale from 0 to 2. Clinical GvHD score was summarized of all five parameters. Error bars show mean ± SEM. n=20 (cGvHD), n=8 (no GvHD). Representative data from one out of two experiments. ****P<0.0001 by unpaired students t-test. Survival was tested by Mantel-Cox-log-rank test. **(B)** Histological quantification of fibrosis and inflammation in liver and lung, based on histo-scoring ranging from 0= no to 4= severe fibrosis/inflammation. Error bars show mean ± SEM. n=8 (cGvHD); n=7 (No GvHD). Representative data from one out of two experiments. *P<0.05 by unpaired students t-test. **(C)** Exemplary photo of eye-involvement in cGvHD pathology. Eyes showed signs of blepharitis and dryness and opacification of lenses. **(D)** Skin thickness was not affected by varying transplanted huPBMC-doses, but was **(E)** increased in cGvHD vs. non-GvHD. Thickness was estimated by measurement of dermis-muscularis-ratio in Masson's Trichrome stainings. Error bars show mean ± SEM. n=12 (cGvHD); n=6 (No GvHD). Pooled data from three independent experiments. *P<0.05 by unpaired students t-test.

Engraftment of donor cells and immune reconstitution after xeno-HCT in the huPBMCs ➔ NSG model

Intending to track the recovery of murine immune cells after irradiation and upon cGvHD development as well as to monitor engraftment and traceability of the transferred huPBMCs in the PB of recipients, blood was sampled from NSGs periodically over 125 days after HCT and immune cell frequencies were analyzed using flow cytometry. As expected, human cell proportions, especially of CD45+ leukocytes and CD3+ and CD8+ T cell subsets, steadily decreased over the examined time,

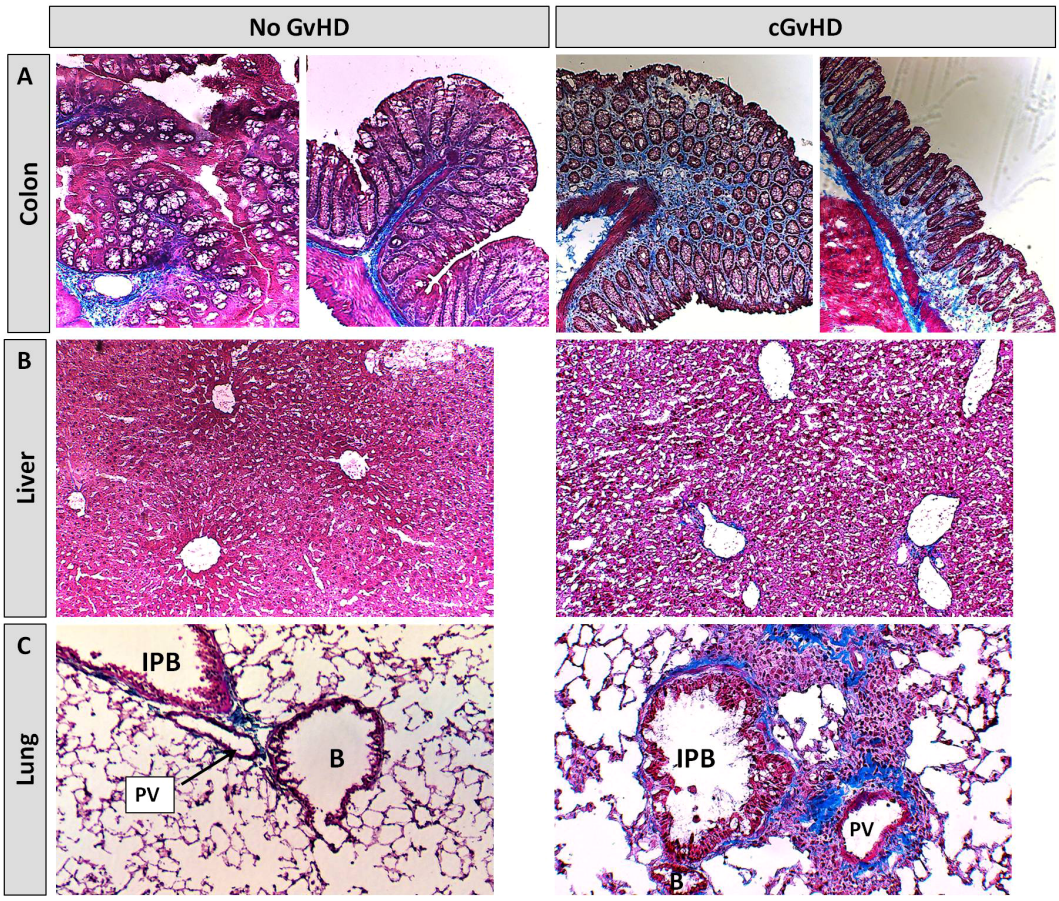

FIGURE 14
Histological characterization of xeno-cGvHD at day+125 after xeno-HCT. Masson's trichrome fibrosis staining in cGvHD target organs **(A)** colon, **(B)** liver and **(C)** lung of xeno-transplanted and only irradiated, but not-transplanted NSG-recipients. Blue, collagen fibres (fibrosis); red, cytoplasm; keratin, muscle fibers and erythrocytes, dark red/black, nuclei; infiltrating immune cells. 20x magnification. PV, Pulmonary vein; IPB, Intrapulmonary bronchus; B, Bronchiolus.

while the frequency of CD4+ T cells remained stable and from day +60 (with cGvHD onset) even slightly expanded (Figure 15A, upper row), indicating a huCD4+-dependent cGvHD-pathophysiology. Around day +60, also the frequency of murine CD45+ leukocytes is elevated in cGvHD, introducing the hypothesis that human T cells can be stimulated by murine tissue and vice versa activate murine immune cells or damage murine tissue in a cross-reactive manner. A remarkably decelerated reconstitution of murine Gr1+ myeloid-derived cells and CD11b-/CD11c+ lymphoid DCs was measured around day +30, but normalized to control-group levels at later stages (Figure 15A, bottom row).

To discern the issue, in which lymphatic organs the transplanted huPBMCs and murine donor-cells home and if there are differences in cell-locations emerging during cGvHD, various cell frequencies were analyzed in PB, BM and spleen at day+125. While huCD4+ T cells and huCD45+ leukocytes were mostly detected to circulate in the periphery and the spleen, but not the BM, huCD8+ T cells were predominantly found to reside in spleens and in small numbers in BM and PB. The majority of murine CD45+ leukocytes were found to home in the BM, indicating complete HC-reconstitution and cell-recurrence after irradiation at day+125 (Figure 15B, upper row). Murine CD11b+ and Gr1+ myeloid-derived cells were measured with similar higher numbers to prevail in the BM and in the PB circulatory system, while both subsets appeared in spleens to a limited extent (Figure 15B; bottom row).

Considerable differences of cellular reconstitution among cGvHD and control group were revealed in murine DCs of distinct origin: while the frequency of myeloid DCs was higher, lymphoid DCs were diminished in spleens of cGvHD-mice (Figure 15B, bottom row).

10.3389/fimmu.2022.1079921

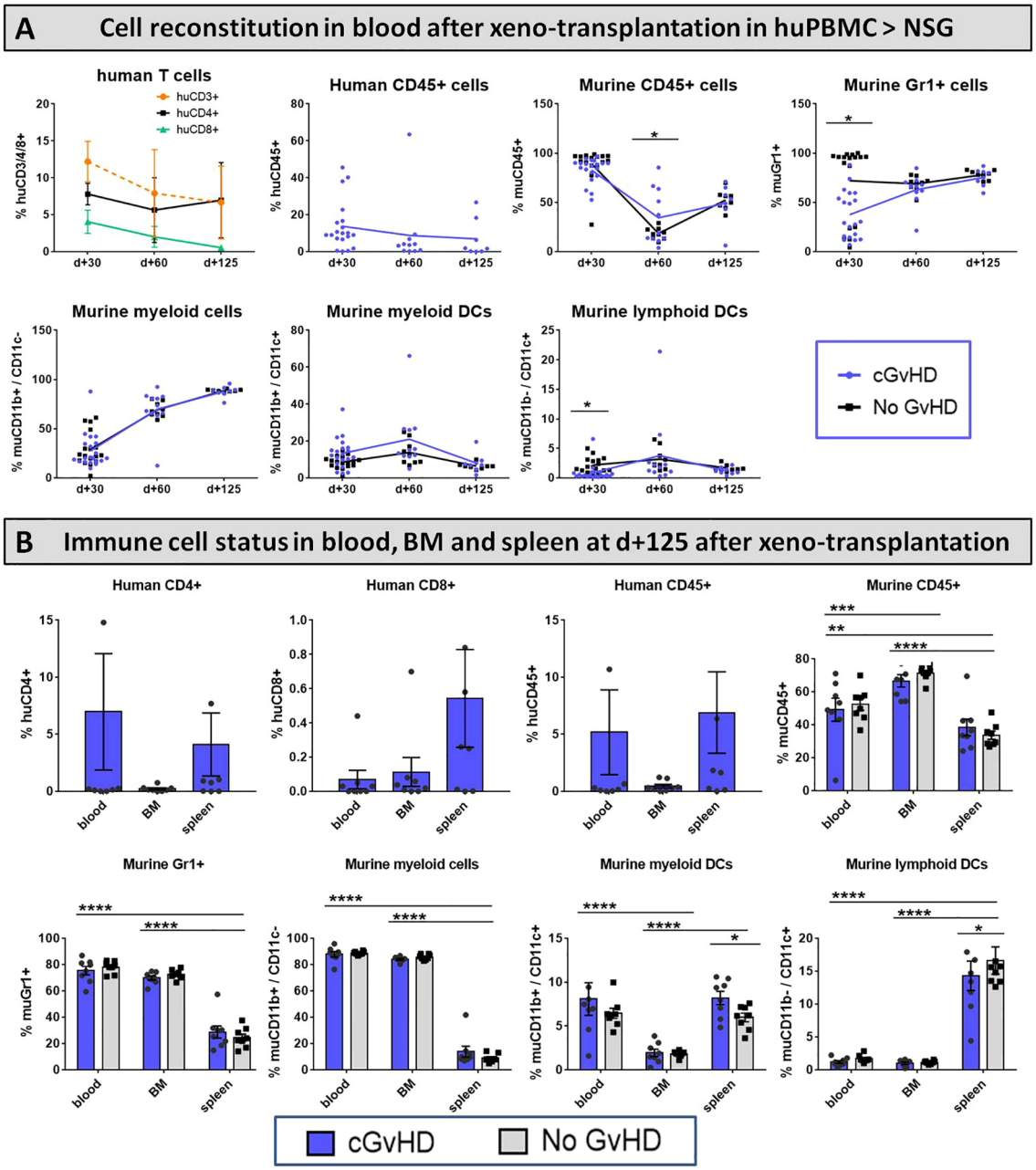

FIGURE 15
Immune cell reconstitution in **(A)** peripheral blood of NSG-recipients over 125 days and **(B)** in PB, BM and spleen at day+125 after xeno-HCT. **(A)** Tail vein blood was collected at three time points, PB cells were isolated, stained with the respective FACS-antibodies and samples were analyzed with flow cytometry. DCs= dendritic cells. **(B)** Blood was collected retrooribitally upon finalization. Spleens were harvested and BM flushed from tibia and femur. Immune cells were isolated, stained with the respective FACS-antibodies and samples were analyzed with flow cytometry DCs= dendritic cells. n=8 per group. Error bars show mean ± SEM. Representative data from one out of two experiments. *P<0.05, **P<0.01, ***P<0.001, ****P<0.0001 by unpaired students *t*-test.

Erythropoietic reconstitution during cGvHD in the huPBMCs NSG model

Monitoring the erythropoietic recovery after xeno-HCT, the differential blood count performed at d+90 displayed a significantly increased frequency of murine lymphocytes in cGvHD, indicating the transferred huPBMCs to effect a 'tissue-crossing' lymphocyte reaction in mice. Murine leukocytes, thrombocytes and neutrophils were decreased in tendency in cGvHD compared to controls, while

other erythropoiesis-related factors were not affected (Supplemental Figure 2).

Discussion

With the overall objective to successfully prevent and treat cGvHD after allo-HCT, the establishment and application of valuable pre-clinical mouse models is key for understanding the systemic diseases' evolution and for translating experimental findings to the human scenario. Over the years, an extensive variety of cGvHD mouse models have been evolved, which fostered the progress of alleviating cGvHD after allo-HCT (15). However, most murine models have both, advances and limitations, so it is important to carefully characterize every single model and to evaluate, which is most appropriate to answer a particular scientific question. Examples of existing limitations are the mere sclerotic phenotype (without other typical features of human cGVHD) in some models, the short duration of 30 to 60 days and the specific target organ tropism (e.g. lung or skin) in other models. Given these limitations, our aim was to develop and characterize models which more closely resemble human cGVHD regarding the type of systemic inflammation and regarding the timing of development of the pathologies.

We established and described two relevant pre-clinical *in vivo* cGvHD models, which display a broad spectrum of the diverse cGvHD symptoms, that may be of advantage for cGvHD research and allow transferability of experimental results from bench to bedside. In the following paragraph, we discuss weaknesses and benefits of the here described haploidentical B6→ BDF1 and the xeno-transplant huPBMC → NSG models.

Most common, patients receive a stem cell infusion from a fully MHC-matched donor (35, 36), partially MHC-matched unrelated donor (37) or haploidentical donor (first-degree relatives, haploidentical in at least one set of genes) (38, 39). The latter scenario of a haploidentical HCT is used increasingly in the last years and is simulated in our B6 [$H2^b$]→; BDF1 [$H2^{b/d}$] model that represents a parent-into F1-generation, thus haploidentical immunologic disparity. The haploidentical setting may therefore be advantageous and more clinically relevant as compared with previous fully MHC-mismatched models (15, 40).

One major difference and potential improvement to other mouse models, which use the transfer of purified BM cells supplemented with purified T cells, is the mobilization of B6- and BDF1 donor-HCs with G-CSF, which allowed us to perform HCT of whole splenocytes. HC recruitment from the BM into the PB applying G-CSF is also exerted in clinical allo-HCT.

In patients, the onset of cGvHD is fluent, beginning approximately 3 months up to 2 years or even later after transplantation (41). Additionally, acute GvHD progresses to cGvHD in 70-80% of patients (42, 43). Our B6→BDF1 mouse model showed acute GvHD around d+20 after allo-HCT with spontaneous improvement afterwards. Later on, the animals developed typical cGVHD symptoms, which progressed until day+125, indicating a transformation of acute to cGVHD, as seen in many humans. Scores in the NSG model continuously increased until day+125 without an initial acute GvHD phase, but mortality rates stayed comparatively moderate. It is still not generally known, after which time cGvHD develops in mice, but the majority of published murine cGvHD models run less than 60 days, which might be too short-timed for a complete progression to robustly manifested cGvHD. The diagnosis of murine cGvHD is mainly defined by a clinical phenotype. At d+125, cGVHD mice of both of our models showed phenotypic as well as histological signs of cGvHD. Diseased NSG- and BDF1 recipients exhibited hunched posture, reduced activity, alopecia, skin scaling, erythema and ocular symptoms as dry and opaque lenses or blepharitis, all of which are frequently described to occur in cGvHD patients (32, 41, 44).

cGvHD simulates characteristics of autoimmune diseases with features of impaired immune tolerance mechanisms, like the involvement of auto- and alloreactive donor-derived T and B cells, the participation of alloantigens and mechanisms of chronic inflammation with subsequent fibrosis (32). The disease mainly manifests in the target organs skin, liver, lung and the gastrointenstinal tract. In addition, a variety of other organ systems, as mouth, joints and fasciae, muscles, eyes, the hematopoetic system or mucosal tissues may be affected (41). Our allo- as well as our xeno-HCT model depicted severe fibrosis and inflammation in the lung, liver, colon and skin of cGvHD mice. In the Masson's Trichrome Stainings, immune cell infiltrates and fibrotic depositions as well as sclerosis were particularly found in cGvHD B6→ BDF1 recipients, where they were related to extensive tissue damage in the respective organ (e.g. epidermal thickening in the skin, hepatitis and steatosis in the liver and bronchiolitis obliterans in the lung and non-infectious colitis in the colon), with all mentioned symptoms contributing significantly to high morbidity and mortality rates after clinical allo-HCT (45–49). Our histopathological observations closely resembled the situation in patients, where fibrosis is mostly systemic, standing in contrast to the majority of published sclerotic mouse models, which mainly comprise a cutaneous pathology (15, 18). It is reported that activated monocytes, macrophages as well as eosinophils may mediate the induction of collagen production leading to systemic fibrosis (50–52). Besides, pro-inflammatory neutrophils contribute to the process of chronic pulmonary fibrosis (53), a manifestation also seen in our cGvHD BDF1 mice. In existing sclerodermatous cGvHD models, mast cell and eosinophilic cell populations have been found increased in the skin (54) and liver (55) of transplanted mice. This theory is in line with our experimental findings in cGvHD from the BDF1

model, where CD11b+Gr1+ myeloid cells and macrophages were measured to be significantly elevated in the PB until day 60 after allo-HCT and also showed signs of increased activation. Furthermore, eosinophils in the PB and neutrophils in the spleen were shown to depict elevated levels in cGvHD. Since application of G-CSF in donors is known to mobilize especially CD11b+ myelomonocytic subsets, this could be an explanation for the high frequency of aforementioned monocytic and myeloid subsets and the augmented rates of fibrosis in our cGvHD mice. Effector T cells as inflammatory triggers and macrophages and monocytes as fibrotic mediators might be recruited by the presence of chemokines, such as CXCL9 and CXCL10, which were both validated as prognostic cGvHD biomarkers in humans (56, 57) and were shown to be significantly increased in cGvHD but not in controls of our BDF1 mouse model.

In flow cytometry experiments of cGvHD BDF1 recipients, we saw a decelerated B cell recovery early as d+20 after allo-HCT during the acute GVHD phase, which is also observed in transplanted patients (58, 59). During cGVHD at d+125 after HCT, we detected massive T and B cell infiltrates in lungs and livers of cGvHD mice in flow cytometry as well as in histological immunofluorescence analyzes. It is known, that impaired B cell tolerance results in persistent activation and exaggerated proliferation of autoreactive and alloreactive B cells and contribute to the human cGvHD pathogenesis, both increasing auto-and alloantibody reactions in cGvHD patients (60, 61). Still, it has to be further elucidated, if the donor B cells in our BDF1 model are allo- or autoreactive, respectively reacting to recipient antigens exclusively or to antigens shared by donor and recipient.

Furthermore, we found an increased frequencies of CD3+, CD4+ and CD8+ T cells, B220+ B cells and neutrophils in the spleens of cGvHD mice, indicating that the observed splenic damage is evoked by inflammatory lymphocytes. While the induction of GvHD in the BDF1 mouse model was assumed to be mainly CD8+ driven, both CD4+ and CD8+ T cell subsets were not found to be significantly elevated in PB of cGvHD mice compared to controls at day+125, although clinical signs of cGvHD were detected in tissues. In a murine cGvHD chemotherapy/TBI-conditioned model Blazar et al. elegantly demonstrated that cGvHD pathology manifests in fibrosis and bronchiolitis obliterans and was associated with CD4+ as well as B220+ B cell infiltration and that germinal center B cell reactions occurring at onset of cGvHD seem to facilitate disease development. Furthermore increased frequencies of follicular T helper cells were assumed to maintain and foster germinal center B cell reactions upon cGvHD progression (62, 63). On the contrary, Zeng et al. showed cGvHD models, which described germinal center reactions as dispensible for cGvHD development, thus recently proposing extrafollicular CD4+ T- and B cell interactions to be responsible for cGvHD induction (64, 65). Given the impressive B cell aggregates that we observed in the lungs, it would be of considerable interest to determine how interactions between T cells and B cells in the spleen and target organs such as the lung contribute to the pathogenesis of cGvHD in our model.

In addition, we detected a diminished DC frequency in spleens of cGvHD BDF1 mice at day+125 after allo-HCT. This resembles the clinical situation, since severe cGvHD is associated with impaired DC recovery and reduced circulating DC numbers, contributing to failing DC-mediated tolerance in allo-HCT patients (66, 67).

Especially xenogeneic models were criticized to be highly artificial, because T cell reactivity by MHC molecules is restricted between species. Human antigen presenting cells are unable to process and present mouse MHC class II antigens to human donor T cells, making this model predominantly CD4+ T cell dependent (28). Actually, our data showed primarily human CD4+ T cells to be proliferated and circulated in the PB of NSG recipients until day+125 after HCT. Interestingly, also the proportion of murine CD45+ leukocytes at day+60 and the population of CD11b+CD11c+ myeloid DCs at day+125 was found increased in cGvHD, supporting the theory that there might be some crosstalk between murine cells, respectively tissue and human cells. Several studies indicate, that human cells can indeed recognize murine xeno-antigens in an MHC I and MHC II dependent manner and that the human CD28 T cell receptor is able to interact with its murine counterpart B7.2, facilitating co-stimulatory signals to donor T cells (68–70).

Moreover, general weaknesses occurring frequently in murine models are differences in the animal suppliers, age of mice, individual handling techniques or a homogenous microbial gut environment in mice when housed under specified, often pathogen-free conditions (71). One risk factor for development of cGvHD is an increased age of both donor and recipient (6, 72). To adapt to this situation, we used B6-donors aged more than 20 weeks and BDF1 and NSG-recipients aged at least 10 weeks. All mice were housed in open-housing cages and handled without tail fixation by tunnel or cupping techniques that might not only reduce anxiety but can help to reduce stress-related weight changes, lethargy and other factors, which can adulterate GvHD scoring results (73).

A potential point to modify in the future is the type of conditioning. Transplanted patients are often administered with cytotoxic drugs as busulfan, cyclophosphamide or fludarabine as conditioning regime prior to allo-HCT (74, 75). To secure reliable engraftment, our BDF1 model received total body irradiation, which could be prospectively refined by applying chemotherapeutic conditioning with busulfan and cyclophosphamide, e.g. as first described in pioneering work by Sadeghi et al. (76) and already further established for acute GvHD models (77).

Conclusion

Mouse models of cGvHD can be criticized to express major differences toward the clinical allo-HCT situation, requiring careful evaluation before translating pre-clinical results into patients. On the other hand, the tight control of standardized experimental conditions and the homogenous nature of murine models, showing less variability contributed to the current knowledge about cGvHD pathogenesis and today's consensus on treatment options. In this study, we established and characterized two improved pre-clinical cGvHD mouse models: one allogeneic, haploidentical B6→ BDF1 and a humanized PBMC→ NSG Xenograft model. Especially our well-described BDF1 model showed various clinical cGvHD manifestations as inflammation, fibrosis and an altered immunological reconstitution and could be utilized for future research on novel promising cGvHD treatment and prophylaxis strategies.

Data availability statement

The raw data supporting the conclusions of this article will be made available by the authors, without undue reservation.

Ethics statement

The animal study was reviewed and approved by Landesamt für Gesundheit und Soziales Berlin.

Author contributions

LV, KR and OP designed the study. LV, KR, MK, SM, CS, JM and CF performed cGVHD experiments. LV and BJ performed histological analyzes. LV and MK performed FACS. LV analyzed data and LV and OP wrote the manuscript. All authors contributed to the article and approved the submitted version.

Funding

This work was supported by Deutsche Krebshilfe (70113055), DKMS Stiftung Leben Spenden (88133122), Kommission für Nachwuchsförderung of the Charité, José Carreras Leukämie-Stiftung (3R/2019, 23R/2021), Deutsche Krebshilfe (70113519), Deutsche Forschungsgemeinschaft (PE 1450/7-1, PE 1450/9-1) and Stiftung Charité BIH (BIH_PRO_549, Focus Group Vascular Biomedicine).

Acknowledgments

The authors would like to thank Felix Heymann (Department of Gastroenterology and Hepatology, Charité, Berlin) for instrumental support in fluorescence microscopy.

Conflict of interest

The authors declare that the research was conducted in the absence of any commercial or financial relationships that could be construed as a potential conflict of interest.

Publisher's note

Supplementary material

The Supplementary Material for this article can be found online at: https://www.frontiersin.org/articles/10.3389/fimmu.2022.1079921/full#supplementary-material

References

1. Passweg JR, Baldomero H, Chabannon C, et al. Impact of the SARS-CoV-2 pandemic on hematopoietic cell transplantation and cellular therapies in Europe 2020. a report from the EBMT activity survey. *Bone Marrow Transplant* (2022) 57 (5):742–52. doi: 10.1038/s41409-022-01604-x

2. Passweg JR, Baldomero H, Chabannon C, et al. The EBMT activity survey on hematopoietic-cell transplantation and cellular therapy 2018. CAR-t's come into focus. *Bone Marrow Transplant* (2020) 55(8):1604–13. doi: 10.1038/s41409-020-0826-4

3. Grube M, Holler E, Weber D, et al. Risk factors and outcome of chronic graft-versus-Host disease after allogeneic stem cell transplantation-results from a single-center observational study. *Biol Blood Marrow Transplant J Am Soc Blood Marrow Transplant* (2016) 22(10):1781–91. doi: 10.1016/j.bbmt.2016.06.020

4. Ferrara JL, Deeg HJ. Graft-versus-host disease. *New Engl J Med* (1991) 324 (10):667–74. doi: 10.1056/NEJM199103073241005

5. Shouval R, Fein JA, Cho C, et al. The simplified comorbidity index: a new tool for prediction of nonrelapse mortality in allo-HCT. *Blood Adv* (2022) 6(5):1525–35. doi: 10.1182/bloodadvances.2021004319

6. Arai S, Arora M, Wang T, et al. Increasing incidence of chronic graft-versus-host disease in allogeneic transplantation: A report from the center for international

blood and marrow transplant research. *Biol Blood marrow Transplant J Am Soc Blood Marrow Transplant* (2015) 21(2):266–74. doi: 10.1016/j.bbmt.2014.10.021

7. Carlens S, Ringdén O, Remberger M, et al. Risk factors for chronic graft-versus-host disease after bone marrow transplantation: a retrospective single centre analysis. *Bone Marrow Transplant* (1998) 22(8):755–61. doi: 10.1038/sj.bmt.1701423

8. Bensinger WI, Weaver CH, Appelbaum FR, et al. Transplantation of allogeneic peripheral blood stem cells mobilized by recombinant human granulocyte colony-stimulating factor. *Blood* (1995) 85(6):1655–8. doi: 10.1182/blood.V85.6.1655.bloodjournal8561655

9. Majolino I, Saglio G, Scimè R, et al. High incidence of chronic GVHD after primary allogeneic peripheral blood stem cell transplantation in patients with hematologic malignancies. *Bone Marrow Transplant* (1996) 17(4):555–60.

10. Storek J, Gooley T, Siadak M, et al. Allogeneic peripheral blood stem cell transplantation may be associated with a high risk of chronic graft-versus-host disease. *Blood* (1997) 90(12):4705–9. doi: 10.1182/blood.V90.12.4705

11. Zeiser R, Blazar BR. Pathophysiology of chronic graft-versus-Host disease and therapeutic targets. *N Engl J Med* (2017) 377(26):2565–79. doi: 10.1056/NEJMra1703472

12. Snell GD. The Nobel lectures in immunology. lecture for the Nobel prize for physiology or medicine, 1980: Studies in histocompatibility. *Scandinavian J Immunol* (1992) 36(4):513–26. doi: 10.1111/j.1365-3083.1992.tb03218.x

13. Kolb HJ, Holler E. Adoptive immunotherapy with donor lymphocyte transfusions. *Curr Opin Oncol* (1997) 9(2):139–45. doi: 10.1097/00001622-199703000-00006

14. Storb R, Rudolph RH, Thomas ED. Marrow grafts between canine siblings matched by serotyping and mixed leukocyte culture. *J Clin Invest* (1971) 50 (6):1272–5. doi: 10.1172/JCI106605

15. Schroeder MA, DiPersio JF. Mouse models of graft-versus-host disease: advances and limitations. *Dis Models Mech* (2011) 4(3):318–33. doi: 10.1242/dmm.006668

16. Hill GR, Ferrara JLM. The primacy of the gastrointestinal tract as a target organ of acute graft-versus-host disease: rationale for the use of cytokine shields in allogeneic bone marrow transplantation. *Blood* (2000) 95(9):2754–9. doi: 10.1182/blood.V95.9.2754.009k25_2754_2759

17. Zeiser R, Blazar BR. Preclinical models of acute and chronic graft-versus-host disease: how predictive are they for a successful clinical translation? *Blood* (2016) 127(25):3117–26. doi: 10.1182/blood-2016-02-699082

18. Chu Y-W, Gress RE. Murine models of chronic graft-versus-host disease: insights and unresolved issues. *Biol Blood marrow Transplant J Am Soc Blood Marrow Transplant* (2008) 14(4):365–78. doi: 10.1016/j.bbmt.2007.12.002

19. Korngold R, Sprent J. Lethal graft-versus-host disease after bone marrow transplantation across minor histocompatibility barriers in mice. *Prev by removing mature T Cells marrow. J Exp Med* (1978) 148(6):1687–98. doi: 10.1084/jem.148.6.1687

20. Jaffee BD, Claman HN. Chronic graft-versus-host disease (GVHD) as a model for scleroderma. *Cell Immunol* (1983) 77(1):1–12. doi: 10.1016/0008-8749(83)90001-1

21. Hamilton BL, Parkman R. Acute and chronic graft-versus-host disease induced by minor histocompatibility antigens in mice. *Transplantation* (1983) 36 (2):150–5. doi: 10.1097/00007890-198308000-00008

22. Via CS, Sharrow SO, Shearer GM. Role of cytotoxic T lymphocytes in the prevention of lupus-like disease occurring in a murine model of graft-vs-host disease. *J Immunol (Baltimore Md. 1950)* (1987) 139(6):1840–9.

23. Slayback DL, Dobkins JA, Harper JM, et al. Genetic factors influencing the development of chronic graft-versus-host disease in a murine model. *Bone marrow Transplant* (2000) 26(9):931–8. doi: 10.1038/sj.bmt.1702661

24. de Wit D, van Mechelen M, Zanin C, et al. Preferential activation of Th2 cells in chronic graft-versus-host reaction. *J Immunol (Baltimore Md. 1950)* (1993) 150(2):361–6.

25. Sakoda Y, Hashimoto D, Asakura S, et al. Donor-derived thymic-dependent T cells cause chronic graft-versus-host disease. *Blood* (2007) 109(4):1756–64. doi: 10.1182/blood-2006-08-042853

26. Zhang C, Todorov I, Zhang Z, et al. Donor CD4+ T and b cells in transplants induce chronic graft-versus-host disease with autoimmune manifestations. *Blood* (2006) 107(7):2993–3001. doi: 10.1182/blood-2005-09-3623

27. Tschetter JR, Mozes E, Shearer GM. Progression from acute to chronic disease in a murine parent-into-F1 model of graft-versus-host disease. *J Immunol (Baltimore Md. 1950)* (2000) 165(10):5987–94. doi: 10.4049/jimmunol.165.10.5987

28. Shultz LD, Lyons BL, Burzenski LM, et al. Human lymphoid and myeloid cell development in NOD/LtSz-scid IL2R gamma null mice engrafted with mobilized human hemopoietic stem cells. *J Immunol (Baltimore Md. 1950)* (2005) 174(10):6477–89. doi: 10.4049/jimmunol.174.10.6477

29. Ito R, Katano I, Kawai K, et al. Highly sensitive model for xenogenic GVHD using severe immunodeficient NOG mice. *Transplantation* (2009) 87(11):1654–8. doi: 10.1097/TP.0b013e3181a5cb07

30. Ullman-Culleré MH, Foltz CJ. Body condition scoring. a rapid and accurate method for assessing health status in mice. *Lab Anim Sci* (1999) 49(3):319–23.

31. Lerner KG, Kao GF, Storb R, et al. Histopathology of graft-vs.-host reaction (GvHR) in human recipients of marrow from HL-a-matched sibling donors. *Transplant Proc* (1974) 6(4):367–71.

32. Cooke KR, Luznik L, Sarantopoulos S, et al. The biology of chronic graft-versus-Host disease: A task force report from the national institutes of health consensus development project on criteria for clinical trials in chronic graft-versus-Host disease. *Biol Blood Marrow Transplant J Am Soc Blood Marrow Transplant* (2017) 23(2):211–34. doi: 10.1016/j.bbmt.2016.09.023

33. Shulman HM, Kleiner D, Lee SJ, et al. Histopathologic diagnosis of chronic graft-versus-host disease. national institutes of health consensus development project on criteria for clinical trials in chronic graft-versus-Host disease: II. *Pathol Working Group Rep Biol Blood Marrow Transplant J Am Soc Blood Marrow Transplant* (2006) 12(1):31–47. doi: 10.1016/j.bbmt.2005.10.023

34. Schindelin J, Arganda-Carreras I, Frise E, et al. Fiji. an open-source platform for biological-image analysis. *Nat Methods* (2012) 9(7):676–82. doi: 10.1038/nmeth.2019

35. Kernan NA, Bartsch G, Ash RC, et al. Analysis of 462 transplantations from unrelated donors facilitated by the national marrow donor program. *N Engl J Med* (1993) 328(9):593–602. doi: 10.1056/NEJM199303043280901

36. Anasetti C, Petersdorf EW, Martin PJ, et al. Trends in transplantation of hematopoietic stem cells from unrelated donors. *Curr Opin Hematol* (2001) 8 (6):337–41. doi: 10.1097/00062752-200111000-00004

37. Petersdorf EW, Anasetti C, Martin PJ, et al. Limits of HLA mismatching in unrelated hematopoietic cell transplantation. *Blood* (2004) 104(9):2976–80. doi: 10.1182/blood-2004-04-1674

38. Henslee-Downey PJ, Abhyankar SH, Parrish RS, et al. Use of partially mismatched related donors extends access to allogeneic marrow transplant. *Blood* (1997) 89(10):3864–72. doi: 10.1182/blood.V89.10.3864

39. Beatty PG, Clift RA, Mickelson EM, et al. Marrow transplantation from related donors other than HLA-identical siblings. *N Engl J Med* (1985) 313 (13):765–71. doi: 10.1056/NEJM198509263131301

40. Reddy P, Negrin R, Hill GR. Mouse models of bone marrow transplantation. *Biol Blood Marrow Transplant J Am Soc Blood Marrow Transplant* (2008) 14(1 Suppl 1):129–35. doi: 10.1016/j.bbmt.2007.10.021

41. Jagasia MH, Greinix HT, Arora M, et al. National institutes of health consensus development project on criteria for clinical trials in chronic graft-versus-Host disease: I. the 2014 diagnosis and staging working group report. *Biol Blood Marrow Transplant J Am Soc Blood Marrow Transplant* (2015) 21(3):389–401.e1. doi: 10.1016/j.bbmt.2014.12.001

42. Ochs LA, Blazar BR, Roy J, et al. Cytokine expression in human cutaneous chronic graft-versus-host disease. *Bone Marrow Transplant* (1996) 17(6):1085–92.

43. Inamoto Y, Flowers MED, Sandmaier BM, et al. Failure-free survival after initial systemic treatment of chronic graft-versus-host disease. *Blood* (2014) 124 (8):1363–71. doi: 10.1182/blood-2014-03-563544

44. Filipovich AH, Weisdorf D, Pavletic S, et al. National institutes of health consensus development project on criteria for clinical trials in chronic graft-versus-host disease: I. diagnosis and staging working group report. *Biol Blood Marrow Transplant J Am Soc Blood Marrow Transplant* (2005) 11(12):945–56. doi: 10.1016/j.bbmt.2005.09.004

45. Strasser SI, Shulman HM, Flowers ME, et al. Chronic graft-versus-host disease of the liver: presentation as an acute hepatitis. *Hepatol (Baltimore Md.)* (2000) 32(6):1265–71. doi: 10.1053/jhep.2000.20067

46. Maung K, Ramalingam S, Chaudhry M, et al. Pre-transplant hepatic steatosis (fatty liver) is associated with chronic graft-vs-host disease but not mortality. *PloS One* (2020) 15(9):e0238824. doi: 10.1371/journal.pone.0238824

47. Dudek AZ, Mahaseth H, Defor TE, et al. Bronchiolitis obliterans in chronic graft-versus-host disease: analysis of risk factors and treatment outcomes. *Biol Blood Marrow Transplant* (2003) 9(10):657–66. doi: 10.1016/s1083-8791(03)00242-8

48. Chien JW, Duncan S, Williams KM, et al. Bronchiolitis obliterans syndrome after allogeneic hematopoietic stem cell transplantation-an increasingly recognized manifestation of chronic graft-versus-host disease. *Biol Blood Marrow Transplant J Am Soc Blood Marrow Transplant* (2010) 16(1 Suppl):S106–14. doi: 10.1016/j.bbmt.2009.11.002

49. Shulman HM, Cardona DM, Greenson JK, et al. NIH Consensus development project on criteria for clinical trials in chronic graft-versus-host disease: II. the 2014 pathology working group report. *Biol Blood Marrow Transplant J Am Soc Blood Marrow Transplant* (2015) 21(4):589–603. doi: 10.1016/j.bbmt.2014.12.031

50. Wynn TA. Fibrotic disease and the T(H)1/T(H)2 paradigm. nature reviews. *Immunology* (2004) 4(8):583–94. doi: 10.1038/nri1412

51. Wynn TA, Barron L. Macrophages: master regulators of inflammation and fibrosis. *Semin Liver Dis* (2010) 30(3):245–57. doi: 10.1055/s-0030-1255354

52. Levi-Schaffer F, Weg VB. Mast cells, eosinophils and fibrosis. *Clin Exp Allergy J Br Soc Allergy Clin Immunol* (1997) 27 Suppl 1:64–70. doi: 10.1111/j.1365-2222.1997.tb01829.x

53. Ding L, Yang J, Zhang C, et al. Neutrophils modulate fibrogenesis in chronic pulmonary diseases. *Front Med* (2021) 8:616200. doi: 10.3389/fmed.2021.616200

54. Choi KL, Giorno R, Claman HN. Cutaneous mast cell depletion and recovery in murine graft-vs-host disease. *J Immunol (Baltimore Md. 1950)* (1987) 138(12):4093–101.

55. Nonomura A, Kono N, Mizukami Y, et al. Histological changes of the liver in experimental graft-versus-host disease across minor histocompatibility barriers. VIII. role of eosinophil infiltration. *Liver* (1996) 16(1):42–7. doi: 10.1111/j.1600-0676.1996.tb00702.x

56. Kitko CL, Levine JE, Storer BE, et al. Plasma CXCL9 elevations correlate with chronic GVHD diagnosis. *Blood* (2014) 123(5):786–93. doi: 10.1182/blood-2013-08-520072

57. Kariminia A, Holtan SG, Ivison S, et al. Heterogeneity of chronic graft-versus-host disease biomarkers: association with CXCL10 and CXCR3+ NK cells. *Blood* (2016) 127(24):3082–91. doi: 10.1182/blood-2015-09-668251

58. Mensen A, Jöhrens K, Anagnostopoulos I, et al. Bone marrow T-cell infiltration during acute GVHD is associated with delayed b-cell recovery and function after HSCT. *Blood* (2014) 124(6):963–72. doi: 10.1182/blood-2013-11-539031

59. Jacobson CA, Sun L, Kim HT, et al. Post-transplantation b cell activating factor and b cell recovery before onset of chronic graft-versus-host disease. *Biol Blood Marrow Transplant J Am Soc Blood Marrow Transplant* (2014) 20(5):668–75. doi: 10.1016/j.bbmt.2014.01.021

60. Sarantopoulos S, Blazar BR, Cutler C, et al. B cells in chronic graft-versus-host disease. *Biol Blood Marrow Transplant J Am Soc Blood Marrow Transplant* (2015) 21(1):16–23. doi: 10.1016/j.bbmt.2014.10.029

61. Sarantopoulos S, Stevenson KE, Kim HT, et al. Altered b-cell homeostasis and excess BAFF in human chronic graft-versus-host disease. *Blood* (2009) 113 (16):3865–74. doi: 10.1182/blood-2008-09-177840

62. Srinivasan M, Flynn R, Price A, et al. Donor b-cell alloantibody deposition and germinal center formation are required for the development of murine chronic GVHD and bronchiolitis obliterans. *Blood* (2012) 119(6):1570–80. doi: 10.1182/blood-2011-07-364414

63. Flynn R, Du J, Veenstra RG, et al. Increased T follicular helper cells and germinal center b cells are required for cGVHD and bronchiolitis obliterans. *Blood* (2014) 123(25):3988–98. doi: 10.1182/blood-2014-03-562231

64. Deng R, Hurtz C, Song Q, et al. Extrafollicular CD4+ T-b interactions are sufficient for inducing autoimmune-like chronic graft-versus-host disease. *Nat Commun* (2017) 8(1):978. doi: 10.1038/s41467-017-00880-2

65. Kong X, Zeng D, Wu X, et al. Tissue-resident PSGL1loCD4+ T cells promote b cell differentiation and chronic graft-versus-host disease-associated autoimmunity. *J Clin Invest* (2021) 131(1):66. doi: 10.1172/JCI135468

66. Reddy V, Iturraspe JA, Tzolas AC, et al. Low dendritic cell count after allogeneic hematopoietic stem cell transplantation predicts relapse, death, and acute graft-versus-host disease. *Blood* (2004) 103(11):4330–5. doi: 10.1182/blood-2003-09-3325

67. Leveque-El Mouttie L, Koyama M, Le Texier L, et al. Corruption of dendritic cell antigen presentation during acute GVHD leads to regulatory T-cell failure and chronic GVHD. *Blood* (2016) 128(6):794–804. doi: 10.1182/blood-2015-11-680876

68. King MA, Covassin L, Brehm MA, et al. Human peripheral blood leucocyte non-obese diabetic-severe combined immunodeficiency interleukin-2 receptor gamma chain gene mouse model of xenogeneic graft-versus-host-like disease and the role of host major histocompatibility complex. *Clin Exp Immunol* (2009) 157(1):104–18. doi: 10.1111/j.1365-2249.2009.03933.x

69. Widmer MB, Bach FH. Allogeneic and xenogeneic response in mixed leukocyte cultures. *J Exp Med* (1972) 135(5):1204–8. doi: 10.1084/jem.135.5.1204

70. Freeman GJ, Borriello F, Hodes RJ, et al. Murine B7-2, an alternative CTLA4 counter-receptor that costimulates T cell proliferation and interleukin 2 production. *J Exp Med* (1993) 178(6):2185–92. doi: 10.1084/jem.178.6.2185

71. Hülsdünker J, Zeiser R. Insights into the pathogenesis of GvHD: what mice can teach us about man. *Tissue Antigens* (2015) 85(1):2–9. doi: 10.1111/tan.12497

72. Kollman C, Howe CW, Anasetti C, et al. Donor characteristics as risk factors in recipients after transplantation of bone marrow from unrelated donors: the effect of donor age. *Blood* (2001) 98(7):2043–51. doi: 10.1182/blood.V98.7.2043

73. Hurst JL, West RS. Taming anxiety in laboratory mice. *Nat Methods* (2010) 7(10):825–6. doi: 10.1038/nmeth.1500

74. Tutschka PJ, Copelan EA, Klein JP. Bone marrow transplantation for leukemia following a new busulfan and cyclophosphamide regimen. *Blood* (1987) 70(5):1382–8. doi: 10.1182/blood.V70.5.1382.1382

75. Santos GW, Tutschka PJ, Brookmeyer R, et al. Marrow transplantation for acute nonlymphocytic leukemia after treatment with busulfan and cyclophosphamide. *N Engl J Med* (1983) 309(22):1347–53. doi: 10.1056/NEJM198312013092202

76. Sadeghi B, Aghdami N, Hassan Z, et al. GVHD after chemotherapy conditioning in allogeneic transplanted mice. *Bone Marrow Transplant* (2008) 42 (12):807–18. doi: 10.1038/bmt.2008.261

77. Riesner K, Kalupa M, Shi Y, et al. A preclinical acute GVHD mouse model based on chemotherapy conditioning and MHC-matched transplantation. *Bone Marrow Transplant* (2016) 51(3):410–7. doi: 10.1038/bmt.2015.279

frontiers | Frontiers in Immunology

TYPE Review
PUBLISHED 14 February 2023
DOI 10.3389/fimmu.2023.1100479

OPEN ACCESS

EDITED BY
Guido Moll,
Charité Universitätsmedizin Berlin,
Germany

REVIEWED BY
Lauren Higdon,
Immune Tolerance Network, United States
Thiago J. Borges,
Massachusetts General Hospital and
Harvard Medical School, United States

*CORRESPONDENCE
Paul A. Keown
paul.keown@ubc.ca

†These authors have contributed
equally to this work and share
first authorship

SPECIALTY SECTION
This article was submitted to
Alloimmunity and Transplantation,
a section of the journal
Frontiers in Immunology

RECEIVED 16 November 2022
ACCEPTED 25 January 2023
PUBLISHED 14 February 2023

CITATION
Wong P, Cina DP, Sherwood KR,
Fenninger F, Sapir-Pichhadze R,
Polychronakos C, Lan J and Keown PA
(2023) Clinical application of immune
repertoire sequencing in solid
organ transplant.
Front. Immunol. 14:1100479.
doi: 10.3389/fimmu.2023.1100479

Clinical application of immune repertoire sequencing in solid organ transplant

Paaksum Wong[1†], Davide P. Cina[2†], Karen R. Sherwood[1,3],
Franz Fenninger[1,3], Ruth Sapir-Pichhadze[4,5],
Constantin Polychronakos[6], James Lan[1,3] and Paul A. Keown[1,3*]

[1]Department of Medicine, University of British Columbia, Vancouver, BC, Canada,
[2]Department of Urologic Sciences, University of British Columbia, Vancouver, BC, Canada,
[3]Department of Pathology and Laboratory Medicine, University of British Columbia, Vancouver,
BC, Canada, [4]Department of Medicine, Division of Nephrology, McGill University, Montreal, QC, Canada,
[5]Department of Epidemiology, Biostatistics and Occupational Health, McGill University, Montreal,
QC, Canada, [6]Department of Pediatrics, The Research Institute of the McGill University Health Centre
and the Montreal Children's Hospital, Montreal, QC, Canada

Background: Measurement of T cell receptor (TCR) or B cell receptor (BCR) gene utilization may be valuable in monitoring the dynamic changes in donor-reactive clonal populations following transplantation and enabling adjustment in therapy to avoid the consequences of excess immune suppression or to prevent rejection with contingent graft damage and to indicate the development of tolerance.

Objective: We performed a review of current literature to examine research in immune repertoire sequencing in organ transplantation and to assess the feasibility of this technology for clinical application in immune monitoring.

Methods: We searched MEDLINE and PubMed Central for English-language studies published between 2010 and 2021 that examined T cell/B cell repertoire dynamics upon immune activation. Manual filtering of the search results was performed based on relevancy and predefined inclusion criteria. Data were extracted based on study and methodology characteristics.

Results: Our initial search yielded 1933 articles of which 37 met the inclusion criteria; 16 of these were kidney transplant studies (43%) and 21 were other or general transplantation studies (57%). The predominant method for repertoire characterization was sequencing the CDR3 region of the TCR β chain. Repertoires of transplant recipients were found to have decreased diversity in both rejectors and non-rejectors when compared to healthy controls. Rejectors and those with opportunistic infections were more likely to have clonal expansion in T or B cell populations. Mixed lymphocyte culture followed by TCR sequencing was used in 6 studies to define an alloreactive repertoire and in specialized transplant settings to track tolerance.

Conclusion: Methodological approaches to immune repertoire sequencing are becoming established and offer considerable potential as a novel clinical tool for pre- and post-transplant immune monitoring.

KEYWORDS

solid organ transplant, alloimmunity, lymphocyte receptor sequencing, B cell receptor (BCR), T cell receptor (TCR)

1 Principal mechanisms of alloantigen recognition

Transplant biopsy is the current gold standard for diagnosing rejection in solid organ transplant, combining histology with more detailed opportunities for cellular, molecular, and spatial biology evaluation of graft injury. But by virtue of its invasive nature, biopsy is normally employed only when clinical data raise diagnostic suspicion. Donor-derived cell-free DNA (dd-cfDNA) has shown potential as a biomarker for early detection of immune activation and serial surveillance (1). Novel solid-phase or cellular assays detecting anti-human leukocyte antigen (HLA) antibodies help to discriminate between cellular (CMR) and antibody mediated rejection (AMR). Unfortunately, current diagnostic methods are limited in utility and application, and typically only confirm rejection once significant organ damage has already occurred. We therefore require novel, less invasive and reliable assays for monitoring the alloimmune response in solid organ transplant to recognize immune events at the earliest possible time prior to the advent of irreversible organ injury. Such assays permit a more precise understanding of the biological mechanisms leading to graft injury, and the opportunity for earlier clinical intervention, mitigating rejection and improving graft outcomes.

Genomic analysis of the T and B cell receptor (TCR, BCR) repertoires promises to further our understanding of immune rejection and allows us to develop clinical biomarkers of graft injury for predicting short- and long-term graft outcomes (2, 3) T and B cells are an attractive target for study because they are cornerstones of the adaptive immune response in the post-transplant period and play key roles in alloreactivity and tolerance. T cells are responsible for cell-mediated rejection (CMR) as well as initiating donor-specific antibody (DSA) formation. In the latter, activated T helper cells trigger the differentiation of B cells and their production of DSAs, leading to antibody-mediated rejection (AMR) (4).

Two main processes underlie T cell-mediated allorecognition, both of which occur through the TCR. In the early post-transplant period, alloreactivity is thought to be driven primarily by direct recognition in which recipient T cells bind HLA-peptide complexes expressed on allogeneic cells. This response gradually transitions to the main driver of long-term allograft rejection (5, 6) considered to be indirect allorecognition, which occurs when recipient antigen-presenting cells (APCs) take up, digest and present donor HLA peptides in the context of self HLA to engage recipient T cells. Recipient T cells recognize this self HLA-foreign peptide complex through the TCR (5, 6) recruiting cytotoxic CD8 T cell responses and driving long-term alloimmune recognition (7). B cell-mediated allorecognition, an extension of this process, occurs *via* B cell receptor (BCR)-mediated recognition of an HLA-peptide complex presented by helper T cells. Once activated, the B cells mature and differentiate into antibody-secreting plasma cells or memory B cells. A single activated B cell may generate 5000 plasma cells in a week and up to 10^{12} antibodies per day (8). These antibodies, directed against structural epitopes on the allogeneic HLA, drive the more destructive AMR with often devastating consequences for the graft. A third less well described pathway is also described, termed the semi-direct pathway (9). In this pathway, recipient APCs uptake intact donor HLA *via* cell-cell contact (10) or extra cellular vesicles (11, 12) and present them on their cell surface to stimulate an alloreactive immune response. Alloantigen-specific recognition events trigger downstream activation of other adaptive immune cells that mount a coordinated antigen-specific response and generate immunologic memory.

Tolerance, a state of immune unresponsiveness to tissues and cells, consists of central and peripheral tolerance. Central tolerance is the deletion of self-reactive clones during negative selection in the thymus, while peripheral tolerance includes peripheral deletion, anergy, and Treg suppression. Operational tolerance can be defined as stable graft function without immunosuppressive treatments and the absence of graft rejection (13). However, it is rare in practice to be safely and completely withdrawn from immunosuppression, and reasons to do so may include non-compliance, malignancies, infections, or serious side effects. Tolerance in liver transplant is relatively frequent in SOTs, and biomarkers of tolerance have been previously described with tolerant patients having increased frequencies of peripheral CD4+CD25+FoxP3+ cells (14). In kidney transplant, recipients who received kidneys from young living donors have seen better tolerance outcomes (15). However, graft function may decrease without prior indication, highlighting the importance of and demand for routine non-invasive monitoring.

2 The T cell immune synapse and selective modulation of molecular signals

T cell allorecognition is among the earliest steps in the adaptive immune response to transplanted tissues. This process is tightly regulated and requires multiple signals acting in concert.

The first and most critical signal is T cell receptor (TCR) recognition of a cognate antigenic peptide presented on a class I or class II major histocompatibility complex (MHC). This interaction is stimulatory, and its strength depends on the density and affinity of the TCR-MHC interaction (16). Antigen analog-MHCs have been explored as TCR antagonists to inhibit antigenic peptide engagement to the TCR as a target for treating allergies or autoimmune diseases (17). However, few studies have investigated its application in transplant immunosuppression likely due to the unique specificities of individual TCRs which are different for every given recipient-donor pair. When compounded with the complexity of identifying potentially alloreactive MHC-TCR combinations, targeting TCR directly as a means of immunosuppression may be difficult.

Once antigen specific recognition occurs, the second signal involves engagement of immune checkpoints which are receptor-ligand pairs belonging to either the TNF or immunoglobulin superfamily. These act to either co-stimulate or co-inhibit the T cell response upon TCR engagement thereby directing and tightly regulating the subsequent T cell response (Figure 1). Because of these properties, immune checkpoints are the target of a new generation of immunosuppressive medications. The most well-described checkpoint is CD28 which engages CD80/CD86 (B7) to stimulate T cell activation (18). CTLA4 is a co-inhibitory molecule

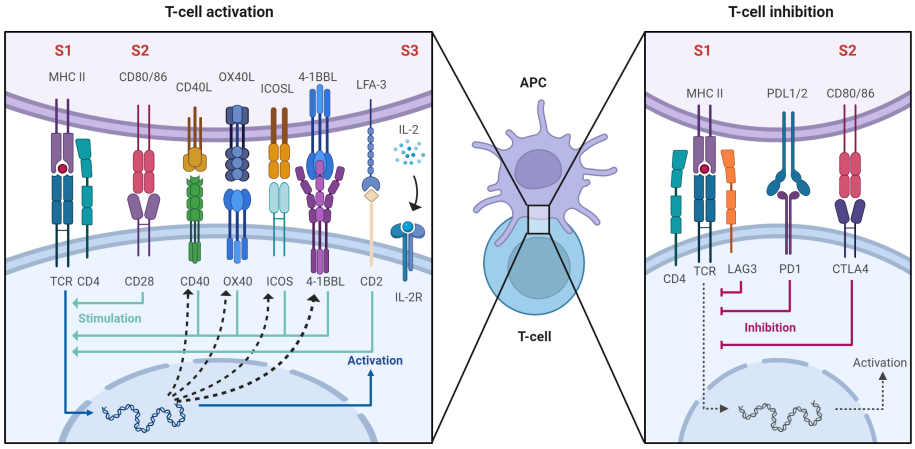

FIGURE 1
After antigen specific allorecognition *via* the antigen-specific TCR-MHC interaction (signal 1, labeled S1) second order signals are required for full T cell activation (S2 and S3). These involve engagement of immune checkpoints which are receptor-ligand pairs belonging to either the TNF or immunoglobulin superfamily. These act to either co-stimulate or co-inhibit the T cell response. Created with BioRender.com.

that competes with CD28 to bind CD80/CD86 and inhibit T cell activation (18). Belatacept is a second generation CTLA4-Fc fusion protein, used in CNI-sparing immunosuppressive regimens, that binds to CD80/CD86 on APCs and blocks engagement of CD28 on T cells thereby inhibiting their activation (19). CD40L is another co-stimulatory checkpoint expressed on T cells that binds to CD40 (CD154) on antigen presenting cells and endothelial cells to stimulate T cell activation (20, 21). Inhibition of CD40 using a humanized monoclonal antibody was sufficient to prevent rejection in nonhuman primate renal transplants (22) but concerns of thromboembolic complications have slowed its translation to clinical use (23). OX40, ICOS, and 4-1BB are so-called 'secondary checkpoints' expressed on activated T cells that are involved in further stimulating T cell activation after initial engagement of CD28. OX40 binds OX40L and is potentially involved in co-stimulation blockade resistant allograft rejection as co-administration of belatacept and anti-OX40L prolongs renal allograft survival in non-human primates relative to either therapy alone (24). ICOS is upregulated upon T cell activation and binds to ICOSL on antigen presenting cells. This interaction facilitates T cell activation, differentiation, and effector functions although its blockade alone or in combination with belatacept is insufficient to prolong renal allograft survival in NHPs (25). 4-1BB is also upregulated upon T cell activation and binds 4-1BBL to preferentially stimulate the CD8 cytotoxic T cell response (26). More recently, interest has turned to CD2 which is a co-stimulatory molecule expressed on T cells and NK cells (27). CD2 binds LFA-3 to regulate positive selection during T cell development and stimulate antigen specific activation in naïve and memory T cells (28–30). While data on the role of CD2 in NK cell function is more limited, it plays a role in antibody-independent and -dependent cytotoxicity (31). Two agents targeting this axis have been tested in the setting of human clinical transplant: Alefacept which is an LFA-3 Fc fusion protein and siplizumab which is a humanized monoclonal antibody targeting CD2. Alefacept has been tested as an induction agent in standard renal transplant agent with equivocal success (32). Siplizumab has been tested for safety in standard human renal transplant (33) and used as part of a pre-conditioning regimen in humans receiving a combined kidney bone marrow transplant to induce tolerance (34, 35). LAG-3 recognizes peptide-bound MHC class II and inhibits T cell activation (36). Last, PD1 is an inhibitory checkpoint expressed on T cells that binds to PDL1 on target cells to block T cell activation. While modulation of this checkpoint has little utility in transplantation, it has been leveraged extensively in cancer immunotherapy (37).

TCR engagement and co-stimulation together lead to downstream activation of the calcineurin/NFAT, MAP kinase, and NF-kB pathways which in turn lead to the transcription of cytokines which provide the third signal for T cell proliferation and differentiation (38). Because all these inputs converge on the calcineurin/NFAT pathway, it is the target of the calcineurin-inhibitors (CNIs) Cyclosporin (39) and Tacrolimus (40) which are the current cornerstones of transplant immunosuppression.

Last, the third signal which occurs upon antigen specific TCR engagement and co-stimulation, is the evolution of cytokines to direct T cell proliferation and differentiation. The prototypical signal responsible for T cell proliferation is IL2 which binds the IL2 receptor (IL2R) on T cells. Downstream activation of the mechanistic target of rapamycin (MTOR) through IL2R favours the proliferation and differentiation of conventional T cells whereas IL2R engagement in the presence of MTOR inhibition favours the proliferation and differentiation of T regulatory cells through STAT5 signaling (41). The IL2R is targeted by basiliximab which is a commonly used form of induction therapy in transplant (42). While many other cytokines are involved in directing further T cell differentiation, an extensive discussion of this topic is beyond the scope of this review (43).

3 The B cell immune synapse and signaling

B cell signaling and activation is a fundamental step in the humoral immune response and in AMR. First, immature B cells released from the bone marrow circulate in the secondary lymphoid

organs (spleen and lymph nodes) until an antigen is encountered (44). Recognition of antigen by the BCR triggers the formation of the immunological synapse where initial cell spreading occurs. Antigens gather into microclusters during this stage and signaling is enhanced at these sites (45). Next, a contraction phase begins where the antigen is concentrated in the centre of the synapse forming the central supramolecular activation cluster (cSMAC), which is surrounded by actin and adhesion molecule-rich peripheral SMAC (pSMAC) (46). B cells are unique in that they can both interact with and act as APCs; a function of BCR-antigen binding is triggering endocytosis and intracellular processing (47). These B cells present processed peptides on MHCII molecules to CD4+ T helper cells through the TCR which signals the T cell to express CD40L, IL-4, and IL-21, promoting B cell proliferation, class switching, and somatic hypermutation (48). Activated B cells may immediately differentiate into plasmablasts for early production of low affinity antibodies for a quick immune response. But they can also form a germinal centre where further somatic hypermutation and class switching occur, eventually differentiating into memory B cells or plasma cells which are both capable of producing higher affinity antibodies (49). Memory B cells are formed when follicular dendritic cells present antigens for extended periods of time, maintaining the germinal centre response.

B cells have also been targeted for immunosuppression in transplant. Rituximab is directed against CD20 on the B cell surface and has been used extensively in treatment of AMR as well as desensitization therapies (50). B cell activation and survival may also be modulated by epratuzumab, an anti-CD22 antibody that depletes naïve and transitional B cells while inhibiting B cell activation and proliferation (51).

4 Receptor rearrangement and sequencing

As mentioned previously, antigen recognition by the TCR is the first crucial step in T cell activation and TCR diversity allows the adaptive immune system to respond to a multitude of antigenic stimuli. The TCR heterodimer consists of an α and β chain which are both generated through random recombination of the α and β genes. β gene recombination involves 3 gene segments: variable (V), diversity (D), and joining (J) while α gene recombination involves V and J segments only. TCR β gene recombination occurs in a stepwise fashion in which D-to-J rearrangement is followed by V-to-DJ rearrangement (Figure 2) (52). Monoallelic rearrangement of the antigen receptors, termed allelic exclusion, involves a mechanism called feedback inhibition whereby further rearrangements of the TCRβ chain are prevented if a functional antigen receptor chain is produced. In the TCRα chain, rearrangement only ceases when the T cell undergoes positive selection. Therefore, multiple functional α chains can be produced and expressed on a cell surface but only one β chain. After successful VDJ recombination, T cells undergo positive and negative selection in the thymus to produce mature T cells that can recognize foreign antigen presented by HLA while sparing self-antigens (53). Thymic output stops in early adulthood after giving rise to around 10^6 to 10^8 unique T cells as identified by their TCR sequence. Such repertoire diversity underlies the breadth of the adaptive immune response against an array of immune targets. BCR diversity is generated *via* a similar V(D)J gene rearrangement process (54).

Considering this profound diversity and specificity, the identification of unique TCR and BCR sequences using lymphocyte receptor sequencing provides an important opportunity to characterize and monitor the dynamic changes in the immune repertoire in response to an antigenic stimulus, particularly HLA molecules, in organ transplantation. This review describes a systematic synthesis of current knowledge and methods for using lymphocyte receptor repertoire sequencing in the setting of solid organ transplantation. First, we summarize different sequencing approaches and compare their relative advantages in a clinical setting. Next, we review current data pertaining to alloreactivity and tolerance in renal transplant and the more limited data in other solid organ transplants. Finally, we discuss promising areas for future study in this space.

5 Methods

Two authors (P.W. and D.P.C) performed the searches in MEDLINE and PubMed Central, SCOPUS and EMBASE library databases. Commencing with T-cell and B-cell receptor sequencing, five refined key search terms were used in combinations for a total of six queries using the Boolean operator "AND", as this allowed for only studies mentioning key search terms to be included (Table 1). Selected search phrases were submitted to PubMed on Oct 27, 2021. All searches were conducted with filters selecting articles that studied humans and English language articles published from January 1, 2010 – Oct 27, 2021. This date range was chosen due to the wide availability of high throughput sequencing post-2010. Total references returned includes replicates. Additional sources were identified by reviewing the reference lists of articles which met inclusion criteria. All studies identified were assessed to determine eligibility based on title and abstract. Potentially eligible studies were retrieved, and the full study report evaluated. Disagreements were resolved by consensus or adjudicated by a third reviewer (K.R.S).

Articles were then evaluated for inclusion in the study according to the workflow process summarized in Figure 3. Once the studies were extracted and reviewed, those that applied TCR or BCR sequencing to solid organ transplant were selected for in-depth review. Studies that focused on non-human species were excluded due to disparities in the nucleotide sequences of receptor genes (55). Articles that focused on hematopoietic stem cell transplantation, cancer or other diseases which mentioned transplant but did not address immune monitoring, lymphocyte receptor repertoire or clonal reactivity were excluded. Likewise, full articles that lacked a detailed methodologic description were excluded from the review.

Study characteristics were categorized and summarized. Details included publication reference (first author, journal, year of publication, article type), receptor type (eg. TCR or BCR), organ transplant, sequencing region (eg. TCRβ sequencing), PCR method (eg. multiplex), starting material (eg. RNA), and whether a mixed lymphocyte reaction was conducted to identify clonal targets. For applicable studies, the subtype of immune cells investigated was

10.3389/fimmu.2023.1100479

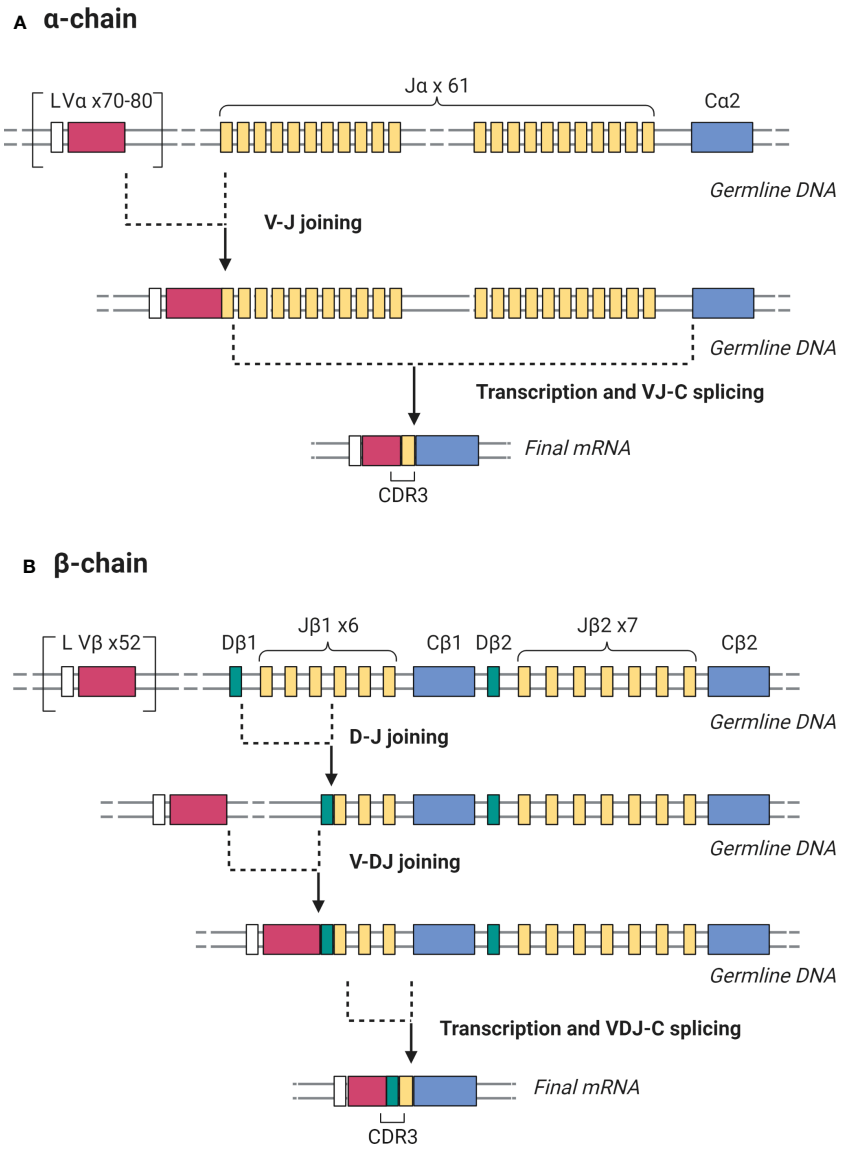

FIGURE 2
Somatic recombination of the germline DNA encoding TCR α and β chains during T cell development generates antigen-binding diversity. **(A)** For the TCR α chain, V-J rearrangement is followed by transcription and splicing to create a complete VJ-C mRNA. **(B)** For the β chain, D-J rearrangement is followed by V-DJ rearrangement, then transcription and splicing to create a complete VDJ-C mRNA. In both cases, the mRNA product is then translated to yield the protein receptor chains. The CDR3 region is the most variable portion of the TCR due to its location in the junction where V-J and V-D-J joining occurs in the α and β chains respectively. Created with BioRender.com.

TABLE 1 Selected search phrases submitted to PubMed on Oct 27, 2021.

Search Phrase	References returned
(Donor reactive) AND (T cell repertoire)	110
(Donor reactive) AND (B cell repertoire)	39
(T cell repertoire) AND transplant*	728
(B cell repertoire) AND transplant*	211
(T cell repertoire) AND clonal*	864
(B cell repertoire) AND clonal*	479
TOTAL	2431

All searches were conducted with filters applied for English language articles published from 2010-2021. Total references returned includes replicates. Truncation symbol used to retrieve search results for all words containing the phrase preceding *.

noted. Other notable study characteristics were documented at the discretion of the reviewer.

6 Results

6.1 Targets and strategies for lymphocyte receptor sequencing

A summary of the studies included in this review and their characteristics are outlined in Table 2. TCR sequencing was performed more frequently than BCR sequencing in most studies (65% *vs* 35%), which could be due to the role of T cells in multiple mechanisms of graft injury, but perhaps also because there are established B cell methods including DSA testing. Not only are T

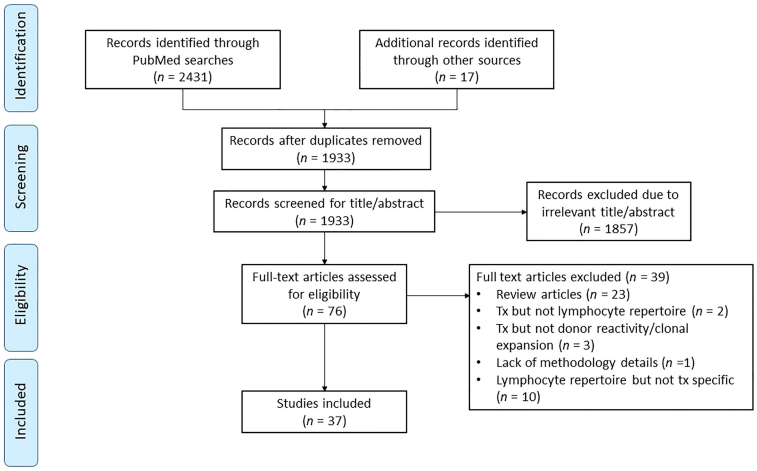

FIGURE 3
Flow diagram for records identified, included, excluded, and reasons for exclusion.

cells involved directly in CMR, but they also play a role in the evolution of antibody-producing B cells that underly AMR. This points to the potential clinical utility of TCR sequencing in monitoring early phases of the alloimmune response with the goal of early intervention to prevent irreversible graft. BCR sequencing may also have clinical potential as it could provide further insight into the dynamics of AMR which is generally a more destructive form of graft injury.

For purposes of identifying alloreactive clones, generation of donor-specific T or B cells could be a valuable resource. Mixed lymphocyte culture (MLC) coupled with receptor sequencing was a common method used amongst studies. Pre-transplant culturing of irradiated donor PBMCs with proliferation dye carboxyfluorescein diacetate succinimidyl ester (CFSE) stained recipient PBMCs over 5-7 days (79, 83, 91) generated an alloreactive fingerprint which could be longitudinally tracked post-transplant for immune monitoring. Morris et al. cultured donor PBMCs with purified T cells as responder cells (75). In terms of culturing conditions, cell plating concentrations were between 1-3 x 10^6 cells/mL, with a 5-fold increase in frequency from seeding to harvesting defined as donor-reactive clones. Harvested cells were then fluorescence activated cell sorted (FACS) to isolate $CFSE^{low}$ proliferating cells as well as CD4+, CD8+, and Tregs. Taken together, MLC approaches have been similar although with slight variations in culturing protocols.

The TCRβ chain was the genomic region sequenced in all 24 TCR sequencing studies, with 4 studies targeting both TCRα and TCRβ chains. Since each T cell can potentially express more than one α chain, but only one β chain, the β chain is considered a precise candidate to uniquely identify a given T cell clone (92). All studies sequenced the complementary determining region 3 (CDR3), a highly polymorphic region in TCRs and immunoglobulins.

Differing approaches were used to generate sequencing reads. Of the 25 studies that detailed PCR methods, 20 (80%) used a multiplex PCR method. This versatile approach accepts either gDNA or RNA input, but the mix of primers targeting only known V gene alleles means that novel alleles cannot be detected. It is also prone to amplification biases which can be mitigated with molecular barcoding (93). Five studies (20%) used nested PCR or 5' rapid amplification of cDNA ends (RACE), the latter of which uses only RNA as starting material. 5'RACE preserves the 5' end of the mRNA by incorporating extra nucleotides at the 3' end of the cDNA molecule and a template-switch oligonucleotide. This enables the reverse transcriptase enzyme to replicate both templates completely and facilitate greater coverage of TCR variants. Ruggiero et al. developed a unique affinity target enrichment approach (94). RNA starting material was used to synthesize cDNA using a biotinylated primer targeting the constant (C) gene, which is adjacent to the rearranged VDJ genes. The cDNA fragments were magnetically captured on streptavidin beads for PCR amplification, allowing for small quantities of cDNA (up to 10 ng) to represent greater repertoire diversity.

6.2 Lymphocyte receptor sequencing in renal transplantation

Lymphocyte receptor sequencing has been applied most extensively in the context of renal transplantation to identify and track the specific alloreactive T cell repertoire, as well as characterize general trends in the peripheral and graft infiltrating T cell repertoire.

To define an 'alloreactive T cell fingerprint' Morris et al. developed a novel method using a MLC of recipient PBMCs labelled with CFSE and irradiated donor PBMCs labeled with Cell Tracer Violet for 6 days. The cultured cells were then FACS sorted for CD4+ and CD8+ CFSE-low cells and then their TCR β-chain CDR3 regions were sequenced. Putative donor-reactive clones are then defined as those that expanded at least 5-fold relative to their abundance in the baseline pre-MLC recipient repertoire (75).

This approach was then used to monitor T cell alloreactivity and identify mechanisms of tolerance in 4 CKBMT patients in whom immunosuppression (IS) was withdrawn, and 2 conventional living donor renal transplant patients. In the two conventional renal transplant patients CD4+ but not CD8+ donor reactive T cells increased in the post-transplant peripheral repertoire over time. In these patients, the magnitude of the *in vitro* alloreactive response, in terms of diversity and expansion of clones, correlated well with the

10.3389/fimmu.2023.1100479

TABLE 2 Summary of findings, methodology and demographic characteristics of included studies.

Author and Year	Cohort	Max Follow-up (months)	Genomic Target	PCR Method	Starting Material	Results	Limitations
Alachkar 2016 (2)	50 ktx	3	TCRβ CDR3	5' RACE	RNA	Expansion of TCR repertoire at time of TCMR compared to pre-tx and 1m	Short follow-up, limited TCMR samples
Arrieta-Bolaños 2018 (56)	3 healthy	–	TCRβ CDR3	Multiplex	DNA	ND in clonality of alloreactive CD4+ against DPB1*02:01 or DPB1*09:01, alloreactive clones low in abundance	Public TCR clones may be alloreactive to DPB1 mismatch
Aschauer 2021 (57)	117 non-sensitized ktx, anti-CD25 induction	12	TCRβ CDR3	5' RACE	RNA	DRC CD4 ↑ 0.72% to 1.89%, graft-infiltrating 6X circulating DRC	Short follow-up
Beausang 2011 (58)	19 highly-sensitized, 7 low-moderately-sensitized ktx	6	BCR IgHV	5' RACE	RNA	Upon depleting B-cell therapy, ↑ proportion IgG/IgA. ↑ frequency mutation IgM/IgD post-tx	Small sample size, bulk RNA seq = cell-to-cell variability in expression level
Bellan 2011 (59)	6 ktx acute TCMR, including 3 AMR	20	BCR IgHV	5' RACE	DNA	CD20+ B cells expressed highly mutated V genes without clonal expansion in TCMR alone or TCMR with AMR	Small sample size
Cappuccilli 2017 (60)	8 HD-Tx 7 HD 6 healthy	–	TCRβ CDR3	Multiplex	RNA	HD-Tx > HD > healthy in altered Vβ spectra	Spectra-alteration pattern is variable between individuals
Emerson 2014 (61)	6 healthy	3	TCRβ CDR3	Multiplex	DNA	Thousands of clones proliferate in MLC, alloreactive repertoire dominated by high abundance clones	Graft-infiltrating clones may not be detected by MLC
Ferdman 2014 (62)	21 ktx with graft failure	–	BCR IgHV	Multiplex	RNA	Clonal expansion and somatic hypermutation ↑ in graft than blood	Only 1 patient analyzed for comparative graft *vs.* blood
Gao 2017 (63)	4 ktx, 3 tolerant upon CKBMT	12	BCR IgHV	Multiplex	RNA	High frequency of transitional B cells and diversified repertoire during B cell recovery, memory B cell prevalent at 6m post-tx	Small sample size
Habal 2021 (64)	4 cardiac allograft vasculopathy at re-tx	–	TCRβ CDR3, BCR IgHV	5' RACE	RNA	Extensive overlap in intragraft and blood TCRβ but minimal overlap in IgHV repertoire	Small sample size, *in vitro* PMA/ionomycin stimulation may modify T cell phenotype
Han 2020 (65)	34 liver tx (11 acute rejection, 23 stable), 20 healthy	3	TCRβ CDR3	Multiplex	RNA	↓ repertoire diversity in rejection cohort and distinct V gene usage	TCRβ repertoire characterization alone may not be enough to distinguish rejecting graft from stable
Huang 2019 (66)	39 IgAN, 13 non-IgAN, 60 healthy	–	TCRβ CDR3, BCR IgHV	Multiplex	RNA	IgAN had ↓ CDR3 length, ↑ IgA1 and hypermutation rate; TCRβ and IgHV clones can distinguish type of nephropathy	No TCRβ data on non-IgAN cohort, may require further studies on involvement of T cells in IgAN pathogenesis
Jones 2021 (67)	180 liver tx	12	TCRβ CDR3	Multiplex	DNA	↑ baseline repertoire clonality associated with sepsis 3m and 12m post-tx, but does not predict mortality	Baseline clonality determined pre-tx, thus repertoire changes post-tx may not be reflected
Kim 2021 (68)	1 hand tx	14	TCRβ CDR3	5' RACE	RNA	↑ alloreactive GILs compared to blood; differential Vβ gene usage between graft and blood T cells	Small sample size, ex vivo expansion of GILs may alter clonal frequency
Lai 2016 (3)	10 ktx, 10 healthy	7 days post-tx	TCRβ CDR3	Multiplex	DNA	↓ diversity, ↑ high abundance clones in pre- and post-ktx compared to healthy, increased specific Vβ usage post-tx	Short follow-up

(Continued)

TABLE 2 Continued

Author and Year	Cohort	Max Follow-up (months)	Genomic Target	PCR Method	Starting Material	Results	Limitations
Lai 2019 (69)	3 ktx with acute rejection	7 days post-tx	BCR IgHV	Multiplex	DNA	↓ diversity, differential IgHV and IgHJ expression post-tx	Short follow-up, limited sample size
Leventhal 2015 (70)	19 CKBMT (12 tolerant and off IS)	18	TCRβ CDR3	Multiplex	DNA	Post-tx diversity of chimeric subjects similar to pre-tx; 97% unique clones post-tx, not present in pre-tx or donor; persistent chimeric patients developed infections while off IS	Only 9 samples had processed TCR data; no timepoints between tx and 2 years post-tx
Link 2016 (71)	4 HSCT	–	TCRαβ CDR3	–	RNA	Half of CD8+ repertoire dominated by CMV-specific T cells; ↓ diversity following CMV infection	Small sample size, CMV-specific CD8+ T cells defined by binding to restricted number of epitopes
Luque 2018 (72)	10 highly-sensitized, 5 non-sensitized	–	BCR Fluorospot	–	PBMC or B cells	Fluorospot assay capable of quantifying anti-HLA donor-reactive memory B cells	Further experiments comparing highly- and non-sensitized in ability to detect various anti-HLAs required
Mathew 2018 (73)	3 healthy	21 days	TCRβγ CDR3	–	DNA	CD40L-activated B cells stimulated AgTregs had ↓ diversity, ↑ polyclonality, demethylated Treg-specific demethylated region CNS2 at day 21 culture	Small sample size; polyclonal stimulation with CD3/CD28 may affect repertoire clonality
Moore 2020 (74)	4 cardiac allograft vasculopathy grafts at tx	–	BCR IgHV	Multiplex	DNA	B cell expansion, ↑ mutated rearrangements in graft but not blood	Small sample size
Morris 2015 (75)	4 CKBMT, 2 ktx	24	TCRβ CDR3	Multiplex	DNA	↓ post-tx donor-reactive clones in 3 CKBMT, ↑ donor-reactive clones in 2 ktx; ↓ diversity in non-tolerant patients	Small sample size, differences in IS between two cohorts
Nguyen 2017 (76)	3 EBV-positive lung tx	13	TCRαβ CDR3	Multiplex	DNA	TCRαβ repertoire biased towards TRVA-5; EBV-specific repertoire stable post-tx in absence or presence of EBV reactivation	Small sample size; repertoire changes not quantifiable due to limitations of bulk RNA TCR seq
Pineda 2019 (77)	27 ktx: 10 NP, 10 progressors (PNR), progressors with rejection (PR)	24	BCR IgHV	Multiplex	DNA/RNA	NP ↑ diversity, PR ↓ diversity; ↑ clonal expansion, presence of specific B cell clones and IGHV genes associated with ↑ risk of rejection	Sample highly selected set of pediatric patients
Pollastro 2021 (78)	1 healthy	10 days	TCRβ CDR3	Multiplex	RNA	*In vitro* expansion of moderate to frequently occurring clones 5-10 days post-stimulation; 15% clones showed ↑ frequency over 10 day culture; IL-4 addition induces expansion of IL-5 producing TCR clones	Short follow-up and sample size
Savage 2018 (79)	3 tolerant, 1 non-tolerant CKBMT; 3 healthy	6	TCRβ CDR3	Multiplex	DNA	ds-Tregs expanded 6m post-tx in tolerant patients, reduced in non-tolerant	Small sample size, large number of pre-tx cells required for assays
Savage 2020 (80)	3 tolerant, 5 non-tolerant liver tx	48	TCRβ CDR3	Multiplex	DNA	↓ donor-reactive TCRβ sequences in both tolerant and non-tolerant, magnitude of ↓ greater than non donor-reactive sequences	Lack of tissue or graft-infiltrating sample to confirm clonal deletion mechanism
Schober 2020 (81)	6 healthy CMV+	170 days	TCRαβ CDR3	Multiplex	RNA	Latent CMV infection resulted in ↑ proportion of larger T cells with low TCR affinity; clones with high affinity dominated acute immune response, low affinity preferred for chronic response	Small sample size; cannot rule out stochasticity as a factor of early/late repertoire dominance due to variability of single-cell-derived T cell populations

(Continued)

TABLE 2 Continued

Author and Year	Cohort	Max Follow-up (months)	Genomic Target	PCR Method	Starting Material	Results	Limitations
Smith 2016 (82)	10 SOT (6 lung, 3 kidney, 1 heart) following CMV-specific ACT	42 weeks	TCRβ CDR3	Multiplex	DNA	ACT responders showed ↑ CMV-specific clonotypes, ↓ diversity, ↑ effector memory T cells; no difference in TRBV usage was seen between responders and non-responders	Small sample size of non-responders (2/10)
Stranavova 2019 (83)	11 CMV+ HLA class I mismatched ktx	12	TCRβ CDR3	Multiplex	DNA	Association between pre-tx presence of CMV IE-1-specific T cells and acute rejection; shared TCRβ sequences between CMV IE-1 and donor-reactive T cells in pre-tx blood and post-tx graft	Lacking clonal frequency data of shared sequences and association with rejecting grafts
Vollmers 2015 (84)	12 heart tx (6 with rejection, 6 without)	15	BCR IgHV	Multiplex	DNA	Proof-of-concept IS monitoring: BCR seq diagnoses acute rejection *via* increased immune activity (71.4% sensitivity, 82% specificity with dd-cfDNA as standard)	Cohort is small and highly selected for rejection status and availability of longitudinal samples
Wang 2019 (85)	10 ESRD, 6 healthy	–	BCR IgHV	Multiplex	DNA	ESRD had ↑ clonal expansion, 5 upregulated and 9 downregulated VDJ genes; no difference in repertoire diversity was observed, although the distribution of ESRD was more skewed	Small sample size, differences in repertoire diversity not significant
Weinberger 2015 (86)	10 nephrectomy patients	–	TCR, BCR IgHV	Multiplex	DNA	Of graft-infiltrating clonotypes, 68% highly expanded T cells and 30% of the highly expanded B cells can be found amongst top 5 abundant clonotypes in blood; ↑ mean diversity in BCR repertoire compared to TCR across blood and kidney	TRBJ frequencies could not be compared to due primer limitations
Yan 2018 (87)	6 hepatitis B-related ACLF, 6 healthy	–	BCR IgHV	Multiplex	DNA	ACLF had ↑ clonal expansion, 6 upregulated and 19 downregulated VDJ genes; no differences in repertoire diversity	Small sample size
Yang 2018 (88)	6 liver tx, 6 healthy	7 days	TCRβ CDR3	Multiplex	DNA	↓ diversity in tx samples, with lowest at 7d post-tx; pre-tx had ↑ highly expanded clones compared to post-tx and healthy; ↑ TRBV expression in public TCRs post-tx	Short follow-up, given repertoire diversity was lowest at last timepoint, further timepoints could be insightful
Zhang 2021 (89)	30 CMV+, 25 CMV-	16	TCRαβ CDR3	Target enrichment	RNA	CMV+ associated with ↓ in naïve CD4+ T cells and ↑ CD4+ and CD45RA+ effector memory T cells, ↑ clonal expansion, and ↓ repertoire diversity	Only peripheral blood samples analyzed
Zuber 2016 (90)	11 intestinal tx, 7 rejectors	26	TCRαβ CDR3	Multiplex	DNA	Non-rejectors had donor T cells enriched for persistent GvH-reactive clones, while rejection was associated with ↑ HvG clones and ↑ T cell turnover	Role of *de novo* HvG clones in graft infiltration not assessed

ACLF, acute-on-chronic liver failure; ACT, adoptive T cell therapy; AMR, antibody-mediated rejection; CKBMT, combined kidney and bone marrow transplant; DRC, donor-reactive cells; ESRD, end-stage renal disease; GIL, graft-infiltrating lymphocytes; HD, hemodialysis; HSCT, hematopoietic stem cell transplantation; IgAN, IgA nephropathy; ND, no difference; NP, non-progressor; PNR, progressors without rejection; PR, progressors with rejection; TCMR, T cell mediated rejection. ↓, decreased; ↑, increased.

magnitude of the alloreactive response post-transplant. CKBMT patients who developed tolerance had a significant reduction in both number and diversity of circulating donor reactive T cells while those who experience rejection after IS withdrawal did not. This supports a role for clonal deletion as a mechanism of tolerance (75).

Savage et al. then leveraged TCR sequencing to study the role of T regulatory cells in maintaining tolerance in the same CKBMT patient population which included 3 tolerant and 1 non-tolerant subject after 10 months of IS withdrawal. They used FACS sorting for CD4+CD25+CD127- Treg lineage markers and TCR sequencing to define Treg repertoires under 3 different conditions: unstimulated, after stimulation with activated donor B-cells, or after stimulation with MLC in the presence of CTLA4Ig. The 'activated donor B-cell method' identified the most biologically relevant repertoire of Tregs that correlated best with tolerance by clonal fraction and cumulative frequency at 6 months. Tregs identified by this method were not expanded in the non-tolerant subject suggesting that tolerance despite lack of persistent mixed chimerism in these CKBMT patients may be in part explained by T regulatory cells (79).

These studies not only highlighted how TCR sequencing can be used to elucidate the biology of tolerance in specialized renal transplant cases, but also provide a basis for further studies using TCR sequencing of the alloreactive repertoire as a biomarker in conventional renal transplant. Aschauer et al. leverage a similar method in a single-center prospective cohort study designed to evaluate the expansion or deletion of alloreactive T cells in the post-transplant repertoire of patients with or without acute TCMR. Secondary outcomes included local T cell expansion in the graft during a rejection episode and changes in clonal diversity over time in rejecting versus non-rejecting patients (95). Using a cohort of 12 patients (3 with TCMR, 3 with borderline rejection, and 6 control patients), they showed that circulating CD4+ alloreactive T cells increased after transplant with no significant difference between controls and rejectors, even at the time of rejection. The biopsy infiltrating repertoire, however, was enriched for donor-reactive T cells at the time of rejection relative to controls (91).

In a separate study aimed at understanding the impact of different induction therapies on the alloreactive repertoire in 5 patients with pre-formed DSA induced with rabbit anti-thymocyte globulin (rATG) plus immunoadsorption and 5 without DSA given Basiliximab. MLC and TCR sequencing was performed at baseline and the alloreactive repertoire tracked for a year. They showed that over 1 year the percentage of peripheral CD4+ but not CD8+ donor-reactive T cells increased at similar frequencies across both groups (57). While these data do not shed further light on the diagnostic utility of TCR sequencing it suggests that there is no significant difference in T cell alloreactivity associated with either induction method alone.

The remaining studies in this space aim to measure general features of the T and B cell repertoire in patients prior to and after transplant. The conclusions that can be drawn from these studies as to the clinical utility of TCR sequencing in transplant are limited by a lack of systematic approaches and standardized metrics.

Two studies examined trends in the T cell repertoire of patients both pre- and post- renal transplant who do experience rejection. Lai et al. characterized the peripheral T cell repertoire in 10 transplant recipients preoperatively, then on postoperative day (POD) 1 and POD 7. These were then compared to a cohort of 10 healthy controls at a single time point. Repertoire overlap between patients, also known as the public repertoire, was minimal. High-abundance clones in individual patients were present at all time points suggesting that abundant clones can be reliably tracked in the peripheral circulation of an individual over time (3). No difference was observed in CDR3 length, VD indel length and DJ indel length between controls and transplant recipients at any time point. Repertoire diversity is a marker of a versatile immune system able to respond to multiple stimuli and is known to be restricted in the setting of autoimmune pathology such as lupus, Crohn's, and psoriasis (96). In this study, diversity was highest in controls and lower in transplants patients at baseline, decreasing further by POD 1, then again by POD 7. While it is difficult to infer the biological significance of this, one might hypothesize that this decreased diversity reflects the relative immune dysfunction previously described in patients with ESRD (97) that is further aggravated by either lymphodepletion or immunosuppression in transplant. Alachkar et al. used a prospective multi-center trial design to study peripheral and graft infiltrating T cell repertoire metrics in renal transplant patients with and without rejections in the first 3 months after transplant. TCR diversity was lower in graft samples than peripheral samples, as expected, but otherwise there was no unifying pattern of TCR diversity in individual patients over time, and no difference in diversity between rejectors and non-rejectors (2). However, this study went on to define recurrent highly abundant clones as the top 10 most frequent clones in each repertoire that occur at all timepoints in both blood and biopsy specimens. They show that these clones were expanded in the peripheral repertoire of transplant patients at the time of rejection but not time-point-matched non-rejectors. They were also able to show in one patient, that 6 of the top 10 most abundant clones infiltrating the graft at the time of TCMR could be identified in the peripheral repertoire of the same patient at multiple earlier time points. The hypothesis here is that highly abundant clones present in both the graft and the peripheral repertoire after transplant are more likely to be alloreactive and therefore interesting from a diagnostic perspective although this cannot be confirmed from these data.

The presumption that graft-infiltrating clones occur in peripheral blood underlies the use of TCR sequencing as a monitoring tool in renal allograft rejection. Weinberger et al. attempted to quantify this using nephrectomy samples from 10 patients of whom one was a transplant patient suffering from acute T cell mediated rejection. They showed poor clonal correlation between the B and T cell receptor profiles of tissue and peripheral samples, but that the correlation was greatest among the top 20 most abundant T cell clones (86). There was however no correlation in frequency between graft-infiltrating and peripheral T cell clones even among the top 20 most abundant clones.

While these studies that quantify general TCR repertoire metrics in renal transplantation suffer from heterogenous study designs, low patient numbers, and highly variable approaches to data analysis, they offer initial guidance to the feasibility and potential of this technology in a clinical setting and several key technical insights. First, TCR repertoire diversity, CDR3 length, and gene usage are all commonly used metrics in this setting. Second, highly abundant clones in the repertoire can be more reliably tracked over time for a given patient. Third, the graft infiltrating profile correlates best with the peripheral repertoire for highly abundant clones but that this correlation is not quantitative. Future studies will have to better define the nature of highly abundant clones and delineate their cognate targets to better understand their role as a clinical tool in renal transplant.

Similar work has also been conducted in B cell repertoire (BCR) sequencing. Pineda et al. performed longitudinal BCR sequencing in renal transplant patients, dividing them into three cohorts consisting of: patients who did not reject and did not sustain chronic graft damage, patients who did not reject but did sustain chronic graft damage, and patients who did reject and sustain chronic graft damage (77). This study showed that higher BCR diversity prior to transplant correlated with the development of rejection, while patients who ultimately rejected their graft had a greater decrease in BCR diversity and increased clonal expansion after transplant. While reduced diversity may be explained by intensification of immunosuppression in rejecting patients, the authors comment that this phenomenon was observed at time-points preceding rejection pointing to the possibility of a causal link. Perhaps the most interesting finding of this study for future

investigation is the association between specific IGHV gene use and rejection. For example, the *IGHV3-23* gene was used significantly more in patients who develop rejection across all time-points (77), in line with prior studies implicating this gene with transplant rejection (98). Moreover, the clonal antibodies arising from this specific IGHV gene, and others found to be clonally expanded in transplant, are known to react with bacterial pathogens and not allogeneic HLA (99). While the cause of this focused clonal expansion remains to be determined, it points to the preferential selection of specific clones over time by an unrelated powerful antigenic stimulus that could in turn contribute to transplant immune mediated pathology. It also raises the potential that certain common antigens are responsible for driving rejection. Further work in this area promises to yield not only potential biomarkers to risk-stratify patients for rejection, but also new insights into the biology of rejection.

6.3 Lymphocyte receptor sequencing in other solid organ transplants

TCR sequencing has also been evaluated in other solid organ transplant studies including liver, intestinal, and heart transplant.

Two studies examined the role of TCR sequencing in liver transplant. Yang et al. investigated general differences in TCR repertoire dynamics between liver recipients and healthy controls (88). TCR sequencing of 6 liver transplant patients pre-transplant and post-transplant day 1 and 7 revealed shared TCR clones between these time points. Few CDR3 sequences were shared amongst individuals, but more were shared amongst healthy people than amongst patients. The distribution of CDR3 and VD/DJ indel length was found to be similar in all controls and patient groups. Clones with a greater than 0.5% frequency were defined as highly expanded clones, but only 10-15% of the total TCR repertoire was found to consist of highly expanded clones, translating to an average of 7.2, 6.8, and 2.3 clones in the pre-transplant, POD1, and POD7 groups respectively. This highly expanded population showed little similarity in DNA or amino acid sequence but had shared V-J gene combinations. The degree of expansion of most expanded clones was highest on POD7 ($p=0.046$). Transplant patients were found to have lower diversity than controls, with significantly decreased diversity on POD7 compared to other groups (88). Savage et al. identified donor-reactive clones by first performing a pre-transplant MLC followed by post-transplant TCR sequencing to track donor-reactive clones in 8 liver allograft recipients (80). Amongst three tolerant and five non-tolerant recipients, all showed significant reductions in donor-reactive TCRβ sequences post-transplant. This is in contrast to data from conventional kidney transplant recipients that shows an increase in alloreactive clones post-transplant (100). Compared to donor-reactive clones, non-specific TCRβ sequences identified in the recipient repertoire by random third-party MLC did not show a distinct pattern of clonal expansion or contraction. Taken together, these data show that TCR sequencing can not only be used to identify general alterations in the T cell repertoire after liver transplant, but also that it can be applied to specifically track donor reactive clones in these patients.

Intestinal allografts are rich in lymphoid tissue, which over time engage in a bidirectional exchange with the recipient in which various degrees of bone marrow and peripheral blood chimerism occur or the allograft can become repopulated with recipient lymphocytes. Two detailed studies from the Sykes group leverage TCR sequencing to understand the biology of this unique case study in SOT. First, using MLC and TCR sequencing they define a graft-versus-host (GvH) and a host-versus-graft (HvG) alloreactive T cell profile (90). Instances of intestinal allograft rejection were correlated with intra-graft donor repertoires enriched for HvG-reactive clones and accelerated T cell turnover, whereas low levels of intra-graft recipient chimerism were associated with immunologic quiescence (90). Furthermore, this study challenges the paradigm that during rejection most graft infiltrating lymphocytes are not allograft specific by showing that up to 80% of CD4 and CD8 T cell clones present in allografts experiencing early cell mediated rejection. They then expand on this study to show that CD8 cytotoxic GvH clones migrating from the graft-lymphoid tissue home to the bone marrow where they create space in the stem cell niche for donor derived hematopoetic stem cells which in turn facilitate bone marrow and peripheral chimerism and graft tolerance (101).

BCR sequencing has been used to monitor the response to immunosuppression in a cohort of 12 heart transplant recipients of whom 6 participants had moderate-to-severe acute rejection (84). This study first set out to characterize immunoglobulin heavy chain (IGH) dynamics in the absence of rejection. IGH transcripts were measured immediately post-transplant then at 6 months after prolonged immunosuppression and categorized into low- and high- expression transcripts. Low-expression transcripts were represented by only one type of Ig molecule and likely expressed by naïve or inactive B-cells. High-expression transcripts were represented by more than one molecule and likely expressed by an activated B cell. While the total number of high-expression IGH transcripts detected did not change between timepoints, the contribution of high-expression IgA, IgE, IgG, mutated IgM sequences diminished relative to total transcripts at late time points and inversely correlated with trough levels of Tacrolimus and Annelovirus load, both of which are previously described markers of immunosuppression (102). Based on these findings the authors defined an activated B cell sequence (ABS) metric as the ratio of highly expressed IgA, IgD, IgE, IgG, and mutated IgM sequences to total sequences. ABS not only inversely tracked with degree of immunosuppression, but the median ABS level rose by 3-fold in the setting of rejection as diagnosed by endocardial biopsy and dd-cfDNA. Moreover, a gradual and significant increase in ABS level was observed in the 4 months leading up to the biopsy proven rejection event, highlighting the potential of this method for early detection of rejection. Last, this study looked at two specific case studies and shows that ABS was also increased in a heart transplant patient with recurrent opportunistic infections, and another who received Filgrastim in the setting of a subsequent bone-marrow transplant for AL amyloidosis (84).

6.4 Infectious complications of solid organ transplant

Opportunistic infections are not only a serious complication of immunosuppression in solid organ transplant but also predispose patients to immune alloreactivity. Common infectious pathogens

include Cytomegalovirus (CMV), Epstein-Barr virus (EBV), BK polyoma virus, Varicella zoster virus (VZV), Herpes simplex virus (HSV), and Pneumocystis jirovecii. Lymphocyte receptor sequencing has the potential of offering insight not only into the risk and dynamics of opportunistic infections in solid organ transplant, but also the mechanistic underpinnings of how viral infections predispose patients to immune rejection.

CMV is a common viral infection that is associated with allograft rejection, although the mechanistic underpinning of this phenomenon is poorly understood. TCR sequencing offers a unique lens through which to interrogate the hypothesis that cross-reactivity of T cells directed at alloantigen and CMV underlies this phenomenon. Using an observational cohort study design, Stranavova et al. showed a significant association between CMV immediate-early protein 1 (IE-1) specific T cell activity by IFNγ ELISPOT and acute renal allograft rejection and function (83). These data confirmed the well-established link between these two pathologies. They followed this with a study of 11 CMV-seropositive and HLA class I mismatched but low immunologic risk renal transplant patients. Using recipient PBMC cultures stimulated with donor cells or CMV antigens they identified several TCR beta sequences that cross-reacted to donor antigens and CMV. Biopsy specimens were available for TCR sequencing in 7 patients. CMV or donor-reactive clones identified from the previous mixed lymphocyte/antigen cultures were found in 6 out of 7 biopsy specimens and 3 of 7 biopsy specimens contained cross-reactive clones. Importantly, the highest number of cross-reactive clones was observed in patients with CMV reactivation with concomitant cellular rejection (83). While these numbers are low, and the absolute number of cross reactive clonotypes are small, these findings support a contributory role for cross-reactive clones in the pathogenesis of CMV associated rejection.

EBV is a common virus that seldom causes pathology in healthy immunocompetent adults. CD8 T cells provide important protection against EBV. GLCTLVAML (GLC) is a highly conserved immunogenic EBV peptide targeted by a restricted T cell repertoire that is highly conserved between individuals. Nguyen et al. leveraged TCR sequencing to quantify clonotypic diversity and abundance of T cells targeting GLC in healthy individuals, then tracked the dynamics of CD8+ GLC-specific clones over time in a cohort of lung transplant recipients before and after EBV exposure. They showed that, on average, the GLC-specific CD8+ TCRαβ repertoire consisted of 10 TCRαβ clonotypes per individual, and that this repertoire was stable before and after immunosuppression in lung-transplant patients without EBV reactivation. In the setting of clinical EBV reactivation, GLC CD8+ T cells expanded in the transplant recipients. There was marked overlap between repertoire at different time points, although the dominant clonotype changed with the onset of profound viremia (76). Another immunodominant EBV epitope, BRLF1, was shown to interact more with TCRα CDR3 sequences than those of TCRβ (103). Further studies are required to understand the immune repertoire changes in SOT associated with EBV and EBV-specific T cell dynamics during rejection.

Reactivation of BK polyoma virus, and BK nephropathy, in the setting of immunosuppression is another important infectious cause of graft loss which is currently best diagnosed with histology. Histological features of BK nephropathy can however mimic those of acute cellular rejection. This is further complicated by the possible co-existence of these conditions. Treatment of acute rejection involves increasing immunosuppression transiently which would worsen BK viremia and BK nephropathy as T cell mediated cellular immunity is the key to controlling BK infection. Indeed, TCR sequencing and flow cytometry with cell-sorting was used to show that BK viral clearance in transplant patients correlates with the repertoire diversity of BK virus specific T cells and markers of exhaustion in BK specific CD4+ T cells (104). This method to evaluate BK viral infection was developed into a diagnostic tool by Dziubianau et al. who used mixed lymphocyte or antigen culture to define an alloreactive and BK reactive T cell repertoire in 5 transplant patients, then evaluated the abundance of these clones in biopsy specimens and urine. They were able to detect BK directed T cell clones in biopsy and urine specimens of two patients with clear biopsy proven BK nephropathy. In one patient with proven BK nephropathy who did not respond to IS withdrawal, alloreactive clones were detected at higher frequency in biopsy and urine specimens suggesting acute cellular rejection to explain this phenomenon. Last, they showed that in chronic cytotoxic nephropathy neither type of clone was detected in either biopsy or urine specimens (105). Excitingly, this approach was used prospectively to influence treatment decision in a patient with a rising creatinine levels 6 weeks after living related donor kidney transplant in the setting of BK viremia and a biopsy consistent with acute TCMR negative for SV40 antigen. Donor and BK virus specific CDR3 sequences were identified by mixed cultures, and then quantified in the T cell repertoire from a graft biopsy. BK virus specific clones dominated the graft repertoire occupying 81.6% of clones. Based on this finding the clinical team tailored their treatment accordingly leading to resolution of the BK viremia and lasting improvement of graft function at 2-year follow-up (104). This work highlights the role of TCR sequencing as an adjunct diagnostic modality in complex differential diagnoses and shows the feasibility of detecting and tracking BK-specific clones in patient urine.

VZV, HSV, and Pneumocystis jirovecii are less studied in SOT through immune receptor sequencing methods. VZV complications are uncommon as most recipients are seropositive (106), but herpes zoster complications are more frequent and may include neuralgias and disseminated zoster. HSV causes more severe clinical manifestations and a slower response to therapy in SOT patients compared to immunocompetent individuals (107). Pneumocystis jirovecii risk is greatest in the first 6 months post-transplant and is higher for those who are seropositive for CMV and/or have low lymphocyte counts (108). Infection has been correlated with higher risk of graft failure and mortality regardless of rejection (109). Prophylactic measures are important in mitigating complications from these infections, giving potential for exploratory TCR/BCR sequencing studies to monitor viral-specific clones.

7 Discussion

In this article, we present a first, formal review of lymphocyte receptor sequencing in SOT to monitor alloreactivity, to describe how the technique is currently being used to monitor renal, liver, intestinal, and heart transplants, and to explore its potential in furthering our understanding of opportunistic infections and immune rejection.

From a methodologic standpoint, sequencing of the CDR3 region of the TCRβ locus was the preferred method for quantifying the T cell repertoire. In both renal and liver transplant recipients, broad alterations are observed in the T cell repertoire with decreased repertoire diversity relative to controls, minimal public repertoire overlap between patients, and reproducible overlap in private repertoire over time (2, 3, 88, 95). Furthermore, MLC and TCR sequencing can be applied to identify putative alloreactive clones and track them over time to evaluate both deletional and Treg induced tolerance among CKBMT and liver transplant patients (75, 79, 80). These studies however lack generalizability as they evaluate very specialized cases in solid organ transplant. The one available prospective study applying this technology to a standard renal transplant cohort is an excellent proof of feasibility and supports a potential role in monitoring alloreactivity but is inconclusive due to low enrollment and short-term follow-up (91). Studies on the effects of lymphodepletion on the T cell repertoire have been in consensus on an increase in donor-reactive CD4+ frequency; one study that investigated repertoire changes in rATG and Basiliximab induced patients found similar increases in alloreactive CD4+ but not CD8+ T cell frequency, supporting an earlier study that found patients receiving ATG showed post-depletional CD4+ CD25+ Treg and CD4+ effector memory phenotype (57, 83). This emphasizes the importance of CD4+ T cells in the alloimmune response and the need to focus monitoring efforts on them. Beyond alloreactivity, several case reports detail the utility of TCR sequencing in studying infectious complications of SOT. Generally, these show that CMV-reactive clones are associated with rejection events (83), and that EBV and BK polyoma virus directed clones can be used to distinguish between alloreactivity and viral injury as well as track viremia (104, 105, 110).

BCR sequencing was less commonly studied and only applied to describe trends in the repertoire before and after transplant. These studies showed an association between specific IGHV gene sequences and class-switched or highly mutated IgM sequences and rejection (77, 84). Somatic hypermutation, the accumulation of point mutations in the Ig variable region, was found to be higher in the graft than in blood and correlated with B cell expansion (62). This presents a further complexity in understanding AMR through BCR sequencing, as detected BCR sequences may have undergone mutation by the time the B cell has infiltrated the graft tissue. Thus, longitudinal tracking of B cell clones may be hindered by somatic hypermutation. No studies were found to have applied BCR sequencing to specifically quantify alloreactivity. However, this could be due to the presence of DSA testing which is an established method already used to detect B cell alloreactivity. This may also explain why there are fewer BCR than TCR studies in transplant overall as DSA testing may be a more efficient method to attain a similar goal. However, BCR sequencing could still hold value in providing earlier information on antigen specificities, which will be discussed later.

Practicality and financial considerations cannot be understated when considering a clinical assay. A TCR/BCR sequencing kit from private biotech companies can cost upwards of several thousand dollars, and sequencing services can cost even more. Meanwhile, Enzyme Linked Immunosorbent Spot (ELISPOT) kits can be more cost-effective (Abcam). In terms of assay time required, ELISPOT can take up to several days for optimal cytokine secretion. Although the initial MLC to establish the alloreactive repertoire can take several days, subsequent receptor sequencing procedures for routine monitoring would only require 2 days. Using nanopore sequencing, this time can be further decreased. While the cost-effectiveness of TCR/BCR sequencing assays may be improved upon as the technology matures, it shows promise as an efficient yet precise monitoring technique for SOT.

An immediate question this research poses is whether tools are available to predict antigen specificity based on TCR or BCR sequences. Studies on antigen prediction are limited, but two studies provide a glimpse for its potential. Grouping of lymphocyte interactions by paratope hotspots (GLIPH) is an algorithm developed by Glanville et al. that defines TCR specificity groups based on a dataset of MHC tetramer-sorted cells with structural data (111). It is also able to define specificities shared between TCRs and individuals, allowing for analysis of T cell responses based on the number and size of specificity clusters. TCRMatch is a TCR specificity analysis tool based on known epitope specificities in the Immune Epitope Database (IEDB) (112). It takes TCRβ CDR3 sequences as input and gives a specificity score for those with a match in the database. These tools could add to future work in immune repertoire sequencing in transplant. However, current databases are developed using well-studied antigens such as common viral and bacterial motifs. Given the complexity conferred by HLA epitopes, predicting how individual repertoires recognize them will require further studies.

Despite the scope and depth of this review, several limitations remain regarding translation to clinical diagnostic practice. First, the conclusions we can draw are limited by the quality of the evidence. While we have performed a comprehensive review of the literature, the studies on this topic are small observational cohort studies and case reports. These studies by their very nature are hypothesis generating. Second, prior to the advent of TCR sequencing, ELISPOT has been used to quantitate the allo-specific memory T cell response. While these data are beyond the scope of this paper, ELISPOT has shown promise in some clinical trials (110, 113, 114), and is another tool with clinical potential for alloimmune risk-stratification and monitoring. Third, the information we can garner from bulk TCR sequencing is limited in two respects. Even in the setting of MLR followed by TCRβ CDR3 sequencing, the antigen specificity of the putative alloreactive clones cannot be determined. Furthermore, once a putative alloreactive clone has been identified, the T cell subtype and phenotype of the clone cannot be ascertained with this method. Single-cell-level cell-surface markers and gene expression data have the power to achieve this. While beyond the scope of this review, early data leveraging this technology in transplant has been reported (101, 115), and provides a promising new direction for the field. And fourth, perhaps one of the most critical points, is that differences in immune activity between the graft and in circulation cannot be overlooked. BCR repertoire overlap has been shown to be small in some instances (64) and number of alloreactive cells and Vβ gene usage can differ between the two sites (68). Thus, sampling site could be a major source of variability in an immune repertoire sequencing assay.

Taken together, the findings outlined above point to the promise of lymphocyte receptor sequencing in detecting and monitoring the early phases of allorecognition and rejection in a clinically relevant setting. While the data is promising, larger prospective studies in a more generalizable SOT population are needed.

Author contributions

KRS and PAK conceived the study idea and PAK obtained research funding. PW developed a search protocol and conducted the review. PW and DPC extracted the data. KRS and PAK supervised the study progress and provided regular feedback. PW and DPC wrote the draft of the manuscript. RS-P and CP were contributing members of the TCR research planning team. All authors contributed to the article and approved the submitted version.

Funding

This study was funded by Genome BC (Genome Canada 273AMR) and the Canadian Institutes of Health Research (CIHR GP1-155871).

Conflict of interest

The authors declare that the research was conducted in the absence of any commercial or financial relationships that could be construed as a potential conflict of interest.

Publisher's note

References

1. Oellerich M, Sherwood K, Keown P, Schütz E, Beck J, Stegbauer J, et al. Liquid biopsies: Donor-derived cell-free DNA for the detection of kidney allograft injury. *Nat Rev Nephrol* (2021) 17:591–603. doi: 10.1038/s41581-021-00428-0

2. Alachkar H, Mutonga M, Kato T, Kalluri S, Kakuta Y, Uemura M, et al. Quantitative characterization of T-cell repertoire and biomarkers in kidney transplant rejection. *BMC Nephrol* (2016) 17:181. doi: 10.1186/s12882-016-0395-3

3. Lai L, Wang L, Chen H, Zhang J, Yan Q, Ou M, et al. T Cell repertoire following kidney transplantation revealed by high-throughput sequencing. *Transpl Immunol* (2016) 39:34–45. doi: 10.1016/j.trim.2016.08.006

4. DeWolf S, Sykes M. Alloimmune T cells in transplantation. *J Clin Invest* (2017) 127:2473–81. doi: 10.1172/JCI90595

5. Baker RJ, Hernandez-Fuentes MP, Brookes PA, Chaudhry AN, Cook HT, Lechler RI. Loss of direct and maintenance of indirect alloresponses in renal allograft recipients: Implications for the pathogenesis of chronic allograft nephropathy. *J Immunol* (2001) 167:7199–206. doi: 10.4049/jimmunol.167.12.7199

6. Ali JM, Negus MC, Conlon TM, Harper IG, Qureshi MS, Motallebzadeh R, et al. Diversity of the CD4 T cell alloresponse: The short and the long of it. *Cell Rep* (2016) 14:1232–45. doi: 10.1016/j.celrep.2015.12.099

7. Siu JHY, Surendrakumar V, Richards JA, Pettigrew GJ. T Cell allorecognition pathways in solid organ transplantation. *Front Immunol* (2018) 9:2548. doi: 10.3389/fimmu.2018.02548

8. Abbas AK, Lichtman AH, Pillai S. Chapter 5: Antibodies and antigens. In: *Cellular and molecular immunology* (2021). Amsterdam, The Netherlands: Elsevier Health Sciences.

9. Ali JM, Bolton EM, Bradley JA, Pettigrew GJ. Allorecognition pathways in transplant rejection and tolerance. *Transplantation* (2013) 96:681–8. doi: 10.1097/TP.0b013e31829853ce

10. Russo V, Zhou D, Sartirana C, Rovere P, Villa A, Rossini S, et al. Acquisition of intact allogeneic human leukocyte antigen molecules by human dendritic cells. *Blood* (2000) 95:3473–7. doi: 10.1182/blood.V95.11.3473

11. Liu Q, Rojas-Canales DM, Divito SJ, Shufesky WJ, Stolz DB, Erdos G, et al. Donor dendritic cell–derived exosomes promote allograft-targeting immune response. *J Clin Invest* (2016) 126:2805–20. doi: 10.1172/JCI84577

12. Marino J, Babiker-Mohamed MH, Crosby-Bertorini P, Paster JT, LeGuern C, Germana S, et al. Donor exosomes rather than passenger leukocytes initiate alloreactive T cell responses after transplantation. *Sci Immunol* (2016) 1:aaf8759. doi: 10.1126/sciimmunol.aaf8759

13. Heidt S, Wood KJ. Biomarkers of operational tolerance in solid organ transplantation. *Expert Opin Med Diagn* (2012) 6:281–93. doi: 10.1517/17530059.2012.680019

14. Martínez-Llordella M, Lozano JJ, Puig-Pey I, Orlando G, Tisone G, Lerut J, et al. Using transcriptional profiling to develop a diagnostic test of operational tolerance in liver transplant recipients. *J Clin Invest* (2008), 118:2845–2857. doi: 10.1172/JCI35342

15. Roussey-Kesler G, Giral M, Moreau A, Subra J-F, Legendre C, Noël C, et al. Clinical operational tolerance after kidney transplantation. *Am J Transplant* (2006) 6:736–46. doi: 10.1111/j.1600-6143.2006.01280.x

16. Dubey C, Croft M, Swain SL. Naive and effector CD4 T cells differ in their requirements for T cell receptor versus costimulatory signals. *J Immunol Baltim Md 1950* (1996) 157:3280–9. doi: 10.4049/jimmunol.157.8.3280

17. Sette A, Alexander J, Ruppert J, Snoke K, Franco A, Ishioka G, et al. Antigen Analogs/MHC complexes as specific T cell receptor antagonists. *Annu Rev Immunol* (1994) 12:413–31. doi: 10.1146/annurev.iy.12.040194.002213

18. Azuma M, Ito D, Yagita H, Okumura K, Phillips JH, Lanier LL, et al. B70 antigen is a second ligand for CTLA-4 and CD28. *Nature* (1993) 366:76–9. doi: 10.1038/366076a0

19. Vincenti F, Rostaing L, Grinyo J, Rice K, Steinberg S, Gaite L, et al. Belatacept and long-term outcomes in kidney transplantation. *N Engl J Med* (2016) 374:333–43. doi: 10.1056/NEJMoa1506027

20. Henn V, Slupsky JR, Gräfe M, Anagnostopoulos I, Förster R, Müller-Berghaus G, et al. CD40 ligand on activated platelets triggers an inflammatory reaction of endothelial cells. *Nature* (1998) 391:591–4. doi: 10.1038/35393

21. Caux C, Massacrier C, Vanbervliet B, Dubois B, Van Kooten C, Durand I, et al. Activation of human dendritic cells through CD40 cross-linking. *J Exp Med* (1994) 180:1263–72. doi: 10.1084/jem.180.4.1263

22. Kirk AD, Burkly LC, Batty DS, Baumgartner RE, Berning JD, Buchanan K, et al. Treatment with humanized monoclonal antibody against CD154 prevents acute renal allograft rejection in nonhuman primates. *Nat Med* (1999) 5:686–93. doi: 10.1038/9536

23. Kawai T, Andrews D, Colvin RB, Sachs DH, Cosimi AB. Thromboembolic complications after treatment with monoclonal antibody against CD40 ligand. *Nat Med* (2000) 6:114–4. doi: 10.1038/72162

24. Kitchens WH, Dong Y, Mathews DV, Breeden CP, Strobert E, Fuentes ME, et al. Interruption of OX40L signaling prevents costimulation blockade–resistant allograft rejection. *JCI Insight* (2017) 2:e90317. doi: 10.1172/jci.insight.90317

25. Lo DJ, Anderson DJ, Song M, Leopardi F, Farris AB, Strobert E, et al. A pilot trial targeting the ICOS–ICOS-L pathway in nonhuman primate kidney transplantation. *Am J Transplant* (2015) 15:984–92. doi: 10.1111/ajt.13100

26. Shuford WW, Klussman K, Tritchler DD, Loo DT, Chalupny J, Siadak AW, et al. 4-1BB costimulatory signals preferentially induce CD8+ T cell proliferation and lead to the amplification *In vivo* of cytotoxic T cell responses. *J Exp Med* (1997) 186:47–55. doi: 10.1084/jem.186.1.47

27. Wang J, Smolyar A, Tan K, Liu J, Kim M, Sun ZJ, et al. Structure of a heterophilic adhesion complex between the human CD2 and CD58 (LFA-3) counterreceptors. *Cell* (1999) 97:791–803. doi: 10.1016/S0092-8674(00)80790-4

28. Gückel B, Berek C, Lutz M, Altevogt P, Schirrmacher V, Kyewski BA. Anti-CD2 antibodies induce T cell unresponsiveness *in vivo*. *J Exp Med* (1991) 174:957–67. doi: 10.1084/jem.174.5.957

29. Teh SJ, Killeen N, Tarakhovsky A, Littman DR, Teh HS. CD2 regulates the positive selection and function of antigen-specific CD4- CD8+ T cells. *Blood* (1997) 89:1308–18. doi: 10.1182/blood.V89.4.1308

30. Sasada T, Yang H, Reinherz EL. CD2 facilitates differentiation of CD4 Th cells without affecting Th1/Th2 polarization. *J Immunol* (2002) 168:1113–22. doi: 10.4049/jimmunol.168.3.1113

31. Binder C, Cvetkovski F, Sellberg F, Berg S, Paternina Visbal H, Sachs DH, et al. CD2 immunobiology. *Front Immunol* (2020) 11:1090. doi: 10.3389/fimmu.2020.01090

32. Rostaing L, Charpentier B, Glyda M, Rigotti P, Hettich F, Franks B, et al. Alefacept combined with tacrolimus, mycophenolate mofetil and steroids in *De novo* kidney transplantation: A randomized controlled trial. *Am J Transplant* (2013) 13:1724–33. doi: 10.1111/ajt.12303

33. Pruett TL, McGory RW, Wright FH, Pescovitz MD, Yang H, McClain JB. Safety profile, pharmacokinetics, and pharmacodynamics of siplizumab, a humanized anti-CD2 monoclonal antibody, in renal allograft recipients. *Transplant Proc* (2009) 41:3655–61. doi: 10.1016/j.transproceed.2009.06.226

34. Kawai T, Sachs DH, Sprangers B, Spitzer TR, Saidman SL, Zorn E, et al. Long-term results in recipients of combined HLA-mismatched kidney and bone marrow

transplantation without maintenance immunosuppression. *Am J Transplant* (2014) 14:1599–611. doi: 10.1111/ajt.12731

35. Kawai T, Cosimi AB, Spitzer TR, Tolkoff-Rubin N, Suthanthiran M, Saidman SL, et al. HLA-mismatched renal transplantation without maintenance immunosuppression. *N Engl J Med* (2008) 358:353–61. doi: 10.1056/NEJMoa071074

36. Maruhashi T, Okazaki I, Sugiura D, Takahashi S, Maeda TK, Shimizu K, et al. LAG-3 inhibits the activation of CD4+ T cells that recognize stable pMHCII through its conformation-dependent recognition of pMHCII. *Nat Immunol* (2018) 19:1415–26. doi: 10.1038/s41590-018-0217-9

37. Pardoll DM. The blockade of immune checkpoints in cancer immunotherapy. *Nat Rev Cancer* (2012) 12:252–64. doi: 10.1038/nrc3239

38. Halloran PF. Immunosuppressive drugs for kidney transplantation. *N Engl J Med* (2004) 351:2715–29. doi: 10.1056/NEJMra033540

39. Starzl TE, Weil R, Iwatsuki S, Klintmalm G, Schröter GP, Koep LJ, et al. The use of cyclosporin a and prednisone in cadaver kidney transplantation. *Surg Gynecol Obstet* (1980) 151:17–26.

40. Starzl TE, Todo S, Fung J, Demetris AJ, Venkataramman R, Jain A. FK 506 for liver, kidney, and pancreas transplantation. *Lancet Lond Engl* (1989) 2:1000–4. doi: 10.1016/s0140-6736(89)91014-3

41. Zeiser R, Leveson-Gower DB, Zambricki EA, Kambham N, Beilhack A, Loh J, et al. Differential impact of mammalian target of rapamycin inhibition on CD4+CD25+Foxp3+ regulatory T cells compared with conventional CD4+ T cells. *Blood* (2008) 111:453–62. doi: 10.1182/blood-2007-06-094482

42. Brennan DC, Daller JA, Lake KD, Cibrik D, Del Castillo D. Rabbit antithymocyte globulin versus basiliximab in renal transplantation. *N Engl J Med* (2006) 355:1967–77. doi: 10.1056/NEJMoa060068

43. O'Shea JJ, Paul WE. Mechanisms underlying lineage commitment and plasticity of helper CD4 $^{+}$ T cells. *Science* (2010) 327:1098–102. doi: 10.1126/science.1178334

44. Charles A Janeway J, Travers P, Walport M, Shlomchik MJ. Survival and maturation of lymphocytes in peripheral lymphoid tissues, in: *Immunobiol immune syst health dis* (2001). Available at: https://www.ncbi.nlm.nih.gov/books/NBK27150/ (Accessed January 23, 2023).

45. Wan Z, Liu W. The growth of b cell receptor microcluster is a universal response of b cells encountering antigens with different motion features. *Protein Cell* (2012) 3:545–58. doi: 10.1007/s13238-012-2054-1

46. Kuokkanen E, Šuštar V, Mattila PK. Molecular control of b cell activation and immunological synapse formation: B cell immunological synapse. *Traffic* (2015) 16:311–26. doi: 10.1111/tra.12257

47. Roberts AD, Davenport TM, Dickey AM, Ahn R, Sochacki KA, Taraska JW. Structurally distinct endocytic pathways for b cell receptors in b lymphocytes. *Mol Biol Cell* (2020) 31:2826–40. doi: 10.1091/mbc.E20-08-0532

48. Crotty S. A brief history of T cell help to b cells. *Nat Rev Immunol* (2015) 15:185–9. doi: 10.1038/nri3803

49. Vinuesa CG, Linterman MA, Goodnow CC, Randall KL. T Cells and follicular dendritic cells in germinal center b-cell formation and selection: Roles of T cells and FDCs in germinal centers. *Immunol Rev* (2010) 237:72–89. doi: 10.1111/j.1600-065X.2010.00937.x

50. Vo AA, Peng A, Toyoda M, Kahwaji J, Cao K, Lai C-H, et al. Use of intravenous immune globulin and rituximab for desensitization of highly HLA-sensitized patients awaiting kidney transplantation. *Transplantation* (2010) 89:1095–102. doi: 10.1097/TP.0b013e3181d21e7f

51. Clatworthy MR. Targeting b cells and antibody in transplantation. *Am J Transplant* (2011) 11:1359–67. doi: 10.1111/j.1600-6143.2011.03554.x

52. Schatz DG, Oettinger MA, Schlissel MS. V(D)J recombination: Molecular biology and regulation. *Annu Rev Immunol* (1992) 10:359–83. doi: 10.1146/annurev.iy.10.040192.002043

53. de Greef PC, Oakes T, Gerritsen B, Ismail M, Heather JM, Hermsen R, et al. The naive T-cell receptor repertoire has an extremely broad distribution of clone sizes. *eLife* (2020) 9:e49900. doi: 10.7554/eLife.49900

54. Alt FW, Oltz EM, Young F, Gorman J, Taccioli G, Chen J. VDJ recombination. *Immunol Today* (1992) 13:306–14. doi: 10.1016/0167-5699(92)90043-7

55. Gkazi AS, Margetts BK, Attenborough T, Mhaldien L, Standing JF, Oakes T, et al. Clinical T cell receptor repertoire deep sequencing and analysis: An application to monitor immune reconstitution following cord blood transplantation. *Front Immunol* (2018) 9:2547. doi: 10.3389/fimmu.2018.02547

56. Arrieta-Bolaños E, Crivello P, Metzing M, Meurer T, Ahci M, Rytlewski J, et al. Alloreactive T cell receptor diversity against structurally similar or dissimilar HLA-DP antigens assessed by deep sequencing. *Front Immunol* (2018) 9:280. doi: 10.3389/fimmu.2018.00280

57. Aschauer C, Jelencsics K, Hu K, Gregorich M, Reindl-Schwaighofer R, Wenda S, et al. Effects of reduced-dose anti-human T-lymphocyte globulin on overall and donor-specific T-cell repertoire reconstitution in sensitized kidney transplant recipients. *Front Immunol* (2022) 13:843452. doi: 10.3389/fimmu.2022.843452

58. Beausang JF, Fan HC, Sit R, Hutchins MU, Jirage K, Curtis R, et al. B cell repertoires in HLA-sensitized kidney transplant candidates undergoing desensitization therapy. *J Transl Med* (2017) 15:9. doi: 10.1186/s12967-017-1118-7

59. Bellan C, Amato T, Carmellini M, Onorati M, D'Amuri A, Leoncini L, et al. Analysis of the IgVH genes in T cell-mediated and antibody-mediated rejection of the kidney graft. *J Clin Pathol* (2011) 64:47–53. doi: 10.1136/jcp.2010.082024

60. Cappuccilli M, Donati G, Comai G, Baraldi O, Conte D, Capelli I, et al. Identification of expanded T-cell clones by spectratyping in nonfunctioning kidney transplants. *J Inflammation Res* (2017) 10:41–7. doi: 10.2147/JIR.S124944

61. Emerson RO, Mathew JM, Konieczna IM, Robins HS, Leventhal JR. Defining the alloreactive T cell repertoire using high-throughput sequencing of mixed lymphocyte reaction culture. *PloS One* (2014) 9:e111943. doi: 10.1371/journal.pone.0111943

62. Ferdman J, Porcheray F, Gao B, Moore C, DeVito J, Dougherty S, et al. Expansion and somatic hypermutation of b-cell clones in rejected human kidney grafts. *Transplantation* (2014) 98:766–72. doi: 10.1097/TP.0000000000000124

63. Gao B, Gu Y, Rong C, Moore C, Porcheray F, Wong W, et al. Dynamics of b cell recovery in Kidney/Bone marrow transplant recipients. *Transplantation* (2017) 101:2722–30. doi: 10.1097/TP.0000000000001789

64. Habal MV, Miller AMI, Rao S, Lin S, Obradovic A, Khosravi-Maharlooei M, et al. T Cell repertoire analysis suggests a prominent bystander response in human cardiac allograft vasculopathy. *Am J Transplant* (2021) 21:1465–76. doi: 10.1111/ajt.16333

65. Han F, Fan H, Ren L, Wang H, Wang C, Ma X, et al. Profiling the pattern of human TRB/IGH-CDR3 repertoire in liver transplantation patients *via* high-throughput sequencing analysis. *Scand J Immunol* (2020) 92:e12912. doi: 10.1111/sji.12912

66. Huang C, Li X, Wu J, Zhang W, Sun S, Lin L, et al. The landscape and diagnostic potential of T and b cell repertoire in immunoglobulin a nephropathy. *J Autoimmun* (2019) 97:100–7. doi: 10.1016/j.jaut.2018.10.018

67. Jones SL, Moore LW, Li XC, Mobley CM, Fields PA, Graviss EA, et al. Pre-transplant T-cell clonality: An observational study of a biomarker for prediction of sepsis in liver transplant recipients. *Ann Surg* (2021) 274:411–8. doi: 10.1097/SLA.0000000000004998

68. Kim JY, Lei Z, Maienschein-Cline M, Chlipala GE, Balamurugan A, McDiarmid SV, et al. Longitudinal analysis of the T-cell receptor repertoire in graft-infiltrating lymphocytes following hand transplantation. *Transplantation* (2021) 105:1502–9. doi: 10.1097/TP.0000000000003535

69. Lai L, Zhou X, Chen H, Luo Y, Sui W, Zhang J, et al. Composition and diversity analysis of the b–cell receptor immunoglobulin heavy chain complementarity –determining region 3 repertoire in patients with acute rejection after kidney transplantation using high–throughput sequencing. *Exp Ther Med* (2019) 17:2206-2220. doi: 10.3892/etm.2019.7183

70. Leventhal JR, Elliott MJ, Yolcu ES, Bozulic LD, Tollerud DJ, Mathew JM, et al. Immune Reconstitution/Immunocompetence in recipients of kidney plus hematopoietic Stem/Facilitating cell transplants. *Transplantation* (2015) 99:288–98. doi: 10.1097/TP.0000000000000605

71. Link CS, Eugster A, Heidenreich F, Rücker-Braun E, Schmiedgen M, Oelschlägel U, et al. Abundant cytomegalovirus (CMV) reactive clonotypes in the CD8+ T cell receptor alpha repertoire following allogeneic transplantation. *Clin Exp Immunol* (2016) 184:389–402. doi: 10.1111/cei.12770

72. Luque S, Lúcia M, Crespo E, Jarque M, Grinyó JM, Bestard O. A multicolour HLA-specific b-cell FluoroSpot assay to functionally track circulating HLA-specific memory b cells. *J Immunol Methods* (2018) 462:23–33. doi: 10.1016/j.jim.2018.07.011

73. Mathew JM, Voss JH, McEwen ST, Konieczna I, Chakraborty A, Huang X, et al. Generation and characterization of alloantigen-specific regulatory T cells for clinical transplant tolerance. *Sci Rep* (2018) 8:1136. doi: 10.1038/s41598-018-19621-6

74. Moore C, Gao B, Roskin KM, Vasilescu E-RM, Addonizio L, Givertz MM, et al. B cell clonal expansion within immune infiltrates in human cardiac allograft vasculopathy. *Am J Transplant* (2020) 20:1431–8. doi: 10.1111/ajt.15737

75. Morris H, DeWolf S, Robins H, Sprangers B, LoCascio SA, Shonts BA, et al. Tracking donor-reactive T cells: Evidence for clonal deletion in tolerant kidney transplant patients. *Sci Transl Med* (2015) 7:272ra210. doi: 10.1126/scitranslmed.3010760

76. Nguyen TH, Bird NL, Grant EJ, Miles JJ, Thomas PG, Kotsimbos TC, et al. Maintenance of the EBV-specific CD8 $^{+}$ TCRαβ repertoire in immunosuppressed lung transplant recipients. *Immunol Cell Biol* (2017) 95:77–86. doi: 10.1038/icb.2016.71

77. Pineda S, Sigdel TK, Liberto JM, Vincenti F, Sirota M, Sarwal MM. Characterizing pre-transplant and post-transplant kidney rejection risk by b cell immune repertoire sequencing. *Nat Commun* (2019) 10:1906. doi: 10.1038/s41467-019-09930-3

78. Pollastro S, de Bourayne M, Balzaretti G, Jongejan A, van Schaik BDC, Niewold ITG, et al. Characterization and monitoring of antigen-responsive T cell clones using T cell receptor gene expression analysis. *Front Immunol* (2021) 11:609624. doi: 10.3389/fimmu.2020.609624

79. Savage TM, Shonts BA, Obradovic A, Dewolf S, Lau S, Zuber J, et al. Early expansion of donor-specific tregs in tolerant kidney transplant recipients. *JCI Insight* (2018) 3:e124086. doi: 10.1172/jci.insight.124086

80. Savage TM, Shonts BA, Lau S, Obradovic A, Robins H, Shaked A, et al. Deletion of donor-reactive T cell clones after human liver transplant. *Am J Transplant* (2020) 20:538–45. doi: 10.1111/ajt.15592

81. Schober K, Voit F, Grassmann S, Müller TR, Eggert J, Jarosch S, et al. Reverse TCR repertoire evolution toward dominant low-affinity clones during chronic CMV infection. *Nat Immunol* (2020) 21:434–41. doi: 10.1038/s41590-020-0628-2

82. Smith C, Brennan RM, Tey S-K, Smyth MJ, Burrows SR, Miles JJ, et al. Coinfection with human cytomegalovirus genetic variants in transplant recipients and its impact on antiviral T cell immune reconstitution. *J Virol* (2016) 90:7497–507. doi: 10.1128/JVI.00297-16

83. Stranavova L, Pelak O, Svaton M, Hruba P, Fronkova E, Slavcev A, et al. Heterologous cytomegalovirus and allo-reactivity by shared T cell receptor repertoire in kidney transplantation. *Front Immunol* (2019) 10:2549. doi: 10.3389/fimmu.2019.02549

84. Vollmers C, De Vlaminck I, Valantine HA, Penland L, Luikart H, Strehl C, et al. Monitoring pharmacologically induced immunosuppression by immune repertoire sequencing to detect acute allograft rejection in heart transplant patients: A proof-of-Concept diagnostic accuracy study. *PloS Med* (2015) 12:e1001890. doi: 10.1371/journal.pmed.1001890

85. Wang L, Dai Y, Liu S, Lai L, Yan Q, Chen H, et al. Assessment of variation in b-cell receptor heavy chain repertoire in patients with end-stage renal disease by high-throughput sequencing. *Ren Fail* (2019) 41:1–13. doi: 10.1080/0886022X.2018.1487862

86. Weinberger J, Jimenez-Heredia R, Schaller S, Suessner S, Sunzenauer J, Reindl-Schwaighofer R, et al. Immune repertoire profiling reveals that clonally expanded b and T cells infiltrating diseased human kidneys can also be tracked in blood. *PloS One* (2015) 10: e0143125. doi: 10.1371/journal.pone.0143125

87. Yan Q, Wang L, Lai L, Liu S, Chen H, Zhang J, et al. Next generation sequencing reveals novel alterations in b-cell heavy chain receptor repertoires associated with acute-on-chronic liver failure. *Int J Mol Med* (2018) 43:243-255. doi: 10.3892/ijmm.2018.3946

88. Yang G, Ou M, Chen H, Guo C, Chen J, Lin H, et al. Characteristic analysis of TCR β-chain CDR3 repertoire for pre- and post-liver transplantation. *Oncotarget* (2018) 9:34506–19. doi: 10.18632/oncotarget.26138

89. Zhang W, Morris AB, Peek EV, Karadkhele G, Robertson JM, Kissick HT, et al. CMV status drives distinct trajectories of CD4+ T cell differentiation. *Front Immunol* (2021) 12:620386. doi: 10.3389/fimmu.2021.620386

90. Zuber J, Shonts B, Lau S-P, Obradovic A, Fu J, Yang S, et al. Bidirectional intragraft alloreactivity drives the repopulation of human intestinal allografts and correlates with clinical outcome. *Sci Immunol* (2016) 1:eaah3732. doi: 10.1126/sciimmunol.aah3732

91. Aschauer C, Jelencsics K, Hu K, Heinzel A, Gregorich MG, Vetter J, et al. Prospective tracking of donor-reactive T-cell clones in the circulation and rejecting human kidney allografts. *Front Immunol* (2021) 12:750005. doi: 10.3389/fimmu.2021.750005

92. Padovan E, Casorati G, Dellabona P, Meyer S, Brockhaus M, Lanzavecchia A. Expression of two T cell receptor α chains: Dual receptor T cells. *Science* (1993) 262:422–4. doi: 10.1126/science.8211163

93. Yaari G, Kleinstein SH. Practical guidelines for b-cell receptor repertoire sequencing analysis. *Genome Med* (2015) 7:121. doi: 10.1186/s13073-015-0243-2

94. Ruggiero E, Nicolay JP, Fronza R, Arens A, Paruzynski A, Nowrouzi A, et al. High-resolution analysis of the human T-cell receptor repertoire. *Nat Commun* (2015) 6:8081. doi: 10.1038/ncomms9081

95. Aschauer C, Jelencsics K, Hu K, Heinzel A, Vetter J, Fraunhofer T, et al. Next generation sequencing based assessment of the alloreactive T cell receptor repertoire in kidney transplant patients during rejection: A prospective cohort study. *BMC Nephrol* (2019) 20:346. doi: 10.1186/s12882-019-1541-5

96. Minervina A, Pogorelyy M, Mamedov I. T-Cell receptor and b-cell receptor repertoire profiling in adaptive immunity. *Transpl Int* (2019) 32:1111–23. doi: 10.1111/tri.13475

97. Betjes MGH. Immune cell dysfunction and inflammation in end-stage renal disease. *Nat Rev Nephrol* (2013) 9:255–65. doi: 10.1038/nrneph.2013.44

98. Cheng J, Torkamani A, Grover RK, Jones TM, Ruiz DI, Schork NJ, et al. Ectopic b-cell clusters that infiltrate transplanted human kidneys are clonal. *Proc Natl Acad Sci* (2011) 108:5560–5. doi: 10.1073/pnas.1101148108

99. Grover RK, Cheng J, Peng Y, Jones TM, Ruiz DI, Ulevitch RJ, et al. The costimulatory immunogen LPS induces the b-cell clones that infiltrate transplanted human kidneys. *Proc Natl Acad Sci* (2012) 109:6036–41. doi: 10.1073/pnas.1202214109

100. Andreola G, Chittenden M, Shaffer J, Cosimi AB, Kawai T, Cotter P, et al. Mechanisms of donor-specific tolerance in recipients of haploidentical combined bone Marrow/Kidney transplantation. *Am J Transplant* (2011) 11:1236–47. doi: 10.1111/j.1600-6143.2011.03566.x

101. Fu J, Zuber J, Shonts B, Obradovic A, Wang Z, Frangaj K, et al. Lymphohematopoietic graft-versus-host responses promote mixed chimerism in patients receiving intestinal transplantation. *J Clin Invest* (2021) 131:e141698. doi: 10.1172/JCI141698

102. De Vlaminck I, Khush KK, Strehl C, Kohli B, Luikart H, Neff NF, et al. Temporal response of the human virome to immunosuppression and antiviral therapy. *Cell* (2013) 155:1178–87. doi: 10.1016/j.cell.2013.10.034

103. Gil A, Kamga L, Chirravuri-Venkata R, Aslan N, Clark F, Ghersi D, et al. Epstein-Barr Virus epitope–major histocompatibility complex interaction combined with convergent recombination drives selection of diverse T cell receptor α and β repertoires. *mBio* (2020) 11:e00250–20. doi: 10.1128/mBio.00250-20

104. Stervbo U, Nienen M, Weist BJD, Kuchenbecker L, Hecht J, Wehler P, et al. BKV clearance time correlates with exhaustion state and T-cell receptor repertoire shape of BKV-specific T-cells in renal transplant patients. *Front Immunol* (2019) 10:767. doi: 10.3389/fimmu.2019.00767

105. Dziubianau M, Hecht J, Kuchenbecker L, Sattler A, Stervbo U, Rödelsperger C, et al. TCR repertoire analysis by next generation sequencing allows complex differential diagnosis of T cell–related pathology. *Am J Transplant* (2013) 13:2842–54. doi: 10.1111/ajt.12431

106. Pergam SA, Limaye APThe AST Infectious Diseases Community of Practice. Varicella zoster virus in solid organ transplantation: Guidelines from the American society of transplantation infectious diseases community of practice. *Clin Transplant* (2019) 33:e13622. doi: 10.1111/ctr.13622

107. Lee DH, Zuckerman RAon behalf of the AST Infectious Diseases Community of Practice. Herpes simplex virus infections in solid organ transplantation: Guidelines from the American society of transplantation infectious diseases community of practice. *Clin Transplant* (2019) 33:e13526. doi: 10.1111/ctr.13526

108. Fishman JA, Gans HThe AST Infectious Diseases Community of Practice. Pneumocystis jiroveci in solid organ transplantation: Guidelines from the American society of transplantation infectious diseases community of practice. *Clin Transplant* (2019) 33:e13587. doi: 10.1111/ctr.13587

109. Kim JE, Han A, Lee H, Ha J, Kim YS, Han SS. Impact of pneumocystis jirovecii pneumonia on kidney transplant outcome. *BMC Nephrol* (2019) 20:212. doi: 10.1186/s12882-019-1407-x

110. Hricik DE, Augustine J, Nickerson P, Formica RN, Poggio ED, Rush D, et al. Interferon gamma ELISPOT testing as a risk-stratifying biomarker for kidney transplant injury: Results from the CTOT-01 multicenter study. *Am J Transplant* (2015) 15:3166–73. doi: 10.1111/ajt.13401

111. Glanville J, Huang H, Nau A, Hatton O, Wagar LE, Rubelt F, et al. Identifying specificity groups in the T cell receptor repertoire. *Nature* (2017) 547:94–8. doi: 10.1038/nature22976

112. Chronister WD, Crinklaw A, Mahajan S, Vita R, Koşaloğlu-Yalçın Z, Yan Z, et al. TCRMatch: Predicting T-cell receptor specificity based on sequence similarity to previously characterized receptors. *Front Immunol* (2021) 12:640725. doi: 10.3389/fimmu.2021.640725

113. Bestard O, Meneghini M, Crespo E, Bemelman F, Koch M, Volk HD, et al. Preformed T cell alloimmunity and HLA eplet mismatch to guide immunosuppression minimization with tacrolimus monotherapy in kidney transplantation: Results of the CELLIMIN trial. *Am J Transplant* (2021) 21:2833–45. doi: 10.1111/ajt.16563

114. Heeger PS, Greenspan NS, Kuhlenschmidt S, Dejelo C, Hricik DE, Schulak JA, et al. Pretransplant frequency of donor-specific, IFN-gamma-producing lymphocytes is a manifestation of immunologic memory and correlates with the risk of posttransplant rejection episodes. *J Immunol Baltim Md 1950* (1999) 163:2267–75. doi: 10.4049/jimmunol.163.4.2267

115. Malone AF, Wu H, Fronick C, Fulton R, Gaut JP, Humphreys BD. Harnessing expressed single nucleotide variation and single cell RNA sequencing to define immune cell chimerism in the rejecting kidney transplant. *J Am Soc Nephrol* (2020) 31:1977–86. doi: 10.1681/ASN.2020030326

frontiers | Frontiers in Immunology

TYPE Original Research
PUBLISHED 27 April 2023
DOI 10.3389/fimmu.2023.1183949

OPEN ACCESS

EDITED BY
Guido Moll,
Charité University Medicine
Berlin, Germany

REVIEWED BY
Manuel Muro,
Hospital Universitario Virgen de
la Arrixaca, Spain
Olga Millán,
Carlos III Health Institute (ISCIII), Spain

*CORRESPONDENCE
Pascal Pedini
pascal.pedini@efs.sante.fr

RECEIVED 10 March 2023
ACCEPTED 04 April 2023
PUBLISHED 27 April 2023

CITATION
Pedini P, Coiffard B, Cherouat N, Casas S, Fina F, Boutonnet A, Baudey JB, Aho P, Basire A, Simon S, Frassati C, Chiaroni J, Reynaud-Gaubert M and Picard C (2023) Clinical relevance of cell-free DNA quantification and qualification during the first month after lung transplantation. *Front. Immunol.* 14:1183949. doi: 10.3389/fimmu.2023.1183949

Clinical relevance of cell-free DNA quantification and qualification during the first month after lung transplantation

Pascal Pedini[1,2]*, Benjamin Coiffard[3], Nicem Cherouat[1], Sylvia Casas[4], Frédéric Fina[5], Audrey Boutonnet[5], Jean Baptiste Baudey[1], Printil Aho[1], Agnes Basire[1], Sophie Simon[1], Coralie Frassati[1], Jacques Chiaroni[1,2], Martine Reynaud-Gaubert[3] and Christophe Picard[1,2]

[1]Immunogenetics Laboratory, Etablissement Français du Sang, Marseille, France, [2]ADES UMR, Aix Marseille Univ, Marseille, France, [3]Aix-Marseille University, Lung Transplant Department, APHM, Marseille, France, [4]Medical Direction, CareDx, Brisbane, CA, United States, [5]Technical Laboratory, ADELIS Tech, Labege, France

Background: Many studies have reported the relevance of donor-derived cfDNA (dd-cfDNA) after lung transplantation (LTx) to diagnose and monitor acute rejection (AR) or chronic rejection or infection (INF). However, the analysis of cfDNA fragment size has not been studied. The aim of this study was to determine the clinical relevance of dd-cfDNA and cfDNA size profiles in events (AR and INF) during the first month after LTx.

Methods: This prospective, single-center study includes 62 LTx recipients at the Marseille Nord Hospital, France. Total cfDNA quantification was performed by fluorimetry and digital PCR, dd-cfDNA by NGS (AlloSeq cfDNA-CareDX®), and the size profile by BIABooster (Adelis®). A bronchoalveolar lavage and transbronchial biopsies at D30 established the following groups: not-injured and injured graft (AR, INF, or AR+INF).

Results: Quantification of total cfDNA was not correlated with the patient's status at D30. The percentage of dd-cfDNA was significantly higher for injured graft patients at D30 (p=0.0004). A threshold of 1.72% of dd-cfDNA correctly classified the not-injured graft patients (negative predictive value of 91.4%). Among recipients with dd-cfDNA >1.72%, the quantification of small sizes (80-120bp) >3.70% identified the INF with high performance (specificity and positive predictive value of 100%).

Conclusion: With the aim of considering cfDNA as a polyvalent non-invasive biomarker in transplantation, an algorithm combining the quantification of dd-cfDNA and small sizes of DNA may significantly classify the different types of allograft injuries.

KEYWORDS

lung transplantation (LTx), graft rejection (MeSH), infections, chimerism, cell-free nucleic acids (cfNAs)

Introduction

In 1948, Mandel and Métais first reported the presence of extracellular nucleic acids in the blood (1). However, due to the lack of sensitive, specific, robust, and reproducible analytical techniques, it was only in 1965 that the first studies identified circulating DNA, cell-free DNA, and extracellular DNA as potential markers of interest in medicine. Almost sixty years later, circulating tumor cfDNA (ctDNA) is at the center of the liquid biopsy concept used routinely in clinical oncology, and fetal-derived cfDNA (cffDNA) has allowed the development of noninvasive prenatal diagnosis (2). In addition to the quantification of cfDNA, the characteristics of the size profiles of cfDNA from fetuses in maternal plasma and the tumor-derived cfDNA molecules (ctDNA) in patient plasma are markers of interest. Indeed, in healthy human subjects, the standard cfDNA fragmentation pattern has a predominant peak at approximately 166 bp and multiples thereof, corresponding to a typical DNA cleavage pattern during apoptosis (3). Fetal DNA and ctDNA have been demonstrated to be shorter (4). The generation of a shorter size would be associated with DNA nuclease activity (5).

In 2019, Knight et al. reported 47 studies (retrospective or prospective) on the analysis of dd-cfDNA after organ transplants (kidney, liver, heart, lung, pancreas) using plasma or urine samples (6). The analyses performed involve the quantification of total cfDNA and an estimation of the percentage of dd-cfDNA by different techniques. Most studies have reported a significant correlation between dd-cfDNA levels and biopsy-proven rejection in kidney, liver, heart, and lung transplants.

In the context of lung transplantation (LTx), De Vlaminck et al. established in 2015 the two basics of the potential utility of dd-cfDNA (7). First, the survival rate after LTx is one of the lowest for all organ transplants, and second, the current diagnostic tests do not distinguish between infection and rejection, which are the two main posttransplant clinical complications. The authors observed a significant relationship between the level of dd-cfDNA and the events of rejection and CMV infection.

Later, Zou et al. (8) performed a digital PCR method according to the HLA mismatch between the donor and the recipient and observed, on the one hand, that there was a significant relationship between dd-cfDNA and acute rejection, but on the other hand, that there was no statistical relationship with bronchiolitis obliterans syndrome (BOS). Other teams have found a correlation between dd-cfDNA and acute rejection (9–12). For other organ transplantation, Agbor-Enoh et al. (13, 14) observed that this relationship is stronger for antibody-mediated rejection (AMR) than for acute cellular rejection (ACR). Moreover, dd-cfDNA was increased before the change in spirometry in recipients for whom the diagnosis of acute rejection will be made, making dd-cfDNA a predictive biomarker of acute rejection. Finally, the authors show that elevated levels of dd-cfDNA before a clinical diagnosis of AMR were associated with a simultaneous increase in DSA levels. Concerning chronic rejection, some authors showed a relationship between dd-cfDNA and the development of chronic lung allograft rejection (CLAD) (15). Finally, in the review by Knight et al. (6), the authors proposed a threshold for the diagnosis of acute rejection at 1%. However, the lack of coherence and consensus among the different preanalytical protocols and the timing for cfDNA analysis is one of the main obstacles to comparing studies and the translation of cfDNA analysis to clinical practice.

This monocentric prospective study investigated the relevance of quantitative and qualitative cfDNA for the diagnosis of early events in LTx in a controlled and reproducible preanalytical process.

Abbreviations: cfDNA, cell free DNA; dd-cfDNA, donor-derived cfDNA; ddPCR, droplet digital PCR; AR, acute rejection; AMR, antibody mediated rejection; ACR, acute cellular rejection; AUC, area under cover; DSA, donor specific antibodies; ROC, receiver operating characteristic; BOS, bronchiolitis obliterans syndrome; LTx, lung transplantation.

Materials and methods

Study design, setting, and participants

Sixty-two recipients were included in the Lung Transplant Department of the Aix-Marseille University Hospital, France, between August 28, 2019, and February 10, 2022 (ancillary study from the LARA protocol: NCT03587493) after signing the consent form. The inclusion criteria were age over 18 years old, registered on the national waiting list for a first lung transplant in the Marseille center, regardless of the indication, and benefit from a mono- or bi-lung transplantation. The exclusion criteria were minors, persons protected by law and deprived of their liberty, patients who are not eligible for a social security number, a previous lung transplant, or a patient who has already benefited from another type of transplantation. Finally, patients were excluded from the evaluation if they died or if they did not benefit from a transbronchial biopsy within 60 days after the LTx. The study was approved by an Institutional Review Board (CPP 2018.04.04 ter).

In the study period, all recipients received a standardized immunosuppressive regimen in accordance with our institutional protocol. Induction therapy consisted of intravenous administration of 20 mg of basiliximab on the day of transplant and day 4 post-transplant associated with high-dose methylprednisolone (7.5 mg/kg before implantation). Standard triple maintenance immunosuppressive regimen consisted of intravenous cyclosporine administered immediately after LTx (to obtain a steady-state serum concentration between 300 and 400 ng/ml) and then switched by oral tacrolimus as soon as possible (to maintain trough blood levels between 12 and 15 ng/ml during the first 3 months and around 10–12 ng/ml thereafter), mycophenolate mofetil, and steroids (prednisone) tapered to 0.5 mg/kg/day over the first month of the study period.

Postoperatively, transplant recipients received a prophylactic antibiotic treatment according to their preoperative and/or concomitant infectious status for at least 7 days. Seropositive CMV recipients and higher-risk CMV-mismatched recipients (donor positive and recipient negative) received prophylactic IV ganciclovir or oral valganciclovir as soon as possible, for the entire study period.

Biological samples

Whole blood samples were collected on the day of transplantation (D0, before surgery) and 15 and 30 days (D15, D30) after transplantation in 8.5 mL Cell-Free DNA Collection tubes (Roche®). DNA isolation from the plasma was completed within 7 days. The samples were double-centrifuged (1600 g, 10 min, and 4500 g, 10 min, room temperature). Plasma was stored at -20°C for less than one month before extraction and at -80°C for longer periods before extraction.

DNA isolation methods

The cfDNA was isolated using a magnetic extraction method (KingFisherTM Flex) with an IDXtract™ Mag kit (ID-Solutions®, Grabels France) according to the supplier's recommendations (16). All cfDNA was stored at 5°C ± 3°C if the PCR was performed immediately or at -20°C for a longer period of storage.

Fluorimetric cfDNA quantification method

All cfDNA was quantified twice by a QUBIT dsDNA HS Assay kit (Thermo Fisher Scientific®, Aalst, Belgium) according to the manufacturer's recommendations.

ddPCR cfDNA quantification methods

The commercial ID kit Quant™ cfDNA (ID. Solutions®, Grabels, France) and the homemade quantification by ddPCR with RPP30 gene amplification were performed. Quantification of cfDNA was performed by ddPCR using the Bio-Rad QX200 System following manufacturer's instructions. Absolute quantities of the cfDNA copies were determined using the QX200™ Droplet Reader.

cfDNA qualification and quantification by BIABooster

Fragment analysis was performed using BIABooster technology (17) (Adelis®, Labege, France). The technology was operated automatically on a commercial capillary electrophoresis instrument using electrohydrodynamic actuation. All the samples were treated with 0.1 U/µl RNase before analysis. BIABooster technology enabled the analysis of cfDNA fragments between 75 and 1649 bp, following the manufacturer's protocol. A reference ladder determines the sizes at each pass. Four peaks and eight areas (<75 bp, 75-111 bp, 111-240 bp, 240-370 bp, 370-580 bp, 580-1650 bp, >1650 bp) were identified and an additional analysis was performed targeting sizes between 80 and 120 bp. The cfDNA concentration (pg/µl) was measured under each area.

dd-cfDNA determination by NGS AlloSeq cfDNA®

The AlloSeq cfDNA kit (CareDx Pty Ltd, WA, Australia) enables relative quantification of the donor-derived cell-free DNA (dd-cfDNA) in a cfDNA sample derived from a transplant recipient. Following cfDNA extraction from plasma, cfDNA was amplified using multiplex PCR that includes PCR primers for 202 single nucleotide polymorphisms. The different reactions, including amplification of targeted regions of interest, indexation, pooling and purification steps were performed, according to the supplier's recommendations. The sequencing reaction used the MiSeq v3 reagent kit for 150 cycles. Data were analyzed using CareDx AlloSeq cfDNA software, which automatically calculates the dd-cfDNA relative quantification. In each run, a positive control (a previous sample with a known dd-cfDNA value) and a negative control (water) were tested.

Identification of HLA antibodies against the donor (DSA)

The identification of antibody specificity was carried out using a LABScan 200 Flow analyzer (Luminex Corporation, Austin, TX). The reagents used were LABScreen Single Antigen HLA Class I and Class II (One Lambda, Canoga Park, CA). The tests were carried out according to the manufacturers' instructions, and the analysis was performed with HLA Fusion 4.4.0 software. The confirmation of DSA was performed by comparing the specificities of the anti-HLA antibodies with the typing of the donor performed using the FluoGene® SSP-PCR technique (Inno-train, Kronberg, Germany) and confirmed by NGS technology (NGmix®, EFS).

Clinical covariables and outcome measures

Clinical data were recorded throughout the study. At inclusion, sex, age, weight, height, blood group, HLA of the recipient and donor, presence of anti-HLA antibodies, underlying lung disease, comorbidities, date of transplantation, type of transplant (single or double), CMV status of the recipient and donor, and type of immunosuppressive induction. At the Day 15 and 30 post-transplant visits, the information collected was the CRP value, the presence of DSA, and the outcome measures: the occurrence of an infection, the occurrence of a CMV infection/disease, and the occurrence of a biopsy-proven rejection. Bronchoalveolar lavage (BAL), bronchial biopsies, and transbronchial biopsies were systematically performed on day 30 and before when infection and/or acute rejection clinically suspected.

Infection was defined by the combination of clinical symptoms, radiological abnormalities (for pulmonary infection), and the identification of a microbe by culture or PCR. CMV infection was defined by the presence of CMV replication in tissue, blood, or other bodily fluids by PCR regardless of symptomatology and CMV disease by the presence of CMV infection that is accompanied by

clinical signs and symptoms according to recent guidelines (18). ACR and AMR were histologically defined according to internationally-accepted definitions but not including clinical parameters (19, 20). For ACR, perivascular and interstitial mononuclear infiltrates were graded as A1-4, small airways inflammation/lymphocytic bronchiolitis as B1R or B2R, and large airways inflammation/lymphocytic bronchitis as E1 or E2 (21).

A status was assigned to each patient at D15 and D30, "AR" (acute rejection including ACR, AMR or both labeled as mixed), "INF" (infection), "AR + INF" for "INJURED", or "NOT-INJURED" (neither rejection nor infection). All outcomes were adjudicated by transplant physicians blinded to dd-cfDNA measurements.

Statistical analysis

For the comparison of methods, linear regression and correlation tests allowed us to establish the correlation between techniques, and the Bland-Altman test allowed us to compare their concordance. Then, a characterization of the data between them allowed an orientation of the statistical tests performed. For the comparison of two quantitative variables, linear regressions and correlation tests were systematically performed. For two qualitative variables, the chi-square test was performed. To establish the link between quantitative data and qualitative data, the Mann-Whitney test was performed. All tests were performed with XLSTAT Life Sciences software, and the significance level was set at alpha = 0.05. All *Pvalue* <0.05 were considered statistically significant.

Results

Patient characteristics

Table 1 presents a summary of the patient characteristics at inclusion and at D15 and D30 according to their status (not-injured, injured, acute rejection or infection). Sixty-two patients were included in the study, the majority of whom received a bilateral LTx (n=54/62, 87%) for an indication of emphysema (n=24/62, 39%), lung fibrosis (n=19/62, 31%) or cystic fibrosis (6/62, 10%). Sixteen percent of patients had pre-transplant DSAs with an average MFI of 11 300 directed against HLA class I or class II.

On day 15, 28/62 (45%) patients had neither acute rejection nor infection, whereas 25/62 (40%), 5/62 (8%), and 4/62 (6%) had infection, acute rejection, or both, respectively. On day 30, 2 patients died, and 2 patients had uninformative biopsies. Forty out of 58 (70%) of the patients were not-injured, while 9/58 (16%), 8/58 (14%), and 1/58 (2%) had acute rejection, infection, or both, respectively (Figure 1).

Table 2 describes the biological and clinical characteristics of AR and INF. Among the AR, five were mixed acute rejection, 3 ACR, and 2 AMR. Only one biopsy showed a histopathological score of 3. Four AR were associated with INF. The INF were either of lung origin, or sepsis (6 cases). The microbiological pathogens were various.

Transplantation status (not-injured *vs.* injured) at D15 was correlated with the presence of DSA on the day of transplantation (p=0.003) and at D15 (p=0.007). In "injured group", there was a stronger level of significance between the AR and non-AR groups (day of transplantation, p=0.002; D15, p=0.003). Transplant status at D30 did not correlate with any other parameter, not even with the presence of pre-transplant DSA (p=0.161), or DSA at D15 (p=0.080) or D30 (p=0.275) (Table 3).

Total cfDNA quantification methods are not associated with early transplant events

A graphical representation revealed a correlation among the four techniques used for quantification (Figure 2A). The ddPCR RPP30 and BIAbooster were the most strongly correlated (r^2=0.934), while the ddPCR RPP30 and Qubit were the least (r^2=0.683). The Pearson correlation test showed a p-value<0.0001 for all techniques.

Analysis with a Bland-Altman plot (Figure 2B) showed good agreement between the techniques. Some outliers were present, especially for the high values of quantification, which were not adapted to the principle of rare events of digital PCR.

No statistical correlation was identified between the quantification of total cfDNA and the parameters collected at D15 and D30, particularly with the transplantation status (Table 3).

The level of %dd-cfDNA at D30 is associated with the transplant status

In the early post-transplant period, there was a high level of % dd-cfDNA, probably related to the surgery. Indeed, at D15, all patients had %dd-cfDNA levels above 1%, and although there was no significant difference regarding the status of the transplantation (Figure 3A), the %dd-cfDNA level was significantly higher (p=0.031) with double transplantation (Supplementary Figure).

The level of %dd-cfDNA at D15 was statistically decreased with the age of the patient (p=0.017), (Table 3).

The level of %dd-cfDNA at D30 was higher when the patient was injured graft than when the patient was not-injured graft (p<0.0001). Moreover, there is a significant difference (Figure 3B) between the AR (p=0.028), INF (p=0.018), and "INF + AR" (p=0.008) groups compared to the "not-injured", but no difference between the "AR" and "INF" groups (p=0.419). A ROC analysis (Figure 4) showed an area under the curve (AUC) of 0.798 (p<0.0001), establishing a threshold of 1.72% of %dd-cfDNA between not-injured and injured graft patients (Figure 4A). Under these conditions, the negative predictive value (NPV) was 91.4% and the positive predictive value (PPV) was 75.0%. Interestingly, the mean %dd-cfDNA levels tended to be higher in AMR than in ACR (mean value: 3.1% *vs.* 1.9%, p=0.10). The *de novo* or pre-transplant DSA, regardless of the level and the type (Class I *vs.* class II HLA antibodies) detected at D15 or D30, was not correlated with the level of %dd-cfDNA at D30 (Table 3).

10.3389/fimmu.2023.1183949

TABLE 1 patient's characteristics at inclusion and at D15 and D30 according to their status.

Recipient demographics	Inclusion	D15 (n=62)				D30 (n=58)**			
		Not-injured	Injured			Not-injured	Injured		
			AR	INF	AR + INF		AR	INF	AR + INF
	n= 62	n=28	n=5	n=25	n=4	n=39	n=6	n=9	n=4
Age (years)									
Mean (SD) *Min - max*	53.6 (11) 20-67	57.2 (8) 35-67	55.0 (6) 47-61	49.1 (14) 20-67	54.8 (11) 39-61	53.0 (13) 20-67	52.0 (11) 37-67	57.7 (9) 36-65	54.5 (4) 51-59
Sex: n (%)									
Male	29 (47)	11 (40)	2 (40)	15 (60)	2 (50)	18 (46)	3 (50)	4 (44)	1 (25)
Female	33 (53)	17 (60)	3 (60)	10 (40)	2 (50)	21 (54)	3 (50)	5 (56)	3 (75)
Weight (kg)									
Mean (SD) *Min-max*	64.8 (14) 35-100	65.6 (11) 48-88	78.6 (5) 74-86	62.2 (15) 35-100	58.8 (16) 40-78	63.1 (14) 35-100	70.0 (13) 54-88	65.8 (12) 48-86	71.5 (9) 62-81
Height (cm)									
Mean (SD) *Min-max*	168 (9.0) 147-185	169 (7) 156-180	168 (10) 157-180	167 (11) 147-185	162 (11) 155-178	168 (9) 147-185	171 (9) 157-180	166 (9) 155-180	165 (10) 154-175
BMI									
Mean (SD) *Min-max*	22.9 (3.9) 13.7-32.3	23.0 (3.1) 18.0-29.8	27.8 (1.7) 26.4-30.0	22.1 (4.5) 13.7-32.3	22.0 (4.0) 16.4-24.6	22.3 (4.2) 13.7-32.3	24.1 (4.4) 18.1-30.0	23.6 (2) 19.7-26.5	26.3 (2) 24.2-27.8
ABOD group: n (%)									
O	26 (42)	10 (36)	3 (60)	11 (44)	2 (50)	16 (41)	3 (50)	3 (33)	2 (50)
A	25 (40)	13 (46)	1 (20)	11 (44)	0 (0)	15 (38)	1 (17)	5 (56)	2 (50)
B	8 (13)	4 (14)	0 (0)	2 (8)	2 (50)	5 (13)	2 (33)	1 (11)	0 (0)
AB	3 (5)	1 (4)	1 (20)	1 (4)	0 (0)	3 (8)	0 (0)	0 (0)	0 (0)
D +	58 (94)	25 (89)	5 (100)	24 (96)	4 (100)	36 (92)	6 (100)	8 (89)	4 (100)
D -	4 (6)	3 (11)	0 (0)	1 (4)	0 (0)	3 (8)	0 (0)	1 (11)	0 (0)
Lung transplantation: n (%)									
Double lung transplantation	54 (87)	24 (86)	5 (100)	21 (84)	4 (100)	33 (85)	5 (83)	9 (100)	4 (100)
Simple lung transplantation	8 (13)	4 (14)	0 (0)	4 (16)	0 (0)	6 (15)	1 (17)	0 (0)	0 (0)
Indications: n (%)									
Emphysema - COPD	24 (39)	14 (50)	2 (40)	7 (28)	1 (25)	15 (38)	1 (17)	4 (45)	2 (50)
Lung fibrosis	19 (31)	7 (25)	3 (60)	7 (28)	2 (50)	12 (31)	2 (33)	3 (33)	2 (50)
Cystic fibrosis	6 (10)	1 (4)	0 (0)	4 (16)	1 (25)	4 (10)	1 (17)	1 (11)	0 (0)
Bronchial dilatation	4 (6)	2 (7)	0 (0)	2 (8)	0 (0)	3 (8)	0 (0)	1 (11)	0 (0)
Alpha anti trypsin deficit	1 (1.5)	1 (4)	0 (0)	0 (0)	0 (0)	0 (0)	1 (17)	0 (0)	0 (0)
Sarcoidosis	1 (1.5)	1 (4)	0 (0)	0 (0)	0 (0)	0 (0)	1 (17)	0 (0)	0 (0)
Other	7 (11)	2 (7)	0 (0)	5 (20)	0 (0)	5 (13)	0 (0)	0 (0)	0 (0)
CMV status: n (%)									
D+/R+	27 (44)	15 (54)	3 (60)	8 (32)	1 (25)	16 (41)	3 (50)	4 (45)	1 (25)
D-/R-	22 (35)	8 (29)	1 (20)	12 (48)	1 (25)	13 (33)	2 (33)	3 (33)	3 (75)

(Continued)

10.3389/fimmu.2023.1183949

TABLE 1 Continued

Recipient demographics	Inclusion	D15 (n=62)				D30 (n=58)**			
		Not-injured	Injured			Not-injured	Injured		
D-/R+	11 (18)	5 (17)	1 (20)	3 (12)	2 (50)	8 (21)	1 (17)	2 (22)	0 (0)
D+/R-	2 (3)	0 (0)	0 (0)	2 (8)	0 (0)	2 (5)	0 (0)	0 (0)	0 (0)
CRP (mg/L)									
Mean (SD) *Min - max*						15.6 (26) 0.3-126.6	6.12 (7) 0.9-19.5	49.8 (91) 4.3-255.2	92.9 (153) 2.5-269.7
DSA D0: n (%)									
No DSA	52 (84)	24 (86)	3 (60)	24 (96)	1 (25)	35 (90)	5 (83)	6 (67)	2 (50)
Class I	6 (10)	3 (10)	2 (40)	0 (0)	1 (25)	2 (5)	1 (17)	1 (11)	2 (50)
Class II	4 (6)	1 (4)	0 (0)	1 (4)	2 (50)	2 (5)	0 (0)	2 (22)	0 (0)
MFI total *Mean (SD)* *Min-max*	11,300 (20,468) 800-68,000	5,675 (7,044) 800-16,000	4,450 (566) 2700-3500	1,100	27,667 (35,020) 5,000-68,000	4,875 (7,424) 800-16,000	2,700	6,433 (3,108) 4,300-10,000	35,750 (45,608) 3,500-68,000
DSA D15: n (%)				n=57*			n=54***		
		n=28	n=5	n=20	n=4	n=35	n=6	n=9	n=4
No DSA		14 (50)	0 (0)	12 (60)	0 (0)	21 (60)	1 (17)	2 (25)	0 (0)
Class I		3 (11)	2 (40)	3 (15)	2 (50)	4 (11)	1 (17)	0 (0)	4 (100)
Class II		5 (18)	1 (20)	4 (20)	1 (25)	6 (17)	0 (0)	4 (50)	0 (0)
Class I + II		6 (21)	2 (40)	1 (5)	1 (25)	4 (10)	4 (66)	2 (25)	0 (0)
MFI total *Mean (SD)* *Min-max*		9,264 (8,387) 550-23,900	27,600 (11,120) 1,500-27,600)	4,036 (3,314) 700-10,400	13,425 (15,942) 500-36,600	6,025 (6,187) 500-18,700	7,475 (6,564) 3,800-17,300	8,333 (6,839) 700-19,800	10,450 (17,444) 1,100-36,600
AR type: n (%)									
Acute cellular rejection (ACR)			1 (20)		2 (50)		3 (50)		0 (0)
A score *B score* *E score*			*A1* *BX* *NR*		*A1* *NR* *NR*	*A1* *BX* *E0*		*A0* *B0* *E1*	*A1* *BX* *NR*	*A0* *B0* *E1*		
Antibody-mediated rejection (AMR)			3 (60)		1 (25)		1 (17)		1 (25)
Mixed rejection (ACR + AMR)			1 (20)		1 (25)		2 (33)		3 (75)
A score *B score* *E score*			*A0* *BX* *E1*		*A4* *BX* *E0*		*A2* *BX* *NR*	*A1* *NR* *NR*		

* 4 patients did not have DSA analysis and one patient died before; **2 patients died, 2 patients have a non-informative biopsy; *** 4 patients did not have DSA analysis. AR, acute rejection; INF, infection; SD, standard deviation; COPD, chronic obstructive pulmonary disease; CMV, cytomegalovirus; D/R, donor/recipient; DSA, donor specific.

The proportion of cfDNA with sizes of 80 to 120 bp is associated with infection at D30

There was no association between the proportion of each DNA fragments size, included 80-120bp and the status of the transplant at D15 (Figure 5A and Table 3). However, the level of %dd-cfDNA tended to correlate with small cfDNA sizes, 80-120 bp (p=0.010). At D30, the proportion of cfDNAs for sizes 80 to 120 bp correlated with INF, allowing us to differentiate between INF and NO-INF patients (p=0.005, Figure 5B). A ROC analysis considering the percentage of 80-120 bp cfDNA sizes associated with the INF group and NO-INF group indicated an AUC of 0.848 (p<0.0001), a NPV of 94.6% and a PPV of 61.1% for a threshold >3.7% (Figure 4B). In

10.3389/fimmu.2023.1183949

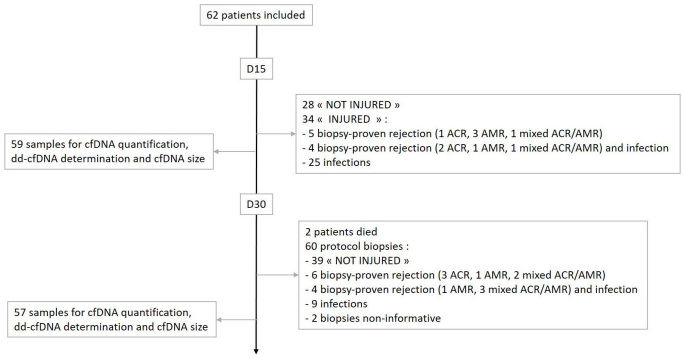

FIGURE 1
Patient and study sample flowchart.

TABLE 2 Description of injured graft patients at D30.

Table 2A Description of injured graft patients at D30: Biological characteristics of Acute Rejection.

Patient	Associated infection	Type of rejection	Biopsy score			Presence of DSA	Total MFI	Type of DSA	%dd-cfDNA	%80-120bp
1	Yes	Mixed	A3	BX	NR	Yes	45,400	A1 A68 B8 B18	3.00%	10.63%
2	Yes	Mixed	A0	B1	E0	No			2.90%	4.36%
3	Yes	AMR	A0	B0	E0	Yes	600	B44	2.70%	4.33%
4	Yes	Mixed	A1	BX	E0	No			3.10%	6.42%
5	No	Mixed	A2	BX	NR	Yes	4,000	B50 Cw5 DR53	5.10%	1.06%
6	No	Mixed	A1	NR	NR	Yes	3,500	A74 DQA1*02	2.20%	1.99%
7	No	ACR	A0	B0	E1	Yes	4,850	A2 DQ8	4.30%	3.41%
8	No	ACR	A1	BX	NR	Yes	7,950	DR15 DQ2 DQ6	0.78%	2.51%
9	No	AMR	A0	B0	E0	Yes	750	B8	4.26%	2.21%
10	No	ACR	A0	BX	E1	No			9.60%	2.04%

ACR, acute cellular rejection; AMR, antibody-mediated rejection; NR, not realized, DSA, donor specific antibodies; MFI, mean fluorescence intensities.

Table 2B Description of injured graft patients at D30: Clinical and biological characteristics of infections.

Patient	Associated rejection	CRP mg/L	Infection diagnosis and microorganism	Treatment	%dd-cfDNA	%80-120bp
1	Yes	269.7	VAP *Enterobacter cloacae*, BSI *Staphylococcus epidermidis*	ertapenem + vancomycin	3.00%	10.63%
2	Yes	2.5	Pneumonia *Klebsiella aerogenes* and *MRSA*	cefepime + linezolid	2.90%	4.36%
3	Yes	6.5	Septic shock without documentation	piperacillin/tazobactam + vancomycin	2.70%	4.33%
4	Yes	NR	Septic shock *Escherichia coli*	cefotaxime	3.10%	6.42%
5	No	NR	Translocation on fecal impaction, *Pseudomonas aeruginosa* and *Stenotrophomonas maltophilia*	amphotericin B + ciprofloxacin + meropenem	2.40%	11.02%
6	No	23.3	Pneumonia *Enterobacter cloacae*	untreated	1.80%	7.22%
7	No	23.1	Presence of mycelial filaments on biopsy	fluconazole	4.50%	4.55%
8	No	4.3	Pneumonia *Pseudomonas aeruginosa* and *Achromobacter xylosoxidans*, BSI *MSSA*	imipenem/cilastatin	3.10%	8.68%
9	No	7.6	Pneumonia *Staphylococcus epidermidis*	piperacillin/tazobactam	2.40%	3.74%

(Continued)

10.3389/fimmu.2023.1183949

TABLE 2 Continued

Patient	Associated rejection	CRP mg/L	Infection diagnosis and microorganism	Treatment	%dd-cfDNA	%80-120bp
10	No	NR	BSI *Serratia marsescens*	cefepime + ciprofloxacin + gentamicin	1.10%	10.10%
11	No	25.2	BSI *Staphylococcus epidermidis*, VAP *Proteus mirabilis*	cefepime + vancomycin	0.90%	11.91%
12	No	255.2	VAP *Corynebacterium*	piperacillin/tazobactam + linezolid	3.30%	2.44%
13	No	10	BSI *Staphylococcus haemolyticus*	vancomycin	2.70%	2.97%

VAP, Ventilator-associated pneumonia; BSI, Bloodstream infections; MRSA, Methicillin-resistant S. aureus; MSSA, Methicillin-sensitive Staphylococcus aureus; NR, not realized.

particular, the test correctly identified 12 of the 14 INF groups (85%), without excluding samples in which AR occurred together with INF.

Combining the association of %dd-cfDNA and %80-120bp cfDNA size is associated with INF occurrence

At D30, a ROC analysis (Figure 4C) considering the percentage of 80-120 bp cfDNA sizes associated with the INF group and NO-INF group when the %dd-cfDNA was >1.72% showed an AUC of 0.960 ($p<0.0001$). Under these conditions, the positive predictive value (PPV) was 100%, and the NPV was 82%. An analysis combining the two biomarkers dd-cfDNA >1.72% and 80-120 bp cfDNA size >3.7% produced the analytical performance described in Figure 6. Interesting, the CRP values tended to correlate only with the %dd-cfDNA and %80-120bp cfDNA sizes ($p=0.15$ and $p=0.08$, respectively) (Table 3).

Discussion

This is, to our knowledge, the first study that attempted to identify the events at D30 post-LTx by combining the level of dd-cfDNA and the cfDNA size fragment profile. In contrast, the total quantification of cfDNA, regardless of the quantification method used, did not seem relevant for the diagnosis of an early transplant event. As proof, there was no statistical variation in this quantification between D15 and D30 after transplantation (data

TABLE 3 Univariate analysis of factors associated to clinical status, cfDNA quantification, % dd-cfDNA, % 80-120 pb size at D15 and D30.

	D15 status	cfDNA quantification D15	dd-cfDNA (%) D15	80-120 pb (%) D15	D30 status	cfDNA quantification D30	dd-cfDNA (%) D30	80-120 bp (%) D30
Sex								
Age			P					
Weight								
Height								
Blood group								
Underlying lung disease								
Type of transplant			P					
CMV status								
DSA D0	P							
DSA D15	P							
DSA D30								
CRP D30								
Status D15	■							
Status D30					■		P	P

Black box: $p>0.15$; Grey box: trend ($0.05<p<0.15$); White box: $p<0.05$, "P" : positive correlation.

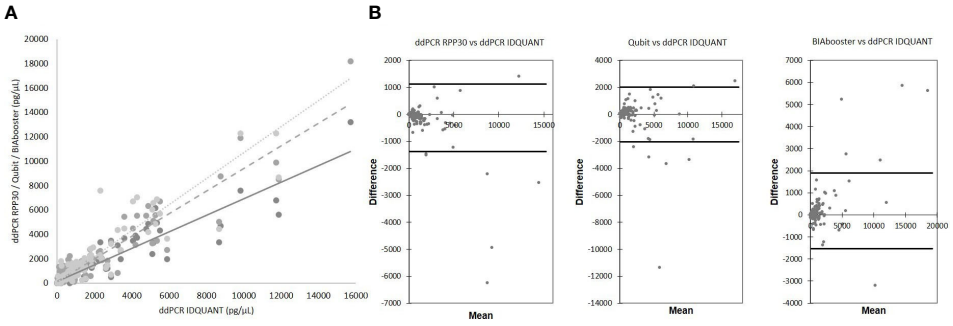

FIGURE 2
Comparison of total cfDNA quantification techniques. **(A)** correlation between techniques ddPCR IDQUANT and ddPCR RPP30 (solid line, y = 0.6776x + 127.9; R^2 = 0.8822, p<0.0001), Qubit (dash line; y = 0.9266x + 137.99; R^2 = 0.8936, p<0.0001) and BIAbooster (dotted line; y = 1.0656x + 39.642; R^2 = 0.871, p<0.0001) **(B)** Bland-Altman plots; concordances between techniques ddPCR IDQUANT and ddPCR RPP30, Qubit and BIAbooster; 95% CI (black solid line).

not shown), suggesting that the patient was in a physiological state of significant cell death or active cfDNA release. It would be interesting to follow this total quantification longer in the post-LTx follow-up to improve our understanding of the pathophysiology of cfDNA in organ transplantation.

Our study showed that the %dd-cfDNA analysis would be an efficient biomarker for the diagnosis of early events past the first 15 days after transplantation. As a reaction to surgery and ischemia-reperfusion, we observed, like other authors, a very high %dd-cfDNA level in the first days of transplantation since all patients exceeded 1% at D15 (7, 8, 14, 22, 23) and that this level was more elevated when the patient received a double lung transplant (24). Although not related to the medical status of the transplant, the % dd-cfDNA level at day 15 was correlated with the percentage of small fragments 80-120 bp in size, suggesting that the donor-derived cfDNA is smaller than that of the recipient.

However, at D30, the %dd-cfDNA levels were significantly lower, and a threshold of 1.72% of %dd-cfDNA was associated with a significant negative predictive value to differentiate not-injured from injured patients, indicating that a %dd-cfDNA value lower than 1.72% would indicate a not-injured transplant with high confidence. This value is very close to those of other studies. Indeed, a review shows thresholds of %dd-cfDNA around 1%, but the clinical events were detected at more distant post-LTx times, and the pre-analytical and analytical processes are unique to this study. Thus, the determination of %dd-cfDNA by clinical-grade NGS allows reproducibility, automation, and above all, the screening of 202 markers without requiring any donor DNA, allowing for good precision. For example, Zou et al. (8) and Sorbini et al. (25) used ddPCR with unitary markers related to HLA-DR mismatches between the recipient and the donor, or Agbor-Enoh et al. (13) used NGS but with the need for donor DNA. According to a review by Knight et al. (6), all previous studies use technologies for which a donor DNA sample is needed.

In our study, a %dd-cfDNA value higher than 1.72% could not differentiate between AR and INF. The threshold analysis was the same when considering or not considering pauci-symptomatic patients and in A1 rejection. Interestingly, as noted by others

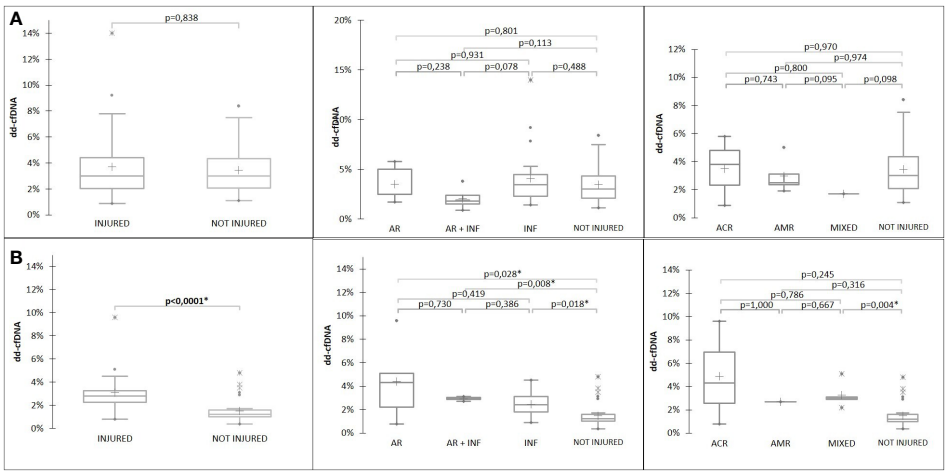

FIGURE 3
%dd-cfDNA at D15 **(A)** and at D30 **(B)** according to patient status.

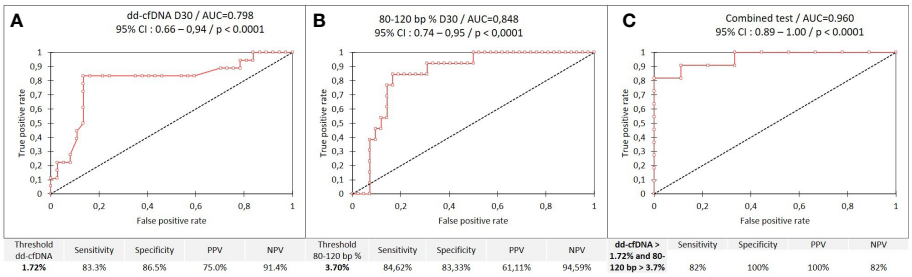

FIGURE 4
ROC curves; **(A)**, %dd-cfDNA between not-injured and injured graft patients **(B)**, %80-120bp size between not-injured and injured graft patients and **(C)**, combined test between infected and uninfected groups.

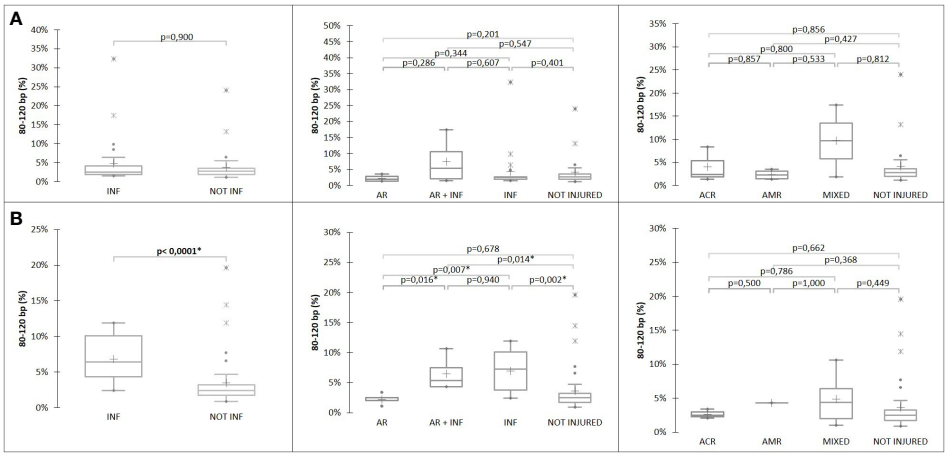

FIGURE 5
%80-120bp cfDNA at **(A)** D15 and **(B)** D30 according to patient status.

(13), the mean %dd-cfDNA levels in AMR were significantly higher than that of ACR, independent of the histologic stage and clinical severity of AR. However, *de novo* or pre-transplant DSA did not induce a change in the %dd-cfDNA levels. In our study, DSA pathogenicity as part of complement activation or the strength of the FcR-mediated ADCC was not investigated. Our teams and others showed that DSA detected after three months was potentially more strongly associated with chronic rejection occurrence in LTx (26). Furthermore the humoral alloimmune-mediated injury seems to be a less important contributor to death-censored graft loss in lung transplant recipients than in kidney transplant recipients (27).

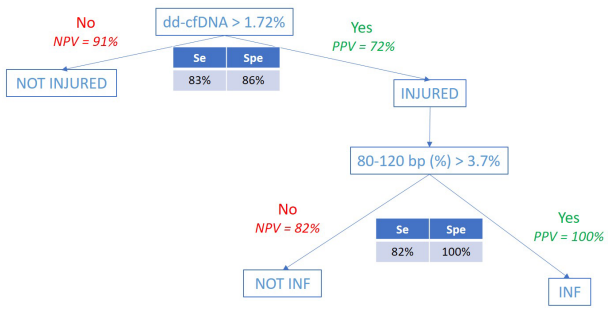

FIGURE 6
Analytical performance of the combined test (%dd-cfDNA and %80-120bp cfDNA).

Some cases considered not-injured (without infection and without acute clinical and histological rejection) at D30 had a high percentage of %dd-cfDNA. Several studies suggest a greater sensitivity of %dd-cfDNA for the detection of clinically silent allograft injury compared to bronchoscopy with transbronchial biopsy; these cases surely would require more frequent clinical follow-up (14). However, in our study, none of these cases reported clinical AR within the first 3 months (data not shown). Thus, our study suggests that in practice, a positive %dd-cfDNA level may serve as a trigger for bronchoscopy and other tests, such as radiologic, histopathologic, and BAL data, to identify allograft injury. In contrast, a %dd-cfDNA value lower than 1.72% may limit the need for clinical and biological investigation.

Interestingly, in our study, the last informative marker related to % dd-cfDNA was the proportion of small cfDNA (80-120bp), which correlated with INF at a threshold of 3.7%. Indeed, when the cutoff was >3.7%, the patients were infected in all cases, and when the cutoff was <3.7%, AR was more frequent than INF. The positive

microbiology was detected not exclusively by different means, such as bronchial aspiration, BAL, histopathology, and blood culture. All blood cultures were positive within 5 days of collection. Several pathogen species, the most found types, were detected, suggesting an absence of a correlation between the pathogen species and the values of the two cfDNA markers. In the two cases with a fragment size 80-120 bp <3.7%, the infections were known to be present for longer than 5 days with adapted antibiotic treatment. Thus, these data may indicate that %dd-cfDNA, and probably even more so the %80-120bp cfDNA size, is elevated in the setting of relevant local lung infection.

Our hypothesis is that small cfDNA fragment sizes are an indirect marker of graft damage, probably as part of the oncology process, due to the activation of DNAse I in the tissue. However, its specificity for the infected tissue may not be that of the lung graft, as evidenced by the high percentage of size fragments, while the %dd-cfDNA value is below that of the threshold. Additionally, it would be relevant to perform the chimerism test specifically on these small sizes, by comparing the results of chimerism from fragments of small sizes and those of large sizes. This size selection would increase the %dd-cfDNA value and make it possible to be more specific for infectious lung lesions. The study by Bazemore et al. (28) showed that % ddcfDNA is higher when isolating high-risk pathogens known to increase the risk of allograft dysfunction. Our study confirms that the level of %ddcfDNA is higher and that %80-120bp is also increased in the case of infection by a high-risk microorganism.

In contrast to other authors (25), the CRP parameter was not associated with %dd-cfDNA or the %80-120bp cfDNA size, suggesting that these infection markers could be interesting when following a local infection evolution, independent of the classical systemic inflammation biochemical marker parameters. Thus, an algorithm approach combining %dd-cfDNA and the %80-120bp cfDNA size is mainly useful to determine an infection occurrence and potentially the source of the infection.

There are few limitations to this study. First, it is a study with preliminary results based on a small cohort. Then the clinical data collected are limited. In a future study, it would be interesting to study the impact of ischemia time, ECMO and length of mechanical ventilation. Also, the impact of the donor-related parameters will be interesting to consider, such as the age of the donor.

Our study shows that the %dd-cfDNA value, measured at D30, is correlated with early transplant events. This analysis is not able to differentiate between infection and rejection, as some authors do. To discriminate the causes of the recipient organ injury (infection in particular), the size of the cfDNA is very promising. A threshold of 3.7% for small fragment sizes from 80 to 120 bp gave a satisfactory positive predictive value to detect infection. This marker could be useful to research local or systemic infections with high-risk pathogens associated or not associated with downstream allograft dysfunction and to follow this clinical evolution after treatment. However, the %dd-cfDNA was the only specific marker of allograft injury. Chimerism analysis of small fragment sizes could reveal the lung origin of infections.

In conclusion, our study suggests, on the one hand, that cfDNA is a very attractive non-invasive marker for the follow-up of transplanted patients and, on the other hand, that this biomarker could finally participate in the decision strategy to perform lung biopsies at D30. Nevertheless, due to its lack of specificity for rejection, it is more prudent to consider this new diagnostic tool as a polyvalent biomarker (%dd-cfDNA, fragmentomics, epigenetic signatures …). As the review by Jimenez-coll et al. (29), our study is a step in the evolution of the biology of organ transplantation towards personalized and predictive medicine based on the use of different panels of biomarkers both before transplantation and for its monitoring.

This study must be validated with a larger replication cohort and by a multicenter study to test the reproducibility of the analytical protocol and to observe the potential "center" effects of the surgical type, which are particularly sensitive when studying early events.

Data availability statement

The original contributions presented in the study are included in the article/Supplementary Material. Further inquiries can be directed to the corresponding author.

Ethics statement

The study was approved by an Institutional Review Board (CPP 2018.04.04 ter). Sixty-two recipients were included in the Lung Transplant Department of the AixMarseille University Hospital, France, between August 28, 2019, and February 10, 2022 (ancillary study from the LARA protocol: NCT03587493) after signing the consent form.

Author contributions

PP supervised the study and performed the technical and statistical analyses. BC and MR-G collected the clinical data from the patients. NC, JB, PA performed the extraction and quantification of cfDNA. SC, FF, AB participated in the technical expertise. ABa, SS, CF, JC, and CP assisted in the interpretation of the results. All authors contributed to the article and approved the submitted version.

Funding

This work was supported in part by "Vaincre la mucoviscidose" and "L'Association Gregory Lemarchal". This study was funded by the Etablissement Français du Sang, Marseille, France.

Acknowledgments

We thank all patients who participated in the study.

Conflict of interest

Author SC was employed by the company CareDX. Authors FF and AB were employed by the company ADELIS Tech.

The remaining authors declare that the research was conducted in the absence of any commercial or financial relationships that could be construed as a potential conflict of interest.

Publisher's note

All claims expressed in this article are solely those of the authors and do not necessarily represent those of their affiliated organizations, or those of the publisher, the editors and the reviewers. Any product that may be evaluated in this article, or claim that may be made by its manufacturer, is not guaranteed or endorsed by the publisher.

Supplementary material

The Supplementary Material for this article can be found online at: https://www.frontiersin.org/articles/10.3389/fimmu.2023.1183949/full#supplementary-material

References

1. Mandel P, Metais P. Les Acides nucléiques du plasma sanguin chez l'homme. *C R Seances Soc Biol Fil* (1948) 142(3–4):241–3.

2. Chitty LS, Lo YMD. Noninvasive prenatal screening for genetic diseases using massively parallel sequencing of maternal plasma DNA. *Cold Spring Harb Perspect Med* (2015) 5(9):a023085. doi: 10.1101/cshperspect.a023085

3. Tamkovich SN, Vlassov VV, Laktionov PP. Circulating DNA in the blood and its application in medical diagnosis. *Mol Biol* (2008) 42(1):9–19. doi: 10.1134/S0026893308010020

4. Jiang P, Lo YMD. The long and short of circulating cell-free DNA and the ins and outs of molecular diagnostics. *Trends Genet TIG* (2016) 32(6):360–71. doi: 10.1016/j.tig.2016.03.009

5. Tamkovich SN, Cherepanova AV, Kolesnikova EV, Rykova EY, Pyshnyi DV, Vlassov VV, et al. Circulating DNA and DNase activity in human blood. *Ann N Y Acad Sci* (2006) 1075(1):191–6. doi: 10.1196/annals.1368.026

6. Knight SR, Thorne A, Lo Faro ML. Donor-specific cell-free DNA as a biomarker in solid organ transplantation. a systematic review. *Transplantation* (2019) 103(2):273–83. doi: 10.1097/TP.0000000000002482

7. De Vlaminck I, Martin L, Kertesz M, Patel K, Kowarsky M, Strehl C, et al. Noninvasive monitoring of infection and rejection after lung transplantation. *Proc Natl Acad Sci USA* (2015) 112(43):13336–41. doi: 10.1073/pnas.1517494112

8. Zou J, Duffy B, Slade M, Young AL, Steward N, Hachem R, et al. Rapid detection of donor cell free DNA in lung transplant recipients with rejections using donor-recipient HLA mismatch. *Hum Immunol* (2017) 78(4):342–9. doi: 10.1016/j.humimm.2017.03.002

9. Levine DJ, Ross DJ, Sako E. Single center « snapshot » experience with donor-derived cell-free DNA after lung transplantation. *biomark Insights* (2020) 15:1177271920958704. doi: 10.1177/1177271920958704

10. Sayah D, Weigt SS, Ramsey A, Ardehali A, Golden J, Ross DJ. Plasma donor-derived cell-free DNA levels are increased during acute cellular rejection after lung transplant: pilot data. *Transplant Direct oct* (2020) 6(10):e608. doi: 10.1097/TXD.0000000000001063

11. Keller M, Agbor-Enoh S. Donor-derived cell-free DNA for acute rejection monitoring in heart and lung transplantation. *Curr Transplant Rep* (2021) 8(4):351–8. doi: 10.1007/s40472-021-00349-8

12. Jang MK, Tunc I, Berry GJ, Marboe C, Kong H, Keller MB, et al. Donor-derived cell-free DNA accurately detects acute rejection in lung transplant patients, a multicenter cohort study. *J Heart Lung Transplant* (2021) 40(8):822–30. doi: 10.1016/j.healun.2021.04.009

13. Agbor-Enoh S, Jackson AM, Tunc I, Berry GJ, Cochrane A, Grimm D, et al. Late manifestation of alloantibody-associated injury and clinical pulmonary antibody-mediated rejection: evidence from cell-free DNA analysis. *J Heart Lung Transplant* (2018) 37(7):925–32. doi: 10.1016/j.healun.2018.01.1305

14. Agbor-Enoh S, Wang Y, Tunc I, Jang MK, Davis A, De Vlaminck I, et al. Donor-derived cell-free DNA predicts allograft failure and mortality after lung transplantation. *EBioMedicine* (2019) 40:541–53. doi: 10.1016/j.ebiom.2018.12.029

15. Keller M, Bush E, Diamond JM, Shah P, Matthew J, Brown AW, et al. Use of donor-derived-cell-free DNA as a marker of early allograft injury in primary graft dysfunction (PGD) to predict the risk of chronic lung allograft dysfunction (CLAD). *J Heart Lung Transplant Off Publ Int Soc Heart Transplant* (2021) 40(6):488–93. doi: 10.1016/j.healun.2021.02.008

16. Pedini P, Graiet H, Laget L, Filosa L, Chatron J, Cherouat N, et al. Qualitative and quantitative comparison of cell-free DNA and cell-free fetal DNA isolation by four (semi-)automated extraction methods: impact in two clinical applications: chimerism quantification and noninvasive prenatal diagnosis. *J Transl Med déc* (2021) 19(1):15. doi: 10.1186/s12967-020-02671-8

17. Andriamanampisoa CL, Bancaud A, Boutonnet-Rodat A, Didelot A, Fabre J, Fina F, et al. BIABooster: online DNA concentration and size profiling with a limit of detection of 10 fg/µL and application to high-sensitivity characterization of circulating cell-free DNA. *Anal Chem* (2018) 90(6):3766–74. doi: 10.1021/acs.analchem.7b04034

18. Razonable RR, Humar A. Cytomegalovirus in solid organ transplant recipients–guidelines of the American society of transplantation infectious diseases community of practice. *Clin Transplant* (2019) 33(9):e13512. doi: 10.1111/ctr.13512

19. Stewart S, Fishbein MC, Snell GI, Berry GJ, Boehler A, Burke MM, et al. Revision of the 1996 working formulation for the standardization of nomenclature in the diagnosis of lung rejection. *J Heart Lung Transplant Off Publ Int Soc Heart Transplant* (2007) 26(12):1229–42. doi: 10.1016/j.healun.2007.10.017

20. Levine DJ, Glanville AR, Aboyoun C, Belperio J, Benden C, Berry GJ, et al. Antibody-mediated rejection of the lung: a consensus report of the international society for heart and lung transplantation. *J Heart Lung Transplant Off Publ Int Soc Heart Transplant* (2016) 35(4):397–406. doi: 10.1016/j.healun.2016.01.1223

21. Greenland JR, Jones KD, Hays SR, Golden JA, Urisman A, Jewell NP, et al. Association of large-airway lymphocytic bronchitis with bronchiolitis obliterans syndrome. *Am J Respir Crit Care Med* (2013) 187(4):417–23. doi: 10.1164/rccm.201206-1025OC

22. Luo J, Liu L, Chen L, Xu X, Wang Y, Wei B, et al. Over-shedding of donor-derived cell-free DNA at immune-related regions into plasma of lung transplant recipient. *Clin Transl Med* (2022) 12(1):e622. doi: 10.1002/ctm2.622

23. Tanaka S, Sugimoto S, Kurosaki T, Miyoshi K, Otani S, Suzawa K, et al. Donor-derived cell-free DNA is associated with acute rejection and decreased oxygenation in primary graft dysfunction after living donor-lobar lung transplantation. *Sci Rep* (2018) 8(1):15366. doi: 10.1038/s41598-018-33848-3

24. Keller MB, Meda R, Fu S, Yu K, Jang MK, Charya A, et al. Comparison of donor-derived cell-free DNA between single versus double lung transplant recipients. *Am J Transplant* (2022) 22:17039. doi: 10.1111/ajt.17039

25. Sorbini M, Togliatto G, Mioli F, Simonato E, Marro M, Cappuccio M, et al. Validation of a simple, rapid, and cost-effective method for acute rejection monitoring in lung transplant recipients. *Transpl Int Off J Eur Soc Organ Transplant* (2022) 35:10546. doi: 10.3389/ti.2022.10546

26. Paul P, Pedini P, Lyonnet L, Di Cristofaro J, Loundou A, Pelardy M, et al. FCGR3A and FCGR2A genotypes differentially impact allograft rejection and patients' survival after lung transplant. *Front Immunol* (2019) 10:1208. doi: 10.3389/fimmu.2019.01208

27. Brugière O, Roux A, Le Pavec J, Sroussi D, Parquin F, Pradère P, et al. Role of C1q-binding anti-HLA antibodies as a predictor of lung allograft outcome. *Eur Respir J* (2018) 52(2):1701898. doi: 10.1183/13993003.01898-2017

28. Bazemore K, Rohly M, Permpalung N, Yu K, Timofte I, Brown AW, et al. Donor derived cell free DNA% is elevated with pathogens that are risk factors for acute and chronic lung allograft injury. *J Heart Lung Transplant Off Publ Int Soc Heart Transplant* (2021) 40(11):1454–62. doi: 10.1016/j.healun.2021.05.012

29. Jimenez-Coll V, Llorente S, Boix F, Alfaro R, Galián JA, Martinez-Banaclocha H, et al. Monitoring of serological, cellular and genomic biomarkers in transplantation, computational prediction models and role of cell-free DNA in transplant outcome. *Int J Mol Sci* (2023) 24(4):3908. doi: 10.3390/ijms24043908

frontiers | Frontiers in Immunology

TYPE Review
PUBLISHED 26 July 2023
DOI 10.3389/fimmu.2023.1201619

OPEN ACCESS

EDITED BY
Guido Moll,
Charité University Medicine Berlin, Germany

REVIEWED BY
Vivek Kasinath,
Brigham and Women's Hospital and Harvard Medical School, United States
Giuseppe Remuzzi,
Istituto Di Ricerche Farmacologiche Mario Negri IRCCS, Italy

*CORRESPONDENCE
George W. Burke III
gburke@med.miami.edu

RECEIVED 06 April 2023
ACCEPTED 26 June 2023
PUBLISHED 26 July 2023

CITATION
Burke GW III, Mitrofanova A, Fontanella A, Ciancio G, Roth D, Ruiz P, Abitbol C, Chandar J, Merscher S and Fornoni A (2023) The podocyte: glomerular sentinel at the crossroads of innate and adaptive immunity.
Front. Immunol. 14:1201619.
doi: 10.3389/fimmu.2023.1201619

The podocyte: glomerular sentinel at the crossroads of innate and adaptive immunity

George W. Burke III[1]*, Alla Mitrofanova[2], Antonio Fontanella[2], Gaetano Ciancio[1], David Roth[3], Phil Ruiz[4], Carolyn Abitbol[5], Jayanthi Chandar[6], Sandra Merscher[7] and Alessia Fornoni[7]

[1]Division of Kidney–Pancreas Transplantation, Department of Surgery, Miami Transplant Institute, University of Miami Miller School of Medicine, Miami, FL, United States, [2]Research, Katz Family Division of Nephrology and Hypertension, Department of Medicine, University of Miami Miller School of Medicine, Miami, FL, United States, [3]Katz Family Division of Nephrology and Hypertension, Department of Medicine, and the Miami Transplant Institute, University of Miami Miller School of Medicine, Miami, FL, United States, [4]Transplant Pathology, Department of Surgery, Miami Transplant Institute, University of Miami Miller School of Medicine, Miami, FL, United States, [5]Division of Pediatric Nephrology, Department of Pediatrics, University of Miami Miller School of Medicine, Miami, FL, United States, [6]Division of Pediatric Kidney Transplantation, Department of Pediatrics, Miami Transplant Institute, University of Miami Miller School of Medicine, Miami, FL, United States, [7]Katz Family Division of Nephrology and Hypertension, Department of Medicine, University of Miami Miller School of Medicine, Miami, FL, United States

Focal segmental glomerulosclerosis (FSGS) is a common glomerular disorder that manifests clinically with the nephrotic syndrome and has a propensity to recur following kidney transplantation. The pathophysiology and therapies available to treat FSGS currently remain elusive. Since the podocyte appears to be the target of apparent circulating factor(s) that lead to recurrence of proteinuria following kidney transplantation, this article is focused on the podocyte. In the context of kidney transplantation, the performance of pre- and post-reperfusion biopsies, and the establishment of *in vitro* podocyte liquid biopsies/assays allow for the development of clinically relevant studies of podocyte biology. This has given insight into new pathways, involving novel targets in innate and adaptive immunity, such as SMPDL3b, cGAS-STING, and B7-1. Elegant experimental studies suggest that the successful clinical use of rituximab and abatacept, two immunomodulating agents, in our case series, may be due to direct effects on the podocyte, in addition to, or perhaps distinct from their immunosuppressive functions. Thus, tissue biomarker-directed therapy may provide a rational approach to validate the mechanism of disease and allow for the development of new therapeutics for FSGS. This report highlights recent progress in the field and emphasizes the importance of kidney transplantation and recurrent FSGS (rFSGS) as a platform for the study of primary FSGS.

KEYWORDS

podocyte, kidney, adaptive immunity, innate immunity, immune pathway

1 Introduction

Legend has it that Blues guitarist extraordinaire Robert Johnson sold his soul to the devil in return for being taught how to play the guitar. The deal was consummated at the crossroads of Highway 49 (known as the Blues Highway) and Route 61 in Clarksdale, Mississippi in 1927. Robert Johnson went on to become the father of American blues music, The King of the Delta Blues, spawning a generation and genre of African-American Blues musicians. It remains to be determined whether the podocyte in being positioned also at the crossroads of innate and adaptive immunity, was by divine intervention, or perhaps a deal made with the devil, similar to that of Robert Johnson. This is of more than passing interest, since it may well relate to podocyte longevity and lifetime/survival. You see, Robert Johnson died at the age of 27, starting a sad legacy of rock musicians who did not make it past their 27th birthday (see Supplemental Appendix). In a similar fashion, the podocyte may live out its functional existence in a normal fashion, or if it is involved in a disease process, for example focal segmental glomerulosclerosis (FSGS), may die young, the equivalent of an unfortunate 27 year-old rock musician. Please indulge this metaphysical conceit (with appreciation to John Donne), placing glomerular podocytes involved in FSGS in a position similar to doomed rock musicians. It is particularly fitting that it was Robert Johnson who wrote the song "Crossroads" (originally "Cross Road Blues"), emphasizing for us the intersection of two key immune pathways. Our mission is to determine how best to protect, preserve, and/or restore the life of our kidney rock star, the podocyte.

Focal segmental glomerulosclerosis (FSGS) is a common glomerular disorder that manifests clinically with nephrotic syndrome and > 80% foot process effacement on electron microscopy (1). FSGS accounts for about 20% of cases of nephrotic syndrome in children and 40% in adults, and is the most common glomerular disorder leading to end stage kidney disease (ESKD) in the United States with a prevalence of 4% (2). Progression to ESKD occurs in 40-60% of patients within 10-20 years from diagnosis, making this the most common primary glomerular disease leading to dialysis in the United States (3). Despite many clinical trials, no effective treatment has been identified (4). Following transplantation, recurrence of FSGS occurs in 20-50% of adults (2, 3, 5) and up to 80% in high-risk pediatric patients (6). Risk factors for recurrent FSGS include younger age (children less than 6 at onset), non-black race, rapid progression to ESKD (less than 3 years from diagnosis), severe proteinuria immediately prior to transplantation, and the loss of a previous allograft(s) to recurrence (2, 3). Recurrence of FSGS increases the risk of renal dysfunction and early graft loss (7, 8).

Abbreviations: APC, Antigen presenting cell; AS, Alport Syndrome; cGAS, Cyclic GMP-AMP synthase; DAMP, Damage-associated molecular pattern; DKD, Diabetic Kidney Disease; ESKD, End stage kidney disease; FSGS, Focal segmental glomerulosclerosis; GBM, Glomerular basement membrane; LPS, Lipopolysaccharide; NFKappa B Nuclear Factor Kappa B; PAMP, Pathogen-associated molecular pattern; SMPDL3b, Sphingomyelin phosphodiesterase acid-like 3b; STING, Stimulator of interferon genes; suPAR, Soluble urokinase receptor; TLR, Toll-like receptor.

2 Pathophysiology of FSGS recurrence

2.1 Circulating factor(s)

Recurrence of FSGS can develop rapidly after transplantation, sometimes within minutes to hours (9), suggesting the presence of a circulating factor(s) that could mediate an early injury to the glomerulus. Further evidence includes the following: 1) plasmapheresis can induce remission of proteinuria (5), and 2) serum from patients with FSGS induces proteinuria in rats, and alters albumin permeability in isolated glomeruli (2, 10). Moreover, in two clinical reports, living donor kidney transplant recipients who experienced severe recurrent FSGS, underwent transplant nephrectomy with re-transplantation of the affected kidney into a non-FSGS recipient (11, 12) resulting in rescue of the donor kidney function with resolution of proteinuria, providing further evidence for a circulating factor(s). Several review articles provide details supporting the existence of circulating factors that are beyond the scope of this article (13, 14).

2.2 Immunology of FSGS

Despite the lack of evidence of immune infiltrates in human FSGS biopsy samples (2, 6), an immune component has been thought to contribute to FSGS (15, 16). For example, the identification of IgM and C3 in glomerular deposits which was associated with both unfavorable response to therapy and worse renal outcomes (17) supports this concept. T-cell involvement has been described in the Buffalo/Mna rat model of FSGS recurrence after renal transplantation (18), and in human recurrent FSGS needle aspirate samples (19). However, neither B cell nor T cell infiltrates are consistently found in FSGS (20). Nonetheless, immunosuppression, which was associated with reduced proteinuria in the Buffalo/Mna rat model (18), has been the main therapy in humans after plasmapheresis or plasma absorption. The most studied immune-directed therapies have included corticosteroids, inhibitors of T lymphocyte calcineurin (cyclosporine A and tacrolimus), alkylating agents (cyclophosphamide and chlorambucil), and mycophenolate mofetil (5, 6). A number of case reports and non-controlled series have reported benefit from rituximab (8, 21, 22) but this has not been universally successful (23). Similarly, it remains unclear if the benefit of these immunosuppressive agents is linked to immunomodulatory functions or to direct podocyte effects.

2.3 At the crossroads of innate and adaptive immunity

2.3.1 Podocyte innate immunity

The glomerular capillary wall consists of three layers: 1) the fenestrated endothelial cell, 2) the glomerular basement membrane (GBM), and 3) the podocyte, the last barrier to prevent loss of protein into Bowman's space. Thus, the podocyte is anatomically located in a position to be a sentinel for the kidney's innate immune system. The mammalian innate immune system was originally intended to protect

its host from outside pathogens, for example viruses, bacteria and fungi – pathogen associated molecular patterns (PAMP's) (24) and in the process distinguish self from non-self. The theory of immunity has since evolved to the recognition of danger signals proposed by Polly Matzinger (25) and more recently to the discontinuity theory (26, 27): that immune activation can be induced by changes (any) in the environment or the cell rather than by detection of specific, defined molecules (24). Ultimately, the innate immune response requires a balance between the appropriate degree of aggression in the face of a serious pathogenic threat, but also the ability to limit local tissue damage with a controlled response.

Podocytes have been shown to express Toll-like receptors (TLRs), which recognize PAMPs, and certain endogenous signals, for example cellular breakdown products (Damage-Associated Molecular Patterns– DAMPs), e.g. reactive oxygen species, mitochondrial or, endoplasmic reticulum stress, DNA, RNA, nucleic acid fragments, etc. (28). TLRs which bind to DAMP's/PAMP's are part of the cellular (host) innate immune defense system, which, once activated, induce secretion of specific cytokines and chemokines that prompt the recruitment of other components of the innate immune response (29, 30). TLR stimulation activates nuclear factor Kappa B (NF Kappa B) in podocytes, and key components of TLR signaling including MyD88, IRAK, TRAF 6, etc. (Figure 1) (31). It has been proposed that the podocyte's role in innate immunity may predispose it to injury, depending on chronicity (32).

This is supported by the demonstration that TLR stimulation leads to podocyte apoptosis, and that blocking this pathway may prevent the progression of fibrosis and disease (33). In addition to TLRs there are a number of other important Pattern Recognition Receptors (PRRs) that are expressed by podocytes. These include the major components of the inflammasome, Nod-like receptors (NLRP3), ASC and caspase 1 (34, 35). The inflammasome is an intracellular protein complex involved in innate immune function including autophagy, apoptosis, fibrosis and secretion of pro-inflammatory cytokines including IL1-Beta and IL18 (28–30, 32). Podocytes also express retinoic acid-inducible gene 1 (RIG-1) that belongs to the family of RIG-I-like helicases that recognize viral RNA (32). Other family members include MDA5 and upon activation by recognition of viral RNA by cytoplasmic sensors,

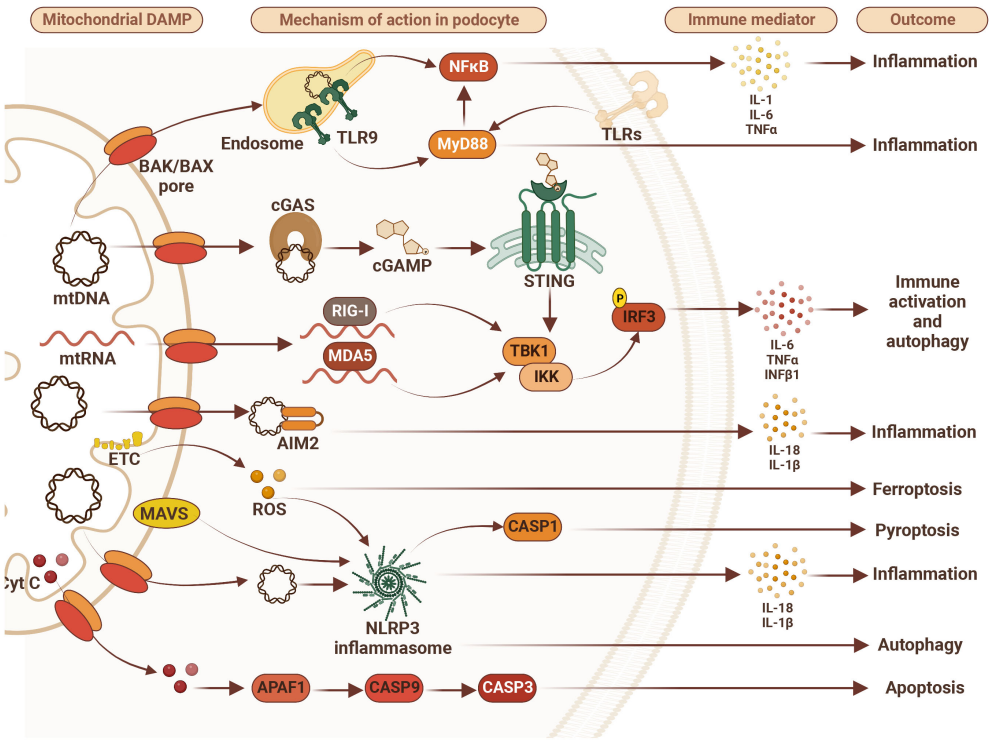

FIGURE 1
Mitochondrial damage-associated molecular patterns (DAMPs) disturb podocyte innate immunity pathways. Mitochondrial DAMPS such as mitochondrial DNA (mtDNA), mitochondrial RNA (mtRNA), cytochrome C (Cyt C), and reactive oxygen species (ROS) contribute to disturbance in podocyte homeostasis via activation of various DNA/RNA-sensing and inflammasome pathways leading to inflammation, immune system activation and different types of cell death including apoptosis, ferroptosis and pyroptosis. Therefore, targeting immune markers such as toll-like receptors (TLRs), tumor necrosis factor alpha (TNFα), NLR family pyrin domain containing 3 (NLRP3), retinoic acid-inducible gene I (RIG-I), melanoma differentiation-associated protein 5 (MDA5), mitochondrial antiviral-signaling protein (MAVS), absent in melanoma 2 (AIM2), stimulator of interferon gene (STING), and/or myeloid differentiation primary response 88 (MyD88) may represent future therapeutic approaches to treat FSGS. AIM2 – absent in melanoma 2; APAF1, apoptotic pepdidase activating factor 1; BAK, Bcl2 homologous antagonist/killer; BAX, Bcl2-associated X protein; CASP1, caspase 1; CASP3, caspase 3; CASP9, caspase 9; cGAS, cyclic GMP-AMP synthase; cGAMP, 2'3'-cyclic GMP-AMP; Cyt C, cytochrome c; ETC, electron transport chain; IL-1β, interleukin 1β; IL6, interleukin 6; IL-18, interleukin 18; IKK, IkB kinase; IRF3, interferon regulatory factor 3; MDA5, melanoma differentiation-associated protein 5; NF-kB, activation of nuclear factor κB; NLRP3, NLR family pyrin domain containing 3; RIG-I, retinoic acid-inducible gene I; ROS, reactive oxygen species; STING, stimulator of interferon gene; TBK1, TANK binding kinase 1; TLR9, toll-like receptor 9; TNFα, tumor necrosis factor alpha.

signal to the mitochondrial adaptor MAVS inducing an Interferon-regulatory factor (IRF)3, and IRF7-mediated type 1 IFN response (Figure 1) (35, 36).

Recently, the cGAS-STING axis has been identified as playing an important role in podocyte innate.

Immunity (37). cGAS, a PRR, is considered to be a key sensor of cytosolic DNA leading to catalyzation of second messenger 2'3'-cGAMP, which binds to the endoplasmic reticulum membrane adaptor STING (encoded by TMEM173) leading to activation of TANK-binding kinase 1 (TBK1), which in turn activates nuclear interferon regulatory factor 3 (IRF3) and leads to the production of type I interferons (Figure 1) (38, 39). The development of the cGAS-STING cytoplasmic defense system provides recognition of foreign nucleic acids, including pathogens/PAMPs (39), and DAMPs, as well as self-mitochondrial DNA leakage (40), cellular stress (24), and senescent break down products (41). This remarkably complex and efficient system based on the spatial coordination of DNA induced-cGAS-STING activity (38) allows for antiviral immunity and balanced innate immune responses toward self-DNA. While the crucial roles of the cGAS-STING pathway in immune cells and the immune defense have been extensively investigated (24, 38, 39), its function in non-immune cells, such as podocytes, remains largely unknown. It is not known if STING contributes to the development and/or progression of glomerular diseases, however, our group has been investigating this, and our work is summarized in this article (37).

2.4 Adaptive immune response

Beyond its role in innate immunity, the podocyte is capable of contributing to the adaptive immune response (16). The podocyte has been shown to possess properties of non-hematopoietic professional antigen-presenting cells (APCs) (42). Expression of both class I MHC antigens and, under certain inflammatory conditions, MHC class II antigens, contributing to the activation of CD8 and CD4 positive T cells, respectively, has been demonstrated on the podocyte. Moreover, podocytes express B7-1 (also known as CD80), a co-stimulatory molecule for T cells which is inducible under conditions of stress and was first reported in the context of the nephrotic syndrome (43). B7-1/CD80 is part of the B cell and APC repertoire and provides the second signal to T cells that allows amplification of the response to peptide antigens presented in the context of the appropriate MHC class I/II background (signal 1). B7-1 binds to CD28 on the T cell membrane, resulting in a positive co-stimulatory signal (signal 2). Interestingly, B7-2 (CD86), a co-stimulatory molecule presents on B cells and APCs that is also capable of binding to CD28 on T cells, is not present on podocytes (43).

The podocyte is in a position to integrate and act upon the range of immune signals, from T/B cell secreted cytokines to DAMPs/PAMPs. When podocytes are activated, through TLR's, cGAS-STING, or B7-1, etc., the change, mediated through the actin cytoskeleton, can affect the slit diaphragm proteins (44), allowing the passage of protein (proteinuria) or potentially danger signals, e.g. pathogens, into Bowman's space, and hence into the urine and excreted (29, 30). This potential for the excretion of danger/pathogen imbues the kidney, by virtue of the podocyte, with the capacity for immune defense mediated through a combination of innate and adaptive immune mechanisms (16). Importantly, clearance of danger into the urine avoids the activation of inflammatory mediators/cytokines that could result in unnecessary local tissue damage (45).

3 Treatment strategies: immunomodulation vs. direct podocyte effect of rituximab for recurrent FSGS

Rituximab is a monoclonal antibody directed against CD20 expressed on B lymphocytes and has been used for the treatment of non-Hodgkin's lymphoma, chronic lymphocytic leukemia and rheumatoid arthritis (46). Rituximab has been used off-label for the treatment of several kidney conditions, including acute allograft rejection and steroid resistant nephrotic syndrome (46). However, the pathogenesis of FSGS has not been demonstrated to be B cell or antibody mediated, suggesting the possibility of a B lymphocyte – independent mechanism of action. To assess the possible role of rituximab in recurrent FSGS, our center began utilizing a single dose of rituximab peri-operatively at the time of kidney transplantation in January 2004. In this study 27 consecutive patients received rituximab and were compared to a historical control group of 14 patients. This group of kidney transplant recipients was comprised predominately of children at high risk for recurrence (47). Nephrotic range proteinuria within the first month post- transplant was reduced from 64% to 26% (p=0.023), and similarly the need for plasmapheresis fell from 71% to 30% (p=0.019).

3.1 Peri-operative use of rituximab: beyond B cell immunity

In an attempt to better understand the mechanism of rituximab in this clinical setting, we pursued two lines of research: one involving pre- and post-reperfusion kidney transplant biopsies, and the other based on the effect of patient serum on podocytes in an *in vitro* assay. We initially expected to identify CD20 on the podocyte membrane, however, we demonstrated direct binding of rituximab to podocytes in the absence of CD20 (47). Screening of a phage display peptide library revealed possible cross reactivity of rituximab with sphingomyelin phosphodiesterase acid-like 3b (SMPDL3b) protein (48). Exposure of lymphoma cells to rituximab regulates the action of acid sphingomyelinase in lipid raft microdomains (49) essential for the organization of signaling molecules in highly specialized cells like podocytes. Based on these findings, we hypothesized that rituximab might have an impact on the filtration barrier in recurrent FSGS via the stabilization of sphingolipids with downstream effect on actin cytoskeleton remodeling. We postulated that rituximab could act as a direct

modulator of podocyte function similar to what has been reported for cyclosporine, that was found to modulate podocyte function by interacting with the podocyte cytoskeleton, independent of its immunosuppressive activity (50).

As part of the protocol for kidney transplantation, a preimplantation biopsy of the allograft was obtained followed by a second biopsy 30 to 60 minutes post-reperfusion, after the completion of the uretero-vesical anastomosis, prior to closure of the incision. We demonstrated membrane and lipid raft specific SMPDL3b expression on podocytes from normal donor kidney biopsies (pre-reperfusion). Interestingly, the number of SMPDL3b-positive podocytes in post-reperfusion biopsies was reduced in patients who later experienced recurrent proteinuria (47). Serum collected in the pretransplant setting from patients who developed recurrent proteinuria resulted in down regulation of SMPDL3b protein expression and acid sphingomyelinase activity in cultured immortalized human podocytes. This was blocked by pretreatment of the podocytes with rituximab. Similarly, pretransplant serum of patients with recurrent disease caused a marked disruption of the actin cytoskeleton which could be prevented by pretreatment with rituximab, or overexpression of SMPDL3b on the podocytes in culture. The protective effect of rituximab was blocked by the addition of siRNA to SMPDL3b (47). Thus, down regulation of SMPDL3b after exposure to patient's serum rendered podocytes more susceptible to actin remodeling, likely caused by a circulating/permeability factor(s). Rituximab appeared to prevent podocyte actin remodeling through stabilization of SMPDL3b (51). In addition, we reported that SMPDL3b may be an important modulator of podocyte function by influencing suPAR-mediated podocyte injury, changing it from a migratory to an apoptotic phenotype (52).

In summary, we have demonstrated that rituximab treatment of high-risk FSGS kidney transplant recipients is associated with a lower incidence of post-transplant proteinuria and could directly protect podocytes in an SMPDL3b-dependent manner (47). The demonstration of SMPDL3b-mediated protection from proteinuria using rituximab in a kidney transplant xenograft (53) and adriamycin-induced nephropathy model (54) further support this. SMPDL3b has also been shown to interact with TLRs and play an important role in down-regulating innate immunity (55).

3.2 Changes identifiable on post-reperfusion biopsies

In those patients who experienced recurrent proteinuria, we identified podocyte foot process effacement by electron microscopy in the post-reperfusion biopsies. Furthermore, we were able to show that the presence of foot process effacement correlated with the degree of proteinuria (9). However, resolution of foot process effacement in the context of recurrent FSGS was not always associated with resolution of proteinuria (56, 57). This suggests that proteinuria related to disruption of the slit diaphragm proteins may be a more subtle injury than that recognized by foot process effacement (9) on electron microscopy. The changes identifiable in the post-reperfusion biopsy emphasize the likelihood of the existence of circulating factor(s) in the kidney recipients with FSGS (9).

3.3 Abatacept rescue in the context of podocyte B7-1 staining

The use of rituximab peri-operatively in high-risk kidney transplant recipients with FSGS resulted in significant reduction in the development of recurrent proteinuria (47). However, 26% of the patients developed nephrotic-range proteinuria despite receiving a single dose of rituximab. This prompted us to further explore the possibility of other podocyte-directed treatment. Based on the demonstration of B7-1/CD80 expression in podocytes that was initially reported in 2004 (43) in the context of the nephrotic syndrome, we stained our pre- and post-reperfusion biopsies in KT recipients with recurrent proteinuria for B7-1. We subsequently identified B7-1 on the post-, but not the pre-reperfusion biopsies. Abatacept (CTLA-4-Ig) is an inhibitor of the T cell costimulatory molecule B7-1 (CD80) and is used to treat rheumatoid arthritis (58). Importantly, abatacept possesses a greater affinity for B7-1 than B7-2 (59). Since podocytes selectively express B7-1, and not B7-2 (43) as described above, we hypothesized that abatacept might be particularly effective in our unique clinical context.

Furthermore, we performed detailed mechanistic *in vitro* studies of podocytes, similar to our efforts with rituximab (47). Podocyte migration *in vitro* is known to correlate with function *in vivo*. We demonstrated that the addition of LPS to podocytes in culture induced B7-1 protein expression and affected migration. This was blocked by abatacept. In addition, B7-1 gene silencing or expression of the truncated construct also suppressed podocyte migration. B7-1 positive podocytes have a reduced capacity to attach to the surrounding matrix through beta 1 integrin. In cell culture studies, B7-1 positive podocytes changed their morphological characteristics and their function, leading to detachment of podocyte foot processes from the GBM. Abatacept appears to act by blocking the B7-1-mediated loss of podocyte Beta 1 integrin activation. Mechanistically, B7-1 promotes disease-associated podocyte migration through inactivation of beta 1 integrin, and this is reversed by abatacept (60).

Four kidney transplant recipients who were at high risk for recurrence (two patients with retransplants; two pediatric patients with rapid progression to ESKD), received a single dose of rituximab peri-operatively (47), and experienced post-transplant nephrotic range proteinuria. The first patient was treated with abatacept and plasmapheresis during the first week following transplantation, and experienced resolution of nephrotic range proteinuria. Treatment with abatacept (60) 10 mg/kg IV, resulted in the partial or complete remission of proteinuria in the three other kidney transplant recipients subsequently. In the two patients who underwent pre- and post-reperfusion biopsies, B7-1 staining was shown on the post-, not the pre-reperfusion biopsy, and B7-1 was found to colocalize with synaptopodin. Similar resolution of proteinuria after abatacept therapy was demonstrated in a non-transplant patient with native FSGS resistant to therapy who was shown to have B7-1 positive staining on biopsy (60). Of the four kidney transplant recipients, two received a single dose of abatacept, while the other two received two doses. All four

recipients received their first dose of abatacept within one week of transplantation. These patients received induction antibody therapy with Thymoglobulin and monoclonal anti-CD25 (IL2R), and maintenance immunosuppression with tacrolimus, mycophenolate mofetil and steroids, as well as plasmapheresis. With follow-up from ten to forty-eight months, the creatinine remained stable, urine protein/creatinine ratio was < 0.1 for two patients, and < 0.5 in the other two patients (60).

3.4 Updated experience with B7-1/abatacept for rFSGS

Since the publication of this experience, a number of articles described difficulty in staining kidney transplant biopsies for B7-1 (61–65) and lack of efficacy of either abatacept or the second-generation anti-costimulatory agent, belatacept (63, 66–69). Over the last decade we have followed 12 patients who experienced recurrent FSGS following KT despite receiving a peri-operative dose of rituximab (70) and found the following:

1) Nine/ten patients with recurrent proteinuria after KT responded to abatacept with improvement or resolution of proteinuria. Of these, two patients did not undergo a KT biopsy. Eight KT recipients were found to be B7-1 positive, one of whom was receiving belatacept at the time of biopsy. This last patient did not respond to abatacept, possibly due to belatacept interference of B7-1 (70).
2) Two patients who remained B7-1 negative on three kidney transplant biopsies during the year following kidney transplantation did not respond to abatacept and lost KT function.
3) None of our patients and no patients from the literature responded favorably to belatacept, regardless of the B7-1 staining (65–69).
4) The resolution of recurrent proteinuria for the second time in two patients who only received abatacept [cases 7 and 8 (70)] adds further strength to support the role for abatacept, since this occurred without plasmapheresis, and in the context of therapeutic calcineurin inhibitor levels (70).

The long-term goal of our program, to optimize treatment of patients with FSGS at risk for recurrent proteinuria after kidney transplantation, has been focused on stratifying patients based on tissue-demonstrated biomarkers. The finding that rituximab binds to SMPDL3b, which is present on healthy podocytes, but is reduced in the context of proteinuria (47) was the first key element. Our clinical experience with rituximab was encouraging, and, to further emphasize the importance of preventing the recurrence of nephrotic range proteinuria, it has been reported that, while a response to rituximab results in 100% five-year graft survival, a lack of response leads to only 36.5% five-year graft survival (8). This concern contributed to our search for a rescue therapy for those kidney transplant recipients who experienced recurrent proteinuria despite receiving a dose of rituximab. In a similar effort to implement biomarker-specific therapy, abatacept, which binds B7-1/CD80, was used in those kidney transplant recipients whose proteinuria recurred despite receiving a peri-operative dose of rituximab. This was done in association with kidney transplant biopsies (when available) to identify podocyte B7-1/CD80 expression (60). In those instances where a kidney transplant biopsy was performed, B7-1 staining was identified on the post-reperfusion, not the pre-reperfusion KT biopsy and treatment with abatacept resulted in improvement/resolution of the proteinuria. This included one example of abatacept treatment-related resolution of proteinuria where B7-1 was demonstrated on a kidney transplant biopsy (70) in which the native kidney disease was not FSGS (series case #3). This suggests that the presence of B7-1 on biopsy in the context of nephrotic range proteinuria may be sufficient to justify treatment with abatacept, regardless of the original disease. Nonetheless, it will be important to continue to study this patient population to confirm the role of both B7-1 expression on podocytes and clinical response to abatacept in those cases of B7-1 positivity.

4 Back to the crossroads: the intersection of innate and adaptive immunity

4.1 Role of SMPDL3b in podocyte cell membrane function

Our experience treating patients with recurrent proteinuria after receiving a kidney transplant for FSGS has led to further study searching for evidence implicating podocyte involvement in the innate immune response. Human podocytes express TLR 1-6 and 9 mRNA [with minimal expression of TLR 7,8,10 (71, 72)], as well as the membrane sphingolipid SMPDL3b (47, 71). In dendritic cells TLR stimulation, for example TLR 4 with LPS, but also with different ligands including CPG, imiquimod, and the pro-inflammatory cytokine IFN-gamma, results in up-regulation of SMPDL3b mRNA and protein levels (55, 73). SMPDL3b plays a negative role in the regulation of TLR activity *in vivo* associated with reduction in IL-6, TNF-alpha, and IL-12p40 (55). SMPDL3b depletion results in profound changes in the cellular lipid composition and membrane fluidity *in vitro*. SMPDL3b-deficient mice show enhanced responsiveness in TLR-dependent peritonitis. Interestingly, the introduction of specific ceramides could restore regulatory control of TLR stimulation in the context of SMPDL3b depletion (54). These features demonstrate the important role of SMPDL3b in cell membrane lipid composition and flexibility linking this with innate immune signaling (55).

There are suggestions that sphingolipids may also be involved in the development of proteinuria, since mutations in sphingosine-1-phosphate (S1P) lyase are associated with the nephrotic syndrome (74). In Fabry disease, the intracellular pathological accumulation of glycosphingolipids led to cellular and tissue damage, ultimately manifesting in proteinuria and progressive nephropathy. This has been reported with increased urinary B7-1 excretion and podocyturia (75), in the context of native kidney biopsy showing podocyte staining for B7-1. Moreover, the addition of lyso-globotriaosylceramide (lyso-

Gb3), present in higher levels in patients with Fabry disease, upregulated the expression of B7-1 mRNA in podocytes *in vitro* (75). The overabundance of sphingolipid was felt to lead *in vivo* to podocyte injury with NF-kappa-B-related B7-1 expression (75). The stimulation of human podocyte TLR3 by poly-IC *in vitro* has also been shown to increase B7-1 mRNA and protein expression in an NF-kappa-B-dependent fashion (72). Thus B7-1 expression appeared to increase with increased levels of NF-kappa-B. Poly-IC injection *in vivo* resulted in proteinuria and increased glomerular expression of B7-1 along with increased urinary B7-1 in mice (76). Podocyte SMPDL3b expression was reduced in biopsies of patients with recurrent FSGS (47). Importantly, SMPDL3b depletion caused a sustained degradation of I-kappa-B-alpha, which led to enhanced NF-kappa-B activity (55). This raised the possibility that the loss of SMPDL3b expression in podocytes in kidneys experiencing recurrence of FSGS (47) may predispose to increased B7-1 expression, possibly NF-kappa-B-mediated. This suggests the intriguing possibility of a connection between sphingolipids and podocyte B7-1 membrane expression in proteinuria. Finally, a recent study using transcriptomic and biological assays in B7-1 transgenic and Adriamycin nephropathy models, found B7-1 mediated podocyte injury through signal transmission to Beta-catenin through a heat shock mediated pathway (Hsp90ab1-LRP-Beta-catenin) (77). This places more biological relevance on the role of B7-1 in podocyte injury. Interestingly, this may also include sphingolipid interaction (76). This area is currently under active study.

4.2 Experimental support for SMPDL3b/B7-1 podocyte biomarker model

Several experimental and clinical studies have recently reported similar biomarkers to those in our work. First, in a series of xenotransplant pig-to-primate kidney transplants, with resultant significant proteinuria, both SMPDL3b and B7-1 were expressed on podocytes (78). Rituximab was used for induction with SMPDL3b-demonstrated specificity (53, 78), and B7-1 was also identified on kidney transplant biopsies (78, 79). In their experiments, belatacept was used to treat their primate recipients. While reducing the degree of proteinuria, belatacept did not result in resolution of proteinuria (78). It would be of interest to test whether abatacept may have been more effective in this setting of B7-1 positive podocyte staining in line with our most recent report (70). Secondly, in a rat model of adriamycin-mediated proteinuric kidney disease, studied separately by two different groups: 1) rituximab was found to significantly reduce proteinuria via SMPDL3b-specific modulation (54), and 2) abatacept significantly reduced proteinuria, although B7-1 was not identified on podocytes, and the mechanism was felt to be related to an effect on peripheral blood Th17 lymphocytes (54). Finally, although the molecular mechanisms resulting in nephrotic syndrome are complex (80), podocyte expression of B7-1 has been suggested as a key therapeutic target for Minimal Change Disease (MCD) (71).

Abatacept treatment of a patient with steroid dependent MCD, resulted in sustained remission of proteinuria (81). However, in this study both endothelial cells and podocytes were found to express B7-1 during relapse of MCD (82), again suggesting B7-1 whether expressed on podocytes or EC, could be a therapeutic target. However, a recent report evaluating circulating factors *in vitro* in FSGS plasma demonstrated changes including actin-cytoskeleton rearrangement and excessive formation of reactive oxygen species (ROS) only in podocytes, not in human glomerular microvascular EC (83).

5 Approach to rFSGS in B7-1 negative KT recipients

5.1 Experience with cGAS-STING in our experimental studies

Although we have observed a reduced incidence of rFSGS in our KT recipients who were treated with a peri-operative dose of rituximab, and subsequently treated with abatacept for those patients identified to express B7-1, we do not yet have effective therapy for those KT recipients who are B7-1 negative. This has led to our next level of investigation, studying the potential role of cGAS-STING in this patient population.

"The cytosol is a highly unusual environment in that it is perhaps the only germ-free location on the planet. In contrast, all extracellular environments have the possibility of being occupied by one or more microbes (84)".

The protection provided by the innate immune system contributed conceptually to this statement and led to our pursuit of the cGAS-STING axis for potential insight into the B7-1-negative development of rFSGS. Perhaps the putative circulating factors (danger) are being recognized by the cGAS-STING system in a B7-1-independent fashion, ultimately leading to slit diaphragm protein dysfunction and proteinuria. The passage of danger equivalents into the urine may provide a less damaging manner of removing pathogen while minimizing local damage. This suggests that interference with cGAS-STING may lead to new therapeutic possibilities.

STING is an adaptor protein involved in DNA-dependent activation of innate immunity against viral or bacterial infection as well as in autoinflammatory diseases such as vasculopathy and systemic lupus erythematosus (37–39). However, the importance of STING in the regulation of local inflammation in the kidney remains largely unstudied. So, we used this to study mouse models of CKD. This study (37) identifies for the first-time activation of the cGAS-STING signaling pathway in podocytes as a significant contributor to the pathogenesis of glomerular disease of either metabolic (Diabetic kidney disease- DKD) or non-metabolic (Alport Syndrome-AS) origin, suggesting that STING targeting represents a potential therapeutic option to prevent kidney function loss in these conditions. This is particularly important given that there is no available treatment for either DKD (85) or AS (86). Activation of the cGAS-STING pathway has previously been shown in non-immune cells such as mouse embryonic fibroblasts and adipocytes (37). Here, we first confirmed that human as well as murine podocytes express all components of the cGAS-STING signaling pathway both at mRNA and protein levels. This included an increase in gene expression of STING, TBK1 and IRF3, along with increased phosphorylation after treatment with cyclic dinucleotides (c-diAMP).

Terminally differentiated human and murine podocytes were utilized as a model system *in vitro* to investigate expression of the

cGAS-STING signaling pathway components and its overall activity. For *in vivo* studies we used db/db type 2 diabetes mice as a model of DKD and Col4a3-/- mice as an experimental Alport syndrome model to determine presence and activity of the cGAS-STING pathway in the kidneys. Activation of STING is associated with proteinuria and podocyte loss in wildtype mice. The cGAS-STING signaling pathway was found to be activated in kidney cortices and glomeruli of db/db mice and mice with AS at baseline and was associated with albuminuria. Pharmacological (with C176) or genetic inhibition ofSTING ameliorated diabetes- or streptozotocin-induced and Alport syndrome-associated glomerular loss of function. Our current findings demonstrate an important role of the cGAS-STING signaling pathway in mediating the detrimental consequences including proteinuria and glomerular dysfunction and point to STING as a potential therapeutic target in glomerular diseases of metabolic and non-metabolic origin (37).

Activation of the cGAS-STING pathway by c-diAMP in podocytes also led to increased expression of type I interferon, a "classic" downstream signal of cGAS-STING. These data confirm the notion that podocytes exhibit features of immune cells and may also be considered as antigen-presenting-like cells. Moreover, increased caspase 3 activity and autophagy markers in c-diAMP treated podocytes suggest that apoptosis and autophagic cell death may be associated with STING activation (37).

While we observed a significant impact of the cGAS-STING pathway on podocyte damage in glomerular diseases of both metabolic (DKD) and non-metabolic (AS and FSGS) origin, the mechanism behind it remains unclear. Some studies indicate that in the kidney, the cGAS-STING pathway may be activated by mitochondrial DNA leakage into the cytosol (40). Thus, it will be important to assess if mitochondrial DNA leakage also occurs in podocytes and contributes to the activation of the cGAS-STING pathway. A recent study suggests that STING is located in the mitochondrial associated membrane, and that this might lead to the specificity of the cellular functions of STING mediated by mitochondrial-ER communication (87). On the other hand, negative regulation of STING signaling is also essential for the prevention of chronic inflammation. Targeting this pathway (cGAS/STING) may represent another therapeutic option to treat or even prevent glomerular disease development and/or progression. We hope that this approach will provide insight into new therapeutic options for those instances of rFSGS that develop despite receiving a peri-operative dose of rituximab, and that are B7-1 negative. Future targets may also include immune markers such as MyD88 (88), CD40 (89), and TNF alpha (90, 91), components of the inflammasome (NLRP1, 3 and 6), RIG-1, MDA5, MAVS, AIM2, RAGE (32, 35), Beta catenin (77) (Figure 1), as well as potential markers of adaptive immunity. It is important to note that antibodies to nephrin (92) and CD40 (89) have also been identified as possible culprits in idiopathic nephrotic syndrome and FSGS after kidney transplantation.

6 Conclusion

Agents known primarily for their immunosuppressive effects clinically, i.e., calcineurin inhibitors, rituximab and abatacept, may be repurposed, and may impact proteinuria through podocyte-specific effects, rather than or in addition to their immunosuppressive actions (93). This paradigm shift may lead to the development of targeted therapies, guided by tissue-biomarker expression, specifically podocyte expression of SMPDL3-b (94), cGAS-STING (37) and/or B7-1 (95). Circulating factor(s) felt to be involved in the pathogenesis of FSGS may be Danger signal (DAMPs/PAMPs) mimetics (96, 97). We have shown these changes in both specific (membrane biomarkers – SMPDL3b, and B7-1) and non-specific (foot process effacement by electron microscopy) fashion in our series of post-reperfusion kidney transplant biopsies (9, 47, 60, 70). Studying the role of the podocyte in FSGS, specifically the innate immune response, with its expression of TLR's, inflammasome components, sphingolipids (SMPDL3b) and cGAS-STING and the adaptive immune response, including co-stimulatory molecules (B7-1/CD80, but not B7-2/CD86), may provide important insights into novel immune mechanisms. Hopefully, this will then lead to the discovery of new therapies based on biomarker-driven approaches (98).

It should be noted that the final song (#13, CD3) on Eric Clapton's live, three-CD set of "Crossroads Revisited" (Eric Clapton and Guests, 2016, Crossroad Concerts LLC, Rhino Entertainment Company) is "Crossroads," and Robert Johnson is appropriately credited with having written it.

Author contributions

GB wrote the manuscript. All authors contributed to the article and approved the submitted version.

Funding

This research was supported by grant NIH 1R01 DK 090316-01A1 (AlF/GB), and also through grants from the Chernowitz Foundation.

Conflict of interest

The authors declare that the research was conducted in the absence of any commercial or financial relationships that could be construed as a potential conflict of interest.

Publisher's note

Supplementary material

The Supplementary Material for this article can be found online at: https://www.frontiersin.org/articles/10.3389/fimmu.2023.1201619/full#supplementary-material

References

1. Sethi S, Glasscock RJ, Fervenza FC. Focal segmental glomerulosclerosis: towards a better understanding for the practising nephrologist. *Nephrol Dial Transplant* (2015) 30 (3):375–84. doi: 10.1093/ndt/gfu035

2. D'Agati VD, Kaskel FJ, Falk RJ. Medical progress focal segmental glomerulosclerosis. *NEngl J Med* (2011) 365:2398–411. doi: 10.1056/NEJMra1106556

3. Cravedi P, Kopp JB, Remuzzi G. Recent progress in the pathophysiology and treatment of FSGS recurrence. *Amer J Transplant* (2013) 13:266–74. doi: 10.1111/ajt.12045

4. DeVriese AS, Wetzels JF, Glassock RJ, Sehti S, Fervenza FC. Therapeutic trials in adult FSGS: lessons learned and the road forward. *Nat Rev Nephrol* (2021) 17:619–30. doi: 10.1038/s41581-021-00427-1

5. Choy BY, Chan TM, Lai KN. Recurrent glomerulonephritis after kidney transplantation. *Am J Transplant* (2006) 6:2535–42. doi: 10.1111/j.1600-6143.2006.01502.x

6. Hubsch H, Montane B, Abitbol C, Chandar J, Shariatmadar S, Ciancio G, et al. Recurrent focal l glomerulosclerosis in pediatric renal allografts: the Miami experience. *Pediatr Nephrol* (2005) 20:210–6. doi: 10.1007/s00467-004-1706-7

7. Abbott KC, Sawyers ES, Oliver JD 3rd, Ko CW, Kirk AD, Welch PG, et al. Graft loss due to recurrent focal segmental glomerulosclerosis in renal transplant recipients in the united states. *Am J Kidney Dis* (2001) 37:366–73. doi: 10.1053/ajkd.2001.21311

8. Garrouste C, Canaud G, Buchler M, Rivalan J, Colosio C, Martinez F, et al. Rituximab for recurrence of primary focal segmental glomerulosclerosis after kidney transplantation: clinical outcomes. *Transplantation* (2017) 101(3):649–56. doi: 10.1097/TP.0000000000001160

9. Chang JW, Pardo V, Sageshima J, Chen L, Tsai HL, Reiser J, et al. Podocyte foot process effacement in postreperfusion allograft biopsies correlates with early recurrence of proteinuria in focal segmental glomerulosclerosis. *Transplantation* (2012) 93 (12):1238–44. doi: 10.1097/TP.0b013e318250234a

10. Sharma M, Sharma R, Reddy SR, McCarthy ET, Savin VJ. Proteinuria after injection of human focal segmental glomerulosclerosis factor. *Transplantation* (2002) 73(3):366–72. doi: 10.1097/00007890-200202150-00009

11. Gallon L, Leventhal J, Skaro A, Kanwar Y, Alvarado A. Resolution of recurrent focal segmental glomerulosclerosis after retransplantation. *N Engl J Med* (2012) 366 (17):1648–9. doi: 10.1056/NEJMc1202500

12. Kienzl-Wagner K, Waldegger S, Schneeberger S. Disease recurrence – the sword of Damocles in kidney transplantation for focal segmental glomerulosclerosis. *Front Immunol* (2019) 10:1669. doi: 10.3389/fimmu.2019.01669

13. Fogo AB. Causes and pathogenesis of focal segmental glomerulosclerosis. *Nat Rev Nephrol* (2015) 11(2):76–87. doi: 10.1038/nrneph.2014.216

14. Konigshausen E, Sellin L. Circulating permeability factors in primary focal segmental glomerulosclerosis: a review of proposed candidates. *BioMed Res Int* (2016) 9:3765608. doi: 10.1155/2016/3765608

15. Bertelli R, Bonanni A, Di Donato A, Cioni M, Ravani P, Ghiggeri GM. Regulatory T cells and minimal change nephropathy: in the midst of a complex network. *Clin Exp Immunol* (2015) 183:166–74. doi: 10.1111/cei.12675

16. Reggiani F, Ponticelli C. Focal segmental glomerular sclerosis: do not overlook the role of immune response. *J Nephrol* (2016) 29:525–34. doi: 10.1007/s40620-016-0272-y

17. Zhang YM, Gu QH, Huang J, Qu Z, Wang X, Meng L-Q, et al. Clinical significance of IgM and C3 glomerular deposition in primary focal glomerulosclerosis. *Clin J Am Soc Nephrol* (2016) 11(9):1582–9. doi: 10.2215/CJN.01190216

18. LeBerre L, Godfrin Y, Gunther F, Buzelin F, Perretto S, Smit H, et al. Extrarenal effects on the pathogenesis and relapse of idiopathic nephrotic syndrome in Buffalo/Mna rats. *J Clin Invest* (2001) 109:491–8. doi: 10.1172/JCI0212858

19. De Oliveira JGG, Xavier P, Carvalho E, Ramos JP, Magalhaes MC, Mendes AA, et al. T Lymphocytes subsets and cytokine production by graft-infiltrating cells in FSGS recurrence post-transplantation. *Nephrol Dial Transplant* (1999) 14:713–6. doi: 10.1093/ndt/14.3.713

20. Benz K, Buttner M, Dittrich K, Campean V, Dotsch J, Amann K. Characterization of renal immune cell infiltrates in children with nephrotic syndrome. *Pediatr Nephrol* (2010) 25:1291–8. doi: 10.1007/s00467-010-1507-0

21. Pescovitz MD, Book BK, Sidner RA. Resolution of recurrent focal segmental glomerulosclerosis proteinuria after rituximab treatment. *N Eng J Med* (2006) 354:1961–3. doi: 10.1056/NEJMc055495

22. Dello Strologo L, Guzzo I, Laurenzi C, Vivarelli M, Parodi A, Barbano G, et al. Use of rituximab in focal glomerulosclerosis relapses after renal transplantation. *Transplantation* (2009) 88:417–20. doi: 10.1097/TP.0b013e3181aed9d7

23. Yabu JM, Ho B, Scandling JD, Vincenti F. Rituximab failed to improve nephrotic syndrome in renal transplant patients with recurrent focal segmental glomerulosclerosis. *Am J Transplant* (2008) 8:222–7. doi: 10.1111/j.1600-6143.2007.02021.x

24. Kufer TA, Creagh EM and Bryant CE. Guardians of the cell: effector-triggered immunity steers mammalian immune defense. *Trends Immunol* (2019) 40(10):939–51. doi: 10.1016/j.it.2019.08.001

25. Matzinger P. Tolerance, danger and the extended family. *Annu Rev Immunol* (1994) 12:991–1045. doi: 10.1146/annurev.iy.12.040194.005015

26. Pradeau T, Jaeger S, Vivier E. The speed of change: towards a discontinuity theory of immunity? *Nat Rev Immunol* (2013) 13:764–9. doi: 10.1038/nri3521

27. Eberl G, Pradeau T. Towards a general theory of immunity. *Trends Immunol* (2018) 39(4):261–3. doi: 10.1016/j.it.2017.11.004

28. Chang A KOK, Clark MR. The emerging role of the inflammasome in kidney diseases. *Curr Opin Nephrol Hypertens* (2014) 23:204–10. doi: 10.1097/01.mnh.0000444814.49755.90

29. Yamashita M, Millward CA, Inoshita H, Saikia P, Chattopadhyay S, Sen GC, et al. Antiviral innate immunity disturbs podocyte cell function. *J Innate Immun* (2013) 5(3):231–41. doi: 10.1159/000345255

30. Anders HJ, Lech M. NOD-like and toll-like receptors or inflammasomes contribute to kidney disease in a canonical and a non-canonical manner. *Kidney Int* (2013) 84(2):225–8. doi: 10.1038/ki.2013.122

31. Bao W, Xia H, Liang Y, Ye Y, lu Y, Xu X, et al. Toll-like receptor 9 can be activated by endogenous mitochondrial DNA to induce podocyte apoptosis. *Sci Rep* (2016) 6:22579. doi: 10.1038/srep22579

32. Xia H, Bao W and Shi S. Innate immune activity in glomerular podocytes. *Front Immunol* (2017) 8:122. doi: 10.3389/fimmu.2017.00122

33. Saurus P, Kuusela S, Lehtonen E, Hyvonen ME, Ristola M, Fogarty CL, et al. Podocyte apoptosis is prevented by blocking the toll-like receptor pathway. *Cell Death Dis* (2015) 6:1–12. E1752. doi: 10.1038/cddis.2015.125

34. Zhang C, Boini KM, Xia M, Abais JM, Li X, Liu Q, et al. Activation of NOD-like receptor protein 3 inflammasomes turns on podocyte injury and glomerulosclerosis in hyper homocysteinemia. *Hypertension* (2012) 60:154–62. doi: 10.1161/HYPERTENSIONAHA.111

35. Thaiss CA, Levy M, Itav S, Elinav E. Integration of innate immune signaling. *Trends Immunol* (2016) 37(2):84–101. doi: 10.1016/j.it.2015.12.003

36. Loo YM, Gale MJr. Immune signaling by RIG-i-like receptors. *Immunity* (2011) 34:680–92. doi: 10.1016/j.immuni.2011.05.003

37. Mitofanova A, Fontanella AM, Tolerico M, Mallela S, David JM, Zuo Y, et al. Activation of stimulator of interferon genes (STING) causes proteinuria and contributes to glomerular diseases. *J Am Soc Nephrol* (2022) 2021:101286. doi: 10.1681/ASN.2021.101286

38. Guey B, Ablasser A. Emerging dimensions of cellular cGAS-STING signaling. *Curr Opin Immunol* (2022) 74:164–71. doi: 10.1016/j.coi.2022.01.004

39. Margolis SR, Wilson SC and Vance RE. Evolutionary origins of cGAS-STING signaling. *Trends Immunol* (2017) 38(10):733–43. doi: 10.1016/j.it.2017.03.004

40. Zhong F, Liang S and Zhong Z. Emerging role of mitochondrial DNA as a major driver of inflammation and disease progression. *Trends Immunol* (2019) 40(12):1120–33. doi: 10.1016/j.it.2019.10.008

41. Gluck S, Ablasser A. Innate immunosensing of DNA in cellular senescence. *Curr Opin Immunol* (2019) 56:31–6. doi: 10.1016/j.coi.2018.09.013

42. Goldwich A, Burkard M, Olke M, Daniel C, Amann K, Hugo C, et al. Podocytes are nonhematopoietic professional antigen-presenting cells. *J Am Soc Nephrol* (2014) 24:906–16. doi: 10.1681/ASN.2012020133

43. Reiser J, von Gersdorff G, Loos M, Oh J, Asanuma K, Giardino L, et al. Induction of B7-1 in podocytes is associated with nephrotic syndrome. *J Clin Invest* (2004) 113:1390–7. doi: 10.1172/JCI20402

44. Moysiadis DK, Perysinaki GS, Beretsias S, Kyriacou K, Nakopoulou L, Boumpas DT, et al. Early treatment with glucocorticoids or cyclophosphamide retains the slit diaphragm proteins nephrin and podocin in experimental lupus nephritis. *Lupus* (2012) 21:1196–207. doi: 10.1177/0961203312451784

45. Paludan SR. Innate antiviral defenses independent of inducible IFN alpha/beta production. *Trends Immunol* (2016) 37(9):588–96. doi: 10.1016/j.it.2016.06.003

46. Salama AD, Pusey CD. Drug insight: rituximab in renal disease and transplantation. *Nat Clin Pract Nephrol* (2006) 2:221–30. doi: 10.1038/ncpneph0133

47. Fornoni A, Sageshima J, Wei C, Merscher-Gomez S, Aguillon-Prada R, Jauregui AN, et al. Rituximab targets podocytes in recurrent focal segmental glomerulosclerosis. *Sci Transl Med* (2011) 2011(3):85ra46. doi: 10.1126/scitranslmed.3002231

48. Perosa F, Favoino E, Caragnano MA, Dammacco F. Generation of biologically active linear and cyclic peptides has revealed a unique fine specificity of rituximab and its possible crossreactivity with acid sphingomyelinase-like phosphodiesterase 3b precursor. *Blood* (2006) 107:1070–7. doi: 10.1182/blood-2005-04-1769

49. Bezombes C, Grazide S, Garret C, Fabre C, Quillet-Mary A, Muller S, et al. Rituximab antiproliferative effect in b-lymphoma cells is associated with acid-sphingomyelinase activation in raft microdomains. *Blood* (2004) 104:1166–73. doi: 10.1182/blood-2004-01-0277

50. Faul C, Donnelly M, Merscher-Gomez S, Chang YH, Franz S, Delfgaauw J, et al. The actin cytoskeleton of kidney podocytes is a direct target of the antiproteinuric effect of cyclosporine a. *Nat Med* (2008) 14(9):931–8. doi: 10.1038/nm.1857

51. Chan AC. Rituximab's new therapeutic target: the podocyte actin cytoskeleton. *Sci Trans Med* (2011) 3(issue 85):P.85ps21. doi: 10.1126/scitranslmed.3002429

52. Yoo TH, Pedigo CE, Guzman J, Correa-Medina M, Wei C, Villareal R, et al. SMPDL3b expression levels determine podocyte injury phenotypes in glomerular disease. *J Am Soc Nephrol* (2015) 26(1):133–47. doi: 10.1681/ASN.2013111213

53. Tasaki M, Shimizu A, Hanekamp I, Torabi R, Villani V, Yamada K. Rituximab treatment prevents the early development of proteinuria following pig-to-baboon xeno-kidney transplantation. *J Am Soc Nephrol* (2014) 25(4):737–44. doi: 10.1681/ASN.2013040363

54. Takahashi Y, Ikezumi Y, Saitoh A. Rituximab protects podocytes and exerts anti-proteinuric effects in rat adriamycin-induced nephropathy independent of b-lymphocytes. *Nephrology* (2017) 22:49–57. doi: 10.1111/nep.12737

55. Heinz LX, Baumann CL, Koberlin MS, Snijder B, Gawish R, Shui G, et al. The lipid-modifying enzyme SMPDL3B negatively regulates innate immunity. *Cell Rep* (2015) 11:1919–28. doi: 10.1016/j.celrep.2015.05.006

56. Alachkar N, Weis C, Arend LJ, Jackson AM, Racusen LC, Fornoni A, et al. Podocyte effacement closely links to suPAR levels at time of posttransplantation focal segmental glomerulosclerosis occurrence and improves with therapy. *Transplantation* (2013) 96(7):649–56. doi: 10.1097/TP.0b013e31829eda4f

57. Burke GW, Chang J-W, Pardo V, Sageshima J, Chen L, Ciancio G, et al. Podocyte foot process effacement in postreperfusion allograft biopsies. *Transplantation* (2014) 97(7):e38–39. doi: 10.1097/TP.0000000000000053

58. Genovese MC, Becker JC, Schiff M, Luggen M, Sherrer Y, Kremer J, et al. Abatacept for rheumatoid arthritis refractory to tumor necrosis factor alpha inhibition. *N Engl J Med* (2005) 353:1114–23. doi: 10.1056/NEJMoa050524

59. Wekerle T, Grinyo JM. Belatacept: from rational design to clinical application. *Transplant Int* (2012) 25:139–50. doi: 10.1111/j.1432-2277.2011.01386.x

60. Yu CC, Fornoni A, Weins A, Hakroush S, Maiguel D, Sageshima J, et al. Abatacept in B7-1-positive proteinuric kidney disease. *N Engl J Med* (2013) 369:2416–23. doi: 10.1056/NEJMoa1304572

61. Baye E, Gallazzini M, Delville M, Legendre C, Terzi F, Canaud G. The costimulatory receptor B7-1 is not induced in injured podocytes. *Kidney Int* (2016) 90:1037–44. doi: 10.1016/j.kint.2016.06.022

62. Novelli R, Gagliardini E, Ruggiero B, Benigni A, Remuzzi G. Any value of podocyte B7-1 as a biomarker in human MCD and FSGS. *Am J Physiol Renal Physiol* (2016) 310:F335–41. doi: 10.1152/ajprenal.00510.2015

63. Salant DJ. Podocyte expression of B7-1/CD80: is it a reliable biomarker for the treatment of proteinuric kidney diseases with abatacept? *J Am Soc Nephrol* (2016) 27:963–5. doi: 10.1681/ASN.2015080947

64. Laszik Z, Dobi S, Vincenti F. B7-1/CD80 is not a reliable immunophenotypical marker of focal segmental glomerulosclerosis, membranous nephropathy, and diabetic nephropathy. *J Am Soc Nephrol* (2014) 25:TH–OR074.

65. Larsen CP, Messias NC, Walker PD. B7-1 immunostaining in proteinuric kidney disease. *Am J Kidney Dis* (2014) 64(6):999–1005. doi: 10.1053/j.ajkd.2014.07.023

66. Grellier J, Del Bello A, Milongo D, Guilbeau-Frugier C, Rostaing L, Kumar N. Belatacept in recurrent focal segmental glomerulosclerosis after kidney transplantation. *Transpl Int* (2015) 28:1109–10. doi: 10.1111/tri.12574

67. Delville M, Baye E, Durrbach A, Audard V, Kofman T, Braun L, et al. B7-1 blockade does not improve post-transplant nephrotic syndrome caused by recurrent FSGS. *J Am Soc Nephrol* (2016) 27(8):2520–7. doi: 10.1681/ASN.2015091002

68. Alachkar N, Carter-Monroe N, Reiser J. Abatacept in B7-1-positive proteinuric kidney disease. *N Engl J Med* (2014) 370:1263–4. doi: 10.1056/NEJMc1400502

69. Benigni A, Gagliardini E, Remuzzi G. Abatacept in B7-1-positive proteinuric kidney disease. *N Engl J Med* (2014) 370:1261–3. doi: 10.1056/NEJMc1400502

70. Burke GW III, Chandar J, Sageshima J, Ortigosa-Goggins M, Amarapurkar P, Mitrofanova A, et al. Benefit of B7-1 staining and abatacept for treatment-resistant post-transplant focal segmental glomerulosclerosis in a predominantly pediatric cohort: time for a reappraisal. *Pediatr Nephrol* (2022) 38(1):145–159. doi: 10.1007/s00467-022-05549-7

71. Cara-Fuentes G, Clapp WL, Johnson RJ, Garin EH. Pathogenesis of proteinuria in idiopathic minimal change disease: molecular mechanisms. *Pediatr Nephrol* (2016) 31:2179–89. doi: 10.1007/s00467-016-3379-4

72. Shimada M, Ishimoto T, Lee PY, Lanaspa MA, Rivard CJ, Roncal-Jimenez CA, et al. Toll-like receptor 3 ligands induce CD80 expression in human podocytes via an NF-kappa-B-dependent pathway. *Nephrol Dial Transplant* (2012) 27:81–9. doi: 10.1093/ndt/gfr271

73. Gorelik A, LX H, Illes K, Superi-Furga G, Nagar B. Crystal structure of the human alkaline sphingomyelinase provides insights into substrate recognition. *J Biol Chem* (2017) 292(17):7087–94. doi: 10.1074/jbc.M116.769273

74. Lovric S, Goncalves S, Gee HY, Oskouian B, Srinivas H, Choi W-I, et al. SGPL1 mutations cause nephrosis with ichthyosis and adrenal insufficiency. *J Clin Invest* (2017) 127(3):912–28. doi: 10.1172/JCI89626

75. Trimarchi H, Canzonieri R, Schiel A, Costales-Collaguazo C, Politei J, Stern A, et al. Increased urinary CD80 excretion and podocyturia in fabry disease. *J Transl Med* (2016) 14:289–96. doi: 10.1186/s12967-016-1049-8

76. Ishimoto T, Shimada M, Gabriela G, Kosugi T, Sato W, Lee PY, et al. Toll-like receptor 3, polyIC, induces proteinuria and glomerular CD80, and increases urinary CD80 in mice. *Nephrol DialTransplant* (2013) 28:1439–46. doi: 10.1093/ndt/gfs543

77. Li J, Niu J, Min W, Ai J, Lin X, Miao J, et al. B7-1 mediates podocyte injury and glomerulosclerosis through communication with Hsp90ab1-LRP-Beta-catenin pathway. *Cell Death Differ* (2022) 29(12):2399–416. doi: 10.1038/s41418-022001026-8

78. Shah JA, Lanaspa MA, Tanabe T, Watanabe H, Johnson RJ, Yamada K. Remaining physiological barriers in porcine kidney xenotransplantation: potential pathways behind proteinuria as well as factors related to growth discrepancies following pig-to-kidney xenotransplantation. *J Immunol Res* (2018), 6413012. doi: 10.1155/2018/6413012

79. Rivard CJ, Tanabe T, Lanaspa MA, Watanabe H, Nomura S, Andres-Hernando A, et al. Upregulation of CD80 on glomerular podocytes plays an important role in development of proteinuria following pig-to-baboon xeno-renal transplantation – an experimental study. *Transpl Int* (2018) 31(10):1164–77. doi: 10.1111/tri.13273

80. Purohit S, Piani F, Ordonez F, de Lucas-Collantes C, Bauer C, Cara-Fuentes G. Molecular mechanisms of proteinuria in minimal change disease. *Front Med December* (2021) 8:761600. doi: 10.33389/fmed.2021.761600

81. Garin EH, Reiser J, Cara-Fuentes G, Wei C, Matar D, Wang H, et al. Case series: CTLA4-IgG1 therapy in minimal change disease and focal segmental glomerulosclerosis. *Pediatr Nephrol* (2015) 30:469–77. doi: 10.1007/s00467-014-2957-6

82. Cara-Fuentes G, Venkatareddy M, Verma R, Segarra A, Cleuren AC, Martinez-Ramos A, et al. Glomerular endothelial cells and podocytes can express CD80 in patients with minimal change disease during relapse. *Pediatr Nephrol 20 June* (2020) 35:1887–96. doi: 10.1007/s00467-020-04541-3

83. Veissi ST, Smeets B, van Wijk JAE, Classens R, van der Velden TJAM, Jeronimus-Klassen A, et al. Circulating permeability factors in focal segmental glomerulosclerosis: in vitro detection. *Kidney Int Rep* (2022) 7(12):2691–703. doi: 10.1016/j.ekir.2022.09.014

84. Franz KM, Kagan JC. Innate immune receptors as competitive determinants of cell fate. *Mol Cell* (2017) 66:750–60. doi: 10.1016/j.molcel.2017.05.009

85. Luyckx VA, Bello AK. Preventing CKD in developed countries. *Kidney Int Reports March* (2020) 5(3):263–77. doi: 10.1016/j.ekir.2019.12.003

86. Chavez E, Rodriguez J, Drexler Y, Fornoni A. Novel therapies for alport syndrome. *Front Med* (2022) 9:848389. doi: 10.3389/fmed.2022.848389

87. Xue C, Dong N, Shan A. Putative role of STING-mitochondria associated membrane crosstalk in immunity. *Trends Immunol* (2022) 43(7):513–22. doi: 10.1016/j.it.2022.04.011

88. Li C, Zhang L-M, Zhang X, Huang X, Liu Y, Li M-Q, et al. Short-term pharmacological inhibition of MyD88 homodimerization by a novel inhibitor promotes robust allograft tolerance in mouse cardiac and skin transplantation. *Transplantation* (2017) 101(2):284–93. doi: 10.1097/TP.0000000000001471

89. Delville M, Sigdel TK, Wei C, Li L, Hsieh S-C, Fornoni A, et al. A circulating antibody panel for pre-transplant prediction of FSGS recurrence after kidney transplantation. *Sci Trans Med* (2014) 6(256):256ra136. doi: 10.1126/scitranslmed.3008538

90. Jain N, Khullar B, Oswal N, Banoth B, Joshi P, Ravindran B, et al. TLR- mediated albuminuria needs TNF alpha-mediated cooperativity between TLRs present in hematopoietic tissues and CD80 present on non-hematopoietic tissues in mice. *Dis Models Mech* (2016) 9:707–17. doi: 10.1242/dmm.023440

91. Pedigo CE, Ducasa GM, Leclercq F, Sloan A, Mitrofanova A, Hashmi T, et al. Local TNF causes NFATc1-dependent cholesterol-mediated podocyte injury. *J Clin Invest* (2016) 126(9):3336–50. doi: 10.1172/JCI185939

92. Watts AJB, Keller KH, Lerner G, Rosales I, Collins AB, Sekulic M, et al. Discovery of autoantibodies targeting nephrin in minimal change disease supports a novel autoimmune etiology. *J Am Soc Nephrol* (2022) 33(1):238–52. doi: 10.1681/ASN.2021060794

93. Salvadori M, Tsalouchos A. How immunosuppressive drugs may directly target podocytes in glomerular diseases. *Pediatr Nephrol July* (2022) 37(7):1431–41. doi: 10.1007/s00467-021-05196-4

94. Li G, Kidd J, Gehr TWB, Li P-L. Podocyte sphingolipid signaling in nephrotic syndrome. *Cell Physiol Biochem* (2021) 55(Suppl 4):13–34. doi: 10.33594/000000356

95. Haraldsson B. A new era of podocyte-targeted therapy for proteinuric kidney disease. *N Eng J Med* (2013) 369(25):2453–4. doi: 10.1056/NEJMe1312835

96. Couser WG, Johnson RJ. The etiology of glomerulonephritis: roles of infection and autoimmunity. *Kidney Int* (2014) 86:905–14. doi: 10.1038/ki.2014.49

97. Reiser J, Mundel P. Danger signaling by glomerular podocytes defines a novel function of inducible B7-1 in the pathogenesis of nephrotic syndrome. *J Am Soc Nephrol* (2004) 15(9):2246–8. doi: 10.1097/01.ASN0000136312.46464.33

98. Wang C-S, Smoyer WE, Cara-Fuentes G. Glomerular B7-1 staining: toward precision medicine for treatment of recurrent focal segmental glomerulosclerosis. *Pediatr Nephrol* (2022) 38(1):13–15. doi: 10.1007/s0047-022-05659-x

frontiers | Frontiers in Immunology

TYPE Original Research
PUBLISHED 29 August 2023
DOI 10.3389/fimmu.2023.1253514

OPEN ACCESS

EDITED BY
Guido Moll,
Charité University Medicine Berlin, Germany

REVIEWED BY
Alexander Hackel,
University of Schleswig-Holstein, Lübeck, Germany
Lionel Le Bourhis,
Institut National de la Santé et de la Recherche Médicale (INSERM), France

*CORRESPONDENCE
Kai Hildner
kai.hildner@uk-erlangen.de

RECEIVED 05 July 2023
ACCEPTED 14 August 2023
PUBLISHED 29 August 2023

CITATION
Matthe DM, Dinkel M, Schmid B, Vogler T, Neurath MF, Poeck H, Neufert C, Büttner-Herold M and Hildner K (2023) Novel T cell/organoid culture system allows *ex vivo* modeling of intestinal graft-versus-host disease. *Front. Immunol.* 14:1253514. doi: 10.3389/fimmu.2023.1253514

Novel T cell/organoid culture system allows *ex vivo* modeling of intestinal graft-versus-host disease

Diana M. Matthe[1,2], Martin Dinkel[1,2], Benjamin Schmid[3], Tina Vogler[1,2], Markus F. Neurath[1,2], Hendrik Poeck[4], Clemens Neufert[1,2], Maike Büttner-Herold[5] and Kai Hildner[1,2]*

[1]Department of Medicine 1, Kussmaul Campus for Medical Research, University Hospital Erlangen, University of Erlangen-Nuremberg, Erlangen, Germany, [2]Deutsches Zentrum Immuntherapie (DZI), University Hospital Erlangen, Erlangen, Germany, [3]Optical Imaging Centre Erlangen (OICE), University of Erlangen-Nuremberg, Erlangen, Germany, [4]Clinic and Polyclinic for Internal Medicine III, University Hospital Regensburg, Regensburg, Germany, [5]Department of Nephropathology, Institute of Pathology, Friedrich-Alexander-University Erlangen-Nuremberg (FAU) and University Hospital, Erlangen, Germany

Acute graft-versus-host disease (GvHD) remains the biggest clinical challenge and prognosis-determining complication after allogeneic hematopoietic stem cell transplantation (allo-HSCT). Donor T cells are acceptedly key mediators of alloreactivity against host tissues and here especially the gut. In support of previous studies, we found that the intestinal intra-epithelial lymphocyte (IEL) compartment was dynamically regulated in the course of MHC class I full mismatch allo-HSCT. However, while intestinal epithelial cell (IEC) damage endangers the integrity of the intestinal barrier and is a core signature of intestinal GvHD, the question whether and to what degree IELs are contributing to IEC dysregulation is poorly understood. To study lymphoepithelial interaction, we employed a novel *ex vivo* T cell/organoid co-culture model system. Here, allogeneic intra-epithelial T cells were superior in inducing IEC death compared to syngeneic IEL and allogeneic non-IEL T cells. The ability to induce IEC death was predominately confined to TCRβ+ T cells and was executed in a largely IFNγ-dependent manner. Alloreactivity required a diverse T cell receptor (TCR) repertoire since IELs genetically modified to express a TCR restricted to a single, non-endogenous antigen failed to mediate IEC pathology. Interestingly, minor histocompatibility antigen (miHA) mismatch was sufficient to elicit IEL-driven IEC damage. Finally, advanced live cell imaging analyses uncovered that alloreactive IELs patrolled smaller areas within intestinal organoids compared to syngeneic controls, indicating their unique migratory properties within allogeneic IECs. Together, we provide here experimental evidence for the utility of a co-culture system to model the cellular and molecular characteristics of the crosstalk between IELs and IEC in an allogeneic setting *ex vivo*. In the light of the emerging concept of dysregulated immune-epithelial homeostasis as a core aspect of intestinal GvHD, this

approach represents a novel experimental system to e.g. screen therapeutic strategies for their potential to normalize T cell/IEC- interaction. Hence, analyses in pre-clinical *in vivo* allo-HSCT model systems may be restricted to hereby positively selected, promising approaches.

KEYWORDS

graft-versus-host disease, GvHD, allogeneic hematopoietic stem cell transplantation, intestinal organoids, epithelial cell death, alloreactive T cell, *ex vivo* model, intraepithelial lymphocytes

1 Introduction

GvHD (graft-versus-host diesase) is a common and severe complication after hematopoietic stem cell transplantation (HSCT) which affects up to 50% of patients and represents the primary cause of post-transplant mortality (1, 2). Pathomechanistically, donor T lymphocytes are considered to function as the central effector cell mediating GvHD development and progression. These so-called alloreactive T cells are activated by recognizing foreign (allogeneic) host antigens presented on MHC molecules, which leads to their secretion of inflammatory cytokines, amongst others IL-2 or IFNγ (3). In turn, these cytokines can induce tissue damage either directly, but also indirectly by sensitizing or activating other immune cells and thereby amplifying the inflammatory process (4).

Recent progress in the field has revealed that T cells and T cell-derived mediators are not only driving systemic and local inflammatory circuits but also actively drive GvHD-associated epithelial cell damage in the gut (5, 6). This is critical as, apart from the skin, the gastrointestinal (GI) tract is most frequently affected, and involvement of the lower GI tract is most associated with non-relapse mortality (7). GI GvHD may clinically present with nausea, diarrhea, abdominal cramps or gastrointestinal bleeding, causing considerable morbidity (8). Moreover, the T cell-mediated destruction of the intestinal epithelium abrogates critical mucosal barrier functions, thereby exacerbating patients' burden by causing malabsorption and malnutrition (8).

Mechanistically, especially T cell-derived type II interferon, IFNγ, has been identified to directly interfere with intestinal epithelial cell homeostasis as it negatively regulates intestinal stem cell maintenance and recovery in the course of intestinal GvHD (5). Interestingly, despite the fact that the intra-epithelial lymphocyte (IEL) compartment contains a significant IFNγ-expressing T cell pool naturally populating the intestinal epithelial cell (IEC) layer (9), the cell type-specific contribution of IELs in the context of IFNγ-driven epithelial cell pathology has not been studied in detail.

Small intestinal (SI) IELs represent a heterogenous cell pool that largely consists of T lymphocytes, which are assumed to be predominately tissue-resident, antigen-experienced T cells (10–12). They can be subdivided into induced ($CD4^+$ or $CD8\alpha\beta^+$ $TCR\alpha\beta^+$) and natural ($CD4^-CD8\alpha\beta^-$ or $CD8\alpha\alpha^+$, $TCR\alpha\beta^+$ or $TCR\gamma\delta^+$) IEL subsets (10, 13). While the development of natural IELs is not yet fully understood, they are considered to predominantly respond to self-antigens rather than foreign ligands (10, 13). Induced IELs originate from conventional $CD4^+$ or $CD8\alpha\beta^+$ $TCR\alpha\beta^+$ MHC-restricted T cells that underwent selection in the thymus and migrated to the gut after encountering non-self antigens in the periphery (10, 13). Due to their unique positioning at the mucosal barrier site, IELs are functionally tissue site-specific memory cells involved in the local protection against recurring infections, thereby ensuring the integrity of the intestinal epithelial lining. However, IELs have been also implicated to exert harmful pro-inflammatory effects under pathologic conditions as e.g. in inflammatory bowel disease or coeliac disease (9, 10, 13).

In the context of allo-HSCT, previous studies by others found that donor T cells indeed populate the recipient IEL compartment (14–16). However, the nature and characteristics of IEL/IEC interaction in the small intestine in the allogeneic setting have not been addressed yet. This is in part attributed to technical difficulties, since IELs are prone to apoptosis *ex vivo* (17). However, groundbreaking work showing that small intestinal (SI) organoids closely mimicking small intestinal epithelial cell structures found *in vivo* can be generated and expanded *ex vivo* from $Lgr5^+$ intestinal stem cells (18) has paved the way for novel methodological approaches to study IEL biology. So progress by our group and others (17, 19, 20) demonstrating that SI organoids offer an appropriate microenvironment to stably culture IELs *ex vivo* has opened up new avenues to analyze IEL biology under physiological conditions, i.e. within the intestinal epithelial layer.

Here we sought to further apply this experimental concept to establish and initially characterize the SI IEL/IEC cross-talk in the allogeneic setting *ex vivo*. Data obtained by employing this novel allogeneic IEL/IEC co-culture model system demonstrate unique functional and migratory properties of IEL-resident T cells and disclose their significant impact on IEC integrity. We propose this model system to be a robust experimental platform providing so far undisclosed insight into IEL/IEC interaction potentially leading to the discovery of new therapeutic targets for the treatment of GvHD in the future.

2 Materials and methods

2.1 Mice

Mouse lines used in this study were either purchased from commercial vendors (Charles River Laboratories, Janvier Labs, The

Jackson Laboratory) or bred in-house. The animals were kept in individually ventilated cages under specific-pathogen free conditions in the animal facilities of either Präklinisches Experimentelles Tierzentrum (PETZ) or Department of Medicine 1, Universitätsklinikum Erlangen. C.B10-H2 b/LilMcdJ mice and B6.129S7-Ifngtm1Ts/J mice were purchased from The Jackson Laboratory. CD45.1/Ly5.1 B6.SJL-*Ptprc*^{a}*Pepc*^{b}/BoyCrl and C57BL/6-Tg(TcraTcrb)1100Mjb/Crl (OTItg) mice were obtained from Charles River Laboratories. C57BL/6J mice are referred to as "B6" throughout the study. Experiments using T cells isolated from Ifng$^{+/+}$ and Ifng$^{+/-}$ littermates yielded comparable results. Therefore, data from mice of both genotypes were pooled and used as a "Ifng$^{+/+}$" control group for Ifng$^{-/-}$ mice. This study was carried out in accordance with the current legislation and the guidelines of the government of Lower and Middle Franconia and animal experiments were approved by the government of Middle Franconia in Bavaria, Germany (54.2532.1 – 24/11-3).

2.2 Murine allo-HSCT and induction of acute GvHD *in vivo*

GvHD was induced as described before (21, 22). In short, female 10-12 week old Balb/c mice were lethally irradiated with 8 Gy total body irradiation at d0. On the next day, recipient mice received 5×10^6 T cell depleted bone marrow (BM) cells from CD45.1/Ly5.1 B6.SJL-*Ptprca Pepcb*/BoyCrl mice intravenously (i.v.). On d2 after irradiation, recipient mice were i.v. injected with 0.7×10^6 allogeneic CD3$^+$ splenocytes from B6 wildtype mice. BM and splenocyte cell suspensions were enriched for the desired cell populations using magnetic separation and anti-CD90.2 microbeads (Miltenyi Biotec) or the Mouse Pan T Cell Isolation Kit II (Miltenyi Biotec), respectively, according to the manufacturer's instructions. Control animals only received T cell depleted BM, but no CD3$^+$ splenocytes.

2.3 Isolation of intestinal crypts and organoid culture

To generate organoids, small intestinal (SI) crypts were isolated from female B6 or Balb/c mice (>8 weeks) to obtain stem cells for the establishment of organoid cultures. For this, mice were sacrificed, the small intestine was removed and placed in cold PBS. The intestine was then flushed with cold PBS, opened longitudinally and the villi were carefully scratched off using a cover slip. The organ was then cut into 0.5 cm pieces and put into a tube with cold PBS. The tissue pieces were thoroughly washed by pipetting up and down with a 25 ml serological pipette, repeating this step with fresh PBS until the solution was clear. SI tissue was then digested for 30-40 min at 4 °C on a MACSmix Tube Rotator (Miltenyi Biotec) in 30 ml PBS + 2 mM EDTA. After the incubation time, the digestion solution was removed by passing through a 100 µm cell strainer. The remaining tissue pieces were then placed into 10 ml fresh cold PBS and vigorously vortexed to mechanically isolate the intestinal crypts. Crypts were collected on ice by passing through a 70 µm cell strainer. The tissue pieces were mixed again with 10 ml fresh cold PBS and the previous step was repeated for a total of five times. The intestinal stem cell-containing crypts were then pelleted by centrifugation at 300 g, 4°C for 5 min and washed one time with PBS and one time with *basal crypt media* (BCM) consisting of Advanced DMEM/F-12 (Gibco) + 1% Penicillin/Streptomycin (Sigma-Aldrich) + 10 mM HEPES (Sigma-Aldrich) + 1% GlutaMAX (Gibco). The presence of successfully isolated crypts was confirmed in a cell culture microscope (Leica DMIL LED) followed by plating crypts in a 1:1 mixture of BCM with Matrigel (Corning) in 24-well-plates. After polymerization of the Matrigel dome at 37° C for 25-30 min, 0.5 ml *crypt culture media* (CCM) consisting of BCM + 1X B-27 supplement (Gibco) + 1 mM N-Acetyl-L-cysteine (Sigma-Aldrich) + 20 ng/ml rmEGF (Immunotools) + 100 ng/ml rmNoggin (PeproTech) + 10% R-Spondin (culture supernatant from R-Spondin producing cell line) was added per well.

To study cytokine-mediated effects on Fas expression regulation by organoids in isolation, organoids generated as described above were passaged by washing in cold PBS and then resuspended in 50 µl of a 1:1 mixture of PBS and Matrigel (Corning). After plating the organoids in a 48-well-plate and polymerization of the Matrigel dome, 300 µl of CCM containing either no additional cytokines as unstimulated control, 10 ng/ml rmTNFα (Immunotools), 10 ng/ml rmIFNγ (Peprotech) or a combination of 10 ng/ml rmTNFα + 10 ng/ml rmIFNγ was added per well. On d2, organoids were harvested and single cell suspensions of organoids were generated as described below (cf. 2.6.4) and stained with EpCAM-Alexa Fluor 488 (Biolegend) and Fas-APC (Biolegend) for 15 min at 4°C in FACS buffer (PBS + 3% FCS).

2.4 Isolation of T cells

T cells for co-cultures were isolated from naïve, unmanipulated mice. As IEL or splenocyte donors, mice irrespective of their sex and between 8 and 17 weeks (mean: 11.2 weeks) of age were used.

2.4.1 Isolation and magnetic-activated cell sorting (MACS)-mediated enrichment of SI IEL T cells

For the isolation of SI IELs, mice were sacrificed and the SI was taken and kept in PBS solution on ice. The intestine was flushed with cold PBS and Peyer's patches were removed. The organ was opened longitudinally, washed by vigorously moving it in PBS, and then cut into 0.5 cm pieces which were placed into 20 ml of pre-warmed predigestion solution consisting of HBSS (Sigma-Aldrich) + 10 mM HEPES + 5 mM EDTA + 5% FCS (Pan Biotech) + freshly added 1 mM Dithiothreitol (Sigma-Aldrich). After 20 min incubation at 37 °C on a shaker, the predigestion solution containing the tissue pieces was vortexed for 20-30 sec and then passed through a 100 µm cell strainer. The flow-through fraction containing IELs was collected and kept on ice. The tissue pieces were placed again in 20 ml of fresh predigestion solution and the described step was repeated one more time. Next, the remaining tissue pieces were incubated for 20 min at 37 °C on a shaker in 10 ml

of HBSS + 10 mM HEPES. In the meantime, approximately 35 ml of the collected flow-through from the predigestion steps were transferred into a new tube, thereby discarding any debris that had sedimented on the bottom. After the last incubation step, the tissue pieces were vortexed and passed through a 100 µm cell strainer. Next, leukocytes were isolated by density centrifugation. For this, the pooled flow-through from the predigestion steps and the HBSS steps was pelleted by centrifugation at 300 g, 4 °C, 5 min, resuspended in 40 % Percoll (Cytiva) in complete media (DMEM high glucose (Gibco) + 10 % FCS + 1 % Penicillin/Streptomycin) and overlayed on 70 % Percoll in HBSS. After centrifugation at 2500 rpm, RT, 20 min without brakes, lymphocytes enriched in the interphase were collected and washed in MACS buffer (PBS + 2 mM EDTA + 0.5 % bovine serum albumin (Sigma-Aldrich)).

To further enrich for T cells of interest within the IEL fraction, positive magnetic cell separation was performed. For this, IELs were labeled either with anti-CD3-Biotin (Biolegend), anti-CD3-PE (Biolegend), anti-CD8a-PE (Biolegend), anti-CD8a-Biotin (Biolegend), anti-TCRγδ-PE (Biolegend) or anti-TCRβ-PE (Biolegend) for 15 min at 4 °C depending on the application as indicated in the figure legends. The cells were then washed with 2 ml MACS buffer, resuspended in 80 µl MACS buffer and 20 µl of respective magnetic beads (anti-PE MicroBeads UltraPure (Miltenyi Biotec) or anti-Biotin MicroBeads (Miltenyi Biotec)) per 10^6 cells and incubated for 15 min at 4 °C. After another washing step with 2 ml MACS buffer, the cells were resuspended in 500 µl MACS buffer and passed through pre-wetted magnetic LS columns, which were washed with 3 x 3 ml MACS buffer. The flow-through fraction containing unlabeled cells was discarded, whereas the magnetically labeled cells of interest were collected by flushing the column with a plunger upon removal of the column from the magnet. Purity was checked by flow cytometry and was routinely >95 % of $CD3^+$ cells within lymphocytes. After magnetic separation, T cells were resuspended in BCM for further steps.

2.4.2 Isolation of splenocytes

Splenocytes were obtained by removing the spleen from sacrificed mice, followed by dissociating the splenic tissue by mashing and passing it through a 40 µm cell strainer. After centrifugation, red cell lysis was performed by resuspending the cell pellet in 3 ml ammonium-chloride-potassium lysis buffer (0.15 M NH_4Cl, 10 mM $KHCO_3$, 100 µM Na_2EDTA) for 3 min. To optimize purity while also maintaining comparability in treatment between IELs and splenocytes, T cells were first enriched by negative magnetic separation using the Pan T Cell Isolation Kit II, mouse (Miltenyi Biotec) according to the manufacturer's protocol and in a second step, positive magnetic cell enrichment (anti-CD8a-Biotin, Biolegend) as described above (2.4.1) was performed.

2.5 Allogeneic T cell/organoid co-culture

Allogeneic co-cultures were started 2-4 days after crypt isolation. At this time point, grown organoids were harvested from the 24-well-plates with cold PBS, washed twice with cold PBS and resuspended in BCM. Approximately 100 organoids were mixed with 2.5 x 10^5 magnetically enriched T cells (cf. 2.4.1/.2) in BCM in a 48-well-plate and incubated for 30 min at 37 °C. After that, organoids and T cells were harvested again from the well with cold PBS, spun down, resuspended in 50 µl of a 1:1 mixture of PBS and Matrigel (Corning) and plated in a 48-well-plate. Lastly, after polymerization of the Matrigel dome, 300 µl of CCM + 10 ng/ml rmIL-7 (Immunotools) + 10 ng/ml rmIL-15 (Immunotools or R&D systems) + 100 IU/ml recombinant human (rh) IL-2 (Immunotools) were added per well.

2.6 Analyses after co-culture

Endpoint analyses were routinely performed on day 2 after start of the co-culture, unless indicated otherwise.

2.6.1 Fluorometric cell death quantification

Fluorometric quantification of cell death among organoids after co-culture was based on Bode, Mueller et al., 2019 (23). In more detail, cell-free supernatants were harvested by carefully pipetting off the liquid phase. The organoids were stained for 30 min at 37 °C in 250 µl/well BCM + 10 µg/ml propidium iodide (Invitrogen) + 10 µg/ml Hoechst 33342 (Invitrogen). After incubation, the wells were carefully washed three times with warm PBS to avoid disruption of the Matrigel dome. Fluorescence intensities within the wells were measured in PBS using a Tecan infinite M200 platereader in the setting "multiple reads per well (circle (filled))" with 1 mm border. For propidium iodide (PI) detection, the excitation wavelength was set to 535 nm and the emission wavelength 617 nm. Hoechst dye was excited at 361 nm and its emission was detected at 486 nm. After the platereader measurement, PBS was replaced by CCM and fluorescence microscopy pictures were taken on a Leica DMI4000 B inverted microscope. The intensity signal of the cell-permeable dye Hoechst was used to normalize for cell numbers in each well, while the extent of the uptake of the cell-impermeable dye PI reported the amount of cell death per well. Thereby, the PI/Hoechst ratio reports the relative cell death present in an assayed well, importantly in a – due to this normalization algorithm – seeding density-independent manner. To correct for physiological baseline cell death, the measured basal cell death, i.e. PI/Hoechst ratio from the respective organoid controls cultured without T cells was subtracted from PI/Hoechst ratios obtained by fluorometric microplate reader measurement from wells of the syngeneic (B6 organoids) and allogeneic (Balb/c organoids) co-culture conditions.

2.6.2 Digital image analysis

To quantify the PI/Hoechst ratios in microscopic images, three representative pictures were taken on a Leica DMI4000 B inverted microscope with a 5X objective and analyzed in Fiji/ImageJ software (version 2.1.0/1.5.3v) by splitting the color channels and measuring the mean intensities for each of the fluorescent dyes. Mean intensities of PI were then normalized to Hoechst intensity, as described above (2.6.1).

2.6.3 Three-dimensional (3D)-rendered images

To obtain 3D-rendered images of co-cultures, B6 (allogeneic) CD3+ enriched IELs were stained with 1 µM Cell Proliferation Dye eFluor 670 (eBioscience) according to the protocol provided by the manufacturer on d0 prior co-culturing. Then, co-cultures of labeled T cells and previously grown B6 (syngeneic)- or Balb/c (allogeneic)-derived SI organoids were started by plating in a µ-Slide 4 Well chamber slide (ibidi). On d2, co-cultures were stained with PI and Hoechst and washed as described above (2.6.1.). Z-stacks of whole organoids were taken at a Leica TCS SP5 II confocal microscope with a 63X objective, with 1 µm distance between slices.

Post-processing of imaging data was performed in Fiji/ImageJ software (version 2.1.0/1.5.3v). To improve the resolution in z, the number of slices was interpolated to approximately match the voxel depth to the pixel width and pixel height. 3D-rendering and -animation were achieved using the plugin 3Dscript (24).

2.6.4 Flow cytometry

To prepare single-cell suspensions for flow cytometry, co-cultures were washed with cold PBS and incubated for 3 x 5 min at 37 °C in 1 ml TrypLE (Gibco). In between incubation steps, co-cultures were vortexed vigorously for 10 sec to mechanically dissociate the organoids. After the last incubation step, TrypLE was stopped by addition of cold PBS, and the cell suspension was spun down (300 g, 5 min, 4 °C). Prior to staining, cells were strained through a 100 µm mesh to remove any residual cell aggregates. To assess apoptotic cells after co-culture, cells were first incubated with CD3-APCCy7 (Biolegend), EpCAM-Alexa Fluor 488 (Biolegend) and Fas-APC (Biolegend) for 15 min at 4 °C in FACS buffer (PBS + 3 % FCS) and then washed with FACS buffer. Then, they were stained for 15 min at RT with Annexin V in Binding Buffer from the eBioscience™ Annexin V Apoptosis Detection Kit eFluor™ 450 (Invitrogen). For the analysis of IEL subpopulations and FasL expression after co-culture, cells were stained with TCRβ-Pacific Blue (Biolegend), TCRγδ-PECy7 (Biolegend), CD4-Brilliant Violet 605 (Biolegend, 100451), CD8a-APCCy7 (Biolegend), CD8b-Alexa Fluor 700 (Biolegend) for 15 min at 4 °C in FACS buffer.

To measure granzyme B and perforin protein expression in T cells by flow cytometry, an intracellular staining protocol was applied. Briefly, single cell suspensions resuspended in DMEM (gibco) + 1 % P/S + 10 % FCS were plated in a 48-well-plate and stimulated with 50 ng/ml phorbol myristate acetate (PMA, Sigma-Aldrich) and 1 µM ionomycin (Sigma-Aldrich) at 37 °C. After 1 h, 1 mg/ml Brefeldin A (Sigma) was added to the cell culture followed by additional 3 h incubation at 37 °C. Then, cells were harvested, washed and stained with a LIVE/DEAD™ Fixable Aqua Dead Cell Stain Kit (Invitrogen) according to the manufacturer's protocol. Next, cells were stained extracellularly with TCRβ-Pacific Blue (Biolegend) and TCRγδ-PECy7 (Biolegend) for 15 min at 4 °C in FACS buffer. After that, cells were fixed in 2 % formaldehyde (Carl Roth) in PBS for 15 min at RT. Subsequent to fixation, cells were washed with FACS buffer and resuspended in 0.05 % saponin in FACS buffer for permeabilization. Cells were stained intracellularly with Perforin-APC (Biolegend) and Granzyme B-FITC (Biolegend) in 0.5 % saponin in FACS buffer for 30 min at 4 °C followed by extensive washing steps prior resuspension in FACS buffer and analysis at the FACS machine.

Stained cells were measured on a LSRFortessa™ Cell Analyzer (BD) and analyzed in FlowJo™ software (FlowJo™ Software (for Windows) [software application] Version 10.6.2. Ashland, OR: Becton, Dickinson and Company; 2019).

2.6.5 Real-time quantitative PCR

For gene expression analysis after co-culture, supernatants were removed and organoids were harvested using 350 µl RLT lysis buffer (Qiagen) + 4 % Dithiotreitol (Sigma-Aldrich) per well. RNA was isolated using the RNeasy Micro Kit (Qiagen) and measured on a Nanodrop. Then, 500-1000 ng of RNA were reversely transcribed to cDNA using the iScript™ cDNA Synthesis Kit (Bio-Rad). Realtime-PCR was performed using iQ™ SYBR® Green Supermix (Bio-Rad) in a CFX Connect or CFX96 Real-Time PCR Detection system (Bio-Rad). Primers included: *Hprt* (for: TGGATACAGGCCAGACTTTGTT, rev: CAGATTCAACTTGCGCTCATC) *Lgr5* (for: GACTTTAACTGGA GCAAAGATCTCA; rev: CGAGTAGGTTGTAAGACA AATCTAGC), *Olfm4* (Mm_Olfm4_2_SG QuantiTect Primer Assay Qiagen, QT01557052), *Ifng* (for: ATCTGGAGGAACTGGCAAAA, rev: TGAGCTCATTGAATGCTTGG), *Tnf* (for: CTTGTGGCAG GGGCCACCAC, rev: CCATGCCGTTGGCCAGGAGG), *Gzmb* (Mm_Gzmb_1_SG QuantiTect Primer Assay Qiagen, QT00114590), *Prf1* (for: CCACTCCAAGGTAGCCAAT, rev: GGAGATGA GCCTGTGGTAAG), *Fasl* (for: CGTGAGTTCACCAACCAAAG, rev: TGTGTCTTCCCATTCCAGAG). Data were analyzed by employing the ddCT method. For epithelial-specific genes (*Lgr5, Olfm4*), the expression levels in the co-cultures were normalized so that the expression levels detected in the respective wells of organoids cultured without T cells equaled 1. That means, the syngeneic condition (B6 T cells + B6 organoids) was normalized to the expression level of B6 organoids alone and the allogeneic sample (B6 T cells + Balb/c organoids) was normalized to the Balb/c organoid w/o T cell control. For the T cell-centered gene expression analyses (*Ifng, Tnf, Gzmb, Prf1, Fasl*), gene expression levels were normalized to levels detected in samples derived from syngeneic co-culture.

2.6.6 Enzyme-linked immunosorbent assay

Cell-free supernatants were assayed for IFNγ protein concentrations *via* ELISA using the IFN gamma Mouse Uncoated ELISA Kit (Invitrogen) according to the manufacturer's protocol and measured in a Tecan infinite M200 platereader. For the quantification of murine IL-2 protein concentration in cell-free supernatants, the ELISA MAX™ Standard Set Mouse IL-2 (Biolegend) was used according to the manufacturer's protocol and measured in a Tecan infinite M200 platereader. It was experimentally verified that this kit was specifically detecting murine IL-2 but not recombinant human IL-2 that was added as a media supplement (cf. 2.5).

2.6.7 Live imaging and migration analysis

Live imaging of the co-culture was performed on d1 on a Zeiss Spinning Disc Axio Observer Z1 microscope at the Optical Imaging Centre Erlangen (OICE) as described before (25). In short, B6

(allogeneic) CD3+ IELs were stained with 1 µM Cell Proliferation Dye eFluor 670 (eBioscience) according to the manufacturer's protocol on d0 and co-cultures of labeled IELs and previously grown B6 (syngeneic)- or Balb/c (allogeneic)-derived SI organoids were plated in a µ-Slide 4 Well chamber slide (ibidi). During the imaging process, the samples were incubated in a 37 °C, 5 % CO_2 chamber and pictures were taken every 30 sec for 45 min using a 25X objective.

Subsequent analysis was also performed as described before (19): Data was imported into Fiji/ImageJ software (version 2.1.0/1.5.3v) using Bio-Formats (26). To assess T cell migration within organoids, the plugin TrackMate (27) was applied with the following settings: LoG (Laplacian of Gaussian) detector with an estimated blob diameter of 7 µm and a threshold of 40-120 (depending on experiment), Simple LAP tracker (Linear Assignment Problem) with linking maximum distance and gap-closing maximum distance both set to 15 µm and gap-closing maximum frame gap of 2 µm. For speed analysis, tracks with a speed below 0.05 µm per second were excluded. To calculate the organoid area patrolled by T cells within the recorded time frame of 45 min, an in-house Fiji macro was applied to the output of TrackMate to sum up the area enclosed by 7 µm around the T cell tracks and relating it to the epithelial area as determined by a manually drawn region of interest, omitting the organoid lumen.

2.6.8 Immunohistochemistry

Staining for CD3ε protein expression was performed on paraffin-embedded co-cultures or SI tissue sections from mice previously undergoing allo-HSCT as indicated (cf. section 2.2). For this purpose, co-cultures were washed with cold PBS, resuspended in HistoGel™ Specimen Processing Gel (Epredia), fixed in ROTI®Histofix 4.5 % formaldehyde (Carl Roth) and embedded in paraffin. After deparaffinization, slides were pre-treated by cooking the slides 2.5 min in Target Retrieval Solution pH 6 (Dako). After blocking endogenous peroxidase by incubation with 30 % H_2O_2 (Carl Roth) for 10 min and subsequently blocking with Avidin/Biotin for 15 min each (Avidin/Biotin Blocking Kit, Vector Laboratories), the slides were incubated with the primary antibody (rat anti-CD3, Bio-Rad) diluted 1:200 in 1% BSA overnight. Thereafter, slides were washed and incubated with the secondary antibody (biotinylated rabbit anti-rat IgG, Vector Laboratories) diluted 1:500 for 30 min. For signal detection, slides were treated with the VECTASTAIN® Elite® ABC-HRP Kit, Peroxidase (Vector Laboratories) according to the manufacturer's protocol and with the ImmPACT® DAB Substrate Kit, Peroxidase (HRP) (Vector Laboratories) as chromogen for 2.5 min. Finally, slides were counterstained with hematoxylin. Representative images were taken on a Leica DMI4000 B inverted microscope.

2.6.9 Immunofluorescence

For immunofluorescence staining of cleaved caspase-3 protein, co-cultures were plated in µ-Slide 8 Well chamber slides (ibidi) on d0. Cleaved caspase-3 staining was performed on d1. For this, samples were fixed for 30-40 min with 4 % paraformaldehyde in PBS at RT, washed with PBS, permeabilized for 10 min with 0.1 % Triton X-100 (Sigma-Aldrich) in PBS at RT and blocked with histobuffer (10 % FCS, 5 % BSA in PBS) for 1 h at RT. Organoids were stained with anti-cleaved Caspase 3 AF648 (BD Biosciences) and anti-EpCAM-AF488 (BioLegend) diluted 1:100 and 1:200, respectively, in histobuffer overnight at 4 °C. The next day, the samples were washed three times with PBS. Nuclei were counterstained for 5 min with Hoechst 33342 (Invitrogen) diluted 1:10000 in PBS. After washing one time with A.d., the slides were mounted with Mowiol 4-88 (Carl Roth). Images were taken with a Leica TCS SP5 II confocal microscope using a 63X objective.

2.6.10 Statistical analysis

Statistical analyses were performed using GraphPad Prism software (version 9.5.1). For the comparison of two groups, a two-tailed unpaired t test was employed with a significance level of 5 %. In case of statistical inequality of variances, a Welch's correction was applied to the t test where indicated in the figure captions. For the comparison of more groups, a one-way ANOVA with a *post-hoc* analysis (Šídák's multiple comparisons test) with a significance level of 5 % was applied.

3 Results

3.1 Allogeneic IEL T cells co-cultured with SI organoids *ex vivo* mirror *in vivo* behavior of donor T cells

Intestinal T cells play a major role in the pathogenesis of intestinal GvHD. However, detailed insight into the disease-specific role of anatomically distinct T cell subsets is sparse. As previously shown by others (14–16), we confirmed that the SI epithelial layer of mice previously undergoing allo-HSCT using a MHC class I full mismatch model system is densely populated with T cells compared to control mice receiving T cell-depleted, allogeneic bone marrow alone (Figure 1A). While this correlative data suggests that IELs may contribute to the dysfunction of small intestinal epithelial cells (IECs) during intestinal GvHD, functional evidence in support of this assumption is lacking. To further explore and characterize allogeneic IEL/IEC interaction *ex vivo*, we adopted a previously reported syngeneic IEL/IEC co-culture model system (19). For this, we magnetically isolated T cells from the SI IEL fraction of healthy naïve B6 mice and cultured those within allogeneic SI organoids that were previously generated *ex vivo* from intestinal stem cell-containing small intestinal crypt preparations of Balb/c (allogeneic) or B6 mice (syngeneic controls) (Figure 1B). On day 2 of co-culture, both allogeneic and syngeneic organoids were densely populated by $CD3^+$ IELs (Figure 1C). Organoid-residing allogeneic IELs expressed significantly higher levels of IL-2 and IFNγ compared to syngeneic T cells both on the transcriptional and on protein level (Figures 1D, E). Overall, our data indicate that IEL-derived allogeneic T cells can be cultured within SI organoids *ex vivo* and show signs of alloreactive activation.

10.3389/fimmu.2023.1253514

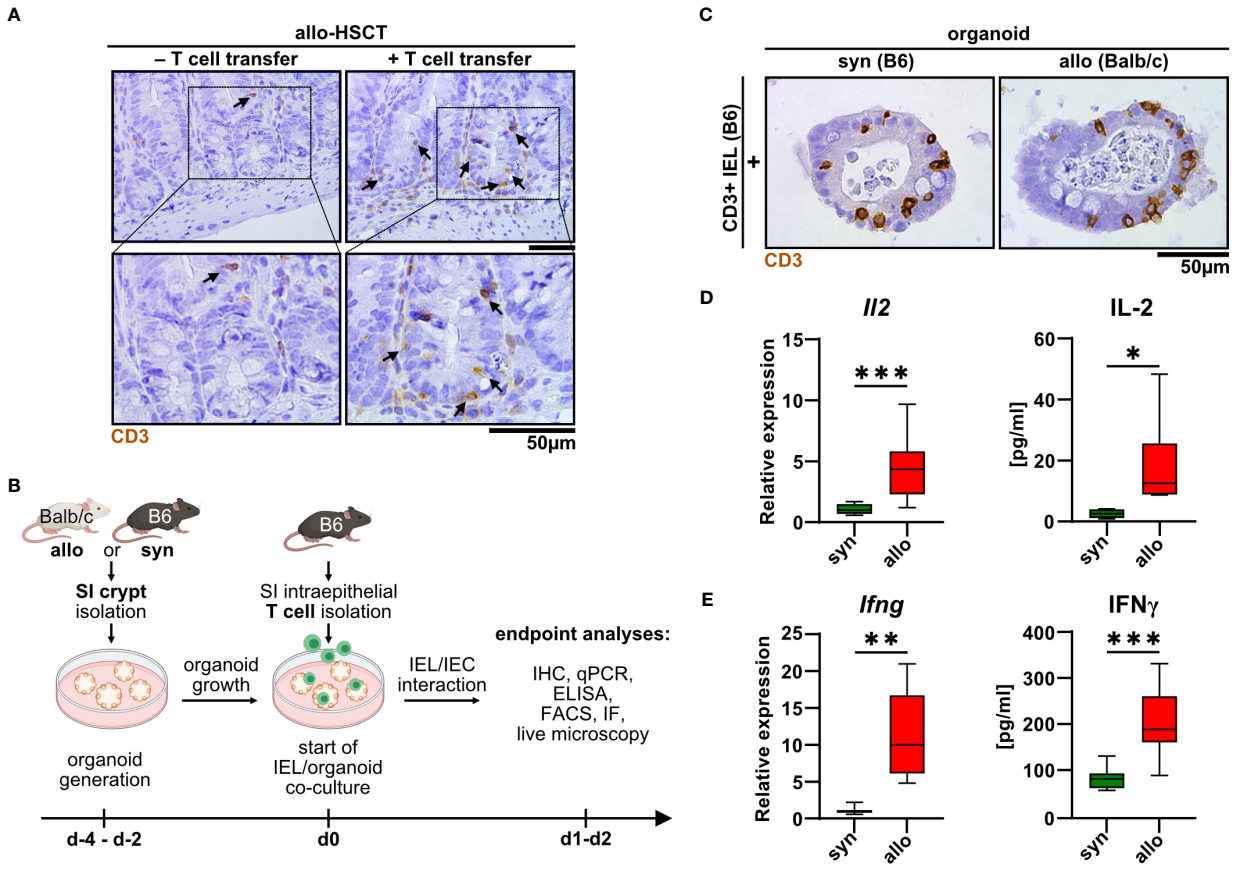

FIGURE 1
Upon allo-HSCT, small intestinal epithelium is infiltrated by allogeneic T cells, which can be mimicked in a novel IEL/organoid co-culture model system *ex vivo*. **(A)** Representative images show immunohistochemical stainings for CD3 protein from the small intestine (SI) of mice in an *in vivo* model of GvHD 30 days after lethal irradiation and rescue through transfer of T cell-depleted bone marrow cells from CD45.1/Ly5.1 B6.SJL-*Ptprc*^{a} *Pepc*^{b}/BoyCrl mice. Mice additionally receiving allogeneic C57BL/6 CD3^{+} splenocytes (+ T cell transfer) serve as experimental group developing GvHD, while untreated mice represent controls without GvHD signs (- T cell transfer). Upper row contains inserts within the images indicating crypt areas that are displayed with magnification in the bottom row. **(B)** Schematic illustration of *ex vivo* IEL/organoid co-culture model workflow. SI organoids from Balb/c or C57BL/6 donor mice are generated from SI Lgr5^{+} stem cell containing crypts and grown for 2-4 days (d-4 – d-2). Allogeneic (Balb/c) organoids or syngeneic (C57BL/6) control organoids are then co-cultured with 2.5 x 10^{5} SI IEL T cell pools freshly isolated from C57Bl/6 donor mice (d0) or were left untreated as controls (not depicted here). Indicated endpoint analyses were performed 1 or 2 days after the start of the co-culture and included immunohistochemistry (IHC), quantitative PCR (qPCR), ELISA, flow cytometry (FACS), immunofluorescence (IF) stainings and live microscopy imaging. Created with BioRender.com. **(C)** Representative images showing immunohistochemical stainings of previously magnetically enriched SI CD3^{+} IELs of C57BL/6 mice (B6) within paraffin-fixed SI organoids on d2 after co-culturing as described in **(B)**, i.e. under allogeneic (Balb/c organoids) or syngeneic (B6 organoids) conditions are displayed. **(D, E)** IEL/organoid co-cultures were generated and cultured under syngeneic and allogeneic conditions as described in **(B)**. At d2, co-cultures were harvested, cell-free supernatant collected and total RNA was isolated from the IEL/organoid total cell pool. **(D)** *Il2* gene expression levels (left panel, n = 13) were determined by qPCR. Obtained data were normalized so that the relative amount detected within syngeneic culture equaled 1. Right panel displays IL-2 protein levels determined by ELISA within cell-free supernatants of syngeneic vs. allogeneic co-cultures (n = 7). **(E)** Left panel shows *Ifng* gene expression levels as determined by qPCR and normalized to the syngeneic condition (n = 8). Right panel depicts IFNγ protein levels (n = 9) in syngeneic vs. allogeneic co-cultures as measured by ELISA in cell-free supernatants. Graphs show median, minimum and maximum values in box and whiskers plots and represent pooled data from independent experiments, *p ≤ 0.05, **p ≤ 0.01, ***p ≤ 0.001 by two-tailed unpaired t test with Welch's correction.

3.2 Allogeneic IEL/IEC co-cultures are characterized by significantly increased cell death rates

The detection of cell death events especially of IECs represents one of the histopathological hallmarks of acute intestinal GvHD (5). Hence, we sought to establish a methodology allowing us to assay, visualize and reliably quantify cell death rates in the IEL/IEC co-culture model system. For this, at day 2, co-cultures were exposed to the dead cell-dye propidium iodide (PI) while we counterstained cell nuclei with Hoechst. As shown in Figure 2A and Supplementary Video 1 by confocal microscopy scanning, organoids cultured alone, i.e. in the absence of T cells, contained only few and small areas with PI-positive cells presumably reflecting physiological cell debris shedding into the crypt lumina. Strikingly, the addition of fluorescently labeled allogeneic T cells led to a noticeable increase of PI^{+} cells. Importantly, PI^{+} areas were anatomically not restricted to the crypt lumen as it appeared to be the case for the majority of the events visible in syngeneic IEL/IEC co-cultures. This data suggested that the observed cell death in allogeneic IEL/IEC co-cultures exceeds physiological epithelial cell turnover as well as cell death due to occasional T cell activation in the syngeneic setting. To address that

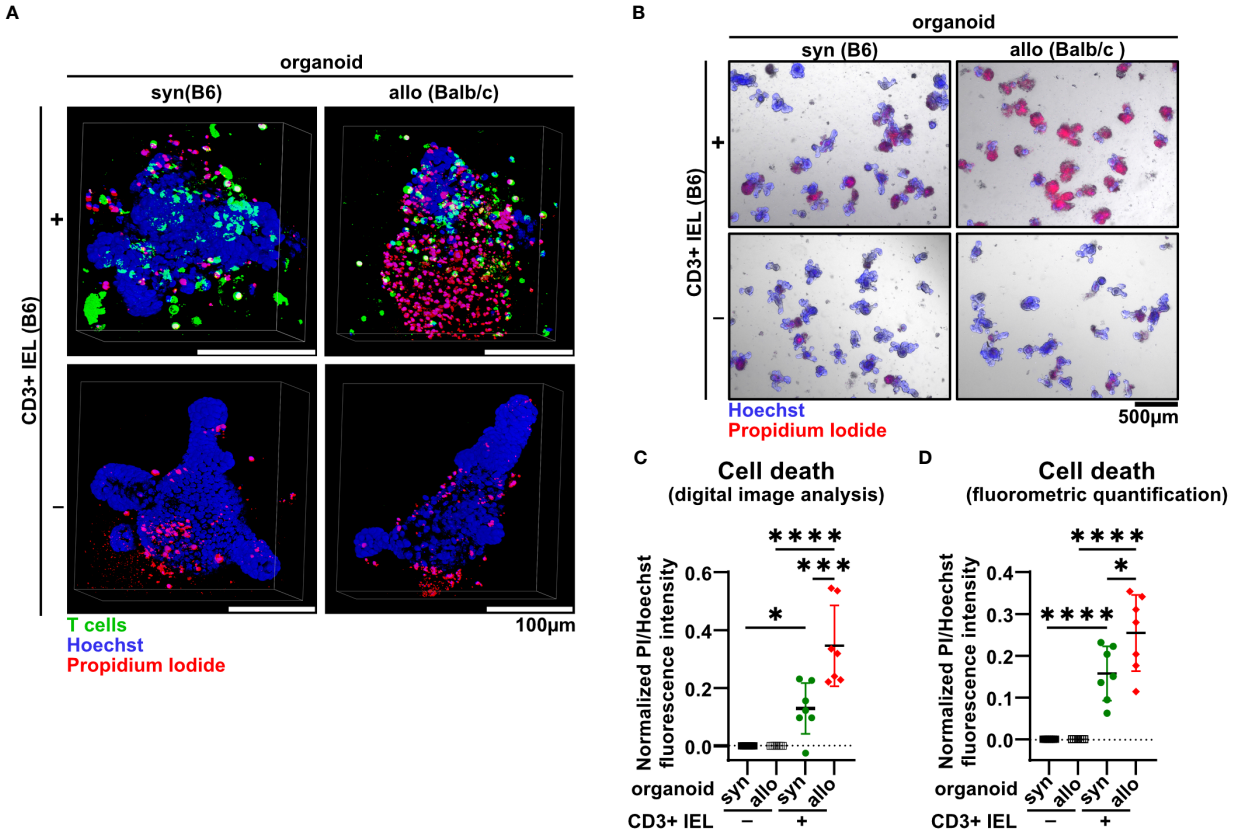

FIGURE 2
IELs induce significantly more organoid cell death under allogeneic compared to syngeneic co-culture conditions. **(A)** Representative 3D-reconstructed images of 2.5 x 10^5 SI IELs from C57BL/6 (B6) mice enriched for $CD3^+$ cells and then co-cultured (+) with syngeneic (B6) or allogeneic (Balb/c) organoids as well as control organoids, i.e. w/o T cells (-) on d2. Prior to co-culturing, T cells were fluorescently labeled with Proliferation Dye eFluor 670 (green). Organoids were stained with Hoechst dye (blue) to visualize cell nuclei while propidium iodide (red) was used to mark dead cells. Z-stacks were taken with a confocal Leica SP5 microscope and reconstructed using Fiji software and the 3Dscript plugin. **(B)** Representative examples of cell death assessment within co-cultures by combined staining with propidium iodide (red) and Hoechst (blue) on d2 of allogeneic vs syngeneic co-cultures or controls (w/o T cells) as described in **(A)** are depicted. Subsequent quantification of cell death rates within organoids was achieved by analysis of the fluorescence intensity in microscopic images using **(C)** Fiji software or **(D)** directly within an individual well using a microplate reader. In **(C, D)**, for normalization, the intensity of propidium iodide (PI) was related to the Hoechst signal (cf. methods section). To account for physiological, spontaneous cell death events, the mean PI/Hoechst ratios were normalized to the respective value obtained within organoid controls cultured in the absence of T cells. Graphs show the mean ± SD from n = 7 independent experiments. * $p \leq 0.05$, *** $p \leq 0.001$, **** $p < 0.0001$ by one-way ANOVA and Šídák's multiple comparisons test.

and objectively quantify cell death rates longitudinally across different experiments, we employed two related analysis protocols as described in detail in the method section. Starting from PI/Hoechst stained co-cultures (Figure 2B), we performed in parallel digital image analysis and fluorometry by normalization of fluorescent signals stemming from PI^+ cells relative to the total cell pool per well represented by Hoechst fluorescence intensity. This fluorometric approach previously reported and validated by Bode, Mueller et al., 2019 (23) allows an objective quantification of organoid death, which, unlike e.g. assays based on metabolic changes due to cell death, is independent of the seeding density. As shown in Figures 2C, D, both assays uniformly revealed that an increase of cell death rates was already detectable after adding syngeneic IELs compared to organoids alone. However, allogeneic IELs induced cell death significantly more, exceeding the level observed after adding syngeneic T cells. Together, allo-IEL/IEC cultures are characterized by a significant increase of cell death events that can be reliably assessed and quantified by the application of PI/Hoechst staining assays.

3.3 Allogeneic $CD3^+$ IEL-induced apoptosis of IECs largely accounts for enhanced cell death *ex vivo*

To shed further light on the cellular compartment contributing to the elevated cell death rates, we stained organoids cultured with or without syn- or allogeneic IELs for the early apoptotic marker cleaved caspase 3. Interestingly, areas corresponding to the epithelial cell layer as identified by membrane-specific expression of the epithelial cell-specific molecule EpCAM (epithelial cell adhesion molecule) stained positive for cleaved caspase 3 (Figure 3A). We further performed flow cytometric analyses of single-cell suspensions of IELs (CD3+) and IEC (EpCAM+) after two days of allogeneic and syngeneic co-culture, respectively (Figure 3B). We found that the apoptotic IEC pool isolated from co-cultures with allogeneic but not syngeneic IELs showed significantly elevated Annexin V binding on their cell surface (Figure 3C). In contrast, the mean fluorescence intensity (MFI) of

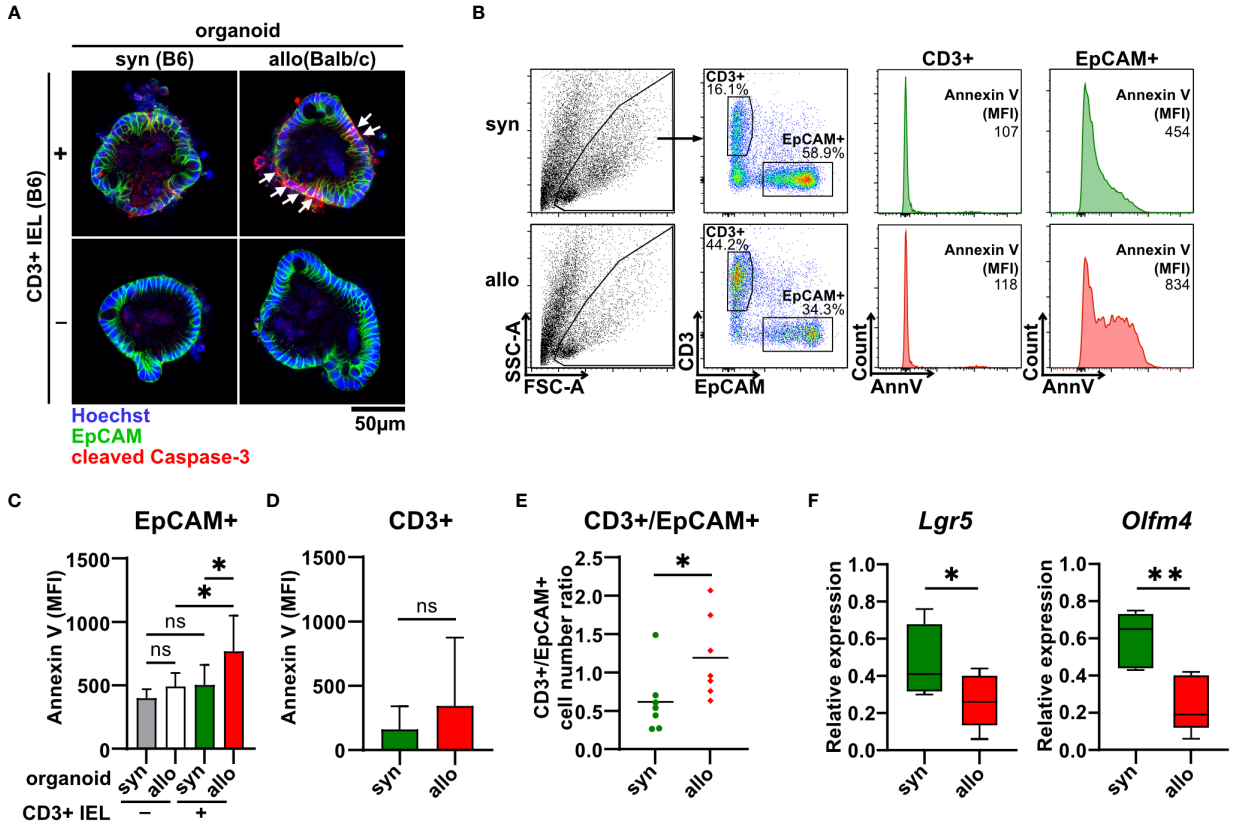

FIGURE 3
Allo-reactive IELs mediate apoptotic IEC death and dysregulation of the intestinal stem cell compartment *ex vivo*. **(A)** 2.5 x 10^5 SI IELs enriched for $CD3^+$ T cells from C57BL/6 (B6) mice were co-cultured (+) with syngeneic (B6) or allogeneic (Balb/c) organoids *ex vivo*. As controls, indicated organoids were cultured w/o T cells (-). To assess apoptotic cell death, co-cultures and controls were stained at d1 for cleaved caspase-3 (red) as well as EpCAM (green) and Hoechst (blue). Representative immunofluorescence stainings are displayed. **(B-E)** Single cell suspensions of co-cultures generated as described under **(A)** were analyzed at d2 of co-culture by flow cytometry. In **(B)**, the gating strategy of flow cytometric analysis of early apoptotic events within $CD3^+$ T cells and $EpCAM^+$ IECs by Annexin V staining is shown. Graph in **(C)** displays MFI for Annexin V staining of $EpCAM^+$ cells; in **(D)** MFI for Annexin V staining within $CD3^+$ cells is illustrated while in **(E)** cell count ratio of $CD3^+$ and $EpCAM^+$ cells is depicted. Graphs in **(C-E)** show mean ± SD from n = 7 biological replicates of independent experiments; **(C)**, *p ≤ 0.05 by one-way ANOVA and Šidák's multiple comparisons test; **(D)** by two-tailed unpaired t test with Welch's correction; **(E)**, *p ≤ 0.05 by two-tailed unpaired t test. **(F)** On d2, co-cultures executed as described under **(A)** were harvested and quantitative gene expression profiling of *Lgr5* (n = 8) and *Olfm4* (n = 5) was performed. For this, expression levels were normalized to levels detected within organoids cultured w/o T cells. Graphs show median, minimum and maximum in box and whiskers plots of pooled data of indicated, independent experiments, ns (not significant) p > 0.05, *p ≤ 0.05, **p ≤ 0.01 by two-tailed unpaired t test.

Annexin V bound to T cells was not increased in allogeneic vs. syngeneic settings (Figure 3D). This data strongly suggests that primarily IEC death accounts for the overall increased cell death fraction after two days of alloreactive IEL/organoid co-culture. Consistent with this interpretation, the T cell/IEC ratio significantly increased in allogeneic compared to syngeneic co-culture conditions (Figure 3E). In addition to our finding of increased IEC death, we wondered whether impaired intestinal stem cell homeostasis might contribute to this shift. Employing *Lgr5* and *Olfm4*, two molecular markers routinely used to robustly identify small intestinal stem cells (28, 29), we observed significantly reduced expression levels of both *Lgr5* and *Olfm4* upon co-culture with allogeneic IELs compared to syngeneic controls (Figure 3F). Overall, our data indicate that allogeneic IELs mediate IEC apoptosis and interfere with the integrity of intestinal epithelial stem cells resulting in a progressive loss of IECs within two days of co-culture.

3.4 Allo-T cell-derived IFNγ drives IEC death and regulates the intestinal epithelial stem cell niche

Type II interferon IFNγ is one of the key effector molecules of cytotoxic T cells but its contribution to intestinal GvHD-associated gut pathology remains controversial (30). Given our finding that allogeneic compared to syngeneic T cells express elevated IFNγ levels when co-cultured with IECs (Figure 1D), we sought to determine its functional impact on allo-IEL-mediated IEC death. Importantly, IFNγ-deficient IELs resulted in significantly less organoid death compared to IFNγ-proficient T cells (Figure 4A). Moreover, the intestinal epithelial stem cell compartment previously shown to be sensitive to IFNγ-mediated damage (31) was protected in co-culture with IFNγ-deficient compared to control allo-IELs as shown by significantly enhanced and hence largely recovered *Lgr5* and *Olfm4* expression levels (Figure 4B).

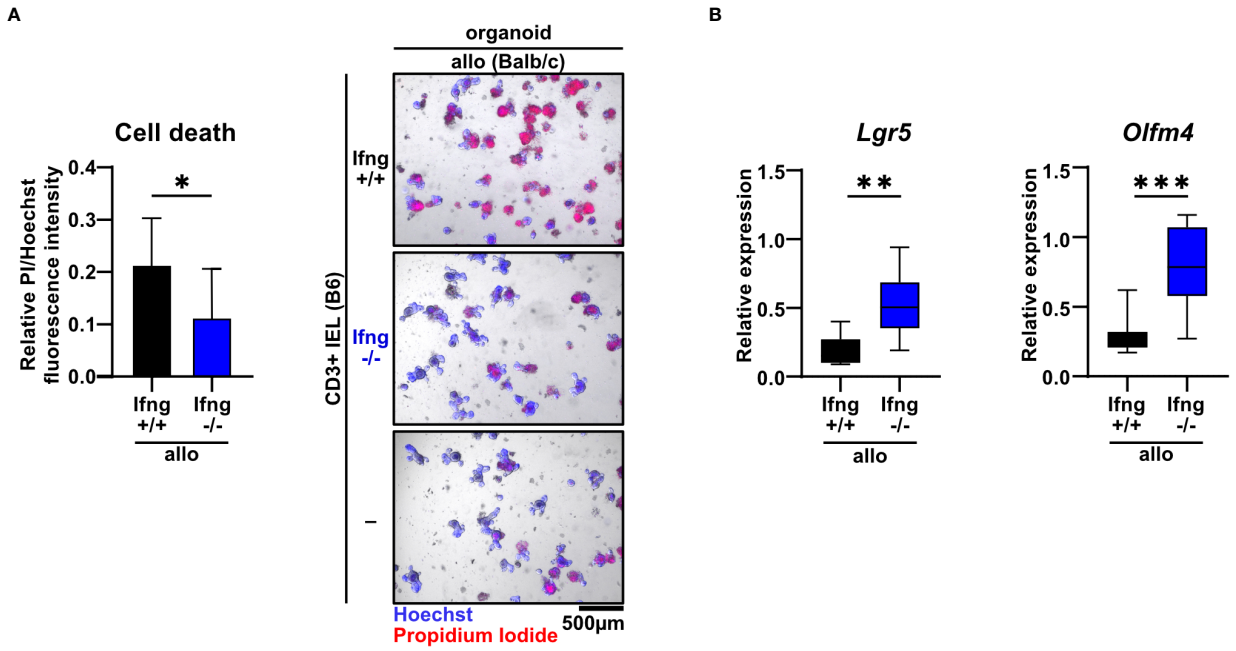

FIGURE 4
Dysregulation of the small intestinal epithelial cell and stem cell compartment in allogeneic co-cultures is dependent on IFNγ. **(A)** 2.5 x 10^5 SI IELs enriched for $CD3^+$ T cells from C57BL/6 (B6) IFNγ-sufficient or IFNγ-deficient mice were co-cultured with allogeneic (Balb/c) organoids *ex vivo*. As controls, Balb/c organoids were cultured alone, i.e. w/o T cells (-). At d2, fluorometric cell death quantification (left) was performed, with the PI/Hoechst fluorescence intensity ratio normalized to the wells with organoids cultured without T cells; representative microscopic images (right) of organoids double-stained with Hoechst and PI after co-culture are displayed. Graph depicts pooled data from n = 9 independent experiments, mean ± SD. *p ≤ 0.05 by two-tailed unpaired t test. **(B)** IEL/IEL co-cultures were performed for 2d as described in **(A)**. Then, total cells were harvested and quantitative gene expression profiling of the stem cell markers *Lgr5* and *Olfm4* was performed. For this, expression levels were normalized to levels detected within organoids cultured w/o T cells. Pooled data from n = 8 independent experiment are depicted as median with minimum and maximum values in box and whiskers plots. **p ≤ 0.01, ***p ≤ 0.001 by two-tailed unpaired t test.

Apart from IFNγ, T cells might additionally employ other soluble factor- or cell-contact-mediated mechanism to execute cytotoxic IEC death, as suggested by several lines of evidence in the literature (32). Assessing TNFα expression on RNA and protein level, we did not observe a differential regulation in our setting (Supplementary Figure 1A). In contrast, granzyme B/perforin gene expression levels were moderately, but significantly increased in allogeneic vs. syngeneic co-culture conditions (Supplementary Figure 1B), but we were unable to monitor equivalent changes in allogeneic IELs on the protein level (Supplementary Figure 1C). Finally, we evaluated whether the FasL/Fas (CD95L/CD95) axis may be involved in mediating T cell-induced target cell death in this model system. Similar to the data on cytotoxic molecules, FasL gene expression was significantly increased in allogeneic compared to syngeneic co-cultures, a finding that could not be confirmed on the protein level (Supplementary Figure 2A). In contrast, however, Fas receptor expression on EpCAM+ epithelial cells was significantly increased in co-cultures with allogeneic compared to syngeneic IELs (Supplementary Figure 2B). To assess whether IFNγ is able to regulate the pool of Fas+ IECs in this setting, we treated organoids with recombinant IFNγ. Strikingly, IFNγ treatment of organoids alone, i.e. in the absence of T cells, strongly increased the pool of Fas+ EpCAM+ epithelial cells (Supplementary Figure 2C). Overall, this data suggests that allogeneic IEL-derived IFNγ is a key molecular signal driving allogeneic IEC death. Mechanistically, IFNγ putatively increases the susceptibility of IECs by sensitizing IECs for FasL/Fas-mediated T cell-driven IEC death thereby strongly interfering with intestinal epithelial cell and stem cell homeostasis.

3.5 $TCR\alpha\beta^+CD8\alpha^+$ IEL-derived T cells are the major executers of allo-mediated IEC death

T cells residing within the SI IEL compartment comprise both $TCR\alpha\beta^+$ and $TCR\gamma\delta^+$ T cells. Interestingly, the TCRαβ/TCRγδ T cell ratio did not differ after the 2d co-culture time period between the allogeneic and syngeneic setting (Supplementary Figures 3A, B). Moreover, within the $TCR\alpha\beta^+$ T cell pool, both $CD4^+$, $CD8\alpha\alpha^+$ and $CD8\alpha\beta^+$ T cell subsets were virtually unaltered (Supplementary Figure 3C). To further elucidate which T cell subsets among IELs largely account for allo-T cell-mediated IEC death, we utilized $TCR\alpha\beta^+$ and $TCR\gamma\delta^+$ T cell-enriched IEL pools and assessed their behavior in the allogeneic co-culture model system. Firstly, we found that $TCR\gamma\delta^+$ IELs expressed significantly less IFNγ compared to $TCR\alpha\beta^+$ IEL pools (Figure 5A). Moreover, $TCR\alpha\beta^+$ IELs were superior in mediating IEC death in comparison to $TCR\gamma\delta^+$ T cells (Figure 5B). Secondly, $CD8\alpha^+$ T cells expressed IFNγ and executed IEC death equally efficient as the total,

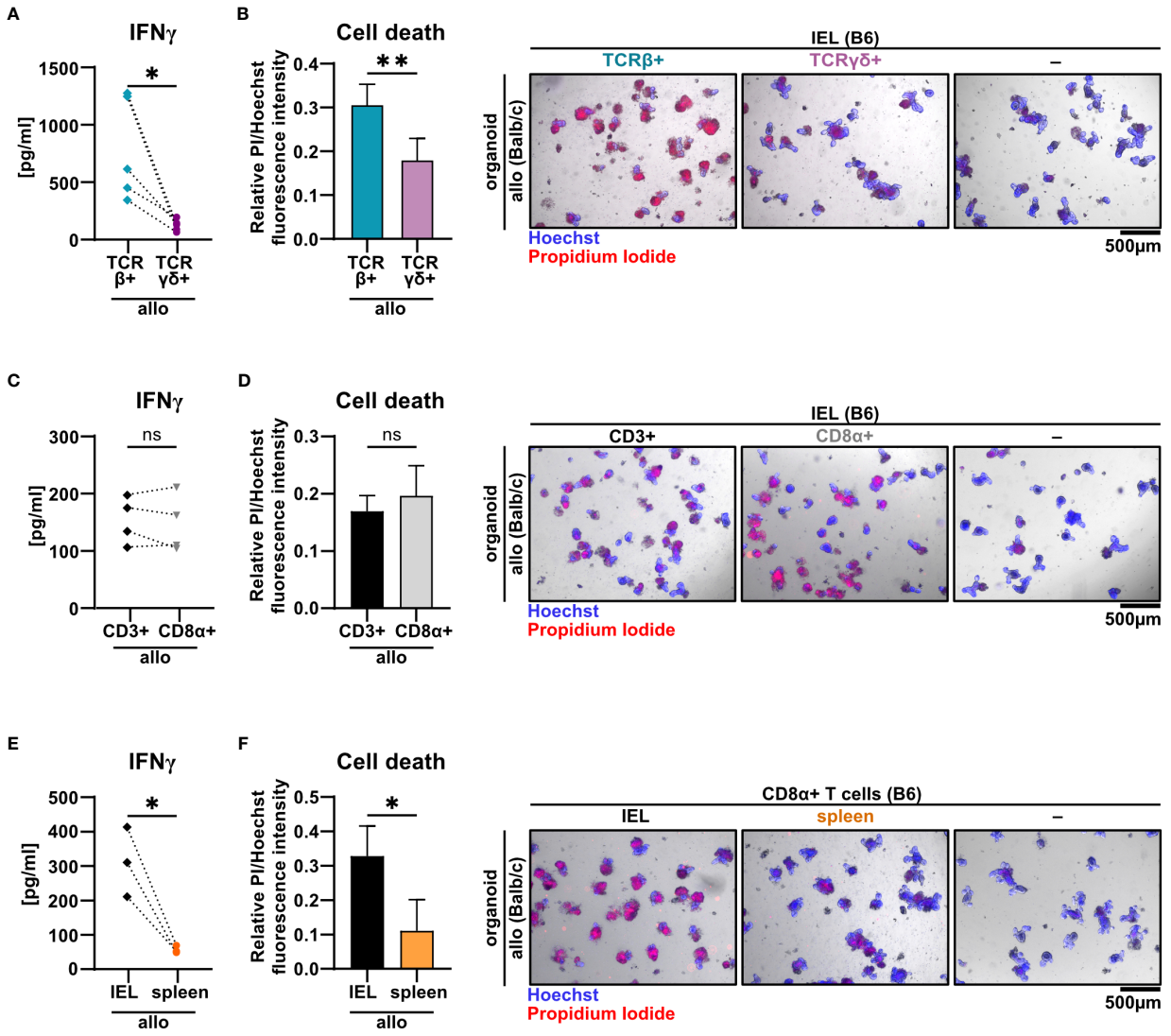

FIGURE 5
TCRβ+ CD8α+ T cells within SI IELs largely account for allo-T cell-mediated organoid cell death *ex vivo*. Balb/c (allo) SI organoids were co-cultured alone (-) or with 2.5 x 10^5 T cells from C57BL/6 (B6) donor mice magnetically enriched for the subsets as indicated below. On d2 after start of the co-culture, cell-free supernatants were analyzed by ELISA and fluorometric cell death quantification was performed. For cell death quantification, the ratio of PI/Hoechst fluorescence intensities was corrected for the baseline cell death in control organoid cultures without T cells. **(A, B)** SI Balb/c organoids were co-cultured with allogeneic SI IELs from B6 donors enriched for TCRβ$^+$ and TCRγδ$^+$ resp. Shown results reflect data from n = 5 independent experiments. **(A)** IFNγ protein quantification in cell-free supernatant by ELISA. **(B)** Organoid cell death assessment (left panel) as determined by fluorometric analysis. On the right panel, representative images of organoids stained with Hoechst and PI after co-culture are displayed. **(C, D)** Data from n = 4 independent co-culture experiments consisting of SI Balb/c organoids and allogeneic B6 SI IELs enriched for CD3$^+$ or CD8α$^+$ T cells are displayed. In **(C)** IFNγ protein was quantified by ELISA in the cell-free supernatant at d2 of co-culture. **(D)** Fluorometric quantification of cell death (left panel) among organoids on d2 of co-culture is shown. In the right panel, representative microscopic images of organoids double-stained with Hoechst and PI after co-culture are displayed. **(E, F)** Results from allogeneic co-cultures of SI organoids from Balb/c mice with CD8α$^+$-enriched IELs vs. CD8α$^+$-enriched splenocytes from B6 mice are displayed. Depicted data were derived from d2 analyses and are pooled from n = 3 experiments. In **(E)**, IFNγ protein levels in the cell-free supernatant were determined by ELISA. In **(F)**, fluorometric cell death quantification (left panel) was performed. Representative microscopic images (right panel) of organoids double-stained with Hoechst and PI after co-culture are depicted. Graphs show pooled data from independent experiments (n = 3-5 as indicated), graphs **(B, D, F)** depict mean ± SD. ns (not significant) $p > 0.05$, *$p \leq 0.05$, **$p \leq 0.01$, by two-tailed unpaired t test or t test with Welch's correction [graphs **(A)** and **(E)**].

unfractionated CD3$^+$ IEL pool suggesting that within the IEL-residing TCRαβ$^+$ T cell fraction, CD8α$^+$ were sufficient, while CD4$^+$CD8α$^-$ T cell subsets were dispensable for the effect observed in the allogeneic setting (Figures 5C, D). Finally, we confirmed that these characteristics were unique properties of bona fide IEL-derived CD8α$^+$ T cells, as splenic CD8α$^+$ T cells failed to comparably mount elevated IFNγ levels and mediate IEC death (Figures 5E, F). Together, small intestinal TCRαβ$^+$ CD8α$^+$ IELs largely account for the death of allogeneic organoids in our *ex vivo* co-culture model system.

3.6 Presence of minor mismatch antigens is sufficient to drive allo-IEL-mediated IEC death

Current pre-clinical models of acute GvHD are either based on a complete mismatch of the major histocompatibility complex (MHC) between host and recipient or on minor histocompatibility antigen (miHA) mismatches alone. Therefore, we aimed to unravel the pathomechanistic requirements underlying allo-IEL mediated IEC death by investigating whether our finding of $CD3^+$ IEL-mediated killing of organoids in a complete MHC mismatch constellation can be recapitulated in a minor mismatch setting *ex vivo*. To achieve this goal, we assayed both killing abilities and IFNγ expression levels of allogeneic IELs cultured either within organoids derived from C.B10-H2b/LilMcdJ mice (minor mismatch) or Balb/c mice (major mismatch). The C.B10-H2b/LilMcdJ strain genetically matches Balb/c mice with the exception that the endogenous MHC complex of Balb/c mice, H2d, has been replaced by H2b, equivalent to the MHC complex of B6 mice. Consequently, tissues derived from this line and B6 mice derived T cells are MHC-matched (H2b) but display a complete mismatch in miHA (33). As shown in Figures 6A, B, both IFNγ protein expression levels and IEC death rates were virtually identical between miHA and MHC mismatch settings *ex vivo*. Given our finding that mismatch in the miHA peptidome is sufficient, we finally wondered whether conversely the TCR specificity is critical for allo-IEL activation as determined by IFNγ release and IEL-mediated cytotoxicity within our model system. To address that question experimentally, we restricted the TCR specificity within the IEL $CD8^+$ T cell pool by making use of a transgenic mouse line in which T cells carry a distinct T cell receptor for murine *Tcra-V2* and *Tcrb-V5* genes recognizing an immuno-dominant peptide of ovalbumin. Strikingly, $CD8\alpha^+$ T cells isolated from the SI IEL compartment of OTI transgenic (tg^+) mice failed to mount IFNγ levels comparable to T cells with an endogenous, polyclonal TCR repertoire (OTI tg^-) (Figure 6C). Consecutively, OTI tg^+ $CD8\alpha^+$ T cells also elicited significantly less cytotoxicity towards IECs in the allogeneic setting compared to non-transgenic IELs (Figure 6D). In summary, allogeneic IEC

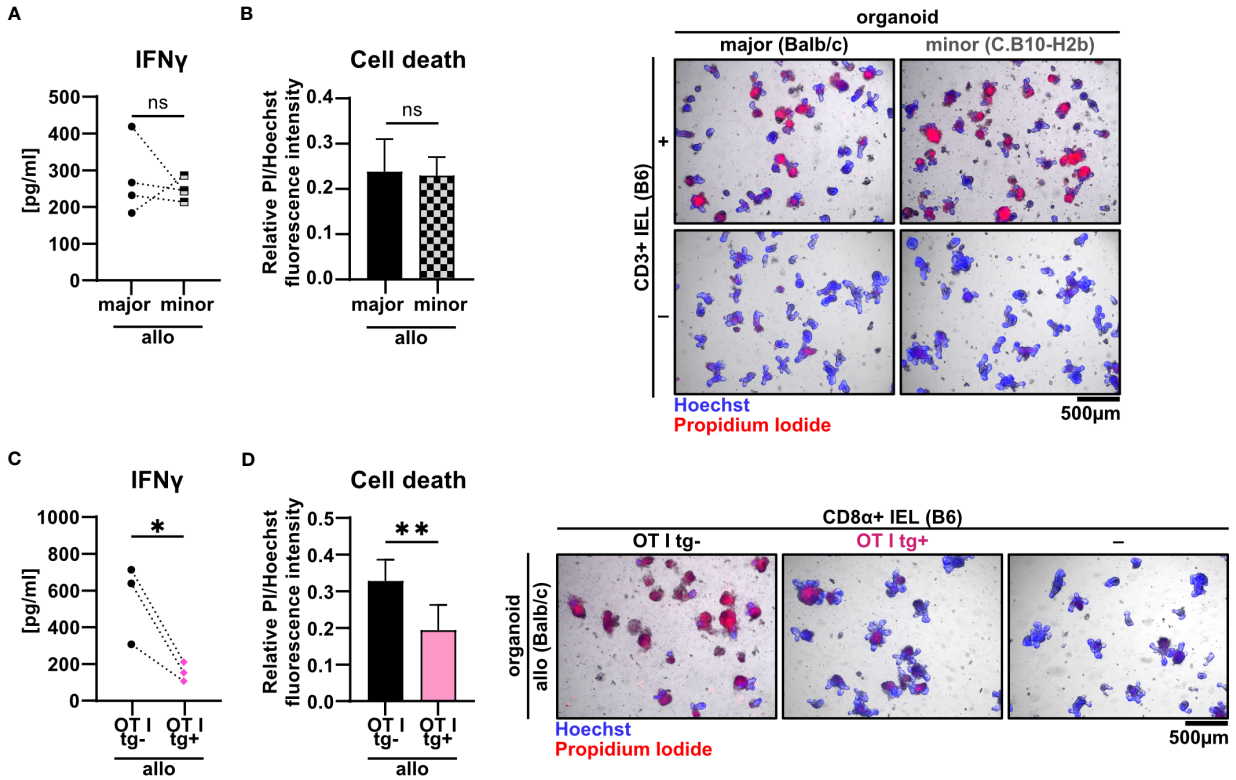

FIGURE 6
Minor mismatch antigens are sufficient for the $CD3^+$ IEL-mediated killing of allogeneic IECs *ex vivo*. **(A, B)** 2.5 x 10^5 C57BL/6 (B6) IELs enriched for $CD3^+$ T cells were co-cultured with SI Balb/c organoids (allogeneic major mismatch, i.e. MHC I-mismatched) vs. SI organoids from C.B10-H2 b/LilMcdJ mice (allogeneic minor mismatch, i.e. MHC I-matched, minor histocompatibility antigen mismatched). Organoids cultured w/o T cells served as controls (-). **(A)** IFNγ protein quantification within cell-free supernatants was performed *via* ELISA at d2; **(B)** fluorometric organoid cell death quantification corrected for the organoid cell death observed in wells with organoids cultured w/o T cells (-) (left panel) and representative microscopic images of organoids stained with Hoechst/PI dyes after 2 days of co-culturing are displayed (right panel). Data represent pooled results from n = 4 independent experiments and depict mean ± SD. Data were analyzed by two-tailed unpaired t test. **(C, D)** Balb/c (allo) SI organoids were co-cultured with 2.5 x 10^5 $CD8\alpha^+$-enriched IELs from OTI tg^+ donor mice or OTI tg^- control mice (B6) or cultured w/o T cells (-) for 2d. Graphs show data from independent experiments as indicated and display **(C)** IFNγ protein quantification within cell-free supernatants performed *via* ELISA at d2 (n = 3); **(D)** organoid cell death after co-culture corrected for baseline organoid death detectable in wells culturing organoids alone, i.e. w/o T cells (-) (left panel, n = 7) as well as representative images of Hoechst and PI dye double-stained organoids (right panel). Data shown in **(D)** represent mean ± SD. ns (not significant) $p > 0.05$, *$p \leq 0.05$, ** $p \leq 0.01$ by two-tailed unpaired t test.

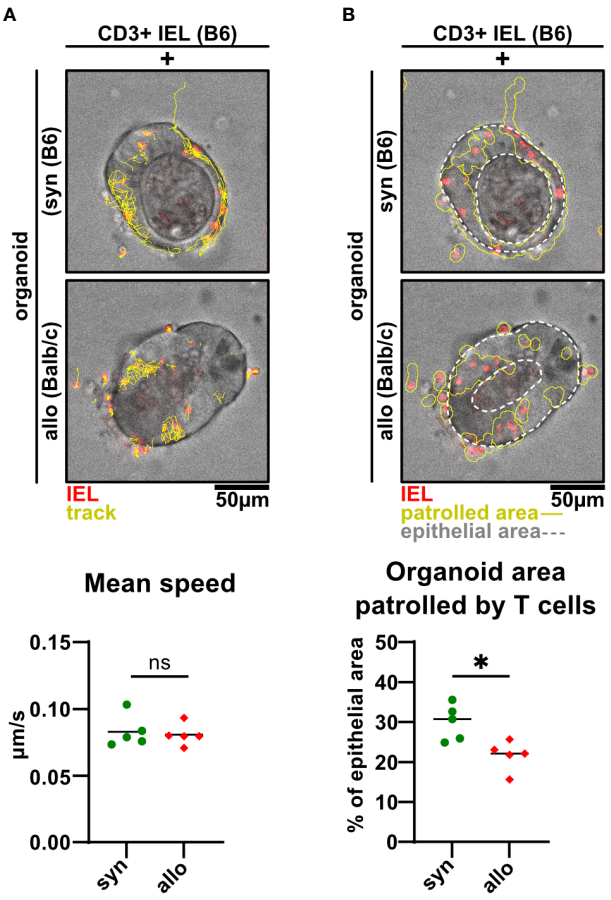

FIGURE 7
Alloreactive intraepithelial T cells display a more restricted patrolling behavior compared to syngeneic controls. **(A, B)** 2.5 x 10^5 $CD3^+$-enriched C57BL/6 (B6) SI IELs were fluorescently labeled with Proliferation Dye eFluor 670 and co-cultured within SI Balb/c organoids for 2d. Representative images and quantitative analyses from live cell imaging time-lapse studies at d2 of co-culturing are displayed. Time series were recorded on a spinning disc microscope with a 25X objective every 30 sec for a period of 45 min on d1 of co-culture. Analyses were performed using Fiji software and the TrackMate plugin as well as an in-house macro script. In **(A)** visualized tracks (yellow) of the movements of T cells (red) within intestinal organoids (top and middle panel) and quantification of their mean speed in µm/s as identified by the TrackMate plugin are shown (bottom panel). In **(B)** organoid area cumulatively covered by migrating IELs (red) over time is depicted (solid, yellow line) while the region of interest is indicated by white dotted lines (top and middle panel). Patrolled areas were quantified by relating this region to the region of interest as determined using an in-house Fiji macro. Graphs show data from n = 5 independent experiments; n = 4 technical replicates per group were recorded in each experiment. ns (not significant) $p > 0.05$, *$p \leq 0.05$ by two-tailed unpaired t test.

killing requires specific antigen recognition of miHA by IELs independent of a complete MHC mismatch.

3.7 Allogeneic IELs display a restricted patrolling behavior within SI organoids *ex vivo*

As previously demonstrated for the syngeneic setting (19), live cell imaging of IEL/IEC co-cultures *ex vivo* offers the opportunity to visualize IEL migratory properties under defined conditions over time. Here, we sought to apply this methodology to decipher whether allogeneic and syngeneic IELs display differential migratory properties. As shown in Figure 7A and Supplementary Video 2, we found IELs to be patrolling SI organoids with a comparable speed irrespective of an allogeneic or syngeneic setting. However, the organoid area scanned by migrating allo-IELs turned out to be significantly smaller compared to syngeneic controls (Figure 7B). Overall, limited area coverage by allo-IELs within organoids might indicate that upon antigen-recognition, defined clones are locally restrained and then exert IEC cytotoxicity as their default functional assignment.

4 Discussion

Intestinal GvHD remains a major challenge in the management of allo-HSCT patients. While donor T cells are acceptedly critical mediators of allogeneic intestinal inflammation, selectively T cell-targeting therapies have not been developed yet despite an urgent medical need for innovative treatment options. One underlying cause represents sparse knowledge on T cell subset-specific roles and here especially insight into their impact on the target tissue mostly affected in the course of GI GvHD, the epithelial layer. Interestingly, some early studies have reported that the intestinal epithelial layer is routinely populated by immune cells, so called IELs, predominately composed of T cells, suggesting that IELs may directly exert IEC damaging effects (14–16). Despite this observation, the behavior within and specific impact of donor T cells on IECs have been poorly explored so far. This is in part due to methodological limitations arising when IELs are studied *in vivo* or *ex vivo* (17, 20). To overcome this shortcoming, we sought to employ a novel IEL/IEC co-culture model system recently reported by us and others as a valuable tool to study IEL function and behavior within syngeneic small intestinal organoids *ex vivo* (17, 19, 20). In this study, we applied this experimental model system to the allogeneic context with the goal to provide a model system that will help to fill this methodological and biological gap, as it enables future studies to explore the lympho-epithelial crosstalk in an allogeneic setting *ex vivo* by mimicking aspects of intestinal GvHD *in vivo*.

Employing our *ex vivo* co-culture model, we found that allogeneic SI IELs readily populated SI organoids while we were unable to detect a noticeable regulation of the IEL composition between syngeneic and allogeneic culture conditions. Of note, we observed significantly elevated IL-2 protein expression levels pointing at robust T cell activation, as IL-2 expression represents a classical landmark of T cell activation downstream of TCR engagement (34), as well as strongly up-regulated IFNγ expression within allogeneic co-cultures. This is in line with previous reports identifying IL-2 as a strong inducer of IFNγ expression and cytotoxic modules within T cells (35, 36).

In delineation from the syngeneic setting, however, our studies were limited to two days as we noticed at this time point significant changes in cell viability in the allogeneic co-cultures: Importantly, we could show that allogeneic IELs induce significantly higher cell death

levels in co-culture compared to syngeneic IELs. Still, we recorded elevated cell death rates also in syngeneic co-cultures when compared to spontaneous, basal cell death events in B6- or Balb/c-derived organoids alone, i.e. in the absence of T cells. As shown by others and our functional studies using IFNγ-deficient IELs, at this point we attribute reduced organoid viability in the presence of syngeneic IELs to the presence of T cell-derived IFNγ. Multiple scenarios may apply to explain this finding: At first, subtle, not traceable genetic differences among different offspring of syngeneic inbred strains serving as B6 IEL and B6 organoid resp. donor mice may be sufficient to trigger T cell activation and concomitant IFNγ expression. Alternatively, IECs that undergo routine shedding upon IEC renewal are *in vivo* physiologically shed to the lumen and are discarded by the stool flow while in our *ex vivo* organoid system they stay *in situ*. Hence, IEC-derived antigens and danger signals e.g. from carried over microbiota might elicit syngeneic IEL activation. Importantly, our characterization of allogeneic IEL-mediated effects on organoids did not only reveal enhanced IEC death but also evidence for a negative regulation of the intestinal stem cell niche given a significant reduction of the expression levels of intestinal stem cell markers Lgr5 and Olfm4 in allogeneic compared to syngeneic conditions. Moreover, and in line with recently published studies, IFNγ expressed by alloreactive IEL T cells turned out to be critical for the abrogated stem cell homeostasis, as IFNγ-deficient IEL T cells did not only elicit reduced cell death but also failed to diminish Lgr5 and Olfm4 expression levels (31, 37). Hence, morphological and molecular characteristics of allogeneic IEL/IEC co-cultures identified by our study overall display aspects that are reminiscent of findings in human intestinal GvHD and highlights IFNγ$^+$ IELs as putatively critical mediators in its pathogenesis (31, 37).

Our studies clearly uncovered that allogeneic T cells isolated from the SI IEL compartment exert cytotoxic effects on IEC that are seemingly unique, as lymphoid-resident spleen-derived T cells were unable to mimic this function. This may be explained by largely unexplored functional properties of IEL T cells compared to splenic T cells somehow adapted to the epithelial environment. However, another obvious argument to explain these cell-type restricted abilities is that IELs largely consist of antigen-experienced, so called tissue-resident memory (Trm) cells that are able to readily exert their default functions upon TCR triggering while splenic T cell pools mainly comprise antigen-unexperienced, naïve cell types requiring additional signals for activation, priming and overall functionality (13, 38, 39). Within the IEL T cell subsets, we found that in fact TCRαβ$^+$ were superior to TCRγδ$^+$ T cells with regard to IFNγ expression and IEC killing abilities in an allogeneic setting. Many studies on their contribution are inconclusive. While there are recently emerging indications for functionally relevant, context-dependent anti-tumoral and anti-leukemic, cytotoxic effects of TCRγδ$^+$ T cells (40, 41), the majority of reports suggests rather immune-regulatory than inflammation-promoting effects of TCRγδ$^+$ T cells during intestinal GvHD (42–44). Therefore, our finding of a seemingly minor role for IEL TCRγδ$^+$ T cells in mediating immune-mediated IEC death in the allogeneic setting is in line with the current state of the field.

Moreover, we found that within TCRαβ$^+$ IELs CD4$^+$CD8α$^-$ T cells are seemingly dispensable for exerting IEC death as IEL CD8α$^+$ T cells lacking CD4$^+$CD8α$^-$ T cells compared to total CD3$^+$ T cells displayed virtually indistinguishable effects albeit there was a trend that the former showed more pronounced cytoxicity. This is in line with recently emerging evidence suggesting that Tregs residing predominately in the lamina propria are able to convert into CD4$^+$CD8α$^-$ intra-epithelial T cells which then exert intestinal inflammation-suppressive functions (45). Future studies, however, will have to determine whether CD4$^+$CD8α$^-$ intra-epithelial T cells are exerting allogeneic IEL-driven IEC death-reducing and intestinal stem cell compartment-protecting effects. Thus, our data show that the CD8α$^+$ Trm population within IEL TCRαβ$^+$ T cells primarily accounts for the cytotoxic effects affecting SI organoids. Importantly, this is in agreement with reports by others showing that donor T cell populations infiltrating the intestinal epithelia during GvHD express transcriptional programs and surface markers (e.g. CD103) characteristic for CD8α$^+$ Trm T cells (46–48).

Having functionally defined the cellular components, we sought to further elucidate the mechanistic cues contributing to IEL-mediated IEC death in our co-culture model system. By additionally applying major and minor mismatch conditions onto the allogeneic setting, we found that major mismatch, i.e. a full MHC mismatch between IEL and organoids, is not a condition sine qua non in our IEL/IEC co-culture model system: We strikingly found that both IFNγ secretion and IEC killing by allogeneic IELs were virtually indistinguishable between MHC-mismatched (major) and MHC-matched (minor, i.e. miHA mismatched) conditions, pointing at the critical role of the presented peptide in this setting.

Over the last decades, alternative pathogenetic concepts have been developed to mechanistically explain direct allorecognition of foreign target cells by T cells. Strikingly, the frequency of alloreactive T cells within a given MHC-mismatched donor is approximately between 1-10%, which is exceptionally high compared to the frequency of T cells specific for a given MHC-peptide complex (49, 50). In the light of this finding, the so-called MHC-centric model suggests that polymorphisms in amino acids between self- and allo-MHC molecules affect the manner in which individual TCRs bind to MHC molecules. In this model, the presented peptide itself only marginally contributes to the recognition process, yielding a high frequency of T cells recognizing the allogeneic MHC molecule with various affinities (50, 51). As opposed to this, the peptide-centric hypothesis presumes that alloreactive T cells are specifically recognizing allopeptides presented on MHC receptors, a model system that is supported by the fact that alloreactive T cell populations are in fact highly peptide specific (50–52). Since both models are supported by functional and structural data, realistically, in most interactions probably both the MHC molecule as well as the peptide contribute to T cell recognition depending on the specific context.

To further assess the relative contribution of the MHC/peptide complex composition on the activation and functionality of allogeneic IELs, we employed OT I transgenic mice on the B6 genetic background carrying a genetically modified, non-endogenous TCR as the source of allogeneic IELs. OT I$^+$ T cells express a TCR that only detects a peptide derived from ovalbumin, i.e. an exogenous antigen that is not present in our co-culture model

system. Importantly, CD8α$^+$ OT I tg$^+$ IELs failed to mount an alloresponse (i.e. IFNγ expression and IEC death induction) in the presence of MHC-mismatched organoids. As the employed OT I transgenic mouse model represented mice not previously back-crossed on a RAG-1/2 deficient background, our data show that OT I tg$^+$ T cells despite containing a minor T cell pool expressing a residual endogenous TCR repertoire are hampered in their ability to induce allo-mediated cell death, indicating that a sufficiently high number and/or diversity of TCR repertoire is required to elicit a robust allo-response in our model system. Together with results derived from the major vs. minor mismatch setting, the shown data suggest that allogeneic IEL activation and functionality rather depend on the TCR recognition of the presented, peptide-derived epitope than alone on the (mismatched) MHC molecule itself. Based on these results, we conclude at this point that allogeneic IELs isolated from B6 donors recognize endogenous peptides on IEC characteristic for the Balb/c genetic background. Our study is certainly limited as it does not ultimately resolve this critical question. Regardless, the IEL/IEC co-culture model system and our initial characterization have certainly laid the methodological basis for more in-depth investigations of the assumed allo-specificity of intestinal IELs in the future.

A major population of IEL T cells express the integrin αEβ7 (CD103) which is known to bind E-Cadherin on IEC thereby presumably conferring IEL tissue retention (10, 39). Moreover, we described earlier that CD103 seems to be a critical component of normal IEL migratory properties within intestinal epithelia, at least *ex vivo* (11, 12). So far, however, the exact mechanisms regulating IEL migration and motility within the epithelial layer both in the steady state and under inflammatory conditions including intestinal GvHD remain only incompletely understood.

One group investigating T cell localization in the context of GvHD-mediated intestinal damage by 3D microscopy found that donor T cells preferentially accumulated in the lower crypt region after allo-HSCT (53). In this study a direct interaction between T cells and intestinal stem cells was described and associated to the occurrence of damaged crypts already 4 days after transplantation, indicating that donor T cell population of the IEL compartment is an early event in GvHD pathology and intestinal stem cells are a primary target of allogeneic T cells (53). Hence, novel experimental platforms and modalities like the IEL/IEC allogeneic co-culture model characterized in our study provide the unique opportunity to further elucidate the lympho-epithelial interaction as e.g. migration also in a spatiotemporal and functional manner *ex vivo*. Therefore, we applied our previously reported live cell imaging microscopy protocol on the allogeneic setting (19). Strikingly, we found that allogeneic T cells displayed a regionally more restricted patrolling behavior contrasting syngeneic T cells covering larger areas within organoids over time. Currently, we cannot provide an analysis with a higher spatiotemporal resolution to e.g. determine whether this is due to the fact that allogeneic IEL T cells orientate themselves *ex vivo* towards the base of the crypts and stem cell niche as described for the *in vivo* behavior (53). Regardless, considering our finding that allogeneic IELs are clearly dependent on allo-peptide recognition and are more strongly activated as evidenced by elevated IFNγ expression levels, for us one explanation model is that upon antigen recognition, IELs may stay more locally confined to exert their cytotoxic effector functions more focused towards their target cells. This is in line with the observation by another group (20), who qualitatively described that OT I tg$^+$ IELs in syngeneic co-culture with small intestinal organoids seemed to arrest in their movement when Ova peptide was added, i.e. upon TCR engagement. However, future studies directly focusing on this aspect will be required but will definitely benefit from the availability of our allogeneic IEL/IEC co-culture model system.

Finally, in delineation from other published studies using allogeneic T cell/organoid co-culture model systems (31, 54, 55), we omitted *in vivo* (e.g. in the course of allo-HSCT) or in a way artificial, broad *ex vivo* activation (e.g. mimicking antigen receptor signaling through PMA/ionomycine or anti-CD3/anti-CD28 stimulation) of the T cells prior to exposition to IECs. By doing so, we focus on the spontaneous, natural activation pattern of alloreactive T cells by epithelial cell structures. In fact, by showing that unstimulated splenic T cells were deficient in inducing IEC death in our co-culture setting, we could demonstrate that mounting a cytotoxic allogeneic response without the requirement of additional (co-)activation is a unique feature of IELs. Hence, our observations strongly indicate that IELs as bona fide antigen-experienced T cells possess reactivity to antigens presented in an allogeneic setting. Importantly, IELs are responsive to those antigen pools upon encountering them in their home tissue without requiring additional priming or signaling by APCs in lymph nodes.

As a limitation, our co-culture system only partially reflects critical aspects closely associated with *in vivo* GvHD pathology. For example, the contribution of innate immune cells such as granulocytes, antigen-presenting cells and ILCs all known to be able to modulate intestinal inflammation in GvHD, is omitted (56). In addition, the role of fungal commensals and enteric viruses, such as CMV reactivation as a common complication in patients previously undergoing allo-HSCT, is not part of the current model system and remains to be integrated in the future (57, 58). Furthermore, IEL/IEC co-cultures are devoid of luminal signals, especially from the intestinal microbiota. Given the nowadays widely accepted, central impact of microbial signals on the initiation and course of intestinal GvHD (59), future attempts to develop this model system further will include the evaluation of modalities allowing the inclusion of both microbiota-derived inflammatory signals and microbial peptides. Lastly, it represents a valuable future goal to apply this model to the human setting, as it has already been achieved successfully for *ex vivo* autologous co-cultures of intestinal T cells and organoids from patients with inflammatory bowel disease (60). Ultimately, the translation to the human system would allow to investigate the IEL/IEC interaction in a more clinical and patient-centered manner.

In summary, our here presented *ex vivo* model system allows multimodal functional studies to investigate the specific regulation of IECs by intestinal allogeneic IEL T cells, thereby overall displaying multiple characteristics reminiscent of intestinal GvHD pathophysiology. We strongly believe that the use of this allogeneic IEL/organoid co-culture model system will facilitate studies designed to elucidate allogeneic pathomechanisms driven by donor-derived IEL T cells with the ultimate goal to pave the way for the identification of novel therapeutic strategies and target structures.

Data availability statement

The original contributions presented in the study are included in the article/Supplementary Material. Further inquiries can be directed to the corresponding author.

Ethics statement

The animal study was approved by government of Lower and Middle Franconia. The study was conducted in accordance with the local legislation and institutional requirements.

Author contributions

DM: Conceptualization, Data curation, Formal Analysis, Investigation, Methodology, Validation, Writing – original draft, Writing – review & editing. MD: Methodology, Resources, Writing – review & editing. BS: Data curation, Methodology, Resources, Software, Writing – review & editing. TV: Investigation, Methodology, Project administration, Resources, Writing – review & editing. MN: Conceptualization, Resources, Supervision, Writing – review & editing. HP: Methodology, Resources, Writing – review & editing. CN: Methodology, Resources, Supervision, Writing – review & editing. MB-H: Conceptualization, Funding acquisition, Investigation, Methodology, Supervision, Writing – review & editing. KH: Conceptualization, Data curation, Formal Analysis, Funding acquisition, Methodology, Project administration, Resources, Supervision, Validation, Visualization, Writing – original draft, Writing – review & editing.

Funding

This study was supported by the Collaborative Research Centers of the Deutsche Forschungsgemeinschaft (DFG, German Research Foundation): TRR 221 (DFG-CRC221, Project-ID 324392634-B03 to KH and -Z01 to MBH); TRR 241 (DFG-CRC241, Project-ID 375876048-A08 to both KH & CN), SFB1181 (DFG-CRC1181, Project-ID 261193037_B05 to KH). Funding was also provided by the IZKF Erlangen: project A84 (to KH & MBH) and A96 (to KH). Spinning disc microscopy was performed on a Zeiss Spinning Disc Axio Observer Z1, funded by Deutsche Forschungsgemeinschaft (DFG, German Research Foundation) - project 248122450.

Acknowledgments

We thank Irena Klaußner, Iris Stolzer and Claudia Günther, Department of Medicine 1, Friedrich-Alexander-University Erlangen-Nürnberg, Erlangen for technical support.

Conflict of interest

The authors declare that the research was conducted in the absence of any commercial or financial relationships that could be construed as a potential conflict of interest.

Publisher's note

Supplementary material

The Supplementary Material for this article can be found online at: https://www.frontiersin.org/articles/10.3389/fimmu.2023.1253514/full#supplementary-material

References

1. Copelan E, Casper JT, Carter SL, van Burik JA, Hurd D, Mendizabal AM, et al. A scheme for defining cause of death and its application in the T cell depletion trial. *Biol Blood Marrow Transplant* (2007) 13(12):1469–76. doi: 10.1016/j.bbmt.2007.08.047

2. Zeiser R, Blazar BR. Acute graft-versus-host disease - biologic process, prevention, and therapy. *N Engl J Med* (2017) 377(22):2167–79. doi: 10.1056/NEJMra1609337

3. Jaksch M, Mattsson J. The pathophysiology of acute graft-versus-host disease. *Scand J Immunol* (2005) 61(5):398–409. doi: 10.1111/j.1365-3083.2005.01595.x

4. Choi SW, Levine JE, Ferrara JL. Pathogenesis and management of graft-versus-host disease. *Immunol Allergy Clin North Am* (2010) 30(1):75–101. doi: 10.1016/j.iac.2009.10.001

5. Ara T, Hashimoto D. Novel insights into the mechanism of GVHD-induced tissue damage. *Front Immunol* (2021) 12:713631. doi: 10.3389/fimmu.2021.713631

6. Jansen SA, Nieuwenhuis EES, Hanash AM, Lindemans CA. Challenges and opportunities targeting mechanisms of epithelial injury and recovery in acute intestinal graft-versus-host disease. *Mucosal Immunol* (2022) 15(4):605–19. doi: 10.1038/s41385-022-00527-6

7. Harris AC, Young R, Devine S, Hogan WJ, Ayuk F, Bunworasate U, et al. International, multicenter standardization of acute graft-versus-host disease clinical data collection: A report from the mount sinai acute GVHD international consortium. *Biol Blood Marrow Transplant* (2016) 22(1):4–10. doi: 10.1016/j.bbmt.2015.09.001

8. Naymagon S, Naymagon L, Wong SY, Ko HM, Renteria A, Levine J, et al. Acute graft-versus-host disease of the gut: considerations for the gastroenterologist. *Nat Rev Gastroenterol Hepatol* (2017) 14(12):711–26. doi: 10.1038/nrgastro.2017.126

9. Ma H, Qiu Y, Yang H. Intestinal intraepithelial lymphocytes: Maintainers of intestinal immune tolerance and regulators of intestinal immunity. *J Leukoc Biol* (2021) 109(2):339–47. doi: 10.1002/JLB.3RU0220-111

10. Cheroutre H, Lambolez F, Mucida D. The light and dark sides of intestinal intraepithelial lymphocytes. *Nat Rev Immunol* (2011) 11(7):445–56. doi: 10.1038/nri3007

11. Masopust D, Choo D, Vezys V, Wherry EJ, Duraiswamy J, Akondy R, et al. Dynamic T cell migration program provides resident memory within intestinal epithelium. *J Exp Med* (2010) 207(3):553–64. doi: 10.1084/jem.20090858

12. Cheng L, Becattini S. Intestinal CD8(+) tissue-resident memory T cells: From generation to function. *Eur J Immunol* (2022) 52(10):1547–60. doi: 10.1002/eji.202149759

13. McDonald BD, Jabri B, Bendelac A. Diverse developmental pathways of intestinal intraepithelial lymphocytes. *Nat Rev Immunol* (2018) 18(8):514–25. doi: 10.1038/s41577-018-0013-7

14. Tsuzuki T, Yoshikai Y, Ito M, Mori N, Ohbayashi M, Asai J. Kinetics of intestinal intraepithelial lymphocytes during acute graft-versus-host disease in mice. *Eur J Immunol* (1994) 24(3):709–15. doi: 10.1002/eji.1830240333

15. Schattenfroh NC, Hoffman RA, McCarthy SA, Simmons RL. Phenotypic analysis of donor cells infiltrating the small intestinal epithelium and spleen during graft-versus-host disease. *Transplantation.* (1995) 59(2):268–73. doi: 10.1097/00007890-199501000-00020

16. Nussler NC, Hoffman RA, McCarthy SA, Simmons RL. Functional changes of intestinal intraepithelial lymphocytes during acute graft versus host disease: correlation with phenotype. *Int Immunol* (1996) 8(11):1767–77. doi: 10.1093/intimm/8.11.1767

17. Nozaki K, Mochizuki W, Matsumoto Y, Matsumoto T, Fukuda M, Mizutani T, et al. Co-culture with intestinal epithelial organoids allows efficient expansion and motility analysis of intraepithelial lymphocytes. *J Gastroenterol* (2016) 51(3):206–13. doi: 10.1007/s00535-016-1170-8

18. Sato T, Vries RG, Snippert HJ, van de Wetering M, Barker N, Stange DE, et al. Single Lgr5 stem cells build crypt-villus structures in *vitro* without a mesenchymal niche. *Nature.* (2009) 459(7244):262–5. doi: 10.1038/nature07935

19. Enderle K, Dinkel M, Spath EM, Schmid B, Zundler S, Tripal P, et al. Dynamic imaging of IEL-IEC co-cultures allows for quantification of CD103-dependent T cell migration. *Int J Mol Sci* (2021) 22(10). doi: 10.3390/ijms22105148

20. Rogoz A, Reis BS, Karssemeijer RA, Mucida D. A 3-D enteroid-based model to study T-cell and epithelial cell interaction. *J Immunol Methods* (2015) 421:89–95. doi: 10.1016/j.jim.2015.03.014

21. Ullrich E, Abendroth B, Rothamer J, Huber C, Buttner-Herold M, Buchele V, et al. BATF-dependent IL-7RhiGM-CSF+ T cells control intestinal graft-versus-host disease. *J Clin Invest* (2018) 128(3):916–30. doi: 10.1172/JCI89242

22. Buchele V, Abendroth B, Buttner-Herold M, Vogler T, Rothamer J, Ghimire S, et al. Targeting Inflammatory T Helper Cells *via* Retinoic Acid-Related Orphan Receptor Gamma t Is Ineffective to Prevent Allo-Response-Driven Colitis. *Front Immunol* (2018) 9:1138. doi: 10.3389/fimmu.2018.01138

23. Bode KJ, Mueller S, Schweinlin M, Metzger M, Brunner T. A fast and simple fluorometric method to detect cell death in 3D intestinal organoids. *Biotechniques.* (2019) 67(1):23–8. doi: 10.2144/btn-2019-0023

24. Schmid B, Tripal P, Fraass T, Kersten C, Ruder B, Gruneboom A, et al. 3Dscript: animating 3D/4D microscopy data using a natural-language-based syntax. *Nat Methods* (2019) 16(4):278–80. doi: 10.1038/s41592-019-0359-1

25. Enderle K, Dinkel M, Spath EM, Schmid B, Zundler S, Tripal P, et al. Dynamic imaging of IEL-IEC co-cultures allows for quantification of CD103-dependent T cell migration. *Int J Mol Sci* (2021) 22(10). doi: 10.3390/ijms22105148

26. Linkert M, Rueden CT, Allan C, Burel JM, Moore W, Patterson A, et al. Metadata matters: access to image data in the real world. *J Cell Biol* (2010) 189 (5):777–82. doi: 10.1083/jcb.201004104

27. Tinevez JY, Perry N, Schindelin J, Hoopes GM, Reynolds GD, Laplantine E, et al. TrackMate: An open and extensible platform for single-particle tracking. *Methods.* (2017) 115:80–90. doi: 10.1016/j.ymeth.2016.09.016

28. Barker N, van Es JH, Kuipers J, Kujala P, van den Born M, Cozijnsen M, et al. Identification of stem cells in small intestine and colon by marker gene Lgr5. *Nature.* (2007) 449(7165):1003–7. doi: 10.1038/nature06196

29. van der Flier LG, Haegebarth A, Stange DE, van de Wetering M, Clevers H. OLFM4 is a robust marker for stem cells in human intestine and marks a subset of colorectal cancer cells. *Gastroenterology.* (2009) 137(1):15–7. doi: 10.1053/j.gastro.2009.05.035

30. Wang H, Asavaroengchai W, Yeap BY, Wang MG, Wang S, Sykes M, et al. Paradoxical effects of IFN-gamma in graft-versus-host disease reflect promotion of lymphohematopoietic graft-versus-host reactions and inhibition of epithelial tissue injury. *Blood.* (2009) 113(15):3612–9. doi: 10.1182/blood-2008-07-168419

31. Takashima S, Martin ML, Jansen SA, Fu Y, Bos J, Chandra D, et al. T cell-derived interferon-gamma programs stem cell death in immune-mediated intestinal damage. *Sci Immunol* (2019) 4(42). doi: 10.1126/sciimmunol.aay8556

32. Chavez-Galan L, Arenas-Del Angel MC, Zenteno E, Chavez R, Lascurain R. Cell death mechanisms induced by cytotoxic lymphocytes. *Cell Mol Immunol* (2009) 6 (1):15–25. doi: 10.1038/cmi.2009.3

33. Freedman HA, Lilly F. Properties of cell lines derived from tumors induced by Friend virus in BALB/c and BALB/c-H-2b mice. *J Exp Med* (1975) 142(1):212–23. doi: 10.1084/jem.142.1.212

34. Jain J, Loh C, Rao A. Transcriptional regulation of the IL-2 gene. *Curr Opin Immunol* (1995) 7(3):333–42. doi: 10.1016/0952-7915(95)80107-3

35. Reem GH, Yeh NH. Interleukin 2 regulates expression of its receptor and synthesis of gamma interferon by human T lymphocytes. *Science.* (1984) 225 (4660):429–30. doi: 10.1126/science.6429853

36. Janas ML, Groves P, Kienzle N, Kelso A. IL-2 regulates perforin and granzyme gene expression in CD8+ T cells independently of its effects on survival and proliferation. *J Immunol* (2005) 175(12):8003–10. doi: 10.4049/jimmunol.175.12.8003

37. Eriguchi Y, Nakamura K, Yokoi Y, Sugimoto R, Takahashi S, Hashimoto D, et al. Essential role of IFN-gamma in T cell-associated intestinal inflammation. *JCI Insight* (2018) 3(18). doi: 10.1172/jci.insight.121886

38. Behr FM, Chuwonpad A, Stark R, van Gisbergen K. Armed and ready: Transcriptional regulation of tissue-resident memory CD8 T cells. *Front Immunol* (2018) 9:1770. doi: 10.3389/fimmu.2018.01770

39. Mueller SN, Mackay LK. Tissue-resident memory T cells: local specialists in immune defence. *Nat Rev Immunol* (2016) 16(2):79–89. doi: 10.1038/nri.2015.3

40. Maniar A, Zhang X, Lin W, Gastman BR, Pauza CD, Strome SE, et al. Human gammadelta T lymphocytes induce robust NK cell-mediated antitumor cytotoxicity through CD137 engagement. *Blood.* (2010) 116(10):1726–33. doi: 10.1182/blood-2009-07-234211

41. de Vries NL, van de Haar J, Veninga V, Chalabi M, Ijsselsteijn ME, van der Ploeg M, et al. gammadelta T cells are effectors of immunotherapy in cancers with HLA class I defects. *Nature.* (2023) 613(7945):743–50. doi: 10.1038/s41586-022-05593-1

42. Minculescu L, Marquart HV, Ryder LP, Andersen NS, Schjoedt I, Friis LS, et al. Improved overall survival, relapse-free-survival, and less graft-vs.-host-disease in patients with high immune reconstitution of TCR gamma delta cells 2 months after allogeneic stem cell transplantation. *Front Immunol* (2019) 10:1997. doi: 10.3389/fimmu.2019.01997

43. Arruda LCM, Gaballa A, Uhlin M. Impact of gammadelta T cells on clinical outcome of hematopoietic stem cell transplantation: systematic review and meta-analysis. *Blood Adv* (2019) 3(21):3436–48. doi: 10.1182/bloodadvances.2019000682

44. Ye W, Kong X, Zhang W, Weng Z, Wu X. The roles of gammadelta T cells in hematopoietic stem cell transplantation. *Cell Transplant* (2020) 29:963689720966980. doi: 10.1177/0963689720966980

45. Sujino T, London M, Hoytema van Konijnenburg DP, Rendon T, Buch T, Silva HM, et al. Tissue adaptation of regulatory and intraepithelial CD4(+) T cells controls gut inflammation. *Science.* (2016) 352(6293):1581–6. doi: 10.1126/science.aaf3892

46. Tkachev V, Kaminski J, Potter EL, Furlan SN, Yu A, Hunt DJ, et al. Spatiotemporal single-cell profiling reveals that invasive and tissue-resident memory donor CD8(+) T cells drive gastrointestinal acute graft-versus-host disease. *Sci Transl Med* (2021) 13(576). doi: 10.1126/scitranslmed.abc0227

47. El-Asady R, Yuan R, Liu K, Wang D, Gress RE, Lucas PJ, et al. TGF-beta-dependent CD103 expression by CD8(+) T cells promotes selective destruction of the host intestinal epithelium during graft-versus-host disease. *J Exp Med* (2005) 201 (10):1647–57. doi: 10.1084/jem.20041044

48. Liu K, Anthony BA, Yearsly MM, Hamadani M, Gaughan A, Wang JJ, et al. CD103 deficiency prevents graft-versus-host disease but spares graft-versus-tumor effects mediated by alloreactive CD8 T cells. *PLoS One* (2011) 6(7):e21968. doi: 10.1371/journal.pone.0021968

49. Abdelsamed HA, Lakkis FG. The role of self-peptides in direct T cell allorecognition. *J Clin Invest* (2021) 131(21). doi: 10.1172/JCI154096

50. Boardman DA, Jacob J, Smyth LA, Lombardi G, Lechler RI. What is direct allorecognition? *Curr Transplant Rep* (2016) 3(4):275–83. doi: 10.1007/s40472-016-0115-8

51. Lechler RI, Garden OA, Turka LA. The complementary roles of deletion and regulation in transplantation tolerance. *Nat Rev Immunol* (2003) 3(2):147–58. doi: 10.1038/nri1002

52. Felix NJ, Allen PM. Specificity of T-cell alloreactivity. *Nat Rev Immunol* (2007) 7 (12):942–53. doi: 10.1038/nri2200

53. Fu YY, Egorova A, Sobieski C, Kuttiyara J, Calafiore M, Takashima S, et al. T cell recruitment to the intestinal stem cell compartment drives immune-mediated intestinal damage after allogeneic transplantation. *Immunity.* (2019) 51(1):90–103 e3. doi: 10.1016/j.immuni.2019.06.003

54. Matsuzawa-Ishimoto Y, Hine A, Shono Y, Rudensky E, Lazrak A, Yeung F, et al. An intestinal organoid-based platform that recreates susceptibility to T-cell-mediated tissue injury. *Blood.* (2020) 135(26):2388–401. doi: 10.1182/blood.2019004116

55. Göttert S, Fischer JC, Eisenkolb G, Thiele Orberg E, Jarosch S, Holler E, et al. IFN-gamma is crucial for the counterbalance of T cell-mediated injury to the intestinal stem cell compartment by regulatory T cells in mice and humans. *Blood* (2022) 140 (Supplement 1):10223–4. doi: 10.1182/blood-2022-169303

56. Peled JU, Hanash AM, Jenq RR. Role of the intestinal mucosa in acute gastrointestinal GVHD. *Hematol Am Soc Hematol Educ Program* (2016) 2016 (1):119–27. doi: 10.1182/asheducation-2016.1.119

57. Cantoni N, Hirsch HH, Khanna N, Gerull S, Buser A, Bucher C, et al. Evidence for a bidirectional relationship between cytomegalovirus replication and acute graft-versus-host disease. *Biol Blood Marrow Transplant* (2010) 16(9):1309–14. doi: 10.1016/j.bbmt.2010.03.020

58. Cho BS, Yahng SA, Kim JH, Yoon JH, Shin SH, Lee SE, et al. Impact of cytomegalovirus gastrointestinal disease on the clinical outcomes in patients with gastrointestinal graft-versus-host disease in the era of preemptive therapy. *Ann Hematol* (2013) 92(4):497–504. doi: 10.1007/s00277-012-1632-x

59. Mathewson ND, Jenq R, Mathew AV, Koenigsknecht M, Hanash A, Toubai T, et al. Corrigendum: Gut microbiome-derived metabolites modulate intestinal epithelial cell damage and mitigate graft-versus-host disease. *Nat Immunol* (2016) 17(10):1235. doi: 10.1038/ni1016-1235b

60. Hammoudi N, Hamoudi S, Bonnereau J, Bottois H, Perez K, Bezault M, et al. Autologous organoid co-culture model reveals T cell-driven epithelial cell death in Crohn's Disease. *Front Immunol* (2022) 13:1008456. doi: 10.3389/fimmu.2022.1008456

frontiers | Frontiers in Immunology

TYPE Original Research
PUBLISHED 19 September 2023
DOI 10.3389/fimmu.2023.1209464

OPEN ACCESS

EDITED BY
Sina Naserian,
Hôpital Paul Brousse, France

REVIEWED BY
Mohamed Essameldin Abdelgawad,
Wake Forest University,
United States
Sara Shamdani,
Hôpital Paul Brousse, France

*CORRESPONDENCE
Guido Moll
guido.moll@charite.de
Rusan Catar
rusan.catar@charite.de

†In memory of Prof. Duska Dragun

‡These authors have contributed equally to this work and share first authorship

§These authors have contributed equally to this work and share senior authorship

RECEIVED 20 April 2023
ACCEPTED 31 August 2023
PUBLISHED 19 September 2023

CITATION
Zhao H, Wu D, Gyamfi MA, Wang P, Luecht C, Pfefferkorn AM, Ashraf MI, Kamhieh-Milz J, Witowski J, Dragun D, Budde K, Schindler R, Zickler D, Moll G and Catar R (2023) Expanded Hemodialysis ameliorates uremia-induced impairment of vasculoprotective KLF2 and concomitant proinflammatory priming of endothelial cells through an ERK/AP1/cFOS-dependent mechanism.
Front. Immunol. 14:1209464.
doi: 10.3389/fimmu.2023.1209464

Expanded Hemodialysis ameliorates uremia-induced impairment of vasculoprotective KLF2 and concomitant proinflammatory priming of endothelial cells through an ERK/AP1/cFOS-dependent mechanism

Hongfan Zhao[1‡], Dashan Wu[1‡], Michael Adu Gyamfi[1], Pinchao Wang[1], Christian Luecht[1], Anna Maria Pfefferkorn[2], Muhammad Imtiaz Ashraf[2], Julian Kamhieh-Milz[3], Janusz Witowski[4], Duska Dragun[1†], Klemens Budde[1], Ralf Schindler[1], Daniel Zickler[1], Guido Moll[1,5*§] and Rusan Catar[1*§]

[1]Department of Nephrology and Internal Intensive Care Medicine, at Charité Universitätsmedizin Berlin, corporate member of Freie Universität Berlin, Humboldt-Universität zu Berlin, and Berlin Institute of Health (BIH), Berlin, Germany, [2]Department of Surgery, at Charité Universitätsmedizin Berlin, Berlin, Germany, [3]Institute of Transfusion Medicine, at Charité Universitätsmedizin Berlin, Berlin, Germany, [4]Department of Pathophysiology, Poznan University of Medical Sciences, Poznan, Poland, [5]BIH Center for Regenerative Therapies (BCRT) and Berlin-Brandenburg School for Regenerative Therapies (BSRT), at Charité Universitätsmedizin Berlin, Berlin, Germany

Aims: Expanded hemodialysis (HDx) therapy with improved molecular cut-off dialyzers exerts beneficial effects on lowering uremia-associated chronic systemic microinflammation, a driver of endothelial dysfunction and cardiovascular disease (CVD) in hemodialysis (HD) patients with end-stage renal disease (ESRD). However, studies on the underlying molecular mechanisms are still at an early stage. Here, we identify the (endothelial) transcription factor Krüppel-like factor 2 (KLF2) and its associated molecular signalling pathways as key targets and regulators of uremia-induced endothelial micro-inflammation in the HD/ESRD setting, which is crucial for vascular homeostasis and controlling detrimental vascular inflammation.

Methods and results: First, we found that human microvascular endothelial cells (HMECs) and other typical endothelial and kidney model cell lines (e.g. HUVECs, HREC, and HEK) exposed to uremic serum from patients treated with two different hemodialysis regimens in the Permeability Enhancement to Reduce Chronic Inflammation II (PERCI-II) crossover clinical trial - comparing High-Flux (HF) and Medium Cut-Off (MCO) membranes - exhibited strongly reduced expression of vasculoprotective KLF2 with HF dialyzers, while dialysis with MCO dialyzers led to the maintenance and restoration of physiological KLF2

10.3389/fimmu.2023.1209464

levels in HMECs. Mechanistic follow-up revealed that the strong downmodulation of KLF2 in HMECs exposed to uremic serum was mediated by a dominant engagement of detrimental ERK instead of beneficial AKT signalling, with subsequent AP1-/c-FOS binding in the KLF2 promoter region, followed by the detrimental triggering of pleiotropic inflammatory mediators, while the introduction of a KLF2 overexpression plasmid could restore physiological KLF2 levels and downmodulate the detrimental vascular inflammation in a mechanistic rescue approach.

Conclusion: Uremia downmodulates vasculoprotective KLF2 in endothelium, leading to detrimental vascular inflammation, while MCO dialysis with the novel improved HDx therapy approach can maintain physiological levels of vasculoprotective KLF2.

KEYWORDS

chronic kidney disease (CKD), end-stage renal disease (ESRD), uremic toxins, cytokine signaling, systemic inflammation, cardiovascular disease (CVD), Krüppel-like factor 2 (KLF2), and expanded hemodialysis therapy (HDx)

1 Introduction

Chronic kidney disease (CKD) and end-stage renal disease (ESRD) are a major public health burden despite recently improved global awareness and better access to kidney care (1–4). In addition to kidney transplantation (KTx) (5), several renal replacement therapies (RRTs), such as peritoneal dialysis (PD) (6) and hemodialysis (HD) (7), offer well-established life-sustaining therapies for ESRD patients (4), which are nonetheless still associated with a considerable need for improvements considering their long-term morbidity and mortality outcomes (8–12).

Even under optimal care, both, CKD and in particular more advanced ESRD patients, suffer from multiple strong cardiovascular disease (CVD) risk factors, which are a leading cause for the underlying high morbidity and mortality (13). These complications can project into the manifestation of chronic microvascular injury, which in turn promotes the cardiovascular and post-inflammatory risks and detrimentally affects patient morbidity and mortality in the long run (14, 15). Thus, in order to optimize existing RRT treatments, intense research is currently ongoing to stepwise overcome any evident RRT-related chronic complications (8–12).

In the case of HD, where uremic toxins are removed *via* membrane-filter systems, uremic interaction with the endothelium and incomplete removal of uremic macromolecules promotes endothelial dysfunction and systemic microinflammation (15, 16). However, the novel expanded hemodialysis therapy (HDx) approach (9–11), which aims for a more efficient removal of middle-sized uremic toxins through use of novel improved middle cut-off (MCO) dialyzers (17), may offer better endothelial protection than the traditional high-flux (HF) dialyzers (7, 17, 18). Thus, more detailed mechanistic studies in this scientific context are of great interest.

As shown in the PERCI-II-MCO study (NCT02084381) (17), compared to HF-dialyzed patients the uremic serum from MCO-dialyzed patients exhibits reduces levels of typical pro-inflammatory mediators and less maladaptive angiogenesis in functional readouts (7, 17). In the current study, we have investigated in detail the role of Krüppel-like factor 2 (KLF2), an important zinc-finger transcription factor expressed in endothelial cells (ECs) (19, 20), considering its putative role in regulating and maintaining vascular homeostasis in the HDx setting.

KLF2 maintains vascular homeostasis and protection against endothelial dysfunction and atherosclerosis by multiple mechanisms (20), e.g. by blocking leukocyte adhesion to endothelium, by inhibiting endothelial inflammation, and by modulating thrombotic pathways and detrimental vascular calcification (20–24). Importantly, KLF2 exerts inhibitory effects on various pro-inflammatory stimuli, such as interleukin-1β (IL-1β), tumor-necrosis-factor-α (TNF-α), transforming-growth-factor-β (TGF-β), and thrombin, thus suggesting a pleiotropic anti-inflammatory and vasculo-protective effect (20, 23, 25). In turn, KLF2-suppression can promote endothelial inflammation and damage of glomerular endothelium (20, 26, 27).

On the transcriptional level, KLF2 has been shown earlier to suppress pulmonary fibrosis and inflammation, and to strongly impede TGF-β signals in the endothelium, through the inhibition of the activator protein 1 (AP-1) (28, 29). However, the potential role of KLF2 in uremia-induced endothelial inflammation, maladaptation, and dysfunction has not been studied in detail yet. Indeed, the modulation of vasculo-protective KLF2 may provide both, an interesting prognostic to either monitor the impact of inflammation and vascular health in advanced CKD/ESRD patients,

but also an interesting therapeutic target to restore vascular health and integrity in uremic patients within vascular crisis.

In this study, we have investigated in detail the effect of uremia-induced regulation of KLF2 on the impact of pro-inflammatory mediators and endothelial function. First of all, we found that endothelial KLF2 expression is strongly downmodulated by uremia compared to healthy serum. Mechanistically, we have explored the underlying signaling mechanisms, and indicating that KLF2 signaling is mediated *via* regulation of AP-1. Eventually, we found that KLF2 expression differs in ECs exposed to uremic serum from patients dialyzed with conventional HF membranes compared to novel MCO dialyzers, thus associating with a reduced release of proinflammatory mediators with the novel improved HDx therapy.

2 Methods

2.1 Study patient description and serum samples

The uremic serum samples were obtained during the Permeability Enhancement to Reduce Chronic Inflammation-II clinical trial (PERCI-II-MCO; ClinicalTrials.gov NCT02084381; https://clinicaltrials.gov/ct2/show/NCT02084381) (17). The clinical study was conducted in accordance with the ethical principles of the Declaration of Helsinki and approved by the Ethics Committees of the Martin-Luther-University Halle-Wittenberg and the Charité Berlin, and written informed consent was given prior to inclusion of subjects into the study, as outlined previously (7, 17). The mean age of the patients in the PERCI-II study was as follows: MCO-first (58.1 +/- 16.5 years, n=23 patients) and HF-first (59.8 +/- 16.5 years, n=25). More detailed study patient parameters, serum sampling procedures, and its experimental use are described in greater detail in our prior publications (7, 17). Briefly, for mechanistic experiments, samples of 20 patients were pooled at equal volumes to obtain a uremic serum pool (USP) and non-uremic serum from 14 healthy donors (Age 36 ± 9.2 years; nine males, five females) was collected at our department, to generate a healthy serum pool (HSP) for comparison (30).

2.2 Endothelial cell culture and experimental readout

The disposable cell culture plastic materials were purchased from Becton Dickinson (Falcon; Franklin Lakes, USA) and basic chemicals from Sigma (St Luis, USA). The specific blocking reagents employed in the cell culture experiments were as follows: AP1-blocker (AP1B; SR-11302), AKT-blocker (AKTB; MK-2206), ERK-Blocker (ERKB; PD-184352), all obtained from Tocris Bioscience (Wiesbaden Germany) (6, 7, 25). The basic media and buffers (e.g. phosphate buffered saline; PBS) and penicillin/streptomycin were purchased from Biochrom-AG (Berlin, Germany) and the fetal calf serum (FCS) from Invitrogen (Darmstadt, Germany). The following specific cell types and respective specialized culture media were used for cell culture expansion and different experimental readouts.

1) Human microvascular endothelial cells (HMECs; catalogue no. CRL-3243; purchased from ATCC®, Manassas, VA, USA) were cultured in MCDB131 basic media for HMECs (Invitrogen and Gibco, Waltham, MA, USA) supplemented with 5% FCS, 10 mM L-glutamine, 10 ng/ml recombinant human EGF, 10nM hydrocortisone, and 1% penicillin/streptomycin (100 U/ml and 100 ug/ml, respectively) (31).

2) Human umbilical vein endothelial cells (HUVECs; Cat. No.: P10961, purchased from Innoprot; Bizkaia, Spain; https://innoprot.com) were cultured in Endothelial Growth Medium for HUVECs (Ca No: CCM027 from Biotechne/R&D Systems, www.rndsystems.com) supplemented with 5% Endothelial Growth Supplement (ECGS; containing human FGF-basic, LR3-IGF-1, VEGF165, EGF, heparin, hydrocortisone, l-ascorbic acid, and FCS, as described in detail by the supplier) and 1% penicillin/streptomycin (100 U/ml and 100 ug/ml, respectively).

3) Human reticular endothelial cells (HRECs; Cat. No.: P10880, from Innoprot) were cultured in Endothelial Cell Growth Medium HRECs (Ca No: P60104 from Innoprot), containing endothelial basic medium, supplemented with 5% FCS, 1% of ECGS (as provided by manufacturer), and 1% penicillin/streptomycin (100 U/ml and 100 ug/ml, respectively).

4) Human embryonic kidney cells (HEK293; Cat. No.: CRL-1573, from ATCC®) were cultured in Dulbecco's Modified Eagle Medium (DMEM; Cat. No.: 30-2003 from ATCC®) supplemented with 10% FCS, 2mM GlutaMax (Gibco), 1mM sodium pyruvate, 10mM HEPES, and 100 U/ml penicillin/100 ug/ml streptomycin (31).

For experimental readout, the different ECs were seeded at standardized densities (20.000 cells per well) and cultured in basic medium with 0.5% FCS, supplemented with or without 5% (vol/vol) HSP, USP, or different types of individual uremic patient serum fractions from the MCO study, as described in detail in figure legends and reported earlier (7). The cell viability was assessed by quantifying mitochondrial activity with the water-soluble tetrazolium (WST-8) salt assay according to the manufacturer's instructions (PromoCell) (30).

2.3 Gene expression analysis with qRT-PCR and Profiler PCR arrays

Gene expression was assessed with reverse transcription and quantitative real-time polymerase chain reaction (qRT-PCR), as outlined earlier (30, 32–37). Total RNA was extracted by using the PerfectPure RNA Cultured Cell Kit (5 Prime, Hamburg, Germany), its concentration and purity was estimated with a spectrophotometer (Nanodrop; Thermo Fisher Scientific), and the RNA reverse transcribed into cDNA with random hexamer primers, and qRT-PCRs performed on a 7500 Fast Block Real-Time PCR system (Applied Biosystems). Human primer sequences can be found in Table 1. The specificity of the qRT-PCR reaction was verified with melting curve analysis and the relative amount of

10.3389/fimmu.2023.1209464

TABLE 1 Sequences of primers used in quantitative-real-time-PCR analysis.

Gene	Sequence Sense Primer 5′→3′	Sequence Antisense Primer 3′→ 5′
TNF-a	gACAAgCCTgTAgCCCATgT	gAggTACAggCCCTCTgATg
UBC	ATTTgggTCgCggTTCTTg	TgCCTTgACATTCTCgATggT
c-FOS (GM)	AggAgAATCCgAAgggAAAg	CTTCTCCTTCAgCAggTTgg
c-JUN (GM)	CCCCAAgATCCTgAAACAgA	CCgTTgCTggACTggATTAT
KLF2 mRNA	CTgCCgTCCTTCTCCACTTT	CCCATggACAggATgAAgTC
AP-1 Oligo for KLF2	CAG CCC TCT CTG AGG CTG GAG CCA	TGG CTC CAG CCT CAG AGA GGG CTG
KLF2_pcDNA3	TAC CGA GCT CGG ATC CAT GGC GCT GAG TGA ACC CA	GAT ATC TGC AGA ATT CCT ACA TGT GCC GTT TCA TGT G
KLF2_2109 + 93	TGGCCTAACTGGCCGGTACCAGCCATTTGGGGTAAGGTACTAT	TCT TGA TAT CCT CGA GCG GGG AGA AAG GAC GCG G
KLF2_1109 + 93	TGGCCTAACTGGCCGGTACCTGCCGCAACTCCAACTTCTCC	Same sequence as KLF2_2109 + 93 above
KLF2_509 + 93	TGGCCTAACTGGCCGGTACCCATGAATCCTGGAGACTCCA	Same sequence as KLF2_2109 + 93 above
KLF2_109 + 93	TGGCCTAACTGGCCGGTACCTTAGGCTGCGCCCGGAGC	Same sequence as KLF2_2109 + 93 above

TNFa, tumor necrosis factor alpha; UBC, Ubiquitin C; c-FOS, early response element; AP-1, activator protein-1; and Oligo, oligonucleotide; KLF2, Krüppel-like factor 2; KLF2_2109-109, different KLF2 promoter 5'-deletion luciferase plasmids.

transcript calculated with the cycle threshold method, using the Applied Biosystems 7500 System v.1.2.3 software and gene expression normalized relative to the endogenous reference gene β2-microglobulin (30). The Human Inflammatory Response and Autoimmunity RT2 Profiler PCR Array kit (Qiagen, Cat. No: PAHS-077ZA-6) was used to evaluate the expression of an exploratory panel of n=84 selected genes involved in the inflammatory response, according to the manufacturer's instructions, as reported earlier (33–35).

2.4 DNA constructs, transient transfection and luciferase assay

The DNA constructs of progressive KLF2 5'-putative promoter region deletion fragments (KLF2_2109, KLF2_1109, KLF2_509, and KLF2_109) were cloned into luciferase plasmid vector (pGL4.10, Promega, Madison, WI, USA), and the isolated plasmids were sent for sequencing (LC Genomics, Houston, TX, USA) to ensure the correct length of promoter segments. The HMECs were cultured in 12-well plates at a density that allowed them to reach 70-80% confluence after 24 hours. Transfections were performed using the TurboFect transfection reagent (Fermentas, Darmstadt, Germany) according to the manufacturer's instructions. The cells were transfected with the constructed reporter plasmid (400ng/well) and co-transfected with the reference pRL-TK renilla plasmid (20ng/well), or the KLF2 overexpression gene, as described earlier (7). Luciferase activity was assessed with the dual-luciferase reporter assay system (Promega, Madison, WI, USA) according to the manufacturer's protocol. Luciferase activity was measured using a microplate luminometer (Fluostar Optima, BMG Labtech, Ortenberg, Germany) and normalized to background levels of Renilla luciferase activity from co-transfected control vectors. The primers sequences are provided in Table 2. The human KLF2 gene promoter region -509 to -110 (Figure S1; GenBank AY738222.1) was analysed with the PROMO virtual laboratory program for the presence and location of potential transcription factor binding sites (http://gene-regulation.com/pub/programs/alibaba2/), accessed on 23 of March 2023 (25).

2.5 Nuclear extracts, electrophoretic mobility shift assay, and immunoassays

Nuclear extracts were prepared using the NE-PER Nuclear and Cytoplasmic Extraction Kit and oligonucleotide probes labelled with Biotin 3' End DNA Labeling Kit (ThermoFisher). For the EMSA (37), the following probe was used (promoter region provided in parentheses): AP-1 - 5'-CAGGCTTCACTGAGCGTCCGCAG-3' (-441 to -464) (Table 2). Each EMSA binding mixture (20 µl) contained 5 µg of nuclear extract, 20 fmol of labeled double-stranded probe, 1 µg of poly (deoxyinosinicdeoxycytidylic) acid, and 2 µl of 10 x reaction buffer, and was incubated at room temperature for 30 min. Protein–DNA complexes were analyzed by electrophoresis in 6% non-denaturing polyacrylamide gels and visualized using a LightShift Chemiluminescent EMSA Kit (ThermoFisher). The Pierce BCA Protein Assay Reagent (Perbio Science, Bonn, Germany) was used to determine the protein concentration for NE-PER and Western Blot analysis.

Cell extracts for KLF2, c-FOS, pAKT and PERK1/2 protein detection in Western blot analysis were prepared as described earlier (38). The cell lysates were electrophoresed on sodium dodecyl sulfate (SDS)-polyacrylamide gels and analyzed by Western blotting using primary antibodies directed against the target proteins KLF2, c-FOS, pAKT and pERK1/2 (Merck-Sigma-Aldrich, Taufenkirchen, Germany, and Cell Signaling Technology, Frankfurt, Germany, respectively) and GAPDH (Hytest, Turku, Finland), and respective secondary peroxidase-conjugated IgG (Dianova, Hamburg, Germany) (Table 2). The bands were visualized with an Enhanced Chemiluminescence Detection System

TABLE 2 Antibodies and reagents used for EMSA and western blot.

Antibody	Target Antigen	Host	Code	Company	Dilution
KLF2	KLF2 protein	Rabbit	SAB210832-100UL	Sigma	1:500
c-FOS	c-FOS Protein	Rabbit	#4384	CST	1:1000
p-AKT	p-AKT Protein	Rabbit	#9272	CST	1:1000
p-ERK	pERK Protein	Rabbit	#9102	CST	1:1000
GAPDH	GAPDH protein	Mouse	#5G4	Hytest	1:50000
2nd Antibody Anti-Mouse	Mouse antigen	Donkey	#715035150	Dianova	1:5000
2nd Antibody Anti-Rabbit	Rabbit antigen	Donkey	#711035152	Dianova	1:10000

KLF2, Krüppel-like factor 2; c-FOS, early response element; AKT, protein kinase B; MAPK/ERK, map-kinase/extracellular signal-regulated kinase; and GAPDH, glyceraldehyde 3-phosphate dehydrogenase.

(Thermo Scientific) and analzed Image J 1.43 software (National Institues of Health, Bethesda, MD, USA). The levels of IL-6, IL-8, and TNF-α in the supernatant of HMEC-conditioned media were measure by enzyme-linked immune assay (ELISA) using respective antibody pair buffer kits (ThermoFisher Scientific, Waltham, MA, USA) according to the manufacturer's instructions.

2.6 Statistical analysis

Data are expressed as mean ± SEM. Non-parametric data are presented as medians. Statistical analysis and visualization was performed using GraphPad Prism (GraphPad®, San Diego, US) and R (version 3.5.1). Analyses of multiple variables were performed by one-way analysis of variance with Student–Newman–Keuls post- or Kruskal–Wallis with Müller–Dunn post-test. A P-value < 0.05 was considered statistically significant.

3 Results

3.1 Uremic serum reduces the transcription and expression of KLF2 in HMECs

The expression of KLF2 in ECs confers endothelial integrity by regulating anti-inflammatory and antithrombotic effects (21), while reduced transcriptional activity of KLF2 exacerbates chronic inflammation and endothelial damage in renal diseases (39). Thus, it is of great interest to study in detail the signaling events and functional effects related to KLF2.

For this purpose, we established a model system (Figure 1), to study the KLF2 response of microvascular HMECs to uremic serum pool (USP) from ESRD patients, as compared to healthy serum pool (HSP), at both the transcriptional mRNA and the translational protein level, employing USP from a well-defined clinical study cohort that has tested novel medium cut-off (MCO) dialyzers with increased molecular cut-off (Figures 1A, B) (7, 17, 18).

First of all, we found a continuous time-dependent downmodulation of KLF2 mRNA in HMECs after 3-24 hour exposure to 5% USP, but not 5% HSP, with a 50% reduction as early as 6 hours post initiation (and 64% decrease by 24 hours), which was thus chosen as the default optimal exposure time for the assessment of changes in KLF2 mRNA transcription in the subsequent experiments (P<0.05 and P<0.1, respectively, Figure 2A).

Next, we tested HMEC exposure to different doses of serum and found that a 6-hour incubation with 5-10% USP, but not similar doses of HSP, led to a strong downmodulation of KLF2 mRNA transcript (around 50% reduction with 5% USP, P<0.01, and more than 80% reduction with 10% USP, P<0.001, Figure 2B). Due to the scarcity of these samples, we chose 5% USP as our standard working concentrations for the subsequent experiments.

Similarly, the exposure of HMECs to 5% USP resulted in a 50% and 66% reduction in KLF2 protein levels at 6 and 12 hours compared to HSP (Both P<0.5, Figure 2C). These results indicate that USP-exposure represses both, the transcriptional and post-transcriptional activity of KLF2 in endothelial cells, which may ultimately aggravate renal injury.

To better understand the mechanism of USP-induced inhibition of KLF2 activity, an exogenous pcDNA3.0-KLF2 (KLF2-OE) plasmid was constructed for this study and applied in our model to restore the inhibition of KLF2 induced by USP (Figure 2D). An amount of 400 ng of plasmid transfected into 50.000 HMECs was found to be the optimal amount to restore KLF2 protein levels in the USP compared to the HSP group.

3.2 Uremic serum induces KLF2 promoter inhibition via AP-1/c-FOS signaling

KLF2 transcriptional activity can be influenced by many regulatory elements and co-dependent genes, including the ubiquitous activator protein-1 (AP-1/c-FOS) family (40–42). Typical transcription factors and signaling cascades that may influence KLF2 transcription and consequent down-stream-signaling in HMECs may include cellular signaling pathways involving the transcription factor AP-1/c-FOS, but also the protein kinase B (AKT) and map-kinase/extracellular signal-regulated kinase 1/2 (MAPK/ERK1/2) signaling (7, 32).

Employing our well-established luciferase-reporter-system (7), we found that treatment of HMECs containing full-length KLF2 promoter constructs with 5% USP, but not 5% HSP, resulted in a strong decrease of luciferase activity in the USP-group (P<0.001,

10.3389/fimmu.2023.1209464

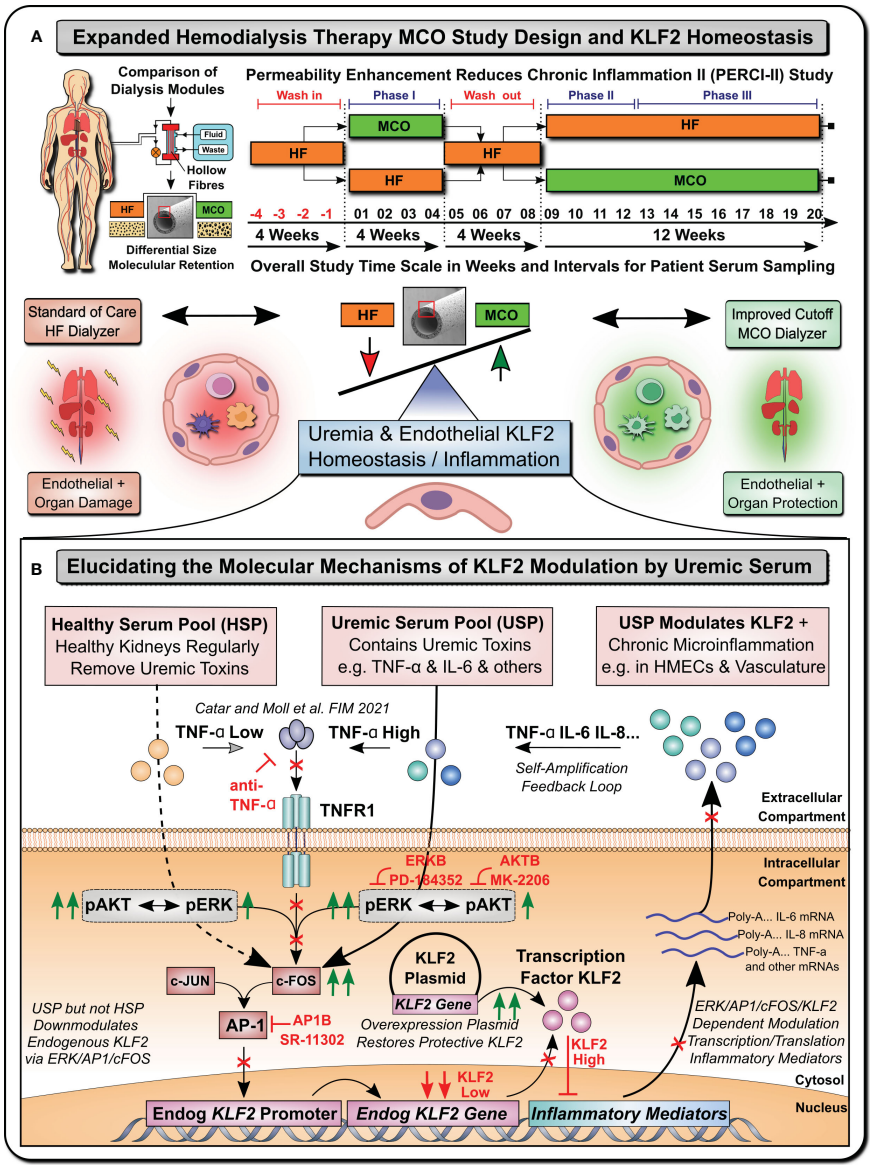

FIGURE 1
Uremia Modulates Vasculoprotective KLF2 Expression (Graphical Abstract). **(A)** Expanded Hemodialysis Therapy (HDx) MCO Study Design and KLF2 Homeostasis: Recently, particular attention has been placed into lowering chronic treatment-associated adverse cardiovascular diseases (CVD) and new optimized treatment concepts, such as "Expanded Hemodialysis Therapy" with improved molecular cut-off hemodialyzers (7, 9, 10). Within the PERCI-II study n=48 hemodialysis patients underwent crossover randomized multi-center comparison employing novel medium-cut-off (MCO; MCOI-Ci400, Gambro) dialyzers in comparison to standard of care high-flux (HF) hemodialyzers (PERCI-II-MCO; ClinicalTrials.gov: NCT02084381) (7, 17). These novel MCO dialyzers have an improved molecular size cut-off, which positively modulates systemic microinflammation and may thus be protective to lower uremia associated endothelial dysfunction and organ damage (7, 17). A key factor in regulating endothelial homeostasis and inflammation is Krüppel-like factor 2 (KLF2), which is the main focus of this mechanistic follow-up study to the PERCI-II clinical trial (7). **(B)** Elucidating molecular mechanisms of vasculoprotective KLF2 modulation by uremic serum: During the biomarker follow-up of the initial PERCI-II clinical trial KLF2 was identified as a potential target for mechanistic follow-up of the molecular signalling mechanisms underlying KLF2 impairment by uremia associated with the conventional HF dialysis regimen, but its improved KLF2 maintenance or restoration with the novel improved MCO dialyzer approach. For the mechanistic studies, to have sufficient amounts of standardized uremic serum available, we compared in detailed signalling pathway analysis and concomitant blocking experiments the response of microvascular endothelial cells (HMECs) to either healthy serum pools (HSP) or uremic serum pools (USP), as described in more detail in an earlier publication that identified TNF-signalling/triggering as a crucial mediator of USP activation in HMECs (7). In the current study, we first-of-all documented a strong impairment of KLF2 expression and concomitant pleiotropic upregulation of a panel of proinflammatory mediators in response to USP but not HSP, thereby triggering a vicious self-amplification loop to trigger the release of more inflammatory uremic toxins from HMECs (e.g. TNF-a, IL-6 etc). Signalling pathway analysis found that this was mediated by preferential engagement of map-kinase/extracellular signal-regulated kinase (MAPK/ERK) instead of protein kinase B (AKT) signalling by employing the respective molecular inhibitors (ERKB: PD-184352 and AKTB: MK-2206). Next, we found that this is mediated by modulation of activator protein 1 (AP-1) and early response element (c-FOS) transcription factor complex (AP-1/c-FOS) signalling (Employing AP1B: SR-11302) and its concomitant binding to the respective promoter region in endothelial KLF2 gene. Importantly, the introduction of a KLF2 overexpression plasmid could restore physiological KLF2 levels and downmodulate the detrimental vascular inflammation in a mechanistic rescue approach. These findings provide new avenues for molecular targets and treatment modalities to reduce chronic microinflammation in the context of hemodialysis.

10.3389/fimmu.2023.1209464

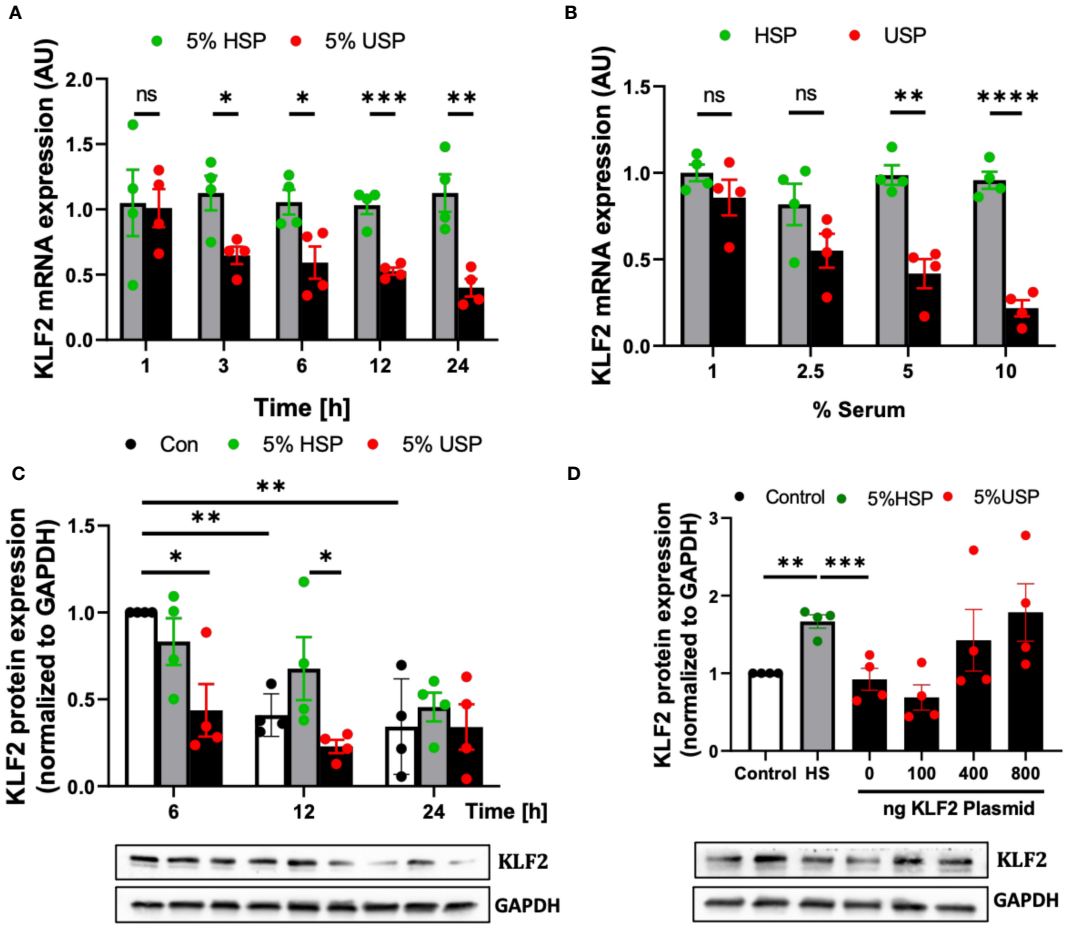

FIGURE 2
Uremic serum inhibits transcription and translation of KLF2 in HMECs. **(A)** Time-dependent downregulation of KLF2 upon USP exposure: KLF2 mRNA expression levels detected in HMECs (AU, arbitrary units, n=4) upon stimulation with either 5% healthy serum pool (HSP) or 5% uremic serum pool (USP), with strong downmodulation of KLF2 mRNA at 3-24 hours (50% reduction at 6 hours); **(B)** Dose-dependent downregulation of KLF2 upon HMEC exposure to USP: KLF2 mRNA expression levels (AU, n=4) after a 6-hours exposure of HMECs to USP or HSP at different serum doses (1%, 2.5%, 5% and 10%), respectively, verifying a strong downmodulation of KLF2 upon exposure to 2.5-10% USP; **(C)** Western blot quantification of time-dependent expression changes of KLF2 protein: KLF2 protein is shown relative to glyceraldehyde-3-phosphate dehydrogenase (GAPDH) house-keeping gene control (AU, n=4) upon cell exposure to either 5% HSP or 5% USP for either 6, 12, and 24 hours (optimal differential readout at 6 hours); and **(D)** Antagonizing KLF2 Downmodulation by USP: Western blot quantification of KLF2 protein expression in HMECs (AU, n=4) after transfection with different concentrations of KLF2 plasmids (100, 400 and 800 ng of KLF2 plasmid) to counteract the KLF2 downmodulation observed upon stimulation with 5% USP. Statistical comparison with ANOVA, Mean ± SEM, with *P<0.05, **P<0.01, ***P<0.001, and ****P<0.0001, ns, not significant.

Figure 3A), while stepwise 5'-deletions of the KLF2 promoter region demonstrate that the deletion of positions from -509 to -109 could fully restore the USP-stimulated inhibitory effect on KLF2 promoter activity (Line 1-3, P<0.001, vs. line 4, ns, Figure 3A). These results suggested that key regulatory elements for KLF2 transcription are located in the -509 to -109 region.

Next, we employed AP-1-, AKT-, and ERK-targeted pharmacological blockade to identify the signaling pathways in HMECs transfected with full-length KLF2-2109 promoter construct that are responsive to stimulation with 5% USP vs. 5% HSP baseline control. The blockade of AP-1 and ERK signaling most effectively restored the USP-induced downmodulation of KLF2 promoter activity (P<0.05 and P<0.01, Figure 3B) and KLF2 mRNA expression (P<0.05, Figure 3C), while blockade of AKT was less effective.

This demonstrates that the USP-induced decrease in KLF2 expression and activity that is depended on the promoter regions -509 to -109 bp engages both AP-1 and ERK signaling. Since AP-1 is a combinatorial transcription factor, the observed promoter region of KLF2 (Entailing the -509 to -109 bp promoter region) was analyzed using the PROMO virtual laboratory (http://alggen.lsi.upc.es/cgi-bin/promo_v3/promo/promoinit.cgi?dirDB=TF_8.3) to determine the DNA-binding switch between AP-1 transcription factor and KLF2 gene (40, 43), and we found that AP-1/c-FOS is a likely candidate could mediate AP-1 action on KLF2.

The specificity of the AP-1/c-FOS binding sites in the KLF2 promoter was confirmed by EMSA (Figure 3D). Semiquantitative EMSA analysis revealed that nuclear extracts from HMECs stimulated with 5% USP contained a DNA-protein complex with

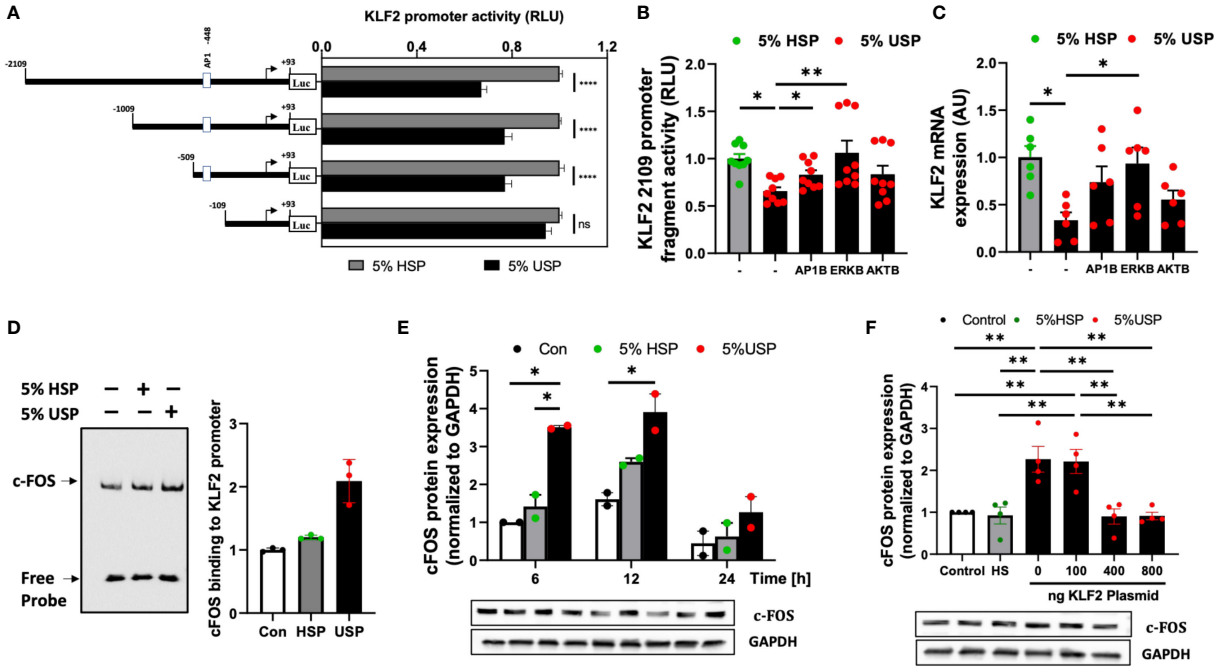

FIGURE 3
USP-inhibition of KLF2 in HMECs occurs in AP-1/c-FOS dependent manner. **(A)** KLF2 Promoter Analysis: Luciferase reporter assays indicate a functional loss of KLF2 activity upon deletion of the -509 to -109 promoter region containing the AP1-/c-FOS transcription factor binding site. HMECs were first transfected with different KLF2 reporter plasmid constructs containing progressive promoter region 5'-deletions, employing either the full-length -2109 construct, or different deletion constructs -1009, -509, -109, and +93, and then incubated with either 5% uremic serum pool (USP) or 5% healthy serum pool (HSP) for 6 hours, to quantify KLF2 promoter activity *via* readout of luciferase activity (RLU, relative luciferase activity, n=12 independent experiments); **(B, C)** Signaling Pathways: Inhibition of KLF2 expression upon a 6-hour exposure to 5% USP can be partially restored by blocking different signaling pathways: e.g. activator protein 1 (AP1B: SR-11302, 1000 nM), protein kinase B (AKTB: MK-2206, 100 nM), or map-kinase/extracellular signal-regulated kinase (MAPK/ERKB: PD-184352, 100 nM) with respective blocking agents (1-hour preincubation) (7, 25, 30), **(B)** Luciferase activity of HMECs containing full-length KLF2 reporter constructs (RLU, n=6) and **(C)** Expression of KLF2 mRNA (AU, arbitrary units, n=6); **(D)** AP-1/c-FOS transcription factor-binding site in the KLF2 promoter region: Biotin-labelled double-stranded oligonucleotides targeting the calculated AP-1/c-FOS positions -464 to -441 of the corresponding KLF2 promoter region were validated using the gel electrophoresis mobility shift assay (EMSA, one representative experiments is shown); **(E)** USP exposure induces a time-dependent upregulation of c-FOS expression in HMECs: Western blot analysis to quantify the expression of c-FOS protein in HMECs (AU, relative to GAPDH, n=2) which were left either untreated (baseline), or incubated for different time intervals (6, 12, and 24 hours) with either 5% USP or 5% HSP, demonstrating the strongest differential response at 6-12 hours; and **(F)** KLF2 overexpression downmodulates c-FOS expression upon USP exposure of HMECs: Different concentrations of KLF2 containing plasmid (100, 400 and 800 ng) were transfected into HMECs, followed by a 6-hour stimulation with 5% USP or 5% HSP, and western blot detection of KLF2 protein expression (AU, relative to GAPDH, n=4). Statistical comparison with ANOVA, Mean ± SEM, with **P*<0.05, and ***P*<0.01, ns, not significant.

more efficient c-FOS probe binding compared to that in the HSP or unstimulated group (Figure 3D). We observed an approximately 2-fold increased intensity of c-FOS-probe in 5% USP-stimulated cells compared to 5% HSP stimulated cells and an approximately 3-fold increased intensity compared to unstimulated HMECs relative to the amount of free probe (P<0.05, Figure 3D). Computational analysis of probe sequences in the EMSA revealed that an AP-1/c-FOS DNA-protein binding site is located at the promoter region -464 to -441 bp (Figure S1).

Time-dependent stimulation of HMECs with 5% USP demonstrated a strong 2-3-fold up-regulation of c-FOS protein compared to stimulation with 5% HSP or untreated baseline, at 6 and 12 hours, but not at 24 hours (First two P<0.05, Figure 3E). Furthermore, we found that transfection and overexpression of 400-800 ng of KLF2 plasmid was effective to reverse the AP1-/c-FOS activity seen with 5% USP stimulation down to the level seen with 5% HSP or baseline control (P<0.01 for both 400 and 800 ng of KLF2 plasmid, Figure 3F).

Altogether, these data indicate that USP-induced inhibition of KLF2 includes binding of AP-1/c-FOS within the KLF2 promoter region -469 to -446 bp (Figures 3A–D), that the AP-1/c-FOS engagement is strongest at 6-12 hours post USP-stimulation (Figure 3E), and that it could be antagonized by overexpression of KLF2 plasmid in HMECs (Figure 3F).

3.3 Uremic serum modulates KLF2 via c-FOS, AKT and MAPK/ERK signaling

Another important component of AP-1 signaling is c-JUN, that can form the alternative transcription factor complex AP1-/c-JUN, as contrasted to the AP-1/c-FOS complex (25, 32, 44). In addition, it is known that ERK activation contributes to EC homeostasis and contributes to the release of inflammatory factors (7, 25, 45), while the role of AKT-signaling in HMECs, is not yet clearly elucidated in the uremic state and conflicting results were reported in the past (46–48).

First, we studied the mRNA expression of c-FOS and c-JUN in response to USP in combination with pharmacological blockers of AKT and MAPK/ERK (Figures 4A, B). We found that c-FOS mRNA was strongly upregulated in response to stimulation with 5% USP (P<0.001, Figure 4A), while c-JUN mRNA was not affected (not significant, Figure 4B). Furthermore, the upregulation of c-FOS mRNA could be inhibited by blocking both AKT and MAPK/ERK signaling pathways (P<0.001, Figure 4A). This indicates that AP-1/c-FOS, but not AP-1/c-JUN, is the key transcription factor complex involved in uremic induction.

Next, we studied the protein levels of c-FOS and KLF2 in response to USP-stimulation in combination with using specific AP-1, AKT, and MAPK/ERK pathway blocking agents (Figures 4C, D). Interestingly, the preincubation of HMECs with AP-1-blocker resulted in a 2-fold amplification of USP-induced c-FOS protein expression compared to HSP or baseline control (P<0.05 and P<0.01, Figure 4C), and the AP-1-blocker could also completely reverse the USP-induced downmodulation of KLF2 protein expression (Figure 4D).

Similar to preventing upregulation of c-FOS mRNA expression (P<0.001, Figure 4A), the blockade of MAPK/ERK-signaling was more effective in preventing upregulation of c-FOS protein upon USP-induction (P<0.05, Figure 4C), while the AKT-blocker was less effective on c-FOS protein than mRNA level, thus indicating that USP-induced c-FOS signaling is more dependent on ERK than AKT signaling. The upregulation of c-FOS protein by USP could be lowered to HSP baseline by transfection of 400 ng KLF2 plasmid (P<0.01, Figure 4C), which could also fully restore KLF2 protein expression (Figure 4D).

Interestingly, stimulation with 5% USP induced a 5-fold increase in phosphorylation of ERK1/2 compared to baseline (P<0.05, Figure 4E), which was approximately 2-fold higher than for stimulation with 5% HSP. In contrast, stimulation with 5% USP induced a 2-fold lower expression of phosphorylated AKT compared to stimulation with 5% HSP (P<0.05 and P<0.001, Figure 4F). Thus, USP and HSP are acting directly opposed on ERK and AKT phosphorylation in HMECs, which may explain the results obtained in Figures 4A–D.

In summary, the diverse components contained in USP compared to HSP (e.g. higher levels of uremic mediators and toxins with on overall more dysbalanced profile vs. healthy blood environment containing less inflammatory or much less uremic mediators) may result in triggering of multiple signaling cascades (e.g. HMEC response to uremic vs. healthy serum). Thereby, USP and HSP trigger differential AP-1/c-FOS signaling through engaging the KLF2 promoter region, and consequently AKT and

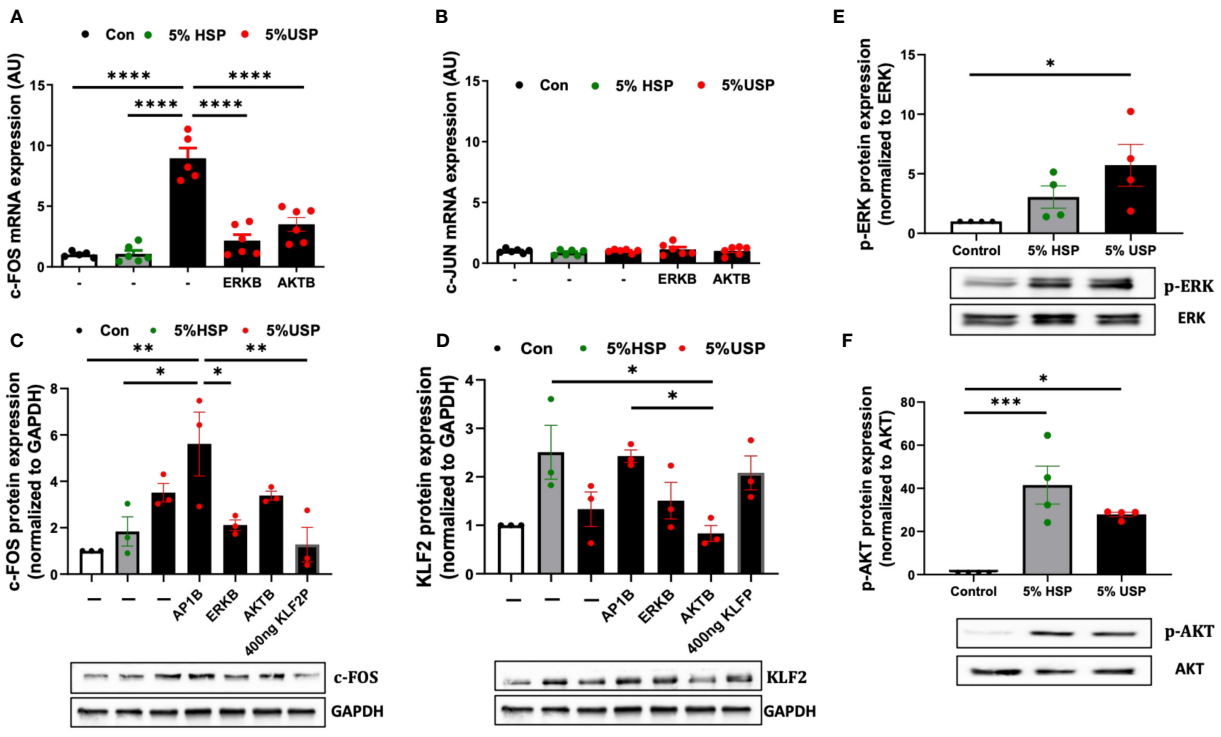

FIGURE 4
USP-induced KLF2 inhibition engages ERK and AKT signaling *via* c-FOS. **(A, B)** Engagement of c-FOS vs. c-JUN: qRT-PCR quantification of mRNA expression levels (AU, n=6) of the key transcription factors c-FOS and c-JUN upon a 6-hour stimulation with either 5% USP or 5% HSP, with or without 1-hour preincubation with blockers of AKT or ERK signaling pathways: protein kinase B (AKTB: MK-2206, 100 nM), or map-kinase/extracellular signal-regulated kinase (MAPK/ERKB: PD-184352, 100 nM), respectively, and **(C, D)** c-FOS and KLF2: Western blot quantification of protein expression levels for KLF2 and c-FOS (AU, relative to GAPDH, n=3 each) after a 12-hour stimulation with either 5% USP or 5% HSP, following a 1-hour preincubation of HMECs with blocking agents against either activator protein 1 (AP1B: SR-11302, 1000 nM), (AKTB: MK-2206, 100 nM), or (MAPK/ERKB: PD-184352, 100 nM), respectively. **(E, F)** Engagement of p-AKT and p-ERK: Western blot quantification for detection of phosphorylated p-AKT and p-ERK, normalized relative to their non-phosphorylated forms (Ratio of pERK/ERK and pAKT/AKT, n=4), upon a 12-hour stimulation with either 5% USP or 5% HSP. Statistical comparison with ANOVA, Mean ± SEM, with **P*<0.05, ***P*<0.01, ****P*<0.001, and *****P*<0.0001, ns, not significant.

MAPK/ERK1/2 canonic signaling pathways, in controlling the expression and regulation of KLF2 expression.

3.4 Uremic serum induces a proinflammatory response in HMECs

Endothelial microinflammation and its beneficial modulation during RRT is critical to the pathophysiology and management of uremia in CKD and ESRD (7). Thus, we studied in representative fashion, the expression changes of a panel of typical inflammatory mediators (e.g. pro/anti-inflammatory cytokines and chemokines) in HMECs in response to stimulation with USP vs HSP, by using the well-defined PCR array technology (33–35).

Out of a panel of 84 target genes (Figure 5A, left panel) a number of proinflammatory activation markers were upregulated in the USP-treated compared to the HSP-treated group (Figure 5A, right panel, cluster analysis: group 2 upregulated transcripts shown in red vs. group 1 unchanged or downmodulated transcripts shown in green, vs. non-treated baseline control group), including targets such as IL-6, CCL2, CCL5, CCL7, CCR2, CXCL1,CXCL8, NFKB1, TLR4 et, while ITGB2 was downregulated compared to the HSP group.

To quantify the changes in specific targets, we measured representative cytokines on mRNA and protein level (e.g. IL6, IL8 and TNF-a, Figures 5B–G) in the presence or absence of the blocking agents or KLF2 plasmid. Indeed, we could confirm that IL-6, IL8, and TNF-a are strongly upregulated in HMECs upon incubation with 5% USP compared to 5% HSP or untreated baseline, on mRNA level (P<0.05 to P0.0001, Figures 5B, D, F) and also on the protein level (P<0.01 to P<0.0001, Figures 5C, E, G).

Incubation with blocking agents directed against AP-1, AKT, or MAPK/ERK1/2 was effective in downmodulating the proinflammatory cytokine mRNA production (P<0.05 to P<0.0001, Figures 5B, D, F), and in particular AP-1- and ERK-blockers were effective in also downmodulating the respective protein production (P<0.01 and P<0.0001, Figures 5C, E, G). The AKT-blocker was effective in blocking IL-6 protein release (P<0.001, Figure 5C), but less effective in blocking IL-8 and TNF-a production (both not significant).

The introduction of the KLF2 overexpression plasmid strongly reduced HMECs' mRNA production of IL-6 and IL-8 in presence of 5% USP (P<0.0001, Figures 5B, D), while TNF-a mRNA expression was unchanged (Figure 5F). The protein production of all three mediators, IL-6, IL-8, and TNF-a was strongly downmodulated upon introduction of KLF2 plasmid (Figures 5C, E, G).

3.5 Compared to HF dialyzers, expanded hemodialysis therapy with novel improved MCO dialyzers normalizes KLF2 transcription in endothelial cells

Our experimental results demonstrate, that USP exposure promotes the inhibition of KLF2 transcription in HMECs by engaging the AP-1/c-FOS transcription factor complex, with activation of ERK and AKT signaling, which is followed by the induction of typical proinflammatory markers such as IL-6. In turn, the blockade of AP1/ERK/AKT-signaling or supplementation of KLF2 overexpression plasmid could reverse the USP-induced activation of inflammatory markers. We next wondered how this would translate in the clinical setting.

We have previously already demonstrated in the PERCI-II clinical study that novel improved medium cut-off (MCO) dialyzers reduce uremic serum (USP)-induced systemic micro-inflammation and endothelial dysfunction (7, 17). Intriguingly, we can here report for the first time that this also translates into beneficial modulation of KLF2 expression (Figure 6).

We first of all found that exposure of HMECs to uremic serum from patients treated either with conventional high-flux (HF) or novel improved MCO dialyzers resulted in normalization of KLF2 mRNA expression with MCO dialyzers (P<0.5 to P<0.001, Figures 6A, B).

When analyzing the individual trial phases, we first of all found that HMECs incubated with uremic serum from patients in the MCO/HF/HF-regimen, starting with MCO dialyzer, had similar KLF2 expression upon incubation MCO serum (end of the first 4-weeks cycle) than upon incubation with HSP, which indicates a beneficial effect of the MCO dialyzer (Figure 6A). In turn, the incubation of HMECs with uremic serum from the following two conventional HF cycles (4 and 8 weeks, respectively, in total 12 weeks long) lead to a strong downmodulation of KLF2 expression in the HMECs (P<0.05 to P<0.0001, Figure 6A).

Vice versa, HMECs incubated with uremic serum from patients in the cross-over HF/MCO/MCO-regimen, starting with HF dialyzer, had a strong downmodulation of KLF2 mRNA expression upon incubation of HMECs with the HF uremic serum collected at the end of the first 4-weeks cycle (P<0.0001, Figure 6B). However, incubation of HMECs with uremic serum from the following two MCO cycles (again 4 and 8 weeks, respectively) was effective in normalizing KLF2 expression to the prior baseline levels observed with HSP (P<0.001 and P<0.0001, Figure 6B).

We next wondered if similar protective effects of MCO-dialysis could be observed with other commonly used endothelial and kidney model related cell types, such as HUVECs, HRECs, and HEK cells (Figures 6C, D). Indeed, we found that in pair-wise analysis improved KLF2 expression could be observed in HMECs, HUVECs, HRECs, and HEKs (P<0.05, P<0.001, P<0.001, and P<0.01, respectively, Figure 6C), comparable to that of HMECs.

In addition, we found that similarly to the signaling pathways employed in HMECs, any detrimental endothelial down-modulation of KLF2 upon exposure to conventional uremic serum from HF dialysis could be mostly reversed by employing selective AP-1-, ERK-, and AKT-blockade in HUVECs, HRECs, and HEKs, respectively (P<0.05 to 0.001, Figure 6D). The ERK-blockade was slightly more effective than the AKT-blockade, thus demonstrating a more dominant signaling through the AP-1/ERK pathway (Figure 6D). Intriguingly, the dominance of ERK signaling was strongest in the HMECs, while this was less evident in the other three cell lines tested,

10.3389/fimmu.2023.1209464

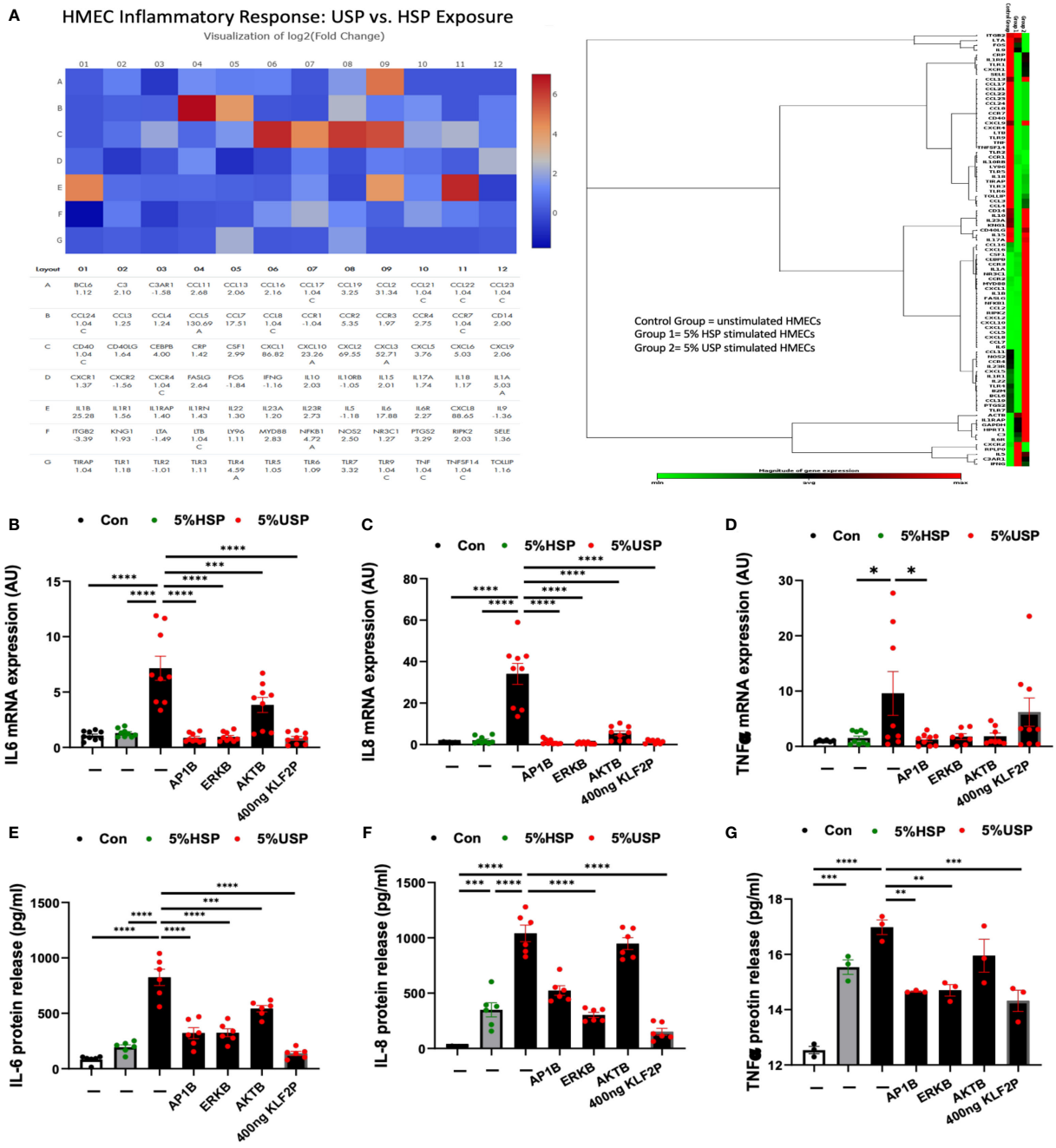

FIGURE 5
KLF2 modulates USP-induced inflammatory response and cytokine release. **(A)** QPCR-Array Readout: differential proinflammatory response of HMECs upon a 6-hour exposure to either 5% USP or 5% HSP, depicting on the left a Heatmap visualization of log2-fold change for n=84 selected genes typically involved in the inflammatory response and to the right the corresponding gene expression cluster analysis to verify relevant inflammatory gene families associated with USP vs HSP stimulation in HMECs; and **(B–G)** Analysis of Key Inflammatory Markers: **(B, D, F)** qRT-PCR analysis of mRNA expression and **(C, E, G)** ELISA quantification of cytokine release for three selected key cytokines (IL-6, IL-8, and TNF-α, respectively) measured after a 6-hour or 24-hour stimulation, respectively, with either 5% USP or 5% HSP, with or without 1-hour preincubation of HMECs with AP1B, ERKB and AKTB blockers. Statistical comparison with ANOVA, Mean ± SEM, with *P<0.05, **P<0.01, ***P<0.001, and ****P<0.0001. ns, not significant.

although in general similar trends considering the dominance of AP-1/ERK signaling could be observed (Figure 6D).

In conclusion, this indicates that MCO dialyzers may offer a better treatment outcome compared to the HF dialyzer, through normalizing KLF2 transcription, which is important for mediating anti-inflammatory and angiogenic effects.

4 Discussion

High cardiovascular morbidity and mortality, caused in part by chronic inflammation associated with endothelial dysfunction, remains a major challenge in the management of CKD and ESRD patients with underlying uremia and systemic microinflammation

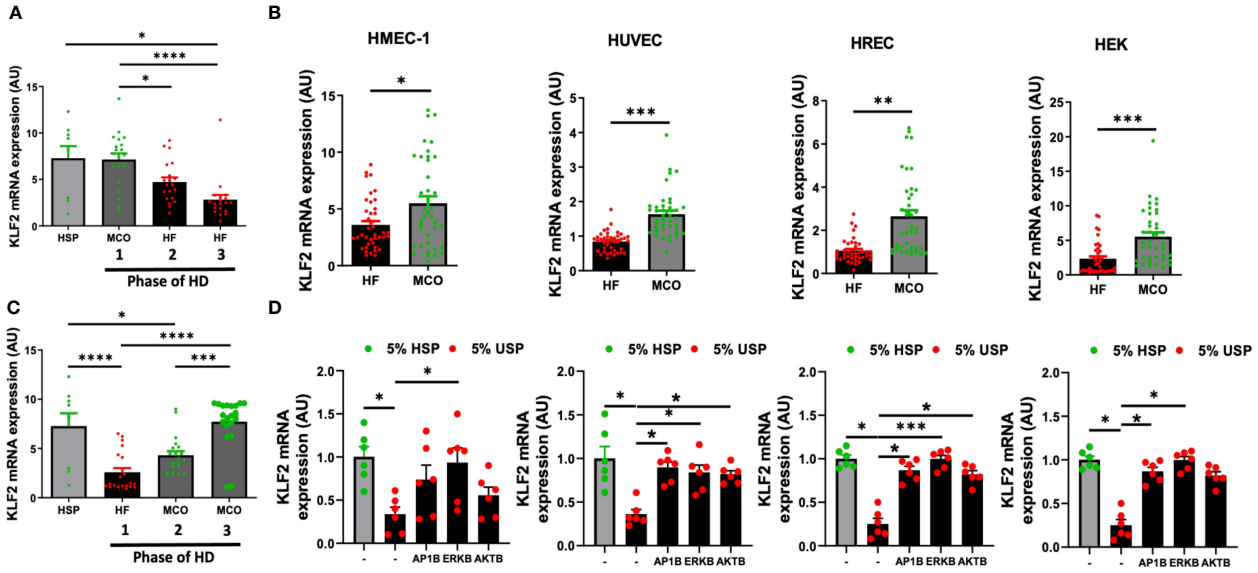

FIGURE 6
Expanded hemodialysis (HDx) therapy with novel improved MCO dialyzers normalizes KLF2 transcription in HMEC, HUVEC, HREC, and HEK cells, by modulating AP-1/c-FOS and AKT/ERK-dependent intracellular signaling. The effect of uremic serum fractions collected from patients undergoing hemodialysis with two different dialyzers/dialysis regimens in the PERCI-II clinical trial on KLF2 expression in different endothelial cell types. The serum fractions were collected from patients first dialyzed with high flux (HF) dialysis during the run-in phase of the trial and then dialyzed either with the conventional HF or the novel improved medium cut-off (MCO) dialyzer for comparison of the two different dialysis regimens in a cross-over clinical study design (n=40 patients included in analysis, comparison of 20 patients in each phase, the inclusion target was 50 patients) (7, 17). **(A, B)** KLF2 mRNA transcript levels at different trial stages were measured after stimulation of HMECs with healthy serum pool HSP reference or individual uremic serum samples from different stages of the PERCI-II trial (n=20 per group), as we previously described in PERCI-II study (A: MCO/HF/HF vs. B: HF/MCO/MCO) (7, 17), **(C, D)** To study if this can be generalized to other cell types, we also compared the effect of HF and MCO on HMECs, HUVECs, HRECs, and HEKs in presence or absence of different inhibitors (AP1B, ERKB, AKTB). KLF2 mRNA transcript levels were measured after a 6-hour incubation of HMECs with 5% uremic serum (n=40 patients) collected at the end of the first HF or MCO phase (each cycle lasted 4 weeks), using ANOVA, Mean ± SEM, with *P<0.05, **P<0.01, ***P<0.001, and****P<0.0001.

(8–12). Endothelial cells (ECs) - as a direct barrier to the uremic substances in the blood - are essential for maintaining vascular homeostasis (49). There is an urgent unmet medical need to reverse endothelial dysfunction and reduce chronic inflammation in the clinical setting of renal replacement therapies (RRTs) (7–13). Thus, we here conducted a detailed study to decipher the major role of KLF2, a key vascular mediator and regulator of inflammatory process (20).

Krüppel-like factor 2 (KLF2), a key transcription factor involved in anti-inflammatory processes in the vasculature, has been proposed to be a critical target in the pathobiology of both CKD and ESRD (39, 50). Intriguingly, the effect of uremic serum (in particular uremic serum from well controlled clinical trials, such as PERCI-I/II) on the regulation and signaling of KLF2 has not been explicitly studied to date. Therefore, we focused in the present study on investigating uremic serum induced transcriptional regulation of KLF2 expression and the engagement of concomitant signaling pathways in microvascular endothelial cells (HMECs), since these cells are typically also a major target of uremic microinflammation (7).

First of all, we found that exposure of HMECs to uremic serum inhibits KLF2 mRNA transcription *via* engaging activating protein-1 (AP-1)/c-FOS signaling, thus resulting in the activation of several canonical signaling pathways, such as MAPK/ERK and AKT signaling, which in turn leads to a strong release of proinflammatory mediators by HMECs, including interleukin-6 (IL-6) and IL-8 and a panel of chemokines, among others. This is in line with our prior results on the response of ECs to uremic microinflammation in the context of endothelial maladaptation (7). Linking the modulation of KLF2, a key vascular transcription factor, to this study provides further insight into the mechanisms underlying the beneficial effect of expanded hemodialysis with improved medium cut-off (MCO) dialyzers (8–12).

Indeed, KLF2 expression is essential for renal vascular integrity and function (20, 39), and upregulation of KLF2 restores glomerular endothelial damage in mice undergoing unilateral nephrectomy (51). In turn, reduced expression of KLF2 potentiates podocyte injury in diabetic nephropathy and increases renal proteinuria (27, 52). Loss of KLF2 expression is also associated with leading to excessive accumulation of uremic solutes in patients with ESRD (53, 54). In support of these results, our current study found a substantial dose- and time-dependent repression of KLF2 transcriptional activity and protein expression in USP-treated HMECs. Thus, chronic accumulation of uremic toxins and inflammatory mediators in USP can lead to a loss of protective anti-inflammatory KLF2 expression in ECs exposed to uremia.

The regulation of KLF2 is complex and may be orchestrated by a variety of genes (39). Thus, the observed downmodulation of KLF2 in response to USP may be coregulated by a multiplicity of genes and signaling pathways. Indeed, biologically, it is not uncommon for genes to share or co-ordinate with similar regulatory binding elements to counter-influence transcriptional regulation. Interestingly, a comparative *de-novo* analysis of

podocyte slit diaphragm molecules revealed that many genes share KLF promoter binding sites (55).

Similarly, downregulation of KLF2 transcription is known to up-regulate several genes and transcription factors such as Binding Endothelial Cell Precursor-Derived Regulator (BMPER) and Suppressor of Mothers against Decapentaplegic (SMAD1) (56, 57), thus also suppressing vascular calcification (57). However, the KLF2 promoter sequence to which regulatory factors bind is still not studied in great detail. Interestingly, an anticalcifying effect on vascular smooth muscle cells (VSMCs) was also reported for the use of uremic serum obtained from patients dialyzed with high- and medium-cut-off HCO/MCO dialyzers (58, 59).

Indeed, early reports suggested that KLF2 promoter activity is influenced by histone methylation or acetylated histones H3 and H4 associated with bare stress or other signals (60, 61). In addition, nuclear factors, including heterogeneous nuclear ribonucleoprotein (hnRNP)-U, hnRNP-D, and P300/CBP-associated factor (PCAF), can also bind to the human KLF2 promoter region (in position -138 and -111 bp) and regulate its transcription (62), while sequestration of the transcriptional coactivator p300/CBP by KLF2 suppresses inflammation through preventing NF-kB/p300 interaction and subsequent activation of the vascular cell adhesion molecule-1 (VCAM-1) (20, 41).

KLF2-p300 interaction also permits KLF2 binding to the endothelial nitric oxide synthase (eNOS) promoter to induce the transcription of this vasculoprotective enzyme (41). These early studies demonstrated KLF2's ability to influence transcription through both, direct DNA-binding and/or indirect cofactor sequestration mechanisms (20). Furthermore, the KLF2 promoter region from -157 to -95 bp is also essential for the induction of fluid shear stress in the endothelium (63). In addition, p53 can also target the KLF2 promoter and repress its transcription in microglial cells (64).

In our study, USP-stimulated HMECs were found to downregulate KLF2 expression through the engagement of the KLF2 promoter sequence region -509 to -109 as a crucial regulatory region. Interestingly, we identified an AP-1 binding site in this region and studied, whether AP-1 is involved in the regulation of KLF2 transcription. Previously, KLF2 was shown to be involved in endothelial inflammation by negatively regulating AP-1 (28), but the specific promoter binding region was unknown. Indeed, targeted deletion analysis in our study indicates that AP-1 and the constitutive element c-FOS rather than c-JUN bind to the KLF2 promoter sequence -464 to -441 to regulate the inhibition of KLF2 in uremia.

Transcription of KLF2 is regulated by proliferative and inflammatory pathways (21, 41). Independent studies have demonstrated the regulation of KLF2 by mitogenic markers, e.g. MAPK/ERK-signaling or through its specific inhibitor PD184352 in mast cells (65). Interestingly, glucose-loading of human umbilical vein endothelial cells (HUVECs) also represses KLF2 transcription *via* attenuated ERK 1/2 activation (66). Shimizu et al. reported that the uremic toxin indoxyl-sulfate can increase monocyte chemoattractant protein-1 (MCP-1) production by activating reactive oxygen species (ROS) and the MAPK/ERK1/2 signaling (67).

MAPK/ERK-signaling is involved in a ricin-induced severe inflammatory response in mouse hemolytic-uremic syndrome in mice (45), thereby suggesting that ERK-signaling may act as a deleterious mediator in the response to uremic toxins. Similarly, enhanced phosphorylation of *p*-AKT has been observed in different stages of both, hemodialysis- and peritoneal-dialysis-treated uremia (68). Interestingly, the uremic toxin indoxyl-sulfate was found to suppress the expression of *p*-AKT, but not ERK in HUVECs (69), while P-cresol, another uremic toxin, was found to activate *p*-AKT and *p*-ERK in VSMCs (70), indicating a certain cell type dependency.

The molecular analysis in our current study indicates, that there exits some crosstalk between USP-stimulation-induced regulation of KLF2 transcription and both ERK and AKT pathway activation. This crosstalk is at least in part mediated *via* AP-1/c-FOS-signaling. Indeed, the suppression of mRNA expression of c-FOS, but not c-JUN, by pharmacological inhibition of ERK-signaling clearly indicated that c-FOS is crucially involved in USP-induced inhibition of KLF2 transcription. Binding of the AP-1/c-FOS complex to the KLF2 promoter region appears to mediate both, the activation of ERK and AKT pathways. Nevertheless, global transcriptomic analysis of KLF2 signaling may be necessary to further uncover additional potential DNA binding elements of the KLF2 promoter sequence.

We found that optimized amounts of KLF2 plasmid transfected into HMECs could attenuate the negative effects of USP-induced proinflammatory cytokine release, e.g. including IL-6, IL-8, and TNF-α. Remarkably, exogenous KLF2 could also inhibit c-FOS expression, indicating a concurrent effect on other regulatory signaling mechanisms, such as ERK and AKT activation. Thus, targeting the modulation of endogenous KLF2 expression (or its activity) could motivate novel therapies to treat the vascular microinflammation induced by uremia. Indeed, several pharmacological approaches, e.g. the use of statins, suberanilohydroxamic acid, tannic acid, and resveratrol, have all been shown to exert atheroprotective and anti-inflammatory effects on the endothelium through induction/targeting of KLF2 (19, 71–75).

The effect of USP on the inhibition of KLF2 mRNA transcription suggested, that dialysis membranes with improved molecular cutoff could offer a better therapeutic outcome. To answer this question, we retrospectively studied USP of patients treated with either high-flux (HF) or medium-cut-off (MCO) dialyzers (7, 41), observing significant improvements in the expression of KLF2 in the MCO group, which is in line with improvements in other inflammatory pathways and reduced endothelial maladaptation (7). This suggests an improved effectiveness of MCO to not only remove small toxic molecules (<0.5kD), but also middle-sized molecules and pro-inflammatory mediators, such as TNF-α, interleukins, β-2-microglobulin, and others (76), compared to the conventional HF hemodialyzers.

In agreement with our prior study (7), MCO may offer a better vasculoprotective role through improved maintenance/upregulation of KLF2 transcription in uremic patients. Indeed, prolonged HD with MCO (for up to 21 weeks) restored KLF2 expression in USP-stimulated HMECs to that found in HMECs stimulated with HSP, which may indicate a beneficial effect for the respective MCO-treated patients. Conversely, extended application

of HF gradually reduced KLF2 to pre-treatment levels. Thus, our study demonstrates that uremic solutes down-regulates KLF2 transcription, leading to upregulation of proinflammatory mediators such as IL-6 *via* triggering AP-1/c-FOS, ERK and AKT signaling. However, maintaining/restoring KLF2 expression levels by use of beneficial MCO dialyzers (or exogenous KLF2 induction) could be a novel treatment approach to restore renal integrity and function in CKD/ESRD.

5 Conclusions and study limitations

Here, we identified that uremia downmodulates vasculoprotective KLF2 expression in common endothelial/kidney model cell lines, such as HMECs, HUVECs, HRECs, and HEKs. We then examined in detail the regulatory signaling mechanisms underlying modulation of KLF2 expression in response to uremic serum (USP). First, we identified the signaling events triggered upon USP-stimulation, including AP-1/c-FOS, MAPK/ERK1/2 and AKT signaling, as respective upstream molecules to regulate the expression of KLF2 in HMECs, and found that this was also applicable to other typical cell lines, such as HUVECs, HRECs, and HEKs.

Next, we demonstrated that any adverse effects of USP-exposure can be effectively attenuated by modulating endogenous KLF2 expression, which was achieved by specific inhibitors or transfection with an exogenous KLF2 plasmid. Further, we compared the inflammatory response to uremic and healthy serum, identifying a panel of mediators involved in uremia-induced chronic vascular inflammation.

Importantly, clinical verification of our results in a well-controlled clinical trial cohort, dialyzed with novel improved medium-cutoff (MCO)-dialysis membranes, was found to better maintain, or even restore KLF2 expression (cross-over design). Indeed, prolonged MCO dialysis eliminated any prior downmodulation of endothelial KLF2 expression observed with conventional HF dialysis membranes or uremic serum before HD treatment.

Thus, novel clinical trials with focus on comparing the therapeutic effects of MCO and HF membranes, but also well-designed pharmacological studies to targeting the respective signaling pathways, may provide new insights for future research and future improvements for patients depending on RRTs, to further reduce the detrimental long-term effects of uremia, chronic vascular inflammation and concomitant organ damage.

Data availability statement

The raw data supporting the conclusions of this article will be made available by the authors, without undue reservation.

Ethics statement

The studies involving humans were approved by Ethics Committees of the Martin-Luther-University Halle-Wittenberg and the Charité Berlin. The studies were conducted in accordance with the local legislation and institutional requirements. The participants provided their written informed consent to participate in this study.

Author contributions

Experiments and investigation: HZ, DW, MG, CL, PW, AP. Writing, review, and editing: HZ, DW, MA, JK-M, JW, GM, RC. Conception and Supervision: JW, DD, KB, RS, DZ, GM, RC. All authors contributed to the article and approved the submitted version.

Funding

The results in this paper have not been published previously, but they are in part complementary to a previously published mechanistic follow-up study to the concomitant clinical trial (7). This manuscript is a follow-up of the published clinical trial: PERCI-II-Medium-Cut-Off (MCO), which is registered at ClinicalTrials.gov NCT02084381 https://clinicaltrials.gov/ct2/show/NCT02084381) (7, 17). The current manuscript focuses on the mechanistic side studies that aim to verify promising biological leads identified in the prior clinical trial. The "lab research" was funded by academic grants through BMBF, DFG, BCRT/BSRT and EU-Project Grants and CGS/CSC-Scholarships, as outlined in detail below. The contributions by GM and RC were made possible by funding from the German Federal Ministry for Education and Research (BMBF) and German Research Foundation (DFG project Nephroproteciton #934046635, subproject A03, as part of CRC 1365, and EXPAND-PD; CA2816/1-1) through the Berlin Institute of Health (BIH)-Center for Regenerative Therapies (BCRT) and the Berlin-Brandenburg School for Regenerative Therapies (BSRT, GSC203), respectively, and in part by the European Union's Horizon 2020 Research and Innovation Program under grant agreements No 733006 (PACE) and 779293 (HIPGEN) and 754995 (EUTRAIN). We also acknowledge financial support from the Open Access Publication Fund of Charité – Universitätsmedizin Berlin and the German Research Foundation (DFG). HZ, DW, and PW were supported by Chinese Scholarship Council (CSC) Stipends (HZ: 202008080251, DW: 202108080082, and PW 202108440113, respectively): https://www.chinesescholarshipcouncil.com/. The 2.1 Million Euro academic financing for the prior PERCI-II clinical study came from the German Ministry for Education and Research (BMBF, Project Codes 1313N11786, 13N11787, 13N11788, and 13N11789) headed on the academic side by RS and DZ at Charité and Prof. Dr. Girndt in Halle, while the clinical study was coordinated by Gambro Dialysatoren GmbH, Hechingen (Gambro AB, including all direct and indirect subsidiaries is now part of Baxter International Inc.) who sponsored parts of the PERCI-II clinical trial (e.g. disposable dialysis materials and standard of care versus newly developed types of MCO dialysis filters from Gambro/Baxter). The subsequent academic research was done independently from Gambro/Baxter, as an academic follow-up study: https://www.gesundheitsindustrie-bw.de/fachbeitrag/pm/dialyseforschung-bmbf-foerdert-von-gambro-koordiniertes-verbundprojekt.

Conflict of interest

The authors declare that the research was conducted in the absence of any commercial or financial relationships that could be construed as a potential conflict of interest.

Publisher's note

All claims expressed in this article are solely those of the authors and do not necessarily represent those of their affiliated organizations, or those of the publisher, the editors and the reviewers. Any product that may be evaluated in this article, or claim that may be made by its manufacturer, is not guaranteed or endorsed by the publisher.

Supplementary material

The Supplementary Material for this article can be found online at: https://www.frontiersin.org/articles/10.3389/fimmu.2023.1209464/full#supplementary-material

SUPPLEMENTARY FIGURE 1
Analysis of the KLF2 promoter region and AP-1 binding site.

References

1. Eckardt KU, Coresh J, Devuyst O, Johnson RJ, Kottgen A, Levey AS, et al. Evolving importance of kidney disease: from subspecialty to global health burden. *Lancet* (2013) 382(9887):158–69. doi: 10.1016/S0140-6736(13)60439-0

2. Remuzzi G, Benigni A, Finkelstein FO, Grunfeld JP, Joly D, Katz I, et al. Kidney failure: aims for the next 10 years and barriers to success. *Lancet* (2013) 382(9889):353–62. doi: 10.1016/S0140-6736(13)60438-9

3. Bikbov B, Purcell CA, Levey AS, Smith M, Abdoli A, Abebe M, et al. Global, regional, and national burden of chronic kidney disease, 1990–2017: a systematic analysis for the Global Burden of Disease Study 2017. *Lancet* (2020) 395(10225):709–33. doi: 10.1016/S0140-6736(20)30045-3

4. Thurlow JS, Joshi M, Yan G, Norris KC, Agodoa LY, Yuan CM, et al. Global epidemiology of end-stage kidney disease and disparities in kidney replacement therapy. *Am J Nephrol* (2021) 52(2):98–107. doi: 10.1159/000514550

5. Roemhild A, Otto NM, Moll G, Abou-El-Enein M, Kaiser D, Bold G, et al. Regulatory T cells for minimising immune suppression in kidney transplantation: phase I/IIa clinical trial. *Bmj* (2020) 371:m3734. doi: 10.1136/bmj.m3734

6. Catar RA, Bartosova M, Kawka E, Chen L, Marinovic I, Zhang C, et al. Angiogenic role of mesothelium-derived chemokine CXCL1 during unfavorable peritoneal tissue remodeling in patients receiving peritoneal dialysis as renal replacement therapy. *Front Immunol* (2022) 13:821681. doi: 10.3389/fimmu.2022.821681

7. Catar R, Moll G, Kamhieh-Milz J, Luecht C, Chen L, Zhao H, et al. Expanded hemodialysis therapy ameliorates uremia-induced systemic microinflammation and endothelial dysfunction by modulating VEGF, TNF-α and AP-1 signaling. *Front Immunol* (2021) 12:774052. doi: 10.3389/fimmu.2021.774052

8. García-Prieto A, de la Flor JC, Coll E, Iglesias E, Reque J, Valga F. Expanded hemodialysis, what´s up, Doc? *Clin Kidney J* (2023). doi: 10.1093/ckj/sfad033

9. Ronco C, Marchionna N, Brendolan A, Neri M, Lorenzin A, Martínez Rueda AJ. Expanded haemodialysis: from operational mechanism to clinical results. *Nephrol Dialysis Transplant* (2018) 33(suppl_3):iii41–7. doi: 10.1093/ndt/gfy202

10. Ronco C, Clark WR. Haemodialysis membranes. *Nat Rev Nephrol* (2018) 14 (6):394–410. doi: 10.1038/s41581-018-0002-x

11. Ronco C, La Manna G. Expanded hemodialysis: A new therapy for a new class of membranes. *Contributions to Nephrol* (2017) 190:124–33. doi: 10.1159/000468959

12. Ronco C. The rise of expanded hemodialysis. *Blood Purif* (2017) 44(2):I–VIII. doi: 10.1159/000476012

13. Jankowski J, Floege J, Fliser D, Bohm M, Marx N. Cardiovascular disease in chronic kidney disease: pathophysiological insights and therapeutic options. *Circulation* (2021) 143(11):1157–72. doi: 10.1161/CIRCULATIONAHA.120.050686

14. de Mattos AM, Prather J, Olyaei AJ, Shibagaki Y, Keith DS, Mori M, et al. Cardiovascular events following renal transplantation: role of traditional and transplant-specific risk factors. *Kidney Int* (2006) 70(4):757–64. doi: 10.1038/sj.ki.5001628

15. Floege J, Gillespie IA, Kronenberg F, Anker SD, Gioni I, Richards S, et al. Development and validation of a predictive mortality risk score from a European hemodialysis cohort. *Kidney Int* (2015) 87(5):996–1008. doi: 10.1038/ki.2014.419

16. Zimmermann J, Herrlinger S, Pruy A, Metzger T, Wanner C. Inflammation enhances cardiovascular risk and mortality in hemodialysis patients. *Kidney Int* (1999) 55(2):648–58. doi: 10.1046/j.1523-1755.1999.00273.x

17. Zickler D, Schindler R, Willy K, Martus P, Pawlak M, Storr M, et al. Medium cut-off (MCO) membranes reduce inflammation in chronic dialysis patients-A randomized controlled clinical trial. *PloS One* (2017) 12(1):e0169024. doi: 10.1371/journal.pone.0169024

18. Kirsch AH, Lyko R, Nilsson LG, Beck W, Amdahl M, Lechner P, et al. Performance of hemodialysis with novel medium cut-off dialyzers. *Nephrol Dial Transplant* (2017) 32(1):165–72. doi: 10.1093/ndt/gfw310

19. Xu S, Liu Y, Ding Y, Luo S, Zheng X, Wu X, et al. The zinc finger transcription factor, KLF2, protects against COVID-19 associated endothelial dysfunction. *Signal Transduct Target Ther* (2021) 6(1):266. doi: 10.1038/s41392-021-00690-5

20. Sweet DR, Fan L, Hsieh PN, Jain MK. Krüppel-like factors in vascular inflammation: mechanistic insights and therapeutic potential. *Front Cardiovasc Med* (2018) 5:6. doi: 10.3389/fcvm.2018.00006

21. Lin Z, Kumar A, SenBanerjee S, Staniszewski K, Parmar K, Vaughan DE, et al. Kruppel-like factor 2 (KLF2) regulates endothelial thrombotic function. *Circ Res* (2005) 96(5):e48–57. doi: 10.1161/01.RES.0000159707.05637.a1

22. Lin Z, Natesan V, Shi H, Dong F, Kawanami D, Mahabeleshwar GH, et al. Kruppel-like factor 2 regulates endothelial barrier function. *Arterioscler Thromb Vasc Biol* (2010) 30(10):1952–9. doi: 10.1161/ATVBAHA.110.211474

23. Nayak L, Goduni L, Takami Y, Sharma N, Kapil P, Jain MK, et al. Kruppel-like factor 2 is a transcriptional regulator of chronic and acute inflammation. *Am J Pathol* (2013) 182(5):1696–704. doi: 10.1016/j.ajpath.2013.01.029

24. Fan Y, Lu H, Liang W, Hu W, Zhang J, Chen YE. Kruppel-like factors and vascular wall homeostasis. *J Mol Cell Biol* (2017) 9(5):352–63. doi: 10.1093/jmcb/mjx037

25. Catar R, Moll G, Hosp I, Simon M, Luecht C, Zhao H, et al. Transcriptional regulation of thrombin-induced endothelial VEGF induction and proangiogenic response. *Cells* (2021) 10(4). doi: 10.3390/cells10040910

26. Wang XQ, Nigro P, World C, Fujiwara K, Yan C, Berk BC. Thioredoxin interacting protein promotes endothelial cell inflammation in response to disturbed flow by increasing leukocyte adhesion and repressing Kruppel-like factor 2. *Circ Res* (2012) 110(4):560–8. doi: 10.1161/CIRCRESAHA.111.256362

27. Zhong F, Chen H, Wei C, Zhang W, Li Z, Jain MK, et al. Reduced Kruppel-like factor 2 expression may aggravate the endothelial injury of diabetic nephropathy. *Kidney Int* (2015) 87(2):382–95. doi: 10.1038/ki.2014.286

28. Shi J, Zhou LR, Wang XS, Du JF, Jiang MM, Song Z, et al. KLF2 attenuates bleomycin-induced pulmonary fibrosis and inflammation with regulation of AP-1. *Biochem Biophys Res Commun* (2018) 495(1):20–6. doi: 10.1016/j.bbrc.2017.10.114

29. Boon RA, Fledderus JO, Volger OL, van Wanrooij EJ, Pardali E, Weesie F, et al. KLF2 suppresses TGF-beta signaling in endothelium through induction of Smad7 and inhibition of AP-1. *Arterioscler Thromb Vasc Biol* (2007) 27(3):532–9. doi: 10.1161/01.ATV.0000256466.65450.ce

30. Zickler D, Luecht C, Willy K, Chen L, Witowski J, Girndt M, et al. Tumour necrosis factor-alpha in uraemic serum promotes osteoblastic transition and calcification of vascular smooth muscle cells *via* extracellular signal-regulated kinases and activator protein 1/c-FOS-mediated induction of interleukin 6 expression. *Nephrol Dial Transplant* (2018) 33(4):574–85. doi: 10.1093/ndt/gfx316

31. Philippe A, Kleinau G, Gruner JJ, Wu S, Postpieszala D, Speck D, et al. Molecular effects of auto-antibodies on angiotensin II type 1 receptor signaling and cell proliferation. *Int J Mol Sci* (2022) 23(7). doi: 10.3390/ijms23073984

32. Catar R, Witowski J, Wagner P, Annett Schramm I, Kawka E, Philippe A, et al. The proto-oncogene c-Fos transcriptionally regulates VEGF production during peritoneal inflammation. *Kidney Int* (2013) 84(6):1119–28. doi: 10.1038/ki.2013.217

33. Connolly-Andersen AM, Moll G, Andersson C, Akerstrom S, Karlberg H, Douagi I, et al. Crimean-Congo hemorrhagic fever virus activates endothelial cells. *J Virol* (2011) 85(15):7766–74. doi: 10.1128/JVI.02469-10

34. Moll G, Rasmusson-Duprez I, von Bahr L, Connolly-Andersen AM, Elgue G, Funke L, et al. Are therapeutic human mesenchymal stromal cells compatible with human blood? *Stem Cells* (2012) 30(7):1565–74. doi: 10.1002/stem.1111

35. Moll G, Ignatowicz L, Catar R, Luecht C, Sadeghi B, Hamad O, et al. Different procoagulant activity of therapeutic mesenchymal stromal cells derived from bone marrow and placental decidua. *Stem Cells Dev* (2015) 24(19):2269–79. doi: 10.1089/scd.2015.0120

36. Moll G, Alm JJ, Davies LC, von Bahr L, Heldring N, Stenbeck-Funke L, et al. Do cryopreserved mesenchymal stromal cells display impaired immunomodulatory and therapeutic properties? *Stem Cells* (2014) 32(9):2430–42. doi: 10.1002/stem.1729

37. Catar R, Witowski J, Zhu N, Lucht C, Derrac Soria A, Uceda Fernandez J, et al. IL-6 trans-signaling links inflammation with angiogenesis in the peritoneal membrane. *J Am Soc Nephrol JASN* (2017) 28(4):1188–99. doi: 10.1681/ASN.2015101169

38. Hegner B, Weber M, Dragun D, Schulze-Lohoff E. Differential regulation of smooth muscle markers in human bone marrow-derived mesenchymal stem cells. *J Hypertens* (2005) 23(6):1191–202. doi: 10.1097/01.hjh.0000170382.31085.5d

39. Mallipattu SK, Estrada CC, He JC. The critical role of Krüppel-like factors in kidney disease. *Am J Physiol Renal Physiol* (2017) 312(2):F259–f265. doi: 10.1152/ajprenal.00550.2016

40. Karin M, Liu Z, Zandi E. AP-1 function and regulation. *Curr Opin Cell Biol* (1997) 9(2):240–6. doi: 10.1016/s0955-0674(97)80068-3

41. SenBanerjee S, Lin Z, Atkins GB, Greif DM, Rao RM, Kumar A, et al. KLF2 Is a novel transcriptional regulator of endothelial proinflammatory activation. *J Exp Med* (2004) 199(10):1305–15. doi: 10.1084/jem.20031132

42. Turpaev KT. Transcription factor KLF2 and its role in the regulation of inflammatory processes. *Biochem (Mosc)* (2020) 85(1):54–67. doi: 10.1134/S0006297920010058

43. Wisdom R. AP-1: one switch for many signals. *Exp Cell Res* (1999) 253(1):180–5. doi: 10.1006/excr.1999.4685

44. Meng Q, Xia Y. c-Jun, at the crossroad of the signaling network. *Protein Cell* (2011) 2(11):889–98. doi: 10.1007/s13238-011-1113-3

45. Korcheva V, Wong J, Corless C, Iordanov M, Magun B. Administration of ricin induces a severe inflammatory response *via* nonredundant stimulation of ERK, JNK, and P38 MAPK and provides a mouse model of hemolytic uremic syndrome. *Am J Pathol* (2005) 166(1):323–39. doi: 10.1016/S0002-9440(10)62256-0

46. Sindhu RK, Ehdaie A, Vaziri ND, Roberts CK. Effects of chronic renal failure on caveolin-1, guanylate cyclase and AKT protein expression. *Biochim Biophys Acta* (2004) 1690(3):231–7. doi: 10.1016/j.bbadis.2004.06.013

47. Li Y, Takemura G, Okada H, Miyata S, Maruyama R, Esaki M, et al. Molecular signaling mediated by angiotensin II type 1A receptor blockade leading to attenuation of renal dysfunction-associated heart failure. *J Card Fail* (2007) 13(2):155–62. doi: 10.1016/j.cardfail.2006.11.005

48. Semple D, Smith K, Bhandari S, Seymour AM. Uremic cardiomyopathy and insulin resistance: a critical role for akt? *J Am Soc Nephrol JASN* (2011) 22(2):207–15. doi: 10.1681/ASN.2009090900

49. Deanfield JE, Halcox JP, Rabelink TJ. Endothelial function and dysfunction: testing and clinical relevance. *Circulation* (2007) 115(10):1285–95. doi: 10.1161/CIRCULATIONAHA.106.652859

50. Dabravolski SA, Sukhorukov VN, Kalmykov VA, Grechko AV, Shakhpazyan NK, Orekhov AN. The role of KLF2 in the regulation of atherosclerosis development and potential use of KLF2-targeted therapy. *Biomedicines* (2022) 10(2). doi: 10.3390/biomedicines10020254

51. Zhong F, Mallipattu SK, Estrada C, Menon M, Salem F, Jain MK, et al. Reduced kruppel-like factor 2 aggravates glomerular endothelial cell injury and kidney disease in mice with unilateral nephrectomy. *Am J Pathol* (2016) 186(8):2021–31. doi: 10.1016/j.ajpath.2016.03.018

52. Guo Y, Pace J, Li Z, Ma'ayan A, Wang Z, Revelo MP, et al. Podocyte-specific induction of kruppel-like factor 15 restores differentiation markers and attenuates kidney injury in proteinuric kidney disease. *J Am Soc Nephrol JASN* (2018) 29(10):2529–45. doi: 10.1681/ASN.2018030324

53. Brunet P, Gondouin B, Duval-Sabatier A, Dou L, Cerini C, Dignat-George F, et al. Does uremia cause vascular dysfunction? *Kidney Blood Press Res* (2011) 34(4):284–90. doi: 10.1159/000327131

54. Saum K, Campos B, Celdran-Bonafonte D, Nayak L, Sangwung P, Thakar C, et al. Uremic advanced glycation end products and protein-bound solutes induce endothelial dysfunction through suppression of krüppel-like factor 2. *J Am Heart Assoc* (2018) 7(1). doi: 10.1161/jaha.117.007566

55. Cohen CD, Klingenhoff A, Boucherot A, Nitsche A, Henger A, Brunner B, et al. Comparative promoter analysis allows *de novo* identification of specialized cell junction-associated proteins. *Proc Natl Acad Sci USA* (2006) 103(15):5682–7. doi: 10.1073/pnas.0511257103

56. Jha P, Das H. KLF2 in regulation of NF-kappaB-mediated immune cell function and inflammation. *Int J Mol Sci* (2017) 18(11). doi: 10.3390/ijms18112383

57. Huang J, Pu Y, Zhang H, Xie L, He L, Zhang CL, et al. KLF2 mediates the suppressive effect of laminar flow on vascular calcification by inhibiting endothelial BMP/SMAD1/5 signaling. *Circ Res* (2021) 129(4):e87–e100. doi: 10.1161/CIRCRESAHA.120.318690

58. Zickler D, Willy K, Girndt M, Fiedler R, Martus P, Storr M, et al. High cut-off dialysis in chronic haemodialysis patients reduces serum procalcific activity. *Nephrol Dial Transplant* (2016) 31(10):1706–12. doi: 10.1093/ndt/gfw293

59. Willy K, Hulko M, Storr M, Speidel R, Gauss J, Schindler R, et al. In vitro dialysis of cytokine-rich plasma with high and medium cut-off membranes reduces its procalcific activity. *Artif organs* (2017) 41(9):803–9. doi: 10.1111/aor.12884

60. Xu M, Chen X, Lin K, Zeng K, Liu X, Pan B, et al. The long noncoding RNA SNHG1 regulates colorectal cancer cell growth through interactions with EZH2 and miR-154-5p. *Mol Cancer* (2018) 17(1):141. doi: 10.1186/s12943-018-0894-x

61. Huddleson JP, Ahmad N, Srinivasan S, Lingrel JB. Induction of KLF2 by fluid shear stress requires a novel promoter element activated by a phosphatidylinositol 3-kinase-dependent chromatin-remodeling pathway. *J Biol Chem* (2005) 280(24):23371–9. doi: 10.1074/jbc.M413839200

62. Ahmad N, Lingrel JB. Kruppel-like factor 2 transcriptional regulation involves heterogeneous nuclear ribonucleoproteins and acetyltransferases. *Biochemistry* (2005) 44(16):6276–85. doi: 10.1021/bi050018s

63. Huddleson JP, Srinivasan S, Ahmad N, Lingrel JB. Fluid shear stress induces endothelial KLF2 gene expression through a defined promoter region. *Biol Chem* (2004) 385(8):723–9. doi: 10.1515/bc.2004.088

64. Zhang X, Liu T, Xu S, Gao P, Dong W, Liu W, et al. A pro-inflammatory mediator USP11 enhances the stability of p53 and inhibits KLF2 in intracerebral hemorrhage. *Mol Ther Methods Clin Dev* (2021) 21:681–92. doi: 10.1016/j.omtm.2021.01.015

65. Marschall JS, Wilhelm T, Schuh W, Huber M. MEK/Erk-based negative feedback mechanism involved in control of Steel Factor-triggered production of Krüppel-like factor 2 in mast cells. *Cell Signal* (2012) 24(4):879–88. doi: 10.1016/j.cellsig.2011.12.007

66. Liu YS, Xu DL, Huang ZW, Hao L, Wang X, Lu QH. Atorvastatin counteracts high glucose-induced Krüppel-like factor 2 suppression in human umbilical vein endothelial cells. *Postgrad Med* (2015) 127(5):446–54. doi: 10.1080/00325481.2015.1039451

67. Shimizu H, Bolati D, Higashiyama Y, Nishijima F, Shimizu K, Niwa T. Indoxyl sulfate upregulates renal expression of MCP-1 via production of ROS and activation of NF-κB, p53, ERK, and JNK in proximal tubular cells. *Life Sci* (2012) 90(13-14):525–30. doi: 10.1016/j.lfs.2012.01.013

68. Martin-Rodriguez S, Caballo C, Gutierrez G, Vera M, Cruzado JM, Cases A, et al. TLR4 and NALP3 inflammasome in the development of endothelial dysfunction in uraemia. *Eur J Clin Invest* (2015) 45(2):160–9. doi: 10.1111/eci.12392

69. Adelibieke Y, Shimizu H, Saito S, Mironova R, Niwa T. Indoxyl sulfate counteracts endothelial effects of erythropoietin through suppression of Akt phosphorylation. *Circ J* (2013) 77(5):1326–36. doi: 10.1253/circj.cj-12-0884

70. Lee CH, Hung YJ, Shieh YS, Chien CY, Hsu YJ, Lin CY, et al. Cilostazol inhibits uremic toxin-induced vascular smooth muscle cell dysfunction: role of Axl signaling. *Am J Physiol Renal Physiol* (2017) 312(3):F398–f406. doi: 10.1152/ajprenal.00258.2016

71. Sen-Banerjee S, Mir S, Lin Z, Hamik A, Atkins GB, Das H, et al. Kruppel-like factor 2 as a novel mediator of statin effects in endothelial cells. *Circulation* (2005) 112(5):720–6. doi: 10.1161/circulationaha.104.525774

72. Parmar KM, Nambudiri V, Dai G, Larman HB, Gimbrone MA Jr., García-Cardeña G. Statins exert endothelial atheroprotective effects *via* the KLF2 transcription factor. *J Biol Chem* (2005) 280(29):26714–9. doi: 10.1074/jbc.C500144200

73. Tuomisto TT, Lumivuori H, Kansanen E, Häkkinen SK, Turunen MP, van Thienen JV, et al. Simvastatin has an anti-inflammatory effect on macrophages *via* upregulation of an atheroprotective transcription factor, Kruppel-like factor 2. *Cardiovasc Res* (2008) 78(1):175–84. doi: 10.1093/cvr/cvn007

74. Xu Y, Xu S, Liu P, Koroleva M, Zhang S, Si S, et al. Suberanilohydroxamic acid as a pharmacological kruppel-like factor 2 activator that represses vascular inflammation and atherosclerosis. *J Am Heart Assoc* (2017) 6(12). doi: 10.1161/jaha.117.007134

75. Gracia-Sancho J, Villarreal G Jr., Zhang Y, Yu JX, Liu Y, Tullius SG, et al. Flow cessation triggers endothelial dysfunction during organ cold storage conditions: strategies for pharmacologic intervention. *Transplantation* (2010) 90(2):142–9. doi: 10.1097/TP.0b013e3181e228db

76. Storr M, Ward RA. Membrane innovation: closer to native kidneys. *Nephrol Dial Transplant* (2018) 33(suppl_3):iii22–7. doi: 10.1093/ndt/gfy228

frontiers | Frontiers in Immunology

TYPE Original Research
PUBLISHED 21 September 2023
DOI 10.3389/fimmu.2023.1243912

OPEN ACCESS

EDITED BY
Guido Moll,
Charité University Medicine Berlin, Germany

REVIEWED BY
Ramin Yaghobi,
Shiraz University of Medical Sciences, Iran
Thomas Jouve,
Centre Hospitalier Universitaire de Grenoble, France
Ross Simon Francis,
Princess Alexandra Hospital, Australia

*CORRESPONDENCE
Eun-Jee Oh
ejoh@catholic.ac.kr

RECEIVED 21 June 2023
ACCEPTED 04 September 2023
PUBLISHED 21 September 2023

CITATION
Bae H, Jung S, Chung BH, Yang CW and Oh E-J (2023) Pretransplant BKV-IgG serostatus and BKV-specific ELISPOT assays to predict BKV infection after kidney transplantation.
Front. Immunol. 14:1243912.
doi: 10.3389/fimmu.2023.1243912

Pretransplant BKV-IgG serostatus and BKV-specific ELISPOT assays to predict BKV infection after kidney transplantation

Hyunjoo Bae[1], Seungwon Jung[2], Byung Ha Chung[3], Chul Woo Yang[3] and Eun-Jee Oh[4,5]*

[1]Department of Biomedicine & Health Sciences, Graduate School, The Catholic University of Korea, Seoul, Republic of Korea, [2]Department of Laboratory Medicine, Uijeongbu Paik Hospital, Uijeongbu, Republic of Korea, [3]Division of Nephrology, Department of Internal Medicine, Seoul St. Mary's Hospital, College of Medicine, The Catholic University of Korea, Seoul, Republic of Korea, [4]Resesarch and Development Institute for In Vitro Diagnostic Medical Devices, College of Medicine, The Catholic University of Korea, Seoul, Republic of Korea, [5]Department of Laboratory Medicine, Seoul St. Mary's Hospital, College of Medicine, The Catholic University of Korea, Seoul, Republic of Korea

Introduction: Polyomavirus (BKV) infection can lead to major complications and damage to the graft in kidney transplant recipients (KTRs). We investigated whether pretransplant BK serostatus and BK-specific cell-mediated immunity (CMI) predicts post-transplant BK infection.

Methods: A total of 93 donor-recipient pairs who underwent kidney transplantation (KT) and 44 healthy controls were examined. Assessment of donor and recipient BKV serostatus and BKV-CMI in recipients was performed prior to transplantation using BKV-IgG ELISA and BKV-specific IFN-g ELISPOT assays against five BK viral antigens (LT, St, VP1, VP2, and VP3). BK viremia was diagnosed when blood BKV-DNA of 104 copies/mL or more was detected during follow-up periods.

Results: Anti-BKV IgG antibody was detected in 74 (79.6%) of 93 KTRs and in 68 (73.1%) of 93 KT donors. A greater percentage of KTRs who received allograft from donors with high levels of anti-BKV IgG had posttransplant BK viremia (+) than KTRs from donors with low anti-BKV IgG (25.5% [12/47] vs. 4.3% [2/46], respectively; P = 0.007). Pretransplant total BKV-ELISPOT results were lower in BK viremia (+) patients than in patients without viremia (-) 20.5 [range 9.9–63.6] vs. 72.0 [43.2 - 110.8]; P = 0. 027). The sensitivity and specificity of the total BKV-ELISPOT assay (cut-off ≤ 53 spots/3×105 cells) for prediction of posttransplant BK viremia were 71.4 (95% CI: 41.9–91.6) and 54.4 (42.8–65.7), respectively. The combination of high donor BKV-IgG, low recipient BKV-IgG, and low total BKV-ELISPOT results improved specificity to 91.1%.

Discussion: Our study highlights the importance of pretransplant BKV-IgG serostatus and BKV-specific CMI in predicting posttransplant BKV infection in KTRs. The combination of high donor BKV-IgG, low recipient BKV-IgG, and low total BKV-ELISPOT results predicted BK viremia after KT. Pretransplant identification of patients at highrisk for BK viremia could enable timely interventions and improve clinical outcomes of KTRs.

KEYWORDS

BK polyomavirus, kidney transplant recipients, pre-transplant BKV-IgG serostatus, BKV-specific ELISPOT, BK viremia

1 Introduction

The BK polyomavirus (BKV) is an opportunistic pathogen of the Polyomaviridae family. After an initial respiratory tract infection with BKV in childhood, which is frequently mild or asymptomatic, the virus persists in a latent state primarily within the renal tubules and epithelial cells of the urinary tract (1–3). Immunosuppressive therapy increases the risk of reactivation in kidney transplant recipients (KTRs) (4, 5). Reactivation of latent BKV in KTRs can lead to BKV-associated nephropathy (BKVAN) and is associated with an increased risk of allograft dysfunction or graft failure in up to 30% of cases (6). Currently, no effective antiviral drugs for BKV infection are available, so the primary strategy for managing the BKV infection is to reduce immunosuppression and restore the immune response against BKV; however, reducing immunosuppressive therapy to limit BKVAN can increase the risk of allograft rejection.

Several posttransplant BKV monitoring strategies have been implemented to improve the management of BKV replication in the immunocompromised host. The most widely used early diagnostic screening method is to periodically measure BKV DNA in the blood and urine up to 1 year after transplantation using quantitative PCR. Despite improvements in screening methods based on regular monitoring of the viral load, the incidence of BKVAN has remained stable over the last few years (5). Therefore, additional indicators to predict the progression of BKV infection are needed for to improve treatment outcomes of KTRs.

Monitoring of BKV-specific humoral and cellular immunity has been considered to assess the risk of BKV infection. However, previous studies have shown that the predictive value of pretransplant BKV-IgG antibodies in KTR is uncertain (2, 6–11). Recently, antibodies against the BKV capsid protein VP1 have been reported to have subtype-specific virus-neutralizing activity in KTRs (12). Some studies have reported that recipient and donor BKV serostatus could be an important predictor of BKV reactivation (2, 13). Since BKV in KTRs may be of donor origin, it is important to assess the donor's serostatus and BKV titer as risk factors for posttransplant BKV infection (13–15). Recently, Saláková et al. reported that the donor BKV-IgG seroprevalence and antibody level were strongly associated with posttransplant BK viremia and BKVAN in a study of 210 KTRs and 130 donors (16). Finally, they confirmed recommendation by Hirsh and Randhawa that KTRs from seropositive donors should be routinely screened for BKV-DNA in plasma much more frequently than KTRs from seronegative donors (5). Regarding the recipient BKV-IgG, Ginevri et al. suggested that the negative antibody status of the recipient was the most substantial predictor of BKV infection in pediatric KTRs (17). Another study has also highlighted the significant association between the recipient's seronegative status for BK viremia and the development of BKVAN (18).

Several studies have assessed BKV-specific cellular immunity (CMI) in KT patients, although typically only after transplantation. An increase in BKV-specific T cells has been associated with resolution of BK viremia, and cellular immunity has been reported to play an important protective role in regulating BKV proliferation and progression of BKVAN (6, 8, 11, 19–21). In addition, low pretransplant BKV-specific T cells and posttransplant BKV-CMV unresponsiveness or loss have been reported to be associated with BK viremia and BKVAN (6, 22). Notably, a recent study has underscored the diminished proliferative response of BKV-specific CD8 T cells as a contributing risk factor for BKVAN (23).

Given the importance of pre-transplant immunity in preventing post-transplant BKV infection, screening both humoral and cellular immunity before transplantation may be an effective measure to predict and prevent BKV infection. In the present study, we assessed the BKV-IgG serostatus of kidney donors and recipients, and also measured BKV-specific ELISPOT responses in KTRs prior to transplantation, which had not been previously investigated. The aim of this study was to identify pretransplant risk factors for posttransplant BKV infection by assessing BKV-specific humoral and cellular immunity.

2 Material and methods

2.1 Study population

This retrospective study included 93 KTRs who consented to donate peripheral blood at the time of their pretransplant cross-

matching test. All KTRs underwent kidney transplantation at Seoul St. Mary's Hospital between January 2016 and October 2019. Pre-transplant serum was also collected from 93 matched donors, and all sera were collected no more than 1 month prior to the kidney transplant. The inclusion criteria were adults aged 20 years or older with available pretransplant blood sampling from both donors and recipients. Patients who had received organ transplants other than the kidney or who did not provide informed consent for the study were excluded. An additional 44 healthy donors were included as controls. This study was approved by the Institutional Review Board at Seoul St. Mary's Hospital (KC19TESI0043).

2.2 Diagnosis of BK viremia and BKVAN

The diagnosis of BKV infection and management of immunosuppression in KTRs were performed according to the protocol of our transplant center (11). Donor and recipient BKV viral loads in whole blood were measured using a Real-Q BK Quantification Kit (Biosewoom, Seoul, Korea) to detect the viral capsid protein (VP-1) gene using an ABI PRISM 7000 real-time PCR system (Applied Biosystems). The recipient's BKV viral load was monitored at 1, 3, 6, 9, and 12 months after transplantation, and then once a year thereafter or when kidney function was impaired. BK viremia was diagnosed when BKV-DNA of 10^4 copies/mL or more was detected during the follow-up period (median 19 [range 18–29) months), and therapeutic intervention was initiated to prevent progression to BKVAN. In the case of BK viremia patients, monitoring using quantitative PCR was performed until BK viremia resolved, and mycophenolate mofetil (MMF) treatment was discontinued. If BK viremia persisted after 1 month, a transplant biopsy was performed, and the dose of calcineurin inhibitor was reduced by 20% while leflunomide was started. A further 2 weeks of BK viremia resulted in a further 50% reduction in tacrolimus. If BK viremia persisted beyond this period, tacrolimus was switched to sirolimus. If BK viremia still persists or increases after an additional 2 weeks, a 5-day course of intravenous immunoglobulin (IVIG) for BKVAN was administered.

In patients with BK viremia, monitoring using quantitative PCR was carried out until BK viremia resolved, and mycophenolate mofetil (MMF) treatment was stopped. If BK viremia persisted after 1 month, a graft biopsy was performed, calcineurin inhibitors were reduced by 20%, and leflunomide was initiated. The diagnosis of BKVAN was made when the following criteria were met: (1) a basophilic intranuclear viral inclusion body suggestive of BKVAN was observed; (2) immunochemical staining for SV40T antigen was positive; (3) there was evidence of BKV proliferation in at least one of the urine cell test, urine PCR, and/or blood PCR results.

2.3 BKV-specific IgG ELISA

Anti-BKV IgG antibody was assessed using the ELISA-VIDITEST anti-BKV IgG kit (VIDIA, Ltd., Czech Republic), which employs recombinant species-specific BKV antigens and targets major BKV type I and IV genotypes for detection. Serum samples were stored at −80°C until use. Diluted serum was dispensed into wells coated with recombinant BKV-specific antigens and incubated for 30 minutes at room temperature. After washing, a secondary antibody (anti-human IgG antibody) labeled with peroxidase was added and incubated at room temperature for 30 minutes. The reaction was detected with 100 µL of 3,3',5,5'-tetramethyl benzidine substrate solution at room temperature for 10 minutes. The optical density (OD) of each well was measured at 450 nm. The cut-off value was determined by multiplying the mean absorbance of the indicated calibrator by the correction factor specified in the quality control certificate.

2.4 BKV-specific IFN- γ ELISPOT

A BKV-specific human IFN-γ ELISPOT (BKV-ELISPOT; ELISPOT Ready-SET-Go kit (eBioscience, San Diego, CA, USA) assay specific for each of the five BKV structural proteins (LT, St, VP1, VP2 and VP3) was performed as described in a previous study (11). Briefly, 96-well ELISPOT plates (Millipore, Cat. No. MAIPS4510) were coated with diluted anti-IFN-γ monoclonal capture antibody at 4°C overnight. After washing the microplate twice with the coating buffer, 200 uL of RPMI-1640 culture solution containing fetal bovine serum and 1% penicillin as a blocking medium was dispensed and left at room temperature for 1 hour. Peripheral blood mononuclear cells (PBMCs) were freshly isolated from heparin-treated whole blood samples by density gradient centrifugation using a Ficoll solution. The PBMCs (3 x 10^5cells/well) were stimulated with phorbol 12-myristate 13-acetate (PMA)/ionomycin as a positive control, RPMI medium as a negative control, and PepMix BKV (1 µg/mL of LT, st, VP1, VP2, and VP3; JPT Peptides Technologies, Berlin, Germany) at 36°C in a CO_2 incubator for 24 hours. After washing the microplate, 100 µL/well of the detection antibody (biotin-labeled anti-human IFN-γ antibody) was dispensed and reacted at room temperature for 2 hours. Further processing was performed according to the manufacturer's instructions. Spot on the dried microplate were counted using an ELISPOT image analyzer (Cellular Technologies Ltd., Cleveland, OH, USA). PBMCs were evaluated in duplicate in each ELISPOT assay and average numbers of spots detected per 3×10^5 PBMCs. Spot numbers were calculated by subtracting the in the negative control from the average number of spots in the test wells. BKV-ELISPOT (sum of the five peptide-specific ELISPOT) results were also calculated.

2.5 Statistical analysis

Counts and percentages were calculated for categorical data, and the data were analyzed using the chi-square test and Fisher's exact test. The median and 95% confidence interval (95% CI)), were calculated for continuous data, and the data were compared using

10.3389/fimmu.2023.1243912

TABLE 1 Demographic characteristics and BK polyomavirus viremia status of the study kidney transplant (KT) recipients.

Characteristics	Total	BK viremia (+)	BK viremia (-)	P value
KT Recipients, n (%)	93	14 (15)	79 (85)	
Primary renal disease, n (%)				
DM	22 (23.7)	2 (14.3)	20 (25.3)	NS
Hypertension	7 (7.5)	4 (28.6)	3 (3.8)	0.009
Polycystic kidney disease	6 (6.5)	3 (21.4)	3 (3.8)	0.042
GN	33 (35.5)	3 (21.4)	30 (38.0)	NS
Unknown	25 (26.9)	2 (14.3)	23 (29.1)	NS
Age at transplantation (years ± SD)	48.4 ± 10.7	54.1 ± 11.3	47.4 ± 10.3	0.028
Gender, male, n (%)	59 (63.4)	12 (85.7)	47 (59.5)	NS
Blood incompatible, n (%)	42 (45.2)	9 (64.3)	33 (41.8)	NS
HLA mismatch number, mean ± SD	4 ± 1.7	4 ± 1.7	3.5 ± 1.7	NS
Prior kidney transplant, n (%)	9 (9.7)	1 (7.1)	8 (10.1)	NS
PRA at pre-KT, n (%)	29 (31.2)	4 (28.6)	25 (31.6)	NS
DSA at pre-KT, n (%)	14 (15.0)	5 (35.7)	9 (11.4)	NS
Induction therapy, n (%)				
Basiliximab	72 (78.5)	11 (78.6)	62 (78.5)	NS
Anti-thymocyte globulin	21 (22.6)	3 (21.4)	18 (22.8)	NS
KT Donor				
Age, years + SD	46.0 ± 11.8	52.1 ± 7.2	44.9 ± 12.2	0.036
Gender, male, n (%)	42 (45.2)	7 (50.0)	35 (44.3)	NS
Deceased donor, n (%)	3 (3.2)	1 (7.1)	2 (2.5)	NS
Acute rejection, n (%)				
AAMR	4 (4.3)	1 (7.1)	3 (3.8)	NS
ATCMR	10 (10.8)	3 (21.4)	7 (8.9)	NS
CAMR	1 (1.1)	0 (0.0)	1 (1.3)	NS
Pretransplant anti-BKV seropositivity				
in donors, n (%)	68 (73.1)	13 (92.9)	55 (69.6)	NS
in recipients, n (%	74 (79.6)	9 (64.3)	65 (82.3)	NS
Pretransplant anti-BKV IgG levels (OD)				
in donors, median (95% CI)		1.80 (1.63-2.65)	1.14 (0.67-1.63)	0.014
in recipients, median (95% CI)		2.14 (0.26-3.11)	1.66 (1.21-2-17)	NS

KT, kidney transplantation; DM, diabetes mellitus; GN, glomerulo-nephritis; BKV, BK polyomavirus; DSA, donor-specific antigen; PRA, panel-reactive antibody; HLA, human leukocyte antigen; AAMR, acute antibody-mediated rejection; ATCMR, acute T cell-mediated rejection; CAMR, chronic active antibody-mediated rejection; NS, not significant (P > 0.05).

Student's t-test and the Mann-Whitney U test. Receiver operating curve (ROC) analyses were used to define the cut-off number of spots for the BKV-ELISPOT assay to predict BKV infection. All statistical analyses were performed using MedCalc® Statistical Software version 20.218 (MedCalc Software Ltd, Ostend, Belgium; https://www.medcalc.org) and GraphPad prism version 9.0 for Windows (GraphPad Software, San Diego, California USA). All statistical analyses were two-tailed tests, and a P value less than 0.05 was defined as statistically significant.

3 Results

3.1 Baseline characteristics of kidney transplant recipients with respect to BK viremia

Among the 93 KTRs, 14 (15.1%) developed BK viremia and 5 (5.4%) were diagnosed with BKVAN. The mean recipient age was 48.4 years (ranging from 20 to 67 years) and 63.4% of recipients

were male. The baseline characteristics of the study participants with respect to BK viremia are summarized in Table 1. In the BK viremia (+) group, both donors and recipients were older than those without BK viremia (-) group; P = 0.028 and P = 0.036, respectively). The incidence of new-onset BK viremia after transplantation was significantly greater in recipients who had primary kidney disease due to hypertension (P = 0.009) or polycystic kidney disease (P = 0.042). There were no significant differences in the baseline characteristics and percentages of recipients who rejected the transplanted kidney between BK viremia (+) and BK viremia (-) patients.

3.2 Pretransplant anti-BKV-specific IgG seropositivity in donors and recipients

Using the cut-off level provided by the manufacturer, the anti-BKV IgG antibody assay was positive in 74 (79.6%) of 93 KTRs and in 68 (73.1%) of 93 KT donors and 31 (70.5%) of 44 healthy controls. There was no significant difference in seropositivity between the 93 KTR and 137 healthy participants (P > 0.05). Next, we analyzed the incidence of post-KT BK viremia according to pre-KT donor or recipient (D or R) anti-BKV serostatus. While not statistically significant, a greater percentage of KTRs who received transplants from seropositive donors (D+) were subsequently diagnosed with BKV infection than those who received transplants from seronegative donors (D−; 19.1% [13/68] vs. 4.0% [1/25]; P = 0.102). The anti-BKV serostatus of KTRs was not associated with post-transplant BK viremia (R+, 12.2% (9/74) vs. R-, 26.3% (5/19); P > 0.05). Five recipients developed BKVAN: three were D+/R−, one was D+/R+, and one was D−/R+.

3.3 Pretransplant anti-BKV-specific IgG levels in donors and recipients

When OD values of BKV-IgG results instead of positivity were analyzed, donors in the BK viremia (+) group had higher anti-BKV-IgG OD values than those in the BK viremia (-) group (median 1.80 [95% CI 1.63-2.65] vs. 1.14 [95% CI 0.67-1.63], P = 0.014; Figure 1). The recipients' anti-BKV-IgG levels were not associated with development of post-KT BK viremia (P > 0.05). Considering the high incidence of anti-BKV-IgG seropositivity, we categorized the KTRs with respect to anti-BKV IgG as those with high OD values (R-H; n = 47, OD range 1.63–2.28) and low OD values (R-L; n = 46, OD range; 0.04–1.56). Donors were also divided into two groups according to anti-BKV IgG levels as D-H (n = 47, OD range 1.63 –3.75) and D-L (n = 46, OD range 0.04–1.56). A greater percentage of KTRs who received a kidney from the D-H group had posttransplant BK viremia than those who received one from the D-L group (25.5% [12/47)] vs. 4.3% [2/46], P = 0.007; Figure 2). Among fourteen BK viremia (+) recipients, 12 (85.8%) received transplants from the high anti-BKV IgG (D-H) group. Among the five patients with BKVAN, four received transplants from D-H donors. When examining D/R pairs, the incidence of BK viremia (+) increased from 4.3% (2/46) in the D-L group to 24.0% (6/25) in the D-H/R-H group and 27.3% (6/22) in the D-H/R-L group.

3.4 Pretransplant BKV-specific INF-γ ELISPOT results

We employed a BKV-specific ELISPOT assay of five BKV peptides in the 93 pretransplant KTRs and 44 healthy controls.

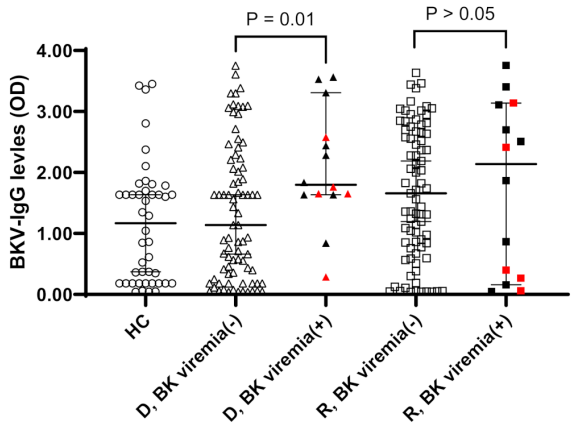

FIGURE 1
Anti-BKV IgG serostatus (optical density, OD) in 44 healthy controls (HC) and 93 donor (D) and recipients (R) prior kidney transplantation. Donors and recipients were stratified according to the development of posttransplant BK viremia development (BK viremia+) or not (BK viremia-). Donors from BK viremia (+) had higher OD values than donors from BK viremia (-) group (P = 0.01). Red symbols indicate results from five patients with BKV-associated nephropathy.

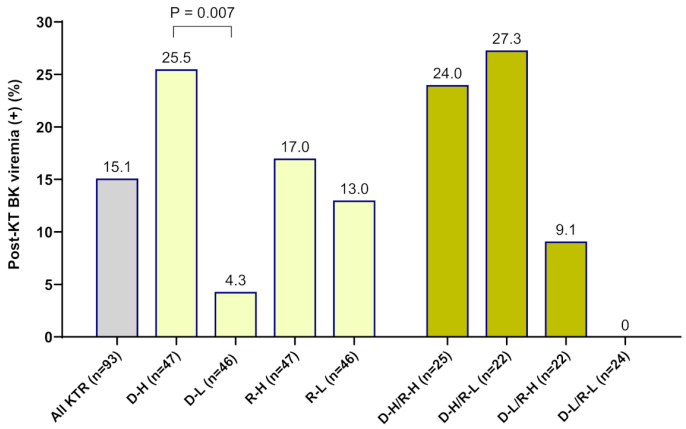

FIGURE 2
The incidence of new-onset posttransplant BK viremia was analyzed in 93 kidney transplant recipients (KTRs) according to the pretransplant anti-BKV-IgG serostatus in donors and recipients. Among KTRs, a greater percentage of the high-anti-BKV-IgG donor (D-H) group had posttransplant BK viremia (+) than those in the low-anti-BKV-IgG donor (D-L) group (P = 0.007). Outcomes were also assessed with respect to recipient anti-BKV-IgG serostatus (high anti-BKV-IgG, R-H; low anti-BKV-IgG, R-L). When examining donor/recipient pairs, the incidence of post-transplant BK viremia (+) was 24.0% (6/25) in the D-H/R-H group and 27.3% (6/22) in the D-H/R-L group.

The results showed a trend toward higher and wider ranges of BKV-ELISPOT values in the KTRs compared to healthy controls (Supplementary Figure 1). Of the five peptide-specific ELISPOT results, the VP2-ELISPOT results (spots/3×10^5 PBMCs) were higher in KTRs compared to healthy controls (median 8.5 [95% CI 6.0–13.0] vs. 5.0 [4.0–8.0], P = 0.040).

When comparing the pre-transplant BKV-ELISPOT results between posttransplant BK viremia (+) and BK viremia (-)

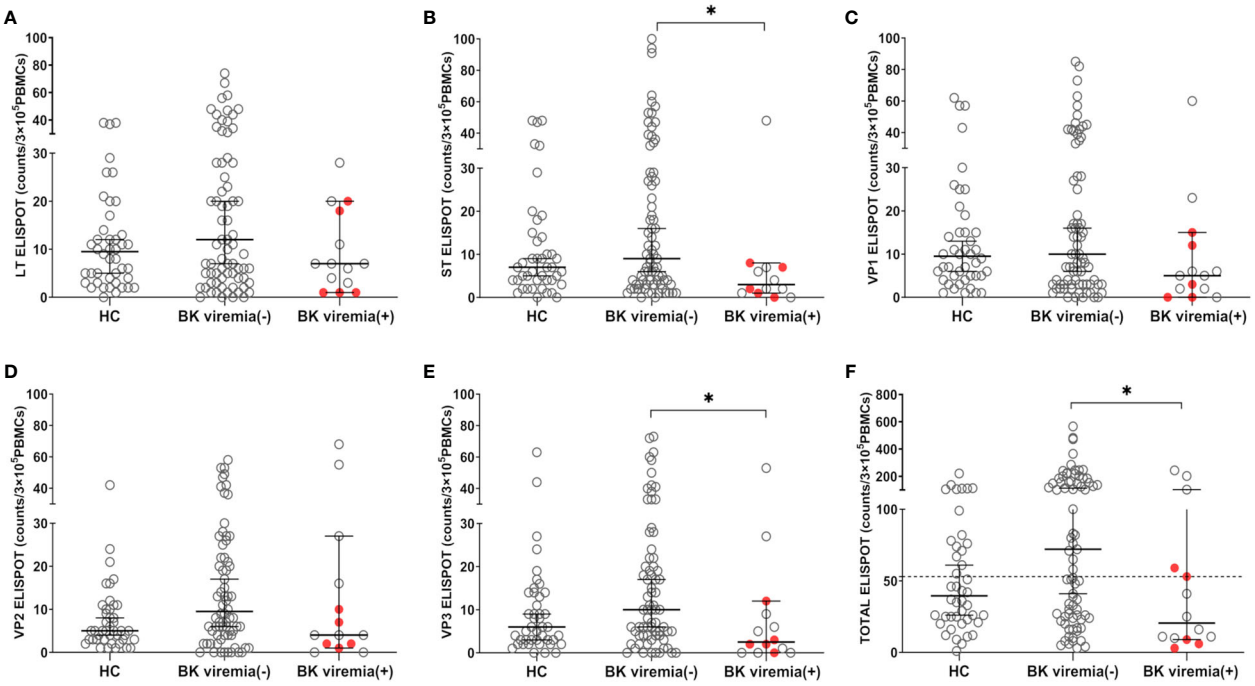

FIGURE 3
Comparisons of pretransplant BKV-ELISPOT assay results for BKV-specific peptides (LT, ST, VP1, VP2, VP3, and peptide totals) in the healthy control (HC), posttransplant-BK viremia (+), and no-posttransplant BK viremia (-) groups after kidney transplantation (KT). The BKV-associated nephropathy group is represented by a red-filled circle symbol. The long line represents the median and short line represents the 95% CI. The dashed line represents the cut-off value of 53 spot numbers/3 x 10^5 cells. BK viremia (+) KT recipients had significantly lower ST**(B)**, VP3**(E)**, and TOTAL**(F)** ELISPOT results than those in the BK viremia (-) group. *P<0.05. CI, confidence interval.

TABLE 2 Diagnostic accuracy of pretransplant donor and recipient anti-BKV-IgG levels and recipient BKV-ELISPOT results in kidney transplant recipients for prediction of BK viremia (>10^4 copies/mL) after kidney transplantation in the study population.

	Sensitivity % (95% CI)	Specificity % (95% CI)	PPV % (95% CI)	NPV % (95% CI)
High donor anti-BKV-IgG	85.7 (57.2-98.2)	55.7 (44.1-66.9)	25.5 (14.4-40.6)	95.7 (84.0-99.2)
Low recipient BKV-ELISPOT*	71.4 (41.9-91.6)	54.4 (42.8-65.7)	21.7 (15.6-29.5)	91.5 (82.1-96.2)
High donor anti-BKV-IgG and low recipient BKV-ELISPOT	57.4 (28.9-82.3)	79.8 (69.2-88.0)	33.3 (21.0-48.4)	91.3 (85.0-95.1)
High donor anti-BKV-IgG, and low recipient anti-BKV-IgG and BKV-ELISPOT	35.7 (12.8-64.9)	91.1 (82.6-96.4)	41.7 (20.9-65.9)	88.9 (84.3-92.2)
High donor anti-BKV-IgG or low recipient BKV-ELISPOT	100.0 (76.8-100.0)	30.4 (20.5-41.8)	20.3 (18.0-22.7)	100.0 (-)

*total BKV-ELISPOT result with spot number ≤ 53/3 x 10^5 PBMCs.
PPV, positive predictive value; NPV, negative predictive value; CI, confidence interval.

patients, BK viremia (+) patients showed a trend toward lower ELISPOT results for all five BKV peptides compared to BK viremia (-) patients, with significant differences for the St- and VP3-ELISPOT results (St-ELISPOT 3.0 [1.0 - 7.1] vs. 9.0 [6.0 -16.0], P = 0.038; VP3-ELISPOT 2.5 [0.0 - 9.3] vs. 10.0 [6.0 - 17.0], P = 0.013; Figure 3). The total BKV-ELISPOT results (sum of the five peptide-specific ELISPOT results) were also lower in BK viremia (+) patients compared to BK viremia (-) patients (20.5 [9.9 - 63.6] vs. 72.0 [43.2 - 110.8], P = 0. 027; Figure 3F). The five patients who developed BKVAN had low total BKV-ELISPOT results of 3, 6, 9, 53 and 59 spots/3×10^5 PBMCs.

Analysis of receiver operating curve (ROC) plots for pretransplant total BKV-ELISPOT results to predict posttransplant BK viremia showed an area under the curve (AUC) of 0.686 (95% CI: 0.581 – 0.778, P = 0.022). At the optimal cut-off value of ≤ 53 spots/3×10^5 cells, the sensitivity and specificity of total BKV-ELISPOT for predicting posttransplant BK viremia were 71.4 (95% CI: 41.9 – 91.6) and 54.4 (42.8 – 65.7). The overall positive predictive (PPV) and negative predictive (NPV) values of the total BKV-ELISPOT results were 21.7% (95% CI: 15.6 – 29.5) and 91.5 (95% CI: 82.1 – 96.2), respectively.

3.5 Prediction of posttransplant BK viremia (+) by combination of pretransplant anti-BKV-IgG levels and BKV-ELISPOT results

When total BKV-ELISPOT results before transplant were compared with anti-BKV-IgG levels in the 93 KTRs, there was no correlation between the two values. The elevated pre-transplant BKV-ELISPOT results in some seronegative patients provided additional evidence that the two risk factors were independent (Supplementary Figure 2). Diagnostic values were determined by combining pretransplant donor/recipient anti-BKV-IgG levels and recipient total BKV-ELISPOT results. For the posttransplant BK viremia prediction, the combination of high donor anti-BKV-IgG (D-H), low recipient BKV-IgG (R-L) and low recipient total BKV-ELISPOT results improved specificity to 91.1%. In case of decreased total BKV-ELISPOT results (≤ 53 spots/3×10^5 PBMCs) or high donor anti-BKV IgG levels, the NPVs for protection from posttransplant BK viremia was 100% (Table 2). Kaplan-Meier analyses demonstrated greater incidence of BK viremia in patients who had lower pretransplant total BKV-ELISPOT results and received a transplant from a donor with high anti-BKV-IgG levels compared with patients who did not (P = 0.003; Figure 4). We suggested an algorithm to predicts the risk of posttransplant BKV infection in KTRs based on pre-transplant BKV-IgG serostatus BKV-specific ELISPOT results (Figure 5).

4 Discussion

The BK polyomavirus is an opportunistic organism that frequently infects immunosuppressed patients after kidney transplantation, with BKVAN being a notable cause of impaired kidney function that may progress to transplant failure in up to 50% of cases (24, 25). Pretransplant risk factors associated with reactivation of BKV have been reported, including anti-thymoglobulin, administration of enhanced immunosuppressants, history of previous acute rejection, old age, HLA mismatch, HLA-C7 deficiency and anti-BKV IgG positivity (26). In the present study, pretransplant risk factors were evaluated using donor/recipient anti-BKV IgG levels and recipient BKV ELISPOT results to predict post-transplant BKV infection.

The BK virus, which causes infection in KTRs, could theoretically originate from both kidney donors and recipients (27). Anti-BKV IgG seropositivity through the manufacturer's suggested cut-off levels was 79.6% in KTR and 72.3% in healthy participants, which are similar to the previous study (28). Regarding the association between pretransplant anti-BKV IgG results and posttransplant BKV infection, in a previous study, KTRs who were negative for anti-BKV IgG had four-fold greater incidence of posttransplant BKV infection when the donor was positive for anti-BKV IgG, compared with donors that were negative for anti-BKV IgG (29). Several studies have reported a significantly higher risk of BKV infection in patients transplanted from anti-BKV-IgG-

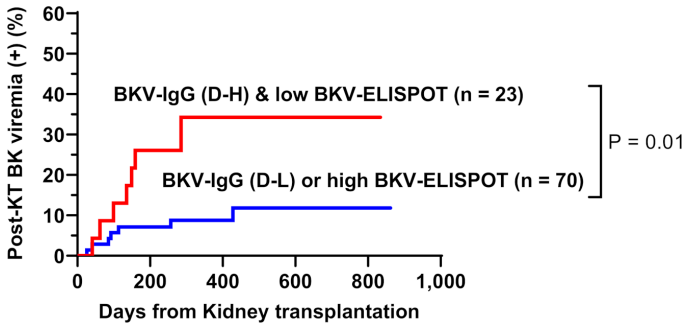

FIGURE 4
Cumulative incidence of posttransplant BK viremia in kidney transplant recipients stratified by donor pretransplant anti-BKV-IgG serostatus (H, high anti-BKV-IgG levels; L, low anti-BKV-IgG levels) and recipient total BKV-ELISPOT result. Recipients who had low BKV-ELISPOT results and received a kidney from high anti-BKV-IgG donors developed posttransplant BK viremia more frequently than the other patient groups.

positive donors (14, 30, 31). However, Hirsch et al. suggested that the D+/R− group is not the highest-risk group (28), and the significance of the donor or the recipient anti-BKV antibody serostatus is still uncertain. In the present study, there was a trend toward a greater percentage of KTRs who received allograft from seropositive donors (D+) developing BK viremia, but the pretransplant serostatus of donor and recipients was not significantly associated with posttransplant BK viremia ($p > 0.05$). However, when anti-BKV IgG levels were examined instead of seropositivity, the D-H/R-L group had the greatest risk of developing BK viremia ($p < 0.001$). These findings are consistent with the those of Saláková et al. (16) who established a significant correlation between donor seropositivity and recipient post-transplant BKV infection. A trend toward donor seropositivity and BKVAN was observed in their study, but lacked statistical significance. However, when assessing BKV IgG levels, both post-transplant BKV infection and BKVAN were more prevalent in recipients with higher donor BKV-IgG levels. They also highlighted a significantly increased risk of BKV infection after transplantation in the D+/R- group. In terms of BKVAN, four out of five BKVAN patients received transplants from the D-H group. These results are consistent with previous studies suggesting that the high risk of posttransplant BKV infection is not limited to the D+/R- group and that anti-BKV IgG levels in both donors and recipients may play an important role (28, 30, 32). Our data consistent with those of previous studies indicating that transplantation from donors with high anti-BKV IgG levels (D-H) into recipients with low anti-BKV IgG levels (R-L) is an independent risk factor for BKV infection

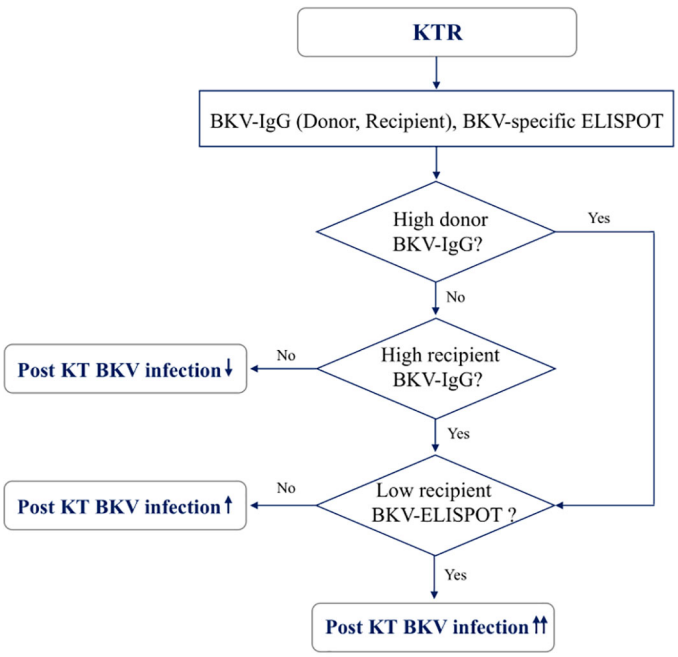

FIGURE 5
A model for predicting risk of BKV infection after transplantation in kidney transplant recipients based on pre-transplant BKV-IgG serostatus and BKV-specific ELISPOT results.

after transplantation by Dakroub et al. (10, 13). Smith et al. (18) also reported that BKV seronegative in 173 pediatric kidney transplant recipients was strongly associated with the incidence of BKVAN after transplantation. These findings suggest the importance of standardized anti-BKV-IgG testing and of clear guidelines for evaluation of anti-BKV-specific IgG levels and the definition of seropositivity. Currently, pretransplant screening of anti-BKV serostatus in kidney donors and recipients is neither mandatory nor routinely performed. Further studies are required to investigate the relationships between posttransplant BK viremia and pretransplant anti-BKV IgG antibody levels measured using standardized assays.

In terms of cellular immunity, BKV-specific T cells play an important role in the control of BKV infection by maintaining a persistent memory T cell response to the virus (19, 33–35). A prior meta-analysis reported that ELISPOT assays could be an effective tool to assess BKV-specific cellular immunity (7). In previous studies, posttransplant monitoring of BKV-specific cellular immune responses were conducted to investigate their associations with posttransplant reactivation of BKV (34, 36, 37). However, there have been few studies assessing whether pretransplant BKV-specific immunity levels can predict posttransplant BKV reactivation. Mutlu et al. (8) analyzed BKV-specific CD4+ T-cell responses of KTRs before transplantation and did not show any association between pre-transplant response and BKV reactivation, like the other two previous studies (6, 38). However, they confirmed that clearance of BK viremia or decrease of viral load corresponds with an increase in BKV-specificCD4+T-cellresponse. Other reports have also suggested that the absence of or low response of BKV-specific T cells may be a risk factor for BKV reactivation, while others have found no clear association (6, 8, 39). Dekeyser et al. found a gradual loss of BKV-specific T-cell polyfunctionality with BKV reactivation, particularly in patients with BKVAN. This exhaustion of BKV-specific T-cell responses is linked to impaired control of viral replication in the kidney (23). In present study, KTRs tended to have greater and broader BKV-ELISPOT results before transplantation compared to healthy controls, with a statistically significant difference for VP2-ELISPOT. Next, we investigated whether the pretransplant BKV-ELISPOT results could predict the development of posttransplant BK viremia. In our study, the 14 BK viremia (+) patients tended to have lower pretransplant ELISPOT responses to all 5 BKV peptides than BK viremia (-) patients. Among the five peptide-specific ELISPOTs, significant differences were observed for the St, VP3 and total BKV-ELISPOT results. The ROC analysis of total BKV-ELISPOT results showed an AUC of 0.686 and sensitivity of 71.4% and specificity of 54.4% using the cut-off value of ≤53 spots/300,000 cells. Also, four of five BKVAN patients had decreased pretransplant BKV-ELISPOT results. Our data are consistent with those of a previous report suggesting that specific T-cells control BKV latency before transplantation, and in this way may influence BKV reactivation after transplantation (40). These results suggest that low BKV-specific cellular responses before transplantation can be used as a risk factor to predict the development of BK viremia after transplantation. Regarding the target antigens of BKV-specific cellular immunity, our data did not identify the dominant target antigen. This finding confirms previous reports that it is not clear whether certain BKV peptides have a more dominant antigenicity (36, 41).

Given both BKV-IgG levels and BKV-ELISPOT results were correlated with BK viremia (> 10^4 copies/mL of BKV-DNA detected during the follow-up period), we analyzed the diagnostic performance of a combination of these biomarkers. Among KTRs who exhibited low levels of anti-BKV-IgG and low total BKV-ELISPOT results, and who received a kidney from the D-H group, the PPV and NPV for BKV viremia after transplantation were found to be 41.7% and 88.9% respectively. The relationship between impairment of BKV-specific cellular immunity and increased BKV replication in BK viremia remains uncertain (39). In a previous study, impaired functionality of cytomegalovirus (CMV) or BKV-specific T cells was evident in some transplant recipients for a prolonged period even after virus control (42–44). In present study, we used threshold of 10^4 copies/mL for BK viremia and initiation of therapeutic intervention. However, several studies have explored alternative thresholds for initiating therapy to prevent the progression to BKVAN. For instance, Hassan et al. reported that the currently suggested plasma viral load cutoff of 10^4 copies/mL for BK virus tends to underestimate the diagnosis of BKVAN (45). Another study by Hirsch et al. also indicated that viral nephropathy was linked to plasma viral loads of 7.7×10^3 copies/mL or higher (28). Randhawa et al. emphasized customized thresholds for medical centers, given their significant impact on predictive BKV infection outcomes (46). When we reexamined the dataset using a threshold of 10^3 copies/mL for BK viremia, two additional patients were reclassified into the BK viremia group. Consequently, the association between donor BKV-IgG levels and BK viremia (> 10^3 copies/mL) after KT was also significant (P value = 0.001). Similarly, BKV-specific ELISPOT results showed comparable diagnostic performances between data using thresholds of 10^3 copies/mL and 10^4 copies/mL (Supplemental Table 1). It is very important to establish risk factors for BKV infection after transplantation and application of proper BKV viral load cutoff, because careful monitoring of serum BKV and early reduction of immunosuppressants can resolve BK viremia and prevent transplant failure due to BKVAN in transplanted kidneys (47). Close monitoring after transplantation is necessary for patients whose donors showed high absorbance before kidney transplantation. Our results indicate anti-BKV-antibody-negative patients with a low ELISPOT results are expected to be at greater risk of BKV reactivation, so thorough monitoring is required. Thus, the application of pretransplant screening tests using anti-BKV-IgG and ELISPOT assays in conjunction with assessment of posttransplant blood BKV-DNA viral load may provide more accurate guidance for therapeutic intervention in KTRs with BKV infection.

This study had some limitations. First, a prospective cohort analysis was conducted at a single center including relatively small number of patients. Second, only five of 14 BK viremia (+) patients developed BKVAN. Therefore, our study could not determine whether pretransplant anti-BKV-IgG and BK-ELISPOT results can identify KTRs who will develop BKVAN. Finally, anti-BKV-

IgG levels were not validated in this study. For clinical application, cut-off values should be investigated with standard methods to stratify individual risk of BKV infection. In addition, our study used a commercially available anti-BKV IgG kit targeting the BKV serotype I and IV genotypes. Therefore, applying our results to other BKV serotypes could potentially introduce variability. Follow-up investigations focusing on all BKV serotypes are essential to comprehensively assess clinical significance of BKV serostatus. Well-designed prospective studies controlling for relevant confounding factors are needed before using anti-BKV-IgG and BKV-ELISPOT assays clinically to predict posttransplant BKV infection. Despite these limitations, our study focused on BKV serostatus and BKV-ELISPOT results before transplantation and demonstrated the diagnostic value of combining these tests. In conclusion, pretransplant donor and recipient anti-BKV-IgG levels and BKV-ELISPOT assay results may be used to identify patients at risk of BKV infection. Further studies are needed to confirm our results and validate the anti-BKV-IgG cut-off levels and BKV-ELISPOT assays as tools to predict post-kidney-transplant BKV infection.

Data availability statement

The raw data supporting the conclusions of this article will be made available by the authors, without undue reservation.

Ethics statement

The studies involving humans were approved by Institutional Review Board at Seoul St. Mary's Hospital (KC19TESI0043). The studies were conducted in accordance with the local legislation and institutional requirements. The human samples used in this study were acquired from a by- product of routine care or industry. Written informed consent for participation was not required from the participants or the participants' legal guardians/next of kin in accordance with the national legislation and institutional requirements.

Author contributions

HB performed the experiments and wrote the paper. HB and SJ analyzed the data. E-JO designed the study and edited the paper. BC and CY supervised specimen selection and the collection of clinical information. All authors contributed to the article and approved the submitted version.

Funding

This work was supported by the National Research Foundation of Korea (NRF) grant funded by the Korea government (MSIP) (NRF-2020R1A2B5B01001859), Republic of Korea. This work was also supported by the Institute of Civil Military Technology Cooperation funded by the Defense Acquisition Program Administration and Ministry of Trade, Industry and Energy of Korean government under grant No. 22-CM-EC-18.

Conflict of interest

The authors declare that the research was conducted in the absence of any commercial or financial relationships that could be construed as a potential conflict of interest.

Publisher's note

All claims expressed in this article are solely those of the authors and do not necessarily represent those of their affiliated organizations, or those of the publisher, the editors and the reviewers. Any product that may be evaluated in this article, or claim that may be made by its manufacturer, is not guaranteed or endorsed by the publisher.

Supplementary material

The Supplementary Material for this article can be found online at: https://www.frontiersin.org/articles/10.3389/fimmu.2023.1243912/full#supplementary-material

References

1. Kean JM, Rao S, Wang M, Garcea RL. Seroepidemiology of human polyomaviruses. *PloS Pathog* (2009) 5:e1000363. doi: 10.1371/journal.ppat.1000363

2. Wunderink HF, van der Meijden E, van der Blij-de Brouwer CS, Mallat MJ, Haasnoot GW, van Zwet EW, et al. Pretransplantation donor-recipient pair seroreactivity against BK polyomavirus predicts viremia and nephropathy after kidney transplantation. *Am J Transplant* (2017) 17:161–72. doi: 10.1111/ajt.13880

3. Hirsch HH, Randhawa P. BK polyomavirus in solid organ transplantation. *Am J Transplant* (2013) 13 Suppl 4:179–88. doi: 10.1111/ajt.12110

4. Fishman JA. BK virus nephropathy–polyomavirus adding insult to injury. *N Engl J Med* (2002) 347:527–30. doi: 10.1056/NEJMe020076

5. Hirsch HH, Randhawa PS, Practice ASTIDCo. BK polyomavirus in solid organ transplantation-Guidelines from the American Society of Transplantation Infectious Diseases Community of Practice. *Clin Transplant* (2019) 33:e13528. doi: 10.1111/ctr.13528

6. Schachtner T, Stein M, Babel N, Reinke P. The loss of BKV-specific immunity from pretransplantation to posttransplantation identifies kidney transplant recipients at increased risk of BKV replication. *Am J Transplant* (2015) 15:2159–69. doi: 10.1111/ajt.13252

7. Udomkarnjananun S, Kerr SJ, Francke MI, Avihingsanon Y, van Besouw NM, Baan CC, et al. A systematic review and meta-analysis of enzyme-linked immunosorbent spot (ELISPOT) assay for BK polyomavirus immune response monitoring after kidney transplantation. *J Clin Virol* (2021) 140:104848. doi: 10.1016/j.jcv.2021.104848

8. Mutlu E, Koksoy S, Mutlu D, Yilmaz VT, Kocak H, Dinckan A, et al. Quantitative analysis of BKV-specific CD4+ T cells before and after kidney transplantation. *Transpl Immunol* (2015) 33:20–6. doi: 10.1016/j.trim.2015.05.005

9. Miettinen J, Lautenschlager I, Weissbach F, Wernli M, Auvinen E, Mannonen L, et al. BK polyomavirus viremia and antibody responses of pediatric kidney transplant recipients in Finland. *Pediatr Transplant* (2019) 23:e13324. doi: 10.1111/petr.13324

10. Dakroub F, Touzé A, Sater FA, Fiore T, Morel V, Tinez C, et al. Impact of pre-graft serology on risk of BKPyV infection post-renal transplantation. *Nephrol Dialysis Transplant* (2021) 37:781–8. doi: 10.1093/ndt/gfab279

11. Bae H, Na DH, Chang JY, Park KH, Min JW, Ko EJ, et al. Usefulness of BK virus-specific interferon-γ enzyme-linked immunospot assay for predicting the outcome of BK virus infection in kidney transplant recipients. *Korean J Intern Med* (2021) 36:164–74. doi: 10.3904/kjim.2019.339

12. Solis M, Velay A, Porcher R, Domingo-Calap P, Soulier E, Joly M, et al. Neutralizing antibody-mediated response and risk of BK virus-associated nephropathy. *J Am Soc Nephrol* (2018) 29:326–34. doi: 10.1681/asn.2017050532

13. Dakroub F, Touzé A, Akl H, Brochot E. Pre-transplantation assessment of BK virus serostatus: significance, current methods, and obstacles. *Viruses* (2019) 11:945. doi: 10.3390/v11100945

14. Sood P, Senanayake S, Sujeet K, Medipalli R, Van-Why SK, Cronin DC, et al. Donor and recipient BKV-specific IgG antibody and posttransplantation BKV infection: a prospective single-center study. *Transplantation* (2013) 95:896–902. doi: 10.1097/TP.0b013e318282ba83

15. Schmitt C, Raggub L, Linnenweber-Held S, Adams O, Schwarz A, Heim A. Donor origin of BKV replication after kidney transplantation. *J Clin Virol* (2014) 59:120–5. doi: 10.1016/j.jcv.2013.11.009

16. Saláková M, Ludvíková V, Hamšíková E, Kolářová M, Šroller V, Viklický O, et al. Pretransplantation seroreactivity in kidney donors and recipients as a predictive factor for posttransplant BKPyV-DNAemia. *Front Immunol* (2022) 13:929946. doi: 10.3389/fimmu.2022.929946

17. Ginevri F, De Santis R, Comoli P, Pastorino N, Rossi C, Botti G, et al. Polyomavirus BK infection in pediatric kidney-allograft recipients: a single-center analysis of incidence, risk factors, and novel therapeutic approaches. *Transplantation* (2003) 75:1266–70. doi: 10.1097/01.Tp.0000061767.32870.72

18. Smith JM, McDonald RA, Finn LS, Healey PJ, Davis CL, Limaye AP. Polyomavirus nephropathy in pediatric kidney transplant recipients. *Am J Transplant* (2004) 4:2109–17. doi: 10.1111/j.1600-6143.2004.00629.x

19. Zhou W, Sharma M, Martinez J, Srivastava T, Diamond DJ, Knowles W, et al. Functional characterization of BK virus-specific CD4+ T cells with cytotoxic potential in seropositive adults. *Viral Immunol* (2007) 20:379–88. doi: 10.1089/vim.2007.0030

20. Zareei N, Miri HR, Karimi MH, Afshari A, Geramizadeh B, Roozbeh J, et al. Increasing of the interferon-gamma gene expression during polyomavirus BK infection in kidney transplant patients. *Microb Pathog* (2019) 129:187–94. doi: 10.1016/j.micpath.2019.02.015

21. Schaenman JM, Korin Y, Sidwell T, Kandarian F, Harre N, Gjertson D, et al. Increased frequency of BK virus-specific polyfunctional CD8+ T cells predict successful control of BK viremia after kidney transplantation. *Transplantation* (2017) 101:1479–87. doi: 10.1097/tp.0000000000001314

22. Comoli P, Basso S, Azzi A, Moretta A, De Santis R, Del Galdo F, et al. Dendritic cells pulsed with polyomavirus BK antigen induce ex vivo polyoma BK virus-specific cytotoxic T-cell lines in seropositive healthy individuals and renal transplant recipients. *J Am Soc Nephrol* (2003) 14:3197–204. doi: 10.1097/01.asn.0000096374.08473.e3

23. Dekeyser M, De Goër M-G, Hendel Chavez H, Boutin E, Herr F, Lhotte R, et al. Heterospecific immunity help to sustain an effective BK-virus immune response and prevent BK-virus-associated nephropathy. *researchSquare [Preprint]* (2022). doi: 10.21203/rs.3.rs-1650939/v1

24. Balba GP, Javaid B, Timpone JGJr. BK polyomavirus infection in the renal transplant recipient. *Infect Dis Clin North Am* (2013) 27:271–83. doi: 10.1016/j.idc.2013.02.002

25. Kuypers DR. Management of polyomavirus-associated nephropathy in renal transplant recipients. *Nat Rev Nephrol* (2012) 8:390–402. doi: 10.1038/nrneph.2012.64

26. Kwak EJ, Vilchez RA, Randhawa P, Shapiro R, Butel JS, Kusne S. Pathogenesis and management of polyomavirus infection in transplant recipients. *Clin Infect Dis* (2002) 35:1081–7. doi: 10.1086/344060

27. Kahan AV, Coleman DV, Koss LG. Activation of human polyomavirus infection — Detection by cytologic technics. *Am J Clin Pathol* (1980) 74:326–32. doi: 10.1093/ajcp/74.3.326

28. Hirsch HH, Knowles W, Dickenmann M, Passweg J, Klimkait T, Mihatsch MJ, et al. Prospective study of polyomavirus type BK replication and nephropathy in renal-transplant recipients. *N Engl J Med* (2002) 347:488–96. doi: 10.1056/NEJMoa020439

29. Andrews CA, Daniel RW, Shah KV. Serologic studies of papovavirus infections in pregnant women and renal transplant recipients. *Prog Clin Biol Res* (1983) 105:133–41.

30. Bohl DL, Storch GA, Ryschkewitsch C, Gaudreault-Keener M, Schnitzler MA, Major EO, et al. Donor origin of BK virus in renal transplantation and role of HLA C7 in susceptibility to sustained BK viremia. *Am J Transplant* (2005) 5:2213–21. doi: 10.1111/j.1600-6143.2005.01000.x

31. Dadhania D, Snopkowski C, Ding R, Muthukumar T, Chang C, Aull M, et al. Epidemiology of BK virus in renal allograft recipients: independent risk factors for BK virus replication. *Transplantation* (2008) 86:521–8. doi: 10.1097/TP.0b013e31817c6447

32. Bohl DL, Brennan DC, Ryschkewitsch C, Gaudreault-Keener M, Major EO, Storch GA. BK virus antibody titers and intensity of infections after renal transplantation. *J Clin Virol* (2008) 43:184–9. doi: 10.1016/j.jcv.2008.06.009

33. Prosser SE, Orentas RJ, Jurgens L, Cohen EP, Hariharan S. Recovery of BK virus large T-antigen-specific cellular immune response correlates with resolution of bk virus nephritis. *Transplantation* (2008) 85:185–92. doi: 10.1097/TP.0b013e31815fef56

34. Schachtner T, Muller K, Stein M, Diezemann C, Sefrin A, Babel N, et al. BK virus-specific immunity kinetics: a predictor of recovery from polyomavirus BK-associated nephropathy. *Am J Transplant* (2011) 11:2443–52. doi: 10.1111/j.1600-6143.2011.03693.x

35. Trydzenskaya H, Sattler A, Müller K, Schachtner T, Dang-Heine C, Friedrich P, et al. Novel approach for improved assessment of phenotypic and functional characteristics of BKV-specific T-cell immunity. *Transplantation* (2011) 92:1269–77. doi: 10.1097/TP.0b013e318234e0e5

36. Binggeli S, Egli A, Schaub S, Binet I, Mayr M, Steiger J, et al. Polyomavirus BK-specific cellular immune response to VP1 and large T-antigen in kidney transplant recipients. *Am J Transplant* (2007) 7:1131–9. doi: 10.1111/j.1600-6143.2007.01754.x

37. Leboeuf C, Wilk S, Achermann R, Binet I, Golshayan D, Hadaya K, et al. BK polyomavirus-specific 9mer CD8 T cell responses correlate with clearance of BK viremia in kidney transplant recipients: first report from the Swiss transplant cohort study. *Am J Transplant* (2017) 17:2591–600. doi: 10.1111/ajt.14282

38. Schachtner T, Stein M, Sefrin A, Babel N, Reinke P. Inflammatory activation and recovering BKV-specific immunity correlate with self-limited BKV replication after renal transplantation. *Transpl Int* (2014) 27:290–301. doi: 10.1111/tri.12251

39. Schmidt T, Adam C, Hirsch HH, Janssen MW, Wolf M, Dirks J, et al. BK polyomavirus-specific cellular immune responses are age-dependent and strongly correlate with phases of virus replication. *Am J Transplant* (2014) 14:1334–45. doi: 10.1111/ajt.12689

40. Šťastná-Marková M, Hamšíková E, Hainz P, Hubáček P, Kroutilová M, Kryštofová J, et al. Pretransplant BK Virus-Specific T-Cell-Mediated Immunity and Serotype Specific Antibodies May Have Utility in Identifying Patients at Risk of BK Virus-Associated Haemorrhagic Cystitis after Allogeneic HSCT. *Vaccines (Basel)* (2021) 9(11):1226. doi: 10.3390/vaccines9111226

41. Mueller K, Schachtner T, Sattler A, Meier S, Friedrich P, Trydzenskaya H, et al. BK-VP3 as a new target of cellular immunity in BK virus infection. *Transplantation* (2011) 91:100–7. doi: 10.1097/tp.0b013e3181fe1335

42. Papadopoulou A, Koukoulias K, Alvanou M, Papadopoulos VK, Bousiou Z, Kalaitzidou V, et al. Patient risk stratification and tailored clinical management of post-transplant CMV-, EBV-, and BKV-infections by monitoring virus-specific T-cell immunity. *EJHaem* (2021) 2:428–39. doi: 10.1002/jha2.175

43. Lee H, Oh E-J. Laboratory diagnostic testing for cytomegalovirus infection in solid organ transplant patients. *Korean J Transplant* (2022) 36:15–28. doi: 10.4285/kjt.22.0001

44. Lee H, Park KH, Ryu JH, Choi AR, Yu JH, Lim J, et al. Cytomegalovirus (CMV) immune monitoring with ELISPOT and QuantiFERON-CMV assay in seropositive kidney transplant recipients. *PloS One* (2017) 12:e0189488. doi: 10.1371/journal.pone.0189488

45. Hassan S, Mittal C, Amer S, Khalid F, Patel A, Delbusto R, et al. Currently recommended BK virus (BKV) plasma viral load cutoff of ≥4 log10/mL underestimates the diagnosis of BKV-associated nephropathy: a single transplant center experience. *Transpl Infect Dis* (2014) 16:55–60. doi: 10.1111/tid.12164

46. Randhawa P, Ho A, Shapiro R, Vats A, Swalsky P, Finkelstein S, et al. Correlates of quantitative measurement of BK polyomavirus (BKV) DNA with clinical course of BKV infection in renal transplant patients. *J Clin Microbiol* (2004) 42:1176–80. doi: 10.1128/jcm.42.3.1176-1180.2004

47. Ali AM, Gibson IW, Birk P, Blydt-Hansen TD. Pretransplant serologic testing to identify the risk of polyoma BK viremia in pediatric kidney transplant recipients. *Pediatr Transplant* (2011) 15:827–34. doi: 10.1111/j.1399-3046.2011.01583.x

frontiers | Frontiers in Immunology

TYPE Case Report
PUBLISHED 26 October 2023
DOI 10.3389/fimmu.2023.1274420

OPEN ACCESS

EDITED BY
Guido Moll,
Charité University Medicine Berlin,
Germany

REVIEWED BY
Helen Latsoudis,
Foundation for Research and Technology
Hellas (FORTH), Greece
Thomas Pfeiffer,
Washington University in St. Louis,
United States

*CORRESPONDENCE
Jia-wei Xu
xujiaweixsl@hotmail.com

†These authors have contributed
equally to this work and share
first authorship

RECEIVED 08 August 2023
ACCEPTED 12 October 2023
PUBLISHED 26 October 2023

CITATION
Zhang M-m, Wang J, Sun D, Wang J-x,
Zhang J-h and Xu J-w (2023) Case Report:
Autoimmune encephalitis and other
neurological syndromes with rare neuronal
surface antibody in children after
hematopoietic stem cell transplantation.
Front. Immunol. 14:1274420.
doi: 10.3389/fimmu.2023.1274420

Case Report: Autoimmune encephalitis and other neurological syndromes with rare neuronal surface antibody in children after hematopoietic stem cell transplantation

Ming-min Zhang[1†], Jing Wang[2†], Dan Sun[2], Jing-xuan Wang[3], Jun-hong Zhang[4] and Jia-wei Xu[1*]

[1]Department of Pediatrics, Union Hospital, Tongji Medical College, Huazhong University of Science and Technology, Wuhan, China, [2]Division of Neurology, Wuhan Children's Hospital, Tongji Medical College, Huazhong University of Science and Technology, Wuhan, China, [3]Wisdom Lake Academy of Pharmacy, Xi'an Jiaotong-Liverpool University, Suzhou, China, [4]Department of Pediatrics, The Central Hospital of Jingmen, Jingmen, China

Introduction: Neuronal surface antibody syndromes (NSAS) encompass a growing set of autoimmune neurological disorders, with their predominant clinical presentation being autoimmune encephalitis (AE). The most extensively documented form within NSAS is anti-N-methyl-D-aspartate receptor (NMDAR) autoimmunity. In contrast, other NSAS, such as anti-metabotropic glutamate receptor-5 (mGluR5) autoimmunity, are less common and less comprehensively characterized, particularly in pediatric cases.

Case description: In this instance, we present the case of a 7-year-old girl who exhibited abnormal behaviors following hematopoietic stem cell transplantation (HSCT). She received a diagnosis of anti-mGluR5 AE, and her Electroencephalogram (EEG) displayed an increased number of generalized slow waves during wakefulness. Treatment involved intravenous administration of gamma globulin and methylprednisolone, followed by oral prednisone tablets. Levetiracetam was introduced as an antiepileptic therapy during the pulse steroid therapy. Notably, the abnormal behaviors exhibited significant improvement after treatment.

Conclusions: To the best of our knowledge, this is the first report of rare pediatric NSAS involving anti-mGluR5 AE following HSCT. Enhancing our understanding and characterization of this condition may facilitate its recognition and treatment in children. Serum antibody testing could enable early identification and treatment of anti-mGluR5 AE.

KEYWORDS

metabotropic glutamate receptor 5, autoimmune encephalitis, hematopoietic stem cell transplantation, epilepsy, graft-versus-host disease

1 Introduction

AE is a disease triggered by an abnormal autoimmune response in the central nervous system's neurons. It is characterized by neuropsychiatric symptoms and seizures. The most common types of AE include anti-NMDAR encephalitis, anti-leucine-rich glioma-inactivating-1 protein encephalitis, and anti-contactin protein-related protein-2 encephalitis (1). In 2011, Lancaster et al. reported the presence of mGluR5 antibodies in the serum and cerebrospinal fluid of two patients with Hodgkin lymphoma and limbic encephalitis (2), thereby raising awareness about anti-mGluR5 AE. In children, AE mediated by anti-mGluR5 is exceedingly uncommon, with merely five documented cases reported since the identification of anti-mGluR5 auto-antibodies in 2011 (3, 4). This report presents the first documented case of the diagnosis and treatment of anti-mGluR5 AE in a child following HSCT. This case serves to enhance clinical awareness of central nervous system complications following HSCT and offers valuable insights into the early diagnosis and treatment of anti-mGluR5 AE.

2 Case presentation

On March 14, 2022, a 7-year-old girl was admitted to Wuhan Children's Hospital, Tongji Medical College, Huazhong University of Science and Technology due to noticeable behavioral changes occurring over the past months. These changes included episodes of eye rolling, mouth twitching, and pronounced mouth breathing, lasting approximately 3-5 minutes, particularly when fatigued, happening about 4-5 times per day. Shortly after these episodes, the child would suddenly rise and move about in a seated position, engaging in self-talk and hand-and-foot movements for several hours. The child had been diagnosed with epilepsy at the age of 1, effectively managed with oral levetiracetam. In March 2021, the patient developed intermittent fever and a decrease in blood cell counts. After a thorough examination, the patient was diagnosed with Shwachman-Diamond syndrome (SDS), a genetic condition marked by bone marrow failure and an elevated risk of hematological malignancies. Using whole-exome sequencing, we identified a homozygous splice site variant and this c.258 + 2T>C variant at the 5' splice site (ss) is associated with aberrant pre-mRNA splicing due to the usage of an upstream cryptic 5'ss at positions c.251-252, eventually resulting in an 8-bp deletion and frameshift (84Cfs3) (5). In November 2021, the patient underwent HSCT from an unrelated HLA9/10-compatible donor at the Department of Pediatrics, Union Hospital Affiliated to Tongji Medical College, Huazhong University of Science and Technology. There were no signs of acute or chronic graft-versus-host disease after HSCT. There was no significant personal history of trauma, infections, tuberculosis exposure, toxin exposure, allergies, or familial metabolic diseases. Upon admission, the patient exhibited stable vital signs, appropriate responsiveness, and normal brain function. Physical examinations revealed a supple neck with non-palpable superficial lymph nodes. Assessments of the heart, lungs, abdomen, and limb muscle strength were normal. Kernig's and Brudzinski signs were negative, and the heel-knee-shin test showed stability. Imaging tests, including diffusion-weighted magnetic resonance imaging (MRI) of the head, computed tomography scans of the chest, abdomen, and pelvis, superficial lymph node ultrasound, and positron emission tomography-computed tomography, showed no significant abnormalities. The EEG indicated a dominant rhythm without prominence, increased slow wave activity during wakefulness, and occasional paroxysmal multi-spike slow waves during sleep (Figure 1A). Integrated sensory and cognitive assessments reported mild proprioceptive and body coordination issues. The self-rating anxiety scale, self-rating depression scale, children's psychological counseling test report, and China-Wechsler children's intelligence scale all exhibited normal results. Laboratory tests, including blood counts, blood coagulation, urine and stool routines, liver and kidney function, thyroid function, C-reactive protein, procalcitonin, electrolyte levels, myocardial enzymes, blood ammonia, lactic acid, blood glucose, anti-nuclear antibodies, and anti-extractable nuclear antigen antibodies, all returned within normal ranges. Lymphocyte subsets detection displayed abnormalities (Table 1). The patient tested positive for Epstein-Barr virus core antigen, Epstein-Barr virus capsid antigen, cytomegalovirus antibodies, and herpes simplex virus I and II immunoglobulin G (IgG). However, fungal glucan, galactomannan tests, pre-transfusion infectious disease screening, tuberculosis microarray, and parvovirus B-19 yielded negative results. Routine cerebrospinal fluid biochemistry, exfoliative cytology, bacterial cultures, and smears (for common bacteria, cryptococci, and fungi) were all unremarkable. Moreover, 12 cerebrospinal fluid AE antibodies, along with oligoclonal bands and myelin basic protein, tested negative (Table 1). Bone marrow cytology and immunophenotypes were generally normal. Double immunofluorescence cell staining revealed elevated anti-mGluR5 antibody levels in the serum (1:1000) (Figure 2). A final diagnosis of anti-mGluR5 AE was established. The patient received treatment with intravenous gamma globulin (400 mg/kg daily for 5 consecutive days) and methylprednisolone (20 mg/kg daily for 5 consecutive days), followed by oral prednisone. During hormonal shock therapy, omeprazole was administered for gastric protection, along with calcium and potassium supplementation. Levetiracetam and trihexyphenidyl were concurrently prescribed for epilepsy and dystonia, respectively. The abnormal behaviors notably improved after treatment, and EEG results improved (Figure 1B). A re-examination in January 2023 revealed the absence of an SBDS gene mutation in peripheral blood. The patient remained symptom-free at the last follow-up in August 2023.

3 Discussion

According to previous reports, central nervous system complications occur in 11–65% of HSCT recipients (90% postmortem), accounting for 9–17% of death. These complications encompass infections, tumors, cerebrovascular issues, and autoimmune diseases (6). In this case, the patient displayed sudden behavioral changes with no prior infection history. The patient had a background of congenital bone marrow

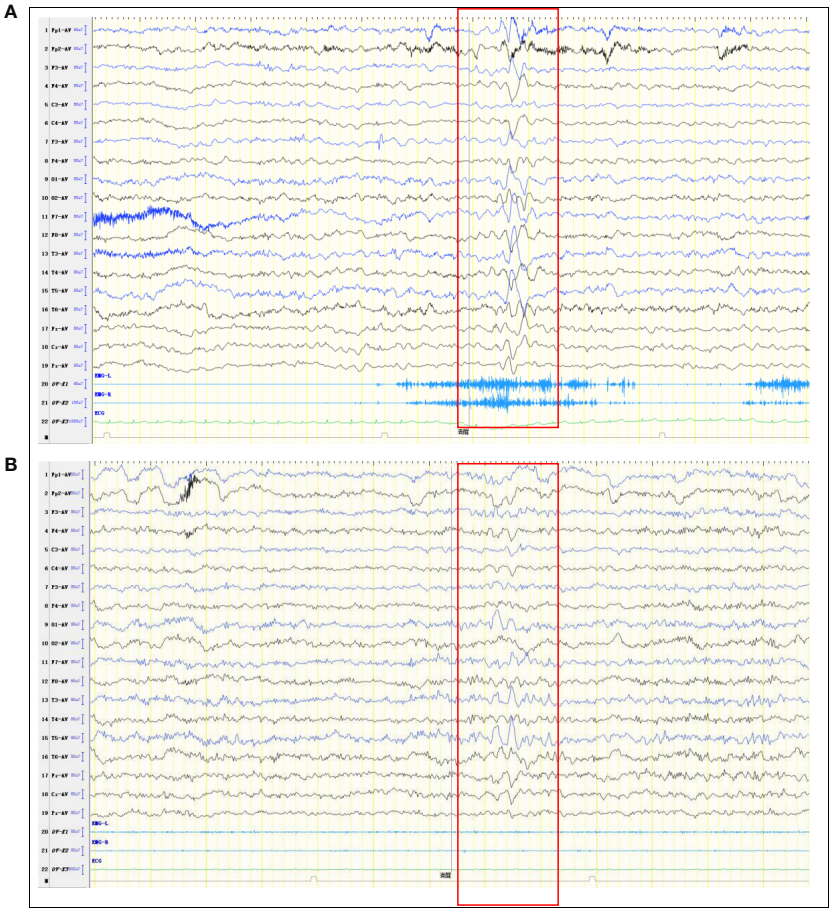

FIGURE 1
Abnormal EEG. **(A)** Pre-treatment EEG shows More extensive slow waves. **(B)** Post-treatment EEG shows slow waves in the left temporal region (limited reduction than pre-treatment slow waves).

TABLE 1 Summary of diagnostic evaluation.

Test	Value	Normal range
Natural killer cell (%)	2.53	6.9-19.3
CD19+ B-lymphocyte (%)	7.78	13.4-23.3
CD3+CD4+ T-lymphocyte (%)	13.43	27.8-44.1
CD3+CD8+ T-lymphocyte (%)	64.76	18.2-30.6
CD4+/CD8+	0.21	1.03-2.09
Anti-nuclear antibody	Negative	<1:80
Extractable nuclear antigens (Jo-1, Ro, La, RNP, Sm)	Negative	
Anti-NMDAR IgG	Negative	
Anti-AMPAR1 IgG	Negative	
Anti-AMPAR2 IgG	Negative	
Anti-LGI1 IgG	Negative	
Anti-C ASPR2 IgG	Negative	
Anti-G ABABR IgG	Negative	
Anti-DPPX IgG	Negative	

(Continued)

10.3389/fimmu.2023.1274420

TABLE 1 Continued

Test	Value	Normal range
Anti-Ig LON5 IgG	Negative	
Anti-Gly Rα1 IgG	Negative	
Anti-mGluR5 IgG	1:1000	Negative
Anti-D2R IgG	Negative	
Anti-GAD65 IgG	Negative	
CSF anti-NMDAR IgG	Negative	
CSF anti-AMPAR1 IgG	Negative	
CSF anti-AMPAR2 IgG	Negative	
CSF anti-LGI1 IgG	Negative	
CSF anti-C ASPR2 IgG	Negative	
CSF anti-G ABABR IgG	Negative	
CSF anti-DPPX IgG	Negative	
CSF anti-Ig LON5 IgG	Negative	
CSF anti-Gly Rα1 IgG	Negative	
CSF anti-mGluR5 IgG	Negative	
CSF anti-D2R IgG	Negative	
CSF anti-GAD65 IgG	Negative	
CSF WBC count (10^6/L)	1	0-10
CSF protein (g/L)	0.18	0.15-0.45
CSF glucose (mmol/L)	3.77	2.2-3.9
CSF oligoclonal bands	0	0–4

CSF, cerebrospinal fluid; NMDAR, N-methyl-D-aspartate receptor; AMPAR1, α-amino-3-hydroxy-5-methyl-4-isoxazole propionic acid type 1 receptor; NMPAR2, α-amino-3-hydroxy-5-methyl-4-isoxazolepropionic acid type 2 receptor; LGI, leucine-rich glioma inactivating 1 protein; CASPR2, contact protein-related protein 2; GABABR, γ-aminobutyric acid type B receptor; DPPX, dihydroxypeptidase-like protein; IgLON5, IgLON family protein 5; GlyR α1, glycine receptor α1 subunit; mGluR5, metabotropic glutamate receptor 5; D2R, dopamine type 2 receptor; GAD65, glutamate decarboxylase 65.

failure and finished HSCT. We ruled out infections, tumors, cerebrovascular abnormalities, graft-versus-host disease, and genetic metabolic issues. The diagnosis of anti-mGluR5 AE was based on clinical symptoms, positive serum anti-mGluR5 IgG levels, and increased slow waves on EEG. This case expands our understanding of central nervous system complications post-HSCT.

Glutamate serves as a primary excitatory neurotransmitter in the central nervous system, accounting for nearly 50% of

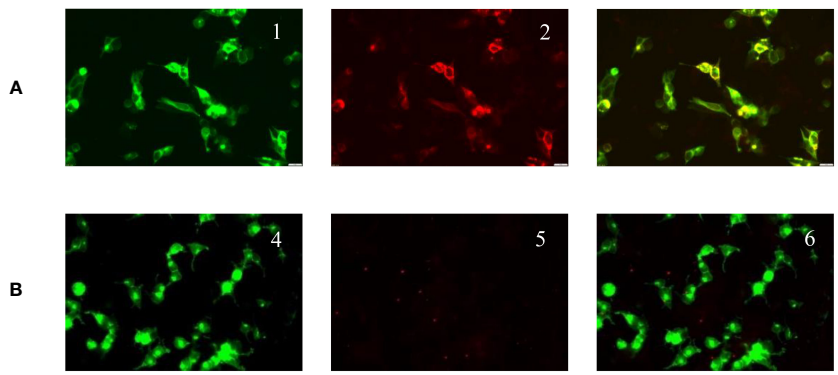

FIGURE 2
Positive serum anti-mGluR5 IgG expression (double immunofluorescence cell staining; original magnification 400×). **(A)** Serum tested. mGluR5 high expression plasmid transfected cells show green fluorescence (1). Anti-mGluR5 antibodies show red fluorescence (2). mGluR5 antigen antibody fluorescence overlap (3). **(B)** Negative control. GFP-transfected cells (4). Negative mGluR5 antibodies immunofluorescence (5). Fluorescence overlap (6).

intercellular synaptic signaling (7). GluRs play a pivotal role in excitatory synaptic transmission and are associated with mental, neurodevelopmental, and neurodegenerative disorders, including schizophrenia, autism, Parkinson's, and Huntington's disease (3). GluRs are classified into glutamate-gated ion channel type receptors and G protein-coupled metabotype receptors (mGluRs). mGluRs are further categorized into three classes based on sequence homology and signaling mechanisms. Class I mGluRs (mGluR1 and mGluR5) activate phospholipase C, triggering intracellular calcium release. Meanwhile, class II (mGluR2 and mGluR3) and class III (mGluR4 and mGluR6–8) mGluRs inhibit adenylyl cyclase (7). Anti-mGluR5 antibodies have been detected in Hodgkin's lymphoma and limbic encephalitis (including Ophelia syndrome) patients but are rare. These antibodies target hippocampal nerve fibers and neuron surface-related antigens in rats, leading to increased synaptic glutamate levels. Excessive glutamate can harm the brain through excitotoxicity, complement fixation, apoptosis, and induce seizures, ataxia, and behavioral and cognitive abnormalities (8, 9). Elevated glutamic acid concentrations can lead to intracellular calcium overload, protease activation, and cellular damage (10).

Autoimmune diseases, such as cytopenia, thyroid dysfunction, and myasthenia gravis, are common post-HSCT. Chronic graft-versus-host disease closely mimics other autoimmune disorders like scleroderma, Sjogren's syndrome, and primary biliary cirrhosis (11). The exact mechanisms of AE after HSCT remain unclear. They could be linked to donor-derived autoimmune lymphocytes or immune dysregulation post-transplantation. Factors contributing to post-transplant autoantibody production are multifaceted and involve genetics, environmental factors, and donor cell characteristics (12). In this case, the patient was still in the immune recovery phase after HSCT, and the imbalance between autoregulatory and autoreactive T lymphocytes led to B cells producing anti-mGluR5 antibodies.

TABLE 2 Clinical characteristics of the six reported pediatric anti-mGluR5 AE cases.

No.	Reference	Gender/ Age (y)	Prodrome	Main clinical manifestations	Concurrent tumor	Cerebrospinal fluid bio-chemistry	Anti-mGluR5 antibody	MRI	Treat-ment method	Prognosis/ relapse (yes or no)
1	Spatola et al. (3)	Male/15	Headache and nausea	Confusion, visual hallucinations, auditory hallucinations, decreased concentration, and status epilepticus	Hodgkin's lymphoma	Nucleated cells: 114×10^6/L; oligoclonal band (+)	Serum: negative; CSF: +	Restricted diffusion in bilateral occipital cortices	Tumor treatment	Full recovery/no
2	Spatola et al. (3)	Male/16	Headache	Mental disturbances, hallucinations, poor sleep, dystonia, and generalized seizures	Hodgkin's lymphoma	Nucleated cells: 31×10^6/L; oligoclonal band (+)	Serum: > 1/ 1280; CSF: 1/20	Normal	Tumor treatment, hormonal therapy, and plasma exchange	Full recovery/ yes
3	Spatola et al. (3)	Female/6	Rash, headache, and flu-like symptoms	Status epilepticus, memory loss, dystonia, ataxia, and degeneration of speech motor function	Hodgkin's lymphoma	Nucleated cells: 21×10^6/L; oligoclonal band (-)	Serum: negative; CSF: 1/10	Bilateral frontal cortex, right occipital cortex, and cerebellar high signals	Hormonal therapy, gamma globulin, and rituximab	Partial recovery/no
4	Spatola et al. (3)	Male/15	None	Facial palsy, abnormal behavior, memory loss, visual hallucinations, and insomnia	Hodgkin's lymphoma	Nucleated cells: 45×10^6/L; oligoclonal band (+)	Serum: 1/ 1280; CSF: 1/640	Normal	Tumor treatment, hormonal therapy, and gamma globulin	Partial recovery/no
5	Chen et al. (4)	Female/ 12	None	Seizures and memory loss	None	Normal nucleated cells; oligoclonal band (+)	Serum: negative; CSF: 1/32	Normal	Hormonal therapy and gamma globulin	Partial recovery/no
6	Present case	Female/7	None	Abnormal behavior and seizures	None	Normal nucleated cells; oligoclonal band (-)	Serum:1/1000; Cerebrospinal fluid: negative	Normal	Hormonal therapy and gamma globulin	Full recovery/no

Neuronal autoantibodies are highly prevalent in both adults and children, with positive anti-mGluR5 antibodies often lead to neuropsychiatric symptoms, encephalopathies, movement disorders, and seizures. Until to 2023, only five cases of pediatric anti-mGluR5 AE have been reported in PubMed, Cochrane Library, and CNKI using the search terms "chlidren", "anti-mGluR5 antibody" and "AE" (3, 4). This report presents the first case of anti-mGluR5 AE following HSCT. Based on previous reports and the current pediatric anti-mGluR5 AE cases, it can be concluded that anti-mGluR5 AE patients may typically exhibit: 1. Prodromal symptoms with headaches; 2. An association with Hodgkin's lymphoma;3. Main clinical features of limbic encephalitis with neuropsychiatric abnormalities; 4. MRI abnormalities; 5. Increased cell count and oligoclonal bands in cerebrospinal fluid; 6. Responsiveness to immunotherapy and/or tumor treatment; 7. Presence of anti-mGluR5 IgG in cerebrospinal fluid, and occasionally in serum; 8. Recurring neurological symptoms. Details are provided in Table 2.

Immunotherapy may be effective due to the direct pathogenic impact of neuronal surface antibodies. Treatment approaches for anti-mGluR5 AE are based on anti-NMDAR encephalitis and include high-dose intravenous corticosteroids, intravenous immunoglobulins, and plasma exchange. Symptomatic and supportive treatments, including antipsychotic and antiepileptic medications, are administered as needed. If initial treatments prove ineffective or recovery is slow, second-line immunotherapy with rituximab or cyclophosphamide may be considered (13, 14). Maintenance therapy with oral steroid is initiated after controlling acute symptoms and gradually tapered over several months. In cases of disease recurrence, mycophenolate mofetil and azathioprine may be used in combination with oral steroid therapy. Given that most anti-mGluR5 AE cases are triggered by tumors, immunotherapy is typically administered in conjunction with standard tumor treatments. Patients with latent tumors, poor responses to immunotherapy, or relapses after initial improvement should be reevaluated after several months.

4 Conclusion

The impairment of glutamatergic synaptic transmission caused by anti-neuronal surface GluR antibodies is now widely acknowledged as a significant factor in AE among humans. Conducting serum antibody tests on HSCT patients, especially those lacking autoimmune antibodies in their cerebrospinal fluid, can facilitate the early detection and treatment of anti-mGluR5 AE.

Data availability statement

The original contributions presented in the study are included in the article/Supplementary Material. Further inquiries can be directed to the corresponding author.

Ethics statement

The studies involving humans were approved by Medical Ethics Committee of the Union Hospital, Tongji Medical College, Huazhong University of Science and Technology (No.2017IEC70). The studies were conducted in accordance with the local legislation and institutional requirements. Written informed consent for participation in this study was provided by the participants' legal guardians/next of kin. Written informed consent was obtained from the individual(s), and minor(s)' legal guardian/next of kin, for the publication of any potentially identifiable images or data included in this article.

Author contributions

M-MZ: Writing – original draft, Writing – review & editing. JW: Writing – review & editing, Conceptualization, Data curation, Software. J-XW: Investigation, Software, Writing – review & editing. DS: Formal Analysis, Supervision, Validation, Writing – review & editing. J-HZ: Writing – review & editing, Investigation, Methodology. JW-X: Formal Analysis, Validation, Visualization, Writing – review & editing.

Funding

The author(s) declare that no financial support was received for the research, authorship, and/or publication of this article.

Conflict of interest

The authors declare that the research was conducted in the absence of any commercial or financial relationships that could be construed as a potential conflict of interest.

Publisher's note

All claims expressed in this article are solely those of the authors and do not necessarily represent those of their affiliated organizations, or those of the publisher, the editors and the reviewers. Any product that may be evaluated in this article, or claim that may be made by its manufacturer, is not guaranteed or endorsed by the publisher.

Supplementary material

The Supplementary Material for this article can be found online at: https://www.frontiersin.org/articles/10.3389/fimmu.2023.1274420/full#supplementary-material

References

1. Ancona C, Masenello V, Tinnirello M, Toscano LM, Leo A, La Piana C, et al. Autoimmune encephalitis and other neurological syndromes with rare neuronal surface antibodies in children: A systematic literature review. *Front Pediatr* (2022) 10:866074. doi: 10.3389/fped.2022.866074

2. Lancaster E, Martinez-Hernandez E, Titulaer MJ, Boulos M, Weaver S, Antoine JC, et al. Antibodies to metabotropic glutamate receptor 5 in the Ophelia syndrome. *Neurology* (2011) 77(18):1698–701. doi: 10.1212/WNL.0b013e3182364a44

3. Spatola M, Sabater L, Planaguma J, Martinez-Hernandez E, Armangue T, Pruss H, et al. Encephalitis with mGluR5 antibodies: Symptoms and antibody effects. *Neurology* (2018) 90(22):e1964–e72. doi: 10.1212/WNL.0000000000005614

4. Chen S, Ren H, Lin F, Fan S, Cao Y, Zhao W, et al. Anti-metabotropic glutamate receptor 5 encephalitis: Five case reports and literature review. *Brain Behav* (2023) 13 (5):e3003. doi: 10.1002/brb3.3003

5. Boocock GR, Morrison JA, Popovic M, Richards N, Ellis L, Durie PR, et al. Mutations in SBDS are associated with shwachman-diamond syndrome. *Nat Genet* (2003) 33(1):97–101. doi: 10.1038/ng1062

6. Uckan D, Cetin M, Yigitkanli I, Tezcan I, Tuncer M, Karasimav D, et al. Life-threatening neurological complications after bone marrow transplantation in children. *Bone Marrow Transplant* (2005) 35(1):71–6. doi: 10.1038/sj.bmt.1704749

7. Scotton WJ, Karim A, Jacob S. Glutamate receptor antibodies in autoimmune central nervous system disease: basic mechanisms, clinical features, and antibody detection. *Methods Mol Biol* (2019) 1941:225–55. doi: 10.1007/978-1-4939-9077-1_15

8. Levite M. Glutamate receptor antibodies in neurological diseases: anti-AMPA-GluR3 antibodies, anti-NMDA-NR1 antibodies, anti-NMDA-NR2A/B antibodies, anti-mGluR1 antibodies or anti-mGluR5 antibodies are present in subpopulations of patients with either: epilepsy, encephalitis, cerebellar ataxia, systemic lupus erythematosus (SLE) and neuropsychiatric SLE, Sjogren's syndrome, schizophrenia, mania or stroke. These autoimmune anti-glutamate receptor antibodies can bind neurons in few brain regions, activate glutamate receptors, decrease glutamate receptor's expression, impair glutamate-induced signaling and function, activate blood brain barrier endothelial cells, kill neurons, damage the brain, induce behavioral/psychiatric/cognitive abnormalities and ataxia in animal models, and can be removed or silenced in some patients by immunotherapy. *J Neural Transm (Vienna)* (2014) 121(8):1029–75. doi: 10.1007/s00702-014-1193-3

9. Meldrum BS. Glutamate as a neurotransmitter in the brain: review of physiology and pathology. *J Nutr* (2000) 130(4S Suppl):1007S–15S. doi: 10.1093/jn/130.4.1007S

10. Manev H, Favaron M, Guidotti A, Costa E. Delayed increase of Ca2+ influx elicited by glutamate: role in neuronal death. *Mol Pharmacol* (1989) 36(1):106–12. doi: 10.1002/med.2610090302

11. Vinzio S, Lioure B, Grunenberger F, Schlienger JL, Goichot B. Auto-immune-like disease post-bone marrow transplantation. *Rev Med Interne* (2004) 25(7):514–23. doi: 10.1016/j.revmed.2003.12.019

12. Rathore GS, Leung KS, Muscal E. Autoimmune encephalitis following bone marrow transplantation. *Pediatr Neurol* (2015) 53(3):253–6. doi: 10.1016/j.pediatrneurol.2015.05.011

13. Dalmau J, Lancaster E, Martinez-Hernandez E, Rosenfeld MR, Balice-Gordon R. Clinical experience and laboratory investigations in patients with anti-NMDAR encephalitis. *Lancet Neurol* (2011) 10(1):63–74. doi: 10.1016/S1474-4422(10)70253-2

14. Titulaer MJ, McCracken L, Gabilondo I, Armangue T, Glaser C, Iizuka T, et al. Treatment and prognostic factors for long-term outcome in patients with anti-NMDA receptor encephalitis: an observational cohort study. *Lancet Neurol* (2013) 12(2):157–65. doi: 10.1016/S1474-4422(12)70310-1

frontiers | Frontiers in Immunology

TYPE Original Research
PUBLISHED 30 October 2023
DOI 10.3389/fimmu.2023.1289744

OPEN ACCESS

EDITED BY
Martin Johannes Hoogduijn,
Erasmus University Rotterdam, Netherlands

REVIEWED BY
Sarah Bruneau,
INSERM U1064 Centre de Recherche en Transplantation et Immunologie, France
Dan Jane-wit,
Yale University, United States

*CORRESPONDENCE
Guido Moll
guido.moll@charite.de
Rusan Catar
rusan.catar@charite.de

†In memory of Duska Dragun

‡These authors have contributed equally to this work and share first authorship

§These authors have contributed equally to this work and share senior authorship

RECEIVED 06 September 2023
ACCEPTED 13 October 2023
PUBLISHED 30 October 2023

CITATION
Moll G, Luecht C, Gyamfi MA, da Fonseca DLM, Wang P, Zhao H, Gong Z, Chen L, Ashraf MI, Heidecke H, Hackel AM, Dragun D, Budde K, Penack O, Riemekasten G, Cabral-Marques O, Witowski J and Catar R (2023) Autoantibodies from patients with kidney allograft vasculopathy stimulate a proinflammatory switch in endothelial cells and monocytes mediated via GPCR-directed PAR1-TNF-α signaling. *Front. Immunol.* 14:1289744. doi: 10.3389/fimmu.2023.1289744

Autoantibodies from patients with kidney allograft vasculopathy stimulate a proinflammatory switch in endothelial cells and monocytes mediated via GPCR-directed PAR1-TNF-α signaling

Guido Moll [1,2*‡], Christian Luecht [1‡], Michael Adu Gyamfi [1‡], Dennyson L. M. da Fonseca [3], Pinchao Wang [1], Hongfan Zhao [1], Zexian Gong [1], Lei Chen [1], Muhamad Imtiaz Ashraf [4], Harald Heidecke [5], Alexander Maximilian Hackel [6], Duska Dragun [1†], Klemens Budde [1], Olaf Penack [7,8], Gabriela Riemekasten [6], Otávio Cabral-Marques [3,9,10,11,12§], Janusz Witowski [1,13§] and Rusan Catar [1*§]

[1]Department of Nephrology and Internal Intensive Care Medicine, Charité Universitätsmedizin Berlin, corporate member of Freie Universität Berlin, Humboldt-Universität zu Berlin, and Berlin Institute of Healthy (BIH), Berlin, Germany, [2]Berlin Institute of Healthy (BIH) Center for Regenerative Therapies (BCRT) and Berlin-Brandenburg School for Regenerative Therapies (BSRT), Charité Universitätsmedizin Berlin, Berlin, Germany, [3]Interunit Postgraduate Program on Bioinformatics, Institute of Mathematics and Statistics (IME), University of São Paulo (USP), São Paulo, Brazil, [4]Department of Surgery, Charité Universitätsmedizin Berlin, Berlin, Germany, [5]CellTrend GmbH, Luckenwalde, Germany, [6]Department of Rheumatology and Clinical Immunology, University of Lübeck, Lübeck, Germany, [7]Department of Hematology, Oncology and Tumorimmunology, Charité Universitätsmedizin Berlin, Berlin, Germany, [8]Berlin Institute of Health (BIH), Berlin, Germany, [9]Department of Clinical and Toxicological Analyses, School of Pharmaceutical Sciences, USP, São Paulo, Brazil, [10]Department of Medicine, Division of Molecular Medicine, USP School of Medicine, São Paulo, Brazil, [11]Laboratory of Medical Investigation 29, USP School of Medicine, São Paulo, Brazil, [12]Department of Immunology, Institute of Biomedical Sciences, USP, São Paulo, Brazil, [13]Department of Pathophysiology, Poznan University of Medical Sciences, Poznan, Poland

Non-HLA-directed regulatory autoantibodies (RABs) are known to target G-protein coupled receptors (GPCRs) and thereby contribute to kidney transplant vasculopathy and failure. However, the detailed underlying signaling mechanisms in human microvascular endothelial cells (HMECs) and immune cells need to be clarified in more detail. In this study, we compared the immune stimulatory effects and concomitant intracellular and extracellular signaling mechanisms of immunoglobulin G (IgG)-fractions from kidney transplant patients with allograft vasculopathy (KTx-IgG), to that from patients without vasculopathy, or matched healthy controls (Con-IgG). We found that KTx-IgG from patients with vasculopathy, but not KTx-IgG from patients without vasculopathy or Con-IgG, elicits HMEC activation and subsequent

upregulation and secretion of tumor necrosis factor alpha (TNF-α) from HMECs, which was amplified in the presence of the protease-activated thrombin receptor 1 (PAR1) activator thrombin, but could be omitted by selectively blocking the PAR1 receptor. The amount and activity of the TNF-α secreted by HMECs stimulated with KTx-IgG from patients with vasculopathy was sufficient to induce subsequent THP-1 monocytic cell activation. Furthermore, AP-1/c-FOS, was identified as crucial transcription factor complex controlling the KTx-IgG-induced endothelial TNF-α synthesis, and mircoRNA-let-7f-5p as a regulatory element in modulating the underlying signaling cascade. In conclusion, exposure of HMECs to KTx-IgG from patients with allograft vasculopathy, but not KTx-IgG from patients without vasculopathy or healthy Con-IgG, triggers signaling through the PAR1-AP-1/c-FOS-miRNA-let7-axis, to control TNF-α gene transcription and TNF-α-induced monocyte activation. These observations offer a greater mechanistic understanding of endothelial cells and subsequent immune cell activation in the clinical setting of transplant vasculopathy that can eventually lead to transplant failure, irrespective of alloantigen-directed responses.

KEYWORDS

chronic kidney disease (CKD), end-stage renal disease (ESRD), kidney transplantation (KTx), kidney allograft vasculopathy, endothelial cells (ECs), non-HLA-directed regulatory autoantibodies (RABs), autoantibodies, tumor necrosis factor-alpha (TNF-α)

1 Introduction

Over the past twenty years, non-HLA-directed regulatory autoantibodies (RABs) with the ability to target G protein-coupled receptors (GPCRs) have evolved as an essential new element in clinical pharmacology and multifaceted clinical pathology, e.g., in the setting of solid organ transplantation (SOT), cardiovascular diseases (CVDs), and in particular for various types of vasculopathy (1–3). This article aims to contribute to a better understanding of the molecular and cellular innate immune crosstalk that RABs can induce in the setting of transplant vasculopathy, which can lead to transplant failure (1).

Initial hallmark studies by Dragun et al. established the crucial functional role of immunoglobulin G (IgG)-derived RABs for the non-HLA-related outcome in kidney transplant (KTx) allograft survival in patients with allograft vasculopathy (4–8). Here, anti-GPCR-directed RABs associated with allograft vasculopathy constitute a distinct phenotype of antibody-mediated rejection (ABMR) (9, 10). After establishing the functional role of RABs directed against the angiotensin II type 1 receptor (AT1R) and endothelin receptor type A (ETAR) for vascular integrity and graft function/survival in the KTx setting (4, 8, 9, 11–16), subsequent studies have identified several RABs directed against GPCR targets typically associated with the vasculature, such as protease-activated receptors (PARs), neuronal and chemokine receptors, and the levels of these RABs are often modulated with patient age and disease status (1, 17, 18). Vasculature-associated RAB targets can be found on different types of micro-/macro-vascular endothelial cells (ECs), vascular smooth muscle cells (VSCMs), and perivascular multipotent mesenchymal stromal/stem cells (MSCs), but also neuronal cells, which are all often employed as model systems to study respective molecular signaling mechanisms (1, 19, 20).

It is now vital to decipher the detailed underlying signaling mechanisms, how these GPCR-specific functional RABs contribute to vascular dysfunction/injury, and the concomitant (auto)immune pathology in patients (1, 21, 22). Recently, we have demonstrated that serum-derived IgG fractions from patients with scleroderma-associated renal crisis stimulate interleukin-6 (IL-6) production by targeting the protease-activated receptor 1 (PAR1) on ECs (23). Intriguingly, histological features of systemic sclerosis (SSc) patients closely resemble those found in KTx recipients without detectable anti-HLA-antibodies but with features of chronic graft rejection (24). The concomitant vascular changes observed in these clinical settings include chronic inflammation, intimal fibrosis, and tissue calcification (1, 21, 22, 25). This pathology resembling a phenotype of chronic rejection must be distinguished from the more common phenotype and risk of acute rejection in the solid organ transplant (SOT) setting, which still accounts for the majority of graft rejections/failures, although overall 1-year allograft survival is now typically >90% (26–28).

A key mediator in (auto)immune pathology is the prototypic proinflammatory cytokine tumor necrosis factor alpha (TNF-α), typically released by activated leukocytes. Its production, underlying signaling mechanisms, and multiple biological effects have been studied extensively over the past three decades (29–32). Typically, ECs are considered to be targets for TNF-α. While TNF receptor 1 (TNFR1) is constitutively expressed on many cell types, expression of TNFR2 is restricted primarily to ECs (31, 32). When

acting directly on ECs, TNF-α stimulates the expression of chemokines, adhesion molecules, and metabolites, such as eicosanoids, that are key to the effective inflammatory response (33). The effect of TNF-α on ECs has been extensively studied in the past (34), but the role of ECs as a significant source of TNF-α has only been tested rather sporadically so far, e.g., TNF-α secretion has been previously reported to occur in human umbilical vein ECs (HUVECs) stimulated with IL-1 and other proinflammatory stimuli (35, 36).

In the present study, we determined whether non-HLA autoantibodies isolated from the serum of KTx recipients with allograft vasculopathy can stimulate ECs and monocytes to release significant amounts of TNF-α. We found an RAB-dependent synergistic TNF-α release from ECs and monocytes mediated via the PAR-1 receptor on ECs (Figure 1).

2 Methods

2.1 KTx patient and healthy serum, IgG isolation, and materials

Blood serum samples from KTx patients or healthy controls were obtained upon written informed consent and ethical approval from the local review board at Charité in agreement with the declaration of Helsinki and respective IgG fractions isolated as detailed earlier (23, 37). The IgG's were suspended in basic culture medium and stored at -80 degrees until use. The IgG for functional studies was prepared from n=7 patients with KTx-associated vasculopathy (KTx-IgG) and compared to IgG from n=7 healthy age and sex-matched controls (Con-IgG) and used in experiments at 1mg/ml as specified in the figure legends (Table S1). Unless stated otherwise, chemicals were from Sigma-Aldrich (Taufkirchen, Germany), and culture plastics were purchased from Corning and Becton Dickinson (Falcon; Franklin Lakes, NJ, USA). Cell culture media and buffers were from Thermo Fisher (Dreieich, Germany), and fetal calf serum (FCS) from Invitrogen (Darmstadt, Germany). The stimulators/inhibitors were as follows: thrombin (19), phorbol-myristate-acetate (PMA), activator protein 1 (AP1) inhibitor (SR-11302), and PAR1 inhibitor (BMS200261). The characteristics of any molecular detection or blocking antibodies employed in this article are given in the supplement (Table S2).

2.2 Culture of THP-1 and HMECs and flow cytometry analysis of CD14 and CD11b expression on THP-1 monocytic cells

The monocytic cell line THP-1 (Merck, Darmstadt, Germany) was cultured in RPMI1640-medium supplemented with 10% FCS and 1% Penicillin/Streptomycin. Human microvascular endothelial cells (HMECs; Catalogue no. CRL-3243) were purchased from ATCC® (Manassas, VA, USA) and used at passages 2-6 and cultured as described previously (19, 38–42).

Primary effect: To measure the direct stimulatory effect of KTx-IgG on HMECs and THP-1, the cells were stimulated for 1-24 hours with 1 mg/ml of KTx-IgG or Con-IgG with subsequent quantification of TNF-α mRNA and cytokine production.

Secondary Effect: The effect of IgG-stimulated TNF-α release from HMECs on THP-1 cells was assessed in three steps. First, to activate the HMECs, the cells were incubated for 6 hours either with or without KTx-IgG or Con-IgG (HMEC activation step) either in the presence or absence of anti-TNF-α blocking antibody or respective IgG isotype control (Table S2), as specified in more detail the figure legends. Second, this was followed by a brief washing step, to remove unbound IgG and thereby prevent autocrine effects of residual IgG on THP-1 cells. The stimulation medium was entirely removed, and the adherent cells briefly washed with IgG-free medium, to remove any remaining residual liquid that could contain unbound IgG. Third, "conditioning medium" was added to the washed cell layer of activated HMECs (anti-PAR1 autoantibody bound to PAR1 receptor on HMECs), to collect the HMEC secreted secretome (including HMEC-secreted TNF-α), to be used as follows.

Coculture of THP-1 with HMEC-conditioned medium: The KTx-IgG-stimulated and HMEC-conditioned medium was then added to the THP-1 cells at a ratio of 10% (v/v). After a 16-hour incubation, the THP-1 cells were assessed with flow cytometry for CD14 and CD11b surface expression, indicative of THP-1 and myeloid cell activation, as described earlier (CD11b more sensitive) (43). Upon the exposure of THP-1 cells to KTx-IgG or Con-IgG conditioned HMEC supernatants, the THP-1 cells were collected by careful mechanical agitation and resuspension, centrifuged for 5min at 1200 rpm, washed with PBS, and checked for viability by using the propidium iodide (PI) exclusion assay (43–45). For the antibody labeling, the THP-1 cells were placed on ice to prevent unspecific changes in CD14 and CD11b surface receptor expression and then labeled for 30 min in the dark with titrated antibodies (0.1 ug/ul) directed against CD14, CD11b, or respective isotype controls (all from Beckman Coulter GmbH, Krefeld Germany) (Table S2). The antibody-labeled THP-1 cells were then washed once more with PBS to remove unbound antibodies and fixed with 1% (v/v) of paraformaldehyde (PFA) diluted in PBS and subsequently analyzed with a flow cytometer (FACS Aria and FASC Calibur; Becton Dickinson, San Jose, CA, USA).

2.3 Detection of cellular TNF-α release with Quantikine ELISA

The concentration of TNF-α protein in the conditioned cell culture supernatants was measured with a high-sensitivity DuoSet immunoassay (Quantikine ELISA Kit; R&D Systems (Minneapolis, MN, USA). The detection limit was 0.049 to 1.6 pg/mL (40, 46).

2.4 Quantitative gene expression mRNA and micro-RNA analysis with qRT-PCR

The *TNF-α* gene and *ß2-microglobulin* (*ß2M*) housekeeping gene expression was assessed with quantitative reverse transcription PCR (qRT-PCR) (38, 44, 46–48). Total RNA was extracted using the PerfectPure RNA kit (5 Prime, Hamburg, Germany), and RNA

10.3389/fimmu.2023.1289744

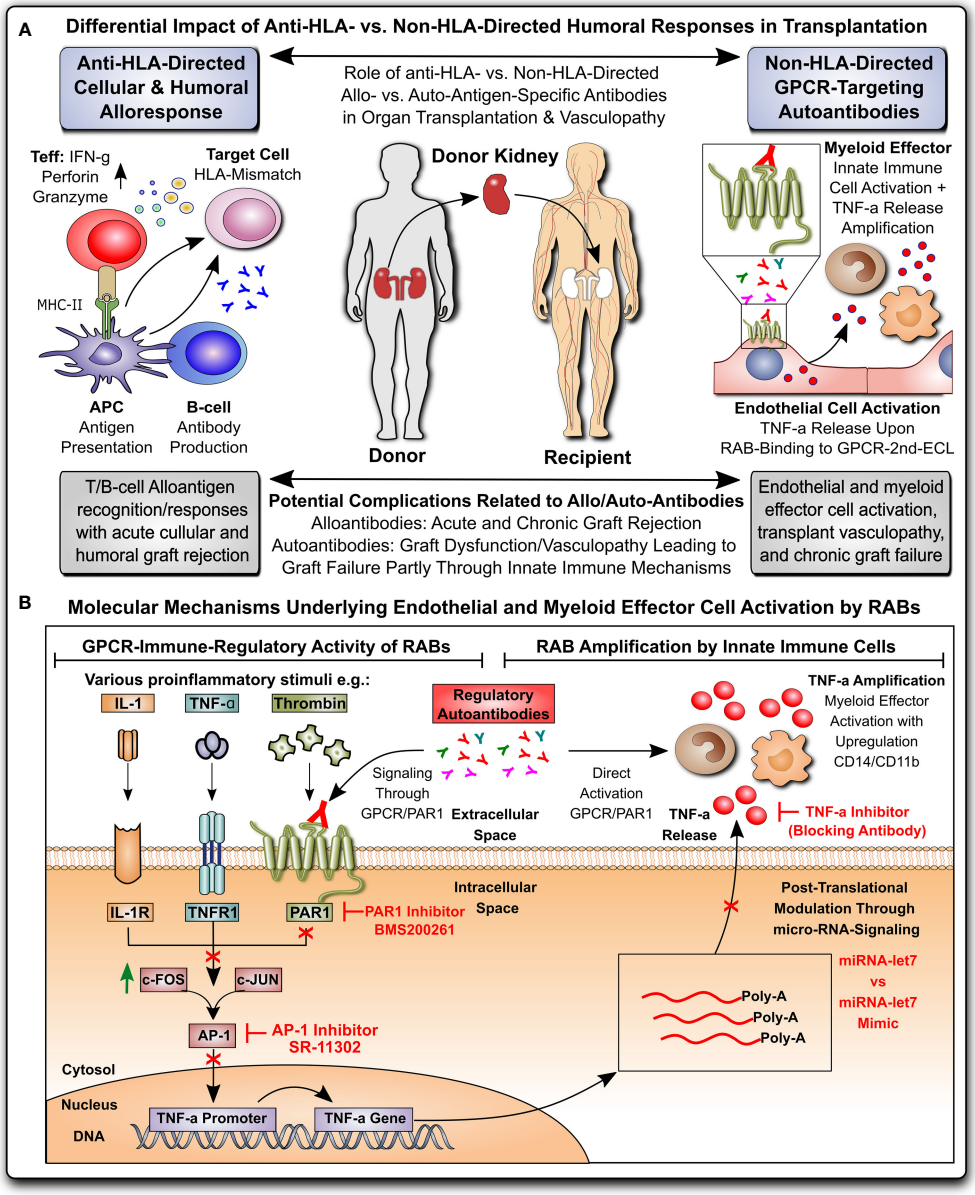

FIGURE 1
Non-HLA-directed autoantibodies from patients with kidney allograft vasculopathy stimulate a proinflammatory switch in endothelial cells and monocytes. **(A)** Differential impact of anti-HLA- vs. non-HLA-directed humoral responses in transplantation: Anti-HLA-directed cellular and humoral alloresponses are mainly effected by T- and B-cells and typically lead to acute humoral and cellular graft rejection in a mismatch transplant setting, while Non-HLA-directed G-protein coupled receptor (GPCR)-targeting regulatory autoantibodies (RAB) predominantly activate vasculature-resident GPCR-expressing endothelial cells to express TNF-α and subsequently activate innate immune effector, leading to chronic graft/transplant failure; and **(B)** Molecular mechanisms underlying endothelial and myeloid effector cell activation by RABs: ECs can be activated by various stimuli (e.g. TNF-α and other cytokines), or as shown here by GPCR-targeting RABs, which in the case of immunoglobulin G (IgG) isolated from transplant patients with transplant vasculopathy and rejection without detection of HLA-directed alloresponses (KTx-IgG), can bind to protease activated receptor 1 (PAR1; a GPCR) on the cell surface of ECs. Binding of KTx-IgG (containing the RABs), but not Con-IgG from healthy controls or KTx-IgG from patients without vasculopathy, activates the intracellular signaling cascades that lead to TNF-production, involving AP-1/c-FOS-signaling, TNF-promoter activation and further posttranscriptional regulation by microRNA-let7f-5g in ECs. The TNF-α secreted by KTx-IgG-activated ECs can kick of other secondary effects, such as THP-1 myeloid effector cell activation (detected by upregulation of surface receptors CD14 and CD11b on THP-1 cells), that may altogether contribute to the development of KTx transplant vasculopathy. AP-1, activator protein 1 transcription factor complex composed of subunits c-FOS and c-JUN; PAR-1, protease activated receptor 1; TNF-α, tumor necrosis factor alpha.

concentration and purity were estimated with a spectrophotometer (Nanodrop; ThermoFischerScientific). The obtained RNA was reverse transcribed into cDNA with random hexamer primers and qRT-PCR performed on a 7500 Fast Block real-time PCR system (Applied Biosystems). The specificity of the PCR reaction was verified with melting curve analysis and relative amount of transcript calculated with the cycle threshold method using the Applied Biosystems 7500 System v.1.2.3 software. Gene expression of the target gene was normalized to that of the housekeeping gene ß2M; Primers were as follows (Table S3): TNF-α (GeneBank

NM_000594.3): forward (5'-GACAAGCCTGTAGCCCATGT-3'), reverse (5'-GAGGTACAGGCCCTCTGATG-3'); ß2M (GeneBank NM_004048.2): forward (5'-GTGCTCGCGCTACTCTCTCT-3'), reverse (5'-CGGCAGGCATACTCATCTTT-3'). For micro-RNA analysis, following cDNA synthesis using the miScript II RT Kit (Qiagen, Hilden, Germany), the expression of 84 miRNAs was analyzed with miSript™ miRNA PCR Array Kit (Qiagen) according to the manufacturer's instructions. Six different snoRNA/snRNA (SNORD61, SNORD68, SNORD72, SNORD95, SNORD96A, and RNAU6-6P) were used as normalization controls. To mimic endogenous miRNA, 1 pmol of synthesized double-stranded has-let-7f-5p miScript miRNA mimic was transfected into cells using HiPerFect transfection reagent, as indicated per the manufacturer's protocol. After 16 hours, the cells were treated with KTx-IgG for 24 hours, and TNF-α release was measured by ELISA, as indicated above.

2.5 DNA constructs, transient transfection, TNF promoter computational analysis, nuclear extracts, and electrophoretic mobility shift assay

The DNA constructs of pre-defined TNF-α promoter fragments (Table S3) were analyzed with Electrophoretic mobility shift assays (EMSA) as described in detail (46). The promoter fragments were first checked for correct segment length by restriction digest. The cells were seeded into 6-well culture plates for transient transfection studies, and transfections were performed at 70-80% cell confluence in the absence of serum using the TurboFect™ transfection reagent (Thermo Fisher). The HMECs were transfected with the TNF-α reporter or reference plasmids and assayed with the dual-luciferase reporter assay system (Promega) (49). The human *TNF-α* promoter region located at -2010 to +50 (GenBank NT_007592.15) was analyzed with PROMO virtual laboratory for presence/location of potential transcription factor binding sites: http://alggen.lsi.upc.es/cgi-bin/promo_v3/promo/promoinit.cgi?dirDB=TF_8.3.

Nuclear extracts were prepared using NE-PER Nuclear and Cytoplasmic Extraction Kit and oligonucleotide probes labeled with Biotin 3' End DNA Labeling Kit (Thermo). For EMSA (38), the following probes were used (Regions of *TNF-α* promoter given in brackets, Figure S3): 5'-CCACACGGAGGCATCTGCACCCTC-3' (-1275 to -1298). Each binding mixture (20 µl) contained 5 µg nuclear extract, 20 fmol labeled double-stranded probe, 1 µg poly-dI/dC, and 2 µl 10 x buffer all incubated at room temperature for 30 min. Protein-DNA complexes were analyzed by electrophoresis in 6% non-denaturing polyacrylamide gels and visualized with LightShift Chemiluminescent EMSA Kit (Thermo). The activity of NFkB and NFAT signaling was analyzed with EMSA and luciferase assays, respectively, as described previously (50, 51).

2.6 Statistics

Statistical analysis was performed using GraphPad Prism 6.05 software (GraphPad Software). The data were analyzed with the t-test or repeated measures analysis of variance. Results were expressed as means ± SD. Differences with a p-value <0.05 were considered significant.

3 Results

3.1 Graphical abstract and synopsis of the major study results

The study background and a summary of the molecular mechanisms identified in this study can be found in Figure 1. In brief, kidney transplant patient-derived IgG (KTx-IgG; from patients with allograft vasculopathy), but not KTx-IgG from patients without allograft vasculopathy or healthy-donor-derived control IgG (Con-IgG), stimulates GPCR-PAR-1-signaling-axis-dependent TNF-α secretion from HMECs and THP-1 monocytic cells. Notably, the KTx-IgG-stimulated TNF-α secretion from HMECs can polarize and amplify THP-1 monocyte activation in response to the HMEC secretome.

3.2 KTx-IgG increases TNF-α production by HMECs and THP-1 monocytic cells

We previously found that non-HLA autoantibodies target vasculature resident GPCRs to induce endothelial injury (1, 52). Here, we focused on the resulting inflammatory milieu. First, we found that the exposure of HMECs to the serum IgG fraction from patients with transplant vasculopathy (KTx-IgG) resulted in both a concentration- and time-dependent increase in *TNF-α* expression (P<0.05 to P<0.001; Figures 2A–C). This increase in *TNF-α* mRNA expression (P<0.01; Figure 2A) was accompanied by a similar KTx-IgG concentration-dependent increase in TNF-α protein release (P<0.01; Figure 2B). Importantly, KTx-IgG from patients without allograft vasculopathy did not stimulate a substantial increase in TNF-α protein release (P<0.05; Figure S1A). This increase in TNF-α occurred rapidly within the first 60 min of exposure and remained well above control levels for the next 12-24 hours, but this did not happen in HMECs treated with a control medium or with IgG from healthy control individuals (Con-IgG) (Figure 2C). To test whether the effect of KTx-IgG was cell-type-dependent, we studied the response of both HMECs and THP-1 monocytes (Figure 2D). Similar to HMECs, the exposure of THP-1 monocytes to KTx-IgG resulted in an increased TNF-α release compared to Con-IgG (P<0.01 vs. P<0.05; Mean increase in TNF-α from 1.0 pg/ml for Con-IgG to 3.5 and 2.2 pg/ml for KTx-IgG, respectively; Figure 2D).

3.3 KTx-IgG modulates TNF-α gene promoter activity in HMECs via AP1-/cFOS

To elucidate the mechanism of KTx-IgG-induced modulation of *TNF-α* expression, HMECs were transfected with reporter constructs corresponding to different fragments of the *TNF-α* reporter, as shown earlier (19, 38, 40, 47, 53). First, we found that

10.3389/fimmu.2023.1289744

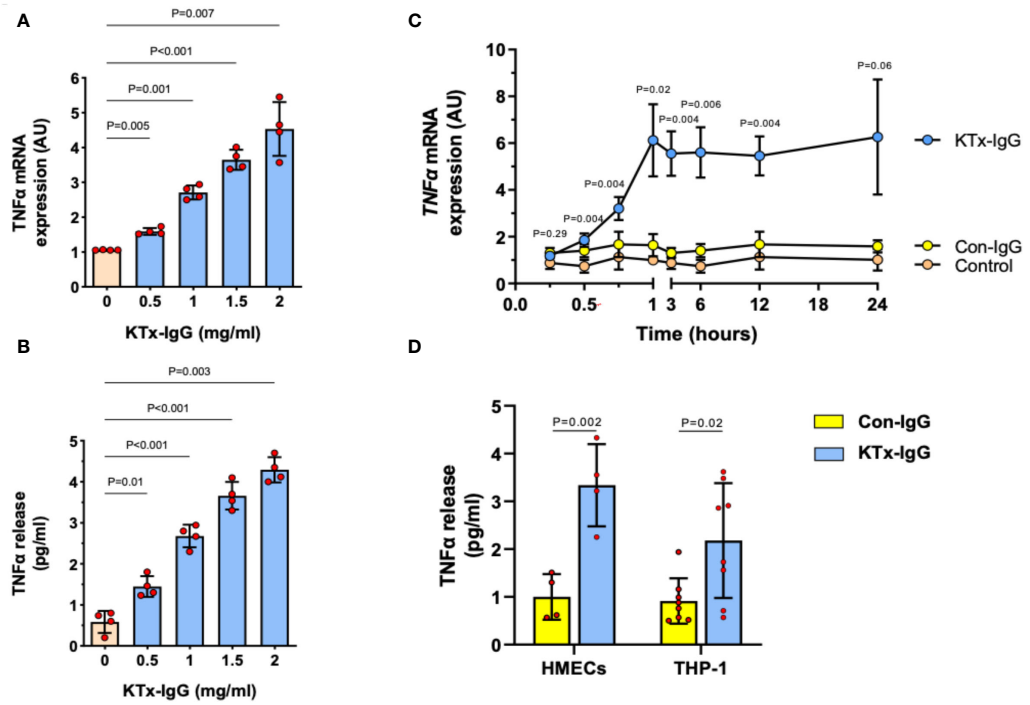

FIGURE 2
Effect of KTx-IgG on TNF-α production by HMECs. **(A, B)** Dose-response-effect of KTx-IgG on *TNF-α* mRNA expression and protein release from HMECs upon a 24-hour incubation with 0.5-2 mg/ml KTx-IgG (AU; arbitrary units, n=4); and **(C)** Kinetics of stimulation with KTx-IgG versus Con-IgG (each 1 mg/ml for 24 hours) on *TNF-α* mRNA expression in HMECs vs. unstimulated baseline (AU; depicting mean +/- SD of n=4); and **(D)** Direct comparison of KTx-IgG vs. Con-IgG (1 mg/ml for 24 hours) on TNF-α release (pg/ml) from both HMECs and THP-1 monocytes. The data were analyzed with repeated measures ANOVA [two-way ANOVA in **(C, D)**] with Šidáks multiple comparison test and are expressed as Mean +/- SD with *P<0.05, **P<0.01, and ***P<0.001.

the activity of full-length *TNF-α* promoter construct (positions -2010 to +50) was substantially increased upon stimulation with KTx-IgG (P<0.001; Figure 3A) and that this activity was retained to position -1511 (P<0.001), while further truncation of the promoter to position -1011 abolished its activity in response to KTx-IgG (P>0.99). Subsequent *in silico* analysis pointed to the presence of high-affinity binding sites for the transcription factor c-FOS. To verify whether c-FOS mediated the effect of KTx-IgG towards the *TNF-α* promoter, an electrophoretic mobility shift assay (EMSA) was performed using a biotin-labeled consensus oligonucleotide for c-FOS binding that corresponded to positions -1286 to -1277 of the promoter (Figure 3B). This demonstrates that nuclear extracts from HMECs stimulated with KTx-IgG form a DNA-protein complex with the c-FOS-specific oligonucleotide. To verify the specificity of c-FOS binding, the EMSA was performed with a 100-fold molar excess of unlabeled oligonucleotide, which resulted in a loss of the c-FOS-DNA complex. The involvement of c-FOS in KTx-IgG-induced TNF-α mRNA expression was confirmed by blocking experiments with the AP-1/c-FOS-inhibitor SR-11302, leading to a strong reduction of TNF-α mRNA expression to baseline (P<0.05; Figure 3C). Additionally, we analyzed the potential activation of NFkB and NFAT signaling in HMECs in response to KTx-IgG from patients with vasculopathy with either EMSA or luciferase assays, respectively (Figures S1C–D). We did not find any substantial activation of either signaling pathway in response to KTx-IgG, e.g. no NFkB EMSA probe shift, but a clear EBNA positive control shift, and no increase in NFAT activity with KTx-IgG in comparison to Con-IgG.

3.4 KTx-IgG modulates the intrinsic expression of selected miRNAs in HMECs

To determine whether miRNAs mediate the effects of KTx-IgG, the expression of a well-defined panel of miRNAs was assessed in HMECs (Figures 4, S2).

Interestingly, along with the strong modulation of endothelial TNF-α expression, exposure to KTx-IgG (1 mg/ml) strongly modulated the expression of several miRNAs (Figure 4A), of whom six were selected for further analysis/validation (Figure S2). Remarkably, miRNA-hsa-let-7f-5p was consistently downregulated by KTx-IgG (P=0.08; Figure 4B), which was also documented upon stimulation with TNF-α (10 pg/ml) (P<0.01; Figure 4C). Interestingly, the downmodulation of miRNA-hsa-let-7f-5p by both KTx-IgG and TNF-α could be abolished by blocking AP-1 (both P<0.01; Figures 4B, C). To verify if the reduction in miRNA-hsa-let-7f-5p is linked to TNF-α production, the HMECs were transfected with miRNA-hsa-let-7f-5p-mimic (1 pM) and then stimulated with KTx-IgG (Figure 4D), which led to a substantial omission of KTx-IgG-mediated induction of TNF-α. Likewise, KTx-IgG did not increase TNF-α release in cells pretreated with AP-1 blocker.

10.3389/fimmu.2023.1289744

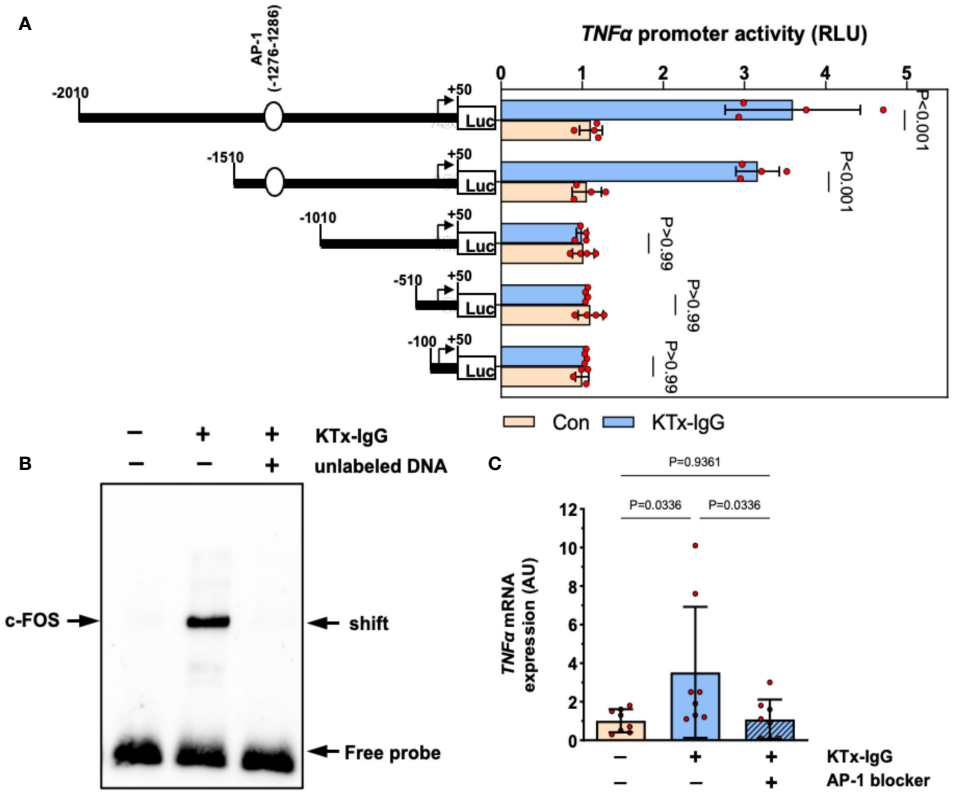

FIGURE 3
Transcriptional regulation of TNF-α expression by KTx-IgG in HMECs. **(A)** HMECs were transfected with either full-length TNF-α promoter construct or with its progressive 5'-deletions and then treated for 6 hours with or without KTx-IgG (1 mg/ml) and the activity of the luciferase reporter fragments was measured (RLI; relative luciferase activity; n=4, ANOVA), documenting that the TNF-α promoter activity is lost from the -1010-promoter-deletion onwards; **(B)** Nuclear fractions of HMECs stimulated as shown in **(A)** were analyzed by using EMSA with a biotin-labelled oligonucleotide with a predicted c-FOS binding sequence corresponding to the positions -1286 to -1277 of the TNF-α promoter. The EMSA was performed in the presence or absence of 100-fold molar excess of unlabeled oligonucleotide with one representative experiment is shown; and **(C)** TNF-α mRNA expression in HMECs stimulated for 12 hours with KTx-IgG (1 mg/ml) in the presence or absence of 1 μM AP-1-inhibitor SR-11302 (n=8; one-way ANOVA). The data are expressed as mean +/- SD with *P<0.05, **P<0.01, and ***P<0.001.

3.5 KTx-IgG-induced TNF-expression in HMECs is mediated via PAR1

Previously, we have identified PAR1 as key mediator of HMEC responsiveness to extracellular stimuli (1, 19). Furthermore, PAR1 is an important target for non-HLA-directed autoantibodies contained in KTx-IgG that can bind to GPCRs (1, 19). To test if the effect of KTx-IgG is mediated via PAR1, HMECs were stimulated with KTx-IgG in the presence of BMS200261, a specific PAR1 blocker, or a competing peptide that corresponds to a sequence motif in the second extracellular loop (ECL2) of PAR1 (Figure 5). Indeed, both treatments abolished KTx-IgG-induced changes in both TNF-α mRNA (Figure 5A) and miRNA-hsa-let-7f-5p (Figure 5B), thus implying that the stimulatory effect of KTx-IgG on HMECs is mediated via the PAR1 GPCR surface receptor. Again, Con-IgG had no effect (Figures 5A, B), thereby iterating that the altered autoantibody homeostasis in KTx patients and their binding to GPCR receptors, such as PAR1 (in particular its ECL2) is crucial for the proinflammatory responses of HMECs. Importantly, the PAR1-mediated stimulatory effect of KTx-IgG was strongly amplified in the presence of its natural activator thrombin and PMA (2-3-fold increase, Figure S1B), and both were strongly reduced in the presence of PAR1-Inhibitor (both P<0.05; Figure S1B).

3.6 KTx-IgG-stimulated HMEC-derived TNF promotes THP-1 monocyte differentiation

Our previous work identified myeloid effector cell activation as an essential amplifier of mesenchymal and endothelial cell modulation of immune responses (34, 43). We employed a similar flow cytometry-based readout to study THP-1 responses to KTx-IgG-stimulated HMEC secretome (Figure 6). As a positive control, stimulation of THP-1 cells with recombinant TNF-α (1 ng/ml, 16 hours) resulted in a substantial increase/doubling in the expression of activated monocyte differentiation markers CD14 and CD11b (Both P<0.001; Figure 6A). To examine whether TNF-α released by KTx-IgG stimulated HMECs could elicit similar biological activity, THP-1 cells were exposed to HMEC conditioned medium, which also led to a similar increase in both CD14 and CD11b expression (Both P<0.05; Figures 6B, C). Importantly, this increase was abolished when the HMEC

10.3389/fimmu.2023.1289744

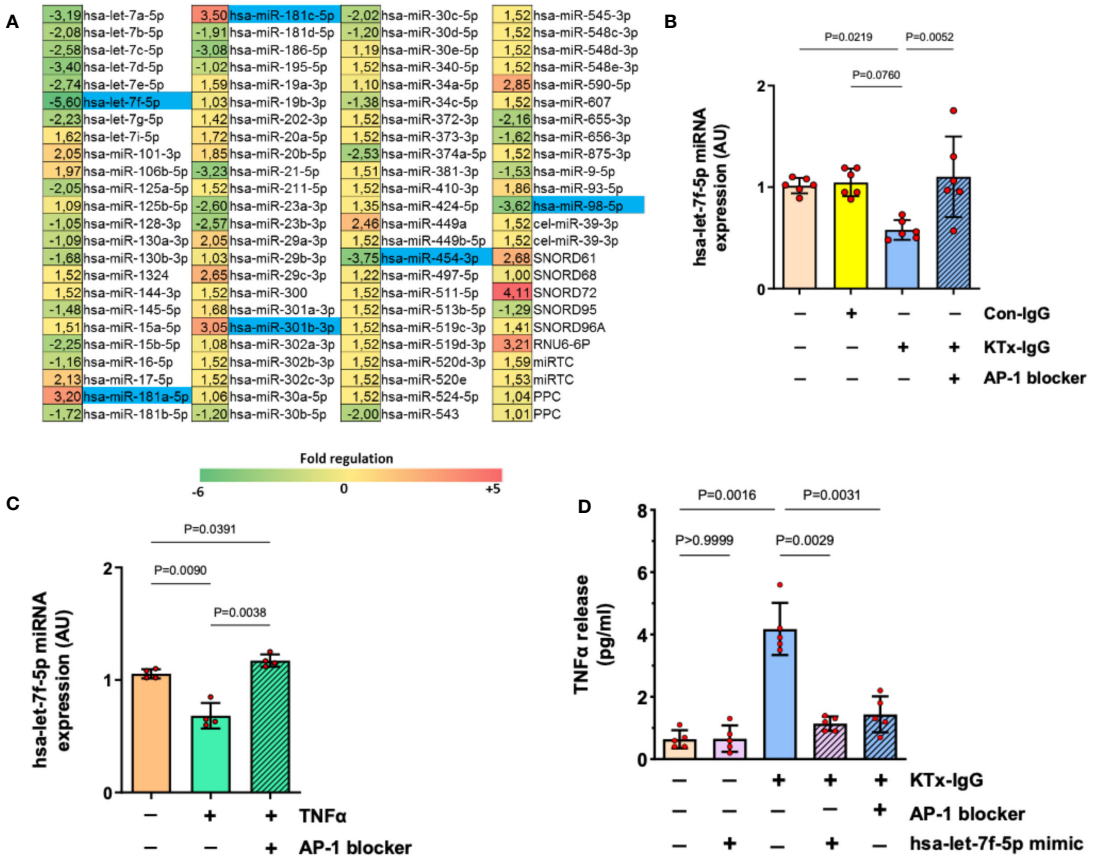

FIGURE 4
AP-1/miRNA-let-7f modulate KTx-IgG-induced TNF-production in HMECs. **(A)** HMECs were incubated for 1-hour with KTx-IgG (1 mg/ml) and miRNAs were isolated and analyzed using a profiler miRNA array, demonstrating no alterations, up- or down-regulation of specific targets (fold upregulation shown in red vs. downregulation shown in green), with the significantly changed targets marked in blue, identifying miRNA-hsa-let-7f-5p as the most strongly modulated target (-5.6 fold-downmodulation; for analysis of other targets please see Figure S1) while there were 2 more potential miRNA targets significantly downmodulated (-3.62 and -3.75) and three more upregulated (+3.05, +3.20, +3.50). **(B, C)** Expression analysis of miRNA-has-let-7f-5p in HMECs in the presence of AP-1 blocker (SR-11302, 1 μM). The cells were stimulated with either **(B)** KTx-IgG (1 mg/ml for 1 hour; n=6), or with **(C)** TNF-α (10 pg/ml for 1 hour; n=4), documenting a normalization/restoration of both KTx-IgG- and TNF-α-induced downmodulation in the presence of the AP-1 blocker. **(D)** Modulatory effect of miRNA-hsa-let-7f-5p and AP-1 on TNF-α production. HMECs were first transfected either with miRNA-hsa-let-7f-5p-mimic (1 pM) or pretreated with AP-1 blocker (SR-11302, 1 μM), and then stimulated with KTx-IgG (1 mg/ml) for 24 hours to quantify the TNF-α release from HMECs (pg/ml; n=5). Statistical testing was done with ANOVA and the data are depicted as mean +/- SD with *P<0.05, **P<0.01, and ***P<0.001.

conditioned medium was treated with an anti-TNF-α antibody but not with the control antibody. Moreover, when the medium was conditioned by HMECs treated with KTx-IgG in the presence of AP-1 inhibitor, PAR1 blocker, or the miRNA-has-let-7f-5p-mimic, the expression of CD14 and CD11b on THP-1 cells was markedly reduced (All P<0.05; Figures 2D, E).

4 Discussion

The present study demonstrates that immunoglobulin G (IgG) antibodies derived from kidney transplant (KTx) recipients with allograft vasculopathy (KTx-IgG), but not IgG antibodies from healthy control individuals (Con-IgG) or KTx-IgG from patients without vasculopathy, are capable of stimulating TNF-α production in HMECs and monocytic cells (THP-1 model). This pathomechanisms may be involved in vascular inflammation during the development of allograft vasculopathy in the absence of donor-specific anti-HLA-antibodies (DSA) and cellular alloresponses (e.g., anti-HLA-directed effector T-cell responses). These anti-HLA directed alloresponses must be clearly distinguished from non-HLA-specific RABs previously identified in hallmark studies from our group to contribute to the pathomechanisms, which lead to non-HLA-related kidney allograft failure and allograft vasculopathy (1, 4, 5, 7–9, 11–15, 54, 55).

Noteworthy, this TNF-α stimulatory effect did only occur upon exposure of HMECs to KTx-IgG from transplant patients with underlying vasculopathy, which has been shown to exhibit disturbed homeostasis in their blood/vasculature-resident RABs (1), but not upon exposure to healthy control IgG (Con-IgG), or KTx-IgG from patients without vasculopathy. The RABs contained in KTx-IgG can not only promote G-protein-coupled receptor (GPCR) activation, but also lead to an altered expression of their highly potent GPCR effector targets (e.g. PAR1 upregulation) in the vasculature, which can then further augment/promote robust

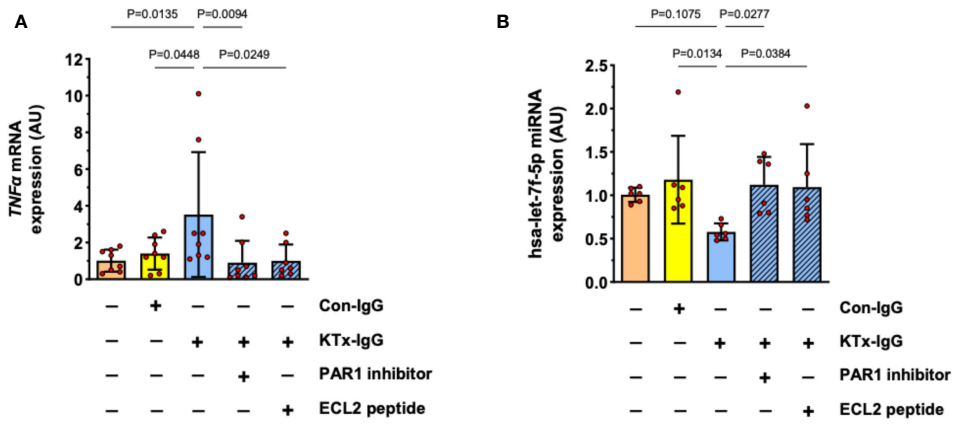

FIGURE 5
Role of cell surface receptor PAR-1 in KTx-IgG-induced responses in HMECs. The protease activated thrombin receptor PAR1 is a typical target for non-HLA autoantibodies contained in patient blood with disturbed autoantibody homeostasis (1, 19). To test whether PAR1 mediates the KTx-IgG-responses, the HMECs were stimulated for 3 hours with patient-derived KTx-IgG or health-donor-derived Con-IgG (both at 1 mg/ml) in the presence of either the PAR1 inhibitor (BMS200261, 1 μM), or small blocking peptide that is specific to the second extracellular loop of the PAR1 receptor (ECL2-specific peptide, 1 μM). After the exposure to the reagents, the HMECs were analyzed for: **(A)** TNF-α mRNA expression (AU, n=8), or **(B)** miRNA-hsa-let-7f-5p (AU, n=6), revealing a PAR1-dependent modulation of both targets. Statistical testing was done with ANOVA and the data are depicted as mean +/- SD with *P<0.05, **P<0.01, and ***P<0.001.

vascular responses upon RAB binding/engagement of their GPCR extracellular loop domains.

These detrimental events, the modulation of GPCR expression and its signaling intensity, can lead to kidney transplant rejection even in the absence of anti-HLA-directed alloantibodies (4). This pathomechanism may explain distinct cases of kidney allograft failure, where specific alloresponses have been ruled out as the underlying cause for allograft failure. Importantly, we here found here for the first time, that the nature of this TNF-α stimulatory effect is related to the ability of these RABs to induce signaling through the thrombin receptor PAR1, a typical protease activated GPCR (56–62).

One of the most important known natural activators of PAR1 is thrombin (19), which cleaves the n-terminus of the PAR1 receptor. Upon cleavage of the n-terminus, the tethered ligand can then bind to the PAR1 receptor to activate the intracellular signaling cascade. In contrast, the KTx-IgG activates the PAR1 receptor by binding to the second extracellular loop, which then leads to conformational changes of the 3D structure of the receptor in the cell membrane. Interestingly, we found that KTx-IgG from patients with vasculopathy increased the TNF-a response of HMECs to their natural activator thrombin and PMA.

Considering the biological *in vivo* relevance of the PAR1-KTx-IgG-signaling-axis-induced endothelial and monocytic TNF-α production and subsequent monocyte activation/differentiation in patients vs. *in vitro* coculture models, it needs to be anticipated that our observations are derived from a static *in vitro* coculture system, where both, the producer and the targets cells, are in close proximity to each other, which facilitates their interaction. It must also be noted that this coculture system is devoid of the vascular flow and fluid-transport condition (e.g. transport of blood or urine), as they are typically observed in the macro-micro-vasculature of the kidneys and kidney nephrons, respectively.

The binding of RABs to GPCRs and the subsequent induction of inflammatory responses may also be a common theme in pathologies other than kidney allograft failure, such as in patients undergoing transplantation of complex vascularized allografts (e.g., full hand Tx) (63), or in patients with dysregulated immune function (e.g., systemic sclerosis, SSc) (23). On the molecular level, RAB-binding to PAR1 resulted in an intracellular signaling cascade involving the transcription factor AP-1 and modulation of miRNA-hsa-let-7f-5p. Indeed, we have previously shown that the AP-1/c-FOS transcription factor complex is a prime relay/modulator of EC inflammatory responses in the vasculature (19, 40, 47).

The dysregulated activity of PARs has been implicated in many different diseases and pathological settings, as reviewed in detail in the following articles (56–62). In addition to serving as a prototypic receptor for its main activating ligand thrombin (19), PAR1 can also respond to other proteases, including plasmin, activate protein C, and matrix-metalloproteinases, to produce either pro-inflammatory or cytoprotective downstream effects, depending on the exact pathophysiological context, as discussed earlier (19). In this respect, we have previously reported an example of biased agonism exerted by IgG from patients with scleroderma (SSc-IgG), which was found to induce IL-6 expression in ECs by signaling through PAR1 (23).

Another exciting aspect of our current study is that we identified HMECs as a source of biologically active TNF-α in the vascular system in the context of binding and stimulation through EC surface resident GPCRs that bind RABs contained in the KTx-IgG but not in Con-IgG from healthy controls. Importantly, TNF-α activation/secretion of ECs will only become evident in the physiological or better said pathophysiological setting *in vivo* when the RAB network homeostasis is somehow disturbed in a particular disease or pathological setting (1). Again, the above-mentioned study on SSc-IgG is exemplary to illustrate how binding of RABs to GPCRs, such as PAR1, can trigger secretion of proinflammatory cytokines, such as IL-6, or in the current KTx-IgG setting secretion of TNF-α from HMECs.

10.3389/fimmu.2023.1289744

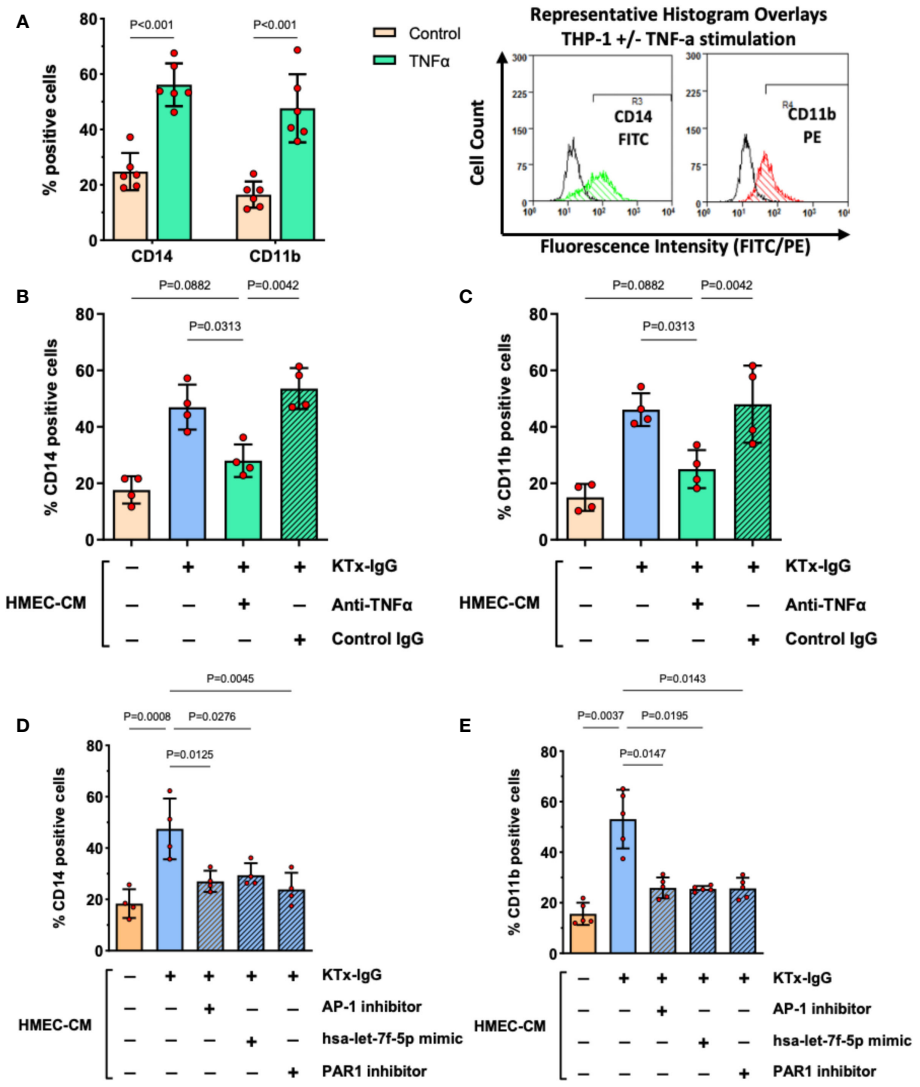

FIGURE 6
KTx-IgG-induced endothelial TNF-α stimulates THP-1 differentiation. **(A)** As positive control, THP-1 cells were treated for 16 hours with or without recombinant TNF-α (1 ng/ml) and then analyzed for the expression of monocyte activation markers CD14 and CD11b, indicating a doubling in the number of cells which are positive for these surface receptors (n=6) with representative histogram overlays shown to the right (CD14 and CD11b expression in TNF-α stimulated cells is depicted in green and red respectively, while the respective unstimulated cells are shown as black lines, in addition respective isotype controls were also included in the assay, not shown here). **(B, C)** The HMECs were preincubated with or without KTx-IgG (1 mg/ml) for 6 hours, washed to remove unbound KTx-IgG, and allowed to condition new culture medium for 24 hours with their secretome (HMEC-CM), which was then collected and added at a ratio of 10% of volume (v/v) together with TNF-α blocking or respective control antibody (Both at 1 µg/ml). After 16 hours of exposure, the THP-1 cells were assessed for either **(B)** CD14-FITC expression or **(C)** CD11b-PE expression with flow cytometry (n=4). **(D, E)** The HMECs were preincubated for 6 hours with or without KTx-IgG (1 mg/ml) in the presence or absence of AP-1 inhibitor (SR-11302, 1 µM), PAR1 inhibitor (BMS200261, 1 µM), or following miRNA-hsa-let-7f-5p-mimic transfection (1 pM). The cells were then washed and allowed to condition their culture media with their secretome for 24 hours (HMEC-CM), which was then collected and added to THP-1 cells at a ratio of 10% of volume (v/v) for 16 hours, after which the THP-1 cells were assessed for either **(D)** CD14-FITC, or **(E)** CD11b-PE expression with flow cytometry. The data in **(A)** were analyzed with t-test and in **(B–E)** with ANOVA, depicting mean +/- SD with *P<0.05, **P<0.01, and ***P<0.001.

The observation that HMECs can secrete TNF-α upon binding of KTx-IgG to their cell surface resident GPCRs is of some biological importance since ECs form the inner lining of the vasculature, measuring 300 to 1000 m2 at the blood-endothelial interface (64, 65). This may imply that the large endothelial surface can respond with TNF-α production in the vasculature, even though the amount secreted per cell is lower than that of immune cells typically implied as source of TNF-α, such as activated macrophages and T-cells (66). This is important, since ECs are not commonly associated with TNF-α secretion, although they have been shown to produce TNF-α upon pathological stimulation (35, 36).

Thus, our finding that ECs can produce TNF-α upon binding of RABs to their GPCRs adds to earlier reports on TNF-α production by ECs exposed to other proinflammatory cytokines or combinations thereof (35, 36). While the quantities of TNF-α released by KTx-IgG-activated ECs seem to be in the low picogram range, these levels may still be of biological significance.

Indeed, we could show here that KTx-IgG-activated HMEC-conditioned medium contained TNF-α at such concentrations, that it can promote activation/differentiation of myeloid cells to activated monocytes/macrophages, but that this effect could be abolished by neutralizing TNF-α in HMEC-conditioned culture media.

Moreover, we were able to delineate some of the underlying signaling pathways leading to TNF-α induction in HMECs and, subsequently monocytes in response to the TNF-α secreted by the HMECs. These signaling events involved the transcription factor AP-1 and miRNA-hsa-let-7f-5p. We have previously demonstrated that the induction of IL-6 by antibodies that target PAR1 in ECs is also controlled by AP-1 (23). This indicates that the early response element AP-1 may act as an early master regulator in the events elicited by KTx-IgG-derived anti-PAR1-RABs. The here-identified involvement of miRNA-hsa-let-7f-5p in underlying anti-PAR1-induced RAB-signaling cascades has not been reported previously and is thus of interest as a mechanistic target for further studies.

Indeed, miRNAs and other noncoding RNAs have been identified as essential modulators of signaling processes in the vasculature, particularly in the context of tissue ischemia/hypoxia and related angiogenic responses (67, 68). MicroRNAs are single-stranded, small noncoding RNAs that can act at the post-transcriptional level to activate or suppress the expression of specific target genes (69). We here found that the stimulation of HMECs with KTx-IgG resulted in the modulation of several miRNAs, but in particular, in a substantial decrease in miRNA-hsa-let-7f-5p, which appeared to be the best target in our subsequent mechanistic validation.

In contrast, supplementation of sufficient amounts of synthetic "miRNA-mimic" agent to replenish the cell endogenous miRNA-hsa-let-7f-5p abolished the stimulating effect of KTx-IgG on TNF-α production. Accordingly, the conditioned medium from HMECs treated with KTx-IgG in the presence of miRNA-hsa-let-7f-5p-mimic did not induce TNF-α-dependent effects on monocytes. Interestingly, the downmodulatory effect of KTx-IgG on miRNA-hsa-let-7f-5p expression could be enhanced by the addition of TNF-α itself, thereby suggesting a feedforward interaction.

Although known for over two decades, let-7 miRNA remains a puzzle (70). In the past, it has been predominantly linked to the development of various cancers but also with the regulation of innate immune responses (70). Our new observations may support the involvement of let-7 miRNA in inflammation and innate immune responses, in which TNF-α and particularly activated monocytes/macrophages are key participants. In this regard, it has been demonstrated earlier that depleting/reducing the number of monocytes and macrophages in animal models can minimize microvascular dysfunction in transplanted kidneys (71, 72).

One of the most promising implications of our findings concerns early disease detection. The correlation between RAB-levels and TNF-α in (kidney) allograft vasculopathy patients should be confirmed in larger clinical studies and potentially serve as valuable, non-invasive biomarkers for monitoring graft health and failure risk (23, 73–75).

The identification of the PAR1-AP-1/c-FOS-miRNA-let7-axis in our study points out the possibility for targeted therapies to minimize the risk of transplant vasculopathy. For instance, Vorapaxar, an FDA-approved PAR1 inhibitor used in cardiovascular events, could be repurposed for transplant patients (76, 77). Similarly, AP-1/c-FOS inhibitors like T-5224 showing promising results and could be explored in this context (78). Furthermore, gene therapies focusing on miRNA let-7 modulators, which are mostly in the research phase for various diseases, could be a novel therapeutic approach (79, 80). On the intercellular level, existing TNF-α inhibitors like the well-studied Infliximab, approved for conditions such as rheumatoid arthritis, offer a promising therapeutic intervention (81, 82). Therefore, our study adds new possibilities for therapeutic interventions and potential targeted therapies in allograft vasculopathy.

5 Conclusions

Our here presented findings suggest that non-HLA-directed GPCR/PAR1-activating regulatory autoantibodies (RABs) that are found in KTx-IgG from transplant patients with vasculopathy can trigger substantial TNF-α production from ECs and myeloid cells, and KTx-IgG from patients with vasculopathy potentiates the response to the natural activator thrombin. Apart from the myeloid TNF-α production, the EC-derived TNF-α production can further promote monocyte activation and differentiation. The here identified detrimental amplification loop induced by GPCR-binding RABs may contribute to allograft vasculopathy, and thus graft failure/rejection irrespective of alloimmuneresponses.

Considering the novel observation of TNF-α production by HMECs; First, this appears to be specific to PAR1-directed stimulation of HMECs with KTx-IgG from patients with underlying kidney graft vasculopathy, which is not a common experimental setting, and may thus not have been noted in earlier studies, and thus this appears to be a very novel finding. For assurance we have also provided the concomitant intracellular signaling analysis. Second, the quantity of TNF-α released by HMEC cells upon stimulation with KTx-IgG is very low (depending on the experimental setting less than 5 pg/mL) and thus it is difficult to detect in the first place, but nonetheless this amount may still be significant. While these levels are very low, they may still be of biological significance as: i) the endothelial surface in humans is very large, and ii) KTx-IgG-activated HMEC-conditioned medium promoted activation/differentiation of myeloid cells *in vitro* and that this effect can be abolished by neutralizing TNF-α.

In contrast to the well-recognized aspects of adaptive immunity in transplantation, the role of innate immunity and humoral autoimmune responses has been somewhat neglected in the past since the activation of its components has been classically seen rather as a consequence than a cause of (subsequent) lymphocyte activation. In line with a few earlier reports (83–85), the here presented new results indicate an often-underestimated role of the innate immune system in transplant rejection that may deserve more attention and further studies. Our new results may lead to a better mechanistic understanding of kidney transplant vasculopathy and thereby reduce any associated detrimental outcomes for patients. Although the relevant HLA barriers and

their associated alloimmuneresponses are of predominant importance in the kidney allograft transplantation setting, we here urge our readers to also consider the potential role of the innate immune responses as a potential negative confounder in the transplant setting, that should not be forgotten.

Further research in this direction may yield fruitful new insights into the regulation of vascular immune homeostasis, particularly on the role of vasculature resident RABs and their targeted GPCRs, to better understand and improve clinical outcomes (1).

Data availability statement

The original contributions presented in the study are included in the article/Supplementary Material. Further inquiries can be directed to the corresponding authors.

Ethics statement

The studies involving humans were approved by the local review board at Charité Universitätsmedizin Berlin. The studies were conducted in accordance with the local legislation and institutional requirements. The participants provided their written informed consent to participate in this study.

Author contributions

GM: Conceptualization, Data curation, Formal Analysis, Funding acquisition, Investigation, Methodology, Resources, Software, Supervision, Visualization, Writing – original draft, Writing – review & editing. CL: Conceptualization, Data curation, Formal Analysis, Investigation, Methodology, Software, Validation, Visualization, Writing – original draft, Writing – review & editing. MG: Conceptualization, Data curation, Formal Analysis, Investigation, Methodology, Software, Writing – original draft, Writing – review & editing, Validation, Visualization. DF: Data curation, Formal Analysis, Investigation, Methodology, Software, Visualization, Writing – original draft, Writing – review & editing, Conceptualization, Validation. PW: Data curation, Formal Analysis, Investigation, Methodology, Conceptualization, Writing – review & editing. HZ: Data curation, Formal Analysis, Investigation, Methodology, Conceptualization, Writing – review & editing. ZG: Data curation, Formal Analysis, Investigation, Methodology, Conceptualization, Writing – review & editing. LC: Data curation, Formal Analysis, Investigation, Methodology, Conceptualization, Writing – review & editing. MA: Conceptualization, Formal Analysis, Funding acquisition, Investigation, Methodology, Resources, Data curation, Writing – review & editing. HH: Data curation, Formal Analysis, Funding acquisition, Investigation, Methodology, Resources, Conceptualization, Writing – review & editing. AH: Conceptualization, Data curation, Formal Analysis, Funding acquisition, Investigation, Methodology, Resources, Writing – review & editing. DD: Conceptualization, Funding acquisition, Investigation, Resources, Supervision, Data curation, Formal Analysis, Methodology, Writing – review & editing. KB: Conceptualization, Funding acquisition, Investigation, Resources, Supervision, Data curation, Formal Analysis, Methodology, Writing – review & editing. OP: Conceptualization, Funding acquisition, Investigation, Methodology, Resources, Supervision, Writing – review & editing, Data curation, Formal Analysis. GR: Conceptualization, Funding acquisition, Investigation, Methodology, Resources, Supervision, Data curation, Formal Analysis, Writing – review & editing. OC-M: Conceptualization, Data curation, Formal Analysis, Funding acquisition, Investigation, Methodology, Resources, Supervision, Visualization, Writing – original draft, Writing – review & editing, Software, Validation, Project administration. JW: Conceptualization, Data curation, Formal Analysis, Funding acquisition, Investigation, Methodology, Project administration, Resources, Software, Supervision, Validation, Visualization, Writing – original draft, Writing - review & editing. RC: Conceptualization, Data curation, Formal Analysis, Funding acquisition, Investigation, Methodology, Project administration, Resources, Software, Supervision, Validation, Visualization, Writing – original draft, Writing – review & editing.

Funding

The author(s) declare financial support was received for the research, authorship, and/or publication of this article. GM's and RC's contributions were made possible by funding from the German Federal Ministry for Education and Research (BMBF) and German Research Foundation (DFG; projects Nephroprotection #394046635, subproject A03, as part of CRC 1365, and EXPAND-PD; CA2816/1-1) and through the BIH Center for Regenerative Therapies (BCRT) and Berlin-Brandenburg School for Regenerative Therapies (BSRT, GSC203), respectively, and in part by the European Union's Horizon 2020 Research and Innovation Program under grant agreements No 733006 (PACE) and 779293 (HIPGEN) and 754995 (EU-TRAIN). OC-M's contributions were made possible by The São Paulo Research Foundation (FAPESP 2018/18886-9, 2020/01688-0, and 2020/07069-0). We acknowledge financial support from the Open Access Publication Fund of Charité Universitätsmedizin Berlin and the DFG.

Conflict of interest

Author HH was employed by CellTrend GmbH.

The remaining authors declare that the research was conducted in the absence of any commercial or financial relationships that could be construed as a potential conflict of interest.

The author(s) declared that they were an editorial board member of Frontiers, at the time of submission. This had no impact on the peer review process and the final decision.

Publisher's note

Supplementary material

The Supplementary Material for this article can be found online at: https://www.frontiersin.org/articles/10.3389/fimmu.2023.1289744/full#supplementary-material

SUPPLEMENTARY TABLE 1
KTx patient and healthy donor serum and IgG samples.

SUPPLEMENTARY TABLE 2
Antibodies and reagents used for flow cytometry and blocking antibody.

SUPPLEMENTARY TABLE 3
Sequences of primers used in quantitative-real-time-PCR analysis.

SUPPLEMENTARY FIGURE 1
Effect of KTx-IgG on HMEC TNF-α production and NFkB/NFAT activation. **(A, B)** Effect of KTx-IgG on TNF-α protein release from HMECs **(A)** Upon a 24-hour incubation with 1.0 mg/ml Con-IgG or KTx-IgG from patients with or without vasculopathy or baseline control (pg/ml, n=3 each) and **(B)** Upon a 24-hour stimulation with 1 mg/ml KTx-IgG from patients with vasculopathy (n=5 each) in the presence or absence of the following stimuli: a) mitogen phorbol-myristate-acetate (PMA, concentration 50 ng/ml), b) thrombin (0.1 U/ml), and c) PAR-1 inhibitor (BMS200261, 1 μM); and **(C, D)** Analysis of NFkB and NFAT activation in response to KTx-IgG from patients with vasculopathy compared to Con-IgG (each 1 mg/ml for 24 hours). The activity of NFkB and NFAT signaling was analyzed with EMSA and luciferase assays, respectively, as described previously (50, 51). The data were analyzed with repeated ANOVA and expressed as Mean +/- SD with *P<0.05, **P<0.01, and ***P<0.001.

SUPPLEMENTARY FIGURE 2
Supplement to Figure 4.

SUPPLEMENTARY FIGURE 3
Supplement to Figure 3 .The TNF-α promoter sequence with the c-FOS binding sites marked in Red, respectively: -1509 ATTTATG AAGGCAAAAAAATTAAATTATTTATTTATGGAGGATGGAGAGAGGGGAA TAATAGAAGAACATCCAAGGAGAAACAGAGACAGGCCCAAGAGATGAAGA GTGAGAGGGCATGCGCACAAGGCTGACCAAGAGAGAAAGAAGTAGGCATG AGGGATCACAGGGCCCCAGAAGGCAGGGAAAGGCTCTGAAAGCCAGCTGC CGACAGAGCCCCACACGGAGGCATCTGCACCCTCGATGAAGCCCAATA AACCTCTTTTCTCTGAAATGCTGTCTGCTTGTGTGTGTGTCTGGGAG TGAGAACTTCCCAGTCTATCTAAGGAATGGAGGGAGGGACAGAGGG CTCAAAGGGAGCAAGAGCTGTGGGGAGAACAAAAGGATAAGGGCTC AGAGAGCTTCAGGGATATGTGATGGACTCACCAGGTGAGGCCGCCAG ACTGCTGCAGGGGAAGCAAAGGAGAAGCTGAGAAGATGAAGGAAAAG TCAGGGTCTGGAGGGGCGGGGGTCAGGGAGCTCCTGGGAGATATGG CCACATGTAGCGGCTCTGAGGAATGGGTTACAGGAGACCTCTGGGGA GATGTGACCACAGCAATGGGTAGGAGAATGTCCAGGGCTATGGAAGT CGAGTATGGGGACCCCCCCTTAACGAAGACAGGGCCATGTAGAGGGC CCCAGGGAGTGAAAGAGCCTCCAGGACCTCCAGGTATGGAATACAGGG GACGTTTAAGAAGATATGGCCACACACTGGGGCCCTGAGAAGTGAGA GCTTCATGAAAAAAATCAGGGACCCCAGAGTTCCTTGGAAGCCAAGAC TGAAACCAGCATTATGAGTCTCCGGGTCAGAATGAAAGAAGAAGGCC TGCCCCAGTGGGGTCTGTGAATTCCCGGGGGTGATTTCACTCCCCGGG GCTGTCCCAGGCTTGTCCCTGCTACCCCCACCCAGCCTTTCCTGAGGC CTCAAGCCTGCCACCAAGCCCCCAGCTCCTTCTCCCCGCAGGGACCCA AACACAGGCCTCAGGACTCAACACAGCTTTTCCCTCCAACCCCGTTTTC TCTCCCTCAAGGACTCAGCTTTCTGAAGCCCCTCCCAGTTCTAGTTCT ATCTTTTTCCTGCATCCTGTCTGGAAGTTAGAAGGAAACAGACCACAG ACCTGGTCCCCAAAAGAAATGGAGGCAATAGGTTTTGAGGGGCATGGG GACGGGGTTCAGCCTCCAGGGTCCTACACACAAATCAGTCAGTGGCCC AGAAGACCCCCCTCGGAATCGGAGCAGGGAGGATGGGGAGTGTGAGG GGTATCCTTGATGCTTGTGTGTCCCCAACTTTCCAAATCCCCGCCCCCG CGATGGAGAAGAAACCGAGACAGAAGGTGCAGGGCCCACTACCGCTTC CTCCAGATGAGCTCATGGGTTTCTCCACCAAGGAAGTTTTCCGCTGGTT GAATGATTCTTTCCCCGCCCTCCTCTCGCCCCAGGGACATATAAAGGCAGTT GTTGGCACACCCAgccagcagacgctccctcagcaaggacagcagaggaccagctaagaggga +50. **Legend:**ATTTATGAAGGCA...TNF-α promoter sequence (-1509bp shown) GAGGCATCTGcFOS binding site (-1277bp bis -1286bp) TaagagggaTNFa gene sequence.

References

1. Cabral-Marques O, Moll G, Catar R, Preuß B, Bankamp L, Pecher AC, et al. Autoantibodies targeting G protein-coupled receptors: An evolving history in autoimmunity. Report of the 4th international symposium. *Autoimmun Rev* (2023) 22(5):103310. doi: 10.1016/j.autrev.2023.103310

2. Lefkowitz RJ, Pierce KL, Luttrell LM. Dancing with different partners: protein kinase a phosphorylation of seven membrane-spanning receptors regulates their G protein-coupling specificity. *Mol Pharmacol* (2002) 62(5):971–4. doi: 10.1124/mol.62.5.971

3. Hermans E. Biochemical and pharmacological control of the multiplicity of coupling at G-protein-coupled receptors. *Pharmacol Ther* (2003) 99(1):25–44. doi: 10.1016/s0163-7258(03)00051-2

4. Dragun D, Müller DN, Bräsen JH, Fritsche L, Nieminen-Kelhä M, Dechend R, et al. Angiotensin II type 1-receptor activating antibodies in renal-allograft rejection. *N Engl J Med* (2005) 352(6):558–69. doi: 10.1056/NEJMoa035717

5. Dragun D, Hegner B. Non-HLA antibodies post-transplantation: clinical relevance and treatment in solid organ transplantation. *Contributions to Nephrol* (2009) 162:129–39. doi: 10.1159/000170845

6. Dragun D, Philippe A, Catar R, Hegner B. Autoimmune mediated G-protein receptor activation in cardiovascular and renal pathologies. *Thromb haemostasis* (2009) 101(4):643–8.

7. Dragun D, Philippe A, Catar R. Role of non-HLA antibodies in organ transplantation. *Curr Opin Organ Transplant* (2012) 17(4):440–5. doi: 10.1097/MOT.0b013e328355f12b

8. Dragun D, Catar R, Philippe A. Non-HLA antibodies against endothelial targets bridging allo- and autoimmunity. *Kidney Int* (2016) 90(2):280–8. doi: 10.1016/j.kint.2016.03.019

9. Lefaucheur C, Viglietti D, Bouatou Y, Philippe A, Pievani D, Aubert O, et al. Non-HLA agonistic anti-angiotensin II type 1 receptor antibodies induce a distinctive phenotype of antibody-mediated rejection in kidney transplant recipients. *Kidney Int* (2019) 96(1):189–201. doi: 10.1016/j.kint.2019.01.030

10. Aubert O, Higgins S, Bouatou Y, Yoo D, Raynaud M, Viglietti D, et al. Archetype analysis identifies distinct profiles in renal transplant recipients with transplant glomerulopathy associated with allograft survival. *J Am Soc Nephrol JASN* (2019) 30(4):625–39. doi: 10.1681/ASN.2018070777

11. Pearl MH, Chen L, ElChaki R, Elashoff D, Gjertson DW, Rossetti M, et al. Endothelin type A receptor antibodies are associated with angiotensin II type 1 receptor antibodies, vascular inflammation, and decline in renal function in pediatric kidney transplantation. *Kidney Int Rep* (2020) 5(11):1925–36. doi: 10.1016/j.ekir.2020.09.004

12. Taniguchi M, Rebellato LM, Cai J, Hopfield J, Briley KP, Haisch CE, et al. Higher risk of kidney graft failure in the presence of anti-angiotensin II type-1 receptor antibodies. *Am J Transplant* (2013) 13(10):2577–89. doi: 10.1111/ajt.12395

13. Reinsmoen NL, Lai CH, Mirocha J, Cao K, Ong G, Naim M, et al. Increased negative impact of donor HLA-specific together with non-HLA-specific antibodies on graft outcome. *Transplantation* (2014) 97(5):595–601. doi: 10.1097/01.TP.0000436927.08026.a8

14. Reinsmoen NL, Lai CH, Heidecke H, Haas M, Cao K, Ong G, et al. Anti-angiotensin type 1 receptor antibodies associated with antibody mediated rejection in donor HLA antibody negative patients. *Transplantation* (2010) 90(12):1473–7. doi: 10.1097/TP.0b013e3181fd97f1

15. Banasik M, Boratyńska M, Kościelska-Kasprzak K, Krajewska M, Mazanowska O, Kamińska D, et al. The impact of non-HLA antibodies directed against endothelin-1

type A receptors (ETAR) on early renal transplant outcomes. *Transplant Immunol* (2014) 30(1):24–9. doi: 10.1016/j.trim.2013.10.007

16. Speck D, Kleinau G, Szczepek M, Kwiatkowski D, Catar R, Philippe A, et al. Angiotensin and endothelin receptor structures with implications for signaling regulation and pharmacological targeting. *Front Endocrinol* (2022) 13:880002. doi: 10.3389/fendo.2022.880002

17. Cabral-Marques O, Halpert G, Schimke LF, Ostrinski Y, Vojdani A, Baiocchi GC, et al. Autoantibodies targeting GPCRs and RAS-related molecules associate with COVID-19 severity. *Nat Commun* (2022) 13(1):1220. doi: 10.1038/s41467-022-28905-5

18. Fonseca DLM, Filgueiras IS, Marques AHC, Vojdani E, Halpert G, Ostrinski Y, et al. Severe COVID-19 patients exhibit elevated levels of autoantibodies targeting cardiolipin and platelet glycoprotein with age: a systems biology approach. *NPJ Aging* (2023) 9(1):21. doi: 10.1038/s41514-023-00118-0

19. Catar R, Moll G, Hosp I, Simon M, Luecht C, Zhao H, et al. Transcriptional regulation of thrombin-induced endothelial VEGF induction and proangiogenic response. *Cells* (2021) 10(4). doi: 10.3390/cells10040910

20. Couto PS, Al-Arawe N, Filgueiras IS, Fonseca DLM, Hinterseher I, Catar RA, et al. Systematic review and meta-analysis of cell therapy for COVID-19: global clinical trial landscape, published safety/efficacy outcomes, cell product manufacturing and clinical delivery. *Front Immunol* (2023). doi: 10.3389/fimmu.2023.1200180

21. Cabral-Marques O, Riemekasten G. Vascular hypothesis revisited: Role of stimulating antibodies against angiotensin and endothelin receptors in the pathogenesis of systemic sclerosis. *Autoimmun Rev* (2016) 15(7):690–4. doi: 10.1016/j.autrev.2016.03.005

22. Cabral-Marques O, Riemekasten G. Functional autoantibodies targeting G protein-coupled receptors in rheumatic diseases. *Nat Rev Rheumatol* (2017) 13 (11):648–56. doi: 10.1038/nrrheum.2017.134

23. Simon M, Lücht C, Hosp I, Zhao H, Wu D, Heidecke H, et al. Autoantibodies from patients with scleroderma renal crisis promote PAR-1 receptor activation and IL-6 production in endothelial cells. *Int J Mol Sci* (2021) 22(21). doi: 10.3390/ijms222111793

24. Crespo M, Llinas-Mallol L, Redondo-Pachon D, Butler C, Gimeno J, Perez-Saez MJ, et al. Non-HLA antibodies and epitope mismatches in kidney transplant recipients with histological antibody-mediated rejection. *Front Immunol* (2021) 12:703457. doi: 10.3389/fimmu.2021.703457

25. Cabral-Marques O, Marques A, Giil LM, De Vito R, Rademacher J, Günther J, et al. GPCR-specific autoantibody signatures are associated with physiological and pathological immune homeostasis. *Nat Commun* (2018) 9(1):5224. doi: 10.1038/s41467-018-07598-9

26. Roemhild A, Otto NM, Moll G, Abou-El-Enein M, Kaiser D, Bold G, et al. Regulatory T cells for minimising immune suppression in kidney transplantation: phase I/IIa clinical trial. *Bmj* (2020). doi: 10.1136/bmj.m3734

27. Pascual M, Theruvath T, Kawai T, Tolkoff-Rubin N, Cosimi AB. Strategies to improve long-term outcomes after renal transplantation. *N Engl J Med* (2002) 346 (8):580–90. doi: 10.1056/NEJMra011295

28. Sayegh MH, Carpenter CB. Transplantation 50 years later–progress, challenges, and promises. *N Engl J Med* (2004) 351(26):2761–6. doi: 10.1056/NEJMon043418

29. Zelova H, Hosek J. TNF-alpha signalling and inflammation: interactions between old acquaintances. *Inflamm Res* (2013) 62(7):641–51. doi: 10.1007/s00011-013-0633-0

30. Kalliolias GD, Ivashkiv LB. TNF biology, pathogenic mechanisms and emerging therapeutic strategies. *Nat Rev Rheumatol* (2016) 12(1):49–62. doi: 10.1038/nrrheum.2015.169

31. Gough P, Myles IA. Tumor necrosis factor receptors: pleiotropic signaling complexes and their differential effects. *Front Immunol* (2020) 11:585880. doi: 10.3389/fimmu.2020.585880

32. Heir R, Stellwagen D. TNF-Mediated Homeostatic Synaptic Plasticity: From *in vitro* to *in vivo* Models. *Front Cell Neurosci* (2020) 14:565841. doi: 10.3389/fncel.2020.565841

33. Sprague AH, Khalil RA. Inflammatory cytokines in vascular dysfunction and vascular disease. *Biochem Pharmacol* (2009) 78(6):539–52. doi: 10.1016/j.bcp.2009.04.029

34. Connolly-Andersen AM, Moll G, Andersson C, Akerstrom S, Karlberg H, Douagi I, et al. Crimean-Congo hemorrhagic fever virus activates endothelial cells. *J Virol* (2011) 85(15):7766–74. doi: 10.1128/JVI.02469-10

35. Imaizumi T, Itaya H, Fujita K, Kudoh D, Kudoh S, Mori K, et al. Expression of tumor necrosis factor-alpha in cultured human endothelial cells stimulated with lipopolysaccharide or interleukin-1alpha. *Arterioscler Thrombosis Vasc Biol* (2000) 20 (2):410–5. doi: 10.1161/01.atv.20.2.410

36. Ranta V, Orpana A, Carpen O, Turpeinen U, Ylikorkala O, Viinikka L. Human vascular endothelial cells produce tumor necrosis factor-alpha in response to proinflammatory cytokine stimulation. *Crit Care Med* (1999) 27(10):2184–7. doi: 10.1097/00003246-199910000-00019

37. Catar RA, Wischnewski O, Chen L, Heidecke H, Rutz C, Schulein R, et al. Non-HLA antibodies targeting angiotensin II Type 1 receptor and endothelin-1 Type A receptors induce endothelial injury via beta2-arrestin link to mTOR pathway. *Kidney Int* (2022) 101(3):498–509. doi: 10.1016/j.kint.2021.09.029

38. Catar R, Witowski J, Zhu N, Lucht C, Derrac Soria A, Uceda Fernandez J, et al. IL-6 trans-signaling links inflammation with angiogenesis in the peritoneal membrane. *J Am Soc Nephrol JASN* (2017) 28(4):1188–99. doi: 10.1681/ASN.2015101169

39. Andrzejewska A, Catar R, Schoon J, Qazi TH, Sass FA, Jacobi D, et al. Multi-parameter analysis of biobanked human bone marrow stromal cells shows little influence for donor age and mild comorbidities on phenotypic and functional properties. *Front Immunol* (2019) 10:2474. doi: 10.3389/fimmu.2019.02474

40. Catar R, Moll G, Kamhieh-Milz J, Luecht C, Chen L, Zhao H, et al. Expanded hemodialysis therapy ameliorates uremia-induced systemic microinflammation and endothelial dysfunction by modulating VEGF, TNF-α and AP-1 signaling. *Front Immunol* (2021) 12:774052. doi: 10.3389/fimmu.2021.774052

41. Catar RA, Bartosova M, Kawka E, Chen L, Marinovic I, Zhang C, et al. Angiogenic role of mesothelium-derived chemokine CXCL1 during unfavorable peritoneal tissue remodeling in patients receiving peritoneal dialysis as renal replacement therapy. *Front Immunol* (2022) 13:821681. doi: 10.3389/fimmu.2022.821681

42. Zhao H, Wu D, Gyamfi MA, Wang P, Luecht C, Pfefferkorn AM, et al. Expanded Hemodialysis ameliorates uremia-induced impairment of vasculoprotective KLF2 and concomitant proinflammatory priming of endothelial cells through an ERK/AP1/cFOS-dependent mechanism. *Front Immunol* (2023) 14:1209464. doi: 10.3389/fimmu.2023.1209464

43. Moll G, Jitschin R, von Bahr L, Rasmusson-Duprez I, Sundberg B, Lonnies L, et al. Mesenchymal stromal cells engage complement and complement receptor bearing innate effector cells to modulate immune responses. *PloS One* (2011) 6(7):e21703. doi: 10.1371/journal.pone.0021703

44. Moll G, Alm JJ, Davies LC, von Bahr L, Heldring N, Stenbeck-Funke L, et al. Do cryopreserved mesenchymal stromal cells display impaired immunomodulatory and therapeutic properties? *Stem Cells* (2014) 32(9):2430–42. doi: 10.1002/stem.1729

45. Crowley LC, Scott AP, Marfell BJ, Boughaba JA, Chojnowski G, Waterhouse NJ. Measuring cell death by propidium iodide uptake and flow cytometry. *Cold Spring Harb Protoc* (2016) 2016(7). doi: 10.1101/pdb.prot087163

46. Zickler D, Luecht C, Willy K, Chen L, Witowski J, Girndt M, et al. Tumour necrosis factor-alpha in uraemic serum promotes osteoblastic transition and calcification of vascular smooth muscle cells via extracellular signal-regulated kinases and activator protein 1/c-FOS-mediated induction of interleukin 6 expression. *Nephrol Dialysis Transplant* (2018) 33(4):574–85. doi: 10.1093/ndt/gfx316

47. Catar R, Witowski J, Wagner P, Annett Schramm I, Kawka E, Philippe A, et al. The proto-oncogene c-Fos transcriptionally regulates VEGF production during peritoneal inflammation. *Kidney Int* (2013) 84(6):1119–28. doi: 10.1038/ki.2013.217

48. Moll G, Rasmusson-Duprez I, von Bahr L, Connolly-Andersen AM, Elgue G, Funke L, et al. Are therapeutic human mesenchymal stromal cells compatible with human blood? *Stem Cells* (2012) 30(7):1565–74. doi: 10.1002/stem.1111

49. Liu J, Schuff-Werner P, Steiner M. Thrombin/thrombin receptor (PAR-1)-mediated induction of IL-8 and VEGF expression in prostate cancer cells. *Biochem Biophys Res Commun* (2006) 343(1):183–9. doi: 10.1016/j.bbrc.2006.02.136

50. Philippe A, Kleinau G, Gruner JJ, Wu S, Postpieszala D, Speck D, et al. Molecular effects of auto-antibodies on angiotensin II type 1 receptor signaling and cell proliferation. *Int J Mol Sci* (2022) 23(7). doi: 10.3390/ijms23073984

51. Hegner B, Kretzschmar T, Zhu N, Kleinau G, Zhao H, Kamhieh-Milz J, et al. Autoimmune activation and hypersensitization of the AT1 and ETA receptors contributes to vascular injury in scleroderma renal crisis. *Rheumatol (Oxford)* (2023) 62(6):2284–93. doi: 10.1093/rheumatology/keac594

52. Catar RA, Wischnewski O, Chen L, Heidecke H, Rutz C, Schülein R, et al. Non-HLA antibodies targeting angiotensin II Type 1 receptor and endothelin-1 Type A receptors induce endothelial injury via β2-arrestin link to mTOR pathway. *Kidney Int* (2022) 101(3):498–509. doi: 10.1016/j.kint.2021.09.029

53. Bonder CS, Ebert LM. Fos-icking for control of angiogenesis: increasing the longevity of peritoneal dialysis. *Kidney Int* (2013) 84(6):1065–7. doi: 10.1038/ki.2013.306

54. Dragun D, Catar R, Kusch A, Heidecke H, Philippe A. Non-HLA-antibodies targeting Angiotensin type 1 receptor and antibody mediated rejection. *Hum Immunol* (2012) 73(12):1282–6. doi: 10.1016/j.humimm.2012.07.010

55. Dragun D, Catar R, Philippe A. Non-HLA antibodies in solid organ transplantation: recent concepts and clinical relevance. *Curr Opin Organ Transplant* (2013) 18(4):430–5. doi: 10.1097/MOT.0b013e3283636e55

56. Willis Fox O, Preston RJS. Molecular basis of protease-activated receptor 1 signaling diversity. *J Thromb Haemostasis JTH* (2020) 18(1):6–16. doi: 10.1111/jth.14643

57. Han X, Nieman MT, Kerlin BA. Protease-activated receptors: An illustrated review. *Res Pract Thromb Haemost* (2021) 5(1):17–26. doi: 10.1002/rth2.12454

58. Chandrabalan A, Ramachandran R. Molecular mechanisms regulating Proteinase-Activated Receptors (PARs). *FEBS J* (2021) 288(8):2697–726. doi: 10.1111/febs.15829

59. Hara T, Sata M, Fukuda D. Emerging roles of protease-activated receptors in cardiometabolic disorders. *J Cardiol* (2023) 81(4):337–46. doi: 10.1016/j.jjcc.2022.09.013

60. Kunze G, Isermann B. Targeting biased signaling by PAR1: function and molecular mechanism of parmodulins. *Blood* (2023) 141(22):2675–84. doi: 10.1182/blood.2023019775

61. Bagang N, Gupta K, Singh G, Kanuri SH, Mehan S. Protease-activated receptors in kidney diseases: A comprehensive review of pathological roles, therapeutic outcomes and challenges. *Chem Biol Interact* (2023) 377:110470. doi: 10.1016/j.cbi.2023.110470

62. Wojtukiewicz MZ, Hempel D, Sierko E, Tucker SC, Honn KV. Protease-activated receptors (PARs)–biology and role in cancer invasion and metastasis. *Cancer Metastasis Rev* (2015) 34(4):775–96. doi: 10.1007/s10555-015-9599-4

63. Sikorska D, Kamińska D, Catar R, Banasik M, Heidecke H, Schulze-Forster K, et al. Non-HLA antibodies in hand transplant recipients are connected to multiple acute rejection episodes and endothelial activation. *J Clin Med* (2022) 11(3). doi: 10.3390/jcm11030833

64. Jaffe EA. Cell biology of endothelial cells. *Hum Pathol* (1987) 18(3):234–9. doi: 10.1016/s0046-8177(87)80005-9

65. Pries AR, Secomb TW, Gaehtgens P. The endothelial surface layer. *Pflugers Arch* (2000) 440(5):653–66. doi: 10.1007/s004240000307

66. Jang DI, Lee AH, Shin HY, Song HR, Park JH, Kang TB, et al. The role of tumor necrosis factor alpha (TNF-α) in autoimmune disease and current TNF-α Inhibitors in therapeutics. *Int J Mol Sci* (2021) 22(5). doi: 10.3390/ijms22052719

67. Uchida S, Dimmeler S. Long noncoding RNAs in cardiovascular diseases. *Circ Res* (2015) 116(4):737–50. doi: 10.1161/CIRCRESAHA.116.302521

68. Bonauer A, Carmona G, Iwasaki M, Mione M, Koyanagi M, Fischer A, et al. MicroRNA-92a controls angiogenesis and functional recovery of ischemic tissues in mice. *Science* (2009) 324(5935):1710–3. doi: 10.1126/science.1174381

69. Bartel DP. MicroRNAs: genomics, biogenesis, mechanism, and function. *Cell* (2004) 116(2):281–97. doi: 10.1016/s0092-8674(04)00045-5

70. Saliminejad K, Khorram Khorshid HR, Soleymani Fard S, Ghaffari SH. An overview of microRNAs: Biology, functions, therapeutics, and analysis methods. *J Cell Physiol* (2019) 234(5):5451–65. doi: 10.1002/jcp.27486

71. Qi F, Adair A, Ferenbach D, Vass DG, Mylonas KJ, Kipari T, et al. Depletion of cells of monocyte lineage prevents loss of renal microvasculature in murine kidney transplantation. *Transplantation* (2008) 86(9):1267–74. doi: 10.1097/TP.0b013e318188d433

72. Stone JP, Ball AL, Critchley WR, Major T, Edge RJ, Amin K, et al. *Ex vivo* normothermic perfusion induces donor-derived leukocyte mobilization and removal prior to renal transplantation. *Kidney Int Rep* (2016) 1(4):230–9. doi: 10.1016/j.ekir.2016.07.009

73. Weigold F, Günther J, Pfeiffenberger M, Cabral-Marques O, Siegert E, Dragun D, et al. Antibodies against chemokine receptors CXCR3 and CXCR4 predict progressive deterioration of lung function in patients with systemic sclerosis. *Arthritis Res Ther* (2018) 20(1):52. doi: 10.1186/s13075-018-1545-8

74. Simon T, Opelz G, Wiesel M, Ott RC, Süsal C. Serial peripheral blood perforin and granzyme B gene expression measurements for prediction of acute rejection in kidney graft recipients. *Am J Transplant* (2003) 3(9):1121–7. doi: 10.1034/j.1600-6143.2003.00187.x

75. Yue X, Yin J, Wang X, Heidecke H, Hackel AM, Dong X, et al. Induced antibodies directed to the angiotensin receptor type 1 provoke skin and lung inflammation, dermal fibrosis and act species overarching. *Ann Rheum Dis* (2022). doi: 10.1136/annrheumdis-2021-222088

76. Tantry US, Bliden KP, Chaudhary R, Novakovic M, Rout A, Gurbel PA. Vorapaxar in the treatment of cardiovascular diseases. *Future Cardiol* (2020) 16 (5):373–84. doi: 10.2217/fca-2019-0090

77. Morrison JT, Govsyeyev N, Hess CN, Bonaca MP. Vorapaxar for prevention of major adverse cardiovascular and limb events in peripheral artery disease. *J Cardiovasc Pharmacol Ther* (2022) 27:10742484211056115. doi: 10.1177/10742484211056115

78. Ishida M, Ueki M, Morishita J, Ueno M, Shiozawa S, Maekawa N. T-5224, a selective inhibitor of c-Fos/activator protein-1, improves survival by inhibiting serum high mobility group box-1 in lethal lipopolysaccharide-induced acute kidney injury model. *J Intensive Care* (2015) 3:49. doi: 10.1186/s40560-015-0115-2

79. Brennan E, Wang B, McClelland A, Mohan M, Marai M, Beuscart O, et al. Protective Effect of let-7 miRNA Family in Regulating Inflammation in Diabetes-Associated Atherosclerosis. *Diabetes* (2017) 66(8):2266–77. doi: 10.2337/db16-1405

80. Gilles ME, Slack FJ. Let-7 microRNA as a potential therapeutic target with implications for immunotherapy. *Expert Opin Ther Targets* (2018) 22(11):929–39. doi: 10.1080/14728222.2018.1535594

81. Syversen SW, Jørgensen KK, Goll GL, Brun MK, Sandanger Ø, Bjørlykke KH, et al. Effect of therapeutic drug monitoring vs standard therapy during maintenance infliximab therapy on disease control in patients with immune-mediated inflammatory diseases: A randomized clinical trial. *Jama* (2021) 326(23):2375–84. doi: 10.1001/jama.2021.21316

82. Gholami A, Azizpoor J, Aflaki E, Rezaee M, Keshavarz K. Cost-effectiveness analysis of biopharmaceuticals for treating rheumatoid arthritis: infliximab, adalimumab, and etanercept. *BioMed Res Int* (2021) 2021:4450162. doi: 10.1155/2021/4450162

83. Callemeyn J, Lamarthee B, Koenig A, Koshy P, Thaunat O, Naesens M. Allorecognition and the spectrum of kidney transplant rejection. *Kidney Int* (2022) 101(4):692–710. doi: 10.1016/j.kint.2021.11.029

84. Venner JM, Hidalgo LG, Famulski KS, Chang J, Halloran PF. The molecular landscape of antibody-mediated kidney transplant rejection: evidence for NK involvement through CD16a Fc receptors. *Am J Transplant* (2015) 15(5):1336–48. doi: 10.1111/ajt.13115

85. Grebe SO, Kuhlmann U, Fogl D, Luyckx VA, Mueller TF. Macrophage activation is associated with poorer long-term outcomes in renal transplant patients. *Clin Transplant* (2011) 25(5):744–54. doi: 10.1111/j.1399-0012.2010.01345.x

frontiers | Frontiers in Immunology

TYPE Review
PUBLISHED 07 August 2024
DOI 10.3389/fimmu.2024.1384137

OPEN ACCESS

EDITED BY
Sophie Paczesny,
Medical University of South Carolina,
United States

REVIEWED BY
Adam Asch,
University of Oklahoma, United States
Sheryl McDiarmid,
The Ottawa Hospital, Canada

*CORRESPONDENCE
Olle Ringdén
olle.ringden@ki.se
Guido Moll
guido.moll@charite.de

RECEIVED 08 February 2024
ACCEPTED 24 July 2024
PUBLISHED 07 August 2024

CITATION
Ringdén O, Svahn B-M, Moll G and Sadeghi B (2024) Better clinical outcomes and lower triggering of inflammatory cytokines for allogeneic hematopoietic cell transplant recipients treated in home care versus hospital isolation – the Karolinska experience.
Front. Immunol. 15:1384137.
doi: 10.3389/fimmu.2024.1384137

Better clinical outcomes and lower triggering of inflammatory cytokines for allogeneic hematopoietic cell transplant recipients treated in home care versus hospital isolation – the Karolinska experience

Olle Ringdén [1]*, Britt-Marie Svahn [1], Guido Moll [2,3,4]* and Behnam Sadeghi [1]

[1]Translational Cell Therapy Research, Division of Pediatrics, Department of Clinical Science, Intervention and Technology (CLINTEC), Karolinska Institutet, Stockholm, Sweden, [2]BIH Center for Regenerative Therapies (BCRT), Charité Universitätsmedizin Berlin, Berlin, Germany, [3]Julius Wolff Institute (JWI), Charité Universitätsmedizin Berlin, Berlin, Germany, [4]Department of Nephrology and Internal Intensive Care Medicine, all Charité Universitätsmedizin Berlin, corporate member of Freie Universität Berlin, Humboldt-Universität zu Berlin, and Berlin Institute of Health (BIH), Berlin, Germany

After allogeneic hematopoietic cell transplantation (Allo-HCT) and conditioning, patients are typically placed in isolated hospital rooms to prevent neutropenic infections. Since 1998, we've offered an alternative: home care for patients living within a one to two-hour drive of the hospital. In Sweden this approach includes daily visits by an experienced nurse and daily phone consultations with a unit physician. When necessary, patients receive transfusions, intravenous antibiotics, and total parenteral nutrition at home. Our initial study report compared 36 home care patients with 54 hospital-treated controls. Multivariate analysis found that home care patients were discharged earlier to outpatient clinics, required fewer days of total parenteral nutrition, had less acute graft-versus-host disease (GVHD) grade II-IV, and lower transplantation-related mortality (TRM) and lower costs. Long-term follow-up showed similar chronic GVHD and relapse rates in both groups, with improved survival rates in the home care group. A subsequent comparison of 146 home care patients with hospital-treated controls indicated that home care and longer home stays were associated with lower grades of acute GVHD. Home care was found to be safe and beneficial for children and adolescents. Over two decades, 252 patients received home care post-Allo-HCT without any fatalities at-home. Ten-year outcomes showed a 14% TRM and a 59% survival rate. In 2020, an independent center confirmed the reduced risk of acute GVHD grades II-IV for patients treated in home care. Here, we report for the first time that home care patients also demonstrate a less inflammatory systemic cytokine profile. We found higher levels of IFN-γ, IL-2, IL-5, IL-13, GM-CSF, and G-CSF, but lower VEGF in hospital-treated patients, which may

contribute to acute GVHD grades II-IV. In conclusion, home-based treatment following Allo-HCT yields multiple promising clinical outcomes and improved systemic inflammatory markers, which may contribute to less development of life-threatening GVHD.

KEYWORDS

allogeneic hematopoietic cell transplantation (alloHCT), graft-versus-host disease (GVHD), steroid-resistant GvHD, inflammation, cytokines, home care, oral nutrition, morbidity and mortality

1 Introduction

Bacterial and fungal infections are common during the pancytopenic phase following allogeneic hematopoietic cell transplantation (Allo-HCT). They are a major risk for treatment related morbidity and mortality and should thus be avoided for optimal patient care.

In-hospital patient isolation practices typically include the use of Laminar Airflow (LAF) rooms or standard protective isolation in single rooms, sometimes with HEPA-filtered air. These rooms, combined with strict handwashing and the use of gloves, gowns, and masks by staff and visitors, aim to reduce any infection risks.

A prospective, randomized study comparing LAF room isolation with standard procedures found significantly fewer cases of septicemia and major local infections in the LAF group, although survival rates were not significantly different (1). Furthermore, a large multicenter study showed that patients in HEPA or LAF rooms had reduced transplantation-related mortality (TRM) and improved survival compared to those in standard isolation (2).

Outpatient chemotherapy has been administered to recipients of autologous hematopoietic cell transplantation (Auto-HCT) (3). In addition, some centers even allow patients to spend a few hours or the night at home (4).

When starting our home care program in the Stockholm region, we suggested that patients could benefit from receiving HCT-related home care instead of hospital isolation. This idea, supported by the hospital's infection control department, was met with a mix of support and skepticism among our peers. However, the Swedish Cancer Society provided financial backing for this project to systematically study the impact of home care versus hospital isolation in the HCT setting.

Consequently, in 1998, we launched a first systematic program offering home care to patients living within a 1-2-hour drive radius of Huddinge Hospital as an alternative to traditional isolation, featuring reversed isolation and HEPA-filtered air.

Outpatient Auto-HCT is well-established (5–7). Patients receiving non-myeloablative conditioning and Allo-HCT were also followed in outpatient settings (8–10). McDiarmid and colleagues reported that auto-HCT and Allo-HCT patients followed in the outpatient clinic post-transplant had fewer infections compared to those isolated in the hospital (11). They concluded that inpatient and outpatient Auto-HCT and Allo-HCT had similar outcomes. Similarly, Solomon et al. reached the same conclusion in an outpatient Allo-HCT study (12). Russell and colleagues opted for a hybrid model, providing a hospital bed for the initial two weeks post Allo-HCT but allowing patients to return home without changing their home environment (13).

Outpatient approaches require frequent, sometimes daily, hospital visits for examinations and blood tests at the outpatient clinic. With outpatient HCT, patients spend time regularly visiting the hospital. In contrast, our home care model allows patients to stay home, with nurses visiting for check-ups, blood sampling, injections, and transfusions as needed. Conditioning, whether myeloablative or reduced intensity (RIC), is administered in the hospital, and following graft infusion, the patients return home. Physicians provide afternoon calls or more frequent contact if necessary.

This article synthesizes our two decades of experience made with patient home care compared to hospital isolation post Allo-HCT in this innovative care setting, illustrating the subsequent iterative steps from the conceptional ideas and first pilot study reported in 2000 to the final long-term outcomes presented in the past years (Figure 1).

2 Home care study long-term follow-up and adjunct results

2.1 Patients receiving home care have decreased risk of moderate to severe acute GVHD

Our initial pilot study assessed the safety of providing home care after Allo-HCT (14). Patients living within a one to two-hour drive from the hospital were eligible for at-home treatment. A requirement for this option was having a caregiver—either a relative or friend—available to assist the patient. Additionally, the home environment had to be approved by the Department of Infection

FIGURE 1
Home Care versus Hospital Isolation in HSCT – Two Decades of Karolinska Experience. This figure summarizes the major achievements made during the past two decades of home care post Allo-HSCT in this innovative care setting, illustrating the subsequent iterative steps from the conceptional idea and first pilot study reported in 2000 to the final long-term outcomes presented in the past years.

Control, which required water temperatures above 50°C, the absence of potted plants and pets, thrice-weekly bedding changes, and weekly cleaning.

Following unit-based conditioning and graft reception, patients were allowed to return home. There, an experienced nurse conducted daily visits to monitor the patient's health, perform blood draws from central lines, and administer intravenous platelet or erythrocyte transfusions, total parenteral nutrition (TPN), and antibiotics when necessary, replicating hospital procedures. A physician reviewed test results daily, consulted with the home-care nurse, and contacted the patient as needed.

Of the 22 patients offered home care in the pilot, 11 accepted and met the inclusion criteria, while the others served as controls (14). In the home care cohort, three patients developed bacteremia compared to nine in the control group ($p<0.01$). Home care patients also had fewer TPN days (median 3 vs. 24, $p<0.001$), required fewer erythrocyte transfusions (median 4 vs. 8, $p<0.01$), and spent fewer days on intravenous antibiotics (median 6 vs. 13 days, $p<0.05$), with no need for analgesics ($p<0.05$) compared to hospitalized controls. These findings led us to conclude that home care was not only safe but also superior to hospital isolation.

The home care initiative continued, comparing 36 home care patients with two control groups: 18 patients who were offered but unable to receive home care for various reasons and 36 patients from other regions treated in the hospital (15). The home care patients typically returned home one day after graft infusion. Two were too ill to leave the hospital, and of the 34 treated at home, 21 were readmitted on 33 occasions (median 1 day, range 0-25 days), primarily due to fever, spending a median of 16 days (range 0-26 days) at home.

Multivariate analysis revealed several benefits of home care, including earlier outpatient clinic discharge ($p=0.03$), fewer TPN days ($p<0.01$), less acute GVHD grades II-IV ($p<0.01$), lower TRM ($p=0.04$), and reduced costs ($p<0.05$, Table 1). The incidence of grades II-IV acute GVHD was 17% among home care patients, significantly lower than the 42% and 45% observed in the control groups ($p<0.05$). Moreover, two-year survival rates were higher in the home care group (70%) compared to the control groups (51% and 57%, respectively, $p<0.05$). Thus, treatment at home, rather than hospital isolation, offered many advantages, most notably a reduced risk of developing acute GVHD grades II-IV.

2.2 Impact of home-based care on post-transplant outcomes: a comparative study of oral nutrition and acute GVHD incidence

Between 1998 and 2006, 601 patients underwent Allo-HCT at the Center for Allogeneic Stem Cell Transplantation (CAST),

TABLE 1 Improvements through home care compared to hospital care in allogeneic hematopoietic cell transplantation.

Univariate analysis			
	Home Care	Hospital Isolation	P-value
Days to discharge, Median	19	26	<0.01
Days with TPN, Median	4	14	<0.01
Acute GVHD II-IV	17%	44%	<0.05
TRM	8%	38%	<0.01
Costs until discharge, USD	25346	32226	<0.001
Multivariate analysis			
Factors	**RR**	**C.I.**	**P-value**
Days of discharge	0.33	0.12 –0.90	0.03
Days of TPN	0.24	0.09 –0.64	<0.01
Acute GVHD II-IV	0.25	0.09 –0.75	0.01
TRM	0.22	0.05 –0.96	0.04
Costs hospital care	2.7	1.01 –7.14	<0.05

From Svahn, BM et al, Blood 2002; 100:4317-4324.
RR, Relative Risk; C.I., Confidence Interval; TPN, total parenteral nutrition; GVHD, graft-versus-host disease; TRM, transplantation-related mortality.
Univariate and Multivariate analysis for outcomes.

Karolinska University Hospital, Huddinge. Of these, 76 were treated at home and compared to a matched control group of 76 hospital-treated patients, matched by age, sex, diagnosis, disease stage, conditioning, cell source, donor type, and immunosuppression (16). This study emphasized oral nutrition, an area where home care patients had previously shown superior oral intake and reduced TPN needs compared to their hospital counterparts (14, 15). Median oral caloric intake was calculated in kcal/kg/day over the first 21 days post-HCT.

Home-treated patients had a median of 20 days (range 10-114) to outpatient clinic discharge post-transplant, compared to 22 days (range 8-104) for the hospital group (p=0.16). The median number of days requiring IV analgesics was zero for both groups, home-treated and hospital controls (0-87 vs. 0-72, p=0.74). Nonetheless, home-treated patients achieved better oral nutrition, with a median intake of 22 (range 4-48) kcal/kg/day versus 19 (range 0-43) kcal/kg/day in the control group (p<0.05) and recorded higher minimum serum albumin levels (p=0.055). A positive correlation was found between the number of days at home and oral nutrition (r=0.33, p=0.004). Additionally, the incidence of acute GVHD grades II-IV was lower in the home care group at 15.9% compared to 33.1% in hospital controls (p=0.03), with five-year survival rates at 65% versus 47%, respectively (p=0.04).

Multivariate analysis showed acute GVHD grades II-IV was associated with poor oral nutrition (p=0.003) and hospital care (p=0.06). Improved oral nutrition was believed to contribute to the lower risk of acute GVHD grades II-IV in home-treated patients (16). Following these findings, we have since encouraged better oral intake among hospital-treated patients, including a dedicated nursing effort to promote improved dietary consumption.

A subsequent study of 146 home care patients, matched with an equal number of hospital controls (17), showed that intensified oral intake efforts since 2006 led to improved hospital patient nutrition (p=0.002), aligning with home care patient intake levels. However, post-2006 data revealed no significant difference in the likelihood of developing acute GVHD grades II-IV between the two groups, with rates of 41% for home care patients and 37% for hospital patients. From 1998 to 2006, home care patients spent a median of 15 days at home, which decreased to 12 days after 2006 (p=0.002).

Multivariate analysis indicated that lower grades of acute GVHD (grades 0-I) were associated with home care (HR 41, p=0.02) and the number of days spent at home (HR 0.92, p=0.005), but not with oral nutrition (HR 0.98, p=0.13). The study also found a five-year survival rate of 61% in the home care group compared to 49% in hospital controls (p=0.07).

In conclusion, the duration of home care was a key factor in reducing the risk of acute GVHD grades II-IV, overshadowing the impact of oral intake.

2.3 Pediatric home care outcomes post-HCT

Initially, the home care project for Allo-HCT was exclusive to adults due to heightened ethical considerations in pediatric novel therapies. However, the program's success led to requests from parents for home-based care for their children scheduled for Allo-HCT, prompting the extension of this option to pediatric patients.

Our study examined 29 children and adolescents receiving home care, matched with 58 hospital controls based on variables like age, diagnosis, disease stage, donor type, HLA compatibility, conditioning, and stem cell source (18). These children typically returned home two days post-HCT (range 1-15). In the home care group, 23 of the 29 children were readmitted to the hospital, primarily due to fever (n=15), with 11 experiencing multiple readmissions.

The median home stay before outpatient clinic discharge was 13 days (range 2-24). Acute GVHD grades II-IV occurred in 21% of the home care group versus 39% in hospital controls (p=0.10), with comparable rates of chronic GVHD at 13% and 8%, respectively (p=0.11). TRM was lower in the home care cohort at 11% compared to 18% among controls (p=0.40), and relapse rates were similar between groups (37% vs. 38%, p=0.81). Survival rates two to four years post-transplant were 77% in the home care group and 62% in hospital controls (p=0.33).

Cost analysis showed median expenses of 38,748 euros for home care patients versus 49,282 euros for hospital controls (p=0.20). The data suggested that home treatment for pediatric Allo-HCT patients was safe, with trends indicating potentially improved outcomes for acute GVHD grades II-IV and survival in the home-based care setting.

2.4 Long-term outcomes in home care post-HCT

After two decades of home care experience following Allo-HCT, we conducted an extensive follow-up (19). The cohort consisted of 252 patients with a median age of 47 (range 0-72). Myeloablative conditioning was administered to 102 patients, while 150 received reduced-intensity conditioning. The donor pool included 71 HLA-identical siblings, 160 matched unrelated donors, and 21 HLA mismatches.

Common complications included bloodstream infections in 54 patients (21%), graft rejection or failure in 12 (4.8%), and hemorrhagic cystitis in 25 (10%). Cytomegalovirus (CMV) PCR positivity occurred in 118 patients (47%), managed with antiviral medications (20). Symptomatic CMV disease was noted in nine patients and proven or probable invasive fungal infections occurred in 17 (6.7%), including aspergillosis (11 cases), Candida albicans (2), and Pneumocystis jirovecii (3).

The cumulative incidence of acute GVHD grades II-IV was 35%, with chronic GVHD at 46%. At the ten-year mark, TRM stood at 14%, with an overall survival rate of 59%. Among the 229 hematologic malignancy patients treated at home, the relapse probability was 34%, the survival rate was 57%, and the relapse-free survival rate was 50% after a decade.

Mortality was primarily due to relapse (51 cases) and infections (17 cases), including pneumonia (6), septicemia (5), invasive fungal infections (4), varicella-zoster encephalitis (1), and toxoplasma encephalitis (1). GVHD claimed ten lives, while Epstein-Barr virus lymphoma, secondary malignancies, graft rejection, and cerebral hemorrhages claimed one death each.

2.5 Cytokine kinetics and GVHD in allo-HCT: home care vs. hospital isolation

Serum cytokine levels in patients receiving home care following Allo-HCT and their hospital-isolated counterparts were assessed using the Luminex platform (Table 2) (21). The home care patients and hospital controls had weekly serum samples stored from the day of transplantation until discharge to the outpatient clinic.

Furthermore, home care patients and hospital controls were matched for age, diagnosis, remission status, timing, HLA match, donor type (sibling or matched unrelated donor), and had similar numbers of female donors to male recipients, G-CSF treatment post Allo-HCT, donor age, CD34+ cell dose, and cell source (21).

Serum samples, collected weekly for the first three weeks post Allo-HCT, revealed that home care patients exhibited significantly lower levels of GM-CSF ($p<0.007$), IFN-γ ($p<0.007$), IL-13 ($p<0.035$), IL-5 ($p<0.04$), and IL-2 ($p<0.07$) (Table 2), altogether indicating less systemic inflammation in their cardiovascular system.

A separate analysis of patients receiving RIC showed that those in home care had higher levels of vascular endothelial growth factor (VEGF) after three weeks compared to hospital-isolated controls ($p<0.001$). Indeed, both, the patient intrinsic or the therapy-induced levels of VEGF in the vasculature may be indicative and of key importance for vascular integrity and vascular tissue healing in GVHD and hemorrhagic cystitis (22–28).

Importantly, survival was significantly higher ($p=0.036$) in patients with median or below-median levels of GM-CSF, being 78% at three years compared to 52% survival in patients with higher levels. This suggests that GM-CSF is crucial for survival following Allo-HCT and may be further somewhat indicative of bone marrow integrity and function (22).

In addition, among hospital-treated patients, those with median or less-than-median levels of the typical pro-inflammatory cytokine IFN-γ had a three-year survival of 75% compared to 44% for those with higher-than-median IFN-γ levels ($p=0.07$), indicating that less inflammation related to IFN-γ signaling may be beneficial, as also observed in other transplant settings (29).

Noteworthy, cytokine responses were influenced by multiple other confounding factors, including bloodstream infections, anti-thymocyte globulin (ATG) therapy, G-CSF treatment, the degree of immunosuppression, conditioning intensity, donor relation, and graft type.

In this cohort, 10% of home care patients experienced acute GVHD grades III-IV, compared to 16% among hospital controls. The cumulative incidence of acute GVHD grades II-IV was 42% and 49% in the two groups, respectively. The five-year survival rates were 69% for home care patients and 57% for those in hospital care.

In summary, hospital-treated patients showed increased levels of inflammatory cytokines implicated in the development of acute GVHD grades II-IV compared to those treated at home.

3 Discussion

The foundational objective of integrating home care into the HCT process was based on the idea that patients would benefit from the comfort and familiarity of their home environment rather than the isolation of hospital stays (Figure 1). This patient-centered approach not only aimed to enhance the quality of life during the treatment period but also aspired to foster a sense of normalcy during a challenging time (14, 15). The lower probability of acute GVHD grades II-IV, lower TRM, reduced costs, and other advantages with home care compared to hospital isolation were welcomed surprises (Table 1). The lower risk of acute GVHD grades II-IV in home care Allo-HCT was recently independently confirmed in a study from Barcelona (30).

There may be several reasons for a lower risk of acute GVHD grades II-IV at home compared to the hospital. One possibility is that patients are more adapted to the bacterial flora at home compared to that in the hospital. The hospital microenvironment may be more hostile and trigger inflammatory cytokines and acute GVHD grades II-IV more than the home environment (21). The microbiome is a predictor of outcome following HCT (31). In HCT patients, the intestinal microbiome is altered by a loss of diversity (32, 33). For instance, gnotobiotic mice have a decreased risk of

TABLE 2 Cytokines decreased in multivariate analysis in home care patients in contrast to patients isolated in the hospital.

Cytokines	Week	Factor	RH	95% CI	P-value
GM-CSF	1	Home care	0.74	0.60 – 0.92	0.007
	2	GVHD II-IV	1.28	1.04 – 1.58	0.02
	2	Home care	0.77	0.63 – 0.95	0.02
IFN-γ	1	Home care	0.74	0.60 – 0.92	0.007
	2	Home care	0.77	0.62 – 0.96	0.02
	2	BSI	0.79	0.63 – 0.98	0.03
IL-13	1	Home care	0.79	0.63 – 0.98	0.035
	2	BSI	0.76	0.62 – 0.95	0.016
	2	Home care	0.82	0.66 – 1.01	0.06
IL-5	1	RIC	0.57	0.44 – 0.73	<0.001
	3	Home care	0.79	0.62 – 0.99	0.04
IL-2	1	Home care	0.81	0.65 – 0.01	0.07
	2	ATG	0.77	0.62 – 0.96	0.02

From O. Ringdén et al., International Journal of Hematology 2021; 113: 712 – 722.
RH, relative hazard; 95% CI, 95% Confidence interval; GVHD, graft-versus-host disease; BSI, blood stream infection; RIC, reduced intensity conditioning; ATG, anti-thymocyte globulin.

developing GVHD (34). In a clinical study, patients with severe aplastic anemia undergoing HCT had a lower probability of acute GVHD grades II-IV if treated in LAF rooms compared to conventional isolation rooms (35).

Nutrition and oral intake, that keeps the gastrointestinal tract functioning, may reduce the risk of gut inflammation, cytokine release, and prevent GVHD (36–38). In an early study, oral nutrition appeared to decrease the risk of acute GVHD grades II-IV in home care patients (16). However, with more patients, oral nutrition was no longer a significant factor, and the number of days spent at home became more important for reducing acute GVHD grades II-IV (17).

The type of antibiotics used also affects the gastrointestinal microbiota and may influence the risk of GVHD (39). Patients treated at home often received gentamicin for fever of unknown origin because it can be given once daily. In contrast, patients in the hospital received imipenem intravenously four times per day. This routine may have affected the gut microbiota in favor of less GVHD grades II-IV in the home care patients.

There is a correlation between moderate to severe acute GVHD and TRM (40, 41). Therefore, it can be expected that a lower incidence of moderate to severe acute GVHD would lead to improved TRM and survival (15). Other factors that may contribute to the development of acute GVHD grades II-IV primarily in the hospital include worse sleep, more stress, and less exercise. We improved the nutrition of the patients treated in the hospital by creating a special team of nurses who encouraged them to eat more and better food instead of relying on TPN. We also had a special kitchen for relatives staying in the hospital with the patients, allowing them to prepare special food that the patients liked.

Additionally, a physical therapist designed exercise programs for the patients, and they were allowed to take walks outside the hospital in the evening when the corridors were not crowded. All these improvements in hospital care were introduced and encouraged to mimic home care as much as possible. These measures may have also reduced the risk of acute GVHD among hospital patients in more recent years. Another reason for a more similar risk of acute GVHD between home care and hospital care patients may be that home care patients have spent significantly less time at home in recent years. In the early era, patients spent a median of 15 days at home during neutropenia, which was significantly longer than a median of 10 days more recently (15, 17, 21).

In the first era, one experienced physician and two experienced nurses cared for all home care patients. When home care was found to be safe, more nurses and physicians were involved. When home care patients came to the ward due to fever of unknown origin, the less experienced doctors were hesitant to send them home after instituting antibiotics. They were more likely to consult infectious disease specialists, who would recommend imipenem to cover pseudomonas aeruginosa. Indeed, the use of antibiotics like imipenem affects the gut microbiota and increases the risk of acute GVHD (39). However, imipenem is given IV four times daily, which precludes home care. The nurse generally goes to the patient's home once but no more than twice a day.

That home care patients in more recent years had a similar probability of grades II-IV acute GVHD (44%) compared to hospital care patients (37%) may only be explained by fewer days spent at home, as tissue typing, HLA matching, donor type, immunosuppression, patient selection, and GVHD treatment were the same in both groups. The number of days spent at home was significant in preventing moderate to severe acute GVHD (17). Furthermore, the probability of grades II-IV acute GVHD among

hospital patients remained unchanged at 32% and 37% in the two time periods, respectively.

It can be discussed whether a special team of doctors and nurses should care for home care patients. It seems advantageous to have the same team caring for all patients, not least so that patients have the same staff throughout the entire HCT journey. Training staff to understand the importance of patients staying at home may be crucial. That home care, with less acute GVHD grades II-IV and shorter time to discharge, was less expensive than hospital care is expected (15). Furthermore, severe complications like GVHD are costly due to long hospital stays and expensive treatments (42, 43). In addition, outpatient Auto-HCT and Allo-HCT was also less expensive than hospital isolation, as were reported in several studies (44–47).

It was debated whether the favorable outcomes in home care patients compared to hospital-treated patients were due to selection bias. We do not believe this is the case because the two groups were very well balanced for treatment characteristics such as donor type, HLA compatibility, immunosuppression, age, and conditioning (15, 17). Furthermore, there is no way to select patients expected to develop acute GVHD grades II-IV, apart from obvious risk factors like HLA match, age, and female donors to male recipients (48–50).

A study comparing cytokine levels in home care and hospital care patients shed some light on the finding that home care patients had less acute GVHD grades II-IV (21). Home care patients had lower levels of GM-CSF compared to hospital controls ($p<0.007$, Table 2). In that study, patients with low GM-CSF levels had improved survival ($p=0.036$). In experimental models, GM-CSF increased GVHD (51), and GM-CSF-licensed myeloid cells induced GVHD (52).

Furthermore, IFN-γ and IL-2 were shown to induce acute GVHD grades II-IV (53–55). Home care patients had lower levels of IFN-γ compared to hospital controls ($p=0.007$, Table 2) and a trend towards lower IL-2 ($p=0.07$). There was also a trend for better survival in hospital controls with lower-than-median levels of IFN-γ (21). Stress was reported to increase IFN-γ levels, and hospital care may induce more stress than staying at home (56).

Both, IL-13 and IL-5 were lowered in home care patients (Table 2). IL-13 induces IgE, has anti-inflammatory properties, and downregulates macrophage activity (57). We found that IgE levels were dramatically increased during acute GVHD grades II-IV (58). The low levels of IL-13 align with low acute GVHD grades II-IV in home care patients. High levels of IL-5 were reported in patients with acute GVHD grades II-IV and fit with the low levels in home care patients (55) (Table 2).

Some studies reported a lower incidence of acute GVHD with RIC as opposed to MAC, due to less damage caused by chemoradiotherapy that triggers acute GVHD (59, 60). If RIC patients were analyzed separately, home care patients had higher VEGF levels ($p=0.001$) and lower G-CSF levels ($p=0.04$) compared to hospital-treated patients (21). High VEGF levels were associated with less acute GVHD grades II-IV (61, 62). In contrast, G-CSF activates T-cells and induces acute GVHD (63, 64).

The low levels of several inflammatory cytokines, especially GM-CSF and IFN-γ, but also to some extent IL-13, IL-5, and possibly IL-2, associated with high levels of VEGF suggest that several mechanisms may be involved in the decreased risk of acute GVHD grades II-IV in home care patients compared to those in hospital isolation.

There are several advantages to home care, like less acute GVHD grades II-IV, lower TRM, and reduced costs. More US centers, such as colleagues at Duke, have started home care programs, including Allo-HCT and Auto-HCT (65). A prospective randomized study comparing home care and hospital care is underway to prove the superiority of home care over hospital isolation.

4 Conclusions

In conclusion, our two decades of experience with home care at Karolinska Hospital and a confirmatory study from Barcelona suggest, that following Allo-HCT, it seems safer to be treated at home than in the hospital. In the Karolinska setting, home care after HCT was found to be safe in adults and children, and it reduced the risk of acute GVHD, decreased transplant-related mortality, improved survival, and led to significantly lower levels of systemic proinflammatory cytokines compared to hospital-treated controls (Figure 1).

Author contributions

OR: Conceptualization, Data curation, Formal analysis, Funding acquisition, Investigation, Methodology, Project administration, Resources, Software, Supervision, Validation, Visualization, Writing – original draft, Writing – review & editing. B-MS: Conceptualization, Data curation, Formal analysis, Investigation, Methodology, Project administration, Resources, Writing – original draft, Writing – review & editing. GM: Conceptualization, Data curation, Validation, Writing – review & editing, Methodology, Software, Visualization. BS: Conceptualization, Data curation, Funding acquisition, Investigation, Supervision, Validation, Writing – original draft, Writing – review & editing.

Funding

The author(s) declare financial support was received for the research, authorship, and/or publication of this article. OR was funded by the Swedish Cancer Society grant (CAN 2018/617), the Cancer Society in Stockholm (111293), and accompanied by the honor of a Distinguished Professor Award from the Karolinska Institutet. GM's contributions were made possible by funding from the German Federal Ministry for Education and Research (BMBF) and German Research Foundation (DFG; projects Nephroprotection #394046635, subproject A03, as part of CRC 1365, and EXPAND-

PD; CA2816/1-1) and through the BIH Center for Regenerative Therapies (BCRT) and Berlin-Brandenburg School for Regenerative Therapies (BSRT, GSC203), respectively, and in part by the European Union's Horizon 2020 Research and Innovation Program under grant agreements No 733006 (PACE), 779293 (HIPGEN), 754995 (EUTRAIN), and 101095635 (PROTO).

Acknowledgments

We want to thank the staff at CAST for compassionate and competent care of our HCT patients. We thank Gunilla Tillinger for her invaluable secretarial assistance. We furthermore acknowledge financial support from the Open Access Publication Fund of Charité Universitätsmedizin Berlin and the DFG.

Conflict of interest

The authors declare that the research was conducted in the absence of any commercial or financial relationships that could be construed as a potential conflict of interest.

Publisher's note

References

1. Buckner CD, et al. Protective environment for marrow transplant recipients: a prospective study. *Ann Intern Med*. (1978) 89:893–901. doi: 10.7326/0003-4819-89-6-893

2. Passweg JR, et al. Influence of protective isolation on outcome of allogeneic bone marrow transplantation for leukemia. *Bone Marrow Transplant*. (1998) 21:1231–8. doi: 10.1038/sj.bmt.1701238

3. Meisenberg BR, et al. Outpatient high-dose chemotherapy with autologous stem-cell rescue for hematologic and nonhematologic Malignancies. *J Clin Oncol*. (1997) 15:11–7. doi: 10.1200/JCO.1997.15.1.11

4. Russell JA, et al. Allogeneic bone-marrow transplantation without protective isolation in adults with Malignant disease. *Lancet*. (1992) 339:38–40. doi: 10.1016/0140-6736(92)90153-T

5. Gilbert C, et al. Sequential prophylactic oral and empiric once-daily parenteral antibiotics for neutropenia and fever after high-dose chemotherapy and autologous bone marrow support. *J Clin Oncol*. (1994) 12:1005–11. doi: 10.1200/JCO.1994.12.5.1005

6. Peters WP, et al. The use of intensive clinic support to permit outpatient autologous bone marrow transplantation for breast cancer. *Semin Oncol*. (1994) 21:25–31.

7. Fernandez-Aviles F, et al. Case-control comparison of at-home to total hospital care for autologous stem-cell transplantation for hematologic Malignancies. *J Clin Oncol*. (2006) 24:4855–61. doi: 10.1200/JCO.2006.06.4238

8. Maris M, Storb R. Outpatient allografting in hematologic Malignancies and nonmalignant disorders–applying lessons learned in the canine model to humans. *Cancer Treat Res*. (2002) 110:149–75.

9. Ruiz-Arguelles GJ, et al. Results of an outpatient-based stem cell allotransplant program using nonmyeloablative conditioning regimens. *Am J Hematol*. (2001) 66:241–4.

10. Petersen SL, et al. Haematopoietic stem cell transplantation with non-myeloablative conditioning in the outpatient setting: results, complications and admission requirements in a single institution. *Br J Haematol*. (2004) 125:225–31. doi: 10.1111/j.1365-2141.2004.04897.x

11. McDiarmid S, et al. Performing allogeneic and autologous hematopoietic SCT in the outpatient setting: effects on infectious complications and early transplant outcomes. *Bone Marrow Transplant*. (2010) 45:1220–6. doi: 10.1038/bmt.2009.330

12. Solomon SR, et al. Outpatient myeloablative allo-SCT: a comprehensive approach yields decreased hospital utilization and low TRM. *Bone Marrow Transplant*. (2010) 45:468–75. doi: 10.1038/bmt.2009.234

13. Russell JA, et al. Early outcomes after allogeneic stem cell transplantation for leukemia and myelodysplasia without protective isolation: a 10-year experience. *Biol Blood Marrow Transplant*. (2000) 6:109–14. doi: 10.1016/S1083-8791(00)70073-5

14. Svahn BM, et al. Is it safe to treat allogeneic stem cell transplant recipients at home during the pancytopenic phase? *A pilot trial Bone Marrow Transplant*. (2000) 26:1057–60.

15. Svahn BM, et al. Home care during the pancytopenic phase after allogeneic hematopoietic stem cell transplantation is advantageous compared with hospital care. *Blood*. (2002) 100:4317–24. doi: 10.1182/blood-2002-03-0801

16. Svahn BM, et al. Case-control comparison of at-home and hospital care for allogeneic hematopoietic stem-cell transplantation: the role of oral nutrition. *Transplantation*. (2008) 85:1000–7. doi: 10.1097/TP.0b013e31816a3267

17. Ringden O, et al. Many days at home during neutropenia after allogeneic hematopoietic stem cell transplantation correlates with low incidence of acute graft-versus-host disease. *Biol Blood Marrow Transplant*. (2013) 19:314–20. doi: 10.1016/j.bbmt.2012.10.011

18. Ringden O, et al. Home care during neutropenia after allogeneic hematopoietic stem cell transplantation in children and adolescents is safe and may be more advantageous than isolation in hospital. *Pediatr Transplant*. (2014) 18:398–404. doi: 10.1111/petr.12262

19. Ringden O, et al. Long-term outcome in patients treated at home during the pancytopenic phase after allogeneic haematopoietic stem cell transplantation. *Int J Hematol*. (2018) 107:478–85. doi: 10.1007/s12185-017-2363-5

20. Ljungman P, et al. Results of different strategies for reducing cytomegalovirus-associated mortality in allogeneic stem cell transplant recipients. *Transplantation*. (1998) 66:1330–4. doi: 10.1097/00007890-199811270-00012

21. Ringden O, et al. Cytokine levels following allogeneic hematopoietic cell transplantation: a match-pair analysis of home care versus hospital care. *Int J Hematol*. (2021) 113:712–22. doi: 10.1007/s12185-021-03087-w

22. Doorn J, et al. Therapeutic applications of mesenchymal stromal cells: paracrine effects and potential improvements. *Tissue Eng Part B Rev*. (2012) 18:101–15. doi: 10.1089/ten.teb.2011.0488

23. Moll G, Le Blanc K. Engineering more efficient multipotent mesenchymal stromal (stem) cells for systemic delivery as cellular therapy. *ISBT Sci Ser*. (2015) 10:357–65. doi: 10.1111/voxs.12133

24. Baygan A, et al. Safety and side effects of using placenta-derived decidual stromal cells for graft-versus-host disease and hemorrhagic cystitis. *Front Immunol*. (2017) 8:795. doi: 10.3389/fimmu.2017.00795

25. Ringden O, et al. Placenta-derived decidua stromal cells for treatment of severe acute graft-versus-host disease. *Stem Cells Trans Med*. (2018) 7:325–32. doi: 10.1002/sctm.17-0167

26. Aronsson-Kurttila W, et al. Placenta-derived decidua stromal cells for hemorrhagic cystitis after stem cell transplantation. *Acta Haematologica*. (2018) 139:106–14. doi: 10.1159/000485735

27. Andrzejewska A, et al. Multi-parameter analysis of biobanked human bone marrow stromal cells shows little influence for donor age and mild comorbidities on phenotypic and functional properties. *Front Immunol*. (2019) 10:2474. doi: 10.3389/fimmu.2019.02474

28. Catar R, et al. Transcriptional regulation of thrombin-induced endothelial VEGF induction and proangiogenic response. *Cells*. (2021) 10. doi: 10.3390/cells10040910

29. Roemhild A, et al. Regulatory T cells for minimising immune suppression in kidney transplantation: phase I/IIa clinical trial. *Bmj*. (2020) 371:m3734. doi: 10.1136/bmj.m3734

30. Gutierrez-Garcia G, et al. A reproducible and safe at-home allogeneic haematopoietic cell transplant program: first experience in Central and Southern Europe. *Bone Marrow Transplant*. (2020) 55:965–73. doi: 10.1038/s41409-019-0768-x

31. Thiele Orberg E, et al. Bacteria and bacteriophage consortia are associated with protective intestinal metabolites in patients receiving stem cell transplantation. *Nat Cancer*. (2024) 5:187–208. doi: 10.1038/s43018-023-00669-x

32. Holler E, et al. Metagenomic analysis of the stool microbiome in patients receiving allogeneic stem cell transplantation: loss of diversity is associated with use of systemic antibiotics and more pronounced in gastrointestinal graft-versus-host disease. *Biol Blood Marrow Transplant*. (2014) 20:640–5. doi: 10.1016/j.bbmt.2014.01.030

33. Stoma I, et al. Compositional flux within the intestinal microbiota and risk for bloodstream infection with gram-negative bacteria. *Clin Infect Dis*. (2021) 73:e4627–35. doi: 10.1093/cid/ciaa068

34. van Bekkum DW, et al. Mitigation of secondary disease of allogeneic mouse radiation chimeras by modification of the intestinal microflora. *J Natl Cancer Inst*. (1974) 52:401–4. doi: 10.1093/jnci/52.2.401

35. Storb R, et al. Graft-versus-host disease and survival in patients with aplastic anemia treated by marrow grafts from HLA-identical siblings. Beneficial effect of a protective environment. *N Engl J Med*. (1983) 308:302–7. doi: 10.1056/NEJM198302103080602

36. Cooke KR, et al. An experimental model of idiopathic pneumonia syndrome after bone marrow transplantation: I. The roles of minor H antigens and endotoxin. *Blood*. (1996) 88:3230–9. doi: 10.1182/blood.V88.8.3230.bloodjournal8883230

37. Mattsson J, et al. Poor oral nutrition after allogeneic stem cell transplantation correlates significantly with severe graft-versus-host disease. *Bone Marrow Transplant*. (2006) 38:629–33. doi: 10.1038/sj.bmt.1705493

38. Reddy P, Ferrara JL. Immunobiology of acute graft-versus-host disease. *Blood Rev*. (2003) 17:187–94. doi: 10.1016/S0268-960X(03)00009-2

39. Shono Y, et al. Increased GVHD-related mortality with broad-spectrum antibiotic use after allogeneic hematopoietic stem cell transplantation in human patients and mice. *Sci Transl Med*. (2016) 8:339ra71. doi: 10.1126/scitranslmed.aaf2311

40. Gratwohl A, et al. Acute graft-versus-host disease: grade and outcome in patients with chronic myelogenous leukemia. Working Party Chronic Leukemia of the European Group for Blood and Marrow Transplantation. *Blood*. (1995) 86:813–8. doi: 10.1182/blood.V86.2.813.bloodjournal862813

41. Ringden O, et al. The highest leukaemia-free survival after allogeneic bone marrow transplantation is seen in patients with grade I acute graft-versus-host disease. Acute and Chronic Leukaemia Working Parties of the European Group for Blood and Marrow Transplantation (EBMT). *Leuk Lymphoma*. (1996) 24:71–9.

42. Svahn BM, Ringden O, Remberger M. Treatment costs and survival in patients with grades III-IV acute graft-versus-host disease after allogenic hematopoietic stem cell transplantation during three decades. *Transplantation*. (2006) 81:1600–3. doi: 10.1097/01.tp.0000210324.44633.b1

43. Svahn BM, et al. Costs of allogeneic hematopoietic stem cell transplantation. *Transplantation*. (2006) 82:147–53. doi: 10.1097/01.tp.0000226171.43943.d3

44. Meisenberg BR, et al. Reduced charges and costs associated with outpatient autologous stem cell transplantation. *Bone Marrow Transplant*. (1998) 21:927–32. doi: 10.1038/sj.bmt.1701191

45. Rizzo JD, et al. Outpatient-based bone marrow transplantation for hematologic Malignancies: cost saving or cost shifting? *J Clin Oncol*. (1999) 17:2811–8. doi: 10.1200/JCO.1999.17.9.2811

46. Jaime-Perez JC, et al. Cost structure and clinical outcome of a stem cell transplantation program in a developing country: the experience in northeast Mexico. *Oncologist*. (2015) 20:386–92. doi: 10.1634/theoncologist.2014-0218

47. Guru Murthy GS, et al. Outcomes of reduced-intensity conditioning allogeneic hematopoietic cell transplantation performed in the inpatient versus outpatient setting. *Biol Blood Marrow Transplant*. (2019) 25:827–33. doi: 10.1016/j.bbmt.2018.12.069

48. Gale RP, et al. Risk factors for acute graft-versus-host disease. *Br J Haematol*. (1987) 67:397–406. doi: 10.1111/j.1365-2141.1987.tb06160.x

49. Ringden O, Nilsson B. Death by graft-versus-host disease associated with HLA mismatch, high recipient age, low marrow cell dose, and splenectomy. *Transplantation*. (1985) 40:39–44. doi: 10.1097/00007890-198507000-00009

50. Hagglund H, et al. Risk factors for acute graft-versus-host disease in 291 consecutive HLA-identical bone marrow transplant recipients. *Bone Marrow Transplant*. (1995) 16:747–53.

51. Ullrich E, et al. BATF-dependent IL-7RhiGM-CSF+ T cells control intestinal graft-versus-host disease. *J Clin Invest*. (2018) 128:916–30. doi: 10.1172/JCI89242

52. Tugues S, et al. Graft-versus-host disease, but not graft-versus-leukemia immunity, is mediated by GM-CSF-licensed myeloid cells. *Sci Transl Med*. (2018) 10. doi: 10.1126/scitranslmed.aat8410

53. Mizuno S, et al. Gamma-interferon production capacity and T lymphocyte subpopulation after allogeneic bone marrow transplantation. *Transplantation*. (1986) 41:311–5. doi: 10.1097/00007890-198603000-00006

54. Piper C, Drobyski WR. Inflammatory cytokine networks in gastrointestinal tract graft vs. *Host Disease Front Immunol*. (2019) 10:163. doi: 10.3389/fimmu.2019.00163

55. Toubai T, et al. Role of cytokines in the pathophysiology of acute graft-versus-host disease (GVHD): are serum/plasma cytokines potential biomarkers for diagnosis of acute GVHD following allogeneic hematopoietic cell transplantation (Allo-HCT)? *Curr Stem Cell Res Ther*. (2012) 7:229–39. doi: 10.2174/157488812799859856

56. Chistiakov DA, et al. The impact of interferon-regulatory factors to macrophage differentiation and polarization into M1 and M2. *Immunobiology*. (2018) 223:101–11. doi: 10.1016/j.imbio.2017.10.005

57. Minty A, et al. Interleukin-13 is a new human lymphokine regulating inflammatory and immune responses. *Nature*. (1993) 362:248–50. doi: 10.1038/362248a0

58. Ringden O, et al. Markedly elevated serum IgE levels following allogeneic and syngeneic bone marrow transplantation. *Blood*. (1983) 61:1190–5. doi: 10.1182/blood.V61.6.1190.1190

59. Ferrara JL, Levy R, Chao NJ. Pathophysiologic mechanisms of acute graft-vs.-host disease. *Biol Blood Marrow Transplant*. (1999) 5:347–56. doi: 10.1016/S1083-8791(99)70011-X

60. Olle Ringdén MU, Sadeghi B, Solders M, Uhlin M, Mattsson J, Remberger M. Decreased risk of acute graft-versus-Host disease using reduced intensity conditioning compared to myeloablative conditioning is independent of donor-Recipient T-cell chimerism. *Transplant Technol Res*. (2014) 4:1000142.

61. Min CK, et al. Vascular endothelial growth factor (VEGF) is associated with reduced severity of acute graft-versus-host disease and nonrelapse mortality after allogeneic stem cell transplantation. *Bone Marrow Transplant*. (2006) 38:149–56. doi: 10.1038/sj.bmt.1705410

62. Nachbaur D, et al. Vascular endothelial growth factor and activin-a serum levels following allogeneic hematopoietic stem cell transplantation. *Biol Blood Marrow Transplant*. (2007) 13:942–7. doi: 10.1016/j.bbmt.2007.04.007

63. Ringden O, et al. Treatment with granulocyte colony-stimulating factor after allogeneic bone marrow transplantation for acute leukemia increases the risk of graft-versus-host disease and death: a study from the Acute Leukemia Working Party of the European Group for Blood and Marrow Transplantation. *J Clin Oncol*. (2004) 22:416–23. doi: 10.1200/JCO.2004.06.102

64. Morris ES, et al. Induction of natural killer T cell-dependent alloreactivity by administration of granulocyte colony-stimulating factor after bone marrow transplantation. *Nat Med*. (2009) 15:436–41. doi: 10.1038/nm.1948

65. Sung AD, et al. Home-based hematopoietic cell transplantation in the United States. *Transplant Cell Ther*. (2022) 28:207 e1–8. doi: 10.1016/j.jtct.2022.01.015

frontiers | Frontiers in Immunology

TYPE Original Research
PUBLISHED 08 October 2024
DOI 10.3389/fimmu.2024.1303746

OPEN ACCESS

EDITED BY
Guido Moll,
Charité University Medicine Berlin, Germany

REVIEWED BY
Josefina M. Alberu,
Tecnológico de Monterrey, Mexico
Yannis Lombardi,
Assistance Publique Hopitaux De Paris, France

*CORRESPONDENCE
Florian Kälble
florian.kaelble@med.uni-heidelberg.de
Christoph F. Mahler
christophfriedrich.mahler@med.uni-heidelberg.de

RECEIVED 28 September 2023
ACCEPTED 22 August 2024
PUBLISHED 08 October 2024

CITATION
Mahler CF, Friedl F, Nusshag C, Speer C, Benning L, Göth D, Schaier M, Sommerer C, Mieth M, Mehrabi A, Renders L, Heemann U, Krautter M, Schwenger V, Echterdiek F, Zeier M, Morath C and Kälble F (2024) Impact of deceased-donor characteristics on early graft function: outcome of kidney donor pairs accepted for transplantation. *Front. Immunol.* 15:1303746. doi: 10.3389/fimmu.2024.1303746

Impact of deceased-donor characteristics on early graft function: outcome of kidney donor pairs accepted for transplantation

Christoph F. Mahler[1*], Felix Friedl[1], Christian Nusshag[1], Claudius Speer[1], Louise Benning[1], Daniel Göth[1], Matthias Schaier[1], Claudia Sommerer[1], Markus Mieth[2], Arianeb Mehrabi[2], Lutz Renders[3], Uwe Heemann[3], Markus Krautter[4], Vedat Schwenger[4], Fabian Echterdiek[3,4], Martin Zeier[1], Christian Morath[1] and Florian Kälble[1*]

[1]Department of Nephrology, University Hospital Heidelberg, Heidelberg, Germany, [2]Department of General, Visceral and Transplantation Surgery, University Hospital Heidelberg, Heidelberg, Germany, [3]Department of Nephrology, Technical University of Munich, Munich, Germany, [4]Department of Nephrology, Hospital Stuttgart, Stuttgart, Germany

Introduction: The impact of deceased donor characteristics on kidney transplant outcomes is controversial. Correspondingly, the predictive performance of deceased donor scores remains moderate, and many transplant centers lack validated criteria for graft acceptance decisions. To better dissect donor-related risk from recipient and periprocedural variables, we analyzed outcomes of kidney donor pairs transplanted in different individuals.

Methods: This study explored (a)symmetry of early outcomes of 328 cadaveric kidney transplant recipients from 164 donor pairs transplanted at three Eurotransplant centers. The primary discriminatory factor was (a)symmetry of partner graft function, defined as early graft loss or impaired graft function [estimated glomerular filtration rate (eGFR) <30 mL/min] 3 months after transplantation. We reasoned that a relevant impact of donor factors would result in a high concordance rate of limited graft function or failure.

Results: The observed number of symmetric graft failure after transplantation was less than statistically expected (3 months: 1 versus 2, p = 0.89; and 12 months: 3 versus 5, p = 0.26). However, we found a trend toward an impaired 5-year graft survival of grafts with good function 3 months after transplantation but a failed or impaired partner graft compared to symmetrically well-functioning grafts (p = 0.09). Subsequently, we explored the impact of individual donor and recipient variables on early transplant outcomes. Generalized estimating

10.3389/fimmu.2024.1303746

equations after feature selection with LassoGEE bootstrap selected donor age, donor body mass index, and donor eGFR as the relevant risk factors.

Discussion: Our findings indicate that donor factors impact early outcomes in kidney transplantation but may have a limited role in long-term graft survival, once a graft has been accepted for transplantation. Utilizing donor-based clinical scores has the potential to aid clinicians in acceptance decisions, giving them an estimate of individual posttransplant outcomes. However, the ultimate decision for acceptance should rest with clinicians, who must consider the complex interplay of donor factors, as well as recipient and periprocedural characteristics.

KEYWORDS

immunology, transplantation - kidney, transplantation, deceased donation, scores

Introduction

Kidney transplantation is the gold-standard therapy for patients with end-stage kidney disease (1). However, clinicians face a difficult decision-making process during organ acceptance, aggravated by a scarcity of optimal donor organs. Development of organ acceptance algorithms to improve individual allocation strategies remains a challenge (2, 3). Different strategies are applied; however, the organ acceptance decisions remain center-specific without universal evidence–based criteria. Applying scoring systems, such as the kidney donor risk index/kidney donor profile index (KDRI/KDPI), has been suggested widely, but its validity in European cohorts is debated. This score calculates the relative risk of individual graft failure compared to a reference donor profile. However, individual donation and procurement factors as well as donor-recipient interactions (e.g., immunological) are omitted (4–6). Beyond these limitations, possibly misleading clinicians within the organ acceptance process, the index interpretation scaled from 0 to 100 is not intuitive and hard to illustrate for patients in a shared decision-making process. In addition to the restrictions of currently used scoring systems, there remains a debate about the general meaning of donor factors. Hence, in this study, we analyzed the outcome of 164 kidney donor pairs transplanted at our center in Heidelberg, at the transplant center of the Technical University in Munich and in Stuttgart. We used kidney function 3 months after transplantation [estimated glomerular filtration rate (eGFR) ≤30 mL/min or early graft loss (EGL) versus eGFR > 30 mL/min] as the discriminatory parameter to select groups and chose graft survival as the primary outcome. We hypothesized that a relevant impact of donor factors would result in (i) an increased rate of symmetric graft failure and (ii) a 5-year survival benefit in pairs with symmetrically good graft function 3 months after transplantation compared to index grafts with good function but an impaired or failed partner graft function (asymmetric early outcome).

Materials and methods

Study cohort

In this study, we retrospectively included N = 1,353 deceased kidney donor transplantations between 2006 and 2021 at our center (605 grafts), Stuttgart transplant center (418 grafts), and the transplant center of the Technical University in Munich (330 grafts). Partner grafts were defined as transplantations where both kidneys from a single donor were transplanted in different individuals. We collected donor and recipient characteristics with their respective clinical outcome after transplantation. The local ethics committees authorized the study without a requirement for individual consent. The following inclusion criteria were applied: recipient age of 18 years or older; offer of a kidney-organ from a deceased donor via Eurotransplant; and transplantation of both kidneys from a single donor at the same center. Exclusion criteria were combined organ offers (heart-kidney and pancreas-kidney).

Outcome

The primary outcome was graft survival. We reasoned that donor-related graft function might be most prominent during the early phase after transplantation, whereas recipient and environmental factors mainly bias late graft failure. Therefore, survival analysis was censored at 5 years from transplantation. The CKD-EPI formula was used for calculation of donor eGFR and recipient eGFR after transplantation. A total of 1,353 transplanted grafts were included in the study. From these, we selected 164 kidney pairs (328 grafts). For survival analysis, 146 grafts were excluded because of symmetric failure or impaired function. Groups were analyzed according to concordance of graft function 3 months after transplantation. Group A: good index graft function with

symmetric (good) partner graft function; and group B: good index graft function with asymmetric (failed or impaired) partner graft function (see Figure 1).

Statistical analysis

The data collection in the context of the presented project was performed with the help of an electronic database system (Microsoft Excel 2018, Microsoft Germany GmbH, Unterschleißheim). A statistical evaluation was then carried out using RStudio (R team 2021).

There were no missing data for 3-month graft function, graft survival, or 3-month recipient survival. There was less than 1.5% of data missing. Merged multiple imputation was used to compute the mean of all imputed values of each missing value. Paired grafts were identified using a unique identifier, and pairs were sorted and merged to ensure correct pairing. For comparisons of groups, we performed the chi-square test for categorical data, the Mann–Whitney rank test for non-parametric data, and the independent t-test for normal distributed data.

Survival analysis

The Kaplan–Meier estimator was used to calculate survival probabilities at 3, 12, and 60 months. The expected versus observed graft outcomes were calculated and compared using chi-square tests. The expected counts of symmetrically failed grafts were calculated using the following formula:

$$\text{Both Grafts Failed} = p_{\text{failure}}^2 \times N_{\text{pairs}}$$

where p_{failure} is the failure probability at the specified time point, and N_{pairs} is the total number of pairs. Survival data were reshaped, combined, and filtered to include only data from 3 months after transplant, and censoring was accounted for. A Cox proportional hazards model with frailty for groups was fitted. Survival functions were plotted and compared using the log-rank tests.

Variable selection and clustered analysis

Univariate generalized estimating equation (GEE) models were employed to calculate odds ratios and confidence intervals for individual variables. For variable selection, we applied Lasso regression, using the GEE model framework, to identify significant predictors. Bootstrapping was used to ensure the stability and reliability of the selected variables. A multivariate GEE model was then fitted on the basis of the previously selected variables. The KDPI was calculated using standard clinical parameters. Descriptive statistics for KDPI and the AUC for 3-month eGFR >30 were generated.

Data availability

The data and code that support the findings of this study are available from the corresponding authors upon reasonable request.

Results

Five-year graft survival based on symmetric versus asymmetric graft function 3 months after transplantation

To assess the impact of donor factors on graft function, we first explored concordance of outcomes for 164 kidney pairs. First,

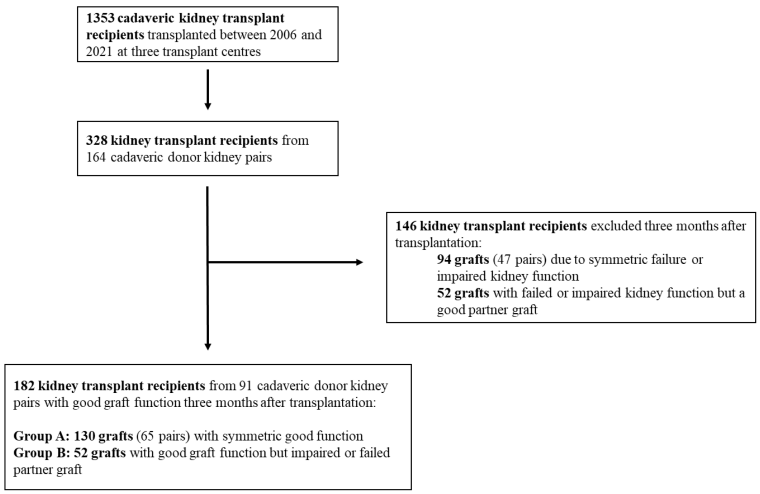

FIGURE 1
Flowchart of patient selection for statistical analysis. Good graft function: eGFR > 30 mL/min; failed or impaired graft function ≤ 30 mL/min.

10.3389/fimmu.2024.1303746

we explored whether outcomes 3, 12, and 60 months after transplantation were donor-dependent, assuming that if the donor plays an important role, then symmetric graft failure would be more frequent than expected for unrelated grafts. The observed and expected frequencies of paired graft failure at the respective time points were (1 versus 2, 3 versus 5, and 11 versus 13; Figure 1). When we completed a chi-square test, there was no significant difference between the observed and expected failure rates and observed failure rates were consistently lower than expected. This would argue against a strong role of donor dependent factors for transplant outcome at these time points.

Second, we explored whether grafts with a good early function differed in their survival rates depending on the partner graft function at 3 months from transplantation. Hence, we compared the survival curves (Figure 2) of group A (symmetric good partner graft function at 3 months) versus that of group B (asymmetric graft function at 3 months, good index graft function). Although there was a trend for reduced graft survival in the asymmetric group, this was not significant (log-rank test, p = 0.09). For illustration of the distribution of eGFR differences within pairs at 3 months after transplantation, see a histogramm in Supplementary Figure 1. Taken together, our statistical analysis demonstrates the complex interplay of donor, recipient, and periprocedural aspects influencing short-term graft function and long-term graft survival. We show a trend toward more graft failure within 5 years after transplantation in patients with a good short-term graft function but an impaired partner graft function compared to patients with a symmetric good graft function 3 months after transplantation. These results thus provide a rationale for further elucidating specific factors that confer donor-associated risks and could improve graft-offer acceptance decisions in deceased-donor kidney transplantation.

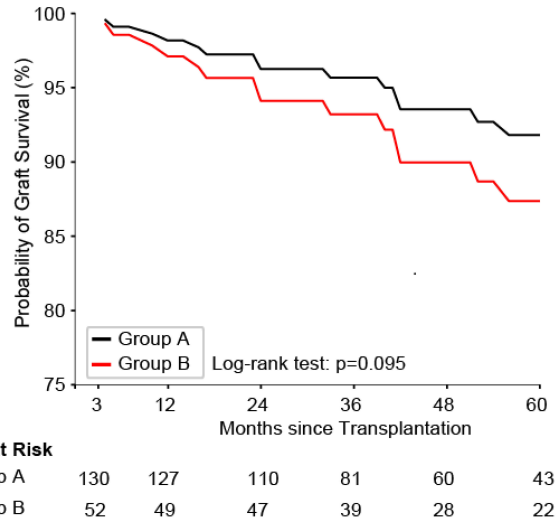

FIGURE 2
Graft survival probability for group A (symmetric good early graft function) versus group B (asymmetric graft function with good index graft at 3 months from transplantation). Kaplan–Meier survival curves comparing graft survival probabilities between groups over 60 months after transplantation. A trend for higher survival probability of group A (black line) compared to that of group B (red line) is shown, although the difference is not statistically significant (log-rank test, p = 0.095). The analysis accounted for the paired nature of the data using a cox frailty model. The number of grafts at risk in each group at different time points is displayed below the graph.

Comparison of donor and recipient characteristics between groups

To assess whether we could identify specific donor and recipient associated risk factors for graft impairment early after kidney transplantation, we performed a statistical comparison between the two groups (group A: index graft with a eGFR > 30 mL/min 3 months after transplantation, partner graft symmetric; group B: index graft with a eGFR > 30 mL/min 3 months after transplantation, partner graft asymmetric; donor characteristics, Table 1). Using this approach, we found that groups differed significantly for the following donor factors: donor age, body mass index (BMI), donor length of stay ≥ 10 days before explantation, and donor eGFR (mL/min). Similarly, groups differed for the recipient factors age, time on dialysis before transplantation, diabetes, ciclosporin, and number of human leucocyte antigen (HLA) mismatches. (recipient characteristics, Table 2). Interestingly, we showed a significant reduction of kidney function in patients with an impaired/failed partner graft compared to both (symmetrical) well-functioning grafts (group A: eGFR 94 mL/min versus group B: eGFR 81 mL/min, p < 0.001).

TABLE 1 Donor characteristics.

	Index graft function (eGFR[b] > 30 mL/min) 3 months after Tx[a]		
	Symmetric partner graft function (N = 130)	Asymmetric partner graft function (N = 52)	P-value
Modifiable and non-modifiable risk factors			
Sex (male)	62 (48)	28 (54)	0.46
Age (year)	57 [54–59]	69 [67–72]	<0.001
Body-Mass-Index	28 [27–28]	27 [26–28]	0.14
Cause of death			0.65
CVA/stroke	76 (59)	33 (63)	
Other	54 (42)	19 (36)	
Hypertension	75 (58)	36 (69)	0.17
Diabetes	20 (17)	3 (7)	0.13
Length of stay ≥ 10 days	8 (6)	2 (4)	0.02
Donor kidney function			
eGFR[b] (mL/min)	95 [91–99]	82 [77–88]	<0.001
Diuresis (mL/h)[c]	168 [149–186]	166 [139–193]	0.94

Data provided as N (%, rounded to integers) or median [IQR] based on available data; p-values underlined if < 0.05; [a]Tx, transplantation; [b]eGFR, estimated glomerular filtration rate (CKD-EPI, Chronic Kidney Disease Epidemiology Collaboration); [c]at day of explantation.

10.3389/fimmu.2024.1303746

TABLE 2 Procedural and recipient characteristics.

	Index graft function (eGFR[b] > 30 mL/min) 3 months after Tx[a]		
	Symmetric partner graft function (N = 130)	Asymmetric partner graft function (N = 52)	P-value
Recipient characteristics			
Sex (male)	91 (70)	36 (69)	0.92
Age (year)	55 [53–57]	63 [61–65]	<0.001
Body mass index	25 [24–26]	26 [25–27]	0.21
Time on dialysis before current tx[a] (years)	7 [5–10]	6 [3–7]	<0.002
PRA[c] > 5%	21 (16)	5 (9)	0.11
Diabetes	21 (16)	18 (35)	0.01
HLA[d] - mismatches	4 [3–4]	4 [4–5]	0.006
Graft function and immunosuppression			
Graft function 3 months after tx[a]			
eGFR[b] (mL/min)	94 (23)	81 (20)	<0.001
Initial graft function			0.94
Primary function	90 (70)	35 (67)	
Delayed graft function	40 (31)	17 (33)	
Ciclosporin	31 (24)	27 (52)	<0.001
Cold ischemia time (h)	12 [11–13]	12 [11–14]	0.98

Data provided as N (%, rounded to integers) or median [IQR] based on available data; p-values underlined if < 0.05; [a]Tx, transplantation; [b]eGFR, estimated glomerular filtration rate (CKD-EPI, Chronic Kidney Disease Epidemiology Collaboration); [c]PRA, panel-reactive-antibody; [d]HLA, human leucocyte antigen.

Regression analysis for early graft failure or reduced graft function at 3 months after transplantation

To explore whether clustered analysis after feature selection with LASSO (least absolute shrinkage and selection operator) bootstrap could reveal distinctive donor-associated risk factors for EGL or reduced graft function (eGFR ≤30 mL/min), we analyzed differentiation parameters for each dimension of graft characteristics (donor age, donor-associated modifiable risk factors, donor kidney function, and HLA mismatches), as well as procedural and recipient factors via univariate analysis for their power to separate different early post-transplant outcomes. In the multivariate model based on the selected variables, optimal differentiation yield was obtained for donor age, donor eGFR, and BMI (Table 3). Using these criteria, the five-fold validated Area under the curve (AUC) was 0.77. Interestingly, as a comparative analysis, KDPI was calculated (see Supplementary Table 1), with an AUC concerning the predictive power of 0.51.

Discussion

EGL after kidney transplantation is a disastrous event with far-reaching consequences for the recipient (7). The primary concern of clinicians involved in the kidney organ allocation process should, therefore, be to optimize organ allocation. In this context, donor-based scoring systems have been developed, such as the KDRI and KDPI. However, despite widespread usage in the United States, the score might underestimate the complexity within the organ allocation process, omitting individual aspects such as procedural factors, immunological constellation, or recipient characteristics. Moreover, the KDRI has been suggested to facilitate increased discard rates in the United States indicating a limited usefulness of the donor-based index (7, 8). A Canadian study by Rose et al. suggests a comparable predictive performance of the donor age compared to the full KDRI (9). Similarly, European studies show limitations of the KDRI usage (10, 11, 19). This is in line with our study; the AUC of the KDPI predicting 3-month graft impairment was 0.5.

The question concerning the general significance of donor factors arises. In this regard, ambiguous data exist (4, 12). Therefore, in this study, we investigated the significance of donor factors using the outcome of kidney donor pairs transplanted at two Eurotransplant centers.

First, we hypothesized donor factors to play a crucial role in case of a higher symmetric rate of failed or impaired partner grafts. However, this correlation could not be proved in our study. The observed rate was even lower than expected. Second, we postulated an important donor relevance if 5-year graft survival differed within grafts with good short-term function in dependence of their partner graft function (good symmetric versus impaired asymmetric). No significant difference was shown, however, at least, a trend toward a better graft survival in case of symmetric good partner graft function ($p = 0.09$). Possibly, the lack of significance is associated with a limited case number. In addition, we showed a significant impaired kidney function 3 months after transplantation of kidney transplant recipients with asymmetric graft function compared to pairs with good symmetric kidney function (81 mL/min versus 94 mL/min, $p < 0.001$).

Hence, we show donor factors not to be the main criterium in the selection of donor organs; it is a more complex interplay of also recipient and periprocedural factors, in predicting short-term graft function. However, donor factors are part and play an important role. This is in line with several other publications. Traynor et al. discussed a relationship of partner graft function and delayed graft function (13). Gourishankar et al. concluded a similarity in kidney function however a missing link between donor factors and rejection rates (14). This fits our data well.

Meanwhile, the influence of donor factors on graft survival has been tested in larger registry studies. OPTN (Organ Procurement and Transplantation Network) and USRDS (United States Renal Data System) data confirm kidney pairs to have similar outcomes concerning Delayed graft function (DGF). However, regarding long-term outcome, the effect weakens, pointing toward a growing importance of recipients factors (15). Similarly, in the present study, graft failure is significantly increased within the first 6

10.3389/fimmu.2024.1303746

TABLE 3 Regression analysis: graft outcome[a] 3 months after Tx.

	Univariate analysis			Clustered analysis with GEE[h] AUC 0.77		
	OR[b]	95% CI[c]	P-value[d]	OR[b]	95% CI[c]	P-value[d]
Donor characteristics						
Age (year)	1.10	1.06–1.13	0.01	1.08	1.05–1.11	0.01
Sex (male)	0.74	0.44–1.24	0.26			
Body mass index	0.96	0.90–1.03	0.03	0.94	0.87–1.01	0.04
eGFR[e] (mL/min)	0.97	0.96–0.99	<0.01	0.98	0.96–0.99	<0.01
Hypertension	0.99	0.59–1.68	0.26			
Diabetes	1.15	0.58–2.28	0.359			
Cause of death	0.77	0.59–1.02	0.13			
Periprocedural characteristics						
Cold ischemia time (h)	0.98	0.93–1.02	0.02			
Delayed graft function	3.00	2.11–4.26	0.14			
HLA-MM[f]	1.24	1.03–1.49	0.09			
Ciclosporin	1.49	0.92–2.41	0.24			
Recipient characteristics						
Age (years)	1.08	1.05–1.11	0.01			
Sex (male)	0.98	0.62–1.53	0.23			
Body mass index	1.04	0.99–1.09	0.02			
Years on dialysis	0.99	0.98–0.99	<0.01			
PRA[g] > 5%	1.00	0.99–1.01	<0.01			
Diabetes	1.38	0.84–2.25	0.26			

[a]Outcome: death-censored early graft loss or eGFR ≤ 30 mL/min 3 months after tx (transplantation) of 328 patients; [b]OR, odds ratio; [c]confidence interval; [d]p-values underlined if <0.05; [e]eGFR, estimated glomerular filtration rate (CKD-EPI) as continuous variable; [f]HLA-MM, human leukocyte antigen mismatch; [g]PRA, panel-reactive antibody; [h]GEE, generalized estimating equations after feature selection with LassoGEE bootstrap.
Tx, transplantation.

months after transplantation if the partner graft failed or shows poor function 3 months after transplantation. Afterward, the incidence of graft failure is similar between groups.

Summarizing, in our opinion, application of purely donor-based indices such as the KDRI in the organ allocation process needs further assessment. Statistical analyses of the KDRI within the Dutch registry showed only the minority of differences in 5-year transplantation outcome are explained by donor factors implied in the KDRI (16).

Hence, in the next step, we determined statistically significant donor and recipient factors using univariate analyses within the whole study population detached from the kidney pair approach. Using GEEs after feature selection with LassoGEE bootstrap, we explored transplantation related variables for an optimal differentiation of early graft outcome. This yielded a combination of donor factors (age, baseline eGFR, and BMI) using these criteria, and the 5-fold validated AUC was 0.77.

The outcome after transplantation seems to be a complex interaction of not only donor but also recipient characteristics and periprocedural factors. In addition, the post-transplantation treatment including the interplay of immunosuppressive medication and recipient compliance as well as the prompt anticipation of clinical complications is of immense importance. Relying on solely donor-derived scores might lead to an unjustified high discard rate of possible donor organs (17, 18). This is in line with recent UK and Dutch data that suggest the impact of donor factors on early graft failure to be limited, once a graft was accepted for transplantation (12).

Our study has several limitations. Mainly, we present a limited number of transplant recipients as we only included cases where both partner grafts were transplanted at the same center. Hence, the number of events fulfilling the primary outcome is low, attenuating the statistical power.

In summary, we show a trend toward an increased risk of graft failure of grafts with good graft function 3 months after transplantation within 5 years after transplantation, if the partner graft shows a poor graft function or failure at 3 months after transplantation. This suggests a relevant effect of donor factors predicting especially the early success after transplantation. However, without statistical significance concerning long-term graft survival, the present study does not justify to rely transplant acceptance decision only on donor factors. Within donor risk factors, present study once again proves donor age to represent the most important predictor.

On the basis of the present data, we suggest to further focus on elaborating the most important donor factors and to translate them into a patient- and clinician-friendly tool to support our organ acceptance strategy. Nevertheless, the final decision should remain with the individual clinician weighing off the complex interplay of not only the donor and the recipient but also periprocedural aspects.

Data availability statement

The raw data supporting the conclusions of this article will be made available by the authors, without undue reservation.

Ethics statement

The studies involving humans were approved by Ethikommission des Uniklinikums Heidelberg. The studies were conducted in accordance with the local legislation and institutional requirements. The ethics committee/institutional review board waived the requirement of written informed consent for participation from the participants or the participants' legal guardians/next of kin because it is a retrospective study, no seperate clinical investigations.

Author contributions

CMa: Conceptualization, Data curation, Formal analysis, Investigation, Methodology, Software, Validation, Visualization, Writing – original draft, Writing – review & editing. FF: Data curation, Writing – original draft, Writing – review & editing. CN: Writing – review & editing. CSp: Writing – review & editing. LB: Conceptualization, Writing – review & editing. DG: Data curation, Writing – review & editing. MS: Writing – review & editing. CSo: Writing – review & editing. MM: Writing – review & editing. AM: Writing – review & editing. LR: Data curation, Project administration, Resources, Writing – review & editing. UH: Data curation, Project administration, Resources, Writing – review & editing. MK: Data curation, Project administration, Resources, Writing – review & editing. VS: Data curation, Project administration, Resources, Writing – review & editing. FE: Data curation, Project administration, Resources, Writing – review & editing. MZ: Writing – review & editing. CMo: Conceptualization, Funding acquisition, Investigation, Resources, Supervision, Validation, Writing – review & editing. FK: Conceptualization, Data curation, Formal analysis, Investigation, Methodology, Project administration, Software, Supervision, Writing – original draft, Writing – review & editing.

Funding

The author(s) declare financial support was received for the research, authorship, and/or publication of this article. CMa is funded by the Clinician Scientist Program of the Heidelberg Faculty of Medicine.

Acknowledgments

We thank Monika Schmid (Transplant Centre, Heidelberg University Hospital, Heidelberg) and Eurotransplant for their support with data-collection. We would also like to thank Lukas Baumann and Johannes Vey from the Institute for Medical Biometry, Heidelberg, Germany as well as Markus Lauer for statistical consulting and review of the statistical methods. We I acknowledge the use of ChatGPT 4.0 (Open AI, https://chat.openai.com) for code-generation in Python and R.

Conflict of interest

The authors declare that the research was conducted in the absence of any commercial or financial relationships that could be construed as a potential conflict of interest.

Publisher's note

All claims expressed in this article are solely those of the authors and do not necessarily represent those of their affiliated organizations, or those of the publisher, the editors and the reviewers. Any product that may be evaluated in this article, or claim that may be made by its manufacturer, is not guaranteed or endorsed by the publisher.

Supplementary material

The Supplementary Material for this article can be found online at: https://www.frontiersin.org/articles/10.3389/fimmu.2024.1303746/full#supplementary-material

References

1. Tonelli M, Wiebe N, Knoll G, Bello A, Browne S, Jadhav D, et al. Systematic review: kidney transplantation compared with dialysis in clinically relevant outcomes. *Am J Transplant*. (2011) 11:2093–109. doi: 10.1111/j.1600-6143.2011.03686.x

2. Wu DA, Watson CJ, Bradley JA, Johnson RJ, Forsythe JL, Oniscu GC. Global trends and challenges in deceased donor kidney allocation. *Kidney Int*. (2017) 91:1287–99. doi: 10.1016/j.kint.2016.09.054

3. Childress JF. Organ donor research: overcoming challenges, increasing opportunities. *JAMA*. (2017) 318:2177–8. doi: 10.1001/jama.2017.16442

4. Lee APK, Abramowicz D. Is the Kidney Donor Risk Index a step forward in the assessment of deceased donor kidney quality? *Nephrol. Dial. Transplant*. (2015) 30:1285–90. doi: 10.1093/ndt/gfu304

5. Zhong Y, Schaubel DE, Kalbfleisch JD, Ashby VB, Rao PS, Sung RS, et al. Reevaluation of the kidney donor risk index. *Transplantation*. (2019) 103:1714–21. doi: 10.1097/TP.0000000000002498

6. Peters-Sengers H, Heemskerk MBA, Geskus RB, Kers J, van der Heide JJH, Berger SP, et al. Validation of the prognostic kidney donor risk index scoring system of deceased donors for renal transplantation in the Netherlands. *Transplantation*. (2018) 102:162–70. doi: 10.1097/TP.0000000000001889

7. Hamed MO, Chen Y, Pasea L, Watson CJ, Torpey N, Bradley JA, et al. Early graft loss after kidney transplantation: risk factors and consequences. *Am J Transplant*. (2015) 15:1632–43. doi: 10.1111/ajt.13162

8. Stewart DE, Garcia VC, Rosendale JD, Klassen DK, Carrico BJ. Diagnosing the decades-long rise in the deceased donor kidney discard rate in the United States. *Transplantation*. (2017) 101:575–87. doi: 10.1097/TP.0000000000001539

9. Rose C, Sun Y, Ferre E, Gill J, Landsberg D, Gill J. An examination of the application of the kidney donor risk index in british Columbia. *Can J Kidney Health Dis*. (2018) 5:2054358118761052. doi: 10.1177/2054358118761052

10. Dahmen M, Becker F, Pavenstädt H, Suwelack B, Schütte-Nütgen K, Reuter S. Validation of the Kidney Donor Profile Index (KDPI) to assess a deceased donor's kidneys' outcome in a European cohort. *Sci Rep*. (2019) 9:11234. doi: 10.1038/s41598-019-47772-7

11. Arias-Cabrales C, Pérez-Sáez MJ, Redondo-Pachón D, Buxeda A, Burballa C, Bermejo S, et al. Usefulness of the KDPI in Spain: A comparison with donor age and definition of standard/expanded criteria donor. *Nefrologia*. (2018) 38:503–13. doi: 10.1016/j.nefro.2018.03.003

12. Schaapherder AF, Kaisar M, Mumford L, Robb M, Johnson R, de Kok MJC, et al. Donor characteristics and their impact on kidney transplantation outcomes: Results from two nationwide instrumental variable analyses based on outcomes of donor kidney pairs accepted for transplantation. *EClinicalMedicine*. (2022) 50:101516. doi: 10.1016/j.eclinm.2022.101516

13. Traynor C, O'Kelly P, Denton M, Magee C, Conlon PJ. Concordance of outcomes of pairs of kidneys transplanted into different recipients. *Transpl. Int*. (2012) 25:918–24. doi: 10.1111/j.1432-2277.2012.01517.x

14. Gourishankar S, Jhangri GS, Cockfield SM, Halloran PF. Donor tissue characteristics influence cadaver kidney transplant function and graft survival but not rejection. *J Am Soc Nephrol*. (2003) 14:493–9. doi: 10.1097/01.ASN.0000042164.03115.B8

15. Kerr KF, Morenz ER, Thiessen-Philbrook H, Coca SG, Wilson FP, Reese PP, et al. Quantifying donor effects on transplant outcomes using kidney pairs from deceased donors. *Clin J Am Soc Nephrol*. (2019) 14:1781–7. doi: 10.2215/CJN.03810319

16. de Kok MJC, Schaapherder AFM, Alwayn IPJ, Bemelman FJ, van de Wetering J, van Zuilen AD, et al. Improving outcomes for donation after circulatory death kidney transplantation: Science of the times. *PloS One*. (2020) 15:e0236662. doi: 10.1371/journal.pone.0236662

17. Aubert O, Reese PP, Audry B, Bouatou Y, Raynaud M, Viglietti D, et al. Disparities in acceptance of deceased donor kidneys between the United States and France and estimated effects of increased US acceptance. *JAMA Intern Med*. (2019) 179:1365–74. doi: 10.1001/jamainternmed.2019.2322

18. Tullius SG, Rabb H. Improving the supply and quality of deceased-donor organs for transplantation. *New Engl J Med*. (2018) 379:693–4. doi: 10.1056/NEJMra1507080

19. Ramspek CL, El Moumni M, Wali E, Heemskerk MBA, Pol RA, Crop MJ, et al. Development and external validation study combining existing models and recent data into an up-to-date prediction model for evaluating kidneys from older deceased donors for transplantation. *Kidney Int*. (2021) 99:1459–69. doi: 10.1016/j.kint.2020.11.016

Frontiers in Immunology

Explores novel approaches and diagnoses to treat immune disorders.

The official journal of the International Union of Immunological Societies (IUIS) and the most cited in its field, leading the way for research across basic, translational and clinical immunology.

Discover the latest Research Topics

See more →

Frontiers

Avenue du Tribunal-Fédéral 34
1005 Lausanne, Switzerland
frontiersin.org

Contact us

+41 (0)21 510 17 00
frontiersin.org/about/contact